

**Cellular and molecular mechanisms underlying
Pax3-related neural tube defects**

Alexandra Jayne Palmer

Thesis submitted for the degree of Doctor of Philosophy in the University
College London

June 2015

Institute of Child Health, 30 Guilford Street, London WC1N 1EH

Declaration

I, Alexandra Jayne Palmer, confirm that the work presented in this thesis is my own. Where information has been derived from other sources, I confirm that this has been indicated in the thesis.

Abstract

The neural tube is the developmental precursor of the central nervous system (CNS). Neural tube defects (NTDs) are among the commonest birth defects, affecting approximately 1 in 1000 pregnancies. They occur when the neural tube fails to close completely during neurulation, and result in an open region of the CNS. Spina bifida is an NTD affecting the spinal region, and it can lead to lifelong disability, including incontinence, motor difficulties, and paralysis below the level of the lesion. Exencephaly is an NTD affecting the cranial region, and is not compatible with life.

Spotch mice carry a mutation in the *Pax3* gene which leads to a functionally null Pax3 protein. Pax3 is important in the development of a number of tissues, and mutant embryos have defects in muscle development, and neural crest-derived tissues, such as the heart, peripheral nervous system and melanocytes. Additionally, embryos develop NTDs; they demonstrate spina bifida with complete penetrance and exencephaly with partial penetrance.

The cellular mechanism behind the development of NTDs in *Spotch* embryos is not well understood. However excess apoptosis, premature neuronal differentiation, and reduced proliferation in the neural tube have all been proposed as potential causes. Furthermore, research has suggested a potential link between Pax3 and canonical Wnt signalling. The aim of this research was to study cellular defects in *Spotch* mice which are potentially causative of NTDs, and also to study the interaction between Pax3 and canonical Wnt signalling.

It was found that excess apoptosis and premature neuronal differentiation are not causative of spina bifida in *Spotch* mice. However, reduced proliferation is present in the neural tube, and may be causative. Additionally, β -catenin loss- and gain-of-function mutations were used to study interaction between Pax3 and canonical Wnt signalling. β -catenin loss-of-function reduces *Pax3* expression, and β -catenin gain-of-function worsens NTDs in *Pax3* mutant embryos, whereas loss-of-function partially rescues exencephaly, but not spina bifida, in these embryos. β -catenin gain- and loss-of-function both also worsen neural crest defects in *Pax3* mutant embryos. Therefore, Canonical Wnt signalling interacts with Pax3 during development, and affects the cranial and spinal regions of the neural tube differently.

In summary, *Pax3* mutation results in a number of defects in developing embryos, including NTDs and neural crest defects. Cellular processes have been studied in this research to identify abnormalities which could be causative of these defects, and a potential molecular link between Pax3 and the canonical Wnt signalling pathway has been identified, which could contribute to the observed phenotype.

Acknowledgements

First and foremost I would like to thank my amazing supervisor, Prof Nick Greene, for his patience, support, and expertise. He has always been there with an open door for a quick question or an impromptu meeting. All the good advice, direction, and help in deciphering odd data has been very much appreciated! I would also like to thank my second supervisor, Prof Andy Copp for his valued suggestions for experiments and help in analysing results.

Huge thanks go to the other members of the lab, past and present, for their invaluable contributions. Particular thanks go to Saba Raza-Knight and Sarah Escuin for teaching me so many protocols and techniques when I first started, and to Dawn Savery for keeping the mouse colonies, and keeping track of all my many genetic crosses. To everyone else, thank you all for the discussions, advice, and willingness to share what you have learnt, as well as the opportunity to vent when things went wrong! In particular I would like to thank you all for going the extra mile for me. Not many people would have been able to continue a mouse-based PhD after developing a serious allergy to mice, but thanks to the contribution of every single member of the lab I was able to finish. I literally couldn't have done this without you, and I am so grateful to all of you. You have made my PhD possible, and you have also made it hugely enjoyable. I will miss you all!

Finally, I would thank my family for being so supportive of my education and my career choice. You have always encouraged me to challenge myself and work hard, both through advice and example. I'm very grateful for your continuing and unwavering support. In particular I would like to thank my Mom, who helped me through serious illness to get to this point. I couldn't have made it without you. This thesis is dedicated to you, and to my two baby nieces, Daisy and April; may you, too, spend your lives doing something you love.

Table of Contents

Declaration.....	II
Abstract.....	III
Acknowledgements.....	IV
Table of Contents.....	V
List of Figures.....	XIII
List of Tables.....	XVII
Abbreviations.....	XVIII

1 General Introduction.....	1
1.1 Neurulation	1
1.1.1 Specification of the neural plate and the neural plate border	1
1.1.2 Convergent extension in the neural plate	4
1.1.3 Development of the hinge points	6
1.1.4 Fusion of the neural folds	9
1.1.5 Cranial closure versus caudal closure	12
1.2 Neural tube defects	13
1.2.1 Commonly observed defects	14
1.2.1.1 Spina bifida.....	14
1.2.1.2 Anencephaly.....	14
1.2.2 Risk factors	15
1.2.2.1 Genetic.....	15
1.2.2.2 Environmental.....	17
1.2.3 Mechanism of tissue damage	18
1.2.4 Folate and neural tube defects.....	20
1.3 The Neural Crest	21
1.3.1 Specification.....	22
1.3.1.1 Induction and Specification.....	22
1.3.1.2 Maintenance and Expansion.....	23
1.3.2 Migration.....	27
1.3.2.1 Signalling in neural crest delamination and migration	28
1.3.2.2 Neural crest cell guidance during migration.....	31

1.3.3 Differentiation.....	33
1.4 Pax3.....	35
1.4.1 The Pax family of transcription factors.....	35
1.4.1.1 The paired domain.....	35
1.4.1.2 Roles of <i>Pax</i> genes in cell function.....	35
1.4.1.3 Roles of <i>Pax</i> genes in tissue development and differentiation.....	36
1.4.2 <i>Pax3</i> gene and protein structure.....	38
1.4.2.1 The paired type homeodomain.....	38
1.4.2.2 Interactions between the binding sites of <i>Pax3</i> protein.....	39
1.4.3 The <i>Spotch</i> mouse.....	39
1.4.3.1 The <i>Spotch</i> phenotype.....	40
1.4.3.2 <i>Pax3</i> mutations in mice.....	40
1.4.4 Processes downstream of <i>Pax3</i>	40
1.4.4.1 Apoptosis.....	40
1.4.4.2 The neural crest.....	43
1.4.4.3 Myogenesis.....	45
1.4.5 Possible mechanisms underlying the development of neural tube defects in <i>Spotch</i> mutant embryos.....	46
1.4.5.1 Excess apoptosis.....	47
1.4.5.2 Premature neuronal differentiation.....	48
1.4.5.3 Reduced proliferation in the neural plate.....	49
1.4.6 <i>Spotch</i> and folate.....	50
1.4.7 Canonical Wnt signalling in <i>Spotch</i>	51
1.5 Waardenburg Syndrome.....	52
1.5.1 Symptoms.....	52
1.5.2 The four types of Waardenburg Syndrome.....	52
1.5.3 <i>Pax3</i> mutations and neural tube defects in Waardenburg Syndrome.....	53
1.5.4 <i>Spotch</i> as a model for Waardenburg Syndrome.....	54
1.6 The canonical <i>Wnt</i> signalling pathway.....	56
1.6.1 Wnt ligands and receptors.....	56
1.6.1.1 Synthesis and secretion of the Wnt ligand.....	59
1.6.1.2 Transport through the extracellular matrix.....	60

1.6.1.3 The Wnt receptors	61
1.6.2 The destruction complex	62
1.6.2.1 Axin	62
1.6.2.2 APC	63
1.6.2.3 GSK3 β	63
1.6.2.4 Dvl	64
1.6.3 β -catenin	65
1.6.3.1 Structure	65
1.6.3.2 β -catenin and adherens junctions	66
1.6.3.3 β -catenin and the destruction complex.....	68
1.6.3.4 Translocation to the nucleus.....	68
1.6.3.5 Transcription factor activity.....	69
1.6.4 Roles of canonical Wnt signalling during development.....	70
1.6.5 Canonical Wnt signalling and cancer	72
1.7 Aims and Hypotheses.....	72
2 Materials and Methods.....	74
2.1 Equipment and Software	74
2.1.1 Laboratory equipment	74
2.1.2 Software	74
2.2 Statistics	74
2.3 Solutions.....	75
2.4 Mouse methods, dissection and histology	76
2.4.1 Mouse husbandry	76
2.4.2 Mutations.....	77
2.4.2.1 The Pax3 ^{Sp2H} allele	77
2.4.2.2 The Pax3 ^{Cre} allele.....	78
2.4.2.3 The β -catenin Gain-Of-Function allele	80
2.4.2.4 β -catenin-null allele	80
2.4.2.5 β -catenin Loss-Of-Function allele	80
2.4.3 Mouse lines	84
2.4.3.1 Pax3 ^{Sp2H/+}	84
2.4.3.2 Pax3 ^{Cre/+}	84

2.4.3.3 β -catenin ^{GOF/GOF}	84
2.4.3.4 β -catenin ^{LOF/+}	84
2.4.3.5 β -catenin ^{+/-}	84
2.4.3.6 BatGal/+	84
2.4.3.7 p53 ^{+/-}	84
2.4.3.8 Sox1 ^{Cre/+}	86
2.4.3.9 Compound mutant mouse lines.....	86
2.4.3.10 Mouse genetic crosses.....	86
2.4.4 Embryo dissection.....	86
2.4.4.1 Dissection for tissue collection	86
2.4.4.2 Dissection for embryo culture	87
2.4.5 Embryo Culture	87
2.4.6 Tissue fixation and dehydration.....	88
2.4.7 Tissue sections	88
2.4.7.1 Paraffin wax sections	88
2.4.7.2 Vibratome sections	89
2.4.7.3 Eosin staining of tissue sections.....	89
2.5 DNA Methods.....	90
2.5.1 DNA Extraction.....	90
2.5.2 PCR	90
2.5.2.1 PCR Cycles	91
2.5.2.2 PCR Primers.....	92
2.5.2.3 Method.....	93
2.5.3 Transformation	93
2.5.4 Plasmid extraction	95
2.5.5 Plasmid linearisation.....	95
2.5.6 Whole mount TUNEL staining.....	95
2.5.6.1 Day 1: Permeabilisation and TdT enzyme incubation.....	95
2.5.6.2 Day 2: Washing, blocking, and antibody incubation.....	96
2.5.6.3 Day 3: Developing	96
2.6 RNA methods	97

2.6.1 Whole mount <i>in situ</i> hybridisation	97
2.6.1.1 Day 1: Embryo pre-treatment and hybridisation.....	97
2.6.1.2 Day 2: Post-hybridisation	98
2.6.1.3 Day 3: Washing	98
2.6.1.4 Day 4: Developing	99
2.6.2 RNA extraction	99
2.6.3 RNA purification.....	100
2.6.3.1 Using the ChromaSpin-100 DEPC-H ₂ O Columns (Clontech, California)	100
2.6.3.2 Using precipitation.....	100
2.6.4 Real time quantitative PCR	100
2.6.4.1 First strand cDNA synthesis.....	100
2.6.4.2 RT-qPCR reaction	101
2.6.5 Transcription for <i>in situ</i> probes.....	103
2.7 Protein Methods	103
2.7.1 Whole mount antibody staining	103
2.7.2 Antibody staining of wax sections	104
2.7.2.1 Day 1: Slide preparation and primary antibody incubation.....	104
2.7.2.1.1 Declere method	104
2.7.2.1.2 Citrate buffer method.....	105
2.7.2.2 Day 2: Secondary antibody incubation and slide mounting	105
2.7.2.3 Analysis of antibody staining of slides	105
2.7.3 Protein extraction and quantification.....	106
2.7.4 Western blot	106
2.7.4.1 Day 1	107
2.7.4.2 Day 2	108
3 Causes of neural tube defects in Pax3 mutant embryos	109
3.1 Results.....	109
3.1.1 Neural tube defects in <i>Spotch</i> mutant embryos.....	109
3.1.1.1 The stage of onset of spinal NTDs in <i>Spotch</i> mutant embryos	111
3.1.1.2 <i>Spotch</i> mutant embryos have an increased frequency of exencephaly	115
3.1.2 Cellular defects during spinal neurulation in <i>Spotch</i> mutant embryos.	115
3.1.2.1 <i>Pax3</i> expression in the neural tube	115

3.1.2.2 Neuronal differentiation is normal in the spinal neural tube of <i>Spotch</i> mutant embryos	115
3.1.2.3 Apoptosis does not cause spina bifida in <i>Spotch</i> mutant embryos	122
3.1.2.4 Proliferation is reduced in the spinal neural tube of <i>Spotch</i> mutant embryos	122
3.1.2.5 Morphological differences between the neural tubes of wild type and <i>Spotch</i> mutant embryos.....	128
3.1.2.5.1 Cross sectional cell number	133
3.1.2.5.2 Neural tube size	133
3.1.2.5.3 Cell density.....	136
3.1.2.5.4 Thickness of the neural folds	136
3.1.2.5.5 Bending and positions of the hinge points	139
3.1.3 The effects of folate deficiency on neural tube closure in <i>Spotch</i> mutant embryos	142
3.1.3.1 Folate deficiency increases the rate of exencephaly in <i>Spotch</i> heterozygous embryos	150
3.1.3.2 Folate deficiency slightly affects spinal neurulation in <i>Spotch</i> heterozygous embryos	150
3.1.4 Canonical Wnt signalling in <i>Spotch</i> mutant embryos	150
3.1.4.1 <i>LacZ</i> RT-qPCR of BatGal embryos.....	150
3.1.4.2 Wnt RT-qPCR plate.....	154
3.1.4.3 RT-qPCR of Wnt genes in <i>Spotch</i> mutant embryos.....	156
3.2 Discussion.....	158
3.2.1 Cellular defects during spinal neurulation in <i>Spotch</i> mutant embryos	158
3.2.2 Consequences of the reduction in proliferation in the neural tube	162
3.2.3 The effects of folate deficiency on neural tube closure in <i>Spotch</i> mutant embryos	165
3.2.4 The <i>Spotch</i> mutation and canonical Wnt signalling.....	166
3.2.5 Conclusions	168
4 Pax3 and β -Catenin Gain-of-Function.....	169
4.1 Results.....	169
4.1.1 Verification of the increase in canonical Wnt signalling in embryos carrying the β -catenin gain-of-function allele	171
4.1.2 β -catenin gain-of-function alone is not able to induce neural tube defects	175

4.1.3 The effect of β -catenin gain-of-function on the development of neural tube defects in <i>Pax3</i> ^{Sp2H/Cre} embryos	180
4.1.3.1 β -catenin gain-of-function affects spinal neurulation in <i>Pax3</i> ^{Sp2H/Cre} and <i>Pax3</i> ^{+/-} embryos, but does not cause spina bifida	180
4.1.3.2 β -catenin gain-of-function increases the rate of exencephaly in both <i>Pax3</i> ^{Sp2H/Cre} and <i>Pax3</i> ^{+/-} mutant embryos	188
4.1.4 Phenotypes resulting from β -catenin gain-of-function	188
4.1.5 β -catenin gain-of-function does not affect proliferation during cranial neurulation	190
4.1.6 β -catenin gain-of-function does not affect neuronal differentiation during neurulation.....	191
4.1.6.1 Spinal neuronal differentiation in embryos with β -catenin gain-of-function...	191
4.1.6.2 Cranial neuronal differentiation in embryos with β -catenin gain-of-function .	192
4.1.7 The effects of β -catenin gain-of-function on the development of the neural crest	198
4.1.7.1 β -catenin gain-of-function causes abnormalities in the neural crest.....	198
4.1.7.2 β -catenin gain-of-function causes an increase in apoptosis in the neural crest	204
4.1.7.3 β -catenin gain-of-function causes a slight decrease in neural crest specification	211
4.1.7.4 Development of the peripheral nervous system	219
4.1.8 β -catenin gain-of-function does not affect <i>Pax3</i> expression.....	219
4.2 Discussion.....	223
4.2.1 The β -catenin gain-of-function allele.....	223
4.2.2 β -catenin gain-of-function and neural tube defects.....	224
4.2.3 β -catenin gain-of-function and neural crest defects	226
4.2.4 The effect of β -catenin gain-of-function on <i>Pax3</i> expression.....	232
4.2.5 Conclusions	233
5 <i>Pax3</i> and β -Catenin Loss-of-Function	234
5.1 Results.....	234
5.1.1 Verification of the decrease in canonical Wnt signalling caused by the β -catenin loss-of-function allele.....	237
5.1.2 The effect of β -catenin loss-of-function on the development of neural tube defects in the <i>Pax3</i> mutant embryo	247
5.1.2.1 β -catenin loss-of-function may delay spinal neurulation in <i>Pax3</i> heterozygous mutant embryos.....	247

5.1.2.2 β -catenin loss-of-function may decrease the frequency of exencephaly in <i>Pax3</i> mutant embryos.....	255
5.1.2.3 The β -catenin loss-of-function phenotype	255
5.1.2.4 An inhibitor of Wnt signalling has no effect on the frequency of exencephaly in cultured <i>Pax3</i> mutant embryos	260
5.1.3 The effect of β -catenin loss-of-function on the development of the neural crest in <i>Pax3</i> mutant embryos.....	261
5.1.4 <i>Pax3</i> signalling is reduced by β -catenin loss-of-function.....	267
5.2 Discussion.....	271
5.2.1 The β -catenin Loss-of-Function allele	271
5.2.2 β -catenin loss-of-function and neural tube defects	272
5.2.3 β -catenin loss-of-function and neural crest defects	274
5.2.4 The effects of β -catenin loss-of-function on <i>Pax3</i> expression.....	275
5.2.5 Conclusions	277
6 General Discussion.....	278
6.1 Neural tube defects	278
6.2 <i>Pax3</i> , Canonical Wnt signalling, and the neural crest.....	282
7 References	285

List of Figures

Chapter 1: General Introduction

Figure 1.1: The neural tube during neurulation.....	2
Figure 1.2: An example of cell intercalation.....	5
Figure 1.3: Modes of neural tube closure.....	8
Figure 1.4: Hinge point formation.....	10
Figure 1.5: A timeline of neural tube closure and neural crest development.....	11
Figure 1.6: The structure of the <i>Pax3</i> gene.....	39
Figure 1.7: Canonical Wnt signalling in the absence or presence of a Wnt ligand.....	58
Figure 1.8: The structures of the β -catenin gene and protein.....	66

Chapter 2: Materials and Methods

Figure 2.1: Structures of the Sp^{2H} allele and protein of <i>Pax3</i>	77
Figure 2.2: Structure of the $Pax3^{Cre}$ allele.....	78
Figure 2.3: Structures of the β -catenin ^{GOF} allele and protein.....	79
Figure 2.4: Structure of the β catenin ⁻ allele.....	82
Figure 2.5: Structures of the β -catenin ^{LOF} allele and protein.....	83

Chapter 3: Causes of neural tube defects in *Pax3* mutant embryos

Figure 3.1: The <i>Splootch</i> phenotype.....	110
Figure 3.2: Closure of the posterior neuropore in the <i>Splootch</i> mouse.....	113
Figure 3.3: The frequency of exencephaly in the <i>Splootch</i> mouse.....	114
Figure 3.4: Region of <i>Pax3</i> expression.....	116
Figure 3.5: Comparing <i>Ngn2</i> expression between $+/+$ and Sp^{2H}/Sp^{2H} embryos.....	117
Figure 3.6: Comparing expression levels of Notch genes between $+/+$ and Sp^{2H}/Cre embryos.....	119
Figure 3.7: Comparing neuronal differentiation between $+/+$ and Sp^{2H}/Cre embryos.....	121
Figure 3.8: Comparing levels of apoptosis in $+/+$ and Sp^{2H}/Sp^{2H} embryos.....	124
Figure 3.9: Phenotypes of embryos from a $Pax3^{Sp2H/+} p53^{+/-}$ x $Pax3^{Sp2H/+} p53^{+/-}$ cross.....	126
Figure 3.10: Comparing levels of apoptosis in $Pax3^{+/+} p53^{+/+}$ and $Pax3^{+/+} p53^{-/-}$ embryos.....	127
Figure 3.11: Proliferation rates in the neural tubes of $+/+$ and Sp^{2H}/Sp^{2H} embryos – 1.....	130
Figure 3.12: Proliferation rates in the neural tubes of $+/+$ and Sp^{2H}/Sp^{2H} embryos – 2.....	131
Figure 3.13: Comparing the morphology of $+/+$ and Sp^{2H}/Sp^{2H} embryos – 1.....	132
Figure 3.14: Comparing the morphology of $+/+$ and Sp^{2H}/Sp^{2H} embryos – 2.....	135
Figure 3.15: Comparing the morphology of $+/+$ and Sp^{2H}/Sp^{2H} embryos – 3.....	137

Figure 3.16: Comparing the morphology of $+/+$ and Sp^{2H}/Sp^{2H} embryos – 4.....	138
Figure 3.17: Comparing the angle of the medial hinge point between $+/+$ and Sp^{2H}/Sp^{2H} embryos.....	141
Figure 3.18: Comparing the angles of the dorsolateral hinge points between $+/+$ and Sp^{2H}/Sp^{2H} embryos – 1.....	144
Figure 3.19: Comparing the angles of the dorsolateral hinge points between $+/+$ and Sp^{2H}/Sp^{2H} embryos – 2.....	145
Figure 3.20: Comparing the positions of the dorsolateral hinge points between $+/+$ and Sp^{2H}/Sp^{2H} embryos.....	147
Figure 3.21: Exencephaly in folate-deficient embryos.....	148
Figure 3.22: Comparing the frequency of exencephaly in embryos of different genotypes with either normal or folate deficient status.....	149
Figure 3.23: Posterior neuropore closure in folate deficient embryos.....	151
Figure 3.24: Comparison of posterior neuropore size in embryos of different genotypes with either normal or folate deficient status.....	153
Figure 3.25: Comparing Wnt signalling levels between $+/+$ and Sp^{2H}/Sp^{2H} embryos.....	154
Figure 3.26: Comparing expressions of Wnt-related genes in $+/+$ and Sp^{2H}/Cre embryos.....	157

Chapter 4: *Spotch* and β -catenin Gain-of-Function

Figure 4.1: A punnet square demonstrating the progeny from the cross $Pax3^{Sp2H/+} \beta$ -catenin ^{GOF/+} x $Pax3^{Cre/+} \beta$ -catenin ^{+/+}	170
Figure 4.2: Pooling of embryo genotypes from the cross $Pax3^{Sp2H/+} \beta$ -catenin ^{GOF/+} x $Pax3^{Cre/+} \beta$ -catenin ^{+/+}	173
Figure 4.3: β -catenin gain-of-function increases expression of <i>Axin2</i>	174
Figure 4.4: β -catenin gain-of-function increases the expression of Wnt markers.....	177
Figure 4.5: The effect of β -catenin gain-of-function on the development of neural tube defects in the absence of <i>Pax3</i> mutation.....	179
Figure 4.6: β -catenin gain-of-function does not affect the size of the posterior neuropore....	183
Figure 4.7: β -catenin gain-of-function increases the frequency of exencephaly but not spina bifida in <i>Pax3</i> mutant and heterozygous embryos.....	187
Figure 4.8: Phenotype of $Pax3^{Sp2H/Cre} \beta$ -catenin ^{GOF/+} embryos.....	189
Figure 4.9: β -catenin gain-of-function does not affect proliferation in the cranial neural tube.....	194
Figure 4.10: β -catenin gain-of-function does not affect the rostro-causal progression of spinal neuronal differentiation in $Pax3^{Cre/+}$ or $Pax3^{Sp2H/Cre}$ embryos.....	195
Figure 4.11: β -catenin gain-of-function does not affect neuronal differentiation in the cranial	

neural tube.....	197
Figure 4.12: β -catenin gain-of-function disrupts expression of <i>ErbB3</i>	200
Figure 4.13: Neuronal differentiation is disrupted by β -catenin gain-of-function.....	203
Figure 4.14: TUNEL assay of 22-24 somite stage embryos.....	206
Figure 4.15: TUNEL assay of 27-29 somite stage embryos.....	208
Figure 4.16: TUNEL assay of 30+ somite stage embryos.....	210
Figure 4.17: β -catenin gain-of-function slightly decreases spinal <i>FoxD3</i> expression in <i>Pax3</i> heterozygous embryos.....	214
Figure 4.18: β -catenin gain-of-function does not affect expression of <i>Ngn2</i>	216
Figure 4.19: β -catenin gain-of-function reduces expression of <i>Brn3a</i> in the spinal region.....	218
Figure 4.20: Positions of primer pairs 1 and 2 within the <i>Pax3</i> gene.....	220
Figure 4.21: β -catenin gain-of-function does not affect <i>Pax3</i> expression levels.....	222

Chapter 5: *Spotch* and β -catenin Loss-of-Function

Figure 5.1: Punnet square demonstrating genotypes and ratios of offspring from the cross <i>Pax3</i> ^{Sp2H/+} β -catenin ^{LOF/+} x <i>Pax3</i> ^{Cre/+} β -catenin ^{+/-}	235
Figure 5.2: Punnet square demonstrating genotypes and ratios of offspring from the cross <i>Pax3</i> ^{Sp2H/+} β -catenin ^{LOF/+} x <i>Pax3</i> ^{Cre/+} β -catenin ^{LOF/+}	236
Figure 5.3: Pooling of embryo genotypes from the cross <i>Pax3</i> ^{Sp2H/+} β -catenin ^{LOF/+} x <i>Pax3</i> ^{Cre/+} β -catenin ^{LOF/+}	241
Figure 5.4: Pooling of embryo genotypes from the cross <i>Pax3</i> ^{Sp2H/+} β -catenin ^{LOF/+} x <i>Pax3</i> ^{Cre/+} β -catenin ^{+/-} - exencephaly.....	243
Figure 5.5: Pooling of embryo genotypes from the cross <i>Pax3</i> ^{Sp2H/+} β -catenin ^{LOF/+} x <i>Pax3</i> ^{Cre/+} β -catenin ^{+/-} - spina bifida.....	245
Figure 5.6: β -catenin loss-of-function results in reduced expression of <i>Axin2</i>	246
Figure 5.7: RT-qPCR was unable to determine if β -catenin loss-of-function reduces the level of canonical Wnt signalling.....	249
Figure 5.8: Punnet squares demonstrating the pooling of genotypes of offspring from the crosses <i>Pax3</i> ^{Sp2H/+} β -catenin ^{LOF/+} x <i>Pax3</i> ^{Cre/+} β -catenin ^{LOF/+} and <i>Pax3</i> ^{Sp2H/+} β -catenin ^{LOF/+} x <i>Pax3</i> ^{Cre/+} β -catenin ^{+/-}	250
Figure 5.9: β -catenin loss-of-function causes minor delays in the closure of the posterior neuropore.....	252
Figure 5.10: β -catenin loss-of-function increases the frequency of spina bifida in <i>Pax3</i> heterozygotes.....	257
Figure 5.11: β -catenin loss-of-function decreases the frequency of exencephaly in <i>Pax3</i> mutant embryos.....	259

Figure 5.12: Phenotype of a *Pax3*^{Sp2H/Cre} *β-catenin*^{LOF/LOF} embryo.....260

Figure 5.13: Culture of *Spotch* embryos with XAV939 does not affect the frequency of exencephaly.....262

Figure 5.14: Culture in 10 μM XAV939 has no detectable effect on canonical Wnt signalling.....264

Figure 5.15: β-catenin loss-of-function disrupts expression of *ErbB3*.....266

Figure 5.16: β-catenin loss-of-function reduces Pax3 expression levels.....269

Figure 5.17: *Pax3*^{Cre/+} *β-catenin*^{+/+} embryos from two different genetic crosses have significantly different expression levels of *Pax3*.....270

List of Tables

Chapter 1: General Introduction

Table 1.1: Abnormal cellular processes found in neural tube defect mouse models.....	16
Table 1.2: Environmental factors which have been linked to neural tube defect development.....	18
Table 1.3: <i>Pax3</i> mutant alleles in mice.....	41

Chapter 2: Materials and Methods

Table 2.1: The effects of the β -catenin gain-of-function allele in different tissue types.....	81
Table 2.2: The effects of the β -catenin loss-of-function allele in different tissue types.....	85
Table 2.3: Compound mutant genotypes and the genetic crosses required to produce them.....	87
Table 2.4: PCR cycles.....	91
Table 2.5: PCR primers.....	92
Table 2.6: Plasmids used for transformation.....	94
Table 2.7: RT-qPCR primers.....	102

Chapter 3: Causes of neural tube defects in *Pax3* mutant embryos

Table 3.1: Genes which passed the threshold of 1.4-fold difference in the RT ² Profiler™ PCR Array Plate for the mouse Wnt signalling pathway from SABiosciences.....	155
---	-----

Chapter 4: *Spotch* and β -catenin Gain-of-Function

Table 4.1: The frequency of neural tube defects in embryos of different genotypes.....	181
Table 4.2: The number of proliferating cells in the dorsal region of the neural tube.....	192
Table 4.3: The number of neurons in the dorsal region of the neural tube.....	198
Table 4.4: Summary of apoptosis data between the 22 and 30+ somite stage.....	212

Chapter 5: *Spotch* and β -catenin Loss-of-Function

Table 5.1: Pooling genotypes from the crosses <i>Pax3</i> ^{Sp2H/+} <i>β-catenin</i> ^{LOF/+} x <i>Pax3</i> ^{Cre/+} <i>β-catenin</i> ^{LOF/+} and <i>Pax3</i> ^{Sp2H/+} <i>β-catenin</i> ^{LOF/+} x <i>Pax3</i> ^{Cre/+} <i>β-catenin</i> ^{+/-}	238
--	-----

Abbreviations

- AP-2 α** – Activating protein 2 α
- APC** – Adenomatous polyposis coli
- bHLH** – Basic helix-loop-helix
- bHLHZ** – Basic helix-loop-helix zipper
- bp** – Base pair
- BMP** – Bone morphogenetic protein
- BSA** – Bovine serum albumin
- CBP** – CREB binding protein
- CIL** – Contact inhibition of locomotion
- CK1** – Casein kinase 1
- CNS** – Central nervous system
- CRD** – Cysteine-rich domain
- CREB** – cAMP response element-binding protein
- CS** – Chondroitin sulphate
- CSPG** – Chondroitin sulphate proteoglycan
- ct** – Curly tail
- ddH₂O** – Double-distilled water
- DEP domain** – Dishevelled, Egl-10, and Pleckstrin domain
- DIX domain** – Dishevelled and Axin domain
- DLHP** – Dorso-lateral hinge point
- Dlp** – Dally-like protein
- DMEM** – Dulbecco's modified eagle's medium
- DMSO** – Dimethyl sulfoxide
- DPX** – Di-n-butyl phthalate
- DRG** – Dorsal root ganglia
- dU** – Deoxyuridine
- Dvl** – Dishevelled
- E** – Embryonic day
- ECM** – Extracellular matrix
- EDTA** – Ethylenediamine tetra-acetic acid
- EGF** – Epidermal growth factor
- EMT** – Epithelial to mesenchymal transition
- ENS** – Enteric nervous system
- ER** – Endoplasmic reticulum

FBS – Fetal bovine serum
FD – Folate deficient diet
FGF – Fibroblast growth factor
FoxD3 – Forkhead box D3
FoxM1 – Forkhead box M1
FRAT – Frequently rearranged in advanced T-cell lymphomas
Fz – Frizzled
GAPDH – Glyceraldehyde 3-phosphate dehydrogenase
GDNF – Glial-derived neurotrophic factor
GOF – Gain-of-function
GPI – Glycosylphosphatidylinositol
Grg – Groucho-related gene
Grhl2 – Grainy head-like 2
GSK3 β – Glycogen synthase kinase-3 β
HAT – Histone acetyltransferase
HD – Homeodomain
HDAC – Histone deacetylase
HDACi – Histone deacetylase inhibitor
Hes1 – Hairy and enhancer of split homologue-1
HS – Heparin sulphate
Hh – Hedgehog
HLH – Helix-loop-helix
HSPG – Heparin sulphate proteoglycan
HTH – Helix-turn-helix
Id – Inhibitor of DNA-binding
ISW1 – Imitation switch 1
LEF1 – Lymphoid enhancing binding factor
LOF – Loss-of-function
MET – Mesenchymal-to-epithelial transition
MHP – Medial hinge point
MITF – Microphthalmia-associated transcription factor
MLL – Mixed lineage leukaemia
MMP – Matrix metalloproteinase
MOMS – Management of Myelomeningocele Study
Msx – Msh Homeobox
MTHFR – Methylene tetrahydrofolate reductase

Myf5 – Myogenic factor 5
NCAM – Neural cell adhesion molecule
ND – Normal diet
NES – Nuclear export sequence
Nf2 – Neurofibromin 2
Ngn2 – Neurogenin 2
NIC – Notch intracellular domain
NLS – Nuclear localisation sequence
Nrg – Neuregulin
NT – Neural tube
NTD – Neural tube defect
Pax – Paired-box protein
PBS – Phosphate-buffered saline
PCP – Planar cell polarity
PCR – Polymerase chain reaction
PD – Paired domain
PDZ domain – post-synaptic density protein 95, Drosophila disc large tumour suppressor 1, zonular occludens 1 domain
PFA – Paraformaldehyde
PG – Proteoglycan
PH3 – Phospho-histone H3
PNP – Posterior neuropore
PNS – Peripheral nervous system
Porc – Porcupine
PSM – Pre-somitic mesoderm
RA – Retinoic acid
RanBP3 – Ran binding protein 3
RGS – Regulator of G-protein signalling
RMS - Rhabdomyosarcoma
rpm – Revolutions per minute
RT-qPCR – Real time quantitative polymerase chain reaction
SCD – Stearoyl desaturase
SDS – Sodium dodecyl sulfate
Shh – Sonic hedgehog
Sox – Sry-related HMG box
Sp2H – Splotch-2H

TAD – Transactivation domain
TBP – TATA binding protein
TBS – Tris-buffered saline
TCF – T-cell-specific transcription factor
β-TrCP – β-transducin repeat-containing protein
TRRAP – Transcription/transformation domain associated protein
Tspan18 – Tetraspanin18
UV – Ultraviolet
Wg – Wingless
Wls – Wntless
Wnt – Wingless-related integration site
WS – Waardenburg Syndrome
Zic – Zinc finger of the cerebellum

1 General Introduction

1.1 Neurulation

The neural tube (NT) is the precursor of the central nervous system (CNS) in the developing embryo. Neural tube closure (neurulation) occurs in mice during the period from embryonic day (E) 8.5 to E10.5, and in humans between 22-28 days following conception (Copp et al., 2003; Mastroiacovo and Leoncini, 2011).

The mechanisms of neurulation differ greatly between organisms. For instance in mammals, amphibians and birds the NT forms from a plate which bends and fuses to form a tube. However, in teleosts such as zebrafish, the NT forms as the result of cavitation of a solid rod. For the purpose of this thesis the focus will be on mammalian neurulation unless stated otherwise.

Neurulation begins with the specification of the neural plate on the dorsal surface of the embryo. This flat region of tissue undergoes convergent extension along the rostro-caudal axis, and bends ventrally along the midline. Further hinge points form along the same axis, in the lateral regions of the neural tube. This brings the edges of the neural folds into close apposition, and they fuse along the midline, forming a tube (**Figure 1A**).

The neural tube extends the full length of the embryo. In the cranial region it forms the brain later in development, and in the spinal region it forms the spinal cord.

1.1.1 Specification of the neural plate and the neural plate border

Neurulation begins with the specification of the neural plate – a flat region of thickened ectodermal tissue on the dorsal surface of the embryo. Signals specifying the neural plate emanate from an organiser. This is the Spemann's organiser in amphibians, the dorsal shield in teleosts, and the node in amniotes (LaBonne and Bronner-Fraser, 1999). Although little research has been carried out regarding neural plate and neural plate border specification in mice, evidence suggests that the mechanisms are conserved between amniotes, such as the mouse and chick (Wilson and Edlund, 2001).

A gradient of bone morphogenetic protein (BMP) signalling is important in early specification of both the neural plate and the neural plate border. BMP-4 has been shown in *Xenopus* to have a ventralising effect on mesodermal tissue (Dale et al., 1992). Until gastrulation in *Xenopus* BMP signalling is active throughout the ectoderm, although the dorsal mesoderm expresses BMP inhibitors, such as noggin, chordin and follistatin. Additional signalling

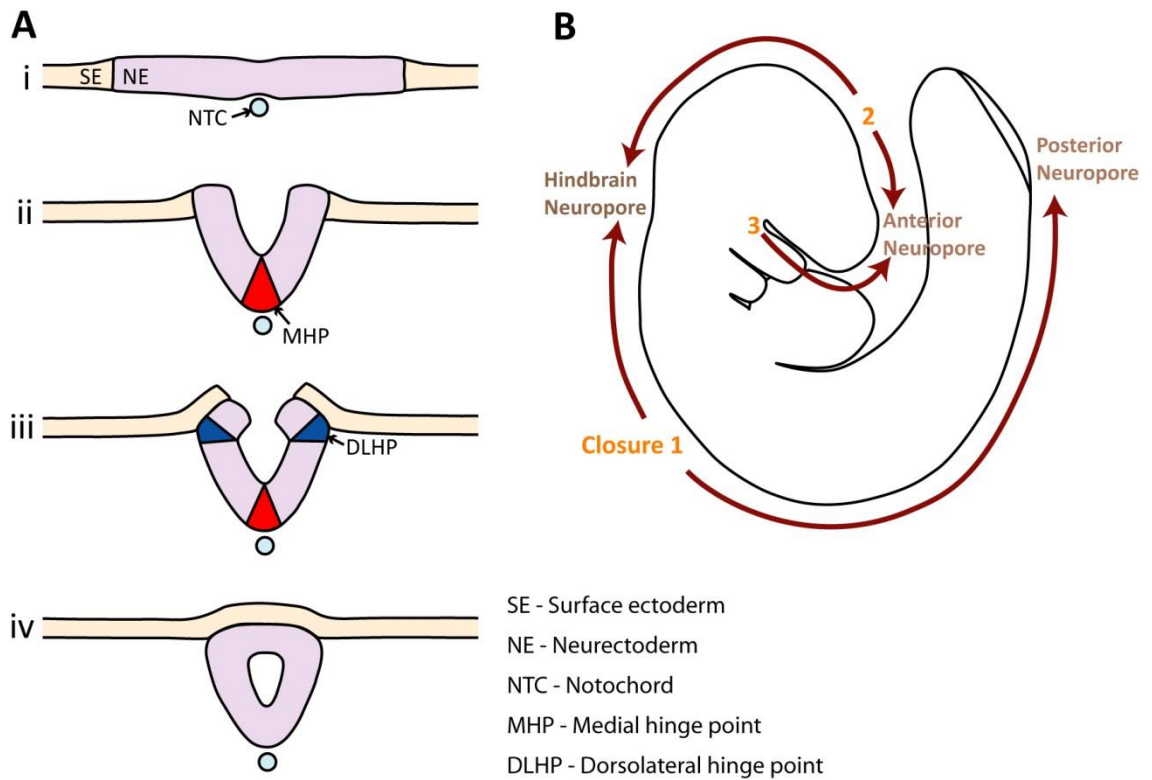


Figure 1.1: The neural tube during neurulation. The neural plate begins as a thickened region of dorsal surface ectoderm (SE), the neurectoderm (NE, **A i**). In the region directly dorsal to the notochord, a hinge point develops – the medial hinge point (MHP) – which causes invagination of the NT (NTC, **A ii**). Dorsolateral hinge points (DLHPs) form in the region of the NT where the neurectoderm is in contact with the surface ectoderm, and this brings the neural folds into apposition (**A iii**). Finally, fusion and remodelling of the NT occurs along the midline to form a closed tube (**A iv**).

NT closure begins at three different closure points (**B**). Closure 1 initiates at the hindbrain-cervical boundary, closure 2 initiates at the midbrain-forebrain boundary, and closure 3 initiates at the rostral limit of the forebrain. These closures spread rostrally and caudally along the midline. Neuropores are open regions of the NT between closure points.

pathways also contribute to the clearing of BMP in the dorsal ectoderm of the NT: Wnt signalling in the dorsal region inhibits BMP-4 expression in this region (Baker et al., 1999), and it has been shown in chick that Fibroblast Growth Factor (FGF) signalling is also required to repress BMP signalling (Wilson et al., 2000). Therefore, a dorso-ventral gradient of BMP-4 is set up in the embryo. It appears that low levels of BMP-4 induce neural plate, intermediate levels induce neural crest (NC) fate, and high levels suppress neural fate while promoting epidermis development (Delaune et al., 2005; Neave et al., 1997; Wilson and Hemmati-Brivanlou, 1995). This was discovered by injecting varying amounts of RNA encoding *Bmp-4* (20-220 pg) into 1-4 cell stage zebrafish embryos, and observing the resulting patterning of the embryos, and the tissues which developed (Neave et al., 1997).

Experiments in the mouse support the theory that BMP signalling plays an important role in neurulation; embryos which are genetically null for Noggin develop spina bifida, and may also develop exencephaly (McMahon et al., 1998; Stottmann et al., 2006). This suggests that BMP inhibition is vital for the correct progression of neurulation in mice. In support of this, ventral expansion of the BMP NT expression domain through use of a *BMP-4* mutant allele in mice has been shown to cause exencephaly (Hu et al., 2004). However, the repression of BMP inhibitor expression, such as that of Noggin or Chordin, does not prevent formation of the neural plate in the mouse. Therefore, it appears that BMP inhibition can promote neural fate, but is not sufficient to induce it (Wilson and Edlund, 2001).

However, BMP-4 expression is highly dynamic. For example, at late gastrula stages in the *Xenopus* it has been shown that expression levels of BMP-4 and the downstream gene *MSX1* are highest in the neural plate border (Suzuki et al., 1997). In order for the neural plate border to develop, it first requires a period of intermediate BMP-4 expression, followed by a period of increased expression. Although low BMP expression is necessary for neural induction, it is not sufficient – BMP inhibition alone is not able to induce neural marker genes in ectodermal tissue *in vivo*, although it suppresses epidermal fate (Delaune et al., 2005; Mayor et al., 1995; Streit et al., 1998).

High levels of FGF signalling and low levels of Wnt signalling are also required to induce border or neural fate in the ectoderm. FGF signalling is seen in the neural plate border region during neural specification in the chick embryo (Eblaghie et al., 2003). Injection of *eFGF* (the *Xenopus* homologue of *FGF4*) RNA into *Xenopus* embryos during the late gastrula phase induces expression of neural marker genes and reduces expression of epidermal marker genes. Additionally, *Xenopus* embryos treated with SU5402 to block FGFR activity fail to develop the neural plate or neural plate border, and develop only ectoderm (Delaune et al., 2005), and a

truncated FGF receptor prevents neural induction in *Xenopus* embryos (Launay et al., 1996). Likewise, in chick, it was found that beads soaked in FGF4 and FGF8 are able to induce expression of early neural markers in ectoderm, but are not able to fully initiate neural induction (Streit and Stern, 1999). FGFs appear to function in the role of neural inducer by blocking BMP signalling on several levels. For instance, FGF signalling has been shown to inhibit expression of *Bmp4* and *Bmp7* (Wilson et al., 2000) as well as inducing expression of the BMP inhibitor *chordin* in zebrafish (Londin et al., 2005). BMP-mediated repression of FGF signalling in the chick is also observed (Wilson et al., 2001).

In chick, genes involved in canonical Wnt signalling, including *Wnt3a*, *Wnt8c* and *Frizzled8* are expressed in the lateral regions of the ectoderm, which will later form non-neural tissue. Chick epiblast explants treated with Wnts developed only ectoderm. Canonical Wnt signalling represses neural fate by preventing FGFs from repressing BMP activity (Wilson et al., 2001).

Positioning of the neural plate border is also dependent on the balance of BMP, FGF and Wnt signalling. Transplantation of cell pellets transfected with the BMP antagonist *chordin* at the neural plate border widens the neural plate at the expense of non-neural ectoderm in the chick embryo (Streit et al., 1998; Streit and Stern, 1999). Additionally, transplantation of BMP-4-secreting cells to the same region will narrow the neural plate (Streit and Stern, 1999). This suggests that positioning of the neural plate border is reliant on the balance between BMP expression and the expression of its antagonists. FGFs, including FGF8, are known to be expressed in the paraxial mesoderm, and are able to induce expression of *msx-1* in the overlying neural plate border. In chick, BMP-4 and *Msx-1* act in a positive feedback loop to increase expression of BMP-4 at the neural plate border (Streit and Stern, 1999). It has been shown that *noggin* in combination with FGF – but not alone – is able to induce NC markers in *Xenopus* animal caps (Mayor et al., 1995). In addition, inhibition of FGF signalling in *Xenopus* reduces expression of NC markers at the neural plate border (Mayor et al., 1997). This suggests that an intact FGF signalling pathway is required for NC specification, and that FGFs interact with the BMP signalling pathway.

Wnt molecules such as *Wnt1* and *Wnt3a* are expressed in the dorsal region of the *Xenopus* NT, and enable competent cells to be specified to a NC fate (Saint-Jeannet et al., 1997). See section 1.3.1 for more information about the specification of the NC, and the role of Wnt signalling in this process.

1.1.2 Convergent extension in the neural plate

Convergent extension is a cellular process that enables tissues to elongate in one axis while narrowing in another. It is important in shaping and patterning the developing NT in vertebrate

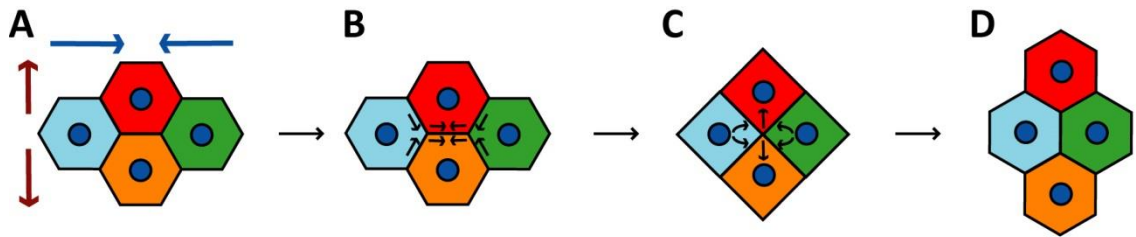


Figure 1.2: An example of cell intercalation. Four cells are shown in common formation. The directions of the change in tissue shape are shown by arrows (**A**). The tissue narrows in one axis (blue arrows) and elongates in another (red arrows). Actin-dependent changes in cell shape (**B**) draw the cell surfaces into a single point, in a rosette formation (**C**). The cells again change shape to form new cell-cell contacts, moving relative to the other cells in the formation (**D**). These alterations in cell-cell contacts change the shape of the tissue.

embryos (Elul et al., 1997). Research into convergent extension has largely been carried out in teleosts and amphibians.

Convergent extension consists of two interlinked processes; convergence and extension. Extension refers to the elongation of the tissue along the antero-posterior axis, and convergence refers to the medio-lateral narrowing of the tissue.

Convergent extension involves multiple cellular processes, including cell shape changes within the tissue. Cells become columnar in shape, which acts to narrow the tissue (Jacobson and Gordon, 1976), and also elongate along the axis of extension. These alterations are caused by changes in the cytoskeletons of the cells in the tissue (Schoenwolf and Powers, 1987). Convergent extension also involves the movement of cells relative to one another in order to form a longer, narrower tissue (**Figure 1.2**). Cytoskeletal changes within cells create directional protrusive activity, which allows cells to interact with and create traction between adjacent cells. Therefore, when it takes place in a stiff tissue, convergent extension can create force to alter the morphology of the developing embryo (Elul et al., 1997; Keller et al., 2000; Keller et al., 1985). This remodelling of the tissue may also involve collective migration of cells as a sheet (Tada and Heisenberg, 2012).

The neural plate is specified as an elliptical tissue, and it elongates into an extended keyhole shape along the antero-posterior axis through convergent extension movements. The neural plate thickens dorso-ventrally, narrows medio-laterally, and extends rostro-caudally, with some medio-lateral widening in the cranial region. These shape changes rely largely on forces generated within the neural tube (Schoenwolf and Alvarez, 1989). Elongation of the cells aids in both the thickening and narrowing of the neural tube (Copp et al., 2003; Schoenwolf, 1985; Schoenwolf and Alvarez, 1989). The movements push the cranial and caudal regions apart, thus contributing to lengthening of the embryo (Keller et al., 2000). Although cell number in the NT stays constant during amphibian neurulation, it is likely that the high level of proliferation seen in the NT during neurulation in birds and mammals contribute to the morphological changes (Schoenwolf and Alvarez, 1989). Convergent extension is thought to be one of the main processes driving gastrulation in *Xenopus* (Keller et al., 1985).

In the mouse convergent extension is dependent on the planar cell polarity (PCP) pathway, which is a non-canonical Wnt signalling pathway. Failure of PCP signalling results in failure of convergent extension in the neural tube (Roszko et al., 2009; Wang et al., 2006). Mice with mutations in the PCP pathway develop severe neural tube defects (NTDs), including craniorachischisis, which occurs when closure 1 fails (Chen et al., 2013; Curtin et al., 2003). This data demonstrates that closure 1 in the mouse is dependent upon convergent extension. Evidence shows that this may also be true in humans, as mutations in genes encoding components of the PCP pathway, such as *VANGL1*, *VANGL2*, *SCRIB* and *CELSR1*, have been found in cases of human NTDs (Cai and Shi, 2014; Lei et al., 2013).

Multiple cell adhesion molecules have been associated with convergent extension. For example, cadherins mediate calcium-dependent cell-cell adhesion. Several cadherins are found in the early *Xenopus* embryo, and both C-cadherin and cadherin-11 are found to be reduced during convergent extension movements. This reduces cell-cell adhesion, which allows for greater freedom in morphological cellular movements (Brieher and Gumbiner, 1994; Hadeball et al., 1998; Lee and Gumbiner, 1995; Zhong et al., 1999). Correct expression of N-cadherin in the early *Xenopus* neural plate also appears to be essential for normal development of the neural tube, and this could be due to effects on cell mixing and convergent extension (Detrick et al., 1990; Keller et al., 2000).

1.1.3 Development of the hinge points

Once the neural plate has been specified, hinge points form along the rostro-causal axis. They form an invagination in the NT, and bend the neural folds into apposition. Fusion of the folds forms a closed tube with a central lumen.

The NT forms two different types of hinge point, and different mechanisms are involved in the formation of each. The medial hinge point (MHP) forms along the midline of the NT, directly above the notochord. The neural folds are elevated either side of the MHP. Two DLHPs form, one on each neural fold, at the point of attachment of the surface ectoderm to the neural folds. They bring the neural folds into apposition in preparation for fusion (**Figure 1.1A**).

Three modes of NT morphogenesis have been described (Shum and Copp, 1996). They differ with developmental stage and position along the rostro-caudal axis. In mode 1 the NT only forms the MHP. In mode 2 the NT exhibits defined DLHPs as well as the MHP, and the closed NT has a diamond-shaped lumen. In mode 3 the hinge points are less clearly defined; bending is observed across the whole of the neural folds, and the closed NT forms a circular lumen (**Figure 1.3**). During early NT closure the posterior neuropore (PNP) closes using mode 1. Later in NT closure the PNP closes using first mode 2, and then mode 3. Modes also differ according to rostro-caudal position along the NT; mode 1 is evident in the rostral spinal NT, mode 2 at mid-spinal levels, and mode 3 in the caudal-most regions of the NT (Shum and Copp, 1996).

Convergent extension requires directional extension, and hinge point formation requires the definition of an apico-basal axis. Therefore coordinated cell polarity within the NT is essential. Polarity is established through mutual exclusion of apical and basolateral polarity complexes, which results in functionally distinct regions containing different populations of proteins (Eom et al., 2013; Margolis and Borg, 2005). The formation of the apico-basal axis allows the cells to act in union as a polarised tissue, which is particularly important for the morphological changes required in hinge point formation.

Cell shape changes within the NT are important for hinge point formation (Karfunkel, 1972; Kinoshita et al., 2008). Cells of the MHP and DLHPs shorten apico-basally, and often form a wedge shape, which aids bending of the tissue. Wedge-shaped cells have undergone apical constriction and basal nuclear positioning in order to narrow the apical region and widen the basal region. The hinge points contain a high proportion of wedge-shaped cells compared to straight regions of the NT (Karfunkel, 1974; Smith and Schoenwolf, 1988).

Apical constriction may play a role in the formation of the hinge points. The polarised cells of the NT have an apical ring of actin and myosin II at the luminal region. This constricts in the cells of the hinge points during neurulation, reducing the apical surface area of the cells (Quintin et al., 2008; Schroeder, 1970). In the presence of either the actin depolymerisation agent cytochalasin or the myosin-II inhibitor blebbistatin apical constriction fails to occur in the chick (Karfunkel, 1972; Kinoshita et al., 2008). However, it is unclear whether apical constriction and the actin cytoskeleton play important roles in mouse

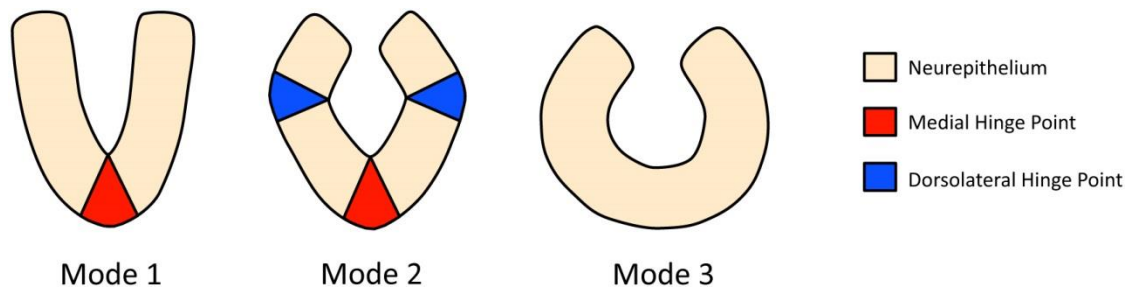


Figure 1.3: Modes of neural tube closure. The shape of the neurepithelium during NT closure is dependent upon developmental stage and position along the rostro-caudal axis. In mode 1 the neurepithelium has a MHP. In mode 2 the neurepithelium exhibits both a MHP and DLHPs. In mode 3 the neurepithelium exhibits bending across the whole medio-lateral axis, and has no clear hinge points.

neurulation, as treatment of mouse embryos with cytochalasin prevented cranial NT closure, but not spinal NT closure. Additionally, cytochalasin-treated embryos still formed hinge points (Ybot-Gonzalez and Copp, 1999). Therefore, the requirement and role of the actin cytoskeleton during neurulation may vary with spinal level.

In addition to the activity of the actin cytoskeleton, microtubules polymerise parallel to the apico-basal axis in the cells of the NT (Messier, 1969). They elongate the cell along this axis, producing the columnar shape typical to cells of the neurepithelium. Disruption of the microtubules in cells of neurulating *Xenopus* embryos through treatment with vinblastine results in the cells losing their columnar shapes and ‘rounding up,’ and the collapse of the hinge points and neural folds (Karfunkel, 1971).

Control of the cell cycle is also likely to have a role in morphogenetic changes of the NT. The wedge-shaped cells seen in the MHP have basally localised nuclei, which is likely to contribute to the narrow apical region and wider basal region (Smith and Schoenwolf, 1987). During the mitosis phase of the cell cycle the nucleus is apically located. Cells in the hinge points spend a shorter time in the mitotic part of the cell cycle compared to cells in non-bending regions, but each cell cycle is longer. This results in a higher proportion of hinge point cells having a basally

localised nucleus at any given time, which contributes to the basal widening of the cell in the hinge point, and the bending of the tissue (Smith and Schoenwolf, 1988).

The notochord releases the morphogen Sonic Hedgehog (Shh), which plays an important role in the development of the MHP. In chicks, removal of the notochord prevents floor plate formation, whereas implantation of a second notochord induces formation of a second floor plate (van Straaten et al., 1985; Wilson and Maden, 2005). Additionally, blocking Shh activity in neural explants using antibodies targeted against the N-terminal region prevents the formation of floor plate cells *in vitro* (Ericson et al., 1996). Likewise, ectopic expression of a Shh-expressing transgene in the dorsal NT of the mouse causes ectopic expression of the floor plate gene *Hnf3β* (Echelard et al., 1993).

Formation of the DLHPs is not well understood, although BMP expression appears to play an important role. In the mouse, low BMP expression is necessary for formation of the DLHPs, but they also appear to require low Shh expression. Therefore the DLHPs form in the lateral regions of the NT, where both BMP and Shh expression are low, and Noggin expression is high (Ybot-Gonzalez et al., 2007) (**Figure 1.4**). Increased BMP expression in the mouse NT caused by a null mutation in *Noggin* inhibits formation of the DLHPs (Stottmann et al., 2006). Additionally, genetic knockout of the *Zic2* gene results in a high frequency of spina bifida due to loss of the DLHPs (Nagai et al., 2000). *Zic2* mutants fail to express dorsal BMP antagonists, which results in the loss of the DLHPs (Ybot-Gonzalez et al., 2007).

In the chick, formation of the MHP occurs in the region of the NT directly dorsal to the notochord, and requires low BMP signalling (Eom et al., 2011). Blocking BMP signalling is able to induce formation of an ectopic MHP, whereas an increase in BMP signalling prevents the formation of the MHP, and thus the floor plate later in development (Eom et al., 2011; Eom et al., 2012). BMP is expressed dorsally in the NT, but is repressed by the BMP antagonist Noggin. Shh from the floor plate and notochord suppress Noggin. Therefore the MHP forms in the region where BMP signalling is low and Shh expression is high (**Figure 1.4**).

1.1.4 Fusion of the neural folds

Fusion between the tips of the neural folds to form a closed tube begins at around E8.5 in the mouse (the 5-7 somite stage). It begins at three defined positions along the rostro-caudal axis, and spreads rostrally and caudally from these points. Closure 1 begins at the hindbrain-cervical boundary, closure 2 at the forebrain-midbrain boundary, and closure 3 at the rostral limit of the forebrain (Greene et al., 2009). The open regions between closure points are known as neuropores, and NT closure should be fully completed by around E10.5 (the 27-30 somite

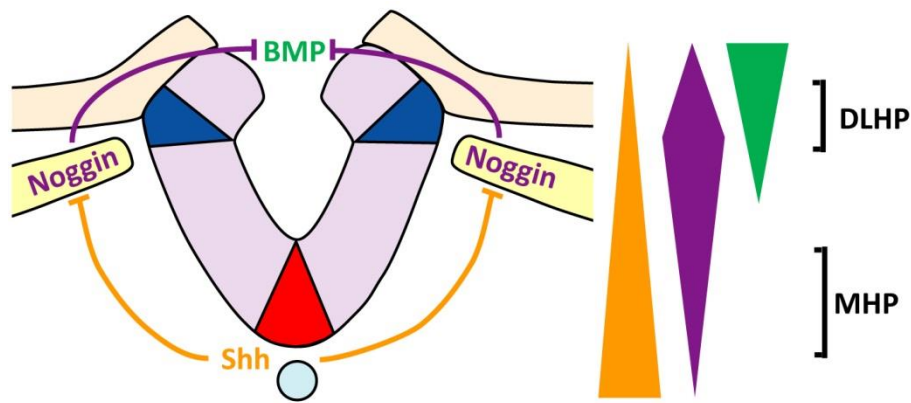


Figure 1.4: Hinge point formation. The MHP (red) forms directly dorsal to the notochord (pale blue), where levels of Shh are high, and BMP is low. The DLHPs (dark blue) form where the NT is in contact with the surface ectoderm, where both Shh and BMP are low. The gold shape indicates the concentration gradient of Shh along the dorso-ventral axis of the NT. The purple shape indicates the concentration gradient of the BMP inhibitor Noggin. The green shape indicates the concentration gradient of BMP. The brackets indicate the positions on the NT and concentration gradients which are optimum for the formation of the MHP and DLHPs.

stage) in the mouse (**Figure 1.1B**). See **Figure 1.5** for a timeline of neuropore closure and NC development.

The behaviour of the tissues involved in fold fusion vary according to their positions on the rostro-caudal axis. For instance, in the rhombencephalon and mesencephalon the non-neural epithelium makes first contact, whereas in the anterior neuropore, the neural epithelium is the first to make contact. However, regardless of the tissue the cells demonstrate the same behaviour at the point of fusion; finger-like projections extend from the cells at the tips of both neural folds, and intercalation of these projections brings the folds into contact (Ray and Niswander, 2012). In the fully closed NT both the neural folds and the surface ectoderm have fused.

Several genes have been implicated in both the initial fusion event and in the maintenance of the fused tissue. Loss- or gain-of-function of the Grainyhead-like gene *Grhl2* in mice results in the development of NTDs due to failure of fusion of the neural folds (Brouns et al., 2011;

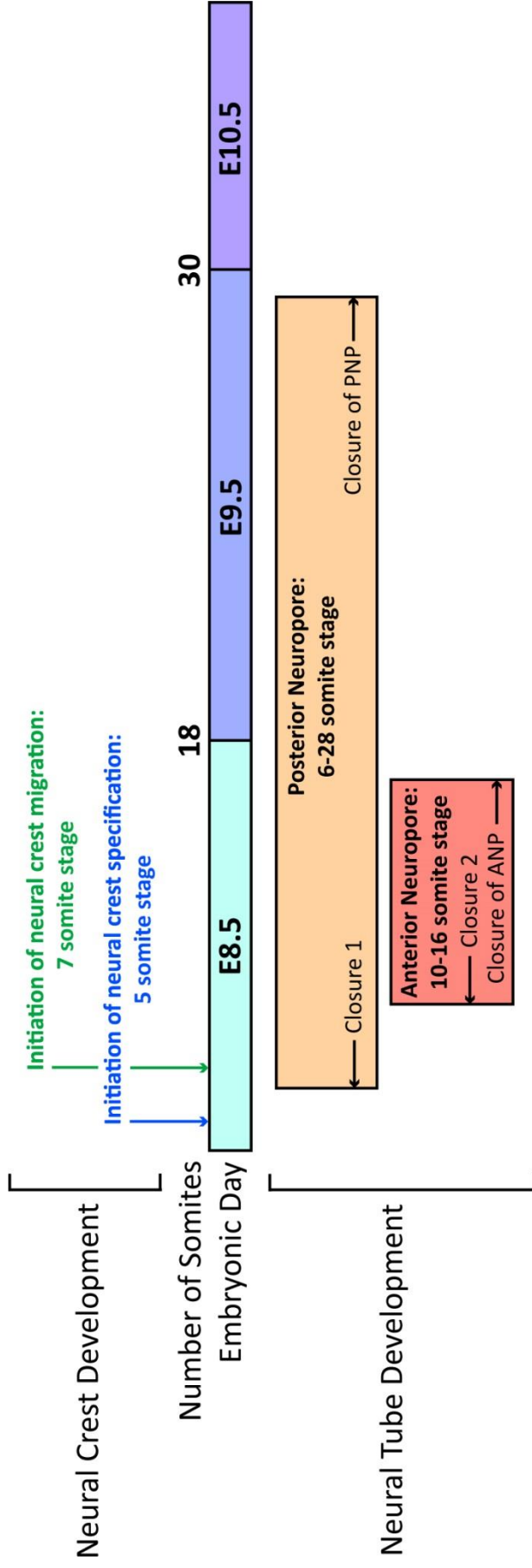


Figure 1.5: A timeline of neural tube closure and neural crest development. All somite stages given in this figure are approximate. Small variations will occur between embryos, genetic backgrounds and mutations.

Neural crest specification and migration varies between populations and positions. Events described in Neural Crest Development describe the first stage at which these processes can be observed in the embryo. Specification and migration of the NC begins in the cranial neural folds and the rostral-most spinal neural folds. Coloured boxes in Neural Tube Development represent the times during which the neuropores are open.

Pyrgaki et al., 2011; Werth et al., 2010). The Grhl2 transcription factor appears to play a general role in tissue fusion, including that of the facial tissues and body wall. It is known to regulate the expression of several genes encoding adhesion molecules, such as *E-cadherin*, *cadherin-3*, *Desmocolin-2* and *Desmoglein-2*, as well as several members of the *Claudin* gene family, which are involved in tight junction formation (Pyrgaki et al., 2011; Werth et al., 2010).

The Ephrin signalling network is necessary for neural fold fusion in the mouse, in particular signalling between ephrin-A and the receptor EphA in the both the cranial and spinal regions (Abdul-Aziz et al., 2009; Holmberg et al., 2000). These molecules may be responsible for the initial adhesion between the neural folds. Signalling with G-protein-coupled receptors also functions in neural fold fusion – mutations in the protein Gpr161 lead to defects in both fusion of the neural folds and the lens of the eye (Matteson et al., 2008).

Further NT fusion defects are found in embryos carrying a mutation in the gene *Nf2*. This mutation causes NTDs due to reopening of the initially fused tissue. This could be due to failure of development of epithelial junctions between cells following the initial fusion event (McLaughlin et al., 2007).

Fusion is followed by remodelling of the neurectoderm and overlying surface ectoderm to form continuous and stable tissues. The processes involved in the remodelling are not well understood, although it appears to be linked to apoptosis of a number of the cells at the fusion site. However the relationship between apoptosis and remodelling during NT closure is uncharacterised (Pai et al., 2012).

1.1.5 Cranial closure versus caudal closure

It would be logical to assume that the same mechanisms are employed in the closure of the neural tube in the cranial and caudal regions. However, research has shown a number of key differences in the mechanisms of NT closure between the cranial and spinal regions, as described below.

In the cranial region, the first stage of NT closure is assisted by an expansion in the surrounding mesenchyme. Proliferation and an expansion of extracellular space in the paraxial mesoderm push the neural folds into a biconvex 'V' shape (Morriss and Solursh, 1978). This mechanism is necessary for closure, as prevention of the proliferation and expansion of the paraxial mesoderm in the cranial region through mutation of the gene *twist* in mouse embryos resulted in open neural folds (Chen and Behringer, 1995). This is not true for the spinal region; the expansion and proliferation of the mesenchyme does not occur in wild type embryos, and removal of the tissue does not affect NT closure (van Straaten et al., 1993).

In the second stage of cranial NT closure the neural folds become convex, and the tips become apposed. This mechanism is dependent on the actin cytoskeleton, and mutation in a number of the proteins involved in the formation and maintenance of a functional actin cytoskeleton cause exencephaly (Brouns et al., 2000; Hildebrand and Soriano, 1999; Stumpo et al., 1995; Xu et al., 1998). However, all these mutant mouse embryos show normal spinal NT closure. In support of this, treatment in culture of mouse embryos with the actin polymerisation inhibitor cytochalasin D prevents closure of the cranial NT, but not the spinal NT (Ybot-Gonzalez and Copp, 1999).

It has been suggested that the direction of cell division may be different between the cranial and spinal regions of the neural plate, with more transverse divisions observed in the cranial region, and more longitudinal divisions observed in the spinal regions of chick embryos (Schoenwolf and Alvarez, 1989).

The cranial region of the NT appears to be more susceptible to morphological abnormalities, whether these abnormalities are genetic or environmental in origin (Copp et al., 2003). Indeed, there are four times as many mouse mutants which develop only exencephaly compared to mutants which develop either spina bifida or both spina bifida and exencephaly (Harris and Juriloff, 2010). This suggests that the mechanisms controlling closure of cranial region are more susceptible to disruption, and/or the closure is less robust when compared to the spinal region. It is possible that the spinal region has more redundant pathways and mechanisms active during closure, which may compensate for mutations and abnormalities. Alternatively, different mechanisms may be responsible for NT closure in the cranial and spinal regions, which have different susceptibilities to teratogens and mutations.

Genetic risk factors for NTDs may be inherited, and a number of studies have been carried out observing NTD occurrence within families (Chatkupt et al., 1993; Hol et al., 2000; Partington and McLone, 1995; Sergi et al., 2013). It is often the case that a single form of NTD is seen within a family. For instance, a family may have a significantly higher rate of spina bifida, but a normal rate of anencephaly, or vice-versa. Risk factors are often specific for a particular type of NTD, which suggests different mechanisms are involved in the closure of the cranial and spinal regions.

1.2 Neural tube defects

Neural tube defects (NTDs) are among the most common birth defects observed today. On average they are seen in around 1 in 1000 pregnancies (Mitchell, 2005), but rates can vary

hugely from around 0.5 in 1000 births in America (Wallingford et al., 2013) to 13.9 in 1000 births in certain areas of China (Li et al., 2006).

NTDs occur when NT closure fails in an embryo, leaving an open region. They vary in type and severity depending on the reason for failure and the position of the open region, and thus may or may not be compatible with life.

1.2.1 Commonly observed defects

The type of NTD which develops depends on the affected region and the severity of the defect. The two most commonly observed NTDs are spina bifida and anencephaly.

1.2.1.1 Spina bifida

Spina bifida occurs when the open lesion is positioned in the spinal region of the NT. With appropriate treatment and medical care, this is often compatible with life, but may cause severe, lifelong disabilities in those affected, including movement difficulties or paralysis below the lesion, hydrocephalus, skeletal abnormalities, and incontinence (Copp et al., 2013).

Spina bifida is usually caused by failure of completion of closure 1, leaving the posterior neuropore open. The size of the open region may govern the severity of the defect. By birth, the lesion may be covered by the meninges (myelomeningocele), or open to the intrauterine environment (myelocele) (Greene and Copp, 2009).

1.2.1.2 Anencephaly

Anencephaly occurs when the cranial region is affected by the NTD, and is not compatible with life. The skull vault fails to close over the open region of the NT, leaving the developing brain open to the intrauterine environment (Copp et al., 2013). Affected embryos usually die during gestation, although some may survive until birth.

Failure of completion of closure 2 (or closure 3 in the murine embryo) results in the development of exencephaly. This develops into anencephaly later in gestation, as the brain tissue is destroyed and the cranial vault remains open.

Exencephaly is more common in females than in males (Janerich, 1975; Tennant et al., 2011), although the reasons for this are unknown. This was initially thought to be due to a slight decrease in the rate of development in female embryos, which would mean that females spent longer in the vulnerable period of neurulation (Toriello and Higgins, 1985). However, it has been found that although females are slightly behind males in developmental stage at neurulation, the rate of development is the same (Brook et al., 1994).

Female embryos undergo X-inactivation through methylation of the second X-chromosome. Recently it has been suggested that the inactive X-chromosome may act as a sink of methyl groups, which could cause a deficit of methyl groups in other systems (Juriloff and Harris, 2012). In support of this, research into the *Trp-53* mutant mouse has shown that the observed disproportion in the occurrence of exencephaly in males and females is reliant on the presence of two X-chromosomes, not on the absence of a Y-chromosome (Juriloff and Harris, 2012). Additionally, folic acid is able to rescue NTDs in some mutant embryos, and the folate cycle is known to affect the availability of methyl groups within the cell (see section 1.2.4 for more information). Therefore, it is possible that increased frequency of exencephaly in female embryos is the result of insufficient methyl group availability. This could affect methylation of both proteins and DNA.

1.2.2 Risk factors

NTDs are an extremely heterogeneous defect, and can develop for a huge variety of cellular or physiological reasons. They are caused by either genetic or environmental factors, or most commonly a combination of the two.

1.2.2.1 Genetic

NTDs in humans are known to have a partially genetic aspect in their occurrence. Women who have been affected by an NTD pregnancy have a 2-5% chance of being similarly affected in a future pregnancy, representing around a 50 times higher risk than the general population (Carter and Evans, 1973; Detrait et al., 2005; Nevin and Johnston, 1980). Additionally, NTDs are often associated with known genetic syndromes and chromosome rearrangements, such as Meckel Syndrome and trisomy 13 (Hume, Jr. et al., 1996; Seller, 1975). However, many of the human risk genes have proved difficult to identify. A number of candidate genes have been used for screening, but few have been associated with NTD development (Boyles et al., 2005). It is likely that many cases show oligogenic inheritance, as cases of NTDs within a family tend to involve individuals related at the second or third degree (Detrait et al., 2005). This makes identification of risk genes even more difficult.

More than two hundred genes have been identified as risk genes for NTDs in mice. However, there is rarely complete penetrance of NTDs for any of the mutations observed. A wide variety of cellular processes can be affected by these genes, later leading to the development of an NTD. Some examples of these processes, and the relevant mouse mutant models, are described in **Table 1.1**.

Mouse Mutant Model	Affected Cellular Process	Reference
<i>Curly tail</i>	Proliferation and gut development: Reduced proliferation in the gut and notochord prior to the 27 somite stage results in excess curvature of the spine, and cause spina bifida.	(Copp et al., 1988a)
<i>Folbp1^{-/-}</i>	Folate one-carbon metabolism: Disruption of folate homeostasis. Embryos develop NTDs at E9.5.	(Piedrahita et al., 1999)
<i>Grhl2</i>	Neural fold fusion: Embryos have downregulation of genes involved in cell adhesion at E9.5, and develop exencephaly and cleft face at this stage.	(Pyrgaki et al., 2011)
<i>Loop tail</i>	Planar cell polarity: Embryos have reduced convergent extension of the NT from E8.5 and develop craniorachischisis.	(Gravel et al., 2010)
<i>Zic2^{Ku/Ku}</i>	Hinge point development: Failure to express BMP inhibitors in the dorsal NT, thus DLHPs don't develop from the 9 somite stage. Embryos have spina bifida.	(Ybot-Gonzalez et al., 2007)
<i>Apaf1^{-/-}</i>	Apoptosis: decreased apoptosis in the cranial region and increased proliferation. Embryos develop exencephaly at E9.5.	(Yoshida et al., 1998)
<i>Dnmt3b^{-/-}</i>	DNA methylation: Disrupted de novo methylation. Embryos develop exencephaly at E9.5.	(Okano et al., 1999)
<i>Palld^{-/-}</i>	Cytoskeletal function: Disruption of the actin cytoskeleton. Embryos develop exencephaly at E9.5.	(Luo et al., 2005)
<i>Cecr2^{Gt45Bic/Gt45Bic}</i>	Chromatin remodelling: Disruption of ATP-dependent chromatin remodelling. Embryos develop exencephaly from E8.5.	(Banting et al., 2005)

Table 1.1: Abnormal cellular processes found in neural tube defect mouse models.

These risk genes can increase the likelihood that an embryo will develop an NTD, especially in combination with other high risk genes, or with environmental factors which also increase the NTD risk. This may even occur in embryos heterozygous for a risk gene: compound heterozygote embryos, or heterozygous embryos exposed to adverse conditions may develop NTDs. For instance, the *Pax3* gene rarely causes NTDs in heterozygous mutant form, but when combined with heterozygous *Grhl3* or *Nf1* mutations, the interaction results in the development of NTDs (Estibeiro et al., 1993; Lakkis et al., 1999). Additionally, *Pax3* heterozygous embryos develop exencephaly when exposed to arsenite (Martin et al., 2003).

Modifier genes may affect the rate of NTD development caused by a mutation, without causing NTDs themselves. This may cause differences in NTD development between mouse genetic backgrounds which carry the exact same mutation. For example, the *Cecr2* mutation causes exencephaly in 74% mutant embryos on a BALB/c genetic background. However, on the FVB/N background, the mutation results in 0% exencephaly. This NTD resistance was found to be linked to a modifier locus on chromosome 19 (Davidson et al., 2007). Additionally, polymorphisms in the position of closure 2 have been found between mouse embryos with different genetic backgrounds, and this has been shown to affect susceptibility to exencephaly (Fleming and Copp, 2000). Most strains develop closure 2 at the midbrain-forebrain boundary, but in embryos with a SWV/Bc background closure 2 is positioned more rostrally. This results in a larger hindbrain neuropore, and thus the strain is more susceptible to exencephaly when exposed to teratogens such as valproic acid or hyperthermia (Finnell et al., 1986; Finnell et al., 1988). On the other hand, the DBA/2 background confers resistance to the teratogenic induction of exencephaly, as the strain initiates closure 2 at a position caudal to the midbrain-hindbrain boundary, resulting in a smaller hindbrain neuropore (Finnell et al., 1986; Finnell et al., 1988; Fleming and Copp, 2000).

1.2.2.2 Environmental

A number of environmental factors and teratogens have been linked to the development of NTDs. Some examples are given in **Table 1.2**.

Environmental factors may have an effect on a variety of cellular processes and pathways. For example, an intact folate cycle is essential in NT development. The drug Carbamazepine is thought to affect the folate status of the mother, thus inducing NTDs in the embryo (Hernandez-Diaz et al., 2001) (see section **1.2.4** for more information about folate and NTDs).

Additionally, the acetylation status of the DNA needs to be tightly regulated, as this contributes to the control of gene expression. The action of histone deacetylases (HDACs) is vital in the control of cellular processes such as proliferation and differentiation through

Environmental Factor/Teratogen	Reference
Maternal diabetes	(Correa et al., 2008)
Vitamin B12 insufficiency	(Ray and Blom, 2003)
Maternal hyperthermia	(Lynberg et al., 1994; Suarez et al., 2004)
Maternal obesity	(Watkins et al., 1996; Watkins et al., 2003)
Carbamazepine (used to treat epilepsy)	(Hernandez-Diaz et al., 2001)
Trimethoprim (antibiotic)	(Hernandez-Diaz et al., 2001)
Valproic acid (used to treat epilepsy)	(Lammer et al., 1987; Menegola et al., 2005)

Table 1.2: Environmental factors which have been linked to neural tube defect development.

chromatin condensation and transcriptional repression (Johnstone, 2002). Inhibition of HDACs with Trichostatin A has been shown to cause NTDs in the chick (Murko et al., 2013). Valproic acid appears to act as a histone deacetylase inhibitor (HDACi), and been found to cause NTDs (Lammer et al., 1987; Menegola et al., 2005).

1.2.3 Mechanism of tissue damage

The mechanism by which exposed neural tissue is damaged in NTD cases is currently under debate. The central nervous system of embryos with spina bifida appears to initially develop normally, and then degenerate later in gestation (Keller-Peck and Mullen, 1996; Stiefel et al., 2007). Research has reported the presence of apparently healthy neural tissue in the open neural tube of an E12 mouse embryo with spina bifida, showing mitotic figures, an intact ependymal surface, and appropriate cell density, although possibly with slightly more intercellular space than seen in wild type embryos. It also appears that neuronal differentiation occurs normally in the open region of spina bifida lesions (Keller-Peck and Mullen, 1996; Stiefel and Meuli, 2007). Nerve fibres develop normally in embryos with spina bifida, and neuronal connections are made between the spinal cord and peripheral tissues (Stiefel et al., 2007).

However, by E16.5 the neural tissue begins to show signs of degeneration, including abrasions and haemorrhage. By approximately E17.5 connections are lost between the spinal cord and the peripheral tissue, and the nerves degenerate. Hind limb pain reactions were observed among only 45% of murine embryos with spina bifida at E18.5, and tail pain reactions in 20%, compared to 100% in wild type embryos of the same gestational age (Stiefel et al., 2007). By E19 the tissue was showing severe damage, including apoptosis and necrosis, and loss of the ependymal surface. Eventually the exposed neural tissue is completely lost (McLone et al., 1997; Stiefel et al., 2007; Stiefel and Meuli, 2007).

It has been suggested that the amniotic fluid itself could be at least partially responsible for the tissue damage seen in the exposed neural tube. The presence of urine in the fluid, or a difference of osmolarity could mediate the toxic effect. However, this is difficult to study using a murine model, as the gestation, and thus the amount of time exposed to the amniotic fluid, is far shorter than that of humans (McLone et al., 1997). Some neuronal loss could be linked to reduced afferent stimulation of neurons in the open neural tube, which could be due to abnormal NC development rather than tissue damage (Moase and Trasler, 1989). Additionally, contact with the uterus wall could cause traumatic injury to the exposed neurons (McLone et al., 1997).

Treatment of spina bifida in which intrauterine fetal surgery is used to cover the lesion is currently practised in several centres (Stiefel et al., 2007). Results have been diverse, with some studies showing improvements in the frequency and severity of hydrocephalus and hindbrain herniation in infants with spina bifida (Bruner et al., 1999; Farmer et al., 2003; Sutton et al., 1999), and a reduction in neuronal damage (Johnson et al., 2003; Verbeek et al., 2012). However, some studies have shown no difference between infants with spina bifida, and those affected by spina bifida who were given the fetal surgery (Holmes et al., 2001; Tubbs et al., 2003). Additionally, many studies have reported a higher rate of premature birth, and complications and mortality during gestation and neonatal life in the infants who have undergone fetal surgery (Bruner et al., 1999; Johnson et al., 2003; Sutton et al., 1999; Verbeek et al., 2012).

A major study in the outcomes of prenatal surgery was the Management of Myelomeningocele Study (MOMS). This was a randomised trial comparing the outcome of prenatal surgery against postnatal surgery for myelomeningocele (Adzick et al., 2011). The trial involved randomly assigned prenatal (prior to 26 weeks of gestation) or postnatal surgery for 158 women. The children were followed for 30 months postnatally, and were assessed for a number of outcomes, including pregnancy complications, premature birth, mental development, motor

development, and the need for the placement of a cerebrospinal shunt. Children in the prenatal surgery group showed an improvement in a number of postnatal outcomes; for example, only 40% required shunt placement compared to 82% in the postnatal surgery group, and they also scored better in a mental development test. Additionally, a higher number of children from the prenatal surgery group performed better than expected for the level of their lesions in motor function tests compared to the postnatal surgery group. However, the prenatal surgery group were more at risk of pregnancy complications; the children had a higher risk of preterm birth, and therefore respiratory distress. There was also a higher risk of chorioamniotic separation, which can result in premature membrane rupture.

Many studies appear to support the conclusion that prenatal surgery to repair spina bifida can improve postnatal outcome in CNS function and complications such as shunt requirement. However, this should be weighed against evidence that prenatal surgery carries a higher risk than postnatal surgery for complications in pregnancy, including a higher risk premature delivery, spontaneous membrane rupture, and fetal mortality. Long term studies will also be required to observe the stability and persistence of the improved outcomes.

1.2.4 Folate and neural tube defects

Folate enters one-carbon metabolism, which plays two main roles in the cell; the synthesis of pyrimidines and purines, and donation of methyl groups to macromolecules (Copp et al., 2013; Kim et al., 2009; Waterland and Jirtle, 2003).

Folic acid is a synthetic and environmentally stable form of folate, which is recommended as a supplement for women during the very early stages of pregnancy. It has been shown to prevent up to 72% NTD recurrence in women who have previously had an NTD pregnancy (MRC, 1991). In America in 1998 it was advised that wheat flour be fortified with folic acid (Food and Drug Administration, 1996), and this has reduced the number of NTD pregnancies by around 19-32% (Boulet et al., 2008; Crider et al., 2011; Williams et al., 2002). However, supplementation is not able to prevent all cases of NTD, which suggests that some forms are folic acid resistant (Heseker et al., 2009).

On average, mothers carrying NTD-affected fetuses have been shown to have a reduction in the plasma levels of folate. Thus, sub-optimal levels are a risk factor, but the levels were consistently above the level of deficiency (Kirke et al., 1993; Mills et al., 1995). This suggests that the defect may be metabolic, rather than caused by a simple deficiency. Several folate-related genes have been identified as potential risk genes for NTDs. Methylenetetrahydrofolate reductase (MTHFR) is a cytoplasmic enzyme involved in folate metabolism, and mitochondrial 10-formyl-tetrahydrofolate synthetase (MTHFD1L) is involved

in mitochondrial one-carbon metabolism. Both of these genes have allelic forms which increase the risk of NTDs (Parle-McDermott et al., 2009; van der Put et al., 1995).

Folate is thought to play a role in cellular proliferation, in part due to its link to pyrimidine and purine synthesis (Beaudin and Stover, 2007). Abnormalities in proliferation can be found in cases of NTD, both in the NT (Smith and Schoenwolf, 1987) and in the surrounding tissues (Copp et al., 1988a). A reduction in proliferation has also been found to induce NTDs after the use of anti-mitotic agents. For example, mouse embryos treated with hydroxyurea, which inhibits DNA synthesis, have a 30% incidence of exencephaly (Copp et al., 1990). Additionally, the anti-mitotic Mytomycin C has been found to increase the rate of exencephaly development in the *curly tail (ct)* mouse (Seller and Perkins, 1986). A reduction in proliferation within the NT is thought to affect the mechanical properties of the NT, for example through the shapes of the cells or the tissue, and thus affect NT closure.

As mentioned previously, folate is essential for the transfer of methyl groups from the one-carbon metabolism to macromolecules for methylation (Copp et al., 2013; Kim et al., 2009; Waterland and Jirtle, 2003). Methylation of macromolecules, including DNA, has been shown to play an important role in NT closure. It has been demonstrated that a reduction in DNA methylation, either genetically (in the mouse) (Okano et al., 1999) or through the use of inhibitors (in the chick) (Afman et al., 2005) can cause NTDs. Abnormal DNA methylation has also been found in some cases of NTD in humans (Zhao et al., 2006). These defects could be related to epigenetic differences which result from abnormal methylation. For example, abnormal DNA methylation could affect the structure of the chromatin and the binding of DNA to certain proteins, which may affect the expression levels of certain genes (Greene et al., 2011). The change in gene expression could contribute to the development of NTDs.

1.3 The Neural Crest

NC cells are a transient, highly migratory subset of cells found in vertebrates during development. They are multipotent cells which are specified at the border of the neural plate and the surrounding ectoderm. During neurulation NC cells undergo EMT (epithelial to mesenchymal transition), and migrate along defined paths to populate target tissues. They contribute to a variety of tissues and organs within the developing embryo, including craniofacial structures, pigmentation cells, and the neurons and glia of the peripheral nervous system, (Basch et al., 2004).

The NC undergo several stages of development. They are first specified at the neural plate border. This involves multiple pathways, including BMP, Wnt and FGF signalling. Specification induces the expression of genes involved in maintenance and expansion of the NC, such as *Pax3*, *FoxD3*, *Sox* and *Snail*. The NC cells then delaminate and migrate to target tissues, which requires the expression of genes involved in EMT, cell polarity and cell guidance, such as *Cadherin* genes, *FoxD3*, *ErbB3*, *Sox9* and *Twist*. Finally, once cells reach the target tissue they differentiate according to migration path, and premigratory and postmigratory positional information.

1.3.1 Specification

The NC are first specified at the border of the neural plate, where it meets the surrounding non-neural ectoderm. Extracellular signalling plays an important role in this specification, and signalling molecules are released from the neural plate, the epidermis, and the underlying mesoderm (Mayor et al., 1995; Moury and Jacobson, 1990; Selleck and Bronner-Fraser, 1995). Indeed, it has been found that in *Xenopus* removal of the paraxial mesoderm underlying the non-neural ectoderm can prevent formation of the NC (Bonstein et al., 1998).

Both the neural ectodermal and presumptive epidermal lineages are able to contribute to the NC population. This has been shown to happen in multiple species *in vitro*, and *in vivo* studies also indicate dual lineage of the NC within the embryo (LaBonne and Bronner-Fraser, 1999; Moury and Jacobson, 1990; Selleck and Bronner-Fraser, 1995).

NC specification involves two stages of signalling – an induction step and a maintenance and expansion step. The signalling pathways BMP, Wnt, and FGF are vital in induction, and molecules such as *Pax3*, *Msx* and *Zic2* enable specification of the NC cells to specific fates. Additionally, molecules such as *Slug*, *Snail* and *Sox10* are important in cell survival and maintenance of the newly acquired NC fate (Steventon et al., 2005). These processes are controlled by a complex gene regulatory network.

1.3.1.1 Induction and Specification

The induction of the neural plate border region is described in section **1.1.1**, as initial specification of the neural plate and the neural plate border are very closely linked. However, once the regions have been induced, gene expression and specification of the cells in the neural plate border begin to deviate from those in the neural plate.

Canonical Wnt signalling appears to have a key function in the specification of the NC. However, its exact role is not fully understood. *Wnt1*, *Wnt3a* and *Wnt3* RNA have all been detected in the dorsal midline of the NT of both mouse and *Xenopus* embryos (Parr et al.,

1993; Roelink and Nusse, 1991; Wolda et al., 1993). This is the region of the NT in which the NC are induced.

In the *Xenopus* embryo overexpression of *Xwnt1* (*Xenopus* Wnt1) and *Xwnt3a* proteins due to injection of RNA increases the expression domain of NC markers in ectoderm tissue neuralised by *noggin* or *chordin*, which inhibit BMP-Smad signalling from the ectoderm (Hegarty et al., 2013; Saint-Jeannet et al., 1997). This suggests that in tissue that has been made competent to respond by BMP antagonists, cells may be specified to form NC by Wnt signalling. In support of this, it was observed that *Xenopus* ectodermal animal caps exposed to both *chordin* and *Xwnt8* expressed NC markers, whereas those exposed only to *chordin* did not (LaBonne and Bronner-Fraser, 1998). Additionally, injection of cells expressing a non-autonomous dominant-negative Wnt1 into the NTs of chick embryos reduced the expression of NC markers (Garcia-Castro et al., 2002).

FGF signalling appears to play a similar role to Wnt signalling in inducing NC specification – *Xenopus* animal caps injected with mRNA for both *chordin* and *eFGF* also expressed NC markers (LaBonne and Bronner-Fraser, 1998). However, this response was not as strong as animal caps expressing *chordin* and *Xwnt8*. A dominant negative *Xwnt8* mutation prevented the NC induction by eFGF. This suggests that eFGF induces the expression of *Xwnt8*, which in turn induces the expression of the NC markers (LaBonne and Bronner-Fraser, 1998).

Evidence suggests that the signalling described may be controlled by the transcription factors Snail and Slug (*Snail2*) in *Xenopus*; *snail2* *Xenopus* morphants show reduced levels of *Xwnt8*, *bmp4*, and *frzb1*, whereas *chordin* was increased (Shi et al., 2011). This could be due to the role of *snail2* in the formation of the mesoderm (Bonstein et al., 1998). On the other hand, it has also been suggested that Wnt signalling may directly induce expression of *slug* in *Xenopus* (Vallin et al., 2001). Therefore, there could be feedback mechanisms tightly connecting and controlling the expressions of these pathways. The exact roles of these proteins in the early development of mammalian NC are unknown.

1.3.1.2 Maintenance and Expansion

Expression of maintenance and expansion genes represents the second stage of NC specification; the cells become firmly specified as NC, and undergo a population expansion prior to migration. The population expansion is vital for the correct development of the NC and NC-derived tissues. This is demonstrated by the NC defects seen in embryos carrying mutations which affect the proliferation of the NC prior to migration (Conway et al., 2000; Ikeya et al., 1997).

The genes involved in maintenance and expansion are expressed solely in the prospective NC cells, and function to maintain and increase the precursor population, while inducing expression of proteins involved in migration. These genes include the transcription factors *FoxD3*, *Hairy2*, *Twist* and *Id3*, and also genes in the families *Msx*, *Sox* and *Snail*. Several of these genes and their functions in NC development are discussed here.

Snail and *Slug* are closely related zinc-finger transcriptional repressors with some functional redundancy (Carl et al., 1999; Gray et al., 1994; Hemavathy et al., 2000). They are expressed in the border region, in NC cells, but the exact timing and function of the proteins appears to differ between vertebrate species. In the mouse *Snail* is expressed in premigratory NC cells, whereas in the chick *Snail* is not expressed in the NC prior to migration. Conversely, *Slug* in the mouse is not expressed in premigratory NC, but is found in premigratory NC in the chick (Sefton et al., 1998). In *Xenopus*, both *Xsnail* and *Xslug* are expressed in the NC long before migration begins (Mayor et al., 1995). *Snail* has also been found to inhibit neurectodermal fate in *Drosophila* (Leptin, 1991), and it may play a similar role in the border region of vertebrates.

The functional roles of *Slug* and *Snail* also differ between species. In *Xenopus* *Xslug* and *Xsnail* are necessary for both NC formation and migration (Aybar et al., 2003; LaBonne and Bronner-Fraser, 2000). However, in the mouse embryo neither *Slug* nor *Snail* expression are necessary for NC formation or migration – E9.5 double mutant mouse embryos which are null for both *Snail1* (*Snail*) and *Snail2* (*Slug*) appear to develop NC cells, which migrate normally (Murray and Gridley, 2006).

Additionally, *Slug* and *Snail* have roles in cell survival. Expression of *SNAIL2* acting as an anti-apoptotic agent in humans has been found in cases of leukaemia (Inukai et al., 1999). Furthermore, aberrant expression of either *SNAIL* or *SLUG* infers resistance to apoptosis due to DNA damage in human cancer cell culture (Kajita et al., 2004).

On the other hand, *Snail* inhibits cell cycle progression in the mouse NC population by repressing *CyclinD2* transcription, thus inhibiting the progression of the cells to late G1 phase (Vega et al., 2004a). This is also true for *Slug* in the chick embryo (Vega et al., 2004a). The genes favour cell shape changes over proliferation, and therefore favour preparation for the impending cell migration over population expansion. However, population expansion still occurs in the NC cells, as the expression of these genes is in balance with the expression of genes which promote proliferation in the NC.

Mouse embryos mutant for both *Wnt1* and *Wnt3a* show a reduction in the number of NC derived cells, which suggests that they may play a role in expansion of the NC population prior

to migration (Ikeya et al., 1997). In support of this, ectopic expression of *Wnt1* in the murine NT resulted in higher than normal proliferation in the affected area (Dickinson et al., 1994). Therefore Wnts may act on proliferation in the NC population. Studies in *Xenopus* show that the effects of *Xwnt1* on the developing NC are mediated by the Wnt receptor *Xfz3* (Deardorff et al., 2001).

c-Myc is a basic helix-loop-helix zipper (bHLHZ) transcription factor which is downstream of Wnt signalling (He et al., 1998). It is involved in a wide variety of cellular processes, including proliferation, differentiation and cell survival (Bellmeyer et al., 2003). c-Myc is expressed early during the formation of the neural plate border, and reduction of expression in *Xenopus* prevents the formation of the NC precursor cells (Bellmeyer et al., 2003). Evidence suggests that c-Myc has no effect on cell proliferation or apoptosis in the neural plate border. However, c-Myc suppression by Morpholinos in the neural plate border of *Xenopus* induced this tissue to form CNS instead of NC precursors, suggesting that c-Myc plays a role in cell fate decisions (Bellmeyer et al., 2003).

The role of Notch in NC induction and maintenance appears to differ between species. In *Xenopus*, it has been shown that HLH transcription factor Hairy2 – a component of the Notch pathway – is expressed downstream of BMP, Wnt and FGF signalling, and is necessary to maintain proliferation and prevent differentiation of the NC, and as a survival factor for these cells. Hairy2 is able to induce Notch signalling, which in turn controls expression of NC genes such as *id3*, *sox9* and *snail2* (Nichane et al., 2008a; Nichane et al., 2008b). In the chick, it appears that the primary role of Notch signalling is to regulate the level of BMP4 expression during the development of the NC, and restrict NC differentiation to the neural plate border (Endo et al., 2002). In the mouse, it represses neuronal differentiation, and may also promote proliferation of the NC population (De Bellard et al., 2002; Yun et al., 2002).

Id3 (Inhibitor of DNA binding) is a helix-loop-helix (HLH) transcription factor. Its expression is induced by Myc activity (Light et al., 2005), and it appears to be necessary for the specification of the NC – Id3 depleted *Xenopus* embryos do not express the NC markers *slug*, *sox10*, *twist*, and *foxD3* (Kee and Bronner-Fraser, 2005; Light et al., 2005). Additionally, NC lacking Id3 fail to proliferate, and instead undergo apoptosis (Kee and Bronner-Fraser, 2005). Therefore, Id3 maintains NC cells as multipotent precursors, preventing differentiation, while also facilitating NC cell survival and population expansion through cell cycle progression.

Several of the Sox transcription factors are expressed in the neural plate border, including Sox8, Sox9 and Sox10. This is true for a variety of organisms, such as *Xenopus*, zebrafish, chick, human, and mouse, but the exact function, timing and expression patterns of the genes differs

between species (Hong and Saint-Jeannet, 2005). For example, in chick and mouse *Sox10* is the earliest Sox gene to be expressed in the developing NC. However, in *Xenopus* and zebrafish *sox10* is one of the final Sox genes involved in NC induction (Hong and Saint-Jeannet, 2005). In many organisms *Sox10* is detected mostly in the peripheral nervous system (PNS) (Cheng et al., 2000; Dutton et al., 2001; Southard-Smith et al., 1998). In *Xenopus* and chick embryos *sox10* is transiently expressed in the migrating cranial NC and the pharyngeal arches (Aoki et al., 2003; Cheng et al., 2000). However in zebrafish and mouse embryos expression is not seen in the pharyngeal arches (Dutton et al., 2001; Southard-Smith et al., 1998).

Several of the Sox mutant embryos generated so far exhibit abnormalities in the NC. For example, conditional deletion of *Sox9* in the NC of mice resulted in craniofacial malformations involving the bone and cartilage tissue derived from the cranial NC (Mori-Akiyama et al., 2003). Similarly, in *Xenopus* injection of Morpholino against *sox9* resulted in the loss of NC derivatives, and craniofacial defects involving the skeleton (Spokony et al., 2002). Furthermore, loss of *Sox10* in several model organisms appears to cause defects in the trunk and vagal NC. The enteric nervous system (ENS) of *Sox10* mutant mice develops abnormally, resulting in aganglionosis of much of the gut (Herbarth et al., 1998). Zebrafish mutants carrying a *sox10* mutation show a similar gut defect, in addition to a pigmentation defect (Kelsh and Eisen, 2000). Many of the Sox mutants studied show relatively normal NC specification and migration, but the NC fail to terminally differentiate once they have reached the appropriate position in the embryo. Some of the Sox genes may also be implicated in cell survival; *Sox9* mutant mouse embryos demonstrate very high levels of apoptosis among the populations of premigratory and early migratory NC cells (Cheung et al., 2005).

FoxD3 is a Forkhead/Winged helix transcription factor, and is expressed in both premigratory and migratory NC, where it acts as a transcriptional repressor (Hochgreb-Hagele and Bronner, 2013; Teng et al., 2008). *FoxD3* is important in the maintenance and migration of the NC population, and conditional deletion of the gene in mouse embryos results in abnormalities of a number of NC derived tissues (including craniofacial structures, PNS and ENS) due to migration failure and apoptosis of the NC (Teng et al., 2008). Similar results were found in zebrafish mutants (Hochgreb-Hagele and Bronner, 2013; Lister et al., 2006; Stewart et al., 2006). Additionally, ectopic expression of *FoxD3* in *Xenopus* and chick NT resulted in the expression of NC markers in the affected cells (Dottori et al., 2001; Sasai et al., 2001). Research has also shown that *FoxD3* suppresses both melanocyte and neural differentiation in chick, suggesting that it acts to maintain the NC as precursors by preventing differentiation (Dottori et al., 2001; Kos et al., 2001; Nitzan et al., 2013). Zebrafish embryos mutant for *foxd3* have

been found to have reduced expression of *snailb* and *sox10*, which suggests that *foxd3* may have a role in controlling the expression of these other NC genes (Stewart et al., 2006).

Pax3 mutant mouse embryos develop a number of NC defects, including pigmentation defects and conotruncal heart defects (Auerbach, 1954; Franz, 1989). For more information on the role of *Pax3* in NC development see section **1.4.4.2**.

Apoptosis in the NC is important during development, and is a highly controlled process. For example, cranial NC cells which are specified in rhombomeres 3 and 5 undergo apoptosis. This is mediated by *Msx2*, which is induced by *BMP4*, and is inhibited by *Snail2* and the Wnt antagonist *Sfrp2*, which act as survival factors. The survival or apoptosis of these hindbrain NC depend on the balance of pro-apoptotic and anti-apoptotic signals (Ellies et al., 2000; Graham et al., 1993; Graham et al., 1994; Morales et al., 2005; Vega et al., 2004b).

1.3.2 Migration

NC migration is closely tied in with the maintenance and expansion stage of NC development. This step prepares the cells for migration, and many genes are common to both stages.

The migration of the NC follows a pre-defined pattern, specified by a 'track' of adhesion molecules in the extracellular matrix (ECM), including fibronectin, laminin-1 and collagen. A variety of different adhesion molecules including integrins and cadherins on the surface of the NC cells allow them to follow this pathway from their region of origin to their target tissue (Maschhoff and Baldwin, 2000; Theveneau and Mayor, 2012). Additionally, repulsive signals, such as those generated by Eph-ephrin signalling or *Twist*, are expressed in tissues surrounding the migration route. This ensures that cells migrate only along the defined path (Smith et al., 1997; Soo et al., 2002).

Migration of the NC is a multi-step process. First EMT of the specified NC allows them to delaminate from the surrounding neural ectoderm, losing epithelial structure and becoming mesenchymal. This process requires a number of cellular alterations, such as loss of polarity, cytoskeletal changes and changes in cell-cell and cell-ECM adhesion. Next, the cells must move through the embryonic tissues, following the specified track laid down for them, to their end position. Once the cells have reached this position, they are able to terminally differentiate (see section **1.3.3**).

In order for delamination and migration to occur, significant changes in cell-cell and cell-matrix adhesion need to occur. Adhesion molecules of both the NC and the ECM through which they move are vital in permitting and promoting migration, and in ensuring the cells reach their target tissue (Lofberg et al., 1985). The NC cells and the surrounding tissues express different

combinations of adhesion molecules. For example, the mammalian NT expresses high levels of N-cadherin, whereas the NC cells have very low expression of N-cadherin (Nakagawa and Takeichi, 1995).

Additionally, different subpopulations of NC cells express different combinations of adhesion molecules, such as integrins and type II cadherins, and migratory paths to different regions of the embryo use different adhesion molecules, including fibronectin, hyaluronic acid, and collagen (Bronner-Fraser, 1985; Nakagawa and Takeichi, 1995; Thiery et al., 1982). This aids the colonisation of separate regions with the appropriate subpopulations of NC (Nakagawa and Takeichi, 1995).

Some NC cells may proliferate as they migrate. Studies of cranial NC in the chick have shown that migrating cells undergo mitotic events at a low frequency, and that the rate of proliferation in the population increases once cells enter the branchial arches. The data also shows that cranial NC cells are able to increase the rate of proliferation during migration to compensate for low numbers of migrating cells (Ridenour et al., 2014). The NC which migrate to the gut and form the ENS have also been examined in the chick, and have been found to proliferate during migration. The migrating cells of the leading edge are reported to proliferate at a higher rate than the trailing cells (Landman et al., 2011).

1.3.2.1 Signalling in neural crest delamination and migration

Levels of Wnt, FGF and BMP signalling appear to be important to allow delamination and migration of the NC. For example, Bmp2 expression is necessary for migration of the cranial NC in mice (Kanzler et al., 2000), and a Bmp4-Noggin balance is necessary for delamination through the control of *rhoB* and *cadherin-6b* expression in chick embryos (Sela-Donenfeld and Kalcheim, 1999). Additionally, Xwnt11 is normally expressed immediately adjacent to the NC population in *Xenopus*; inhibition of Xwnt11 activity represses NC migration, whereas ectopic expression induces migration of the NC towards the Xwnt11 activity (De et al., 2005). In chick FGF8 has been found to be chemotactic for migrating cardiac NC - FGF8 is expressed in the pharyngeal ectoderm and endoderm, and NC from NT explants migrate towards sources of FGF8 (Sato et al., 2011).

FoxD3 is described previously, as it has a role in maintenance of the newly specified NC. FoxD3 is also important in NC migration. Some research has shown that transfection of *FoxD3* into chick NT explants is able to induce ectopic expression of NC markers, but is not sufficient to enable delamination and migration of these NC cells (Cheung et al., 2005). On the other hand, *in vivo* studies of electroporated chick NTs have demonstrated disassembly of the basement membrane and migration of the affected cells (Dottori et al., 2001). Therefore, the exact role

of FoxD3 during migration is not known. However, FoxD3 is able to induce changes in the cell-cell and cell-ECM adhesion molecules which favour migration. For example, FoxD3 downregulates N-cadherin, and upregulates Integrin- β 1 and Laminin expression in mouse embryos (Cheung et al., 2005). Additionally, research has shown FoxD3 to be a promoter of EMT in the NC through the activity of Tetraspanin18 (Tspan18). Tspan18 is a scaffolding protein which maintains cadherin-6b. This protein is unfavourable to EMT. The NTs of chick embryos which have been electroporated with an anti-FoxD3 Morpholino fail to downregulate Tspan18 at the appropriate time. Thus it appears that FoxD3 downregulates Tspan18 expression, which in turn downregulates cadherin-6b, enabling EMT to occur (Fairchild et al., 2014; Fairchild and Gammill, 2013).

The Sox genes are discussed previously, as they have a role in maintenance and expansion of the NC. In addition to this role, Sox9 is expressed in premigratory NC, and is important in initiation of migration in these cells (Cheung and Briscoe, 2003). Expression of Sox9 in chick neural explants induced the expression of NC marker genes. The tissue explants demonstrated basement membrane disassembly in the regions expressing Sox9, and a small proportion of the cells displayed migratory behaviour (Cheung and Briscoe, 2003). Sox9 mutant mouse embryos have lower expression levels of *Snail* in premigratory NC, which suggests that Sox9 may control expression of *Snail* in these cells (Cheung et al., 2005). Sox9 is not able to efficiently induce delamination and migration of NC when transfected alone. However, when combined with certain other signalling molecules Sox9 is able to induce this more efficiently than either molecule alone (Cheung et al., 2005).

RhoB is a member of the rho family of GTP binding proteins, and is expressed in the premigratory NC, and transiently in the migratory NC. Its expression in the NC is induced by BMP, and inhibition of *RhoB* activity in chick NT explants by use of the Rho inhibitor *Clostridium botulinum* exotoxin C3 prevents delamination of the NC cells (Liu and Jessell, 1998). Research has also shown that *RhoB* can induce NC migration at low efficiency, and may promote apoptosis in transfected cells (Cheung et al., 2005). However, when expression constructs were transfected together, *RhoB* and Sox9 produce dramatic changes in NT cells of chick explants; cells expressed NC markers, lost polarity, became rounded in shape, and migrated out of the explant at much higher efficiency than when expressing either *RhoB* or Sox9 alone. Apoptosis was also reduced compared to *RhoB*-transfected explants (Cheung et al., 2005).

The role of Notch signalling in NC maintenance and expansion is described previously. The function of Notch signalling during NC migration is not well understood, and appears to differ a

great deal between species. However, it has been shown in mice that loss of Delta-1 results in abnormalities in the development of the dorsal root ganglia (DRG) and sympathetic ganglia, suggesting that Notch signalling plays a role in the migration of these cells (De Bellard et al., 2002).

The genes *Snail* and *Slug* are discussed previously relating to their roles in premigratory NC. They are also involved in NC migration, and again, the exact role is dependent upon species. In the chick the NC marker *Slug* – but not the closely related *Snail* – is expressed in the migratory NC, and the repression of *Slug* prevents EMT in these cells (Nieto et al., 1994; Sefton et al., 1998). Studies have shown that electroporation of *Slug* into the chick hindbrain NT increased the population of migratory NC, but no difference is seen in the spinal region (Cheung et al., 2005; del Barrio and Nieto, 2002).

Conversely, the mouse expresses both *Slug* and *Snail* in migrating NC, although deletion of neither *Slug* nor *Snail* in the mouse inhibits the delamination or migration of the NC (Murray and Gridley, 2006; Sefton et al., 1998). However, mouse *Snail* has been shown to induce EMT in carcinomas through the downregulation of E-cadherin, and ectopic expression of *Snail* or *Slug* has been found to initiate EMT *in vitro* (Bolos et al., 2003; Cano et al., 2000). Downregulation of *Cadherin-6b* and upregulation of *Cadherin-7* are important steps in EMT. *Slug* expression in chick is important for the downregulation of *Cadherin-6b* (Taneyhill et al., 2007). Similarly, *Snail* is able to downregulate several members of the matrix metalloproteinase (MMP) family *in vitro* (Miyoshi et al., 2004). The MMPs are important for the breakdown of the ECM, thus allowing the NC to migrate. The role of the *Snail* family of transcription factors is still not completely understood.

Cotransfection of *Sox9* and *Slug* into chick NT explants induced strong expression of NC marker genes. Additionally, higher numbers of rounded and migratory cells were seen when compared to explants transfected with *Sox9* or *Slug* alone. Cotransfection of *Sox9* and *Snail* gave similar results (Cheung et al., 2005).

Twist is a basic helix-loop-helix (bHLH) transcription factor, and is expressed early in the development of the NC (Hopwood et al., 1989; O'Rourke and Tam, 2002). *Twist* is thought to play an important role in EMT both in the NC and in cancers; expression has been found in metastatic cancer cell lines, and repression of *Twist* inhibits metastasis when these cells are transplanted into mice. Additionally, *Twist* is known to downregulate E-cadherin, much like *Slug* and *Snail*, which also induce EMT (Yang et al., 2004).

ErbB2 and ErbB3 are members of the epidermal growth factor (EGF) family of proteins. They dimerise to form a heterodimer in order to bind the EGF-like proteins Neuregulin (Nrg) 1 or Nrg2 (Carraway, III and Cantley, 1994). *erbB2* or *erbB3* mutant zebrafish lack DRG and sympathetic neurons (Honjo et al., 2008). In wild type zebrafish embryos the migrating NC usually pause in the location of presently differentiating DRG, but this pause was not seen in embryos mutant for *erbB3*. This suggests that in zebrafish ErbB3 is necessary for recognition of the positional signal which retains migrating NC in the correct region for DRG differentiation (Budi et al., 2008; Honjo et al., 2008). Murine embryos mutant for *ErbB2* or *ErbB3* also exhibit reduced DRG and sympathetic neurons. However, this appears to be due to failure of the NC to migrate to this region; NC cells leave the NT, but migrate only a short distance (Britsch et al., 1998). Therefore, ErbB3 is important in migration of the NC population, but its exact role appears to differ between species.

1.3.2.2 Neural crest cell guidance during migration

The guidance of NC migration is necessary to ensure that NC cells which have been made competent for a particular fate migrate towards the tissue in which that fate will be possible and appropriate. Multiple mechanisms are in place to ensure that the NC migrate in streams towards the correct tissues.

Specific adhesion molecules are often expressed only in certain tissues, or in certain subpopulations of NC. This specificity aids the guidance of the subpopulations to their target tissue. For example, in *Xenopus* the adhesion molecule Cadherin-11 is expressed only in the cranial NC (Vallin et al., 1998), and its suppression results in failure of the migrating cranial NC to reach their target tissue, the pharyngeal pouches (Kashef et al., 2009). Also, α 7-integrin is observed on a subpopulation of migrating trunk NC in the chick (Kil and Bronner-Fraser, 1996).

The NC cells migrate in a highly directional manner, and show polarisation of the cytoskeleton parallel to the direction of travel. In *Xenopus* and zebrafish, this polarisation is dependent on the PCP pathway, and suppression or deletion of components of this pathway, such as Wnt11, inhibits NC migration (De et al., 2005; Matthews et al., 2008). However, mouse embryos which lack PCP signalling have normally migrating NC cells. Therefore, PCP signalling is non-essential in mammalian NC migration (Pryor et al. Submitted manuscript). PCP signalling usually acts to polarise tissues through its effects on the cytoskeleton, and it has been suggested that in *Xenopus* and zebrafish NC cells may interact in some way which allows them to act as a 'tissue' regarding PCP signalling (Kuriyama and Mayor, 2008).

Indeed, evidence suggests that the NC may interact through tissue-specific attractive-repulsive forces, which enable them to move in a stream. NC cells demonstrate the repulsive force CIL

(contact inhibition of locomotion) which induces a change in the direction of migration if cell-cell contact is made between the NC (Carmona-Fontaine et al., 2008). In addition to CIL, NC cells also exhibit coattraction. This is an attractive force between NC cells, mediated by the complement protein C3 – which acts as a chemoattractant for the NC – and its receptor C3aR, both of which are expressed by migrating NC cells (Carmona-Fontaine et al., 2011). In combination, CIL and coattraction are able to explain the collective migration of NC cells seen *in vivo*.

Chemotaxis is also used to attract NC to their destination. For instance, as mentioned previously, FGF8 is expressed in the pharyngeal ectoderm and endoderm, and attracts chick cardiac NC cells to their destination (Sato et al., 2011). Additionally, Glial-derived neurotrophic factor (GDNF) and netrins act as chemoattractants for migrating ENS-fated NC cells in the gut of mouse embryos (Jiang et al., 2003; Young et al., 2001).

Repulsive molecules in surrounding tissues and the ECM prevent NC cells from migrating away from their path. Eph receptors and the ephrin ligands are cell surface molecules which provide repulsive cues. For example, in *Xenopus* the cells of the third branchial arch and a subset of cranial NC express EphA4 and EphB1. The adjacent second arch expresses the ligand for these receptors, Ephrin-B2. Therefore, this tissue repels the subpopulation of NC cells, and prevents mixing of the second and third arch NC populations (Smith et al., 1997). The Semaphorin family of proteins plays a similar role; Collapsin-1 in chick is a Semaphorin which is expressed in regions surrounding NC migration routes for both hindbrain and trunk NC cells. A Collapsin-1 receptor, Neuropilin-1, is expressed in the NC cells which migrate along these pathways (Eickholt et al., 1999).

Twist expression is found in both the NC cells and the paraxial mesoderm surrounding the NC migration path, and it appears to act on both tissues individually to enable correct migration in mouse embryos. *Twist* mutant mouse embryos show a merging of NC streams into the first and second branchial arches, which form two distinct streams in the wild type embryo. However, wild type NC cell transplants into the *Twist* mutant embryos showed that the wild type NC cells were more likely to follow the correct path, but also merged streams. This suggests that *Twist* expression is required in the NC cells to enable them to follow the correct migration path, but also in the surrounding paraxial mesenchyme to produce a repulsive signal which maintains the tight migration path (Soo et al., 2002).

In the spinal region, NC cells are able to migrate through or around different regions of the somite. The migration path is representative of their fate. For instance, NC cells which travel through the medial region of the somite develop sensory and sympathetic ganglia, and

Schwann cells, whereas cells which travel between the somite and the surface ectoderm form melanocytes (Kuriyama and Mayor, 2008; Le Douarin and Teillet, 1974). Control of which pathway the NC cells follow is largely dependent upon Eph-ephrin signalling between the NC cells and the surrounding tissue (Santiago and Erickson, 2002). However, *Slit/Robo* signalling is also implicated; this is a repulsive signalling pathway which is active during early NC cell migration in the trunk. In chicks the Slit ligands are expressed in the dermomyotome, whilst the early migrating NC express the Slit receptors Robo1 and Robo2. *Slit2* is essential for preventing migration through the dorsal pathway, between the surface ectoderm and the dermomyotome (Jia et al., 2005).

1.3.3 Differentiation

The NC contribute to almost every tissue in the embryo, and are able to form an enormous variety of cell types. NC cells are multipotent *in vitro*, but *in vivo* the differentiation is highly controlled and context dependent (Anderson, 1994).

Upon initial specification the NC appear to be multipotent. However they become more specified with development. Prior to migration, the cells begin to demonstrate some lineage restriction (Schilling and Kimmel, 1994), and upon migration to a particular target tissue become increasingly constrained to a particular fate through a series of environmental and epigenetic factors (Koblar et al., 1999).

Upon completion of migration NC cells may undergo another round of proliferation prior to terminal differentiation. For example, it was shown that NC-derived neural precursors in the developing DRG are Sox10-positive until terminal differentiation, upon which they lose Sox10 expression and become Tuj1-positive. Sox10-positive cells were found to be proliferative, and become Tuj1-positive upon the final cell division (Britsch et al., 2001; Gonsalvez et al., 2014; Membregh and Hall, 1995).

Once cells have reached the target tissues they terminally differentiate into the fated cell type. Many of the mechanisms and signalling pathways which regulate this progressive acquisition of cell fate and final differentiation are not well understood, but a selection are discussed below.

The spatial position of NC on the rostrocaudal axis as they become specified is central to the fate of the cells. Additionally, as discussed previously, NC cells of different fates migrate past the somites via different pathways – either between the surface ectoderm and the dermomyotome, or through the sclerotome (Kuriyama and Mayor, 2008; Le Douarin and Teillet, 1974).

The Hox genes play an important role in the rostrocaudal patterning of the NC, as they control the rostrocaudal patterning of much of the embryo. For example, in the cranial region of the mouse embryo each branchial arch expresses a different combination of Hox genes. The NC of branchial arches 2 and 3, but not branchial arch 1 show similar expression patterns and express *Hox2.8*, *Hox2.7* and *Hox2.9*, whereas *Hox2.6* is only expressed caudally of the branchial arches (Hunt et al., 1991). Additionally, electroporation of *Hoxb1* into the NT of chick embryos was able to upregulate *Slug* expression, which indicates NC specification (Gouti et al., 2011).

The cardiac NC arise from the NT adjacent to somites 1-3, and migrate into branchial arches 3, 4 and 6 (McKeown et al., 2013). In the mouse cardiac NC subpopulation *Twist1* is able to directly interact with *Sox10*, which binds the promoter of the neurogenic *Phox2b* gene. In doing so it represses *Phox2b* transcription, and inhibits neuronal differentiation in the cardiac NC (Vincentz et al., 2013). The cardiac NC cells provide signalling to aid in embryonic cardiogenesis, and also contribute to the heart valves and form parasympathetic nerves (Brade et al., 2013).

Timing of migration may also be crucial for differentiation in some NC subpopulations. In the zebrafish, early migrating cranial NC cells differentiate to form the facial skeleton and connective tissue, whereas later migrating cranial NC form the PNS of the cranial region (Bhatt et al., 2013).

Sensory neurons are derived from the trunk NC and differentiate in the DRG. Differentiation of these NC cells occurs in three waves, each of which is controlled by different neurogenic signalling molecules. The first wave of differentiation generates large-diameter touch and movement neurons. The second wave generates more large-diameter touch and movement neurons, but also small-diameter pain neurons. The third wave generates mostly nociceptive neurons (Bhatt et al., 2013). The first two waves of differentiation are controlled by the bHLH transcription factors *Neurogenin2* (*Ngn2*) and *Neurogenin1* (*Ngn1*) respectively (Fode et al., 1998; Ma et al., 1996). Mutation of *Ngn2* disrupted differentiation of the sensory neurons in mice (Fode et al., 1998). Additionally, overexpression of *ngn1* in *Xenopus* resulted in ectopic neurogenesis (Ma et al., 1996).

1.4 Pax3

1.4.1 The Pax family of transcription factors

The Paired-box (*Pax*) genes encode a family of transcription factors which have important roles in a wide variety of processes during embryonic development. They share sequence homology, and have conserved structural domains (Balczarek et al., 1997). Pax proteins have an N-terminal paired domain and a C-terminal transactivation domain (Thompson and Ziman, 2011).

Different isoforms of the Pax proteins can be produced through alternate splicing of the RNA as a response to certain environmental cues. These isoforms can have slightly different DNA binding properties and responses (Thompson and Ziman, 2011).

1.4.1.1 The paired domain

The paired domain (PD) is a conserved DNA-binding domain found in Pax proteins. The N-terminal and C-terminal regions of the PD act as two independent globular domains. The N-terminal domain is the larger of the two, and consists of a short region of parallel β -sheet, a β turn, three α -helices, and an extended C-terminal tail. The C-terminal domain has three α -helices. The helical units of both regions show similarity to the homeodomain (Xu et al., 1995).

The N-terminal domain is concerned with sequence-specific DNA binding. The β -sheet region contacts the sugar phosphate backbone of the DNA, and the β turn and extended C-terminal tail of the region contact the minor groove. The first helix contains a helix-turn-helix (HTH) domain, the second helix contacts the phosphate molecules, and the third helix binds the major groove (Xu et al., 1995).

Like the N-terminal region, the C-terminal domain also contains three α -helices, and shows similarities to the structure of the homeodomain. However, the region does not necessarily bind to DNA, and shows a higher degree of physical flexibility. There are also longer loops of amino acids between the helices compared to the standard homeodomain. This site shows DNA binding in some PD-containing proteins, and is thought to contribute to the binding site-specificity of the PD as a whole (Xu et al., 1995).

1.4.1.2 Roles of *Pax* genes in cell function

The *Pax* genes are involved in multiple developmental processes. Their expression is confined to tightly controlled regions, which suggests a potential role in the patterning of the embryo. Antero-posterior, as well as dorso-ventral restrictions in expression of the *Pax* genes suggests roles in patterning along multiple axes. *Pax* genes are frequently found to hold cells in a non-apoptotic progenitor state until environmental signals are able to induce either proliferation or

full differentiation and maturation of the population (Blake and Ziman, 2014). Thus, they are important for maintaining the correct balance of proliferation and differentiation in developing tissues. Additionally, repressive interactions between *Pax* genes helps to establish and stabilise boundaries between regions, whereas coordinated expression can reinforce patterning (Thompson and Ziman, 2011). Organisms which are heterozygous for mutations in *Pax3* genes often show a phenotype, which suggests that, not just the presence, but the dosage of the genes is also important (Bernasconi et al., 1996).

A number of *Pax* genes are known to play roles in cell survival and apoptosis. This is seen in embryonic development, but also in the development of carcinomas. For instance, research on rhabdomyosarcoma (RMS) cells has found that *Pax3* or *Pax7* may be upregulated in these cancerous cells, and that downregulation can increase the rate of cell death, suggesting that the *Pax* genes are necessary for their survival (Bernasconi et al., 1996).

Pax genes are known to act as survival factors in some tissues. For example, *Pax7* is necessary for the maintenance of satellite cells in adult muscle. These cells are quiescent stem cells, and are able to proliferate and differentiate in the event of muscle damage in the adult. However, in *Pax7* mutant mice the satellite cells rapidly apoptose after birth, suggesting that *Pax7* is a necessary anti-apoptotic factor for these cells (Relaix et al., 2006).

Pax gene misexpression may also occur in cystic or proliferative disorders. *Pax2* would usually be downregulated in the kidney following differentiation, but it is known to be expressed in the epithelial cells of cystic kidneys. It also upregulates expression of BCL2, which protects cells against apoptosis in the hyperproliferative epithelia of cystic kidneys (Winyard et al., 1996).

1.4.1.3 Roles of Pax genes in tissue development and differentiation

The *Pax* transcription factors have roles in a huge variety of development processes and systems. They act on aspects such as cell survival – as described above – and the proliferation differentiation balance, but also induce expression of certain differentiation genes to control cell fate.

Most *Pax* genes (with the exception of *Pax1*) have roles in the development of the CNS, including the NC. They are able to affect migration, specification and proliferation, as well as differentiation of specific cell types, and they play key roles in patterning of the developing brain and spinal cord.

Research has suggested that both *Pax6* and *Pax7* are involved in the specification of large regions of the CNS during early development, and at later stages in the differentiation of specific cell types (Kawakami et al., 1997). *Pax3* and *Pax7* are expressed in the dorsal region of

the neural tube, whereas *Pax6* is expressed in the mid-ventral region (Goulding et al., 1991; Jostes et al., 1990; Walther and Gruss, 1991). In chick embryos *Pax7* is required for the specification of NC cells prior to gastrulation (Basch et al., 2006), and in mouse embryos *Pax6* is expressed in the early developing forebrain and hindbrain, in closed regions of the neural tube, and in the developing eye (Walther and Gruss, 1991). As development progresses, expression of the genes can be associated with specific cellular populations; for instance, in the mouse *Pax7* is expressed in the mesencephalon, and *Pax6* is expressed in the olfactory bulbs, the telencephalon and the diencephalon in the developing brain (Jostes et al., 1990; Walther and Gruss, 1991).

Pax2, *Pax5* and *Pax8* are expressed later in neurulation, at approximately E10. The difference in the timing of expression between the *Pax* genes occurs because *Pax3*, *Pax6* and *Pax7* are expressed in the precursor cells of the CNS, whereas *Pax2*, *Pax5* and *Pax8* are expressed in post-mitotic neuroblasts (Goulding, 1992).

Some *Pax* genes are involved in the development of the NC and their derivatives. All NC cells require *Pax3* for correct migration and expansion of the progenitor population (Conway et al., 2000). A subset of the NC migrating to the craniofacial region from the cephalic region of the neural tube additionally require *Pax7*, and it has been found that mouse embryos lacking a functional copy of this gene develop craniofacial abnormalities, including skull and cartilage abnormalities (Mansouri et al., 1996).

Many *Pax* proteins are also involved in the differentiation of non-neuronal cell types. *Pax5* is expressed in much of the developing CNS, the fetal liver, B-lymphocytes and adult testis (Adams et al., 1992). *Pax5* mutant mice lack B-lymphocytes, as the development of these cells is arrested at an early precursor stage (Urbanek et al., 1994). Therefore, B-lymphocytes require *Pax5* in order to differentiate. It has been shown that *Pax5* is necessary both for the induction of expression of B-lymphocyte-specific differentiation genes, and the inhibition of gene expression linked to other cell fates (Nutt et al., 1999).

Pax2 is expressed in the CNS and the urogenital system in the developing embryo (Dressler et al., 1990). *Pax2* mutant embryos have been found to lack the ureter, genital tract, and kidneys (Torres et al., 1995). Evidence suggests that *Pax2* acts through epigenetic means during urogenital development; association of *Pax2* with its binding elements results in H3K4 histone methylation, which will alter expression of genes relating to urogenital development (Patel et al., 2007).

The *Pax6* gene is important in the development of the CNS, the eyes, and the pancreas. Heterozygosity in humans leads to Aniridia – a disorder which comprises a number of eye defects. Homozygous mutation in mice causes much more severe eye defects, and in *Drosophila* prevents eye development altogether (Shaham et al., 2012). Pax6 is required in multiple processes during eye development. For example, research has shown Pax6 to be necessary for the maintenance and differentiation of both the iris and ciliary body cells (Davis et al., 2009).

1.4.2 Pax3 gene and protein structure

This project focusses on one of the Pax genes, Pax3. The Pax3 gene is located on chromosome 1 in the mouse, and chromosome 2 in the human (Walther et al., 1991; Wilcox et al., 1992). The Pax3 protein contains another active site, the paired-type homeodomain, in addition to the PD (**Figure 1.6**). The protein is important in the development of a number of tissues, including the CNS, the NC, and some muscles, such as those of the limbs.

Seven different isoforms of Pax3 exist in man – PAX3 a-h. PAX3e is full length, containing 10 exons. The remaining isoforms are alternatively truncated and spliced (Wang et al., 2007). The isoforms may be expressed in different tissues in the body. For example, a report describes how the human PAX3b protein was found in most tissues studied, but PAX3a was found only in the cerebellum, oesophagus and skeletal muscle (Tsukamoto et al., 1994). Additionally, the isoforms may play different roles during development; it has been found that the isoforms PAX3c, PAX3e and PAX3g have different effects on the expression of downstream genes (Wang et al., 2007), and isoforms PAX3a-h appear to differentially affect cellular mechanisms in cultured melanocytes, including proliferation, migration and apoptosis (Wang et al., 2006). The cues which initiate alternative splicing in Pax3 are unknown.

1.4.2.1 The paired type homeodomain

Although the Pax proteins are characterised by the presence of the PD, Pax3, Pax4, Pax6, and Pax7 contain an additional domain known as the paired-type homeodomain (HD) (**Figure 1.6**). It contains three α -helices, called α 1, α 2 and α 3, which are connected by short loops. There is also an N-terminal arm, which inserts into the minor groove and interacts with DNA in a sequence-specific manner. Upon interaction of the N-terminal arm, helix α 3 inserts into the major groove, and interacts with the bases and the sugar-phosphate backbone of the DNA (Birrane et al., 2009; Kissinger et al., 1990).

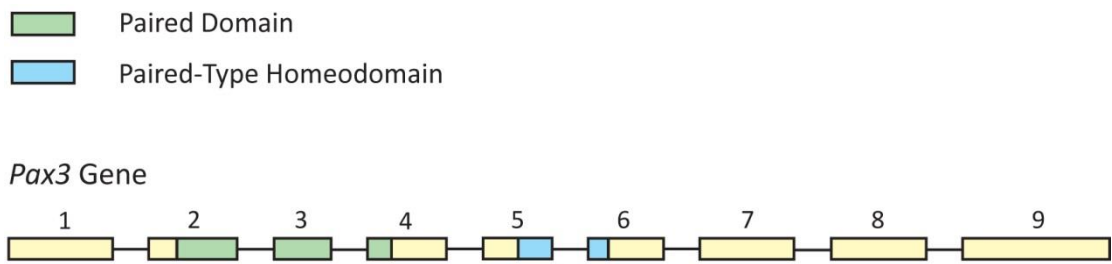


Figure 1.6: The structure of the *Pax3* gene. The *Pax3* gene consists of 9 exons, which encode two DNA binding domains – the paired domain, and the paired-type homeodomain.

1.4.2.2 Interactions between the binding sites of Pax3 protein

The PD and HD of Pax3 are structurally independent, and have separate roles in the functioning of the protein, but they are also able to influence the function of the other. This has been demonstrated in the *Spotch-delayed* mouse, which has an amino acid substitution at position 9 of the PD; the glycine to arginine substitution dramatically reduces DNA binding of both active sites (Underhill et al., 1995). This mutation was found to be contained within a β -turn, which contributes to a β -hairpin motif (Xu et al., 1995). It was discovered that the PD contributes to the sequence-specificity of homeodomain DNA binding in the Pax3 protein (Underhill and Gros, 1997). The substitution within the β -turn disrupts the folding of the β -hairpin motif, which reduces the DNA binding of both the PD and the HD. It has also been found that in wild type Pax3 protein helix 2 of the PD is closely apposed to the amino terminus of the homeodomain (Apuzzo and Gros, 2007). This suggests the possibility of interaction. Additionally, small structural alterations in the PD impairs the ability of the HD to bind DNA, which suggests some functional interdependence (Apuzzo and Gros, 2002).

1.4.3 The Spotch mouse

The *Spotch* mouse was first identified in 1947 (Russell, 1947), and then described in detail a few years later (Auerbach, 1954). The mutant embryos were identified through the development of spina bifida, lack of pigmentation in tissue transplants, and lethality at E14.0 in gestation (Auerbach, 1954). The embryos carry a mutation in the *Pax3* gene, and show defects in *Pax3* positive tissues.

1.4.3.1 The *Spotch* phenotype

Pax3 mutant mice are known as *Spotch* mice due to a white belly patch seen on the adult heterozygotes (Russell, 1947). This is caused by a mild pigmentation defect, but the heterozygous mice are otherwise healthy and breed normally.

Spotch mutant embryos die at around E13.5-14.0 in gestation, and demonstrate fully penetrant spina bifida and partially penetrant exencephaly (Auerbach, 1954). Lethality is due to the presence of heart defects, such as persistent truncus arteriosus and outflow tract malformations (Conway et al., 1997b; Franz, 1989).

The heart defects seen in the mutant embryos are the result of NC abnormalities. Other NC defects include lack of pigmentation and abnormalities of the PNS and ENS (Auerbach, 1954; Lang et al., 2000; Moase and Trasler, 1989). Mutant embryos also have defects of the musculature, in particular affecting the limbs (Franz et al., 1993).

1.4.3.2 *Pax3* mutations in mice

In 1991, a *Pax3* mutation was found in the *Spotch* mouse (Epstein et al., 1991). It was later demonstrated that no recombination took place between the *Spotch* locus and *Pax3*, indicating very close linkage, and *Pax3* gene mutations were also found in multiple alleles of *Spotch* (Goulding et al., 1993). This evidence identified *Pax3* as the key mutated gene in the *Spotch* mouse.

Since the discovery of *Pax3* as the mutant gene in the *Spotch* mouse, multiple *Pax3* mutant alleles have been discovered or developed. They differ slightly in phenotype and severity. The alleles are described in **Table 1.3**.

1.4.4 Processes downstream of Pax3

Pax3 influences a number of signalling pathways and cellular processes, including general mechanisms such as apoptosis and proliferation, and more tissue-specific mechanisms, such as differentiation of certain cell types, and cellular migration. Understanding the phenotype of the *Spotch* mouse requires an understanding of processes downstream of *Pax3* during embryonic development.

1.4.4.1 Apoptosis

There is a great deal of debate about the role of *Pax3* in cell survival, and the implications of this in the development of NTDs in *Pax3* mutant mouse embryos. Several studies have shown links between *Pax3* expression and apoptosis, suggesting that – like many *Pax* genes – *Pax3* is important in cell survival in multiple tissues

Table 1.3: Pax3 mutant alleles in mice. The table describes Pax3 mutant alleles currently in use. The usual phenotype of Pax3 mutant includes the NTDs spina bifida and exencephaly, muscle defects, and NC defects, with lethality at around E13.5. Any divergence or additional aspects to the phenotype are described in the column labelled 'Phenotype.' Lack of a description in this column indicates that the mutant phenotype is as described here.

Allele	Mutation	Phenotype	Reference
Sp	5 bp mutation at splice acceptor site of intron 3, leading to aberrant splicing.		(Auerbach, 1954; Epstein et al., 1993; Russell, 1947)
Sp ^{1H}	32 bp deletion from exon 5.		(Vogan et al., 1993)
Sp ^{2H}	32 bp deletion from exon 5.		(Beechey and Searle, 1986; Epstein et al., 1991)
Sp ^{4H}	Deletion of Pax3 and other genes.	Preimplantation lethal.	(Goulding et al., 1993)
Sp ^d (Spotch delayed)	Point mutation leading to amino acid substitution in the paired box.	Perinatal lethal. Lower severity of phenotype. No exencephaly.	(DICKIE, 1964; Vogan et al., 1993)
Sp ^r (Spotch retarded)	Deletion of Pax3 and other genes.	Preimplantation lethal.	(Beechey and Searle, 1986)
Sp ^{2G}	LacZ knock-in replacing exon 1. Null allele.	Expression of LacZ in Pax3-expressing tissues.	(Mansouri et al., 2001)
Pax3 ^{Cre}	Cre knock-in replacing exon 1. Null allele.	Expression of Cre in Pax3-expressing tissues.	(Engleka et al., 2005)
Pax3 ^{neo}	TK-neo(R) cassette inserted into intron 5. Hypomorphic.	Defective myogenesis in the tongue and limbs. Perinatal lethality.	(Zhou et al., 2008)

(Borycki et al., 1999; Scholl et al., 2001; Underwood et al., 2007). However, whether this has any significance in NT closure remains unclear.

It is known that mothers with pre-gestational diabetes mellitus (PGDM) have a higher incidence of birth defects and NTDs in their offspring compared to the general population (Correa et al., 2008). This is a complication known as diabetic embryopathy. Mothers with PGDM are defined as having been diagnosed by a physician with either type 1 or type 2 diabetes mellitus prior to pregnancy. It has been shown that embryos from diabetic mice had not only an increased incidence of NTDs, but also reduced *Pax3* expression and increased NT apoptosis (Phelan et al., 1997). Oxidative stress was found to reduce *Pax3* expression, which demonstrates that these effects are caused by hypoxia in the embryo as a result of high levels of glucose just prior to NT closure (Chang et al., 2003; Chappell, Jr. et al., 2009; Fine et al., 1999; Li et al., 2005). Hyperglycemia-induced oxidative stress increases the activity of the methyltransferase Dnmt3b. This protein was found to be required for methylation of *Pax3* regulatory elements, and thus silencing of *Pax3*, which allows differentiation of the neuroepithelial tissue to occur. Therefore, in the hyperglycemic condition of diabetic pregnancy, *Pax3* regulatory elements are hypermethylated, and *Pax3* expression is reduced (Wei and Loeken, 2014). Oxidative stress has been previously linked to the development of NTDs. For example, exposure of embryos to either valproic acid or arsenic causes oxidative stress, which leads to NTD development (Han et al., 2011; Tung and Winn, 2011). It is possible that these teratogens also mediate their NTD-inducing effects through a reduction in *Pax3* expression.

Research has shown that apoptosis is increased in *Pax3*-deficient pre-somitic mesoderm (PSM) both *in vitro* and *in vivo*, suggesting that *Pax3* plays a role in cell survival in this tissue (Borycki et al., 1999). Increased levels of apoptosis were also observed in the NC-derived DRG of *Pax3*-deficient E11.5 embryos. However, the same research found no difference in the level of apoptosis in the NT of *Pax3*-deficient embryos, both *in vitro* and *in vivo* (Borycki et al., 1999).

Pax3 expression has been found to affect the levels of p53 protein. *Pax3* overexpression suppresses p53-dependent transcription and reduces p53 protein levels *in vitro* (Underwood et al., 2007). Additionally, suppression of *Pax3* activity by mutation increases p53 protein levels *in vivo* (Pani et al., 2002). This demonstrates a method by which *Pax3* may exert control on the levels of apoptosis in a developing embryo. Thus, loss of *Pax3* is hypothesised to lead to an increase in p53-dependent apoptosis. p53 mutation has been shown to rescue both NTDs (Pani et al., 2002) and cranial NC cell migration (Morgan et al., 2008) in *Pax3* mutant mice.

Aberrant *Pax3* expression has been reported in a range of cancers, such as rhabdomyosarcoma and melanoma. For instance, upregulation of *Pax3* has been reported in melanoma tissue, but

not in surrounding healthy tissue, and was found to contribute to the survival of the malignant cells (Scholl et al., 2001). Additionally, fusions of *Pax3* and a member of the Forkhead gene family have been observed in alveolar rhabdomyosarcoma, leading to abnormal *Pax3* transcription factor activity (Galili et al., 1993; Shapiro et al., 1993). The presence of *Pax3* is usually associated with survival of cancerous tissue.

1.4.4.2 The neural crest

Pax3 mutation causes defects in a range of NC-derived tissues, including the PNS, heart, pigmentation cells, and the ENS (Auerbach, 1954; Conway et al., 1997b; Koblar et al., 1999; Lang et al., 2000; Lang et al., 2005). This suggests it plays an important role early in the development of the NC. Some examples of the functions of *Pax3* in NC differentiation are given here.

Overexpression of *pax3* in *Xenopus* has been found to upregulate expression of the NC specification genes *slug*, *snail*, and *foxd3* adjacent to the neural plate border. Additionally, knockdown of *pax3* expression in *Xenopus* through the use of Morpholinos resulted in a reduction in the expression of *slug* and *foxd3*, but not *msx1*. Further research suggests that *Msx1* induces the expression of both *pax3* and *zic1* in *Xenopus*, and that these proteins act together to induce NC fate. This activity requires Wnt signalling (Dottori et al., 2001; Monsoro-Burq et al., 2005; Sato et al., 2005).

Schwann cells develop from a subset of NC cells, and act as an insulating sheath for neuronal fibres in the CNS and the PNS. First, Schwann cell precursors differentiate from the NC population, and these then develop into immature Schwann cells. Finally the immature cells mature postnatally into myelinating or nonmyelinating Schwann cells (Jessen and Mirsky, 1998). *Pax3* expression is necessary for the development of the nonmyelinating Schwann cells, which sheathe small diameter axons. Reduction in *Pax3* expression results in the loss of embryonic Schwann cells (Kioussi et al., 1995).

Pax3 mutant mouse embryos develop heart defects due to NC abnormalities (Conway et al., 1997a; Conway et al., 1997b). These abnormalities include septation defects and outflow tract defects (Conway et al., 1997b; Conway et al., 2000). The mutant embryos were found to have reduced migration of the NC into the developing heart (Conway et al., 1997a). This is thought to be due to a reduction in the proliferation of the NC prior to migration (Conway et al., 2000). This defect could also be due to abnormalities in the environment through which the NC migrate (see below) (Henderson et al., 1997; Mansouri et al., 2001). As discussed previously, research has found that *Pax3* mutant embryos have excessive p53-mediated apoptosis in the migrating NC. Additionally, reduction in p53 expression rescued the migration defect seen in

Pax3 mutant embryos, suggesting that Pax3 acts to suppress apoptosis in these cells (Morgan et al., 2008).

The microphthalmia-associated transcription factor (MITF) is a 'master regulator' of melanocyte fate. Pax3 promotes the development of melanocytes by binding to the promoter of the *MITF* gene in combination with Sox10, and initiating the expression of MITF (Bondurand et al., 2000). However, Pax3 is also able to repress melanocyte fate by forming a repressor complex which prevents transcription of MITF target genes (Lang et al., 2005). Therefore Pax3 initiates the development of melanogenic precursors, but prevents terminal differentiation.

There are several possible explanations for the NC defects seen in *Pax3* mutant mice. Undoubtedly there are abnormalities in specification and differentiation, but research has also suggested defects in NC migration (Moase and Trasler, 1990). Evidence suggests that *Pax3* mutant NC are capable of migration through both the dorso-ventral and dorso-lateral migration pathways (Chan et al., 2004). However, abnormalities are present in the ECM, and also in the migration abilities and adhesive properties of the NC. For example, the ECM protein Versican is overexpressed in *Pax3* mutant embryos, which reduces NC migration (see below) (Henderson et al., 1997). Additionally, Pax3 has been shown to control cell surface properties of the NC, which affect interactions between the NC and the ECM (Mansouri et al., 2001).

Pax3 has been associated with cell aggregation and mesenchymal-to-epithelial transition (MET). It has been reported that *Pax3* mutant embryos lose the epithelial structure of the dermomyotome in the somites (Daston et al., 1996; Mansouri et al., 2001). Moreover, ectopic *Pax3* expression *in vitro* has been shown to induce cells to form an epithelial-like aggregate through activation of a PCP Wnt signalling cascade (Wiggan et al., 2002; Wiggan and Hamel, 2002). This suggests changes in cell-cell interactions induced by Pax3 signalling. Indeed, these cells were found to show reduced cadherin-11 expression at sites of cell-cell contact, which is consistent with epithelial identity (Wiggan et al., 2002). Additionally, fractionation of the cellular components revealed that ectopic *Pax3* signalling induced the change of cadherin and catenin positioning from the detergent-soluble cytoplasmic fraction to the detergent-insoluble cytoskeletal fraction (Wiggan et al., 2002). This change is associated with an increase in cell adhesion.

The neural cell adhesion molecule (NCAM) is a direct transcriptional target of Pax3 (Bennett et al., 1998). Expression of NCAM is finely controlled, and the level of expression is particularly important during NC migration. EMT requires low expression of NCAM, and so it is downregulated just prior to migration of the NC, and in the migrating cells (Edelman, 1986). It is later upregulated on the cell surfaces of multiple differentiated NC-derived cell types,

including Schwann cells and neurons (Edelman, 1986). *Pax3* mutant embryos still express NCAM, but of an altered size (Moase and Trasler, 1991). Research suggests that *Pax3* is involved in post-translational modification of NCAM, specifically in sialylation (Glogarova and Buckiova, 2004; Moase and Trasler, 1991); *Pax3* mutant mouse embryos show lower levels of polysialylated NCAM compared to wild type (Glogarova and Buckiova, 2004). This is likely to affect the adhesive properties of the NC population.

The protein Versican is a chondroitin-sulphate proteoglycan (CSPG) expressed in the ECM (Zimmermann and Ruoslahti, 1989). It is expressed in regions outside the normal migratory paths of the NC, and acts as a repulsive molecule to maintain the pathway (Henderson et al., 1997). Versican is overexpressed in *Spotch* mutant mouse embryos; *Versican* and *Pax3* are expressed reciprocally in wild type embryos, but *Pax3* mutation results in the expansion of the regions expressing *Versican* (Henderson et al., 1997). This disrupts the migration of the NC population.

1.4.4.3 Myogenesis

Vertebrates have three stages of limb muscle differentiation, all of which appear to involve *Pax3* in some role. During primary myogenesis cells are specified as muscle precursors in the somite, and then they migrate to the limb buds, where they express muscle markers and differentiate. Secondary myogenesis involves growth of the fetal muscle from a subset of undifferentiated myogenic precursor cells within the developing muscle tissue. Adult myogenesis occurs following muscle damage, and also involves undifferentiated muscle precursor cells, known as satellite cells (Yokoyama and Asahara, 2011).

Muscles in the vertebrate trunk and limbs are derived from the myotome of the somite. The myotome itself consists of two populations of myogenic precursor cells. The medial region of the myotome contains cells fated to form the muscles of the back, whereas the lateral region contains cells which migrate into the limb buds to form the limb musculature (Ordahl and Le Douarin, 1992).

Pax3 is expressed in the pre-somitic mesoderm, and then following somitogenesis is expressed throughout the newly-formed somite. However, as development continues the expression becomes restricted to the dermomyotome in the dorsal region of the somite (Buckingham and Relaix, 2007), and then to the lateral region of the dermomyotome (Bober et al., 1994). The cells of this region later form the limb musculature. Shh signals from the notochord and Wnt1/Wnt3 signals from the NT are sufficient for initiating the expression of *Pax3* and *Pax7* in the somites (Goulding et al., 1994; Maroto et al., 1997; Munsterberg et al., 1995). In mice

lacking *Pax3* expression the population of myogenic precursors doesn't develop. Therefore, the mice do not form limb muscles (Bober et al., 1994; Goulding et al., 1994).

Pax3 appears to be necessary for the migration of muscle progenitor cells from the somites into the limb buds (Bober et al., 1994; Tajbakhsh et al., 1997). The migrating cells express *Pax3*, but no muscle markers or differentiation genes until they have reached their positions in the limb buds (Bober et al., 1994). *Pax3* is required for the migration of the specified myogenic precursors, but experiments have shown that the cells from the appropriate region are competent to form myoblasts when they are transplanted into the limb bud (Daston et al., 1996). Therefore *Pax3* is not necessary for the final differentiation of the cells. The gene *c-met* appears to act downstream of *Pax3*, and is necessary for migration of the myogenic precursors into the limb bud (Bladt et al., 1995).

Pax3 and the closely related *Pax7* have been found to regulate the onset of myogenesis through induction of the expression of the myogenic determination genes *MyoD* and *Myf5* (Myogenic factor 5) (Bajard et al., 2006; Maroto et al., 1997). This has been demonstrated in both embryonic myogenic precursor cells, and in adult muscle progenitor cells – satellite cells – which aid in muscle healing and growth (Maroto et al., 1997; Tajbakhsh et al., 1997). Both *Pax3* and *Myf5* are thought to act upstream, and therefore be necessary for the induction of *MyoD* expression in muscle precursor cells (Tajbakhsh et al., 1997). The loss of both *Myf5* and *MyoD* results in loss of the myoblasts during development (Daston et al., 1996).

Myogenic precursors and satellite cells express both *Pax3* and *Pax7*, and in the absence of this gene expression only the very earliest embryonic muscle forms (Relaix et al., 2005). This *Pax3*⁺, *Pax7*⁺ cell population is derived from the dermomyotome of the somite, and constitutes the majority of proliferating cells in the embryonic or adult muscle tissue, allowing both secondary myogenesis and adult muscle healing to occur (Ben-Yair and Kalcheim, 2005). Cells which fail to express these genes either apoptose or adopt non-myogenic fates (Relaix et al., 2005).

On the other hand, muscle development in the cranial region appears to be *Pax3*-independent. The gene is not expressed in cranial muscles (Tajbakhsh et al., 1997). Additionally, *Pax3* mutant mice fail to develop trunk muscles, but the muscles in the head develop normally (Tajbakhsh et al., 1997).

1.4.5 Possible mechanisms underlying the development of neural tube defects in *Spotch* mutant embryos

Given the roles of *Pax3* during embryonic development, there are a number of cellular defects which could potentially cause NTDs in *Spotch* mutant (*Sp*^{2H}/*Sp*^{2H}) embryos.

1.4.5.1 Excess apoptosis

The link between apoptosis and NTDs is unclear. Some research has shown an increase in NTDs in embryos with reduced apoptosis. For example, it was observed that embryos homozygous for a mutation in the pro-apoptotic gene *p53* developed exencephaly with a penetrance of between 8 and 16%. This NTD was found to only affect the female embryos (Sah et al., 1995). On the other hand, rat embryos with retinoic acid-induced NTDs had increased apoptosis in the neural folds (Wei et al., 2012). Therefore, excess apoptosis may also be associated with NTDs.

However, a number of publications argue against a causative link between insufficient apoptosis and NTDs. Apoptosis is unnecessary to complete the closure of either the cranial or caudal regions of the NT (Massa et al., 2009). Additionally, some studies have found *p53* null mice to be phenotypically normal, although they have an increased risk of cancerous tumour development (Donehower et al., 1992).

Previous research has shown that diabetes reduces *Pax3* expression, and that this, in turn, increases apoptosis in the NT (Phelan et al., 1997). Further research suggested that excess *p53*-mediated apoptosis in the neural tubes of *Pax3* mutant embryos could cause the NTDs seen in these mice (Pani et al., 2002). This theory is supported by evidence discussed in section 1.4.4.1, which suggests that *Pax3* plays an important role in cell survival.

Pax3 has been found to reduce *p53*-mediated gene expression, and reduce levels of *p53* protein (Underwood et al., 2007). It was also reported that the *Pax3* mutation resulted in raised levels of the *p53* protein, and increased apoptosis in the neural folds (Pani et al., 2002; Phelan et al., 1997). *Pax3*^{Sp/+} *p53*^{+/-} mice were intercrossed to generate double mutant embryos lacking both *Pax3* and *p53* function. NTDs occurred with lower frequency in *Pax3*^{Sp/Sp} *p53*^{-/-} embryos, (Pani et al., 2002). These results suggest that the reduction in apoptosis caused by the *p53* mutation could rescue the NTDs in the *Spotch* mutant mice, and the conclusion was that *Pax3* acts to inhibit apoptosis during neural tube closure. Further research from this lab suggests that *Pax3* protein is responsible for the ubiquitination and degradation of the *p53* protein, thus reducing the rate of apoptosis in the neural tube (Wang et al., 2011).

On the other hand, unpublished data from our laboratory suggests that *p53*-mediated apoptosis is not involved in NTD development in *Spotch* mice. TUNEL staining has shown no increase in apoptosis in the neural folds of *Sp*^{2H}/*Sp*^{2H} embryos, and inhibition of apoptosis with the pan-caspase inhibitor Z-VAD-FMK (Zhu et al., 1995) did not rescue NTDs in these mice.

1.4.5.2 Premature neuronal differentiation

The timing of neuronal differentiation is known to be important in controlling the development of the NT, and premature neuronal differentiation has been associated with several models of NTDs. Multiple genes have been found to inhibit neuronal differentiation in the developing NT, and mutation in these genes may result in premature neuronal differentiation and NTD development. For example, mutations in several of the *Zic* genes have been associated with NTDs, including *Zic2*, *Zic3* and *Zic5*, and these genes are known to maintain neuroepithelial cells in a proliferative, undifferentiated state during NT development (Aruga et al., 2002a; Aruga et al., 2002b; Aruga, 2004; Nagai et al., 2000). Additionally, teratogens may alter the expression of genes which control the timing of neuronal differentiation. For example, excess glucose induces NTDs in developing embryos, and has been found to induce premature neuronal differentiation in the NT. Exposure to high glucose concentration causes changes in the expression levels of genes such as *Shh*, *Bmp4*, *Neurog1/2*, *Hes1/5* and *Olig1*, which control differentiation and proliferation in the NT (Fu et al., 2006).

On the other hand, the protein Geminin is thought to promote neuronal differentiation in the NT, but its mutation causes spina bifida in mouse embryos (Patterson et al., 2014). This suggests that developmental timing of neuronal differentiation is important in the formation and closure of the NT.

Pax3 is known to play a role in the patterning and differentiation of the PNS, which is NC-derived (discussed in section 1.4.4.2). *Pax3* is normally associated with the maintenance of multipotency and the prevention of differentiation. Therefore, loss of *Pax3* expression is often accompanied by differentiation; *in vitro* studies have shown that loss of *Pax3* expression induces multipotent cells to differentiate into neurons (Reeves et al., 1999), and *in vivo* studies have demonstrated premature neuronal differentiation in *Sp^{2H}/Sp^{2H}* embryos (Nakazaki et al., 2008).

Loss of *Pax3* expression prevents sensory neuronal differentiation in the ophthalmic trigeminal placode. Ectopic expression of *Pax3* in other placodes induces expression of the markers of ophthalmic trigeminal placode development, but no neurons differentiate (Dude et al., 2009). In addition, *Pax3*-negative NC cell culture produces 5-fold fewer sensory neurons than *Pax3*-positive NC cell culture (Koblar et al., 1999). These results suggest that *Pax3* expression is necessary for the determination of certain neuronal fates, but that it holds the cells in a precursor state and prevents differentiation.

Pax3 is able to regulate the expression of genes involved in the terminal differentiation of PNS neurons. It binds to *cis*-regulatory elements of the proneural bHLH genes *Hairy and enhancer of split homologue-1 (Hes1)* and *Neurogenin2 (Ngn2)* (Nakazaki et al., 2008), which are involved in determination of neuronal cell fate. The expression levels of *Hes1* and *Ngn2* are reduced in *Pax3* mutant mouse embryos, and these embryos exhibit premature neuronal differentiation (Nakazaki et al., 2008), suggesting that Pax3 is involved in regulating the acquisition of neuronal fate.

Ngn2 is involved in the acquisition of sensory neuronal fate (Fode et al., 1998). It acts in part through induction of *Delta1* expression, which leads to initiation of Notch signalling to induce neuronal differentiation (Ma et al., 1996). Expression of Delta induces *Notch* expression in adjacent cells, and Notch promotes the expression of the *Hes* genes, including *Hes1*, which inhibit *Ngn2* expression, and maintain cells in a neural progenitor state. Thus the oscillation of these genes controls the patterning and timing of neuronal differentiation (Kageyama et al., 2008; Shimojo et al., 2008). Pax3 induces expression of both *Hes1* and *Ngn2*, and therefore regulates lateral inhibition and neural differentiation through the activity of the Notch pathway.

Unpublished research in our laboratory has shown premature neuronal differentiation in the cranial region of the neural tube of *Sp^{2H}/Sp^{2H}* embryos. This neuronal differentiation occurs prior to cranial NT closure, and may be the cause of exencephaly in these embryos; neurons are not epithelial cells, and so premature neuronal differentiation may alter the morphology and behaviour of the neurepithelium prior to fusion, thus making fusion more likely to fail. This defect is particularly prominent in the prospective midbrain. However, neuronal differentiation in the spinal region of the NT in *Sp^{2H}/Sp^{2H}* embryos has not previously been studied.

1.4.5.3 Reduced proliferation in the neural plate

The rates of proliferation in tissues including the NT and tissues surrounding the NT are known to play a role in NT closure and in the development of NTDs. For instance, the drug valproic acid is known to cause NTDs in embryos, and evidence suggests that it reduces proliferation in the developing neurepithelium (Wlodarczyk et al., 1996). On the other hand, the *humpty dumpty* mouse mutant carries a mutation in the protein phosphatase Phactr4, and the embryos develop exencephaly. In this case, the NTD is caused by an increase in proliferation in the ventral NT caused by loss of Phactr4 activity (Kim et al., 2007). Therefore it appears that the rate of proliferation in the NT must be finely balanced for closure to occur successfully.

Changes in the relative rates of proliferation between tissues can also cause NTDs. For example, a reduction in proliferation in the gut and notochord of the *curly tail (ct)* mouse leads

to spina bifida. This is due to the imbalance in proliferation in the gut and notochord compared to the NT, which causes curvature of the spinal region. Thus the NT is mechanically prevented from closing (Copp et al., 1988a). NTDs in *ct* embryos can be rescued through growth retardation caused by food deprivation in the mothers; the reduction in proliferation is greater in the more rapidly proliferating NT. Therefore, the proliferation imbalance is corrected, and spina bifida does not develop (Copp et al., 1988b).

Changes in proliferation have been widely reported in *Pax3*-negative tissues. For example, a reduction in the proliferation rate of myogenic precursors has been demonstrated in cultured *Pax3*-deficient cells (Collins et al., 2009), and there is also a reduction in the expansion of the NCC population in *Spotch* mice prior to NCC migration (Conway et al., 2000).

In the NT, *Sp^d* mutant embryos first show a reduced proliferation rate compared to controls, and then later in development, an increased rate compared to controls, resulting in overexpansion of the neural tissue (Keller-Peck and Mullen, 1997). These mice develop spina bifida.

Alterations to proliferation have been reported in NTDs in multiple animal models (Murko et al., 2013; Wang et al., 2013; Wei et al., 2012). However, these proliferation defects are accompanied by other cellular defects, such as alterations in apoptosis or differentiation. Therefore, little is known about proliferation in the NT of the *Spotch* mouse, or about the effects of altered proliferation on the development of NTDs as separate from apoptosis or premature differentiation.

Unpublished data from our laboratory has shown that premature neuronal differentiation observed in the cranial NT of *Sp^{2H}/Sp^{2H}* embryos is accompanied by reduced proliferation. This does not clarify which – if either – of these mechanisms is causative, but the data presents a possible causative mechanism for study in the spinal region of the NT in *Sp^{2H}/Sp^{2H}* embryos.

1.4.6 *Spotch* and folate

The *Spotch* mouse model is known to be sensitive to folate levels – supplementation has been found to rescue the NTDs usually seen in these mice. However, more unusually, folate deficiency has been found to increase the frequency of NTD development (Burren et al., 2008; Fleming and Copp, 1998). Additionally, *Spotch* embryos have an abnormal result on the dU (deoxyuridine) suppression test, which is a measure of thymidylate synthesis and can indicate abnormalities in the folate cycle. Exposure to folic acid results in a dU suppression test result closer to wild type, suggesting that folate supplementation is able to rescue some of the folate cycle defects which result in NTD development in the *Spotch* mouse (Fleming and Copp, 1998).

As mentioned previously (section 1.2.4) folate may be related to NTDs due to its influence on proliferation. As the proliferation-differentiation balance is disrupted in the *Spotch* mouse it may be this mechanism that is rescued by folate supplementation, or worsened by deficiency. In support of this, *Pax3* mutant neurospheres generated from *Spotch* NTs show increased NC cell proliferation when exposed to folate (Ichi et al., 2012). Furthermore, folate supplementation reverses abnormal epigenetic alterations seen in *Spotch* embryos which affect the *Pax3* downstream proneural effectors *Hes1* and *Ngn2* (Ichi et al., 2010).

1.4.7 Canonical Wnt signalling in *Spotch*

Evidence suggests that canonical Wnt signalling may interact with *Pax3* signalling. Both pathways are important in regulation of the proliferation-differentiation balance in the NT, and indeed, both promote the maintenance of the proliferative state while repressing differentiation (Keller-Peck and Mullen, 1997; Megason and McMahon, 2002). See section 1.6 for more detail regarding the canonical Wnt signalling pathway.

Several studies have been published which demonstrate a link between *Pax3* and the Wnt signalling pathway. For example, the region of *Pax3* expression in the neural plate has been shown to expand upon ectopic expression of *Wnt8* in *Xenopus*, and shrink when *Wnt8* expression is inhibited (Bang et al., 1999). In addition, Wnt signalling was shown to induce *Pax3* expression in *Xenopus* NC, which are derived from the neural plate border (Monsoro-Burq et al., 2005). It has also been suggested that Wnt signalling may influence *Pax3* signalling through the activity of *Msx1* in mouse limb muscle development, and *Ap2a* in the NC (de et al., 2011; Miller et al., 2007). Cultured chick neural plate cells have been shown to upregulate *Pax3* along with other NC markers in response to supplementation of either *Wg* or *Wnt3a* (Taneyhill and Bronner-Fraser, 2005)

Ectopic *Wnt1* expression in the ventral NT increased the rate of proliferation of the cells in this region by acting through β -catenin to shorten the cell cycle. Transfection of *Wnt1* into one half of the NT caused lateral bulging of the transfected half due an increase in the number of cells in this region. Furthermore, the expression pattern of *Pax3* is overlapping with that of *Wnt1* and *Wnt3a* in the neural folds, and *Pax3* has been reported to directly induce *Wnt1* expression (Fenby et al., 2008; Megason and McMahon, 2002). Therefore, it is possible that *Pax3* and canonical Wnt signalling may have interlinking roles in the development of the NT. Since both premature neuronal differentiation and reduced proliferation have been suggested as potential mechanisms of NTD development, it is also possible that canonical Wnt signalling may be involved in the formation of NTDs.

Recent evidence suggests that β -catenin may function upstream of Pax3. Conditional knock-out of β -catenin using a *Pax3^{Cre}* allele resulted in the development of NTDs, and the knockdown of *Pax3* and *Cdx2* expression. Binding sites for TCF/LEF1 were found in the *Pax3* promoter, which suggests that *Pax3* may be a direct target of β -catenin (Zhao et al., 2014).

1.5 Waardenburg Syndrome

Pax3 mutation in humans has been associated with certain types of the developmental disorder Waardenburg syndrome (WS). WS was first described in 1951 by the Dutch ophthalmologist and geneticist Petrus J. Waardenburg (WAARDENBURG, 1951). It is an autosomal dominant developmental disorder with a frequency in the general population of around 1 in 40 000, and accounts for approximately 2% cases of congenital deafness (Van et al., 1995).

1.5.1 Symptoms

WS has a number of characteristic symptoms. Additionally, a number of symptoms are seen with varying penetrance, and can be rare, or particular to a certain family. Even the most common symptoms have highly variable penetrance between families.

Common characteristics of WS include total or partial heterochromia irides (abnormal iris pigmentation), synophrys (hyperplasia of the medial portion of the eyebrows), poliosis (a white forelock), patches of skin hypopigmentation, dystopia canthorum (broad nasal root), and unilateral or bilateral sensorineural deafness. However, many other symptoms have been associated with the disease, including premature greying, limb defects, gut defects, microphthalmia, facial clefts, and genito-urinary abnormalities (Asher, Jr. and Friedman, 1990; Delezoide and Vekemans, 1994).

1.5.2 The four types of Waardenburg Syndrome

WS is a heterogeneous disease which can be caused by mutations in many different genes. However, mutations in certain genes are associated with particular groups of symptoms. Therefore, the syndrome has been clustered into four types according to common symptoms (Read and Newton, 1997).

Type I WS (WS1) usually exhibits the common symptoms listed above. It differs from WS2 only by the absence of dystopia canthorum in type II (Farrer et al., 1994; Tassabehji et al., 1993). WS3 is also known as Klein-Waardenburg syndrome, and shows limb abnormalities. WS4 is

also known as Shah-Waardenburg, or Waardenburg-Hirschprung disease, and is characterised by the presence of an aganglionic megacolon.

Both WS1 and WS3 have been associated with mutations in the *Pax3* gene (Farrer et al., 1994; Hoth et al., 1993; Tassabehji et al., 1992). Despite similarities to WS1, WS2 has been shown not to be linked to *Pax3* mutation (Arias, 1993; Farrer et al., 1994). However, mutations in the *MITF* gene have been found in some, but not all WS2 patients (Tassabehji et al., 1994). It is likely that a diagnosis of WS2 is given to a large group of heterogeneous melanocyte defects. WS4 has been associated with mutations in several different genes, including *Sox10*, *Endothelin-3*, and the *Endothelin-B receptor* gene (Edery et al., 1996; Pingault et al., 1998; Puffenberger et al., 1994).

1.5.3 *Pax3* mutations and neural tube defects in Waardenburg Syndrome

Pax3 mutations are known to cause WS1 and WS3 (Farrer et al., 1994; Hoth et al., 1993; Tassabehji et al., 1992). The majority of cases of WS1 and WS3 which have been described have been heterozygous for *Pax3* mutation. The disease has a dominant inheritance pattern, and one affected allele will produce a phenotype. A large number of different *Pax3* mutations have been reported in humans, and these are often family specific. WS is known to be an extremely heterogeneous disease, and it is probable that position and severity of the mutation within the protein is linked to the nature of the phenotype which develops.

Pax3 mutation in the population is relatively rare. According to the ExAC database a large number of missense mutations have been identified, the majority of which have been found in a single individual. However, very few mutations have been identified which are predicted to be deleterious. The database lists 8 loss-of-function mutations, 5 of which were found in just one individual. The remaining loss-of-function mutations are predicted to have a frequency of around 1/10 000 or less. The most common of the loss-of-function alleles is also reported to have occurred in homozygous form in one individual.

Pax3 mutations found in affected families tend to cluster around the sites of the paired-type homeodomain and the paired domain. There are three common types of mutation (Read and Newton, 1997). The first includes deletions, frameshift mutations, splice site mutations and nonsense mutations which result in a null allele. These mutations can be found anywhere between exons 2-6, but rarely affect the 3' region of the gene. The second common type of mutation consists of an amino acid substitution in the N-terminal region of the paired domain (Xu et al., 1995). The third common type of mutation involves the third α -helix of the homeodomain, which is important in the recognition of the target DNA sequence (Kissinger et al., 1990). These mutations all result in loss of function to some degree, and all result in the

same group of symptoms. Variations in symptoms are likely to be due to the Pax3 dosage sensitivity of different tissues. For example, the frontal bone (the skull bone which encompasses the forehead and part of the eye sockets) must be highly sensitive to Pax3 dosage, and is therefore almost always affected by mutation. Thus dystopia canthorum is virtually universal in cases of *Pax3* mutation. However, other symptoms such as pigmentation defects and limb abnormalities are much more variable, which suggests that melanocytes and limb bud mesenchyme are less sensitive to Pax3 dosage (Read and Newton, 1997).

Several cases of suspected homozygosity of *Pax3* mutation have been reported, and a small number have been confirmed. A case was reported in 1995 of a fetus showing severe symptoms of WS3, and also anencephaly. The parents were siblings with WS1, and the pregnancy was terminated at 15 weeks. The fetal tissue was not genotyped, but it is likely that the fetus was homozygous for mutations in *Pax3* (Ayme and Philip, 1995). Another case was described in 1995 in which a baby was born with suspected homozygous mutation of *Pax3*. The pregnancy was normal, but the child was born with severe symptoms of WS3. The parents were cousins who were both affected with WS1. Genotyping confirmed that the baby carried two copies of the *Pax3* mutant allele found in other members of the family, including the parents (Zlotogora et al., 1995).

Whether there is a link between NTDs and *Pax3* mutation in humans is not well established. Individuals have been reported with both WS and spina bifida (Ayme and Philip, 1995; Carezani-Gavin et al., 1992; Hol et al., 1995; Moline and Sandlin, 1993). In some cases, the two defects have been inherited together within a family (Begleiter and Harris, 1992; Chatkupt et al., 1993). It is not known whether the NTD is part of the syndrome of WS, or whether it could be associated with a different susceptibility locus, possibly closely linked to the *Pax3* locus. Linkage analysis has suggested no linkage between spina bifida and the *Pax3* gene, which suggests that it is not a major susceptibility gene in the development of NTDs in humans (Chatkupt et al., 1995). However, it may still act as a risk gene; recent studies have shown that single nucleotide polymorphisms in *Pax3* are more common in the genomes of patients with spina bifida than the general population (Agopian et al., 2013; Lu et al., 2007). NTDs in humans are known to be multigenic. Thus Pax3 mutations could be associated with the development of spina bifida in combination with other risk alleles and/or environmental factors.

1.5.4 *Spotch* as a model for Waardenburg Syndrome

Pax3 mutations are the cause of defects observed in both the *Spotch* mouse and in cases of WS1 and WS3. Several common phenotypic aspects occur in these disorders in both mice and humans. For instance, pigmentation abnormalities affecting the skin and hair/fur are seen in

both cases, and WS3 individuals also have limb abnormalities, which are seen in *Spotch* mice (Auerbach, 1954; Bober et al., 1994; Hoth et al., 1993; WAARDENBURG, 1951). Additionally, heart defects are very common in *Spotch* mutant embryos, and are occasionally seen in WS individuals (Banerjee, 1986; Mathieu et al., 1990).

Although the *Spotch* mouse carries a mutation in the gene responsible for WS1 and WS3, several differences in phenotype are also apparent. These differences could in part be due to the position and nature of the mutations, or due to the fact that *Spotch* mice are often studied in homozygous form, whereas most affected WS individuals are heterozygous for the mutation.

One of the major disabilities commonly found in WS in humans is sensorineural deafness (WAARDENBURG, 1951). Inner ear abnormalities have been reported in *Spotch* homozygous mutant embryos, and are usually seen in combination with exencephaly; the inner ear of *Spotch* embryos with closed NTs often develop normally (Deol, 1966). The abnormalities are likely due to the effects of the *Pax3* mutation on NC and probably also neurectodermal cells which contribute to inner ear development (Freyer et al., 2011). For instance, higher levels of apoptosis and lower levels of polysialylated NCAM in the developing inner ear have been reported in *Spotch* mutant embryos (Buckiova and Syka, 2004). However, the development of the inner ear is normal in heterozygotes, and their hearing is unaffected (Buckiova and Syka, 2004; Steel and Smith, 1992).

The *Spotch* mouse is frequently used as an experimental model for NTDs. However, the link between NTDs and WS appears to be weak, and *Pax3* is not known as a susceptibility gene for NTDs in humans (Chatkupt et al., 1995). However, NTDs are rare in heterozygous *Spotch* mice, and most WS patients studied are also heterozygous. Additionally, sample sizes of human homozygous *Pax3* mutant cases are very low. Studies have shown that certain gene variations of *Pax3* in humans may increase the risk of spina bifida (Agopian et al., 2013; Lu et al., 2007). Therefore *Pax3* may act as a risk gene in humans, and certain *Pax3* alleles may increase the risk of developing an NTD in combination with other risk alleles.

The study of *Spotch* mice enables cellular mechanisms to be identified which result in defects in WS patients. For example, neural crest defects present in *Spotch* embryos are equivalent to some of the defects identified in WS patients, including pigmentation abnormalities, and defects in limb development in *Spotch* embryos are likely to be equivalent to the limb defects seen in WS3 patients (Auerbach, 1954; Bober et al., 1994; Hoth et al., 1993; WAARDENBURG, 1951). Study of these abnormalities in the *Spotch* mouse has shed light on the mechanisms

behind the defects seen in WS patients. Additionally, *Spotch* embryos provide a useful model for the study of developmental defects which result in NTDs.

1.6 The canonical *Wnt* signalling pathway

The Wnt signalling pathways are highly evolutionarily conserved, and are found in a huge range of organisms, from *Drosophila* and *C. elegans* to mammals. There are two main branches of Wnt signalling – the canonical and non-canonical pathways. All Wnt signalling involves binding of an extracellular secreted Wnt ligand to a Frizzled cell-surface receptor, and can change the behaviour and fate of cells in a multicellular organism. Wnt signalling often acts over a short distance, such as between neighbouring cells, but is also able to act as a longer range morphogen (Clevers and Nusse, 2012; Tabata and Takei, 2004).

Canonical Wnt signalling involves the protein β -catenin (**Figure 1.7**). In the absence of Wnt ligand, β -catenin is sequestered by a protein complex called the destruction complex, whose components include Axin, Adenomatous polyposis coli (APC), Glycogen synthase kinase-3 β (GSK3 β), and Dishevelled (Dvl) (see section 1.6.2). The β -catenin protein is then phosphorylated, ubiquitinated, and targeted for degradation by the proteasome.

When Wnt ligand is present, the Wnt receptors sequester the components of the destruction complex. This process requires the protein Dishevelled (Dvl). This sequestration enables β -catenin to build up in the cytoplasm of the cell without being targeted for degradation. β -catenin is then transported to the nucleus, where, in combination with other transcription factors and cofactors, including T-cell-specific transcription factor (TCF)/lymphoid enhancing binding factor (LEF), it is able to initiate the transcription of certain Wnt-responsive genes, including transcription factors important during embryonic development (MacDonald et al., 2009).

1.6.1 Wnt ligands and receptors

Humans and most other mammals have 19 Wnt genes, which form 12 subfamilies. The Wnt proteins are hydrophobic, cysteine-rich secreted glycoproteins of around 40 kDa in size (Clevers and Nusse, 2012).

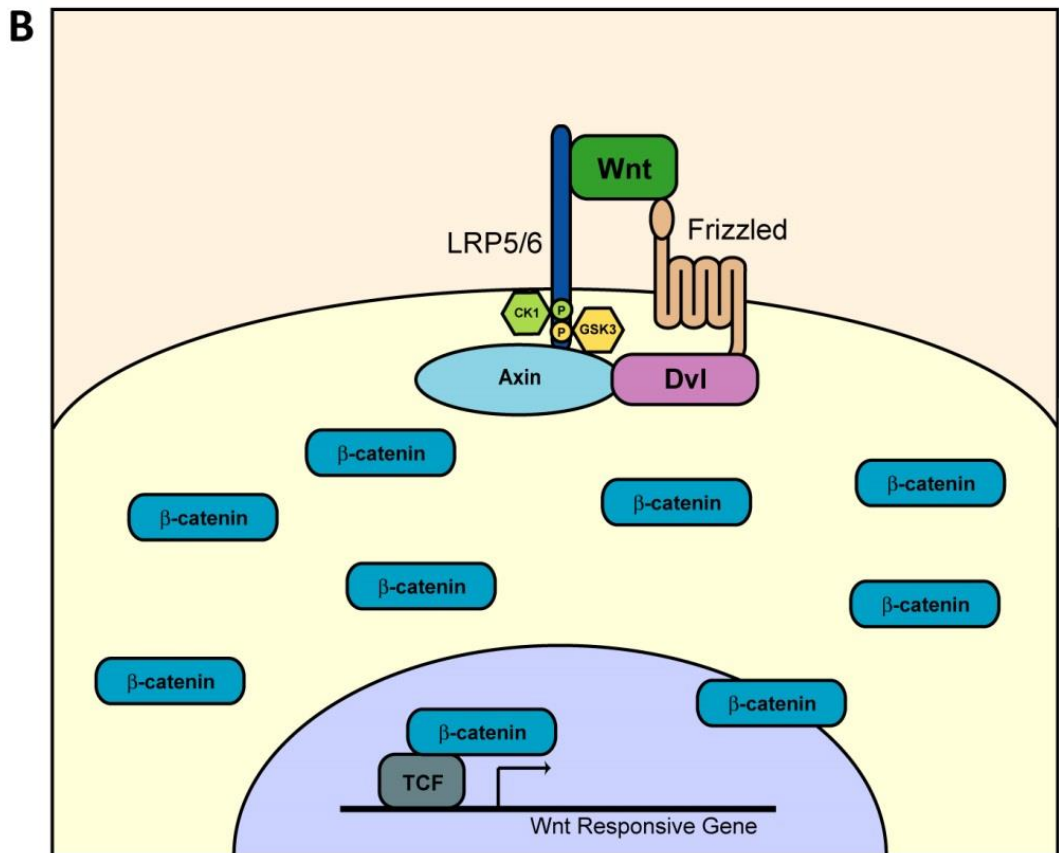
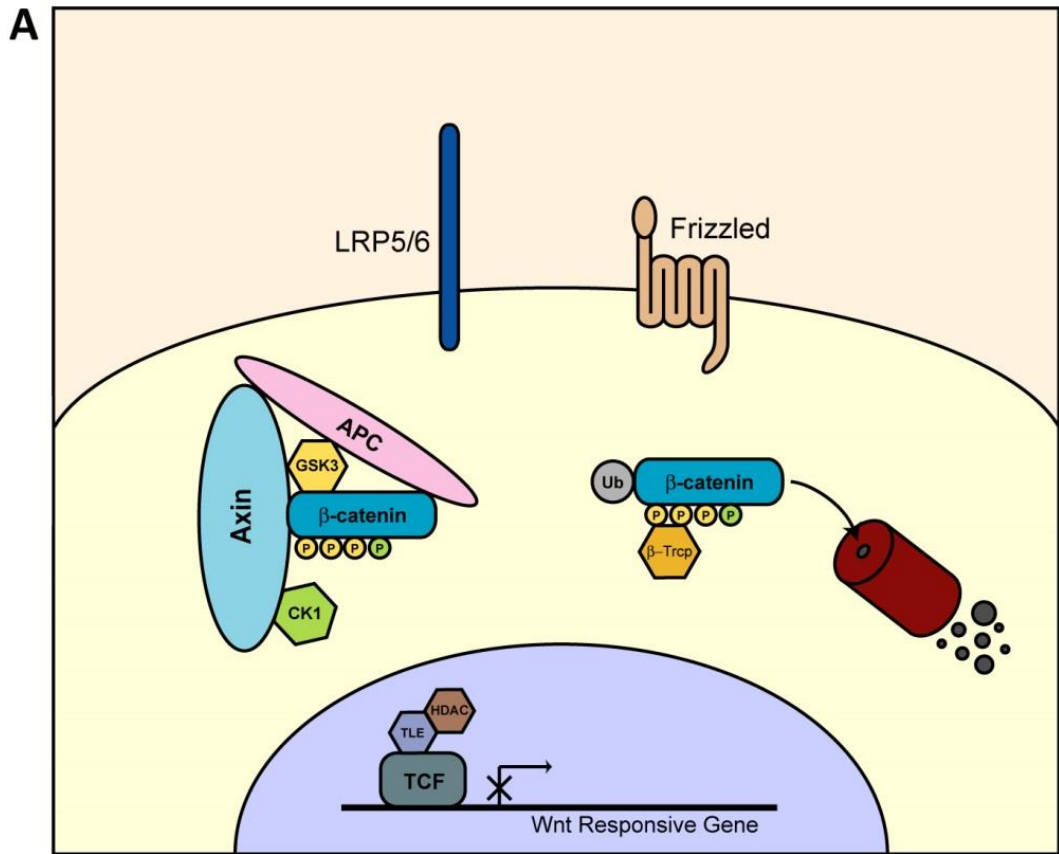
In canonical Wnt signalling the Wnt ligands bind to a heterodimeric receptor, consisting of a Frizzled (Fz) protein and an LRP5/6 protein. There are 10 mammalian Fz proteins, which are 7-membrane pass proteins with a cysteine-rich N-terminal domain (CRD) (Bhanot et al., 1996). LRP5 and LRP6 are low-density lipoprotein receptor-related proteins. They are both

Figure 1.7: Canonical Wnt signalling in the absence (A) or presence (B) of a Wnt ligand.

Canonical Wnt signalling alters the fate and activity of the β -catenin protein. When Wnt ligand is absent (**A**) the destruction complex forms in the cytoplasm. This protein complex consists of a number of molecules, including Axin, APC, GSK3, and CK1. The destruction complex binds cytoplasmic β -catenin, and phosphorylates it. This targets the β -catenin for degradation by the proteasome, and it becomes scarce within the cell. Absence of β -catenin in the nucleus results in the binding of repressors to the promoters of the Wnt-responsive genes, and transcription is inhibited.

When Wnt ligand is present (**B**) it binds to the cell surface receptors Frizzled and LRP5/6. The intracellular regions of these receptors sequester components of the destruction complex, and prevent it from forming. β -catenin is not targeted for degradation, and its concentration within the cytoplasm increases. β -catenin translocate to the nucleus, where it displaces repressors on the promoters of Wnt responsive genes. In combination with a number of co-factors, β -catenin recruits components of the cell's transcriptional machinery, and activates transcription of these genes.

Figure modified from (MacDonald et al., 2009).



approximately 180 kDa in size, and have single-pass transmembrane domains (Brown et al., 1998; Kim et al., 1998; Wehrli et al., 2000).

1.6.1.1 Synthesis and secretion of the Wnt ligand

Wnt ligands are synthesised in the endoplasmic reticulum (ER). They undergo a number of post translational modifications in the ER, including protein folding, glycosylation and acylation.

Folding is enabled through interactions with molecular chaperones, such as GRP78, which binds Wnt3a (Verras et al., 2008). Wnts are cysteine rich, which supports evidence that disulphide bonds are an important part of Wnt folding (Mason et al., 1992).

In *Drosophila* the transmembrane protein Porcupine (Porc) is necessary for N-glycosylation of the Wnt1 homologue Wingless (Wg) at multiple sites. It acts by anchoring Wg at the ER membrane (Tanaka et al., 2002). The role of glycosylation of Wnt ligands is controversial; some research has shown that prevention of Wnt3a glycosylation inhibits secretion and signalling (Komekado et al., 2007). However, alternative research suggests that lack of Wnt glycosylation has no effect on either secretion or signalling abilities of the ligand (Tang et al., 2012).

Wnt ligands, including Wnt3a, have been shown to bind the lipid group palmitic acid at a conserved cysteine residue (Cys77 in murine Wnt3a). The lipid imparts hydrophobic properties on the protein, and removal results in a loss of signalling ability of the ligand (Willert et al., 2003). Wnt3a is also modified at Ser209 with the monounsaturated fatty acid palmitoleic acid. This Ser209 palmitoylation has been found to be essential for secretion of the ligand. In cells lacking the Ser209 acylation, Wnt3a is retained in the endoplasmic reticulum (ER) and is not transported for secretion (Takada et al., 2006). For example, the enzyme stearoyl desaturase (SCD) generates monounsaturated fatty acids, which are then attached to Wnt ligands as the palmitic and palmitoleic acids described above (Rios-Esteves and Resh, 2013). Porc acts as an acyltransferase for this attachment, and is thus necessary for the secretion of Wnt3a in mice (Hofmann, 2000; Takada et al., 2006). In the absence of either of these proteins Wnt ligands, such as Wnt3a, show reduced secretion and signalling.

Additionally, the seven-pass membrane protein Wntless (Wls) is essential for Wnt ligand secretion (Banziger et al., 2006; Bartscherer et al., 2006). Wls is a putative orphan G protein coupled receptor (Jin et al., 2010) which is found in the ER (Coombs et al., 2010). The protein is able to bind to the hydrophobic palmitoleic acid group at Ser209 of Wnt ligands to enable release from the ER and secretion from the cell (Das et al., 2012).

The protein Oto is able to promote the anchorage of Wnt ligands to the membrane of the ER through the addition of the phospholipid glycosylphosphatidylinositol (GPI), thus preventing

secretion. Cleavage of the GPI anchor allows secretion of the Wnt ligand. In this way, Wnt ligand may be accumulated and then secreted in a burst (Zoltewicz et al., 2009). Additionally, accumulation of the Wnt ligand may be achieved through the use of cholesterol- and glycosphingolipid-rich domains of the plasma membrane known as lipid rafts; acylation of Wnt1 by Porc results in the targeting of the ligand to lipid rafts, which enables accumulation for secretion (Zhai et al., 2004).

1.6.1.2 Transport through the extracellular matrix

Cell surface proteins and the ECM play important roles in transduction of the secreted Wnt signal between cells.

The proteoglycans (PGs) are protein components of the cell surface and the ECM which play important roles in cell adhesion and the regulation of intercellular signalling (Reichsman et al., 1996). They consist of a core protein bound by covalently linked glycosaminoglycan chains. These chains may be chondroitin sulphate (CS), heparin sulphate (HS), dermatan sulphate or keratin sulphate. Some PGs, such as glypicans and syndecans, are found at the cell surface, whereas others, such as versican and perlecan, tend to be associated with the ECM (Theocharis et al., 2010). The cell surface PGs in particular bind to a large number of molecules involved in cell signalling, and can influence processes such as proliferation and migration (Theocharis et al., 2010). Heparin sulphate proteoglycans (HSPGs) are PGs which are commonly found on the surface of cells. They are able to act as cofactors in a number of interactions between proteins, such as between growth factors and their receptors, and between various enzymes and structural proteins (David, 1993).

Wnt ligand is found mostly associated with components of the matrix; around 50% at the cell surface, 33% with the ECM, and only around 17% in solution surrounding the cells (Reichsman et al., 1996). *Drosophila* Wg has been found to be released from the cell surface and the ECM by the addition of small amounts of exogenous glycosaminoglycan chains, such as heparin, HS, and CS. Thus it was discovered that Wg is bound by the HS and CS components of the proteoglycans, and that this binding promotes signalling by Wg (Reichsman et al., 1996). Furthermore, research suggests that the *Drosophila* HSPGs dally and dally-like potentiate Wg signalling by acting in combination with the Wnt receptor Dfz2 (Baeg et al., 2001; Lin and Perrimon, 1999). This mechanism probably acts through the sequestration and stabilisation of Wg at the cell surface, which makes the ligands more available for receptor binding (Baeg et al., 2004).

Wnt ligands are known to be hydrophobic, and yet they are able to move through the ECM – sometimes long distances – in order to bind receptors. Wg ligands in *Drosophila* have been

found to co-localise with extracellular lipoprotein particles called argosomes, which appear to aid movement of Wg through the ECM (Panakova et al., 2005). The HSPGs dally and dally-like may stabilise the ligands during transport (Mikels and Nusse, 2006).

1.6.1.3 The Wnt receptors

The Wnt ligands bind to a heterodimer consisting of the Fz and LRP5/6 Wnt receptors (Mao et al., 2001; Tamai et al., 2000). Wnts induce co-clustering of the Wnt receptors, thus increasing the likelihood of a response to further Wnt signalling (Bilic et al., 2007).

The CRD of Fz plays an important role in the binding of Wnt to its receptor (Bourhis et al., 2010; Dann et al., 2001; Hsieh et al., 1999; Janda et al., 2012). It is thought that binding of the site shields Wnt lipid groups from the aqueous environment (Janda et al., 2012). In *Xenopus*, the Fz8-CRD binds the Xwnt8 ligand in a doughnut shape, with two binding domains. In the first binding domain, a palmitoleic acid group at Ser187 of Xwnt8 (the equivalent of S209 of Wnt3a) binds into a hydrophobic groove in the Fz8-CRD. The second site consists of a rigid β -strand on the Xwnt8 protein, which enables hydrophobic interactions with residues in a pocket of the Fz8-CRD (Bienz and He, 2012; Janda et al., 2012).

The extracellular domain of LRP6 has been shown to bind Wnt1 and Wnt3a, and – when bound to a Wnt ligand – the CRD of Fz8 (Bourhis et al., 2010; Tamai et al., 2000). However, LRP6 appears to have multiple binding sites for different Wnt ligands, and indeed may bind multiple Wnt ligands simultaneously (Bourhis et al., 2010).

Binding strength differs greatly between the different Wnt ligands and the different receptors. For example, Wnt3a binds more tightly to the Fz8-CRD than Wnt5a and Wnt5b, and much more tightly than Wnt9b. However, Wnt9b binds very tightly to LRP6, whereas Wnt5a and Wnt5b appear not to interact with LRP6 at all (Bourhis et al., 2010).

It has been shown that the C-terminal cytoplasmic domain of LRP6 is necessary for transducing the Wnt signal (Tamai et al., 2000). Following Wnt signalling the intracellular domain of LRP6 is phosphorylated by CK1 (casein kinase 1). This activates LRP6 and induces Axin recruitment (Bilic et al., 2007; Tamai et al., 2004). Similarly, Fz proteins are able to recruit and directly bind Dishevelled (Dvl) at the cell surface in response to Wnt ligand binding (Chen et al., 2003). Dishevelled is able to bind Axin, and so this reinforces – or possibly enables – the recruitment of Axin at the cell surface during Wnt signalling, and facilitates clustering of the Wnt receptors (Angers and Moon, 2009; Choi et al., 2010).

1.6.2 The destruction complex

The destruction complex is a cytoplasmic protein complex including the proteins Axin, APC, GSK3 β , and Dvl. The purpose of the destruction complex is to bind β -catenin in the absence of Wnt ligand, and phosphorylate β -catenin for targeting to proteosomal degradation. In the absence of Wnt ligand components of the destruction complex are sequestered at the cell membrane by the Wnt receptors, thus stabilising β -catenin for transcriptional activity (MacDonald et al., 2009).

1.6.2.1 Axin

The protein Axin acts as a molecular scaffold to which the other components of the destruction complex can bind. It significantly downregulates β -catenin when overexpressed, such as in cancer (Hart et al., 1998). Axin has several binding domains; an N-terminal Regulator of G-protein signalling (RGS) domain, a GSK3 β -binding domain, and a C-terminal DIX (Dishevelled and Axin) domain (Behrens et al., 1998; Fagotto et al., 1999; Kishida et al., 1999).

The N-terminal half of Axin has been found to bind to GSK3 β , β -catenin, and the central region of APC (Hart et al., 1998). The RGS domain directly binds APC (Behrens et al., 1998; Hart et al., 1998), and the DIX domain is able to bind other DIX domains, forming either a homodimer or a heterodimer with molecules such as Dvl (Choi et al., 2010). In binding β -catenin and GSK3 β in close proximity, Axin promotes phosphorylation of β -catenin by GSK3 β , thus targeting β -catenin for degradation (Ikeda et al., 1998).

The C-terminal region of Axin has been found to bind to the intracellular domain of LRP5 as a result of canonical Wnt signalling (Cliffe et al., 2003; Mao et al., 2001). The RGS, DIX and GSK3 β binding domains are all thought to be important for this interaction (Mao et al., 2001). The binding is also facilitated by the presence of the Wnt ligand and by GSK3 β (Mao et al., 2001). The interaction between Axin and LRP5 prevents the formation of the destruction complex, and thus β -catenin is stabilised.

Additionally, GSK3 β is able to phosphorylate the Axin protein, resulting in a more stable form which binds β -catenin with higher affinity (Willert et al., 1999; Yamamoto et al., 1999). In the presence of the Wnt ligand Wnt3a the phosphorylation of Axin by GSK3 β is suppressed, resulting in Axin protein with a shorter half-life, and a reduction in overall Axin levels within the cell (Yamamoto et al., 1999). This aids the increase in intracellular β -catenin seen following canonical Wnt signalling. In addition, Axin is dephosphorylated in response to Wnt signalling, causing it to bind β -catenin with lower affinity, also increasing the concentration of free β -catenin within the cell (Willert et al., 1999).

1.6.2.2 APC

Adenomatous polyposis coli (APC) is a large protein of around 311.8 kDa (Grodén et al., 1991). It has numerous domains and motifs, including armadillo repeats, a basic domain, an oligomerisation domain, and 15 and 20 amino acid repeats (Polakis, 1997). These domains facilitate interactions with a number of proteins, including itself (Joslyn et al., 1993), GSK3 β (Rubinfeld et al., 1996), β -catenin (Rubinfeld et al., 1993), and microtubules (Smith et al., 1994). The Armadillo repeats are necessary for association of APC with the plasma membrane during active canonical Wnt signalling (Cliffe et al., 2003). APC also binds Axin in a region between residues 1554 and 1698, near the C-terminal region (Hart et al., 1998). Many cancers have a mutation in APC, which results in the aberrant stabilisation of β -catenin (Peifer and Polakis, 2000).

A region of 15 amino acid repeats acts as a binding site for β -catenin (Su et al., 1993). Additionally the protein contains a series of 7 repeats of 20 amino acids (Grodén et al., 1991). These repeats contain some sequence similarity to the 15 amino acid repeats, and may also bind β -catenin (Rubinfeld et al., 1995).

APC is phosphorylated by GSK3 β in the 20 amino acid repeat region, which allows this region to bind β -catenin (Hart et al., 1998; Rubinfeld et al., 1993; Rubinfeld et al., 1997; Su et al., 1993). This phosphorylation is promoted by Axin, which binds GSK3 β and APC in close proximity (Hart et al., 1998).

1.6.2.3 GSK3 β

Glycogen synthase kinase-3 β (GSK3 β) is a serine/threonine kinase which can phosphorylate multiple proteins, including many of those involved in the canonical Wnt signalling pathway. The GSK3 β protein consists of an N-terminal β -sheet, which forms a barrel shape, and a C-terminal α -helical domain (Dajani et al., 2001).

GSK3 β is able to phosphorylate several of the proteins involved in the destruction complex, including APC, Axin, and β -catenin. The binding of these proteins to the Axin scaffold brings them into close proximity, which promotes their GSK3 β -mediated phosphorylation (Ikeda et al., 1998; Rubinfeld et al., 1996; Yamamoto et al., 1999). GSK3 β binds to Axin via a hydrophobic groove in the α -helical region (Dajani et al., 2003).

GSK3 β activity needs to be inhibited in order for canonical Wnt signalling to occur, and this can be achieved through a number of mechanisms. For example, the protein FRAT (frequently rearranged in advanced T-cell lymphomas) is able to bind to a region overlapping the binding site of Axin. Thus it acts as an inhibitor of GSK3 β activity by competing with Axin for occupation

of the site (Dajani et al., 2003). The activity of GSK3 β can also be inhibited by phosphorylation of the serine-9 residue (Sutherland et al., 1993). This can be induced by Wnt and FGF2 signalling (Shimizu et al., 2008). Additionally, endocytosis of GSK3 β is induced by Wnt signalling. This results in a decrease in GSK3 β activity in the cell, and also sequestration of GSK3 β into multivesicular bodies (Taelman et al., 2010).

1.6.2.4 Dvl

Dvl has three main signalling domains; an N-terminal DIX domain, a central PDZ (post-synaptic density protein 95, Drosophila disc large tumour suppressor 1, zonula occludens 1) domain, and a more C-terminal DEP (Dishevelled, Egl-10, and Pleckstrin) domain (Kishida et al., 1999; Li et al., 1999). All three domains are necessary for the upregulation of β -catenin protein levels during Wnt signalling (Li et al., 1999; Yanagawa et al., 1995). The DIX domain allows Dvl, like Axin, to form either a homodimer or a heterodimer (Kishida et al., 1999).

Dvl plays a role in Wnt signal transduction at the cell surface. When Wnt ligand is present the PDZ domain of Dvl binds to Fz (Wong et al., 2003). This interaction is stabilised by association between the DEP domain of Dvl and the plasma membrane (Simons et al., 2009). The receptor aggregation results in the accumulation of other proteins, including the Axin-GSK3 β complex at the cell surface, which appears to enable GSK3 β - and then CK1-dependent phosphorylation of LRP6 (Bilic et al., 2007; Davidson et al., 2005; Julius et al., 2000; Zeng et al., 2005; Zeng et al., 2008).

Dvl is phosphorylated by kinases such as CK1 or CK2 in response to Wnt signalling (Bryja et al., 2007; Willert et al., 1997; Yanagawa et al., 1995), and it acts as an antagonist of Axin through multiple methods; it is not able to directly bind GSK3 β , but through its interaction with Axin, Dvl is able to inhibit the Axin-mediated, GSK3 β -dependent phosphorylation of both β -catenin and APC (Kishida et al., 1999). Additionally, as described above, Dvl aids recruitment of Axin to the cellular membrane through DIX-domain binding in response to canonical Wnt signalling (Bilic et al., 2007; Cliffe et al., 2003; Julius et al., 2000; Zeng et al., 2008). Dvl also inhibits the GSK3 β -mediated phosphorylation of Axin, preventing the formation of its more stable form. The PDZ domain is necessary for this role (Yamamoto et al., 1999). Through these multiple mechanisms, Dvl is able to agonise canonical Wnt signalling, and increase the intracellular concentration of β -catenin.

Dvl also plays a role in the activity of β -catenin as a transcription factor. Nuclear localisation of Dvl was found to occur following Wnt stimulation, and this was essential for its function in canonical Wnt signalling (Itoh et al., 2005). Additionally, Dvl was found to upregulate transcription of a reporter gene when co-transfected with LEF-1, compared to transfection of

LEF-1 alone (Li et al., 1999). These results are explained by the discovery that Dvl forms a complex with c-Jun, TCF and β -catenin, which stabilises the formation of the β -catenin-TCF complex at the promoters of Wnt-responsive genes (Gan et al., 2008).

1.6.3 β -catenin

β -catenin has functions in both the canonical Wnt signalling pathway and in adherens junctions between cells in epithelia. The balance between these different roles can affect availability of cytoplasmic β -catenin for canonical Wnt signalling. The structure of β -catenin is vital for interaction with other proteins, including those of the adherens junction, components of the destruction complex, and cofactors for the control of downstream gene transcription.

1.6.3.1 Structure

The β -catenin protein consists of 781 amino acids. Residues 138-671 form a compact central domain containing 12 armadillo repeats (**Figure 1.8**). Each repeat contains three α -helices, and the armadillo repeat region consists of a right-handed superhelix of these α -helices. The superhelix has a hydrophobic core and an external positively charged groove, which acts as an active site for a number of interactions. It also has a slight bend around the region of repeats 9-10 (Huber et al., 1997).

The N- and C-terminal domains are smaller and less organised when compared to the central domain. However, they too play roles in interactions with proteins. The C-terminal domain is involved in both the stabilisation of β -catenin in response to a canonical Wnt signal, and in the transcriptional activity of β -catenin (Cox et al., 1999). It was found that the C-terminal region may stabilise the protein by interacting with the β -catenin armadillo repeats, shielding this region from the destruction complex (Mo et al., 2009). This also shields the domain from binding E-cadherin in the adherens junction complex (Piedra et al., 2001).

The N-terminal domain of β -catenin is also able to interact with the armadillo repeat region, although not as strongly as the C-terminal domain. The C-terminal region potentiates this interaction, but the binding of the N-terminal to the armadillo repeats hinders the binding of the C-terminal (Castano et al., 2002). Interaction of the terminal regions with the armadillo domain alters the specificity of the armadillo domain for various ligands and cofactors, including TBP (TATA binding protein), Tcf-4 and E-cadherin (Solanas et al., 2004).

The C-terminal domain is necessary for the transcriptional activity of β -catenin because it binds to the transcription factors TBP (Hecht et al., 1999), and TCF/LEF (Solanas et al., 2004), enabling recruitment of transcription machinery to Wnt-target genes. This interaction is facilitated by the N-terminal region (Castano et al., 2002; Xing et al., 2008).

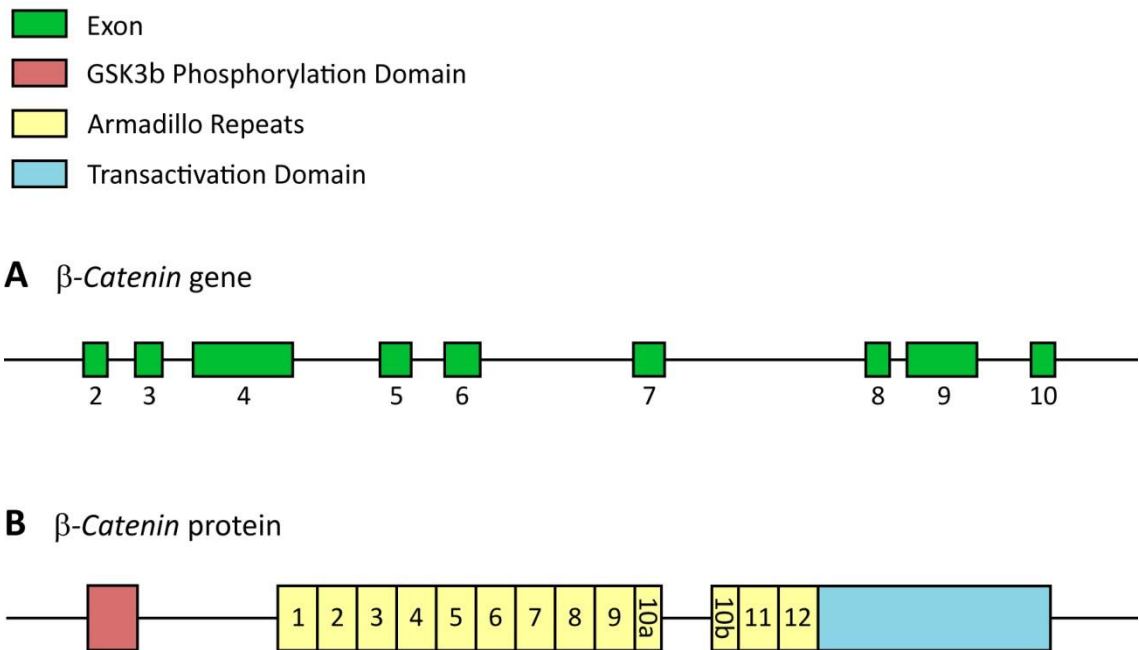


Figure 1.8: The structures of the β -catenin gene (A) and protein (B). β -catenin has a number of domains which enable it to interact with other proteins. The Armadillo repeats facilitate binding with proteins such as Axin and APC, and the GSK3 β phosphorylation domain enables degradation by the proteasome. The transactivation domain recruits components of the transcriptional machinery, thus supporting the activity of β -catenin as a transcription factor.

The N-terminal region of β -catenin also binds to α -catenin in the adherens junction (Aberle et al., 1996), and deletion of the N-terminal region prevents binding to α -catenin. However, deletion of the C-terminal domain increases binding, which suggests that the C-terminal inhibits interaction between the N-terminal domain of β -catenin and α -catenin (Castano et al., 2002).

1.6.3.2 β -catenin and adherens junctions

Adherens junctions are found in epithelial and endothelial tissue, and form between the lateral surfaces of neighbouring cells. They consist of E-cadherin bound to p20, α -catenin, β -catenin and γ -catenin (plakoglobin) and are known to interact with the actin network (Capaldo et al., 2014; Knudsen and Wheelock, 1992).

The N terminal region of β -catenin is known to be important for adherens junction formation as it binds to α -catenin (Aberle et al., 1996). Additionally, the armadillo repeats 3-8 are required for binding to E-cadherin (Graham et al., 2000).

The protein Bcl9-2 appears to act as a molecular switch between the translation and adhesion roles of β -catenin; Bcl9-2 expression causes EMT and translocation of β -catenin to the nucleus for signalling. Reduction in Bcl9-2 results in membrane localisation of β -catenin, where it functions in adherens junctions (Brembeck et al., 2004). Additionally, phosphorylation of β -catenin at Tyr-86 and Tyr-654 by tyrosine kinases inhibits the formation of the β -catenin/E-cadherin complex at the adherens junction, and thus is another level of control (Roura et al., 1999). The level of E-cadherin expression is usually the rate limiting factor for the formation of adherens junctions, and so controlling E-cadherin expression can alter the rate of junction formation, and thus β -catenin sequestration (Heasman et al., 1994).

β -catenin which functions in adherens junctions and that which functions in canonical Wnt signalling come from the same pool. Therefore, changes in one mechanism may alter the other. For example, an increase in canonical Wnt signalling in mammalian cell culture through transfection of Wnt1 cDNA resulted in an increase in cytoplasmic β -catenin. This in turn caused saturation of β -catenin binding cadherin at the adherens junctions, and increased cell-cell adhesion (Hinck et al., 1994). Research has shown that even very low levels of β -catenin expression (around 12.5% of wild type) are sufficient to maintain adherens junctions, whereas higher levels (more than 25%) are required for canonical Wnt signalling and the maintenance of downstream gene expression (Rudloff and Kemler, 2012). This suggests that E-cadherin is able to outcompete components of the canonical Wnt signalling pathway for the binding of β -catenin.

Experiments which manipulate canonical Wnt signalling and β -catenin expression in the NT have demonstrated that this can affect the formation of the adherens junctions. For example, it was found that conditional null β -catenin disrupted the formation of the adherens junctions in the dorsal NT (Valenta et al., 2011). In addition, conditional mutation of β -catenin in the posterior region of the embryo reduced formation of adherens junctions (Hierholzer and Kemler, 2010). On the other hand, an increase in Wnt7a expression in neural progenitors through use of a transgene in mice also reduced the formation of adherens junctions in these cells (Shariatmadari et al., 2005). However, given that Wnt7a functions in both canonical and non-canonical Wnt signalling, this defect could be due to abnormalities in cell polarity caused by alterations in non-canonical Wnt signalling.

Plakoglobin and β -catenin demonstrate some functional redundancy. Plakoglobin functions in both the adherens junction, and another cell-cell junction called the desmosome. In plakoglobin mutant mouse embryos, β -catenin is able to replace plakoglobin in the desmosome, and thus was able to partially compensate for the loss of plakoglobin (Bierkamp et al., 1999). Additionally, plakoglobin was upregulated and partially compensated for conditional β -catenin deletion in the mouse heart (Zhou et al., 2007) and liver (Wickline et al., 2011; Wickline et al., 2013). Plakoglobin appears able to replace β -catenin in the adherens junction, but is not able to compensate for its role in canonical Wnt signalling (Wickline et al., 2013).

1.6.3.3 β -catenin and the destruction complex

Multiple components of the destruction complex are able to directly interact with β -catenin. The armadillo repeats of β -catenin bind to Axin (Ikeda et al., 1998). More specifically, Armadillo repeats 3-7 have been found to be responsible for binding the Axin homologue Conductin (Behrens et al., 1998). β -catenin also binds directly to APC via the central Armadillo repeats (Rubinfeld et al., 1995). β -catenin is phosphorylated by both CK1 α and GSK3 β . Phosphorylation by CK1 α at residue Ser45 primes β -catenin for phosphorylation by GSK3 β in the N-terminal region, at residues Ser29, Ser33, Ser37, and Thr41 (Amit et al., 2002; Liu et al., 2002; Yost et al., 1996).

Phosphorylation of β -catenin is crucial for its degradation. β -catenin which has been phosphorylated by GSK3 β is recognised by the E3 ubiquitin ligase β -TrCP (β -transducin repeat-containing protein), and only phosphorylated β -catenin is recognised (Hart et al., 1999). Once bound to β -catenin, β -TrCP recruits the ubiquitination complex protein Skp1 (Liu et al., 1999), which poly-ubiquitinates the β -catenin protein. This ubiquitination targets the β -catenin protein for degradation by the proteasome (Aberle et al., 1997; Orford et al., 1997).

1.6.3.4 Translocation to the nucleus

If β -catenin accumulates in the cytoplasm, it is transported to the nucleus via mechanisms which are not well understood. However, a number of proteins have been identified which modify the cellular response to canonical Wnt signalling by controlling either the influx or efflux of β -catenin from the nucleus.

It is known that Rac1 activation is necessary for the translocation of β -catenin; activated Rac1 is able to activate KNK2, which phosphorylates β -catenin at residues Ser191 and Ser605. This phosphorylation is necessary for the translocation of β -catenin, and its ablation reduces Wnt-induced nuclear localisation of β -catenin (Wu et al., 2008).

Additionally, Armadillo repeats 1-12 of β -catenin have been found to interact with the Forkhead box domain of FoxM1 (Forkhead box M1). The cytoplasmic concentration of FoxM1 increases in response to canonical Wnt signalling, and the interaction between β -catenin and FoxM1 has been shown to be necessary for the Wnt-dependent nuclear translocation of β -catenin (Zhang et al., 2011).

Other proteins promote the nuclear export of β -catenin. Axin and APC have both nuclear localisation sequences (NLS) and nuclear export sequences (NES), which allow them move in and out of the nucleus (Henderson, 2000; Wiechens et al., 2004). Therefore they are able to shuttle β -catenin into the cytoplasm from the nucleus (Cong and Varmus, 2004; Henderson, 2000). Additionally, the proteins RanBP3 (Ran binding protein 3) and Menin directly bind β -catenin and facilitate its transport from the nucleus into the cytoplasm (Cao et al., 2009; Hendriksen et al., 2005).

1.6.3.5 Transcription factor activity

Nuclear β -catenin is able to act as a transcription factor alongside numerous cofactors. Transcriptional repressors inhibit this activity.

The transcription factors TCF and LEF are closely related proteins of the High Mobility Group-box transcription factor family. They play an important role in the transcriptional activity of β -catenin, and in the transcription of Wnt-responsive genes. LEF-1 is able to create bends of 130° in DNA by binding and widening the minor groove. This change in shape allows binding and interaction between DNA-bound proteins which would otherwise be too distant to interact (Giese et al., 1992; Giese et al., 1995).

In the absence of canonical Wnt signalling, nuclear β -catenin is very low, and TCF/LEF acts as a transcriptional repressor in combination with the proteins of the Groucho-related genes (Grg) (Cavallo et al., 1998). Grg is able to recruit proteins to aid repression of the transcriptional activity. For example, Grg can recruit the HDAC Rpd3 (Chen et al., 1999), which compacts local chromatin structure, making the DNA less available to the core transcriptional machinery of the cell (Braunstein et al., 1993).

When canonical Wnt signalling is active, and β -catenin nuclear concentration increases, Grg is displaced by β -catenin, which allows TCF/LEF to function as a transcriptional activator (Brantjes et al., 2001; Cavallo et al., 1998). Armadillo repeats 1-7 of β -catenin bind to the N-terminal domain of LEF-1 in a yeast 2-hybrid screen (Behrens et al., 1996). Likewise, the N-terminal region of Xctf-3 has been found to bind the armadillo repeats of β -catenin in *Xenopus*

(Molenaar et al., 1996), and the N-terminal region of *Drosophila* dTCF binds to the armadillo repeats of the *Drosophila* β -catenin, Armadillo (van de Wetering et al., 1997).

The interactions between TCF/LEF and β -catenin result in transcription of the Wnt-responsive genes, including cyclin-D1 (Tetsu and McCormick, 1999), siamois (Brannon et al., 1997), Xnr3 (McKendry et al., 1997), and c-MYC (He et al., 1998). One mechanism by which this occurs is the recruitment of histone acetyltransferases (HATs), such as p300 and CBP (CREB binding protein) (Hecht et al., 2000). These proteins are able to induce transcription in two ways: acetylation of the surrounding histones, and recruitment of the transcriptional machinery, such as the protein TBP (Hecht et al., 2000). Histone acetylation produces a more open structure in the chromatin. This allows the core transcriptional machinery to access the DNA (Hebbes et al., 1988).

HATs are able to recruit the core transcriptional machinery to Wnt-responsive genes during canonical Wnt signalling. The acetyltransferases of the p300/CBP family bind TBP and TFIIB (Kwok et al., 1994; Yuan et al., 1996). Additionally, the protein complex formed by β -catenin and TCF/LEF is able to recruit transcriptional machinery to DNA. β -catenin supplies a transactivation domain (TAD) to the complex, which is able to recruit proteins such as TBP to induce transcription of the region (Hecht et al., 1999; Willert and Nusse, 1998).

As well as binding histone acetyltransferases, β -catenin binds a variety of other transcriptional coactivators. Many of these proteins – like the HATs – play a role in restructuring the local chromatin (Mosimann et al., 2009). For example, TRRAP (transcription/transformation domain associated protein), MLL (mixed lineage leukaemia) proteins, and ISW1 (imitation switch 1) are all able to bind β -catenin, and all play roles in the dynamics of chromatin structure (Sierra et al., 2006).

1.6.4 Roles of canonical Wnt signalling during development

Canonical Wnt signalling plays a vital role in the patterning and development of a wide variety of embryonic tissues. It is usually associated with the maintenance of stem cell fate and multipotency, and the inhibition of differentiation. Complete deletion of β -catenin in mouse embryos causes developmental arrest at gastrulation (Haegel et al., 1995).

Canonical Wnt signalling plays important roles in a number of morphogenetic events during development. For example, it is necessary for the partitioning of the somites, and posterior extension of the body axis (Agathon et al., 2003; Aulehla et al., 2008; Takada et al., 1994)

One of the more well-known Wnt assays involves duplication of the *Xenopus* antero-posterior body axis as a result of ectopic Xwnt1 expression (McMahon and Moon, 1989). This result is

reproducible using a number of different components of the canonical Wnt pathway, including β -catenin, Dvl, and dominant-negative GSK3 β (Guger and Gumbiner, 1995; He et al., 1995; Sokol et al., 1995). Additionally, ectopic expression of Axin in *Xenopus* inhibits canonical Wnt signalling, and therefore also inhibits formation of the body axis (Zeng et al., 1997). These results verify the role of active canonical Wnt signalling in the formation and patterning of the embryonic antero-posterior axis (Kiecker and Niehrs, 2001).

In this project, the research was focussed on the role of canonical Wnt signalling after gastrulation and the determination of the axes. On a tissue and cellular level, canonical Wnt signalling has numerous roles in patterning and differentiation of the developing CNS. It appears to largely be involved in the maintenance of multipotent, proliferating cells. For example, β -catenin is able to promote neural precursor cell proliferation when it binds to TCF/LEF proteins. It activates transcription of cyclin-D1, which allows the cell to pass from G1 into S phase in the cell cycle (Arber et al., 1997; Tetsu and McCormick, 1999). Furthermore, canonical Wnt signalling increases expression of the ID, MSX and REST/NRSF proteins, which are all able to repress neuronal differentiation (Chong et al., 1995; Odelberg et al., 2000; Rockman et al., 2001; Schoenherr and Anderson, 1995; Willert et al., 2002). β -catenin is also able to interact with the Notch intracellular domain (NIC), and thus contribute towards the expression of the antineurogenic *hes1* and *hes5* genes by binding to the promoter (Shimizu et al., 2008).

Publications suggest that canonical Wnt signalling is necessary for CNS angiogenesis, but not non-CNS angiogenesis. Canonical Wnt-related genes are expressed in the CNS, and loss of expression of these genes results in reduced angiogenesis and poor blood-brain barrier formation (Daneman et al., 2009). Additionally, an increase in β -catenin causes upregulation of the Notch signalling pathway and abnormalities in the development of the vessels, including the formation of blind-ended tubes, and elongation and branching defects (Corada et al., 2010).

Although canonical Wnt mutations commonly cause CNS defects, NTDs appear to be rarer, and the link between canonical Wnt signalling and NT development is not well understood. However, several studies suggest that such a link exists. For example, LRP6 mutant mouse embryos have a number of neural defects, including exencephaly and/or spina bifida with approximately 50% penetrance (Pinson et al., 2000), although it is possible that this effect is mediated through the non-canonical Wnt signalling pathway (Gray et al., 2013). Recent research indicates that β -catenin mutation may cause NTDs through the influence of canonical Wnt signalling on NT genes, including *Pax3* (Zhao et al., 2014).

Canonical Wnt signalling is also involved in the development of the PNS. The role of Wnt signalling in early NC specification is discussed in section 1.3. However, it also appears to have a role in NC differentiation; mice with a conditional deletion of β -catenin in the NC fail to develop sensory neurons in the DRG (Hari et al., 2002). On the other hand, overexpression of β -catenin in the NC results in the almost complete differentiation of sensory neurons at the expense of other NC-derived tissue types (Lee et al., 2004). Thus β -catenin appears to promote sensory neuronal fate in the NC. Pax3 is also known to be important in the development of the NC and sensory neuronal fate (Auerbach, 1954; Nakazaki et al., 2008). Therefore, this evidence may support an interaction between the canonical Wnt signalling pathway and Pax3.

1.6.5 Canonical Wnt signalling and cancer

As discussed above, canonical Wnt signalling is associated with the maintenance of multipotency and proliferation, and the inhibition of differentiation. Cancer occurs when cells become proliferative, and often migratory, in inappropriate contexts. It is a disease caused by imbalance between proliferation, differentiation and apoptosis, and abnormal canonical Wnt signalling is often implicated.

Cancers are usually associated with inappropriately activated canonical Wnt signalling. For example, stabilisation of β -catenin has previously been shown to induce transformation of mammary epithelial cells to a cancer-like state (Shimizu et al., 1997). Additionally, β -catenin stabilisation in the epidermis of mice was reported to cause hair follicle tumours (Gat et al., 1998).

Loss of components of the destruction complex may lead to accumulation of β -catenin in the absence of Wnt ligand. This can lead to constitutively active canonical Wnt signalling, and thus cancerous transformation. For example, loss of APC is a common cause of colon cancer (Nakamura et al., 1992), and loss of Axin2 has also been associated with the development of colorectal cancer (Lammi et al., 2004).

Canonical Wnt signalling may also affect the ability of cancer cells to metastasise; metastatic cells have been reported to exhibit hyperactive canonical Wnt signalling, and reduction of TCF activity reduced the ability of the cancerous cells to metastasise (Nguyen et al., 2009).

1.7 Aims and Hypotheses

In this thesis I aim to use *Pax3* mutant mice to observe why and how these embryos develop NTDs. This will include study of the *Spotch-2H* mutant mouse and the cellular and

morphological effects of the mutation. I will also study the potential interaction between Pax3 and canonical Wnt signalling using the development of NTDs and NC defects in β -catenin loss- and gain-of-function embryos.

In the first results chapter (**Chapter 3**) I intend to study the development of NTDs in Pax3-mutant *Spotch* mice in detail, and identify abnormal cellular processes which could be causing the NTDs in these embryos. I will also compare morphology of the NT between genotypes to attempt to elucidate if the cellular defects result in a physical defect which could prevent NT closure.

Hypothesis 1: Premature neuronal differentiation and reduced proliferation in the NT of the *Spotch* embryo cause spina bifida.

In the second results chapter (**Chapter 4**) I will study the effects of β -catenin gain-of-function (GOF) on the development of the NT and NC in combination with Pax3 mutation. I will use a conditional β -catenin GOF allele in combination with a Pax3^{Cre} allele to increase canonical Wnt signalling in Pax3-expressing tissues, including the NC and the dorsal region of the NT. I will then study NT and NC development in embryos with a variety of allele combinations to observe if any defects occur due to interaction between the pathways.

In the third results chapter (**Chapter 5**) I will study the effects of β -catenin loss-of-function (LOF) on the development of the NT and NC in combination with Pax3 mutation. I will use a conditional β -catenin LOF allele in combination with a Pax3^{Cre} allele to reduce canonical Wnt signalling in Pax3-expressing tissues. Again, I will study the development of the NT and NC in embryos with a variety of allele combinations to observe if any defects occur due to interaction between the pathways. The results using both β -catenin GOF and LOF may be clearer than using either GOF or LOF alone.

Hypothesis 2: Interaction between Pax3 and the canonical Wnt signalling pathway reduces proliferation and induces premature neuronal differentiation in the NT and NC, resulting in NTDs and NC defects.

2 Materials and Methods

2.1 Equipment and Software

2.1.1 Laboratory equipment

Microscopes used for dissection were Zeiss (Oberkochen) Stemi SV11 and Zeiss (Oberkochen) Stemi SV6. Microscopes used for whole mount bright field micrographs were the Zeiss (Oberkochen) Stemi SV11 microscope connected to a Leica (Wetzlar) DFC 490 camera, or the Leica (Wetzlar) MZ FLIII microscope connected to a Leica (Wetzlar) DC500 camera. The microscope used for whole mount fluorescent micrographs was the Leica (Wetzlar) MZ FLIII microscope connected to a Leica (Wetzlar) DC500 camera. The microscope used for bright field histology and micrographs was the Zeiss (Oberkochen) Axioplan 2 microscope connected to a Zeiss (Oberkochen) AxioCam HRc camera. The microscope used for fluorescent immunohistochemistry and micrographs was the Zeiss (Oberkochen) AxioPhot microscope connected to a Leica (Wetzlar) DC500 camera.

Room temperature centrifuging was carried out in the Fisher Scientific (New Hampshire) Accuspin Micro centrifuge. Cold centrifuging (at 4°C) was carried out in the Thermo Scientific (Massachusetts) Heraeus Fresco 21 centrifuge. Thermal cyclers used were the Techne (Staffordshire) TC-512 and MJ Research (Quebec) PTC-200. The Sonics (Connecticut) Vibra Cell sonicator was used. Spectrophotometers used were the Shimadzu (Kyoto) UV mini 1240 and the NanoDrop (Massachusetts) ND-1000.

The microtomes Microm (Bicester) HM325 and Microm (Bicester) HM330 were used for wax sectioning, and the vibratome Leica (Wetzlar) VT 1000S was used for gelatin-albumin sectioning.

2.1.2 Software

Adobe Photoshop CS3 and Adobe Photoshop Lightroom 2 were used to process images. SigmaPlot 2001 was used to create graphs and charts. SigmaStat 3.5 was used for statistical analysis.

2.2 Statistics

SigmaStat 3.5 was used for all statistics described in this thesis. The statistical tests carried out for each experiment are described in figure legends. The t-test was used to compare two

groups of data. One-way ANOVA was used to compare for more than two groups, as this corrects for multiple comparisons; false positives are more likely when carrying out multiple comparisons between groups. A power calculation was used to estimate required sample size. The Chi Square and Fisher Exact Tests were used to compare proportions and assess for significance. If the sample size of at least 20% of the groups was greater than 5 then the Chi Square Test was used. If not, then the Chi Square test loses accuracy, and so the Fisher Exact Test was used instead. Where advised by the software, additional tests were carried out in order to confirm results. These are described in the figure legends.

2.3 Solutions

Regularly used solutions are described here. More specific solutions are described in the relevant sections.

10x Phosphate-buffered saline (PBS, 1000 ml)

100x PBS tablets (Oxoid, Cheshire)
1000 ml Milli-Q water
Stir until fully dissolved. Autoclave.

1x PBS (1000 ml)

100 ml 10x PBS
900 ml Milli-Q water
1 ml Diethyl pyrocarbonate (DEPC, Sigma, Missouri)
Stir for several hours. Autoclave.

PBT (1000 ml)

1000 ml PBS
1 ml Tween-20

4% Paraformaldehyde (PFA, 500 ml)

20 g PFA (Sigma, Missouri)
500 ml PBS
Dissolve at 60-65°C.

DEPC-treated water (1000 ml)

1000 ml Milli-Q water
1 ml DEPC

Stir for several hours. Autoclave.

10x Tris-buffered saline (TBS, 1000 ml)

250 ml 1M Tris-HCl (pH 7.5)

80 g NaCl (Fisher Scientific, New Hampshire)

2 g KCl (Sigma, Missouri)

Milli-Q water to 1000 ml

Autoclave.

TBST (1000 ml)

100 ml 10x TBS

1 ml Triton X-100 (Sigma, Missouri)

Milli-Q water to 1000 ml

2.4 Mouse methods, dissection and histology

2.4.1 Mouse husbandry

The mice used in this project were housed according to the Home Office Code of Practice. Ambient temperature was maintained between 19°C and 23°C, and humidity was kept between 40% and 70%. A 24 hour diurnal cycle of 12 hours light and 12 hours dark was used. Food and water were freely available.

A standard pellet feed was used for most of the mice (Harlan breeding diet). Some of the mice were given a folate deficient (FD) diet for experimental purposes. This feed was produced in Harlan Laboratories, and contained no folate and 1% succinyl sulfathiazole (Burren et al., 2008). Female mice were maintained on the folate deficient diet for at least 3 weeks prior to mating.

Males were housed with other male littermates until sexual maturity, after which they were housed individually for studing. Females were housed in groups with other females. Mice were mated from sexual maturity at 6 weeks of age.

A single male was housed with one or more females for breeding. A vaginal plug was taken as a sign of pregnancy. Pregnant females were housed individually, or with other pregnant females from the same group.

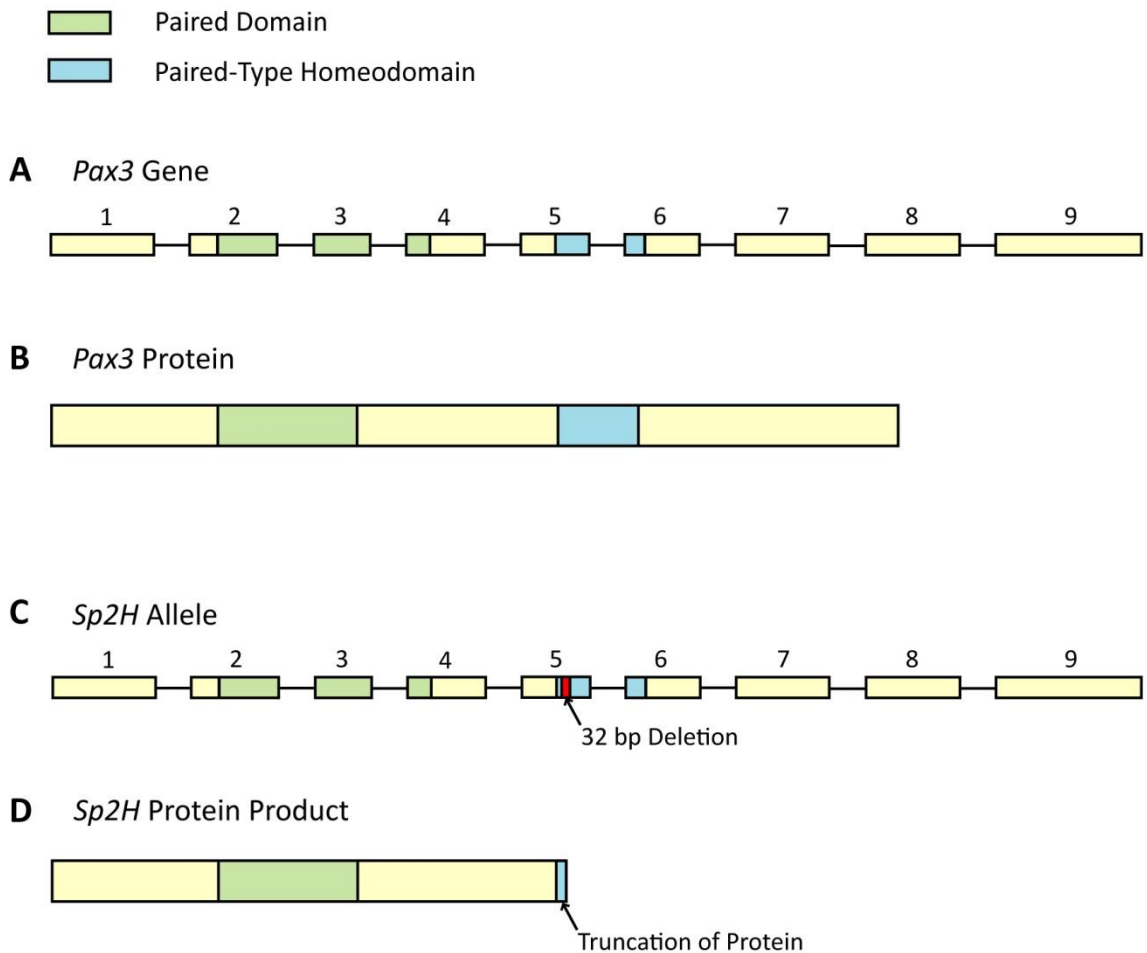


Figure 2.1: Structures of the Sp^{2H} allele and protein of Pax3. The structures of the wild type Pax3 gene (A) and protein (B) are provided for reference. The Sp^{2H} allele has a 32 bp deletion (shown in red) in the paired-type homeodomain region of exon 5 (C). This deletion causes a frame shift, and creates a stop codon. This results in the formation of a truncated, functionally null Pax3 protein (D).

2.4.2 Mutations

Several mutations will be referred to frequently in this thesis. These mutations are described in detail below.

2.4.2.1 The Pax3^{Sp2H} allele

The Pax3^{Sp2H} allele (also referred to in this thesis as Sp^{2H}) was generated through X-ray irradiation (Beechey and Searle, 1986). The allele has a 32 bp deletion from the region of the

gene which encodes the HD (**Figure 2.1**). The deletion results in creation of a stop codon. Therefore, the Sp^{2H} protein is truncated and functionally null.

2.4.2.2 The Pax3^{Cre} allele

The Pax3^{Cre} allele used in this research was generated in 2005 (Engleka et al., 2005). It is a knock-in gene, in which the first exon of *Pax3* is replaced with a *Cre-recombinase* (*Cre*) gene (**Figure 2.2**). The *Pax3* gene is functionally null, and embryos which are homozygous for Pax3^{Cre} have the same phenotype as other *Pax3*-null mice, including those homozygous for Pax3^{Sp2H}. They display loss of Pax3 protein expression, and mouse reporter lines demonstrate effective Cre-dependent recombination in the appropriate tissues (Engleka et al., 2005).

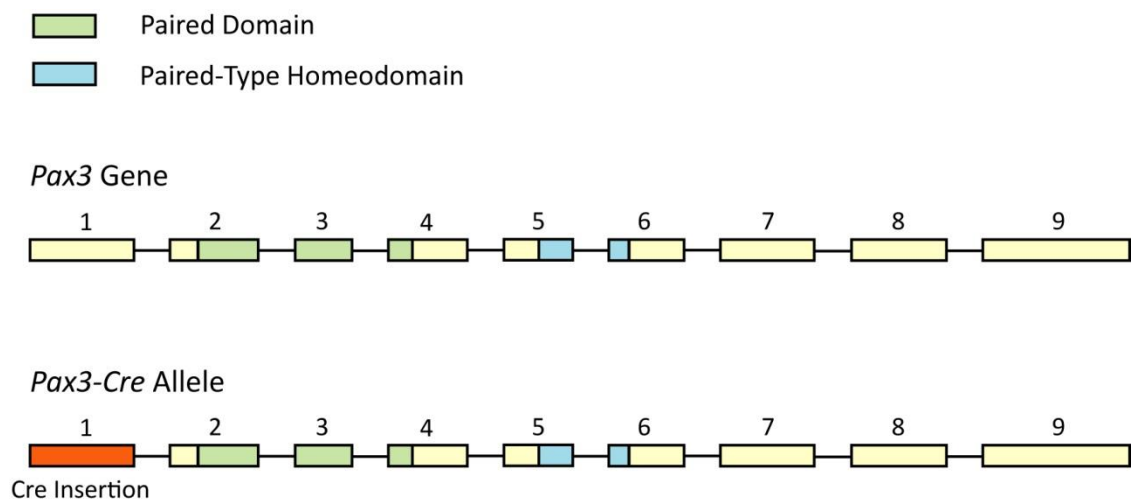


Figure 2.2: Structure of the Pax3^{Cre} allele. The structure of the wild type *Pax3* gene is provided for reference. The *Pax3-Cre* allele has exon 1 replaced with the *Cre* gene. Expression of this allele results in a functional Cre protein, but no functional Pax3 protein.

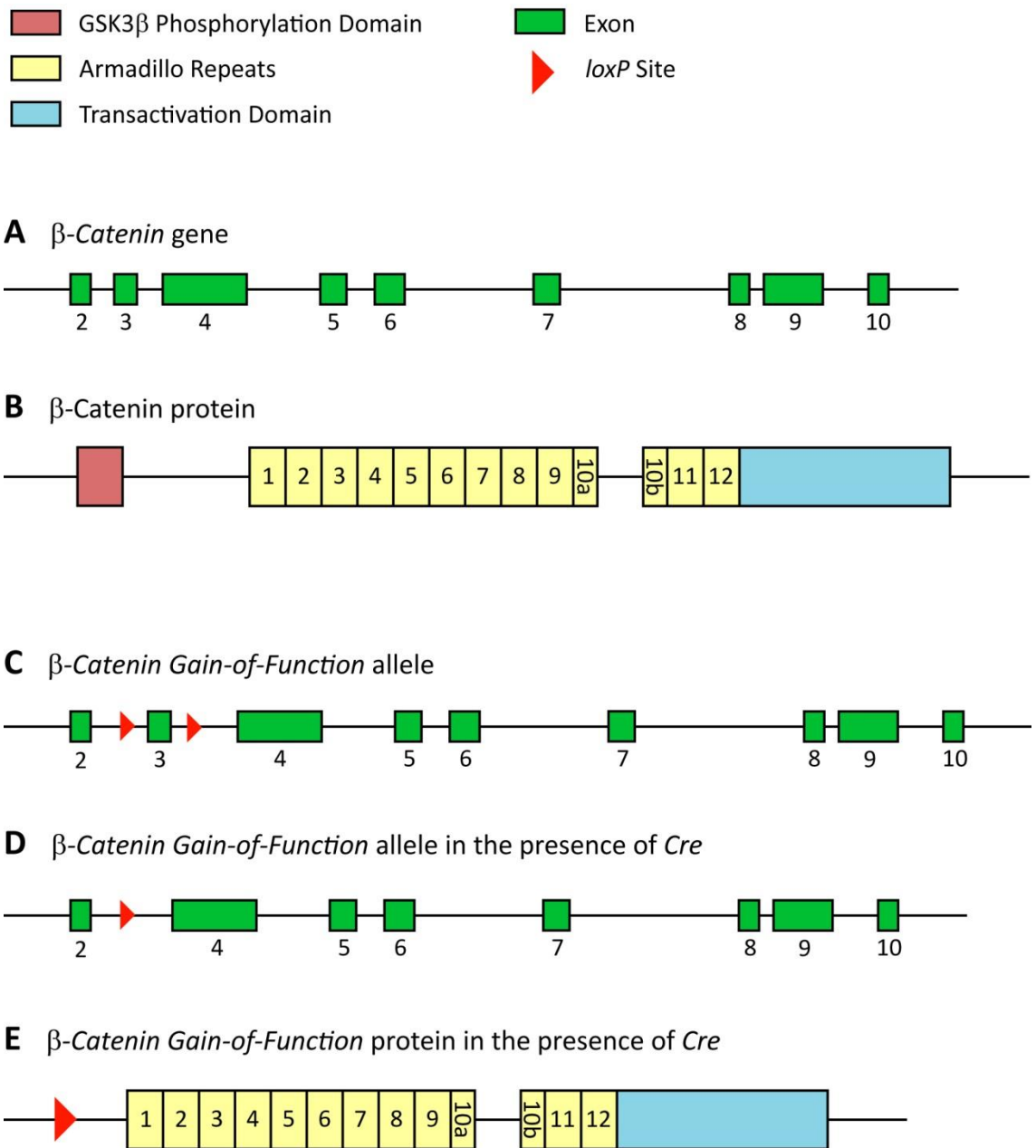


Figure 2.3: Structures of the β -catenin^{GOF} allele and protein. The wild type β -catenin allele (A) and protein (B) are shown for reference. In the intact β -catenin^{GOF} allele loxP sites surround exon 3, which contains the GSK3 β phosphorylation domain (C). When the Cre allele – and thus the Cre recombinase enzyme – is present, exon 3 is removed from the allele (D). This results in a protein lacking the GSK3 β phosphorylation domain (E).

2.4.2.3 The β -catenin Gain-Of-Function allele

The β -catenin allele used in the research described in this thesis was developed in 1999. The *Pax3*^{GOF} mouse was generated through the development of chimaeric mice and germline transmission (Harada et al., 1999). LoxP sites are positioned on either end of exon 3 along with a neo selection cassette. This results in the deletion of 76 amino acids from the protein, including the phosphorylation sites targeted by GSK3 β (**Figure 2.3**). Thus, when a Cre is present and the region between the LoxP sites excised the β -catenin protein is no longer able to be phosphorylated by GSK3 β . This reduces the targeting of β -catenin for ubiquitination and degradation, and the protein is stabilised (Harada et al., 1999).

The β -catenin GOF allele was originally created to study the effects of Wnt signalling activation in the gut (Harada et al., 1999). The allele was used in combination with a cytokeratin-19 Cre allele, which allowed the β -catenin^{GOF} allele to be expressed in the gut epithelium from early in development. Mice carrying the cytokeratin-19 Cre and β -catenin^{GOF} alleles developed intestinal polyposis shortly after birth (Harada et al., 1999).

Since the original research, this β -catenin^{GOF} allele has been used in combination with a large number of different Cre recombinase-expressing alleles for expression in a wide variety of tissues. A selection of these studies are summarised in **Table 2.1**.

2.4.2.4 β -catenin-null allele

The β -catenin-null (β -catenin⁻) allele was developed in 1995. The mice were generated through creation of a chimaeric germline mutant (Haegel et al., 1995). The allele contains an IRES- *β geo* cassette in place of exon 2 and part of exon 3 (**Figure 2.4**). A stop codon prevents translation of the remaining β -catenin allele (Haegel et al., 1995). Murine embryos which are homozygous for the β -catenin⁻ allele die around the time of gastrulation (Haegel et al., 1995).

2.4.2.5 β -catenin Loss-Of-Function allele

The β -catenin loss-of-function (β -catenin^{LOF}) allele contains *loxP* sites flanking exons 2-6, which are thus removed in the presence of Cre recombinase enzyme (Brault et al., 2001). Exons 2-6 contain a number of important regions, including the ATG translation start site, the GSK3 β phosphorylation domain, and part of the armadillo repeat domain (**Figure 2.5**). Its deletion prevents the production of a functional β -catenin protein (Brault et al., 2001).

The mice were generated through creation of a chimaeric germline mutant (Brault et al., 2001). The β -catenin^{LOF} allele was originally used in combination with Wnt1-Cre to study β -catenin LOF in the CNS. *Wnt1*^{Cre/+} β -catenin^{LOF/LOF} embryos developed a number of CNS defects, including failure to develop regions of the midbrain and hindbrain, and lack of craniofacial

Tissue	Cre Allele	Affected Cell Type	Phenotype	References
Bone/cartilage	<i>Col2a1</i>	Chondrocytes	Generalised chondrodysplasia, reduced proliferation. Perinatal lethal. Ectopic synovial joint formation.	(Akiyama et al., 2004; Guo et al., 2004)
Eye	<i>lens</i>	Lens surface ectoderm	Lens agenesis.	(Smith et al., 2005)
Limbs	<i>Prx1</i>	Limb mesenchyme	Premature regression of the apical ectodermal ridge, limb truncations.	(Hill et al., 2006)
Teeth	<i>K14</i>	Oral and dental epithelium	Supernumerary tooth generation.	(Jarvinen et al., 2006)
Kidney	<i>Hoxb7</i>	Kidney epithelium	Hypoplastic/cystic/absent kidneys. Reduced differentiation.	(Marose et al., 2008)
Heart	<i>Mef2c</i>	Second heart field	Small right ventricle. Thickened, hypercellular outflow tract and right ventricle myocardium.	(Ai et al., 2007)
Reproductive system	<i>MMTV</i>	Prostate epithelium	Hyperproliferation and transdifferentiation.	(Bierie et al., 2003)

Table 2.1: The effects of the β -catenin gain-of-function allele in different tissue types. Modified from (Grigoryan et al., 2008).

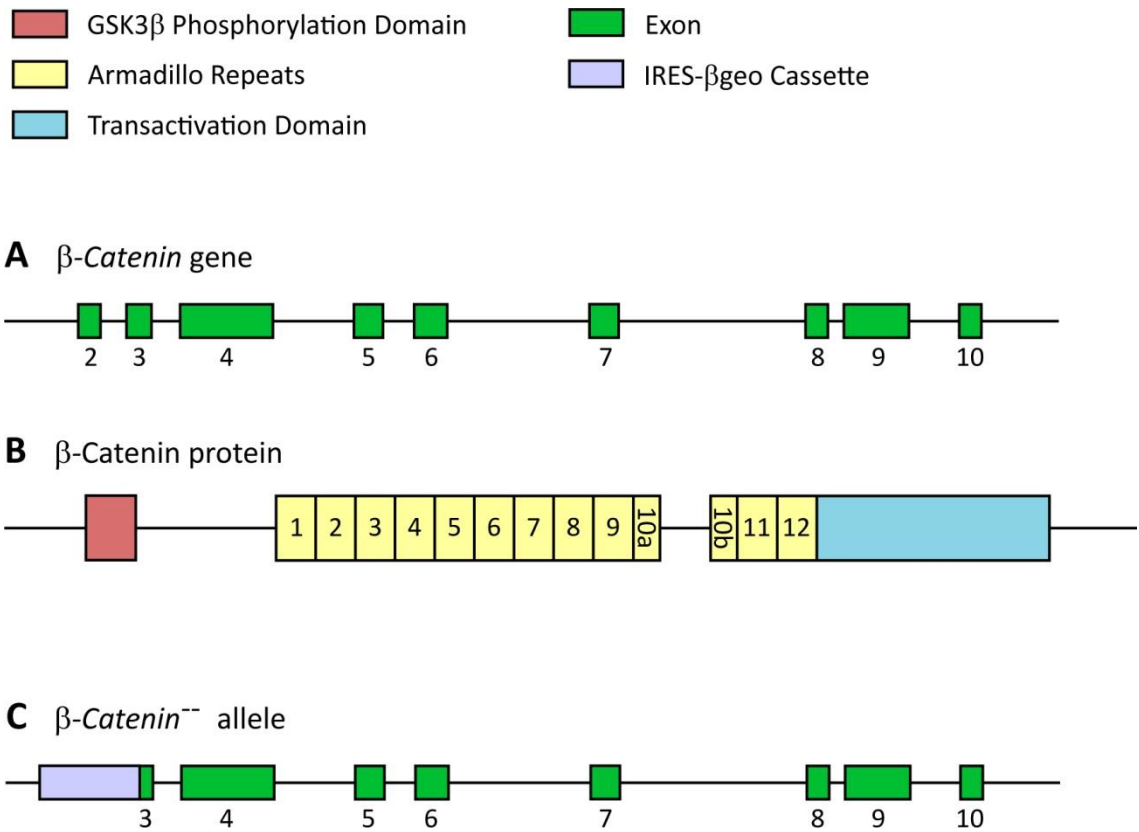


Figure 2.4: Structure of the β -catenin^{-/-} allele. The wild type β -catenin allele (A) and protein (B) are shown for reference. In the β -catenin^{-/-} allele the IRES- β geo cassette replaces exon 2 and part of exon 3 (C). A stop codon in the IRES- β geo cassette prevents translation of the remaining β -catenin protein. This results in a null allele.

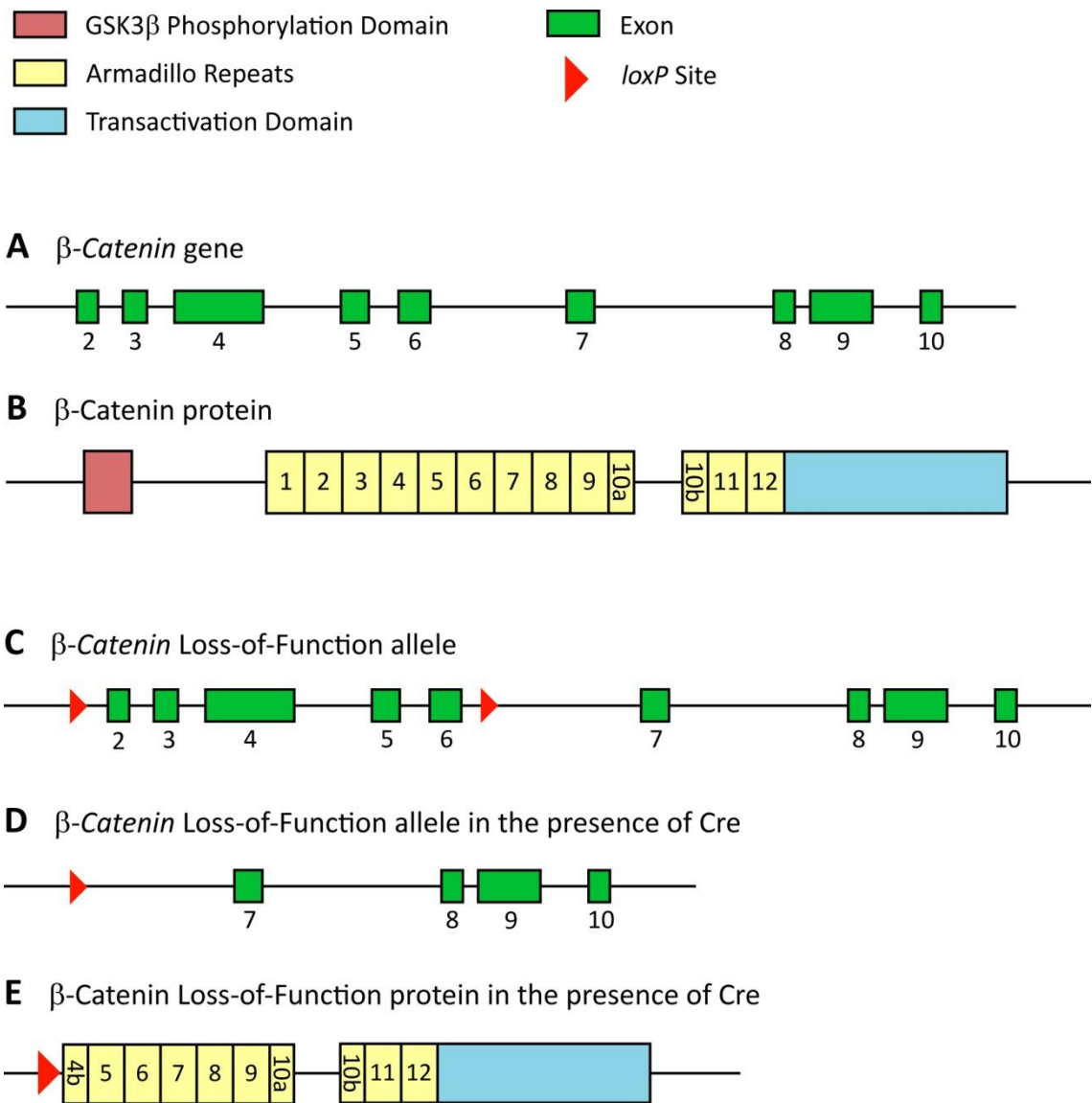


Figure 2.5: Structures of the β -catenin^{LOF} allele and protein. The wild type β -catenin allele (**A**) and protein (**B**) are shown for reference. In the intact LOF allele *loxP* sites flank exons 2-6, which encode the GSK3 β phosphorylation domain and part of the armadillo repeat domain (**C**). When the Cre recombinase enzyme is present the region is removed (**D**). This results in a functionally null protein (**E**).

structures (Brault et al., 2001). This latter aspect indicated a role for canonical Wnt signalling in the specification and/or differentiation of the NC.

Since its generation, the β -catenin^{LOF} allele has been used to study the role of canonical Wnt signalling in a number of different tissues and organ systems. Several examples of its use are summarised in **Table 2.2**.

2.4.3 Mouse lines

The mice described have been used for experiments discussed in this thesis.

2.4.3.1 *Pax3*^{Sp2H/+}

The *Spotch-2H* mutation is carried on a mixed background which includes CBA/Ca, 101 and C3H/He. The heterozygous colony is maintained through the cross *Pax3*^{Sp2H/+} x *Pax3*^{+/+}.

2.4.3.2 *Pax3*^{Cre/+}

The *Pax3*^{Cre} allele (Engleka et al., 2005) is carried on a C57BL/6 background. The heterozygous colony is maintained through the cross *Pax3*^{Cre/+} x *Pax3*^{+/+}.

2.4.3.3 β -catenin^{GOF/GOF}

The *Pax3*^{GOF} allele is carried on a C57BL/6 background, and the homozygous colony is maintained through the cross β -catenin^{GOF/GOF} x β -catenin^{GOF/GOF}.

2.4.3.4 β -catenin^{LOF/+}

The β -catenin^{LOF} allele is carried on a C57BL/6 background, and the heterozygous colony is maintained through the cross β -catenin^{LOF/+} x β -catenin^{+/+}.

2.4.3.5 β -catenin^{+/-}

This allele is carried on a C57BL/6 background, and the heterozygous colony is maintained through the cross β -catenin^{+/-} x β -catenin^{+/+}.

2.4.3.6 *BatGal*⁺

These mice were generated through DNA microinjection into the pronuclei of single-cell embryos (Maretto et al., 2003). The allele is carried on a C57BL/6 background, and the heterozygous colony is maintained through the cross *BatGal*⁺ x *+/+*.

2.4.3.7 *p53*^{+/-}

This allele was originally conditional, and the mice were generated by the production of germline chimaeras (Jonkers et al., 2001). The mutation is carried on a mixed CBA/101 background. Embryos carrying the conditional allele were first bred to β -actin^{Cre/+} embryos to remove p53 expression ubiquitously, including the germ cells. These animals were then

Tissue	Cre Allele	Affected Cell Type	Phenotype	References
Bone/cartilage	<i>Col2a1</i>	Chondrocytes	Perinatal lethal. Hypoproliferative chondrocytes. Embryos have a form of dwarfism.	(Akiyama et al., 2004)
Eye	<i>lens</i>	Lens surface ectoderm	Microphthalmia. Ectopic lens. Abnormal lens morphogenesis.	(Smith et al., 2005)
Heart	<i>Mef2c</i>	Second heart field	Reduced right ventricle with thin myocardium. Defective outflow tract formation.	(Ai et al., 2007)
Kidney	<i>Hoxb7</i>	Kidney epithelium	Absent or unbranched ureter. Kidney hypoplasia/aplasia. Cystic kidneys.	(Marose et al., 2008)
Limb	<i>Brn4</i>	Apical ectodermal ridge	Malformed/absent hindlimbs. Dorsalised hindlimbs. Loss of apical ectodermal ridge.	(Soshnikova et al., 2003)
Tate buds	<i>K14</i>	Tongue epithelium	Loss of fungiform papilla.	(Liu et al., 2007)
Lung	<i>Dermo1</i>	Lung mesenchyme	Small, misshapen lungs. Less epithelial branching. Degenerated trachea. Reduced mesenchyme.	(Yin et al., 2008)

Table 2.2: The effects of the β -catenin loss-of-function allele in different tissue types. Modified from (Grigoryan et al., 2008).

interbred to remove the β -actin^{Cre} allele. The heterozygous colony is maintained through the cross $p53^{+/-}$ x $p53^{+/+}$.

2.4.3.8 Sox1^{Cre/+}

The mice were generated through homologous recombination in ES cells, followed by the generation of germline mutant mice (Takashima et al., 2007). The allele is carried on a C57BL/6 background, and the heterozygous colony is maintained through the cross $Sox1^{Cre/+}$ x $Sox1^{+/+}$.

2.4.3.9 Compound mutant mouse lines

Some of the genetic crosses carried out require breeding with mice carrying more than one mutation. Compound mutants are generated only for experimental breeding. The crosses required to generate the compound mutants are described in **Table 2.3**.

2.4.3.10 Mouse genetic crosses

The following crosses were carried out in the research described in this thesis.

- $Pax3^{Sp2H/+}$ x $Pax3^{Sp2H/+}$
- $Pax3^{Sp2H/+}$ $p53^{+/-}$ x $Pax3^{Sp2H/+}$ $p53^{+/-}$
- $Pax3^{Sp2H/+}$ $BatGal/+$ x $Pax3^{Sp2H/+}$
- $Pax3^{Sp2H/+}$ β -catenin^{GOF/+} x $Pax3^{Cre/+}$ β -catenin^{+/+}
- $Pax3^{Sp2H/+}$ β -catenin^{LOF/+} x $Pax3^{Cre/+}$ β -catenin^{+/-}
- $Pax3^{Sp2H/+}$ β -catenin^{LOF/+} x $Pax3^{Cre/+}$ β -catenin^{LOF/+}
- $Pax3^{Sp2H/+}$ β -catenin^{GOF/+} x $Sox1^{Cre/+}$

2.4.4 Embryo dissection

Litters were obtained from timed matings. The matings were carried out either overnight or during the day, and the time of plug detection was designated embryonic day (E) 0.5. Females were killed using cervical dislocation, and the embryos were removed from the female through hysterectomy. Dissection of the embryos from the uterus was carried out in Dulbecco's Modified Eagle's Medium (DMEM, Invitrogen, Massachusetts) containing 10% heat-inactivated fetal bovine serum (FBS, Invitrogen, Massachusetts), which was pre-warmed to 37°C. Dissection was carried out using a dissection microscope.

2.4.4.1 Dissection for tissue collection

The decidua was removed from the uterus, and then placed in fresh DMEM and FBS. Embryos were removed from the decidua, the trophoblast, and Reichert's membrane. The yolk sac was usually collected for genotyping by PCR (see section 2.5.2). The embryo was then finally removed from the chorion. Measurements were taken using an eyepiece graticule. The

Compound Mutant Genotype	Genetic Cross
<i>Pax3</i> ^{Sp2H/+} <i>p53</i> ^{+/-}	<i>Pax3</i> ^{Sp2H/+} x <i>p53</i> ^{+/-}
<i>Pax3</i> ^{Sp2H/+} <i>BatGal</i> /+	<i>Pax3</i> ^{Sp2H/+} x <i>BatGal</i> /+
<i>Pax3</i> ^{Sp2H/+} <i>β-catenin</i> ^{GOF/+}	<i>Pax3</i> ^{Sp2H/+} x <i>β-catenin</i> ^{GOF/GOF}
<i>Pax3</i> ^{Sp2H/+} <i>β-catenin</i> ^{LOF/+}	<i>Pax3</i> ^{Sp2H/+} x <i>β-catenin</i> ^{LOF/+}
<i>Pax3</i> ^{Cre/+} <i>β-catenin</i> ^{LOF/+}	<i>Pax3</i> ^{Cre/+} x <i>β-catenin</i> ^{LOF/+}
<i>Pax3</i> ^{Cre/+} <i>β-catenin</i> ^{+/-}	<i>Pax3</i> ^{Cre/+} x <i>β-catenin</i> ^{+/-}

Table 2.3: Compound mutant genotypes and the genetic crosses required to produce them.

embryo was then washed in PBS, and either immediately frozen at -80°C without liquid, or fixed and dehydrated (see section 2.4.6).

2.4.4.2 Dissection for embryo culture

Embryos for culture were dissected late on day E8.5. The decidua was removed from the uterus, and then placed in fresh DMEM and FBS. Embryos were removed from the decidua, the trophoblast, and Reichert's membrane without puncturing the yolk sac or damaging the ectoplacental cone. The embryo in the yolk sac was then removed to fresh DMEM and FBS for a short time until culture.

2.4.5 Embryo Culture

Prior to embryo culture rat blood was collected, and the serum separated and heat-treated for 30 minutes at 56°C. This rat serum was stored at -20°C until use.

Embryos were dissected down to the yolk sac and ectoplacental cone as described previously (section 2.3.3.2). Rat serum was defrosted and warmed to 37°C, and then syringed through a 0.45 µm filter. 0.5-1.0 ml rat serum was allowed per embryo. The rat serum was separated into culture tubes, no more than 3 ml per tube, and the top of the tube was greased to seal the lid against gas exchange. Gas containing 5% CO₂ and 5% O₂ was gently blown onto the surface of the rat serum for 1 minute. The embryos were added, no more than 4 to a tube, and then gassed again, before being placed in a 37°C incubator on a roller to keep the fluid moving.

Cultures were carried out for approximately 42 hours. The tubes were gassed approximately every 12 hours, and the composition of the gas changed with embryonic age: E8.5 embryos were gassed with 5% O₂ and 5% CO₂, E9.5 embryos with 20% O₂ and 5% CO₂, and E10.5 embryos with 40% O₂ and 5% CO₂.

Some cultures included the canonical Wnt inhibitor XAV939 (Sigma, Missouri). In these cultures, XAV939 was first mixed with dimethyl sulfoxide (DMSO) to give a suspension at a concentration of 125 mM. A 1 in 50 dilution of the XAV939 suspension was made using PBS-DEPC, to give a working solution at a concentration of 2.5 mM. This working solution was diluted into the rat serum at the desired concentration.

Once the culture was complete the embryos were removed from the culture tubes into DMEM and FBS, and then dissected as in section **2.4.4.1**. The embryos were either frozen at -80°C without liquid, or fixed and dehydrated (see section **2.4.6**).

2.4.6 Tissue fixation and dehydration

Fresh tissue was fixed by placing it immediately in cold paraformaldehyde (PFA), and incubating overnight at 4°C.

The fixed tissue was dehydrated on ice using cold solutions. It was first washed twice for 15 minutes in PBS to removed PFA, and then incubated in increasing concentrations of methanol in DEPC-treated water. Once the tissue was in 100% methanol, it was stored at -20°C.

2.4.7 Tissue sections

2.4.7.1 Paraffin wax sections

Embryos were previously fixed and dehydrated (see section **2.4.6**), and then stored in 100% methanol at -20°C prior to embedding.

Embryos were incubated in 100% ethanol through two 30 minute washes, and then incubated twice in a glass embedding mould in Histoclear (National Diagnostics, Georgia) – once at room temperature and once at 60°C. The length of the Histoclear washes was dependent on the stage of the embryo; 15 minutes for E8.5, 20 minutes for E9.5, and 30 minutes for E10.5. The embryos were then incubated in the embedding moulds in molten wax at 60°C for three hours, with fresh wax every 45 minutes.

Following the incubations, the moulds were moved to room temperature, and the embryo positioned for sectioning as the wax set. The wax was left to set in the moulds for at least 24 hours at room temperature prior to sectioning. Brief incubations at -20°C allowed the wax-embedded embryos to be removed from the moulds.

Wax blocks were shaped to a cube containing the embryo, and then mounted onto wooden blocks using molten wax. Sections were cut to a thickness of 7 μm , and then incubated on a water-covered slide over a heater for a few minutes to smooth out wrinkles in the wax. The water was then removed, and the slides were left to dry at 37°C for at least 24 hours.

2.4.7.2 Vibratome sections

Embryos were fixed prior to embedding (see section **2.4.6**), and then washed in PBS. If they were also dehydrated for storage at -20°C, they were then rehydrated through a series of incubations in decreasing concentrations of methanol in PBS, and then washed twice in PBS.

Embryos (or pieces of embryo) were incubated overnight in a gelatin-albumin mix (0.45% gelatin, 27% albumin, 18% sucrose in PBS) at 4°C. The following day, 200 μl gelatin-albumin mix was pipetted into a mould. 20 μl glutaraldehyde (Sigma, Missouri) was then added and very quickly mixed before the embryo was placed and positioned in the mould. The block set at room temperature for 30 minutes, and was then removed from the mould and stored in PBS at 4°C.

The gelatin-albumin blocks were incubated in PBS at 4°C for at least 1 hour prior to sectioning. Blocks were trimmed and mounted, and sectioned using a vibratome at a thickness of 40 μm (frequency 8, speed 7). Sections were mounted in 50% glycerol in distilled water.

2.4.7.3 Eosin staining of tissue sections

Embryos were first embedded and sectioned in wax (see section **2.4.7.1**), and mounted onto glass slides. The slides were dewaxed by incubating them twice in HistoClear for 10 minutes per wash, and then rehydrated by incubating them briefly in decreasing concentrations of ethanol in water. They were then washed twice in water.

To develop the colour, the sections were incubated in 1% eosin Y (Acros Organics, Geel) in distilled water for 3-5 minutes. They were then washed twice very briefly in water and checked under a microscope. If the colour needed further development they were again incubated in eosin. Once the colour was a little darker than desired the sections were dehydrated by incubating them for 10 seconds per step in increasing concentrations of ethanol in distilled water, until they were in 100% ethanol. This step fades the colour a little. The sections were then transferred briefly to HistoClear, before being washed in fresh HistoClear for 5-10 minutes. The slides were mounted using di-n-butyl phthalate (DPX, BDH).

2.5 DNA Methods

2.5.1 DNA Extraction

DNA was extracted from yolk sac tissue collected during dissection of embryos. A Lysis mixture was made using 1 in 5 DNareleasey (Anachem, Luton) in PBS, and 20 µl of this mixture was added to each yolk sac, covering the tissue. The mixture and yolk sac were then put into a thermal cycler, and the appropriate program was run.

2.5.2 PCR

PCR was used to genotype embryos. DNA extracted from the yolk sac was used for the reaction.

2.5.2.1 PCR Cycles

Program No.	Start		Cycle		No. of Cycles	Finish	
	Temp (°C)	Time (mins)	Temp (°C)	Time (s)		Temp (°C)	Time (mins)
1	94	2	94 60 72	30 30 45	32	72	5
2	94	4	96 62 72	20 20 30	40	72	10
3	94	1.5	94 60 72	30 60 60	35	72	2
4	94	2	94 60 72	30 30 150	31	72	10
5	94	2	94 58 72	30 30 45	35	72	5
6	94	5	94 60 72	60 60 60	35	72	5
7	94	2	94 63 72	30 30 45	29	72	5
8	65	15	96 65 96 65 96	120 240 60 60 30	1	-	-

Table 2.4: PCR cycles.

2.5.2.2 PCR Primers

Allele	Primer	Primer Sequence	Wild Type band size (bp)	Mutant band size (bp)	Cycle
Sp2H	Forward	CCTCGGTAAGCTTCGCCCTCTG	122	90	1
	Reverse	CAGCGCAGGAGCAGAACCACCTTC			
Pax3-Cre	1	CTGCACTCGGTGTCACG	~300	~600	1
	2	AAGCGAGCACAGTGCGGC			
	3	GAAACAGCATTGCTGTCACTTGTCGTGGC			
β -catenin GOF	Forward	AGAATCACGGTGACCTGGGTAA AA	600	800 (550 when floxed)	2
	Reverse	CATTCATAAAGGACTTGGGAGGTGT			
β -catenin LOF	Forward	AAGGTAGAGTGATGAAAGTTGTT	221	324	3
	Reverse	CACCATGTCTCTGTCTATTC			
p53 deleted	Forward	CACAAAAACAGGTTAAACCCAG	None	~600	1
	Reverse	GAAGACAGAAAAGGGGAGGG			
p53 wild type	Forward	CACAAAAACAGGTTAAACCCAG	300	None	1
	Reverse	AGCACATAGGAGGCAGAGAC			
β -catenin null	1	CATGGACAGGGTGGCCTGA	220	150	4
	2	TGTTTTTCGAGCTTCAAGGTTTCAT			
	3	AGAATCACGGTGACCTGGGTAAAA			
BatGal	Forward	TTATCGATGAGCGTGGTGGTTATGC	None	400	5
	Reverse	GCGCGTACATCGGGCAAATAATATC			
GAPDH	Forward	ATGACATCAAGAAGGTGGTG	177	NA	6
	Reverse	CATACCAGGAAATGAGCTTG			
Cre	A	ACCCTGATCCTGGCAATTTCCGG C	None	500	7
	B	GATGCAACGAGTGATGAGGTTC GC			

Table 2.5: PCR primers. All primers are from Sigma, Missouri.

2.5.2.3 Method

The following PCR mixture was used.

PCR mixture (50 μ l)

2 μ l DNA

5 μ l 10x PCR Rxn buffer (Invitrogen, Massachusetts)

1.5 μ l 1.5 mM MgCl₂ (45 μ M, Invitrogen, Massachusetts)

5 μ l 2mM dNTP mix (dATP, dCTP, dGTP and dTTP, all Promega, Wisconsin)(0.2 mM)

0.3 μ l 40 μ M Forward primer (0.24 μ M)

0.3 μ l 40 μ M Reverse primer (0.24 μ M)

0.25 μ l 5 U/ μ l Taq DNA polymerase (0.025 U/ μ l, Invitrogen, Massachusetts)

Milli-Q water to 50 μ l

Distilled water was used as a negative control. The tubes containing the mixture were placed in a thermal cycler, and an appropriate PCR program was run. 2.5% agarose gels were made by heating together 2.5 g agarose powder per 100 ml TAE buffer until the agarose was fully dissolved. Once it had cooled slightly 6 μ l ethidium bromide (Sigma, Missouri) was added per 100 ml agarose mixture. This was left to cool until solid with a comb to form wells. The PCR samples were then loaded onto the 2.5% agarose gel for electrophoresis, and imaged under ultraviolet (UV) light.

2.5.3 Transformation

20-100ng target plasmid was added to the bottom of a chilled 1.5 ml tube. Competent cells (DH5 α) were thawed on ice, and then a 50 μ l aliquot was added to the plasmid and gently mixed. The tube containing plasmid and competent cells was incubated on ice for 20 minutes, heat shocked at 42°C for 45 seconds, and then returned to ice for at least 2 minutes. 950 μ l LB broth (2.5% LB Broth, Invitrogen, Massachusetts, in Milli-Q water) was added to the tube, and the mixture was incubated with shaking at 37°C for 1 hour. The cells were then ready to be plated.

Probe Gene Name	Vector	Insert Size	Partial or Full Length	Antibiotic Resistance	Linearisation Enzyme		Polymerase		Obtained From
					Sense	Anti-sense	Sense	Anti-Sense	
Pax3	pGEM-T	186 bp	Partial	Ampicillin					Cloned previously in our lab by Deborah Henderson.
Axin2						NotI		T3	
FoxD3	pBlueScript	558 bp	Partial	Ampicillin	HindIII	BamHI	T7	T3	
ErbB3	pBS-DR3	1.4 kb	Partial	Ampicillin	XhoI	EcoRI	T3	T7	Carmen Birchmeier, Berlin.
Ngn2	pBlueScript-SK	2.2 kb	Full	Ampicillin		NotI		T7	Dr David J. Anderson, California Institute of Technology
Brn3a	pBS	220 bp		Ampicillin	NotI	HindIII	T3	T7	Supplied by Shanie.

Table 2.6: Plasmids used for transformation. These plasmids contains probes for use in *in situ* hybridisation.

2.5.4 Plasmid extraction

Transformed cells were plated under sterile conditions onto LB agar plates (32% LB agar, Invitrogen, in Milli-Q water) containing an appropriate antibiotic, and allowed to grow overnight at 37°C. Individual white colonies from the plates were picked into 5 ml LB broth containing the same antibiotic, and incubated overnight in a 37°C shaker. Around 3 ml of the resulting mixture was treated using the Qiagen (Venlo) QIAprep Spin Miniprep Kit (following the kit protocol), and the concentration of DNA in the final elution was estimated using a NanoDrop. The plasmid was stored at -20°C.

2.5.5 Plasmid linearisation

An appropriate restriction enzyme was chosen, and the following restriction digest set up.

Restriction digest (200 µl)

5 – 10 µg Plasmid DNA

1 x Restriction Enzyme Buffer (Promega (Wisconsin), Fermentas (Massachusetts) or New England Biolabs (Massachusetts))

20 - 50 U Restriction Enzyme (Promega (Wisconsin), Fermentas (Massachusetts) or New England Biolabs (Massachusetts))

1 x Bovine serum albumin (if recommended by manufacturer)

Milli-Q water to 200 µl

The digest was incubated for 2 – 4 hours at the optimal temperature for the restriction enzyme, as recommended by the manufacturer. The plasmid was either cleaned immediately, or stored at -20°C until it was cleaned. The plasmid was cleaned using the QIAquick PCR Purification kit, following the recommended protocol. The concentration of the cleaned plasmid could be estimated using a NanoDrop.

2.5.6 Whole mount TUNEL staining

TUNEL staining was carried out using the Millipore (Massachusetts) ApopTag Peroxidase *in situ* Apoptosis Detection Kit. Prior to this assay, embryos were fixed in 4% PFA, dehydrated into 100% methanol, and stored at -20°C.

2.5.6.1 Day 1: Permeabilisation and TdT enzyme incubation

Embryos were rehydrated into PBT using decreasing concentrations of methanol. They were then incubated in 10 µg/ml proteinase K diluted in PBT. The length of the incubation was dependent on the developmental stage of the embryo, as shown below.

E8.5: 1 minute

E9.5: 4 minutes

E10.5: 8 minutes

The embryos were washed in 2 mg/ml glycine in PBT immediately following the proteinase K incubation. This ensures cessation of the proteinase K reaction. The embryos were then incubated for 20 minutes in 4% PFA, washed, and then fixed in an ice-cold 2:1 mixture of ethanol and asetic acid on ice for 10 minutes. Following further washing, the embryos were incubated in equilibration buffer from the kit for 1 hour at room temperature, and then left overnight at 37°C in working strength TdT enzyme, also from the kit.

2.5.6.2 Day 2: Washing, blocking, and antibody incubation

The TdT enzyme reaction was halted by washing the embryos in working strength stop/wash buffer from the kit for 3 hours with several changes of solution. They were then blocked for at least 1 hour in a blocking solution containing 5% heat-treated sheep serum and 2 mg/ml bovine serum albumin (BSA) in PBT.

After blocking, the embryos were incubated in 0.5 µl/ml Anti-digoxigenin AP-conjugated Fab Fragments (Roche, Penzberg) in a blocking solution containing 1% heat-treated sheep serum and 2 mg/ml BSA in PBT. This incubation was carried out for 2 hours at room temperature. They were then washed in 2 mg/ml BSA in PBT overnight at 4°C with multiple changes of solution.

2.5.6.3 Day 3: Developing

Embryos were equilibrated in NTMT by washing three times for 5 minutes. They were then incubated in the dark in a developing solution containing NBT/BCIP in NTMT for around 10 minutes, or until the stain had developed sufficiently, and then the reaction was stopped using washes in PBT.

NTMT (50 ml)

1 ml 5M NaCl (100 mM, Fisher Scientific, New Hampshire)

2.5 ml 2M Tris HCl pH 9.5 (100 mM)

1.25 ml 2M MgCl₂ (50 mM, Fluka Analytical, Buchs)

0.5 ml Tween-20 (Sigma, Missouri)

DEPC-treated water to 50 ml

Developing solution (5 ml)

5 ml NTMT

85 µl NBT/BCIP (0.32 µg/µl NBT, 0.16 µg/µl BCIP, Roche, Penzberg)

Finally, the embryos were fixed for 30 minutes at room temperature in 4% PFA, and then washed in PBT.

2.6 RNA methods

2.6.1 Whole mount *in situ* hybridisation

Prior to whole mount *in situ* hybridisation embryos were fixed in 4% PFA, dehydrated into 100% methanol, and stored at -20°C.

2.6.1.1 Day 1: Embryo pre-treatment and hybridisation

Embryos were rehydrated on ice into PBT using decreasing concentrations of methanol in PBT. They were then bleached in 6% hydrogen peroxide (Sigma, Missouri) in PBT on ice for 1 hour, and washed in PBT. The embryos were then treated with 5 µg/ml proteinase K depending on their developmental stage, as shown below.

E8.5: 1 minute

E9.5: 2 minutes

E10.5: 7 minutes

The embryos were washed in glycine solution (Fisher Scientific, New Hampshire, 2 mg/ml in PBT) to stop the proteinase K reaction, and then in PBT. They were then fixed in 4% PFA containing 0.2% glutaraldehyde (Sigma, Missouri) for 20 minutes at room temperature, and then again washed in PBT.

Embryos were pre-hybridised in hybridisation mixture at 70°C for at least 2 hours. Hybridisation mixture containing the RNA probe was then applied to the embryos, and they were incubated overnight at 70°C. Sense probe was used as a negative control where necessary.

Hybridisation Mixture (50 ml)

25 ml Formamide (Sigma, Missouri)

12.5 ml 20x SSC pH 4.5

5 ml 10% SDS

25 µl 10 mg/ml Yeast RNA (50 µg/ml)

100 µl 25 mg/ml Heparin (50 µg/ml)

DEPC-treated water to 50 ml

20x SSC pH 4.5 (500 ml)

87.7 g NaCl

44.1 g Sodium Citrate (Fluka Analytical, Buchs)

500 ml DEPC-treated water

Adjust to pH 4.5 using hydrochloric acid. Autoclave.

10% Sodium dodecyl sulfate (SDS, 500 ml)

50 g SDS (Sigma, Missouri)

500 ml DEPC-treated water

2.6.1.2 Day 2: Post-hybridisation

The following solutions were made and heated to hybridisation temperature.

Solution 1 (50 ml)

25 ml Formamide

12.5 ml 20x SSC

5 ml 10% SDS

DEPC-treated water to 50 ml

Solution 2 (50 ml)

25 ml Formamide

5 ml 20x SSC

5 ml 10% SDS

DEPC-treated water to 50 ml

The probe-hybridisation mixture was removed from the embryos for storage at -20°C and future use, and solution 1 was applied to the embryos for a 15 minute wash at hybridisation temperature. This is followed by two further washes in solution 1 for 30 minutes each at hybridisation temperature, and then two 30 minute washes in solution 2 at a temperature 5° lower than hybridisation temperature.

Embryos were washed in TBST, and then blocked for at least 1 hour at room temperature in 10% heat-treated sheep serum in TBST. They were then incubated overnight at 4°C in a 1:2000 concentration Anti-digoxigenin AP-conjugated Fab Fragments (Roche, Penzberg) in TBST containing 1% heat-treated sheep serum.

2.6.1.3 Day 3: Washing

The embryos were washed several times briefly, and then for longer incubations, all in TBST, and all at room temperature. They were then washed overnight in TBST at 4°C.

2.6.1.4 Day 4: Developing

Embryos were equilibrated in NTMT. They were then incubated in developing solution, described below.

NTMT (50 ml)

1 ml 5M NaCl (100 mM)
2.5 ml 2M Tris HCl pH 9.5 (100 mM)
1.25 ml 2M MgCl₂ (50 mM)
0.5 ml Tween-20
DEPC-treated water to 50 ml

Developing solution (5 ml)

5 ml NTMT
22.5 µl NBT (4.5 µl/ml, Roche, Penzberg)
17.5 µl BCIP (3.5 µl/ml, Roche, Penzberg)

The embryos were incubated in this solution protected from light.

2.6.2 RNA extraction

Tissue was previously stored without liquid at -80°C. It was kept on ice throughout RNA extraction (unless otherwise stated) to minimise RNA degradation.

Frozen tissue (from dry ice) was homogenised in 500 µl Trizol (Ambion, Massachusetts) through vigorous pipetting in a fine pipette tip, and the sample was then incubated at room temperature for 5 minutes. 100 µl chloroform was added, and the tube was shaken vigorously for 15 seconds. The sample was then incubated at room temperature for a further 2-3 minutes, before being centrifuged at 12000 x g for 15 minutes at 4°C. Following centrifugation the upper aqueous phase contained the RNA and was removed to a fresh tube.

In order to precipitate the RNA from the solution, 250 µl isopropyl alcohol was added to the sample. The mixture was vortexed and incubated for 10 minutes at room temperature, and then centrifuged at 14000 x g for 10 minutes at 4°C to pellet the RNA. The supernatant was removed, and the pellet washed using 500 µl 75% methanol (in DEPC-treated water). The RNA was pelleted again by centrifugation at 12000 x g for 5 minutes at 4°C. The supernatant was removed, and the pellet left to air-dry for around 15 minutes, before being resuspended in 20 µl RNase-free water.

The sample was then DNase-treated using the Ambion (Massachusetts) DNasefree kit, following the protocol given by the manufacturer, and the resulting elution was analysed with a NanoDrop to estimate the concentration of the RNA.

2.6.3 RNA purification

2.6.3.1 Using the ChromaSpin-100 DEPC-H₂O Columns (Clontech, California)

The manufacturer recommended protocol was used. Then 40 µl formamide and 1 µl RNase inhibitor (Roche, Penzberg) were added to the cleaned RNA, and the probe was stored at -20°C.

2.6.3.2 Using precipitation

4 µl 0.2M EDTA (Sigma, Missouri) was added to stop the transcription, then the RNA was precipitated using 4 µl 4M lithium chloride (Sigma, Missouri), 1 µl tRNA (Sigma, Missouri) and 100 µl 100% ethanol, and overnight incubation at -20°C. The precipitated RNA was pelleted by centrifugation at 13000 rpm for 10 minutes at 4°C. The pellet was washed first with 70% ethanol, and then with 100% ethanol, centrifuging the pellet as described above, and discarding the supernatant for each step. The pellet was dissolved in a suitable volume of RNase-free water for 15 minutes at 65°C. 1 µl RNase Inhibitor (Roche, Penzberg) was added, and the RNA was stored at -20°C.

2.6.4 Real time quantitative PCR

2.6.4.1 First strand cDNA synthesis

The VILO Superscript cDNA Synthesis Kit (Invitrogen, Massachusetts) was used for this reaction, and the manufacturer recommended protocol was used. The following reaction mixture was made.

cDNA Synthesis (20 µl)

2 µg RNA

4 µl 5x VILO Reaction mix (Invitrogen, Massachusetts)

2 µl 10x SuperScript enzyme mix (Invitrogen, Massachusetts)

Nuclease-free water to 20 µl

The reaction was incubated at room temperature for 10 minutes, and then put into a thermal cycler. The cycler held the reaction at 42°C for 1 hour, and then terminated the reaction by incubating it at 85°C for 5 minutes. Samples were stored at -80°C.

The quality of the resulting cDNA was tested using PCR for the gene *GAPDH*. See section 2.5.2 for details.

2.6.4.2 RT-qPCR reaction

The real time quantitative PCR (RT-qPCR) was carried out using the following mixture per well.

- 12.5 µl RealTime PCR Mesa Blue qPCR Master Mix Plus for SYBR Assay
- 1.5 µl Forward primer (10 µM stock solution)
- 1.5 µl Reverse primer (10 µM stock solution)
- 2 µl cDNA
- 7.5 µl DEPC-treated water

DEPC-treated water was used as a negative control for each primer pair. The following thermal cycle was used for the reaction. Primers were designed to function at the following temperatures, and were tested before use.

- 2 minutes at 50°C
 - 5 minutes at 95°C
 - 15 seconds at 95°C
 - 1 minute at 60°C
 - 1 minute at 60°C
- } x 40

The gene *GAPDH* (*glyceraldehyde 3-phosphate dehydrogenase*) was used as a house-keeping gene for normalisation of expression of the genes. *β-Actin* was used as a second house-keeping gene for *Axin2* to verify the results. See **Table 2.7** for information about the primer pairs used.

Each reaction was carried out in triplicate. A dissociation curve was also observed for each reaction to check for primer dimerization or other failure of the experiment. Any reaction in which the qPCR result for C_T differed from the other repeats by 0.2 or more was not included in the data. An RQ was calculated for each embryo by averaging the RQs for the replicates included in the data (discussed with individual experiments, at least 2 replicates per condition). An RQ was then calculated for each genotype or group by taking the average of the embryos in the group. All results were normalised to the average RQ for the control group, which was given the value 1.

Gene	Forward primer sequence (5' – 3')	Reverse primer sequence (5' – 3')	Region Amplified (bp)	Reference
<i>GAPDH</i>	ATGACATCAAGAAGGT GGTG	CATACCAGGAAATGA GCTTG	1001-1177	(Gustavsson et al., 2007)
<i>Axin1</i>	CCTCTACCTCACATTCC TCGCACTT	TCAACCGTTCTCCTCAA CTTTTCT	1534-1676	(Sun et al., 2012)
<i>Axin2</i>	AAGCCTGGCTCCAGAA GATCACAA	TTTGAGCCTTCAGCA TCCTCTGT	2560-2694	
<i>Cdx2</i>	TCCTGCTGACTGCTTTC TGA	CCCTTCCTGATTTGTG GAGA	1639-1802	(Koch et al., 2012)
<i>Fzd6</i>	GCGGCGTTTGCTTCGT T	CACAGAGGCAGAAG GACGAAGT	1380-1454	(Hayashi et al., 2009)
<i>Sfrp4</i>	ATCCTGGCCATCGAAC AGTATGAA	GCACCATCATATCTG GTGTGAT	421-742	(Johnston et al., 2010)
<i>Dll1</i>	GGATCTGAACTACTGC ACTC	GAGCACACTCACTAC CTC	1594-1733	Designed by Nick Greene
<i>Fos1</i>	GTCGACCTAGGGAGGA CCTTAC	CATCTCTGGAAGAGG TGAGGAC	1391-1498	(Watanabe et al., 2009)
<i>Pax3: 1</i>	GGCTTTTCGAGAGAACC CACT	AGGTCTCCGACAGCT GGTAT	1093-1316	
<i>Pax3: 2</i>	GTGCTCGCTTTTCGTC TCG	CAGAGGCCTGCCGTT GATAA	325-538	

Table 2.7: RT-qPCR primers. All primers are from Sigma (Missouri). *Pax3: 1* and *Pax3: 2* primers were designed using Primer-BLAST online software (<http://www.ncbi.nlm.nih.gov/tools/primer-blast/>). Primers were designed to work using the thermal cycle described above.

2.6.5 Transcription for *in situ* probes

The following transcription reaction was set up.

Transcription (20 µl)

- 1 µg Linearised DNA
- 2 µl DIG labelling mix (Roche, Penzberg)
- 2 µl 10x Transcription buffer (Roche, Penzberg)
- 0.5 µl RNase inhibitor (Roche, Penzberg)
- 2 µl relevant polymerase (Roche, Penzberg)
- Nuclease-free water to 20 µl

The reaction was incubated at 37°C for 2-4 hours. The RNA was either cleaned immediately following transcription, or stored at -20°C until it could be cleaned.

2.7 Protein Methods

2.7.1 Whole mount antibody staining

The embryos were fixed in 4% PFA, dehydrated (see section 2.1.4) and stored at -20°C prior to use. They were fixed again in DMSO (Sigma, Missouri) + methanol (in a 1:4 ratio) at 4°C overnight the evening before the antibody staining. The embryos were then incubated for 2 x 2 hours in a 1:1:4 ratio of DMSO + H₂O₂ + methanol at room temperature, followed by 2 x 2 hours in PBXMS at room temperature. An appropriate concentration of primary antibody was added to PBXMS (Tuj1 was used at a dilution of 1:1000), and the embryos were incubated in 1 ml or less of this primary antibody solution overnight at 4°C. They were washed for 3 x 10 minutes followed by 3 x 1 hour in PBX at room temperature, and then 2 x 1 hour in PBXMS, also at room temperature. An appropriate concentration of secondary antibody was added to PBXMS and the embryos were incubated in 1 ml or less of this secondary antibody solution overnight at 4°C. They were then washed for 3 x 10 minutes followed by 3 x 1 hour in PBX at room temperature. Finally, the embryos were washed for 3 x 10 minutes in PBS at room temperature.

PBXMS (50ml)

- 45 ml PBS
- 5 ml Heat Treated Sheep Serum (10% final volume)
- 1 g Fat-free Dried Milk (2% final volume, Premier Foods, St. Albans)
- 0.25 ml Triton X-100 (0.5% final volume, Sigma, Missouri)

PBX (100 ml)

100 ml PBS

0.5 ml Triton X-100

2.7.2 Antibody staining of wax sections

2.7.2.1 Day 1: Slide preparation and primary antibody incubation

Sections were first dewaxed and rehydrated, and the antigens were unmasked. This was done using either Declere (Cell Marque, California) (see section **2.7.2.1.1**) or HistoClear, methanol and citrate buffer (see section **2.7.2.1.2**). The method depended on the primary antibody being used. The antibody anti-phospho-histone H3 (rabbit, Millipore, Massachusetts) requires the Declere method, and the antibody Tuj1 (Neuronal class III β -tubulin rabbit polyclonal antibody, Covance, New Jersey) requires the citrate buffer method.

Sections were washed in TBST, and incubated in blocking solution for at least 1 hour at room temperature.

Blocking solution (50 ml)

5 ml 20 mg/ml BSA in MilliQ water (2 mg/ml, Sigma, Missouri)

5 ml 1.5% Glycine in MilliQ water (0.15%)

5 ml 10x TBS

50 μ l Triton X-100

2.5 ml Heat-inactivated sheep serum

Milli-Q water to 50 ml

To conserve blocking solution a humidity chamber was used for the incubation; 200 μ l blocking solution was added to each slide, and a Parafilm coverslip applied. This method was also used for the antibody incubations.

Following the blocking procedure, the slides were incubated in an appropriate concentration of the primary antibody in blocking solution overnight at 4°C. Tuj1 was used at a concentration of 1:1000, and anti-phospho-histone H3 was used at a concentration of 1:250. When testing the antibodies the negative control was incubated overnight in blocking solution without primary antibody.

2.7.2.1.1 Declere method

Declere was diluted 1:20 in distilled water prior to use. Slides were placed in the diluted Declere at room temperature, and then heated in a steamer for 50 minutes. 10 minutes prior to the end of the incubation fresh Declere was placed in the steamer to heat. The slides were

then removed from the steamer and placed in the fresh, heated Declere, then left to cool to room temperature. The Declere dewaxes the slides, rehydrates the sections, and unmasks antigens.

2.7.2.1.2 Citrate buffer method

Slides were dewaxed by two 10 minutes incubations in Histoclear. They were then rehydrated by a series of 2 minute incubations in decreasing concentrations of ethanol in distilled water (two incubations in 100% ethanol, followed by 90%, 70%, 50%, and 25%, and two washes in distilled water). Slides were then moved to cold citrate buffer, and microwaved on medium power for 3 minutes. Slides were left to cool for 1 minute, then again microwaved on medium power for 3 minutes. Finally, slides were left to cool for 1 minute, microwaved on high power for 3 minutes, and left to cool to room temperature.

Citrate Buffer (1000 ml)

2.1 g Citric Acid (11 mM, Sigma, Missouri)

1000 ml MilliQ water

Use NaOH to alter the pH to 6.0.

2.7.2.2 Day 2: Secondary antibody incubation and slide mounting

Slides were washed in TBST, and then incubated in the dark in a 1:500 concentration of the secondary antibody, Invitrogen (Massachusetts) Alexa Fluor 488 Goat anti-Rabbit IgG. This incubation was carried out for 1 hour at room temperature. The slides were then washed again in TBST, still protected from light, and mounted using Vectashield Mounting medium for Fluorescence with DAPI (Vector Laboratories, California). They were stored at 4°C protected from light.

2.7.2.3 Analysis of antibody staining of slides

Antibody staining of slides was carried out using sections of different orientations and regions for various experiments. Some analysis was centred on the closure point of the PNP, using transverse caudal sections. In this analysis, the first section (in a rostral-caudal direction) which showed an open NT was designated section 0. Contiguous sections positioned more rostrally, in the closed region, were designated -1, -2, -3, etc. Contiguous sections positioned more caudally, in the open region, were designated 1, 2, 3 etc. Analysis of the hinge points used at least 4 sections out of sections 0, 1, 2, 3, 4 and 5. Sections 0, 1 and 2 were classed as proximal sections, and sections 3, 4 and 5 were classed as distal sections. These positions were relative to the closure point of the PNP. All other analysis of this region used at least 4 sections out of sections -6, -4, -2, 0, 2 and 4.

Other analysis used sections from the cranial region of the embryo using coronal sections. In these sections, the first section (in a dorso-ventral direction) in which the lumen of the optic vesicle is visible on both sides was designated section 0. Contiguous sections positioned more ventrally were designated sections 1, 2, 3, etc. Analysis was carried out on at least 4 sections out of sections 0, 2, 4, 6 and 8.

Analysis involving cell counting or measurements was carried out on between 4 and 6 sections per embryo. Cell counts were carried out individually for each section, and then an average figure per section was calculated for each embryo, thus accounting for differences in the number of sections used per embryo. Likewise, measurements were taken for each section, and then an average per section was calculated for each embryo. Analysis for genotypes or groups of embryos used an average of the embryos in the group, giving each embryo equal weight, regardless of the number of sections included.

2.7.3 Protein extraction and quantification

Protein was extracted from whole embryos which had previously been stored without liquid at -80°C. Embryos were kept on dry ice throughout protein extraction.

Around 50 µl RIPA buffer was added to E9.5 embryos, and then the frozen samples were homogenised using a sonicator. Homogenates were stored at -80°C.

RIPA Buffer

50mM Tris pH 7 - 8

150 mM NaCl

0.1% SDS

0.5% sodium deoxycholate

1% Triton X-100

Protease inhibitors

The protein in the samples was quantified using the Pierce (Massachusetts) Bicinchoninic acid (BCA) Kit. Standard solutions of a known protein concentration were made using BSA, and small samples of the extractions were mixed with the reagents using the protocol recommended by the manufacturer's instructions. The samples and standards were incubated at 60°C for 3 minutes, and then the absorption was measured at 562 nm using a spectrophotometer.

2.7.4 Western blot

Protein extractions were previously stored at -80°C.

2.7.4.1 Day 1

Protein extractions were prepared for the Western blot gel by mixing a known quantity of protein in the extract with 0.5 μ l β -mercaptoethanol and loading buffer (BioRad, California, Laemmli sample buffer) to a final volume of 25 μ l. These mixtures were then incubated at 100°C for 2-3 minutes to denature the proteins.

Western blots were carried out using Invitrogen (Massachusetts) NuPage system Bis-Tris gels with a 4-12% gradient, and either 10 or 15 wells. A working solution of NuPage MOPS running buffer (Invitrogen, Massachusetts) was made as follows:

NuPage MOPS Running Buffer (500 ml)

25 ml NuPage 20x running buffer (Invitrogen, Massachusetts)

475 ml MilliQ water

The gel was loaded with 5 μ l protein marker (BioRad, California, Precision Plus Protein Standard) and the samples. Distilled water was used as a negative control in place of the protein. Other possible negative controls which could be used are a p53-negative protein sample, or a separate blot minus the antibody. Positive controls could include a sample of p53 protein. The gel was run under the following conditions.

20 minutes: 100 volts, 120 mA, 25 W.

1 hour: 150 volts, 120 mA, 25 W.

A 1 hour wet transfer was carried out to transfer proteins to the membrane. The following transfer buffer was used.

20x Transfer buffer (125 ml)

10.2 g Bicine (25 mM)

13.1 g Bis-Tris (25 mM, Sigma, Missouri)

0.75 g EDTA (1 mM, Sigma, Missouri)

Milli-Q water to 125 ml.

pH adjusted to 7.2.

1x Transfer buffer (1000 ml)	1 gel (10% methanol)	2 gels (20% methanol)
20x Transfer buffer	50 ml	50 ml
Methanol	100 ml	200 ml
Milli-Q water	850 ml	750 ml

Following transfer, the membrane was blocked at room temperature for at least 1 hour in blocking solution containing TBST with 5% dried milk powder. The membrane was then

incubated overnight at 4°C in blocking solution containing primary antibody (1:1000 concentration of Santa Cruz anti-p53 rabbit polyclonal antibody).

2.7.4.2 Day 2

The membrane was washed in TBST and then incubated for 1 hour at room temperature in blocking solution containing secondary antibody (1:50 000 concentration of Roche, Penzberg, goat anti-rabbit HRP-conjugated antibody).

The membrane was again washed in TBST, and then incubated for 5 minutes at room temperature in chemiluminescent solution (Amersham ECL Prime Western blotting detection reagents, GE Healthcare, Little Chalfont). The membrane was imaged using chemiluminescence-sensitive film (Kodak, New York, Standard chemiluminescent BioMax light film) and an X-ray developer.

3 Causes of neural tube defects in Pax3 mutant embryos

3.1 Results

In this chapter, the *Spotch-2H* mouse will be studied during embryonic development. The work is based on the following hypothesis: premature neuronal differentiation and reduced proliferation in the NT of the *Spotch* embryo cause spina bifida.

The aim of this research is to ascertain the cellular mechanism or mechanisms which are defective in the *Spotch* embryo, and possibly result in the development of NTDs. Based on previous research (see section 1.4.5) it appears likely that excess apoptosis, premature neuronal differentiation or reduced proliferation in the NT could occur in these embryos, and potentially cause NTDs. Therefore, in this chapter each process will be studied to identify abnormalities in the *Spotch* mutant embryos in comparison to wild type embryos. Previous research on the cranial region of *Spotch* embryos and the development of exencephaly (Nicholas Greene, unpublished data) found that there was no difference in the rate of apoptosis between wild type and *Spotch* mutant embryos, but that premature neuronal differentiation and reduced proliferation were both present in the cranial NT of *Spotch* mutant embryos. Therefore, the hypothesis above assumes that the mechanism is the same in the spinal region.

Morphological differences are also studied in this chapter in the spinal NT of *Spotch* mutant embryos compared to wild type embryos. The aim of this is to identify any morphological changes in the NT caused by the cellular defects which could prevent closure of the NT.

In addition, other pathways are briefly studied in relation to the *Pax3* mutation. Folic acid has previously been reported to rescue exencephaly, but not spina bifida in *Spotch* mutant embryos (Burren et al., 2008). This is confirmed here. The Notch and canonical Wnt signalling pathways have also been linked to Pax3 (Ma et al., 1996; Megason and McMahon, 2002; Nakazaki et al., 2008; Zhao et al., 2014), and so qualitative studies are used to assess if these pathways are affected by the *Pax3* mutation in *Spotch* embryos.

3.1.1 Neural tube defects in *Spotch* mutant embryos

The *Pax3* mutation found in *Spotch* mice results in partial penetrance of exencephaly and complete penetrance of spina bifida (Auerbach, 1954) (**Figure 3.1**). These NTDs were studied for frequency, and also for cellular defects which could be causal.

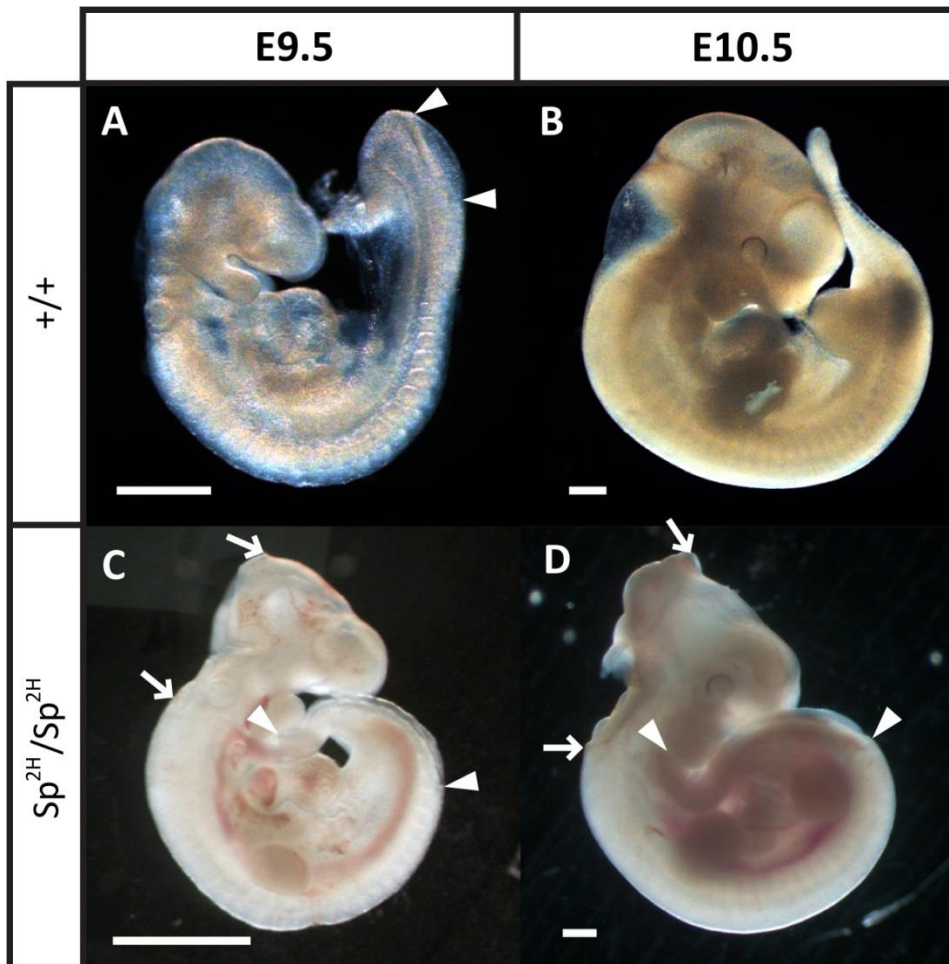


Figure 3.1: The *Splotch* phenotype. $+/+$ (**A** and **B**) and Sp^{2H}/Sp^{2H} (**C** and **D**) embryos are shown at E9.5 and E10.5. The PNP is shown between white arrowheads and the open cranial region is shown between white arrows. Scale bars represent 500 μ m.

At E9.5, $+/+$ embryos have a closed cranial region, and a relatively small PNP (**A**). However, Sp^{2H}/Sp^{2H} embryos at the same stage often have an open cranial NT, and the PNP is significantly larger (**C**). At E10.5, $+/+$ embryos have a completely closed NT (**B**). However, Sp^{2H}/Sp^{2H} embryos at the same stage usually display an open spinal region, referred to as spina bifida at E10.5, and also frequently have an open cranial NT (**D**).

3.1.1.1 The stage of onset of spinal NTDs in *Spotch* mutant embryos

In order to study the molecular mechanisms which are abnormal in NTD development in Sp^{2H}/Sp^{2H} embryos, it was important to determine the period of time during NT development in which the mechanism is abnormal. The longer the NT is exposed to the intrauterine environment, the greater the potential for secondary effects leading to differences in the cellular processes of the tissue when compared to wild type (+/+) NT. Therefore, it is important to study the tissue before it has been affected by the exposure, but when the cellular defect is present. Thus, embryos were studied to identify the somite stage at which phenotypic differences are first apparent between Sp^{2H}/Sp^{2H} and +/+ embryos.

Spinal NT closure occurs prior to cranial NT closure, and spina bifida occurs when the spinal NT fails to fully close (Greene et al., 2009). Therefore, the earliest observable difference between +/+ and Sp^{2H}/Sp^{2H} embryos is an increase in the length of the PNP in the Sp^{2H}/Sp^{2H} embryos (unpublished observations). The PNP eventually closes in +/+ embryos, but remains open in the Sp^{2H}/Sp^{2H} embryo, and develops into spina bifida.

Due to these observations, differences in PNP length were used to estimate the stage at which progression of closure in Sp^{2H}/Sp^{2H} embryos begins to diverge from that observed among +/+ embryos. Experimental litters containing embryos of each genotype were generated through intercross of *Spotch* heterozygous ($Sp^{2H}/+$) mice. The number of somites and the length of PNP were recorded for each embryo, and then analysed according to genotype. The embryos were also grouped according to number of somites (8-9 somites, 10-11 somites, etc.), and the PNP sizes were plotted for each genotype within the group (**Figure 3.2**). This allowed statistical analysis to be carried out to compare PNP sizes between genotypes.

A significant difference in PNP size is first seen between wild type and Sp^{2H}/Sp^{2H} embryos at the 10-11 somite stage, although a trend toward a larger PNP in mutant embryos is seen even earlier than this. The results suggest that the cause of the NTD is present from very early during NT closure, possibly from soon after the initiation of closure at approximately 7 somites.

A significant increase in PNP size is seen between wild type and $Sp^{2H}/+$ embryos from the 12-13 somite stage. This difference is consistently smaller than that between +/+ and Sp^{2H}/Sp^{2H} embryos, but is present and significant until the 20-21 somite stage, which is the latest stage that was measured.

NTDs are rare in $Sp^{2H}/+$ embryos (Auerbach, 1954). Therefore the results suggest that the progression of neurulation may be slightly delayed in $Sp^{2H}/+$ compared to +/+ embryos, but is

Figure 3.2: Closure of the posterior neuropore in the *Spotch* mouse. Experimental litters were generated containing a mixture of genotypes by intercrossing $Sp^{2H}/+$ mice. The graph demonstrates the length of the PNP (as shown in **Figure 3.1**, the distance between the white arrowheads) of embryos of different genotypes at different somite stages during development, between 8 and 23 somites. The graph begins in **A** and continues in **B**. Asterisks indicate significant difference from $+/+$ embryos of the same somite stage. The first significant difference between $+/+$ and Sp^{2H}/Sp^{2H} embryos is seen at the 10-11 somite stage. The first significant difference between $+/+$ and $Sp^{2H}/+$ embryos is seen at the 12-13 somite stage. The size of the PNP decreases as the NT closes in $+/+$ and $Sp^{2H}/+$ embryos between 8 and 23 somites. However, the PNP slightly increases in size between these time points in Sp^{2H}/Sp^{2H} embryos.

Error bars indicate standard error. * $p \leq 0.05$, ** $p \leq 0.01$, *** $p \leq 0.001$. One-way ANOVA was used to test for significant difference.

8-9 somites – $+/+$: n = 2. $Sp^{2H}/+$: n = 8. Sp^{2H}/Sp^{2H} : n = 6.

10-11 somites – $+/+$: n = 9. $Sp^{2H}/+$: n = 21. Sp^{2H}/Sp^{2H} : n = 12.

12-13 somites – $+/+$: n = 17. $Sp^{2H}/+$: n = 30. Sp^{2H}/Sp^{2H} : n = 8.

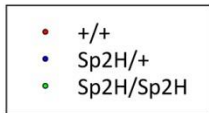
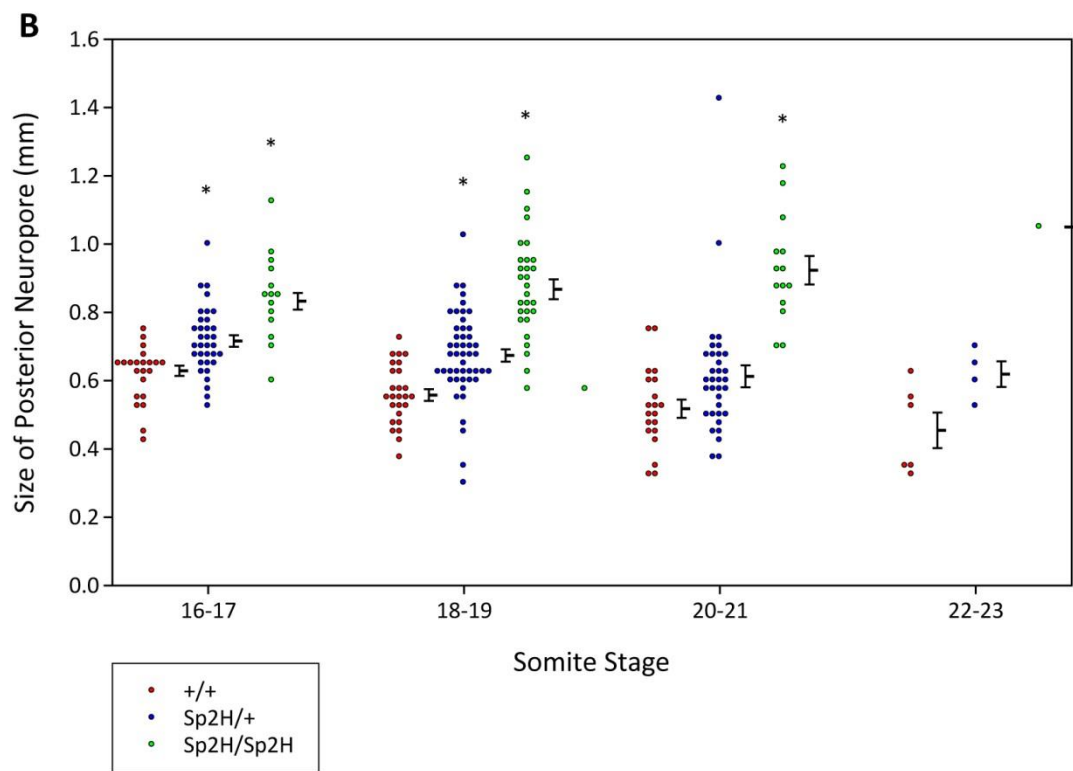
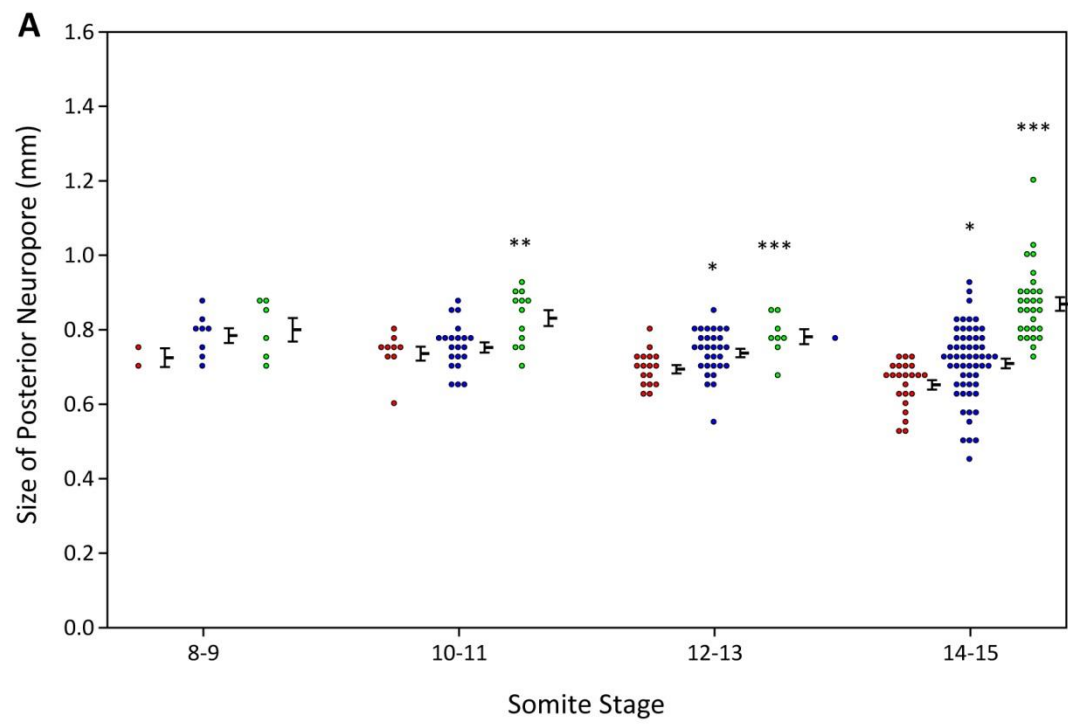
14-15 somites – $+/+$: n = 23. $Sp^{2H}/+$: n = 58. Sp^{2H}/Sp^{2H} : n = 29.

16-17 somites – $+/+$: n = 27. $Sp^{2H}/+$: n = 34. Sp^{2H}/Sp^{2H} : n = 20.

18-19 somites – $+/+$: n = 26. $Sp^{2H}/+$: n = 50. Sp^{2H}/Sp^{2H} : n = 30.

20-21 somites – $+/+$: n = 20. $Sp^{2H}/+$: n = 34. Sp^{2H}/Sp^{2H} : n = 14.

22-23 somites – $+/+$: n = 6. $Sp^{2H}/+$: n = 4. Sp^{2H}/Sp^{2H} : n = 1.



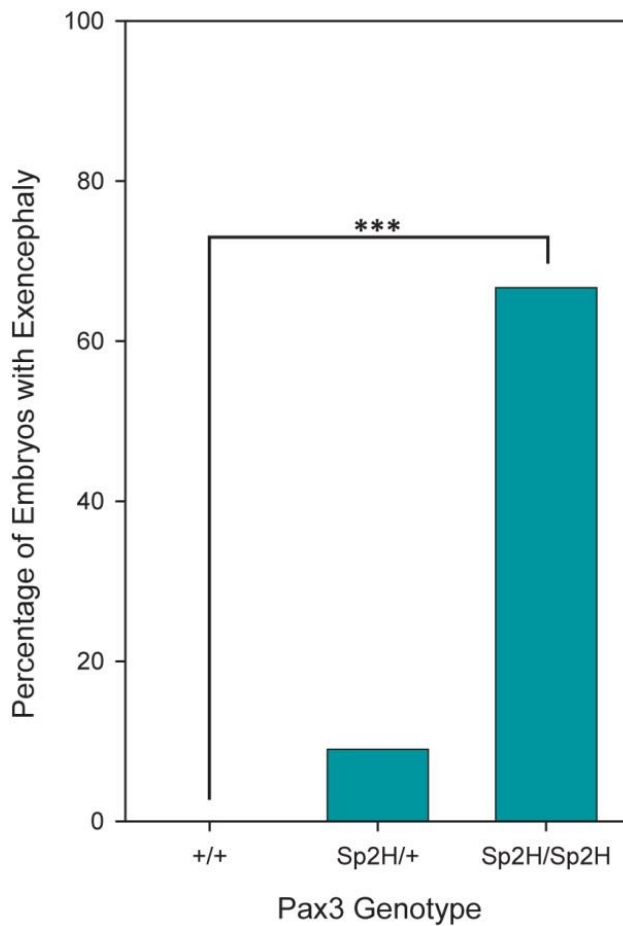


Figure 3.3: The frequency of exencephaly in the *Splotch* mouse. Experimental litters were generated containing a mixture of genotypes by intercrossing $Sp^{2H}/+$ mice. Exencephaly was defined as an open cranial NT at the 18 somite stage or later.

The graph describes the rate of exencephaly in embryos from these litters, with the different genotypes analysed separately. Exencephaly does not occur in $+/+$ embryos, but a small percentage of $Sp^{2H}/+$ embryos develop the NTD (9.0%), although this difference is not significant. However, a significantly higher percentage of Sp^{2H}/Sp^{2H} embryos develop exencephaly (66.7%).

* $p \leq 0.05$, ** $p \leq 0.01$, *** $p \leq 0.001$. The chi-square was used to test for significant difference. $+/+$: $n = 54$. $Sp^{2H}/+$: $n = 94$. Sp^{2H}/Sp^{2H} : $n = 46$.

still completed. However, flexion defects have not been reported in $Sp^{2H}/+$ mice, which suggests that closure itself is not overtly delayed. On the other hand Sp^{2H}/Sp^{2H} embryos have nearly complete penetrance of spina bifida (Auerbach, 1954; Greene et al., 2009), so NT closure is not completed.

3.1.1.2 *Spotch* mutant embryos have an increased frequency of exencephaly

Although $Sp^{2H}/+$ embryos have a slightly higher frequency of exencephaly than $+/+$ embryos, this difference does not reach significance (**Figure 3.3**). This could be due to sample size, and it is possible that with higher numbers of embryos the difference would become significant. However, Sp^{2H}/Sp^{2H} embryos have a significantly higher frequency of exencephaly than $+/+$ embryos. These results suggest that the presence of the Sp^{2H} allele – particularly when in homozygous form – predisposes the mouse embryo to develop exencephaly.

3.1.2 Cellular defects during spinal neurulation in *Spotch* mutant embryos.

As discussed in section 1.4.5, a number of theories have been suggested to explain the development of NTDs in Sp^{2H}/Sp^{2H} mice. Some of these theories have been tested in the cranial region, but the research described here focusses on cellular defects observed in the spinal region as potential causes of spina bifida.

3.1.2.1 *Pax3* expression in the neural tube

In order to study the effects of *Pax3* mutation in these mice, the region in which *Pax3* is expressed in wild type embryos must be defined. Whole mount *in situ* hybridisation was carried out on $+/+$ embryos at E9.5 to identify the region of *Pax3* expression (**Figure 3.4**). Expression was detected in the NT and the segmented mesoderm.

Embryos were sectioned in transverse or coronal orientation, and *Pax3* expression was observed in the dorsal region of both the caudal and cranial NT. A small area of expression was also observed in the ventral region of the cranial NT (**Figure 3.4C**). However, due to the angle of the section this most likely represents the dorsal region of the NT which curves back underneath the forebrain. Therefore the dorsal region of the NT was studied as the *Pax3* expressing region.

3.1.2.2 Neuronal differentiation is normal in the spinal neural tube of *Spotch* mutant embryos

Premature neuronal differentiation has been suggested as a potential cause of NTDs in Sp^{2H}/Sp^{2H} embryos (see section 1.4.5.2). Cells exit the cell cycle upon differentiation, and also exhibit differences in cell properties, such as cell-cell adhesion and communication, from the precursor cells of the neuroepithelium (Yamashita, 2013). These changes could modify the

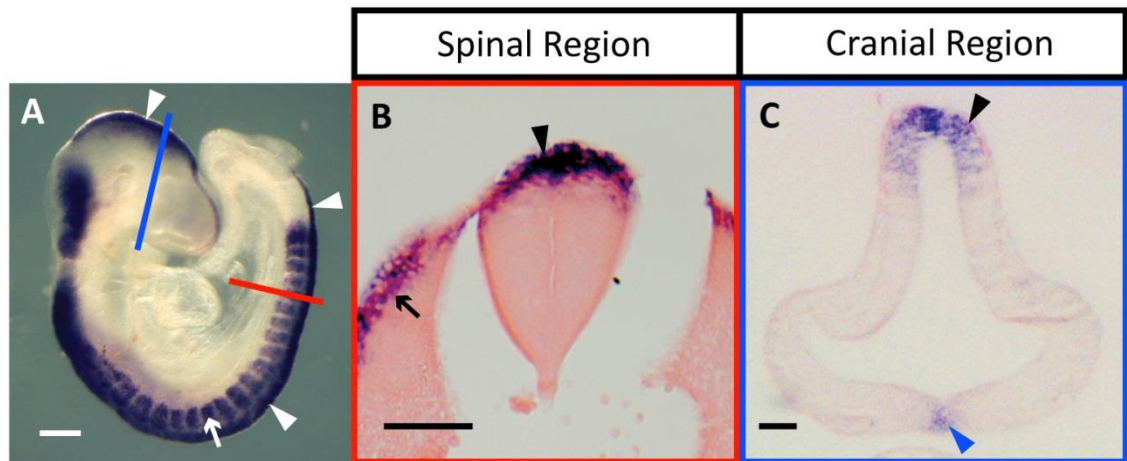


Figure 3.4: Region of *Pax3* expression. **A** shows a wild type embryo at E9.5 which has undergone whole mount *in situ* hybridisation for *Pax3*. Expression can be seen in the NT (white arrowheads) and the segmented mesoderm (white arrow). The white scale bar represents 250 μm .

B and **C** show eosin-stained wax sections taken from the embryo. **B** shows a caudal section through the neural tube, at the level indicated by the red line in **A**. *Pax3* expression can be seen in the dorsal region of the NT (black arrowhead), and in the paraxial mesoderm (black arrow). **C** shows a section through the cranial region. The position of the section is indicated by the blue line in **A**. *Pax3* expression can be seen in the dorsal midbrain region of the NT (black arrowhead), and also in a small area of the ventral forebrain region (blue arrowhead). The black scale bars represent 50 μm .

properties of the NT, either through a reduction in cell number, or through alteration of the cell types within the tissue.

Neuronal differentiation in the NT was examined using whole mount *in situ* hybridisation with a probe to identify the *Ngn2* gene. This is a proneural gene, and acts as marker for differentiating neurons. It is also downstream of *Pax3* signalling (Nakazaki et al., 2008). Therefore, changes in *Ngn2* expression could be due solely to *Pax3* mutation, and will not necessarily indicate neuronal defects. However, alterations in the expression pattern of *Ngn2* at this stage could be an early indicator of the kind of *Pax3*-related neuronal defects which might be present at later stages of development.

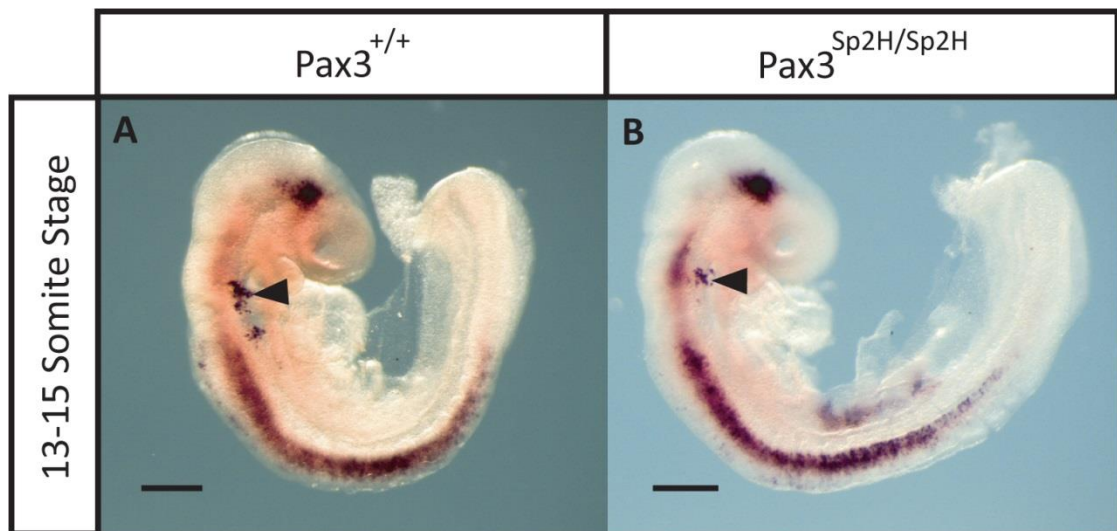


Figure 3.5: Comparing *Ngn2* expression between *+/+* and *Sp^{2H}/Sp^{2H}* embryos. Experimental litters were generated containing a mixture of genotypes by intercrossing *Sp^{2H}/+* mice. 13-15 somite stage embryos underwent whole mount *in situ* hybridisation for *Ngn2*. The embryos shown are at the 15 somite stage. The scale bars represent 250 μ m. n = 3 for each genotype.

Ngn2 expression can be seen in the spinal region and the midbrain, and a small patch of surface-level cells near the branchial arches (arrowhead). There are no differences between the genotypes in the spinal expression pattern of *Ngn2*. There is possibly excess cranial expression of *Ngn2* in *Pax3^{Sp2H/Sp2H}* embryos. Sections of this region could provide more information. However, this study focusses on the development of the spinal NT.

Ngn2 expression is studied at the 13-15 somite stage. At this stage neuronal specification is beginning to occur in the cranial and spinal regions of the NT. At the time of study, statistics showed 14-15 somites to be the stage at which the PNPs of *Sp^{2H}/Sp^{2H}* embryos were first statistically larger than those of their wild type counterparts. Therefore many of the studies described in this thesis use the same somite stage. Later statistical analysis showed the divergence between genotype to be earlier, at the 10-11 somite stage (**Figure 3.2**). Although the 14-15 somite stage is less than ideal for the studies, it is likely that any cellular defects will still be present and identifiable at this stage.

Expression in *+/+* embryos is seen in the spinal region and the midbrain, as well as a small subset of surface-level cells near the branchial arches (**Figure 3.5**). No difference is seen in the pattern of *Ngn2* expression between the wild type and *Spotch* mutant embryos at this stage.

Notch signalling is important in controlling the timing of neuronal differentiation (de la Pompa et al., 1997). Pax3 and Ngn2 act upstream of the Notch pathway during neuronal differentiation (Ma et al., 1996). Additionally, deletion of Notch in mouse has been found to exacerbate the *Spotch* phenotype (Nicholas Greene, unpublished data). Therefore the relative expression levels of two Notch target genes – *Dll1* and *Fos1* – were compared between *+/+* and *Sp^{2H}/Cre* embryos. The expression of these genes was previously identified as potentially altered in *Sp^{2H}/Sp^{2H}* embryos (Nicholas Greene, unpublished data). *Sp^{2H}/Cre* embryos were used as these were generated using an alternative genetic cross (explained in **Figure 3.6**). This cross is used mostly in **Chapter 4**, but the embryos were also used for RT-qPCR data in this chapter. The genetic crosses used each experiment are described in the figure legends.

Expression levels of *Dll1* and *Fos1* were studied using real time quantitative PCR (RT-qPCR), comparing between the genotypes at the 23-24 somite stage (**Figure 3.6**). No significant differences were found in relative expression levels of these genes when comparing genotypes. However, the original study was carried out using 14-15 somite stage embryos. Therefore it could be interesting to repeat the study at multiple stages, as the expression differences between genotypes could change with developmental stage.

Additionally, immunohistochemistry was used on both whole mount embryos and transverse sections to study neuronal differentiation in *+/+* and *Sp^{2H}/Sp^{2H}* embryos (**Figure 3.7**). The antibody Tuj1 binds β III-tubulin, and was used to identify differentiated neurons.

Whole mount immunohistochemistry was used to compare neuronal differentiation between *+/+* and *Sp^{2H}/Sp^{2H}* embryos at 23-24 somite stage. This developmental stage was used due to availability of somite stage matched embryos. Although the defect is well established at this stage, it may be easier to identify differences in the extent of the spinal neuronal differentiation between genotypes, as differentiation has extended further along the axis, and differences may be more exaggerated or more quantifiable. β III-tubulin expression was studied in both the cranial and spinal regions of the embryos. No differences were seen in either the pattern or the extent of cranial expression (**Figure 3.7**).

Neuronal differentiation in the spinal region progresses in a rostral-to-caudal wave. Therefore the extent of the differentiation was quantified by observing the furthest somite level which

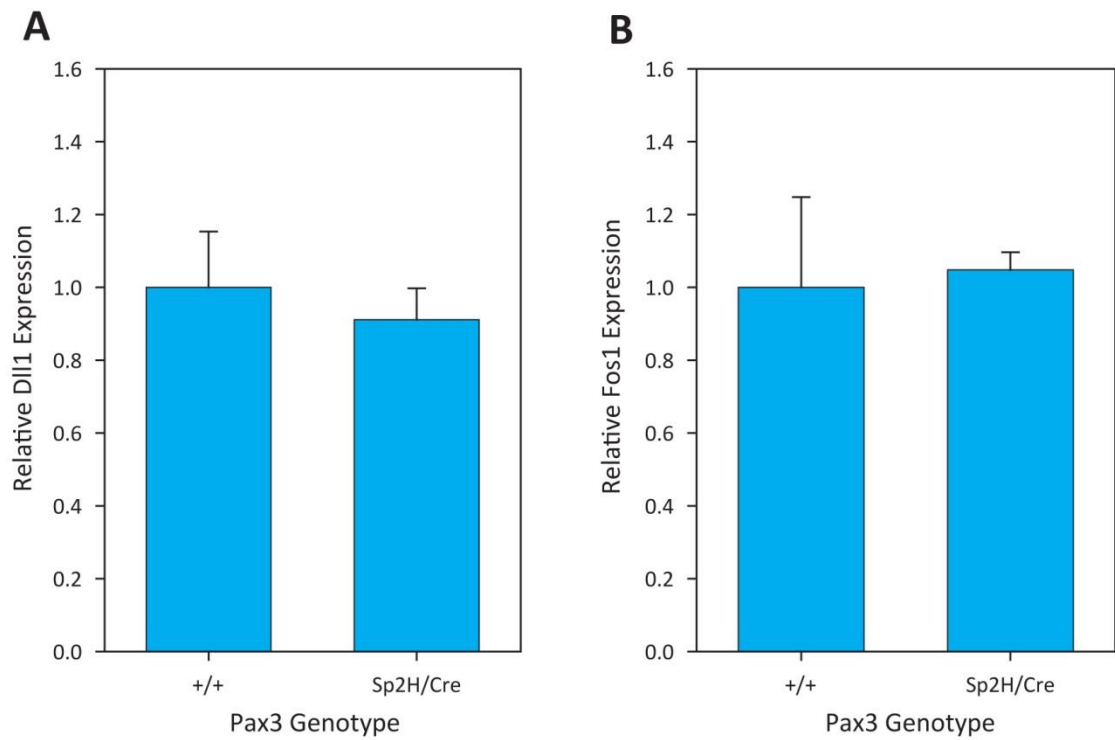


Figure 3.6: Comparing expression levels of Notch genes between +/+ and Sp^{2H}/Cre embryos. Experimental litters were generated containing a mixture of genotypes through the cross $Pax3^{Sp2H/+} \beta\text{-catenin}^{GOF/+} \times Pax3^{Cre/+} \beta\text{-catenin}^{+/+}$. This cross was used for the experiments described in **Chapter 4**. Sp^{2H}/Cre embryos are – like Sp^{2H}/Sp^{2H} embryos – Pax3-null. Relative expression levels are normalised to wild type embryos.

The expression levels of *Dll1* (**A**) and *Fos1* (**B**) were compared using whole embryo RNA extractions and RT-qPCR analysis. *GAPDH* was used as the housekeeping gene. No significance was seen in gene expression between the genotypes for either *Dll1* or *Fos1*.

The t-test was used to test for significant difference. $n = 4$ for each genotype. Error bars show standard error.

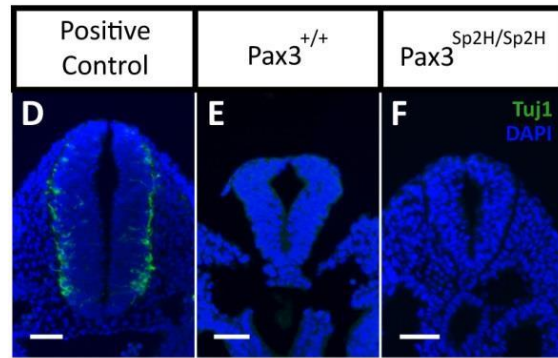
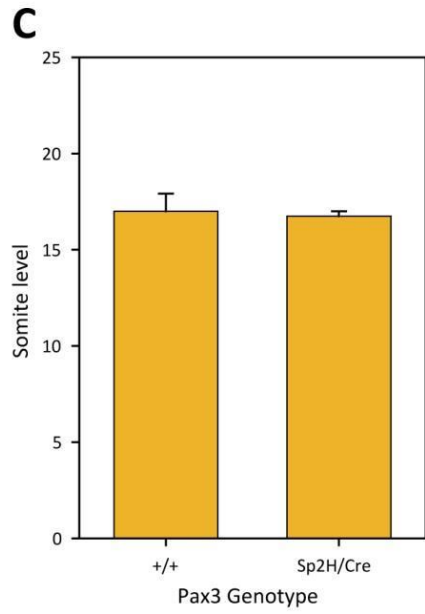
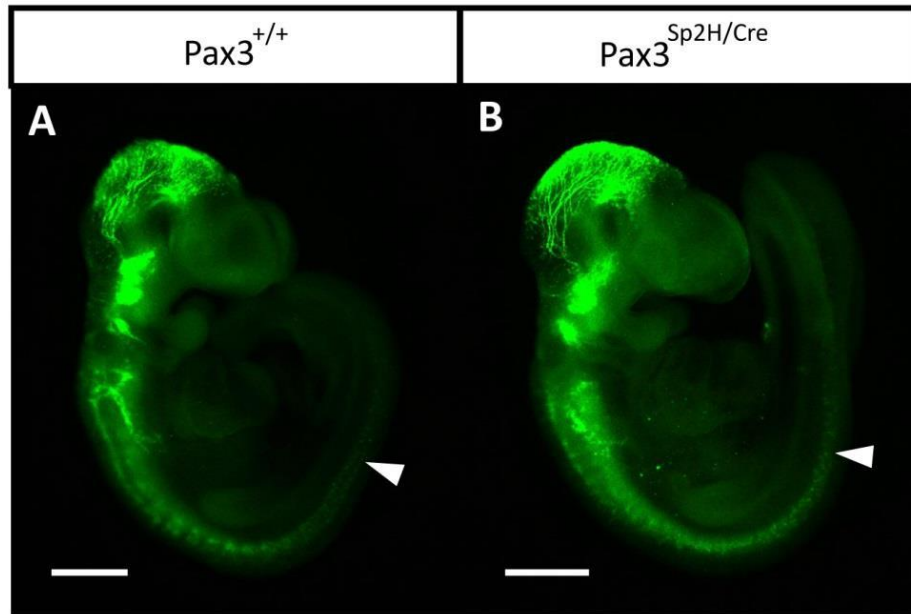
Figure 3.7: Comparing neuronal differentiation between $+/+$ and Sp^{2H}/Cre embryos.

Experimental litters were generated containing a mixture of genotypes through the cross $Pax3^{Sp2H/+}$ β -catenin^{GOF/+} x $Pax3^{Cre/+}$ β -catenin^{+/+}. This cross was used for the experiments described in Chapter 4. Sp^{2H}/Cre embryos are – like Sp^{2H}/Sp^{2H} embryos – Pax3-null.

A and **B** are 24 somite stage embryos which have undergone whole mount immunohistochemistry with the antibody Tuj1, a neuronal marker. Scale bars in **A** and **B** represent 500 μ m. The pattern and extent of neuronal differentiation do not differ greatly between $+/+$ (**A**) and Sp^{2H}/Cre (**B**) embryos. Embryos used were 23-24 somite stage, embryos shown are 24 somite stage. n = 2 per genotype.

Neuronal differentiation in the spinal region develops in a rostro-caudal direction. Therefore, the extent to which neuronal differentiation had progressed was examined (marked by arrowheads in **A** and **B**). The most caudal somite level which displayed robust Tuj1 staining was compared between the genotypes at the 23-24 somite stage. The results are shown in **C**. No significant difference was seen between the genotypes in the extent of the neuronal differentiation. Student t-test was used to test for significant difference. n = 4 for each genotype.

Immunohistochemistry using Tuj1 was also carried out on sections of the NT of 17-21 somite stage embryos (**D-E**). The region surrounding the rostral limit of the PNP was examined for neuronal differentiation. Scale bars in **D-F** represent 50 μ m. The positive control (**D**) is a section from the cranial NT of a $+/+$ embryo, and Tuj1 staining is seen particularly in neuronal cell bodies around the basal surface of the NT. However, no neuronal differentiation is seen in the sections around the PNP in either $+/+$ (**E**) or Sp^{2H}/Sp^{2H} (**F**) embryos. $+/+$: n = 2. Sp^{2H}/Sp^{2H} : n = 3.



demonstrated β III-tubulin expression. No significant difference was seen when comparing $+/+$ and Sp^{2H}/Sp^{2H} embryos (**Figure 3.7C**).

The embryos were sectioned in a transverse orientation through the region surrounding the rostral limit of the PNP. Tuj1 was used for immunohistochemistry of this region. If neuronal differentiation were seen in this region it could potentially affect NT closure. However, no β -tubulin expression was seen in the region for either the $+/+$ or Sp^{2H}/Sp^{2H} embryos (**Figure 3.7D-F**).

3.1.2.3 Apoptosis does not cause spina bifida in *Spotch* mutant embryos

As described in section **1.4.5.1**, excess apoptosis in the spinal NT has been suggested as a cause of NTDs in *Spotch* mutant embryos.

Whole mount TUNEL stains were carried out on whole mount embryos at the 15-16 somite stage in order to compare levels of apoptosis in the spinal neural tube of $+/+$ and Sp^{2H}/Sp^{2H} embryos (**Figure 3.8**). This stage was chosen as it is reasonably early in the development and closure of the spinal NT, and embryos were available to allow the developmental stages to be matched. Although the TUNEL assay showed variation in the staining – particularly regarding the wild type embryos – the results were consistent; no excess apoptosis was observed in Sp^{2H}/Sp^{2H} embryos.

A genetic cross was carried out similar to that published previously (Pani et al., 2002) combining the Sp^{2H} allele with a *p53* mutant allele. If excess apoptosis were causing the development of NTDs in Sp^{2H}/Sp^{2H} embryos it would be expected that the reduction in apoptosis caused by the *p53* mutation would rescue the NTDs in Sp^{2H}/Sp^{2H} embryos. However, such a rescue was not seen (**Figure 3.9**). On the other hand, the *p53* mutation did not appear to greatly reduce apoptosis in wild type embryos (**Figure 3.10**).

3.1.2.4 Proliferation is reduced in the spinal neural tube of *Spotch* mutant embryos

Research has suggested that *Pax3* may have a role in regulation of proliferation (see section **1.4.5.3**). Therefore, proliferation in the *Pax3*-expressing dorsal region of the caudal NT was studied to observe if a change in proliferation could be involved in the development of spina bifida in Sp^{2H}/Sp^{2H} mice.

Two different developmental stages were studied; the 14-15 somite stage and the 19-20 somite stage. As mentioned earlier, the 14-15 somite stage was initially chosen as at the time experiment commenced, this was the stage at which a significantly bigger PNP was first seen in the Sp^{2H}/Sp^{2H} embryos compared to the wild type embryos. At 14-15 somite stage the PNP is significantly bigger in Sp^{2H}/Sp^{2H} compared to $+/+$ embryos. However, as this is reasonably early

Figure 3.8: Comparing levels of apoptosis in $+/+$ and Sp^{2H}/Sp^{2H} embryos. Experimental litters were generated containing a mixture of genotypes by intercrossing $Sp^{2H}/+$ mice. TUNEL staining has been used to observe apoptosis in 15-16 somite stage embryos. **A** and **B** show examples of wild type embryos, and **C** and **D** show examples of *Spotch* mutant embryos. **A'**, **B'**, **C'** and **D'** show close-up images of the caudal region and PNP. Scale bars represent 250 μ m. n = 4 per genotype.

Apoptosis in the cranial region may be slightly increased in Sp^{2H}/Sp^{2H} (**C** and **D**) embryos compared to $+/+$ (**A** and **B**) embryos, but this result is inconsistent between embryos. In addition, although there is a great deal of variation between embryos, there does not appear to be a consistent difference in the levels of apoptosis in the spinal regions and PNPs of Sp^{2H}/Sp^{2H} embryos (**C**, **C'**, **D** and **D'**) and $+/+$ embryos (**A**, **A'**, **B** and **B'**).


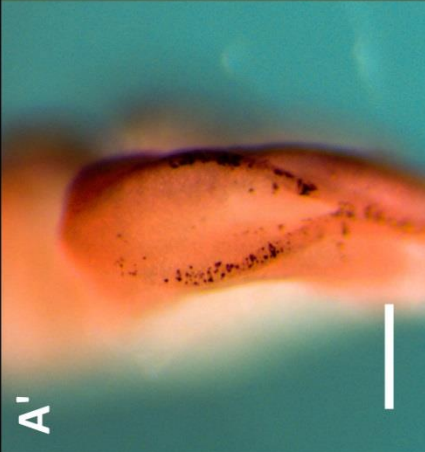

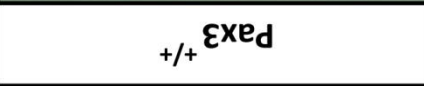

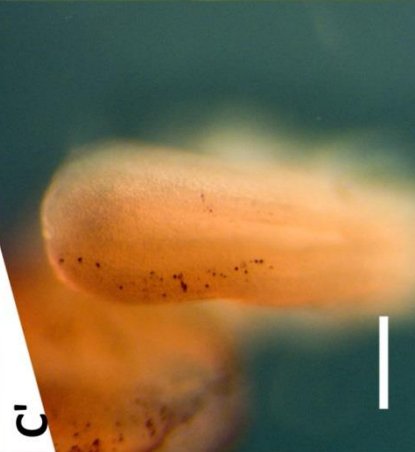

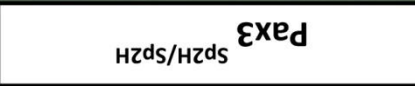
	Whole Embryo View	Caudal View	Whole Embryo View	Caudal View
Pax3 ^{+/+}	 <p>A</p>	 <p>A'</p>	 <p>C</p>	 <p>C'</p>
Pax3 ^{sp2H/sp2H}	 <p>B</p>	 <p>B'</p>	 <p>D</p>	 <p>D'</p>

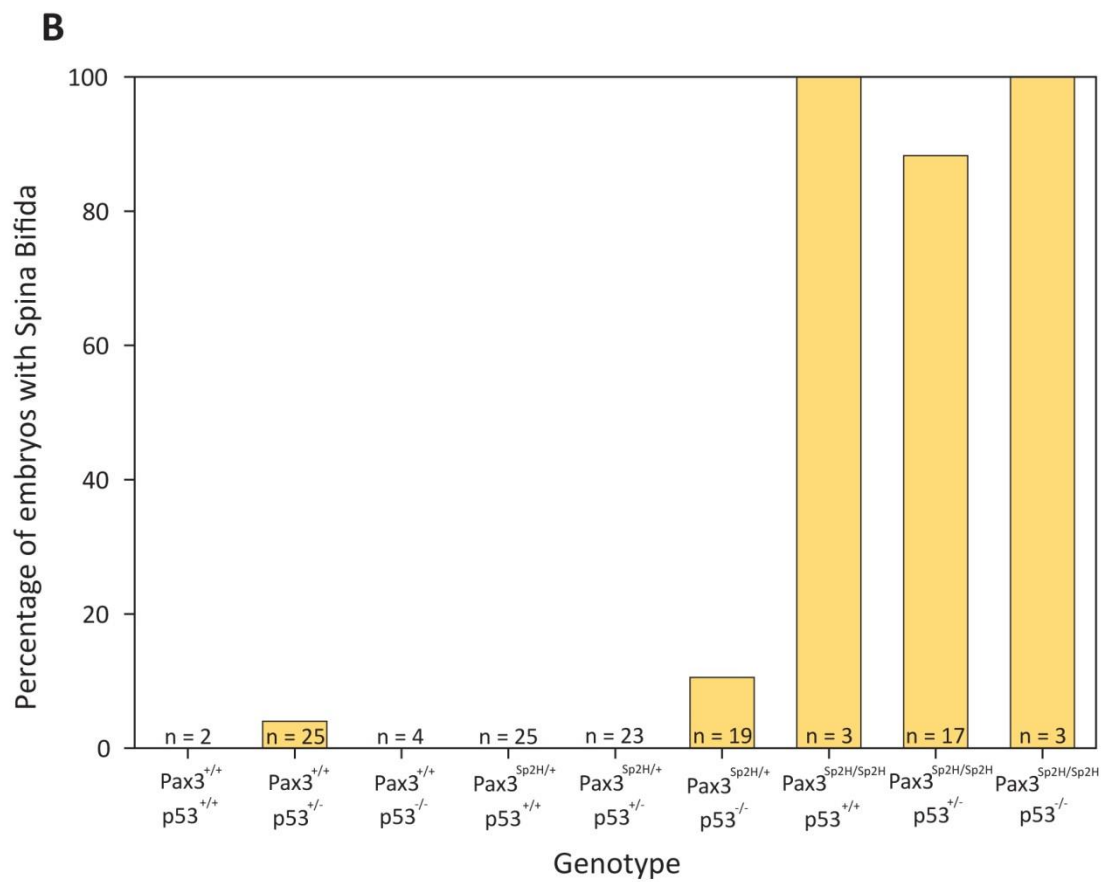
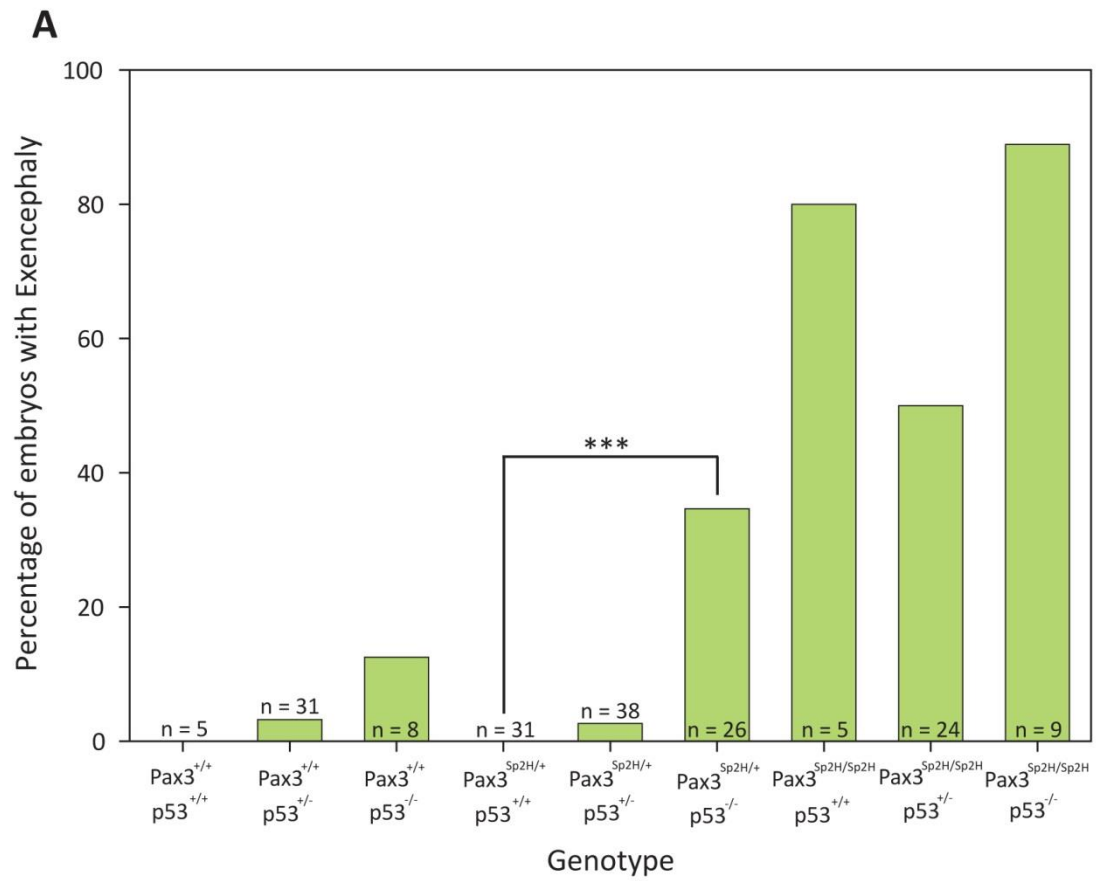
Figure 3.9: Phenotypes of embryos from a $Pax3^{Sp2H/+}$ $p53^{+/-}$ x $Pax3^{Sp2H/+}$ $p53^{+/-}$ cross.

Exencephaly is defined as an open cranial NT at the 18 somite stage or older. Spina bifida is defined as an open spinal NT at the 30 somite stage or older.

Graph **A** displays the frequency of exencephaly in the embryos of different genotypes from this cross. Significance was analysed between embryos of the equivalent *Pax3* genotype, but with different *p53* genotypes. Although significance was only seen in the $Sp^{2H}/+$ embryos, it appears that a decrease in *p53* expression increases the frequency of exencephaly.

Graph **B** displays the frequency of spina bifida in the embryos of different genotypes from this cross. Significance was analysed between embryos of the equivalent *Spotch* genotype, but with different *p53* status. Very little difference was seen that could be attributed to the presence or absence of *p53*. Therefore, *p53* expression appears to have no effect on the development of spina bifida.

*** $p \leq 0.001$. The Fisher Exact Test was used to test for significant difference.



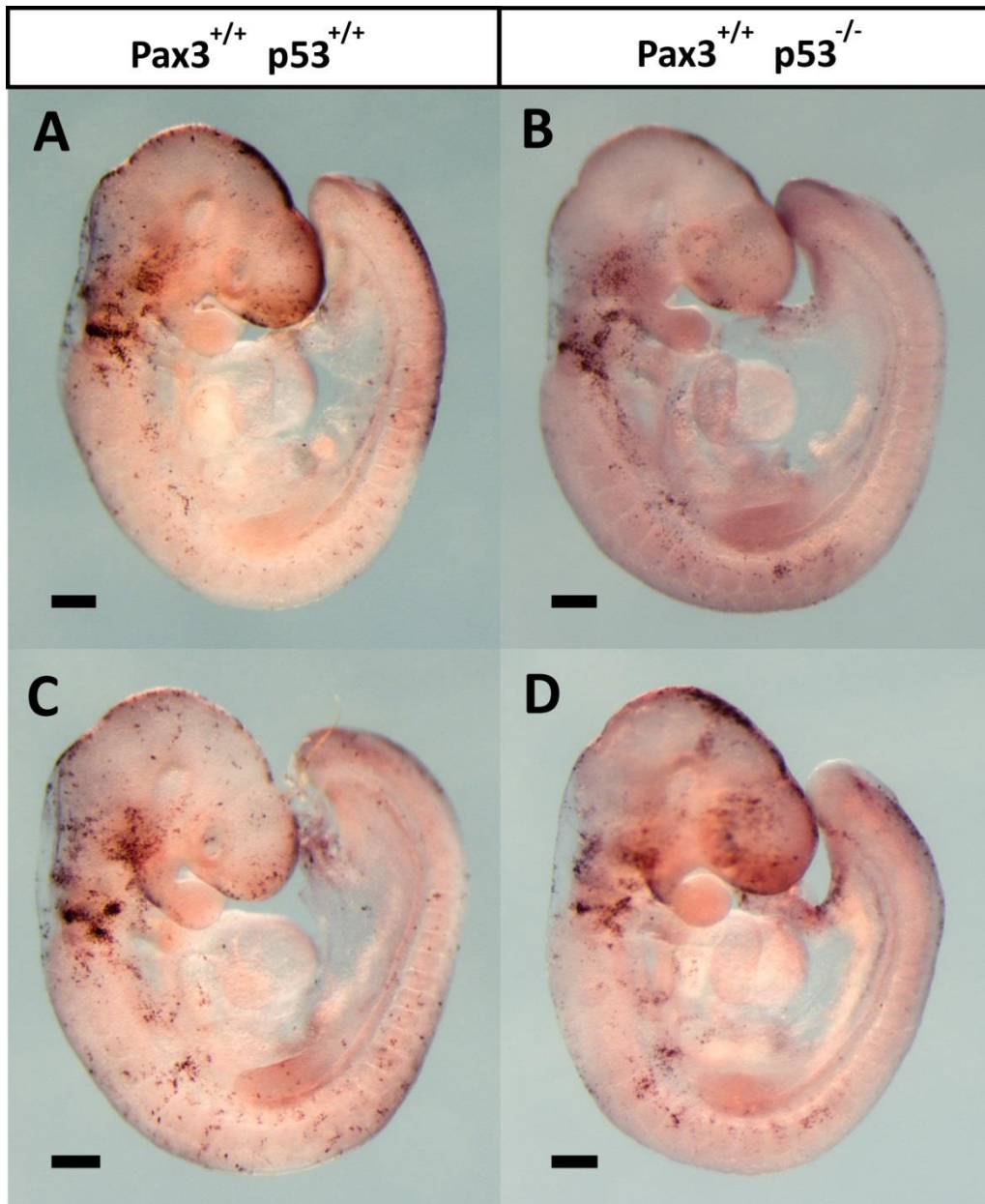


Figure 3.10: Comparing levels of apoptosis in $Pax3^{+/+} p53^{+/+}$ and $Pax3^{+/+} p53^{-/-}$ embryos. Experimental litters were generated containing a mixture of genotypes by intercrossing $Pax3^{Sp2H/+} p53^{-/-}$ mice. TUNEL staining has been used to observe apoptosis in 21-24 somite stage embryos. **A** and **C** show $Pax3^{+/+} p53^{+/+}$ embryos, and **B** and **D** show $Pax3^{+/+} p53^{-/-}$ embryos. Scale bars represent 250 μ m. It is clear that the levels of apoptosis are highly variable between embryos, but do not appear to differ between $Pax3^{+/+} p53^{+/+}$ embryos and $Pax3^{+/+} p53^{-/-}$ embryos.

$Pax3^{+/+} p53^{+/+}$: n = 2. $Pax3^{+/+} p53^{-/-}$: n = 3.

in NT closure secondary effects in the NT of Sp^{2H}/Sp^{2H} embryos caused by exposure to the intrauterine environment are unlikely. At 19-20 somite stage the PNP is considerably larger in Sp^{2H}/Sp^{2H} embryos, and the cellular defect has been present for some time, and therefore may be more apparent.

Sections were taken of the region surrounding the rostral limit of the PNP in mouse embryos of the appropriate ages and genotypes (See section **2.7.2.3** for more information). Immunohistochemistry was carried out on these sections to identify cells positive for phosphohistone H3 (PH3). This protein marks late G2 and M phase cells, and is often used to calculate mitotic index (Colman et al., 2006).

The dorsal-most 25% of each section was designated the *Pax3*-expressing region, and the ventral-most 33% was used as a *Pax3*-negative control region. For each region a count was taken for the total number of cells (using DAPI) and the number of PH3-positive cells. The results for the sections were totalled to give a percentage of PH3-positive cells for each embryo, referred to from now on as the mitotic index.

At 14-15 somite stage, *+/+* embryos showed a significantly higher mitotic index in the *Pax3*-expressing dorsal region than in the *Pax3*-negative ventral region. However, this proliferation gradient appears to be lacking in Sp^{2H}/Sp^{2H} embryos (**Figure 3.11C, E and G**). The dorsal index for Sp^{2H}/Sp^{2H} embryos resembled the ventral region, with no significant difference in mitotic index between the two regions in these embryos (**Figure 3.11E**).

Mitotic index for 14-15 somite stage *Pax3*-negative ventral control regions showed no significant difference between *+/+* and Sp^{2H}/Sp^{2H} embryos. However the rate of proliferation in the Sp^{2H}/Sp^{2H} embryos was significantly reduced compared to wild type in the *Pax3* expression domain (**Figure 3.11C**).

At the 19-20 somite stage, analysis of *+/+* embryos shows that the proliferation gradient present in the younger 14-15 somite stage *+/+* embryos is no longer present (**Figure 3.11D, F and H**). In the 19-20 somite stage *+/+* embryos there was no significant difference between the mitotic indices of the *Pax3*-positive dorsal and *Pax3*-negative ventral regions. Likewise, no such difference was seen in the 19-20 somite stage Sp^{2H}/Sp^{2H} embryos (**Figure 3.11F**).

3.1.2.5 Morphological differences between the neural tubes of wild type and *Splotch* mutant embryos

The neural tube cross sections of *+/+* and Sp^{2H}/Sp^{2H} embryos were analysed further. This was in order to examine any morphological effects of reduced proliferation on the Sp^{2H}/Sp^{2H} NTs, and

Figure 3.11: Proliferation rates in the neural tubes of $+/+$ and Sp^{2H}/Sp^{2H} embryos – 1.

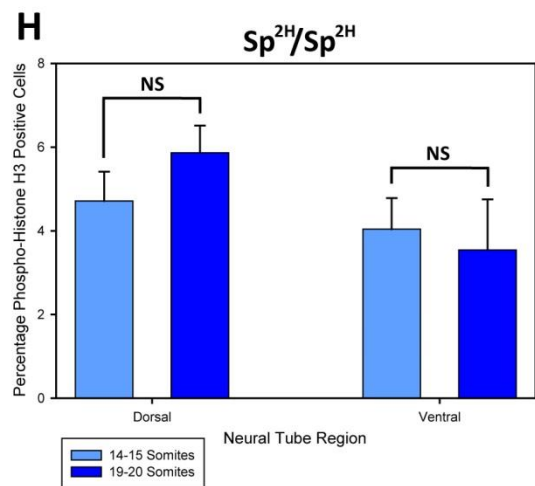
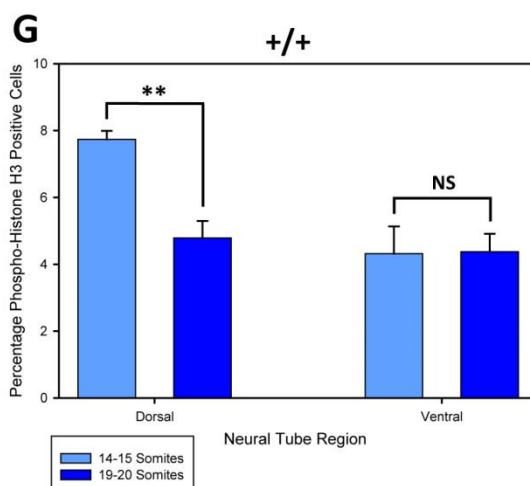
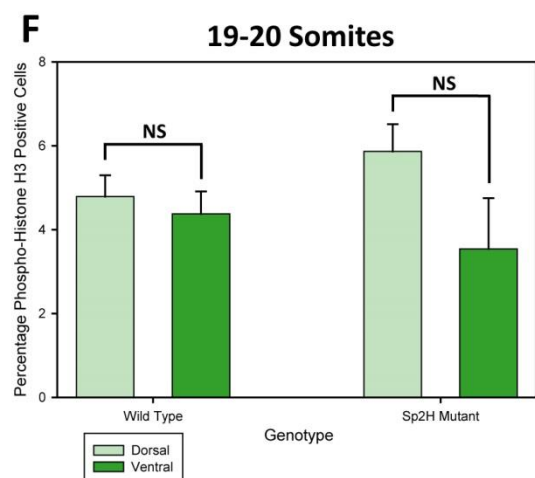
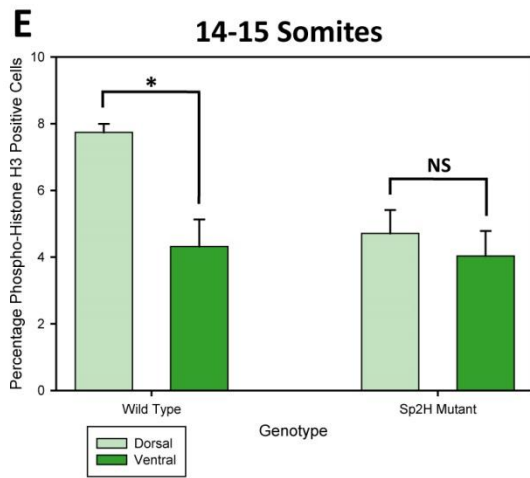
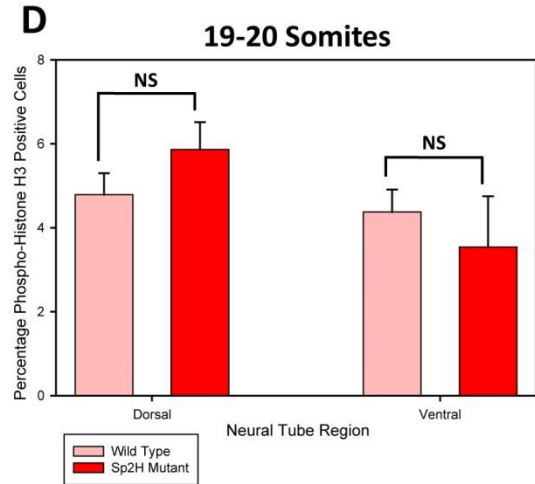
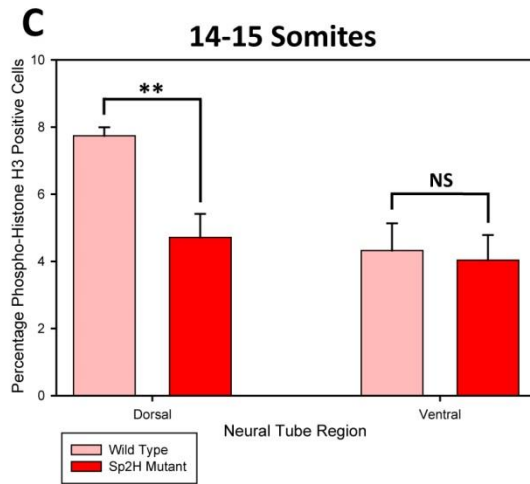
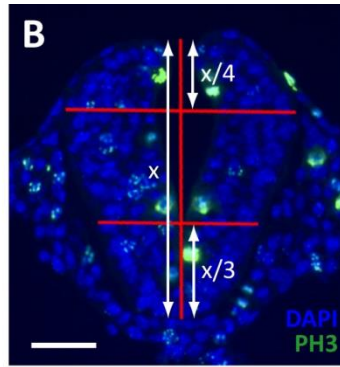
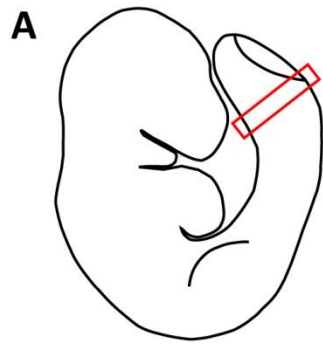
A shows the region of the embryo studied. Transverse sections were taken from the region surrounding and including the closure point of the PNP ($n = 4-6$ per embryo). **B** shows one such section, and demonstrates how the section was divided for the study. The total dorso-ventral 'height' of the NT was measured (x). The 'Dorsal' region was taken as the dorsal-most quarter of the NT ($x/4$), and the 'Ventral' region was taken as the ventral-most third of the NT ($x/3$). The proliferation studies were carried out in these regions. Scale bar represents $50 \mu\text{m}$. PH3 is phospho-histone H3 staining. Data is replicated in **C-D**, **E-F** and **G-H** to show different genotype and stage comparisons.

C and **D** compare the rates of proliferation between $+/+$ and Sp^{2H}/Sp^{2H} embryos in the dorsal and ventral regions at the 14-15 somite stage (**C**) and 19-20 somite stage (**D**). A significant difference is only seen in the dorsal region at the 14-15 somite stage (**C**) – the Sp^{2H}/Sp^{2H} embryos show a reduction in the rate of proliferation.

E and **F** compare the rates of proliferation between the dorsal and ventral regions in $+/+$ and Sp^{2H}/Sp^{2H} embryos at the 14-15 somite stage (**E**) and 19-20 somite stage (**F**). $+/+$ embryos show a significant reduction in proliferation in the ventral region at the 14-15 somite stage. No other significant differences were seen between regions.

G and **H** compare the rates of proliferation between the two time points in the dorsal and ventral regions in the $+/+$ (**G**) and Sp^{2H}/Sp^{2H} embryos (**H**). $+/+$ embryos show a reduction in proliferation in the dorsal region of 19-20 somite stage embryos compared to 14-15 somite stage embryos. No other significant differences were seen.

* $p \leq 0.05$, ** $p \leq 0.01$, *** $p \leq 0.001$. NS: no significance. $n = 6$ for each genotype within each time point ($n = 24$ in total). Error bars show standard error. The t-test was used to test for significant difference. This data follows a Gaussian distribution apart from dorsal data in the 19-20 somite stage Sp^{2H}/Sp^{2H} embryos.



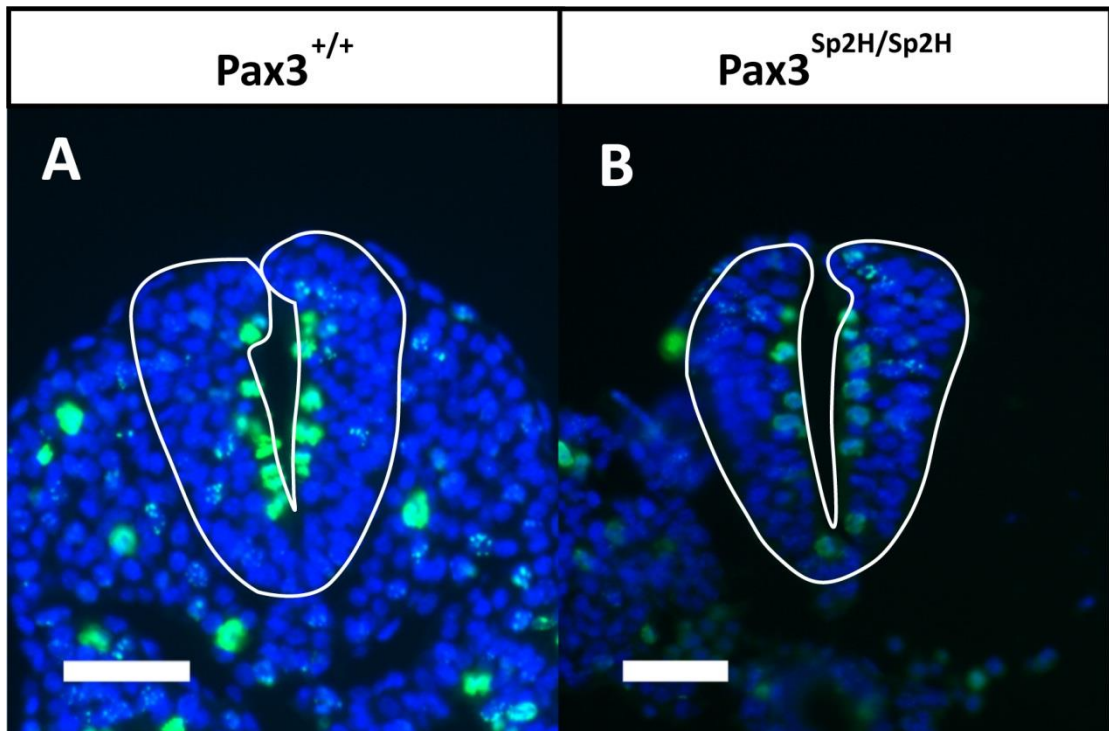


Figure 3.12: Proliferation rates in the neural tubes of $+/+$ and Sp^{2H}/Sp^{2H} embryos – 2. Experimental litters were generated containing a mixture of genotypes by intercrossing $Sp^{2H}/+$ mice. Scale bars represent 50 μm . Cell nuclei are stained with DAPI and show as blue. The Phospho histone H3 antibody marks proliferating cells and shows as green.

A and **B** show examples of the NTs of wild type and *Spotch* mutant embryos respectively. The NT is outlined in white for clarity. *Spotch* mutant embryos (**B**) have a reduced mitotic index (proportion of green cells compared to blue cells) in the dorsal NT compared to wild type embryos (**A**) at the 14-15 somite stage.

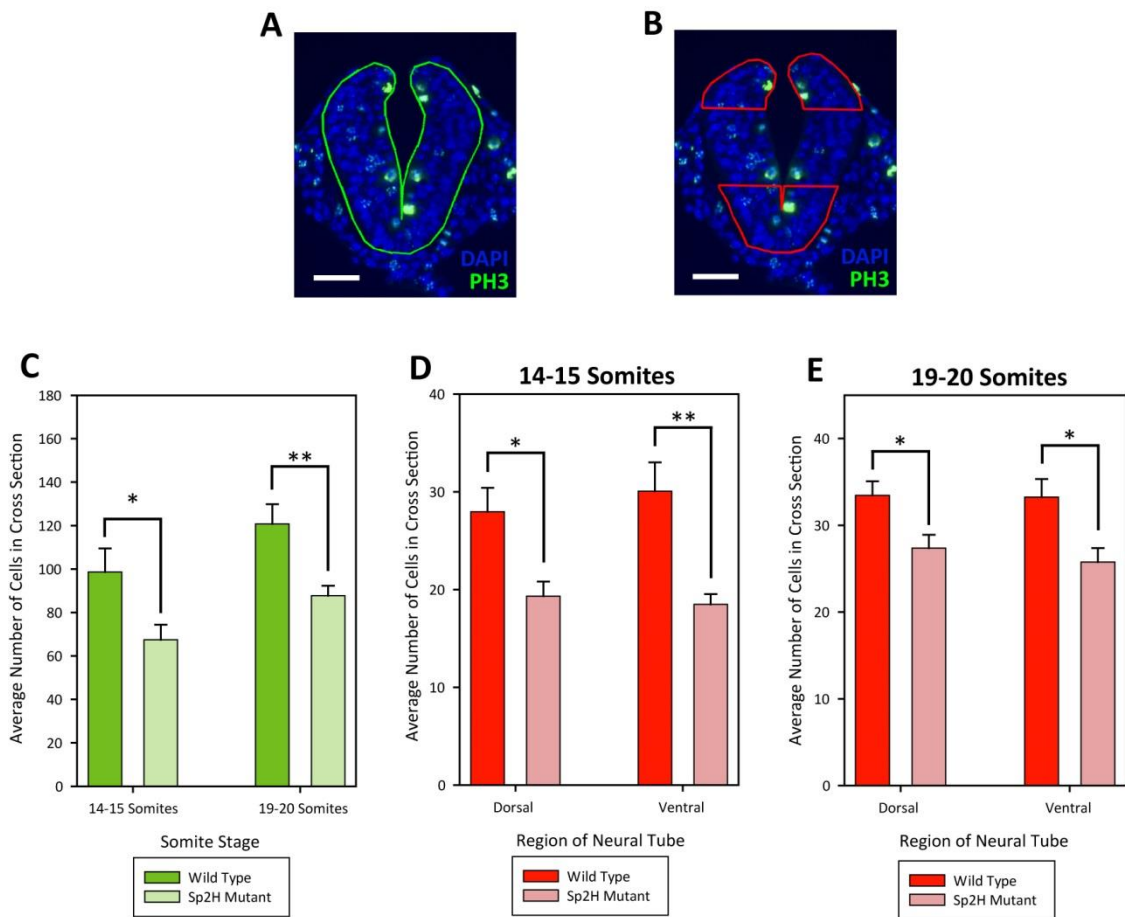


Figure 3.13: Comparing the morphology of $+/+$ and Sp^{2H}/Sp^{2H} embryos – 1. Experimental litters were generated containing a mixture of genotypes by intercrossing $Sp^{2H}/+$ mice. The numbers of cells in neural tube cross sections were analysed using the DAPI antibody as a nuclear marker. Results were compared between $+/+$ and Sp^{2H}/Sp^{2H} embryos.

A and **B** show the regions studied. **A** delineates the area of the entire NT. Graphs shown in green pertain to this area. **B** demonstrates the dorsal and ventral regions, as described in **Figure 3.13C**. Graphs shown in red pertain to these areas. PH3 is phospho-histone H3 staining. Scale bars represent 50 μm .

C shows the results for cell numbers in the whole NT. Cell numbers are significantly lower in Sp^{2H}/Sp^{2H} embryos compared to $+/+$ embryos at both the 14-15 and 19-20 somite stages.

D and **E** show the results for the cell numbers in the specified region of the NT at the 14-15 somite stage (**D**) and the 19-20 somite stage (**E**). Cell numbers are significantly reduced in Sp^{2H}/Sp^{2H} embryos in both the dorsal and ventral regions, and at both the 14-15 and 19-20 somite stages.

* $p \leq 0.05$, ** $p \leq 0.01$. NS: no significance. $n = 6$ for each genotype within each time point ($n = 24$ in total). Error bars show standard error. The t-test was used to test for significant difference. This data follows a Gaussian distribution.

to potentially identify any abnormalities which could contribute to the development of spina bifida.

3.1.2.5.1 Cross sectional cell number

If cell proliferation is reduced in the dorsal region of the NT in Sp^{2H}/Sp^{2H} embryos, it seems likely that these embryos may have fewer cells in the NT. DAPI staining was used to enable cell counts for cross sections of the NT (**Figure 3.13**).

Sp^{2H}/Sp^{2H} embryos show a significant reduction in the total number of cells in the cross section of the NT. This difference is seen at both the 14-15 and 19-20 somite stages (**Figure 3.13C**). Therefore it appears that a reduction in cell number occurs in the younger embryos, but continues into the older embryos, even once the difference in proliferation is no longer present.

Previously the sections had been divided into dorsal and ventral regions for the proliferation counts. Cell counts were taken for each of these regions separately, and compared between $+/+$ and Sp^{2H}/Sp^{2H} embryos in order to determine if the proliferation defect affected cell numbers in just the *Pax3*-positive dorsal region, or throughout the NT.

Statistically significant reductions in cell number are seen in both the dorsal and ventral regions of 14-15 and 19-20 somite stage embryos (**Figure 3.13D-E**). These results suggest that cell number is reduced not just in the *Pax3*-positive dorsal region of the NT, but throughout the NT of Sp^{2H}/Sp^{2H} embryos. The reduction in cell number is likely to be caused by the reduced dorsal cell proliferation in these embryos. It could result in either a reduction in cell density, or a smaller NT, or both.

3.1.2.5.2 Neural tube size

Dorso-ventral height and left-right width of the NT were compared between $+/+$ and Sp^{2H}/Sp^{2H} embryos. The measurements were taken from the cross sections. Height was measured down the centre line of the NT, through the MHP. Width was measured at the widest point of the NT cross section, perpendicular to the centre line (**Figure 3.14**).

At the 14-15 somite stage, both height and width were significantly reduced in Sp^{2H}/Sp^{2H} embryos compared to $+/+$ embryos (**Figure 3.14D-E**). At the 19-20 somite stage the height of the NT was significantly reduced, but not the reduction in width does not reach significance (**Figure 3.14D-E**). Possibly this difference would be significant with larger sample sizes.

The ratio of height to width was analysed to determine if the proportions of the NT were changed in any way in the Sp^{2H}/Sp^{2H} embryos. However no statistically significant differences

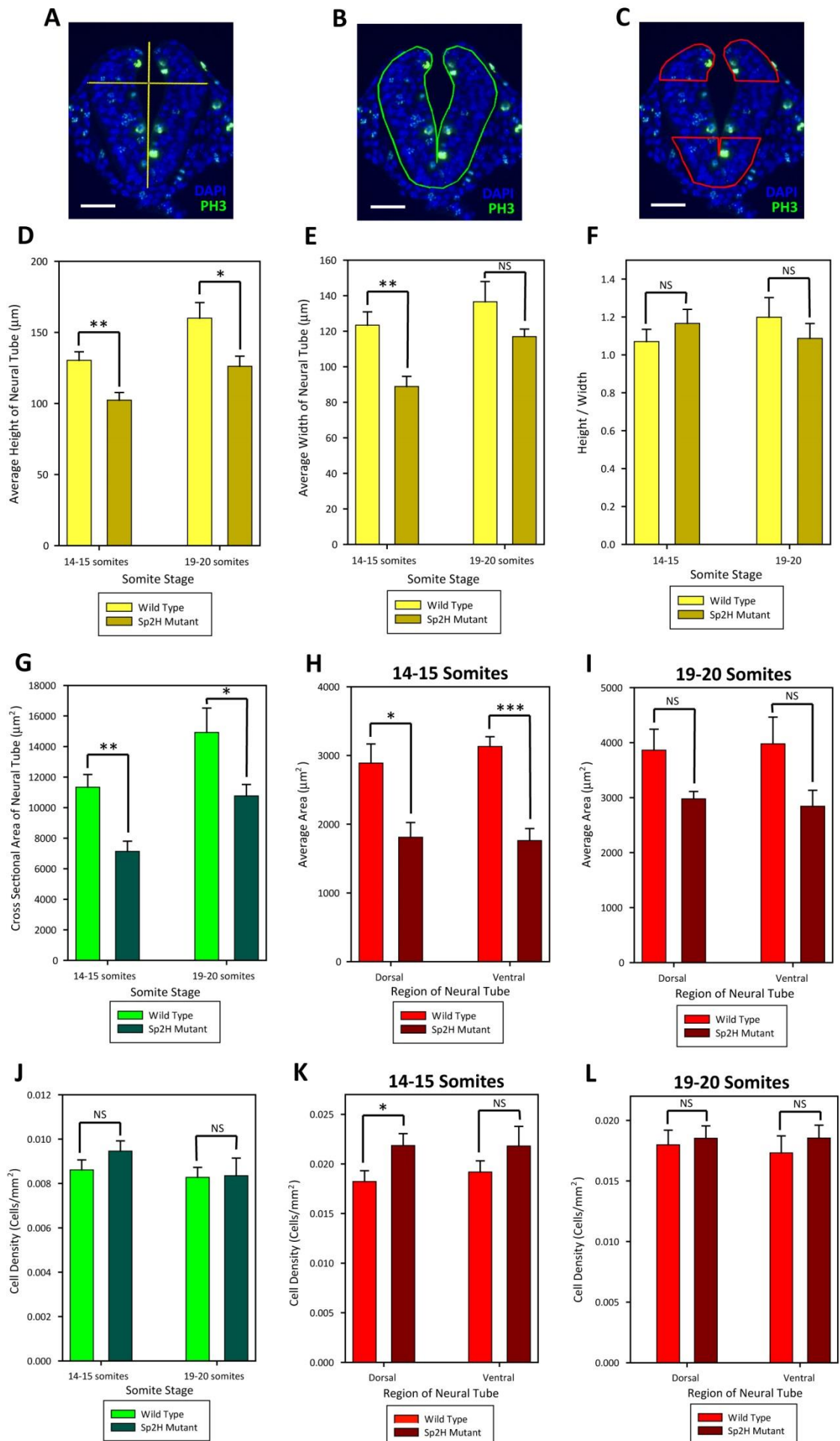
Figure 3.14: Comparing the morphology of $+/+$ and Sp^{2H}/Sp^{2H} embryos – 2. A-C show measurements and regions which were compared. The scale bar represents 50 μm . PH3 is phospho-histone H3 staining. **A** shows the lengths which were taken for height and width. Height was measured from the MHP along the dorso-ventral axis. Width was taken at the widest point of the NT perpendicular to the height measurement. All graphs shown in yellow pertain to these measurements. **B** shows the total area of the NT. Graphs shown in green pertain to this area. **C** shows the partial regions measured; the dorsal-most 25% and the ventral-most 33%. Graphs shown in red pertain to these areas.

D compares height and width of the NTs between $+/+$ and Sp^{2H}/Sp^{2H} embryos at the 14-15 and 19-20 somite stages. A significant reduction in height is seen in Sp^{2H}/Sp^{2H} embryos at both somite stages. **E** compares the width at both somite stages. A reduction in width is seen in the mutants at both stages, but the difference is only significant at the 14-15 somite stage. **F** looks at the height/width ratio, comparing the genotypes at the two time points. No significant difference is seen in the height/width ratios, which suggests that although the NTs are smaller in Sp^{2H}/Sp^{2H} embryos, they are similarly proportioned.

G compares the total area of the NTs between the genotypes at both time points. Sp^{2H}/Sp^{2H} embryos have a significantly reduced surface area at both time points. **H** and **I** compare the partial areas – dorsal and ventral – between the genotypes at the 14-15 somite stage (**H**) and the 19-20 somite stage (**I**). Sp^{2H}/Sp^{2H} embryos show significantly reduced area in both the dorsal and ventral regions at 14-15 somite stage. However, although both regions are reduced in area at the 19-20 somite stage, the differences are not significant.

J-L: Cell density is measured as the number of cells contained within a region/area of that region. There are no significant differences in cell density between the genotypes at either time point (**J**). **K** and **L** compare cell density between the genotypes in the partial regions at the 14-15 somite stage (**K**) and the 19-20 somite stage (**L**). **K** shows that there is an increase in cell density in Sp^{2H}/Sp^{2H} embryos at the 14-15 somite stage, although this difference is only significant in the dorsal region. However this difference is no longer present at the 19-20 somite stage (**L**).

* $p \leq 0.05$, ** $p \leq 0.01$, *** $p \leq 0.001$. NS: no significance. $n = 6$ for each genotype within each time point ($n = 24$ in total). Error bars show standard error. The t-test was used to test for significant difference. All data follows a Gaussian distribution except for the total area of 14-15 somite stage Sp^{2H}/Sp^{2H} embryos, and the total cell density of 19-20 somite stage Sp^{2H}/Sp^{2H} embryos.



were seen in this ratio for either the 14-15 or 19-20 somite stages, suggesting that the overall shape of the NT remains in proportion, although it is reduced in size in the Sp^{2H}/Sp^{2H} embryos (**Figure 3.14F**).

The area of the NT was also measured. A statistically significant reduction was seen in the cross sectional area of the NT of Sp^{2H}/Sp^{2H} embryos at both the 14-15 and 19-20 somite stages compared to $+/+$ embryos (**Figure 3.14G-I**). This is consistent with a smaller NT.

3.1.2.5.3 Cell density

Cell density was measured as $\frac{\text{number of cells}}{\text{cross sectional area}}$. First the overall density of the cross section was analysed, using the total cell count and the total area of the cross section. There is no significant difference between the $+/+$ overall density and the Sp^{2H}/Sp^{2H} overall density at either the 14-15 or 19-20 somite stages (**Figure 3.14J**).

Next the regional densities of the NT were analysed, considering the dorsal region and the ventral region separately. Cell counts and area measurements were taken for these regions. At the 14-15 somite stage there is a statistically significant increase in cell density in the *Pax3*-expressing dorsal region of the neural tube in Sp^{2H}/Sp^{2H} embryos compared to the dorsal region of the NT in $+/+$ embryos (**Figure 3.14K**). Although the cell density in the *Pax3*-negative control domains of these embryos appears to also be increased, the data does not reach significance. Therefore the mutation appears to increase the cell density in the NT at this stage in development, but it appears to affect the dorsal region more than the ventral region.

Regional cell density in 19-20 somite stage embryos appears to be more equal across the genotypes compared to 14-15 somite stage embryos (**Figure 3.14L**). There is no statistically significant difference in cell density in either the dorsal or ventral regions.

3.1.2.5.4 Thickness of the neural folds

Another property of the NT which was analysed was the thickness of the neural folds. This was measured on both folds using the cross sections at three different points on the dorso-ventral axis; at the boundary of the dorsal region (25% total height from the dorsal-most point), at the midpoint (50% total height from the dorsal-most point), and at the boundary of the ventral region (33% total height from the ventral-most point). These will be referred to as the dorsal, mid, and ventral measurements respectively. See **Figure 3.15A-B** for illustration.

At the 14-15 somite stage there is a strong trend for Sp^{2H}/Sp^{2H} embryos to have thinner neural folds at all three measurement points. However, the difference narrowly fails to reach

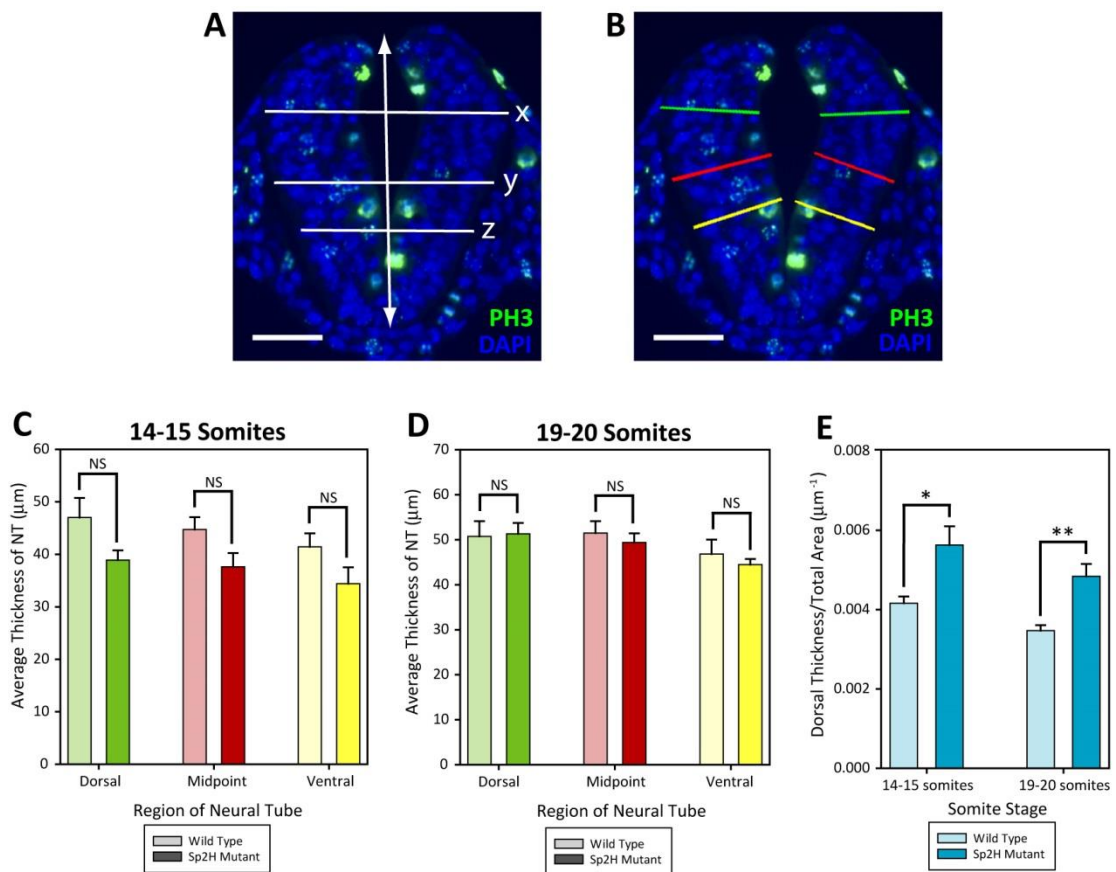


Figure 3.15: Comparing the morphology of $+/+$ and Sp^{2H}/Sp^{2H} embryos – 3. A demonstrates how the NT was divided up for the thickness studies. The scale bars represent 50 μm . The total height of the NT was measured (white double-ended arrow), and lines were drawn perpendicular to this, across the width of the NT; one below the dorsal quarter (x), one at midway (y), and one above the ventral third (z). Measurements were taken perpendicular to the neural folds, from the points where the lines met the basal surface of the NT (B) – dorsal, midpoint and ventral measurements.

C and D compare thickness measurements between $+/+$ and Sp^{2H}/Sp^{2H} embryos at the 14-15 somite stage (C) and the 19-20 somite stage (D). Comparisons were made for each of the three measurements points. No significant differences were seen between the genotypes.

E compares the ratio of dorsal thickness to total NT area between genotypes. Comparisons were made for each of the time points. A significantly increased ratio is seen at both the 14-15 and 19-20 somite stages in Sp^{2H}/Sp^{2H} embryos compared to $+/+$ embryos.

* $p \leq 0.05$, ** $p \leq 0.01$. NS: no significance. $n = 6$ for each genotype within each time point ($n = 24$ in total). Error bars show standard error. Student t-test was used to test for significant difference. This data follows a Gaussian distribution.

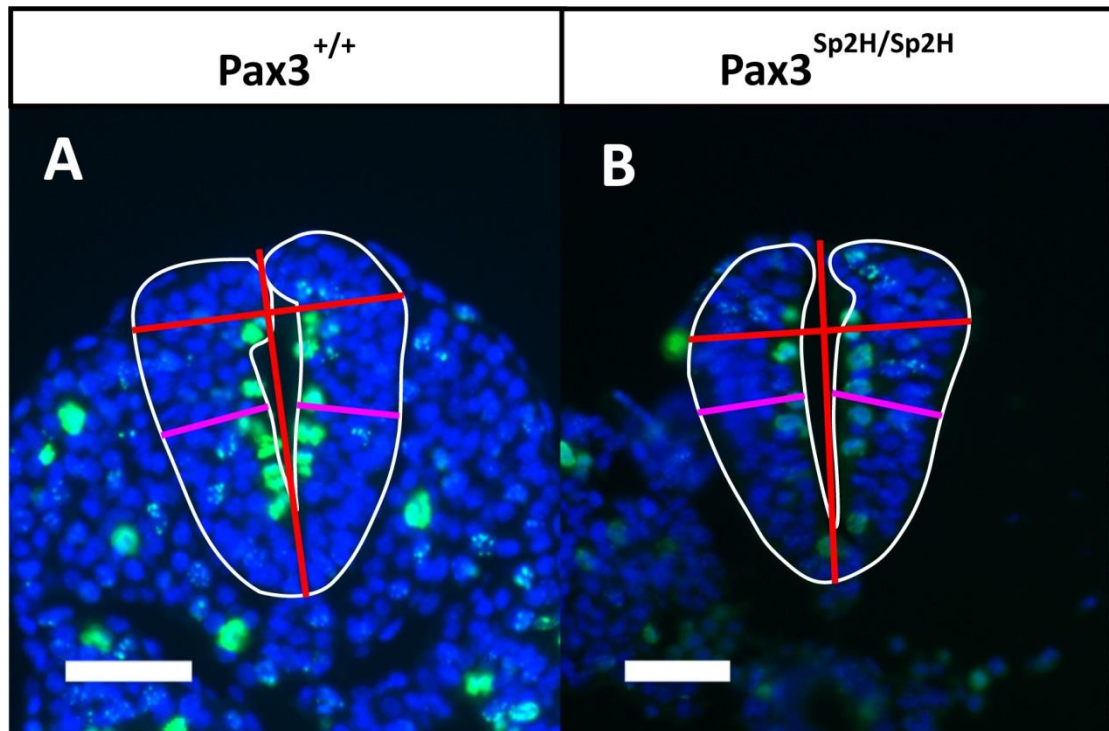


Figure 3.16: Comparing the morphology of $+/+$ and Sp^{2H}/Sp^{2H} embryos – 4. Experimental litters were generated containing a mixture of genotypes by intercrossing $Sp^{2H}/+$ mice. Scale bars represent 50 μm . Cell nuclei are stained with DAPI and show as blue. The Phospho histone H3 antibody marks proliferating cells and shows as green. **A** and **B** show examples of the NTs of wild type and *Splotch* mutant embryos respectively. The NT is outlined in white for clarity.

Splotch mutant embryos (**B**) have reduced numbers of cells in cross section, and a smaller cross-sectional area in the NT compared to wild type embryos (**A**). In addition, the density of cells in the dorsal region of the NT is reduced in *Splotch* embryos (**B**) at the 14-15 somite stage compared to wild type embryos (**A**).

The height and width of the NTs are shown in red. *Splotch* mutant embryos have reduced height at both 14-15 and 19-20 somite stages, and reduced width at the 14-15 somite stage compared to wild type embryos (**A**). The thickness of the NT (shown in pink) is also reduced at the 14-15 somite stage in *Splotch* mutant embryos (**B**) compared to wild type embryos (**A**).

statistical significance for the dorsal, mid, and ventral measurements (**Figure 3.15C**). Possibly the differences would be statistically significant with larger sample sizes.

By the 19-20 somite stage the difference has decreased, and there are no significant differences in the thickness of the neural folds between $+/+$ and Sp^{2H}/Sp^{2H} embryos for the dorsal, mid, or ventral measurements (**Figure 3.15D**).

Although the NT was found to be significantly smaller in Sp^{2H}/Sp^{2H} embryos at both the 14-15 and 19-20 somite stages, the neural folds of these embryos are not significantly thinner. Therefore, the thickness of the neural folds was analysed in relation to the size of the NT for $+/+$ and Sp^{2H}/Sp^{2H} embryos. $\frac{\text{Dorsal thickness}}{\text{Total area}}$ was calculated for each embryo, and the results were compared between the genotypes. Dorsal area was chosen as the thickness measurement most likely to be affected by the presence of the Sp^{2H} allele, as this involves the region of the NT which expresses *Pax3* in wild type embryos.

Analysis showed a statistically significant increase in the dorsal thickness to area ratio for both the 14-15 and 19-20 somite stage Sp^{2H}/Sp^{2H} embryos (**Figure 3.15E**). This suggests that the neural folds are proportionally thicker for their size in the NTs of Sp^{2H}/Sp^{2H} embryos when compared to $+/+$ embryos, and that this difference is present at the 14-15 somite stage, and continues to be present at the 19-20 somite stage.

3.1.2.5.5 Bending and positions of the hinge points

As the neural folds are proportionally thicker in Sp^{2H}/Sp^{2H} embryos compared to $+/+$ embryos, it is possible that this affects the bending of the hinge points; thicker neural folds may exhibit a lower degree of bending, thus resulting in failure of the NT to close. In this way, the change in proportions of the neural folds of Sp^{2H}/Sp^{2H} embryos compared to $+/+$ embryos may cause the higher frequency of spina bifida seen in these mice. In order to examine if this may be the case, the angles of the MHPs were measured, along with the angles and positions of the DLHPs, in the open region of the spinal NT.

In order to calculate the angle of the MHP, several points were defined in the neural folds. The thicknesses of the neural folds were calculated halfway along the dorso-ventral axis, and the midpoint of each fold was marked at this point. Likewise, the midpoint of the neural folds was calculated at the MHP. The angle of the MHP was calculated by measuring the angle between these three points (**Figure 3.17A-B**).

Figure 3.17: Comparing the angles of the medial hinge points between $+/+$ and Sp^{2H}/Sp^{2H} embryos. **A** and **B** show how the MHP angle was defined. The scale bar represents 50 μm . Blue staining is DAPI. Green staining is anti-phospho histone H3. **A** shows how the length of the NT is measured along the midline, and then the NT is bisected halfway along this midline (yellow lines). The thickness of the neural folds is measured at the MHP and the bisection points (red lines), and then the centres of the neural folds are calculated in these regions (blue circles). The MHP is measured as an angle between these points (**B**, blue circles, red lines and yellow angle).

The angles of the MHPs have been compared between $+/+$ and Sp^{2H}/Sp^{2H} embryos at the 14-15 (**C**) and 19-20 (**D**) somite stages. No significant differences in angle are present between the genotypes at either somite stage.

In **E-H** the MHPs have been analysed separately according to whether they are proximal or distal to the closure point of the PNP (see section 2.7.2.3 for more details). **E** and **F** show that there are no significant differences between the MHP angle of proximal or distal sections in either $+/+$ or Sp^{2H}/Sp^{2H} embryos at the 14-15 (**E**) or 19-20 (**F**) somite stages. **G** and **H** show that there are no significant differences in MHP angle between the genotypes at either the 14-15 (**G**) or 19-20 (**H**) somite stages when comparing proximal and distal sections separately.

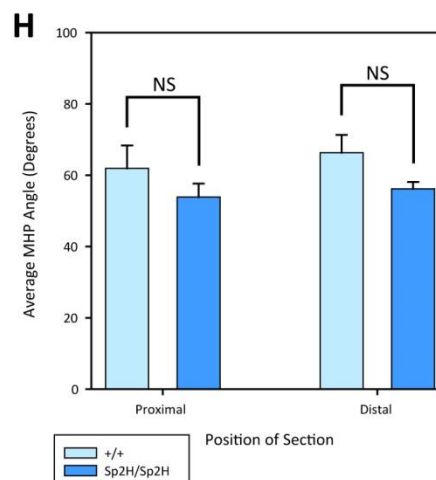
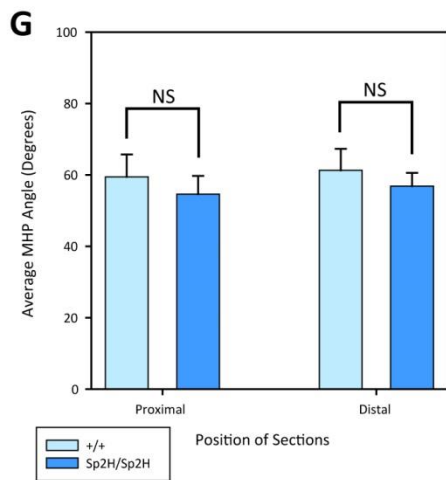
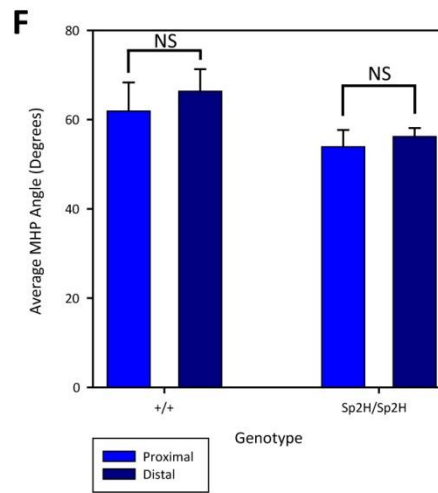
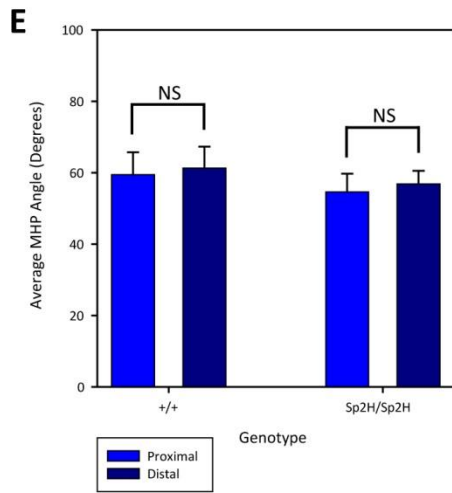
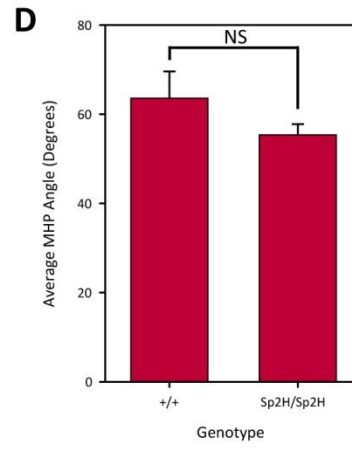
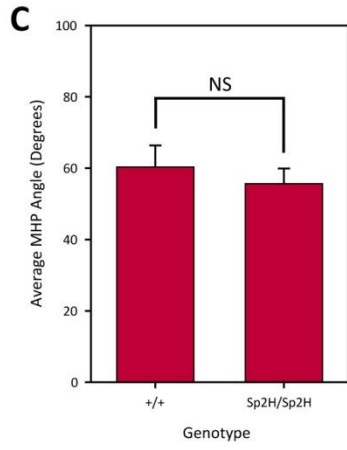
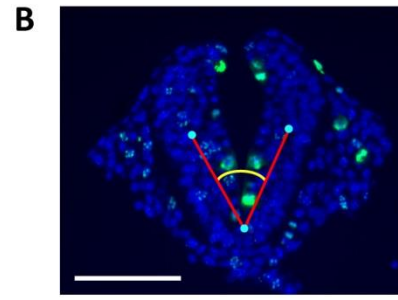
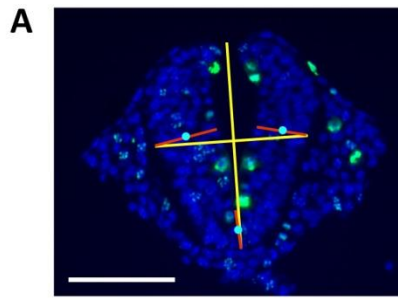
NS: no significance. Error bars show standard error. The t-test was used to test for significant difference. This data follows a Gaussian distribution, apart from the unseparated MHP angles of 14-15 somite stage $+/+$ embryos.

$+/+$ 14-15 somite stage: n = 6.

Sp^{2H}/Sp^{2H} 14-15 somite stage: n = 5.

$+/+$ 19-20 somite stage: n = 5.

Sp^{2H}/Sp^{2H} 19-20 somite stage: n = 5.



The angle of the MHP was compared between Sp^{2H}/Sp^{2H} and $+/+$ embryos at both the 14-15 and 19-20 somite stages. At both of these somite stages, there were no significant differences in MHP angle between Sp^{2H}/Sp^{2H} and $+/+$ embryos (**Figure 3.17C and D**).

Additionally, the angle of the MHP was compared between sections proximal and distal to the closure point of the PNP. Within each genotype, no significant differences were observed between the angles of the MHPs in proximal or distal sections in either 14-15 or 19-20 somite stage embryos (**Figure 3.17E and F**). Additionally, no differences were found between genotypes when comparing either proximal or distal sections separately (**Figure 3.17G and H**).

The DLHP angle was calculated by marking the midpoint of the neural fold at the DLHP, and finding the angle between lines which are parallel to the neural folds around the DLHP and meet at this point (**Figure 3.18A and B**). The DLHPs are not always present in the NT at the level of the PNP closure point in 14-15 somite stage embryos, so this analysis was only carried out on 19-20 somite stage embryos. It was found that the angles of the DLHPs are significantly smaller in Sp^{2H}/Sp^{2H} embryos compared to $+/+$ embryos, indicating greater bending in the *Spotch* mutant embryos. (**Figure 3.18C**) However, these differences between the genotypes do not reach significance when considering proximal and distal sections separately, although this could possibly be overcome by greater sample sizes as there appears to be a trend, despite the absence of statistical significance (**Figure 3.18E**).

The dorso-ventral position of the DLHPs was calculated by connecting a line between the outermost points of the DLHPs, at the basal edge of the NT. The distance was then measured between the ventral-most point of the NT and the intersection of this line with the midline. This distance was calculated as a proportion of the total length of the NT (**Figure 3.20A and B**). It was found that the DLHPs of Sp^{2H}/Sp^{2H} embryos are located significantly more dorsally when compared to those of $+/+$ embryos (**Figure 3.20C**). No significant differences were seen within genotypes when comparing proximal and distal sections (**Figure 3.20D**). However, significant differences are present between the genotypes when comparing proximal and distal sections separately (**Figure 3.20E**).

3.1.3 The effects of folate deficiency on neural tube closure in *Spotch* mutant embryos

Folate levels are known to affect the closure of the NT in Sp^{2H}/Sp^{2H} embryos (Burren et al., 2008; Fleming and Copp, 1998). Folate deficient embryos were generated by feeding a folate deficient diet (FD) to the mother for three weeks before mating, and during gestation. The effects of folate deficiency on NTD development were studied in these embryos.

Figure 3.18: Comparing the angles of the dorsolateral hinge points between $+/+$ and Sp^{2H}/Sp^{2H} embryos – 1. **A** and **B** show how the DLHP angles were defined. The scale bar represents 50 μm . Blue staining is DAPI. Green staining is anti-phospho histone H3. **A** shows how the thicknesses of the neural folds were measured at the DLHPs (yellow lines) and the midpoints of the neural folds were calculated at these points (blue circles). **B** shows how lines were drawn centred on these midpoints (blue circles) lying parallel with the neural folds dorsal and ventral to the DLHPs (red lines). The angles between these lines were calculated to give a value for the DLHPs (yellow angles).

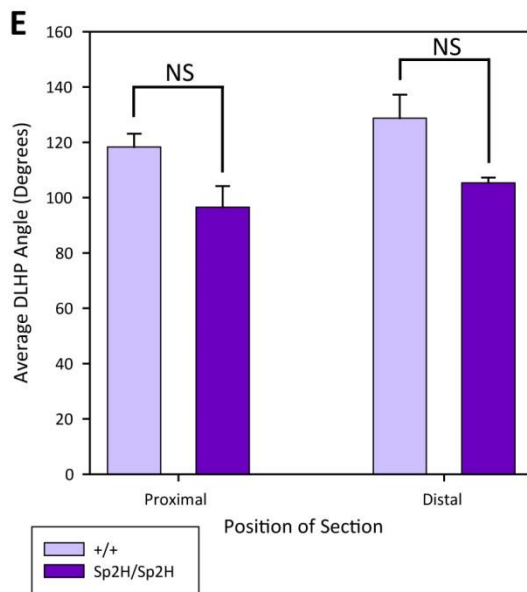
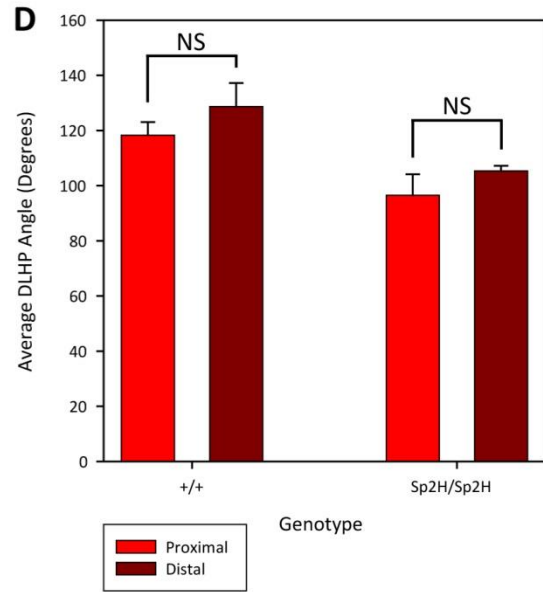
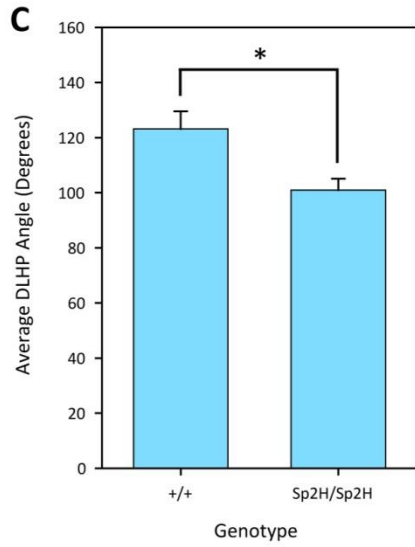
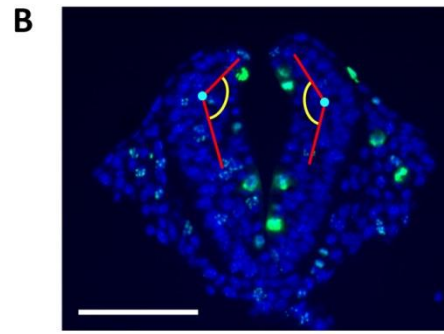
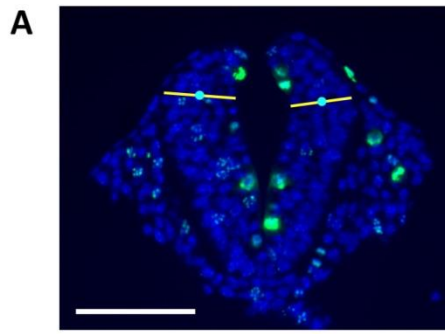
The angles of the DLHPs at the 19-20 somite stage have been compared between $+/+$ and Sp^{2H}/Sp^{2H} embryos (**C**). Sp^{2H}/Sp^{2H} embryos have significantly smaller DLHP angles when compared to $+/+$ embryos.

In **D** and **E** the DLHPs have been analysed separately according to whether they are proximal or distal to the closure point of the PNP (see section 2.7.2.3 for more details). **D** shows that there are no significant differences between the DLHP angles of proximal or distal sections in either $+/+$ or Sp^{2H}/Sp^{2H} embryos at the 19-20 somite stage. **E** shows that there are no significant differences in DLHP angle between the genotypes when comparing proximal and distal sections separately.

* $p \leq 0.05$. NS: no significance. Error bars show standard error. The t-test was used to test for significant difference. This data follows a Gaussian distribution.

$+/+$: $n = 4$.

Sp^{2H}/Sp^{2H} : $n = 3$.



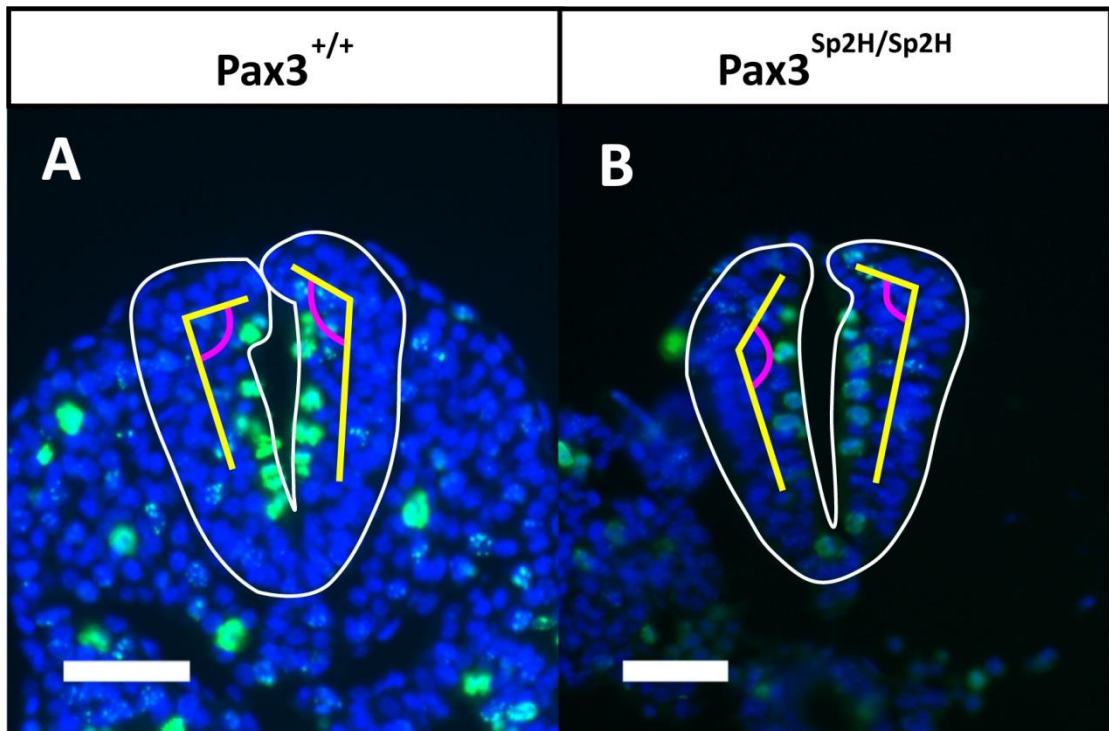


Figure 3.19: Comparing the angles of the dorsolateral hinge points between $+/+$ and Sp^{2H}/Sp^{2H} embryos – 2. Experimental litters were generated containing a mixture of genotypes by intercrossing $Sp^{2H}/+$ mice. Scale bars represent 50 μm . Cell nuclei are stained with DAPI and show as blue. The Phospho histone H3 antibody marks proliferating cells and shows as green. **A** and **B** show examples of the NTs of wild type and Splotch mutant embryos respectively. The NT is outlined in white for clarity.

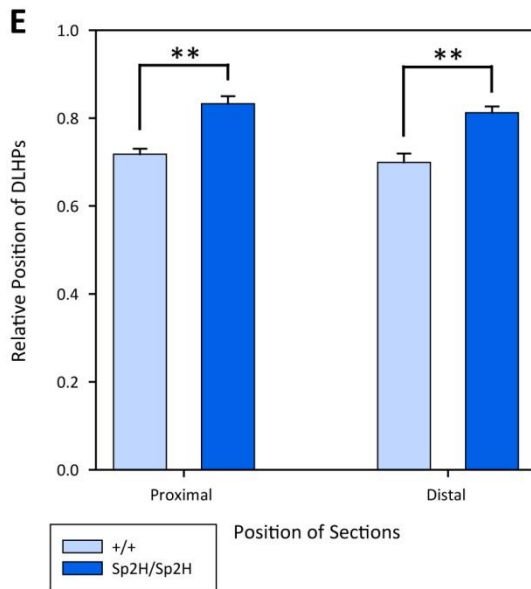
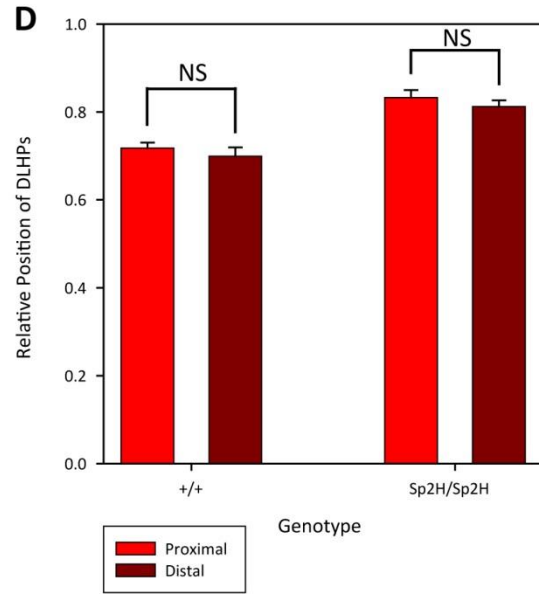
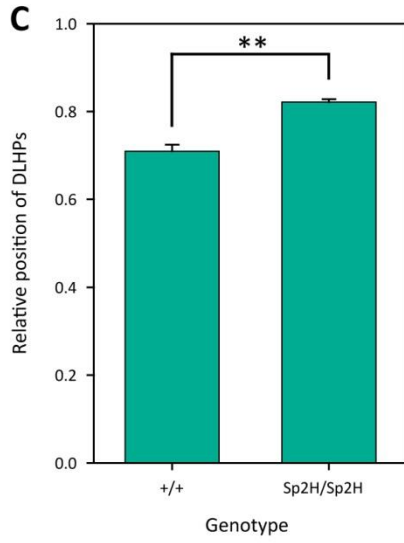
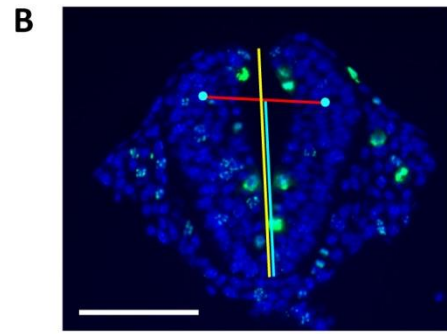
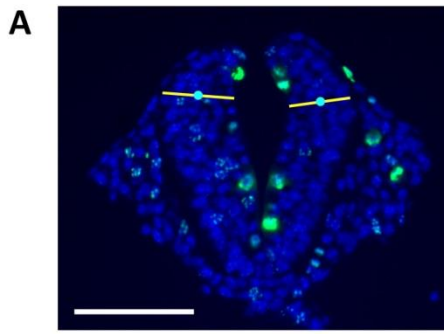
The positions of the DLHPs are shown in yellow, and the measured angles are shown in pink. The average DLHP angles of *Splotch* mutant embryos (**B**) are smaller than those of wild type embryos (**A**).

Figure 3.20: Comparing the positions of the dorsolateral hinge points between $+/+$ and Sp^{2H}/Sp^{2H} embryos. **A** and **B** show how the DLHP positions were defined. The scale bar represents 50 μm . Blue staining is DAPI. Green staining is anti-phospho histone H3. **A** shows how the thicknesses of the neural folds were measured at the DLHPs (yellow lines) and the midpoints of the neural folds were calculated at these points (blue circles). **B** shows how these points were joined (blue circles, red line). The midline of the NT was measured (yellow line), and the distance from the ventral limit of the NT to the line joining the DLHP midpoints was also measured (blue line). The position of the DLHPs was calculated as $\frac{\text{blue line}}{\text{yellow line}}$.

The positions of the DLHPs at the 19-20 somite stage have been compared between $+/+$ and Sp^{2H}/Sp^{2H} embryos (**C**). Sp^{2H}/Sp^{2H} embryos have significantly more dorsal DLHPs when compared to $+/+$ embryos.

In **D** and **E** the DLHPs have been analysed separately according to whether they are proximal or distal to the closure point of the PNP (see section 2.7.2.3 for more details). **D** shows that there are no significant differences between the DLHP positions of proximal or distal sections in either $+/+$ or Sp^{2H}/Sp^{2H} embryos at the 19-20 somite stage. **E** shows that the DLHPs are significantly more dorsal in Sp^{2H}/Sp^{2H} embryos compared to $+/+$ embryos when considering proximal and distal sections separately.

** $p \leq 0.01$. NS: no significance. Error bars show standard error. The t-test was used to test for significant difference. $n = 3$ per genotype. This data follows a Gaussian distribution.



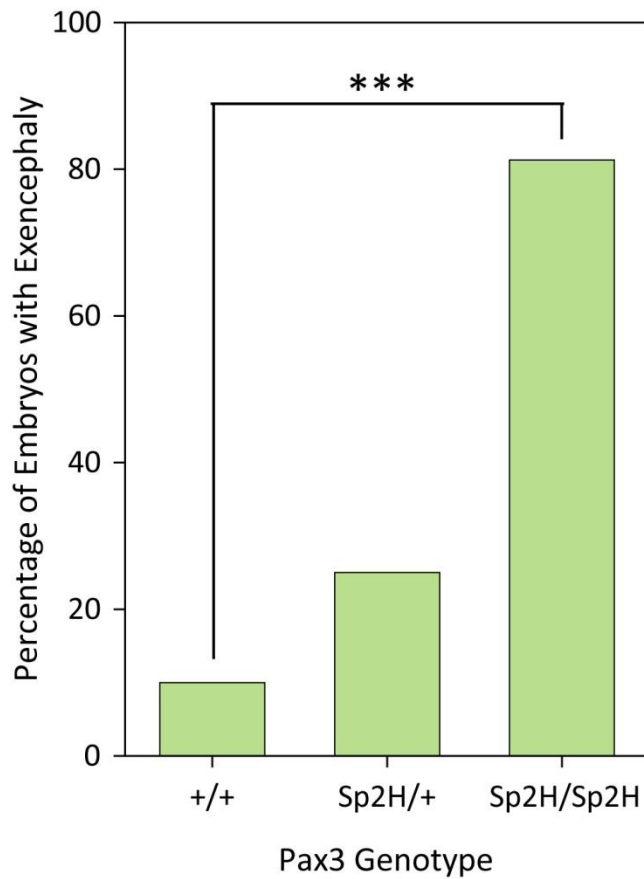


Figure 3.21: Exencephaly in folate-deficient embryos. Experimental litters containing multiple genotypes were generating through intercross of $Sp^{2H}/+$ mice.

The graph shows frequency of exencephaly in the different genotypes from this cross. Exencephaly is defined as an open cranial NT at the 18 somite stage or older. Sp^{2H}/Sp^{2H} embryos have a significantly higher frequency of exencephaly when compared to $+/+$ embryos. The frequency in $Sp^{2H}/+$ embryos also appears to be higher, but the difference has not reached significance. The Fisher Exact Test was used to test for significant difference. *** $p < 0.001$. $+/+$: $n = 10$. $Sp^{2H}/+$: $n = 28$. Sp^{2H}/Sp^{2H} : $n = 16$.

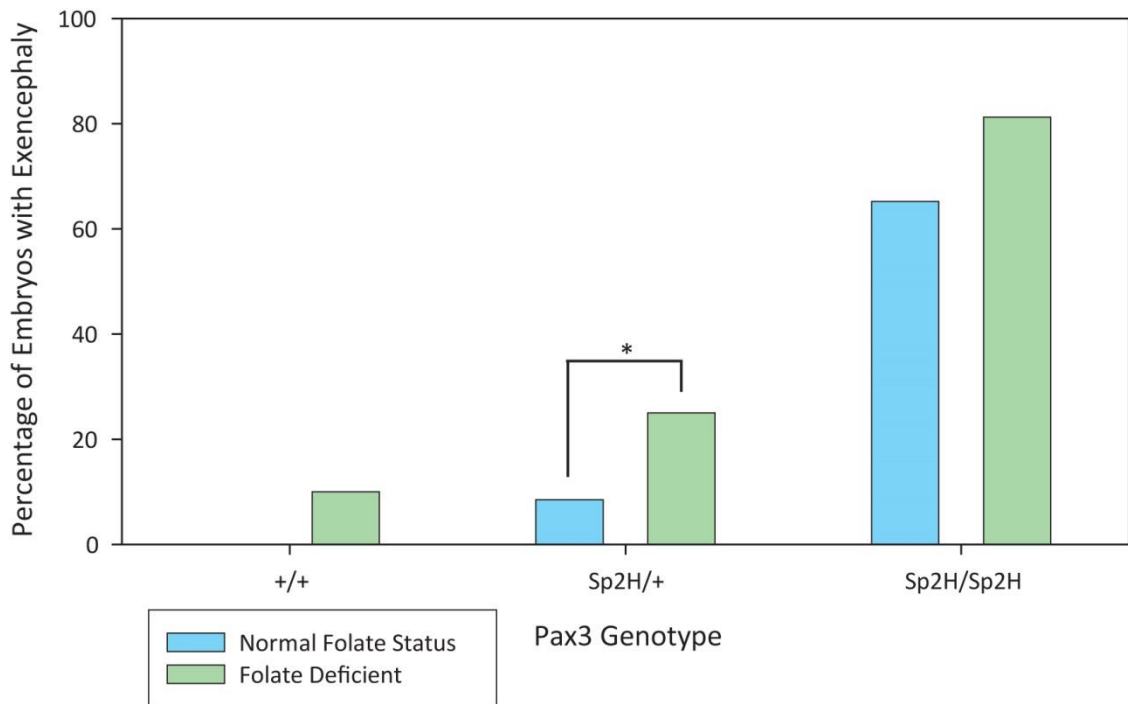


Figure 3.22: Comparing the frequency of exencephaly in embryos of different genotypes with either normal or folate deficient status. Experimental litters were generated through intercross of $Sp^{2H}/+$ embryos. Progeny of the resulting genotypes were compared to embryos of equivalent genotype with folate deficiency. FD and ND embryos were collected concurrently, although ND embryos were collected for a longer period of time.

$+/+$ and Sp^{2H}/Sp^{2H} embryos showed an increase in the frequency of exencephaly in the FD embryos when compared to the ND embryos of the equivalent genotype. However, this difference was not significant. $Sp^{2H}/+$ embryos, on the other hand, show a significant increase in exencephaly in the FD embryos.

* $p < 0.05$. The Fisher Exact Test ($+/+$ and $Sp2H/Sp2H$) or the Chi-Square Test ($Sp2H/+$) were used to test for significant difference.

Normal folate status - $+/+$: $n = 54$. $Sp^{2H}/+$: $n = 94$. Sp^{2H}/Sp^{2H} : $n = 46$.

Folate deficient - $+/+$: $n = 10$. $Sp^{2H}/+$: $n = 28$. Sp^{2H}/Sp^{2H} : $n = 16$.

3.1.3.1 Folate deficiency increases the rate of exencephaly in *Spotch* heterozygous embryos

FD embryos were monitored for exencephaly. A significant increase in the frequency of exencephaly is seen when comparing Sp^{2H}/Sp^{2H} embryos to $+/+$ (**Figure 3.21**). An increase is also seen in $Sp^{2H}/+$ embryos compared to $+/+$, but this difference does not reach significance.

The frequency of exencephaly within genotypes was compared between normal diet (ND) and FD embryos to observe the effect of the folate deficiency on exencephaly development. An increase was seen in the frequency of exencephaly in $+/+$ and Sp^{2H}/Sp^{2H} FD embryos, although these differences did not reach significance. However, a significant increase in the frequency of exencephaly was seen in $Sp^{2H}/+$ FD embryos when compared to the ND embryos of the same genotype (**Figure 3.22**). This data validates previous findings (Burren et al., 2008).

3.1.3.2 Folate deficiency slightly affects spinal neurulation in *Spotch* heterozygous embryos

The effect of FD on spinal neurulation has not previously been studied. The PNP was measured for each embryo, and the embryos were grouped according to somite stage (6-8, 9-11, etc.) (**Figure 3.23**). The PNP sizes of $+/+$ embryos on ND and FD were compared to examine whether the FD may have an effect on NT closure without any influence of the *Pax3* mutation.

The PNP sizes were also compared within the genotypes between embryos on ND or FD. No significant differences in PNP size were found between $+/+$ ND or FD embryos (**Figure 3.24A**). However, a significant reduction in PNP size was found in $Sp^{2H}/+$ FD embryos at the 15-17 and 18-20 somite stages (**Figure 3.24B**). FD Sp^{2H}/Sp^{2H} embryos also showed a significant reduction in PNP size at the 9-11 somite stage when compared to ND embryos (**Figure 3.24C**).

3.1.4 Canonical Wnt signalling in *Spotch* mutant embryos

It is possible that canonical Wnt signalling is disrupted in Sp^{2H}/Sp^{2H} embryos (see section 1.4.7 for more information). Therefore, canonical Wnt signalling levels, and expression of related genes, were studied in Sp^{2H}/Sp^{2H} mice.

3.1.4.1 *LacZ* RT-qPCR of BatGal embryos

Embryos were collected at the 18-19 somite stage from a $Pax3^{Sp2H/+} LacZ^{BatGal/+} \times Pax3^{Sp2H/+}$ cross. The BatGal allele is a LacZ-expressing gene under the control of β -catenin responsive elements (Maretto et al., 2003). Therefore, the β -galactosidase gene is expressed in regions of canonical Wnt signalling, and the amount expressed should indicate the level of canonical Wnt signalling.

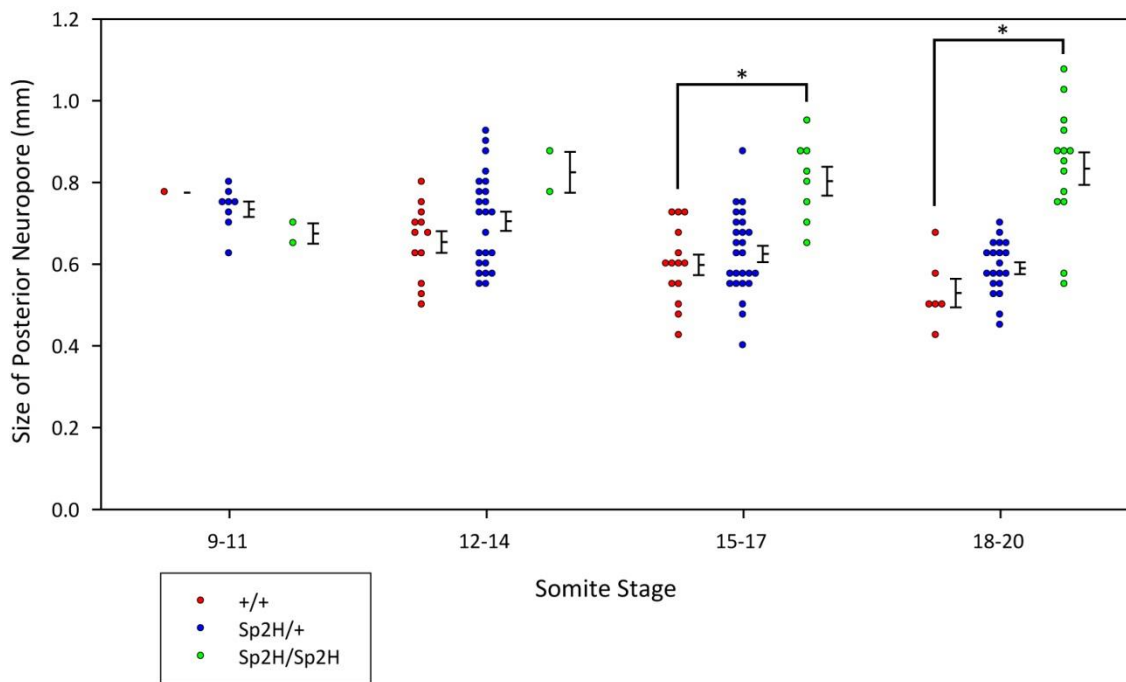


Figure 3.23: Posterior neuropore closure in folate deficient embryos. Experimental litters containing multiple genotypes were generated through intercross of $Sp^{2H}/+$ mice.

The graph shows PNP length in embryos of the different genotypes in grouped somite stages. Although the Sp^{2H}/Sp^{2H} embryos appear to have a larger PNP at the 12-14 somite stage, a significant increase in size is first seen at the 15-17 somite stage. No significant difference is seen in PNP size between $+/+$ and $Sp^{2H}/+$ embryos. One-way ANOVA was used to test for significant difference. Error bars show standard error. * $p < 0.05$.

9-11 somites – $+/+$: $n = 1$. $Sp^{2H}/+$: $n = 8$. Sp^{2H}/Sp^{2H} : $n = 2$.

12-14 somites – $+/+$: $n = 12$. $Sp^{2H}/+$: $n = 24$. Sp^{2H}/Sp^{2H} : $n = 2$.

15-17 somites – $+/+$: $n = 14$. $Sp^{2H}/+$: $n = 26$. Sp^{2H}/Sp^{2H} : $n = 8$.

18-20 somites – $+/+$: $n = 6$. $Sp^{2H}/+$: $n = 20$. Sp^{2H}/Sp^{2H} : $n = 14$.

Figure 3.24: Comparison of posterior neuropore size in embryos of different genotypes with either normal or folate deficient status. Experimental litters were generated through intercross between $Sp^{2H}/+$ embryos. FD and ND embryos were collected concurrently, although ND embryos were collected for a longer period of time. The graphs show data for the resulting genotypes – $+/+$ (A), $Sp^{2H}/+$ (B), and Sp^{2H}/Sp^{2H} (C). Data has been grouped according to the somite stage of the embryo.

$+/+$ embryos show no significant differences in PNP size between the two different folate statuses. However the $Sp^{2H}/+$ and Sp^{2H}/Sp^{2H} embryos both show significant differences at certain somite stages when compared to the ND embryos. A significant reduction in PNP size is seen in the FD embryos at the 15-17 and 18-20 somite stages in the $Sp^{2H}/+$ embryos, and at the 9-11 somite stage in the Sp^{2H}/Sp^{2H} embryos.

* $p \leq 0.05$, ** $p \leq 0.01$. Error bars show standard error. The t-test was used to test for significant difference.

A – 9-11 somites – ND: n = 10. FD: n = 1.

12-14 somites – ND: n = 29. FD: n = 12.

15-17 somites – ND: n = 38. FD: n = 14.

18-20 somites – ND: n = 40. FD: n = 6.

21-23 somites – ND: n = 12. FD: n = 4.

B – 6-8 somites – ND: n = 4. FD: n = 3.

9-11 somites – ND: n = 26. FD: n = 8.

12-14 somites – ND: n = 59. FD: n = 24.

15-17 somites – ND: n = 63. FD: n = 26.

18-20 somites – ND: n = 66. FD: n = 20.

21-23 somites – ND: n = 22. FD: n = 7.

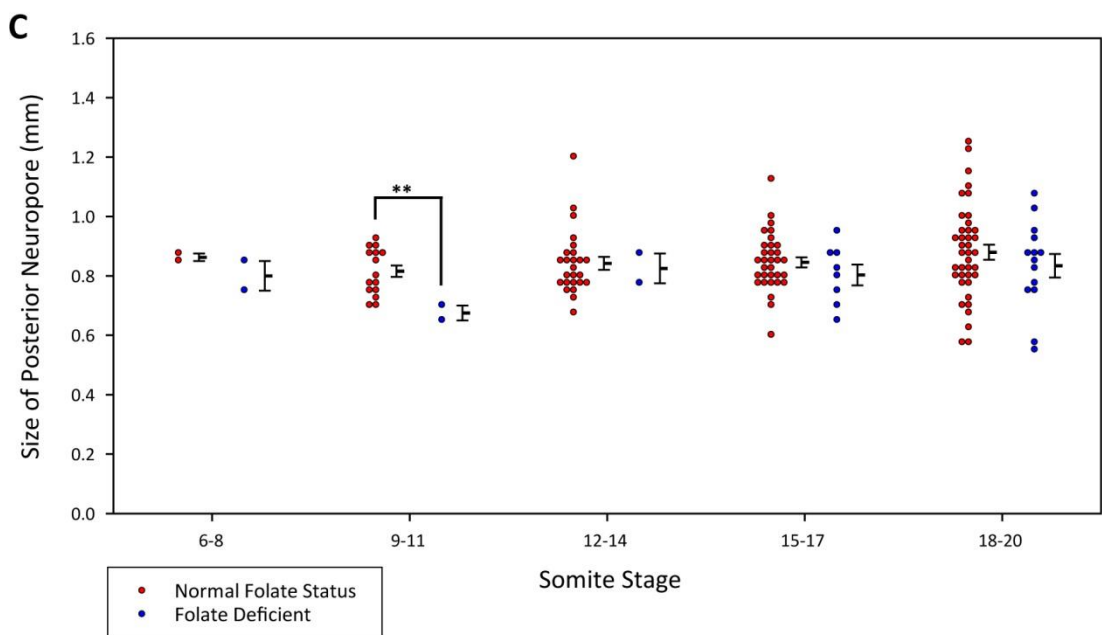
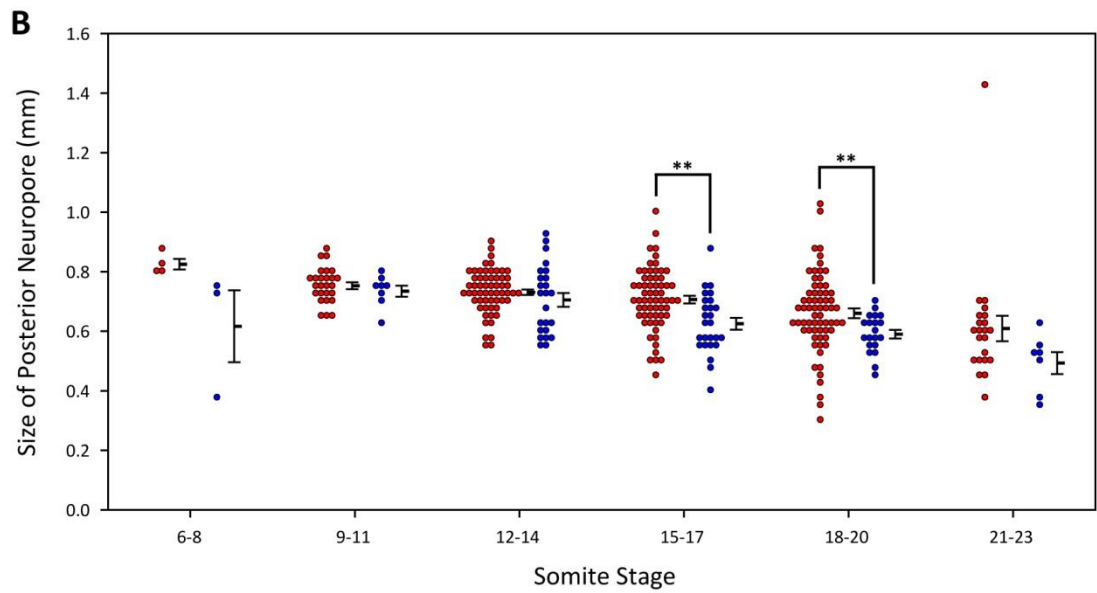
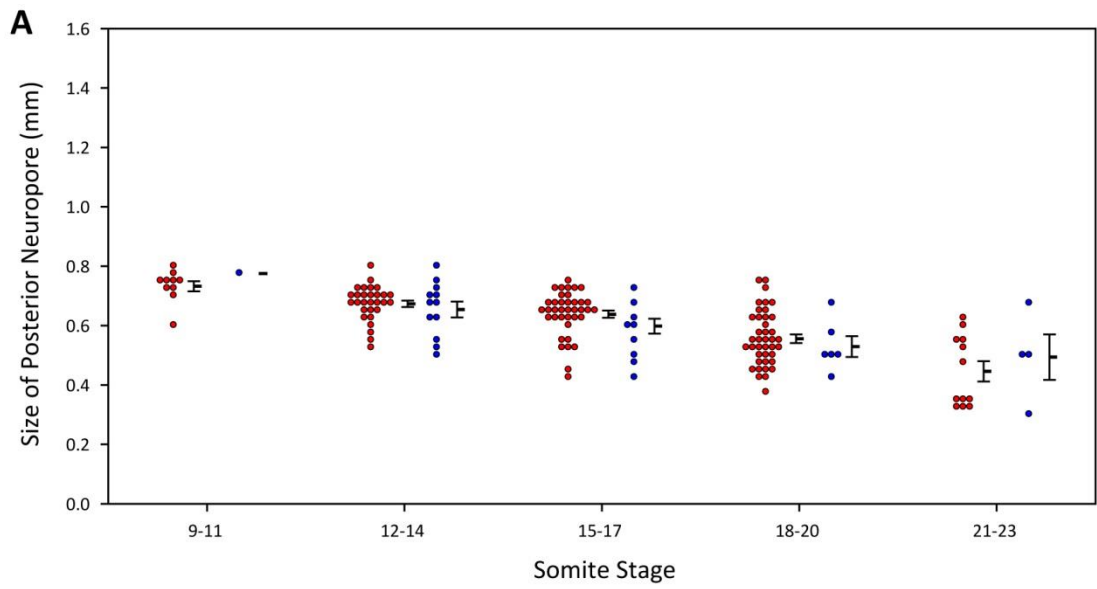
C – 6-8 somites – ND: n = 2. FD: n = 2.

9-11 somites – ND: n = 16. FD: n = 2.

12-14 somites – ND: n = 25. FD: n = 2.

15-17 somites – ND: n = 32. FD: n = 8.

18-20 somites – ND: n = 39. FD: n = 14.



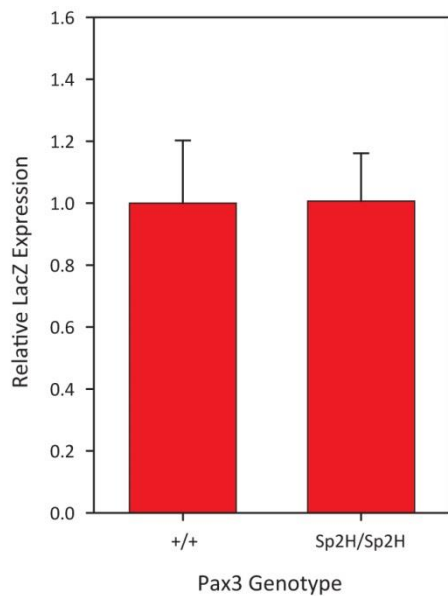


Figure 3.25: Comparing Wnt signalling levels between +/+ and Sp^{2H}/Sp^{2H} embryos.

Experimental litters were generated containing a mixture of genotypes by crossing $Sp^{2H}/+$ +/+ mice to $Sp^{2H}/+$ *BatGal*/+ mice. RT-qPCR was carried out on whole embryo RNA extractions from 18-19 somite stage +/+ and Sp^{2H}/Sp^{2H} embryos carrying the *BatGal* Wnt reporter allele. No significant difference in LacZ expression was seen between the genotypes.

The t-test was used to test for significant difference. n = 3 for each genotype. Error bars show standard error.

RNA was extracted from whole embryos of genotypes $Pax3^{+/+}$ *BatGal*/+ and $Pax3^{Sp2H/Sp2H}$ *BatGal*/+. RT-qPCR was used to compare the relative expressions of LacZ in these embryos, to observe if *Pax3* expression affects levels of canonical Wnt signalling in the embryos as a whole. No significant difference was seen in the levels of LacZ expression between these genotypes (Figure 3.25).

3.1.4.2 Wnt RT-qPCR plate

RT-qPCR was carried out using the RT² Profiler™ PCR Array Plate for the mouse Wnt signalling pathway from SABiosciences. This array allowed a broad readout of the expression of genes

implicated in or downstream of Wnt signalling in the *Spotch* embryo. The array does not allow for replicates, and thus is simply used to indicate genes which may be worth further study. The RT-qPCR was carried out using RNA extracted from 14 somite stage embryo heads, and $+/+$ embryos were compared to Sp^{2H}/Sp^{2H} embryos. The 14 somite stage was used as this was the main stage of interest (as discussed previously), and the cranial region was used as this is what was available at the 14 somite stage. Although the spinal region is the main area of study in the *Spotch* embryos in this thesis, it is possible that using the cranial region could also give insight into gene expression in the embryo as a whole, including the spinal region.

Gene	Relative Expression
Axin1	0.60
Fgf4	0.69
Fosl1	5.28
Foxn1	1.74
Fshb	1.47
Fzd6	0.68
Sfrp4	1.44
Wnt2	0.24
Wnt6	0.71
Wnt7a	1.73
Wnt8a	1.72
Wnt9a	0.51

Table 3.1: Genes which passed the threshold of 1.4-fold difference in the RT² Profiler™ PCR Array Plate for the mouse Wnt signalling pathway from SABiosciences. Experimental litters were generated by intercrossing $Sp^{2H}/+$ embryos. Sp^{2H}/Sp^{2H} embryos were compared to control embryos, which had the genotype $+/+$. n = 3 per genotype.

RNA was extracted from the cranial regions of 14 somite stage embryos, and then pooled according to genotype. The threshold was a 1.4-fold difference, which is equivalent to relative expression levels of 1.4 (upregulated gene) or 0.71 (downregulated gene).

A threshold of 1.4-fold difference was chosen to define genes with differences in relative expression levels. This should allow dismissal of genes which are exhibiting small natural fluctuations in expression. Several genes passed the set threshold of 1.4-fold difference (see **Table 3.1** for a list of these genes), and some of these were studied further (see section below). However, Wnt-related gene expression appeared largely very similar between *+/+* and *Sp^{2H}/Sp^{2H}* embryos.

3.1.4.3 RT-qPCR of Wnt genes in *Spotch* mutant embryos

A number of canonical Wnt-related genes were chosen from amongst those which appeared to be disrupted on the Wnt RT-qPCR plate (see section above). The potential genes were narrowed down by choosing those which were related to canonical Wnt signalling specifically, and which appeared to show an expression pattern which could overlap with that of *Pax3*. The genes *Axin1*, *Sfrp4*, and *Fzd6* were chosen to study, and the genes *Axin2* and *Cdx2* were chosen to monitor the overall levels of Wnt signalling, as these are established measures of canonical Wnt signalling levels; *Cdx2* is known to be downstream of canonical Wnt signalling, and *Axin2* has been shown to be downregulated in the NTs of embryos with β -catenin loss-of-function (Benahmed et al., 2008; Hart et al., 1998; Wang and Shashikant, 2007; Zechner et al., 2003). *Axin2* is commonly used to monitor levels of canonical Wnt signalling, as expression of *Axin2* is induced by canonical Wnt signalling. This is supported by the identification of TCF/LEF binding sites in the *Axin2* promoter region (Jho et al., 2002). Although several genes showed greater fold changes in the Wnt RT-qPCR plate study these were not examined further due to lack of connection to the canonical Wnt signalling pathway or due to differences in expression pattern between the gene and *Pax3*.

RNA was extracted from whole embryos of 23-24 somite stage and genotypes *+/+* and *Sp^{2H}/Cre*, and RT-qPCR was used to compare relative expressions of the chosen genes (**Figure 3.26**). Although embryos at approximately the same somite stage as used previously (14 somites) would be ideal for carrying out the validation, these were not available in sufficient numbers to allow comparison between the genotypes. 23-24 somite stage embryos were available in numbers which enabled comparison. However, no significant differences were seen in the gene expressions when compared between the genotypes.

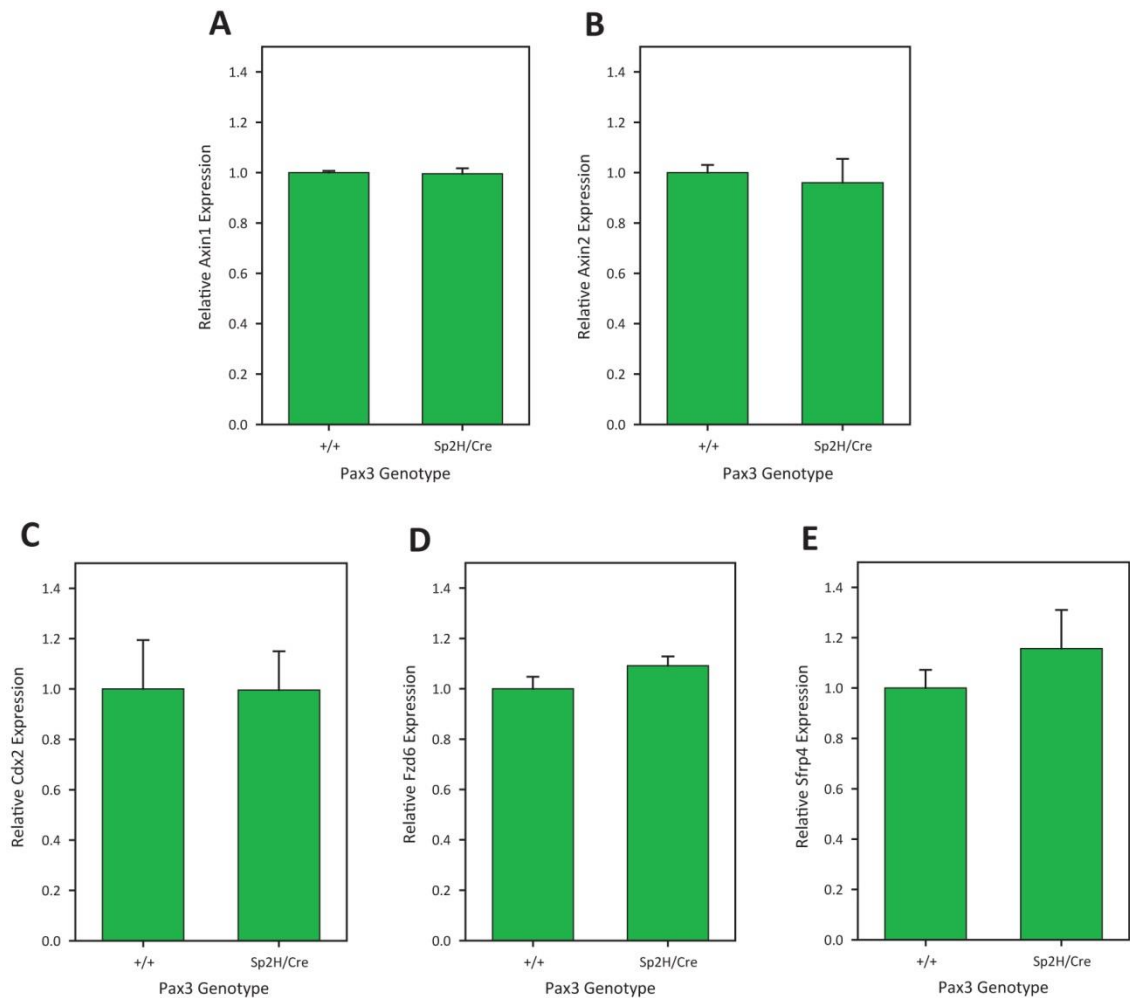


Figure 3.26: Comparing expressions of Wnt-related genes in *+/+* and *Sp^{2H}/Cre* embryos.

Experimental litters were generated containing a mixture of genotypes through the cross *Pax3^{Sp2H/+} β-catenin^{GOF/+} × Pax3^{Cre/+} β-catenin^{+/+}*. This cross was used for the experiments described in **Chapter 4**. *Sp^{2H}/Cre* embryos are – like *Sp^{2H}/Sp^{2H}* embryos – *Pax3*-null.

Gene expression was analysed using RT-qPCR on whole embryo (23-24 somite stage) RNA extractions. The gene expressions analysed were *Axin1* (A), *Axin2* (B), *Cdx2* (C), *Fzd6* (D), and *Sfrp4* (E). No significant differences were seen in expression between the genotypes for any of the genes studied.

n = 4 for each genotype. Error bars show standard error. The t-test was used to test for significant difference.

3.2 Discussion

3.2.1 Cellular defects during spinal neurulation in *Spotch* mutant embryos

Three main theories have been put forward as potential cellular mechanisms which could cause exencephaly in Sp^{2H}/Sp^{2H} embryos; increased apoptosis, premature neuronal differentiation, and reduced proliferation in the NT. This study analysed each of these cellular processes in the spinal region of Sp^{2H}/Sp^{2H} embryos during neurulation to investigate whether they could possibly play a causal role in the development of spina bifida.

Apoptosis was studied using both observational and experimental methods. TUNEL staining detected no increase in apoptosis in the PNP of Sp^{2H}/Sp^{2H} embryos, although quantification of apoptosis in the spinal region by cell counting using sections could confirm this more definitively. Additionally, higher sample numbers could help to clarify the results, as apoptosis is highly variable, even within a genotype. It is possible that higher levels of apoptosis occur in the cranial region of Sp^{2H}/Sp^{2H} embryos compared to $+/+$ embryos. However this result was inconsistent, and would require quantitation of apoptotic cells and larger sample sizes to confirm.

If excess apoptosis was present in the caudal NT of Sp^{2H}/Sp^{2H} embryos, then experimentally reducing apoptosis may have constituted a rescue effect. This effect has been previously reported through use of a p53-null allele (Pani et al., 2002). However, attempts to replicate these results proved unsuccessful; Sp^{2H}/Sp^{2H} embryos developed both spina bifida and exencephaly regardless of p53 expression levels. This suggested that the p53-null allele used in these crosses had no rescuing effect on NTDs in Sp^{2H}/Sp^{2H} mice.

However, p53 has additional functions unrelated to apoptosis, including cell cycle arrest, induction of senescence, and regulation of metabolism (Chen et al., 2005; el-Deiry, 1998; Hu et al., 2010; Matoba et al., 2006). Therefore, p53 mutation will have effects on other cellular processes in addition to apoptosis, and any of these may have contributed to NTD rescue in Sp/Sp embryos. Inhibitors which target apoptosis specifically, such as Z-VAD-FMK, may provide information on the role of apoptosis in NTD development in *Spotch* embryos, while leaving other p53-mediated processes intact.

There are several reasons why the research described here could disagree with that reported previously (Pani et al., 2002). For example, the original research used mice carrying the Pax3^{Sp} allele, whereas the mice used in the research described here carry the Pax3^{Sp2H} allele. Differences in Pax3 protein activity or severity of NTDs could affect the results. Additionally, the mice in the original research had a C57 genetic background, whereas those used in the

research described here had a mixed CBA/101 background. As discussed previously (Section 1.2.2.1) differences in genetic background can alter the effects of mutations due to the presence of different modifier genes (Davidson et al., 2007; Finnell et al., 1986; Finnell et al., 1988; Fleming and Copp, 2000). Therefore, it is possible that any rescue effects caused by the p53 mutation in *Splotch* embryos are more prominent on particular genetic backgrounds. Following these results, attempts were made to verify the knock-down of the p53 protein in the mice used in the study. However, endogenous p53 protein present at a concentration which was too low to detect using Western blot, despite attempts to concentrate the protein. Additionally, no reduction in apoptosis was noted in Pax^{+/+} p53^{-/-} embryos compared to Pax3^{+/+} p53^{+/+} embryos, so verification was not possible. Immunohistochemistry to detect the p53 protein in whole embryos or sections could possibly be used to verify p53 knockdown in the mutant embryos.

Neuronal differentiation in the neural tube was compared in *+/+* and *Sp^{2H}/Sp^{2H}* embryos during neurulation. Theoretically premature neuronal differentiation in the spinal region of *Sp^{2H}/Sp^{2H}* mice could interfere with the closure of the PNP and cause spina bifida. Indeed, premature neuronal differentiation in the cranial region has been previously found in *Splotch* embryos (Nicholas Greene, unpublished data). However, no differentiating cells were observed in the region surrounding the closure point of the PNP, either in *+/+* or *Sp^{2H}/Sp^{2H}* embryos. Therefore, even if premature neuronal differentiation were present in the spinal NT of *Sp^{2H}/Sp^{2H}* embryos it would be unlikely to be causal for spina bifida.

Sp^{2H}/Sp^{2H} embryos were assessed for the presence of premature neuronal differentiation in the spinal region. The extent of the differentiation was measured by observing the somite level at which neuronal differentiation was visible through immunohistochemistry. However, no significant difference was seen when comparing this between the *+/+* and *Sp^{2H}/Sp^{2H}* embryos. This makes it unlikely that there is premature neuronal differentiation in the spinal region of *Sp^{2H}/Sp^{2H}* embryos.

Finally, proliferation of the cells in the spinal NT was compared between *+/+* and *Sp^{2H}/Sp^{2H}* embryos during neurulation. Reduced proliferation has been previously found in the cranial NT of *Splotch* embryos (Nicholas Greene, unpublished data). A gradient of proliferation was observed in the cells of the spinal NT in *+/+* embryos at the 14-15 somite stage; proliferation was high in the dorsal Pax3-expression region, and lower in the ventral Pax3-negative region. However, this gradient is lost by the 19-20 somite stage; embryos demonstrate a uniform rate of proliferation throughout the NT, equivalent to the lower ventral rate of proliferation in 14-15 somite stage *+/+* embryos. The proliferation gradient is absent in 14-15 somite stage

Sp^{2H}/Sp^{2H} embryos – the mutant NT has a uniform rate of proliferation throughout, which is equivalent to the lower ventral rate of proliferation in $+/+$ embryos. There were no significant differences in proliferation between $+/+$ and Sp^{2H}/Sp^{2H} embryos at 19-20 somite stage; proliferation is uniform throughout the NT in both genotypes at this stage of development.

As mentioned previously, experiments to study proliferation and differentiation in the *Splotch* embryos were carried out the 14-15 somite stage and 13-15 somite stage respectively, as this originally appeared to be the developmental stage at which significant differences in the size of the PNPs were first seen between genotypes. As more data was collected this point during development was found to be earlier than originally thought, at the 10-11 somite stage. Ideally, the experiment quantifying proliferation in the spinal region of the NT would be repeated using embryos at the 8-9 somite stage, prior to the onset of the defect. At this stage during development there are no significant differences in the size of the PNP between $+/+$ and Sp^{2H}/Sp^{2H} embryos. The defect must be present prior to the detection of the morphological defect. Therefore, at the 8-9 somite stage the cellular defect would likely be present, but there would be no morphological differences to potentially affect the results. However, the data presented in this thesis has merit, as it demonstrates cellular differences in the NT soon after the onset of the morphological defect.

It would be interesting to carry out the proliferation experiments using 13-15 and 19-20 somite stage embryos, and sections a fixed distance from the caudal extremity. In the experiments described in this thesis the focus of study was the closure point of the PNP. However, due to the differences in the size of the PNP between genotypes this point will be in a different position on the rostro-caudal axis depending on genotype. Therefore, it could be informative to observe proliferation in the NT a set distance from the caudal tip of the embryo. This would eliminate the possibility that the position of the sections on the rostro-caudal axis causes changes in proliferation between genotypes, as opposed to the genotypes themselves. However, the method used in this thesis is useful, as it enables direct comparison between genotypes of proliferation in the actively closing regions of the PNP. This is essential, as the closure appears to be slowed in Sp^{2H}/Sp^{2H} embryos, and so this is a critical region.

It would also be interesting to study whether the proliferation defect seen in Sp^{2H}/Sp^{2H} embryos causes the NTDs in these embryos, or whether it is an unrelated additional defect. A reduction in proliferation could prevent NT closure through a wide range of mechanisms. For example, it could alter the morphology of the NT (as was studied), thus mechanically preventing closure. Alternatively, the rate of proliferation could be coupled with another cellular mechanism, such as differentiation, apoptosis, or migration (such as that of the NC).

Alteration of proliferation could alter the activity of other mechanisms, which could affect the behaviour or proportions of cell types, or the properties of the tissue. Any of these alterations could potentially prevent closure of the NT. Experiments to observe the expression of genes, such as those expressed in the NC, those related to migration, or those expressed in the ECM for example, could provide more information about other disrupted mechanisms in the NT and surrounding tissues of *Spotch* mutant embryos. Alternatively, the proliferation defect seen in the *Spotch* mutant embryos may not be limited to the NT. Proliferation studies of surrounding tissue, such as the notochord or the gut, could show if these tissues may also have altered proliferation in the mutant embryos. For example, reduced proliferation in the gut of *ct* embryos causes spina bifida (Copp et al., 1988a). Therefore, it is possible that proliferation defects in tissues other than the NT in the *Spotch* embryos may cause NTDs.

Reducing proliferation in embryos at the critical stages of NT closure could mimic the defect seen in the Sp^{2H}/Sp^{2H} mice, and it would be interesting to observe if NTDs develop. For example, culture of embryos in an anti-mitotic agent, such as Mitomycin, would reduce proliferation. However, this reduction might be seen in all tissues, and could potentially cause a large number of defects. Therefore, NTDs would not necessarily be indicative of causation by reduced proliferation in the NT specifically. Alternatively, an interesting experiment could be to slightly reduce proliferation in $Sp^{2H}/+$ embryos; these embryos are more susceptible to NTDs than $+/+$ embryos. Therefore, if reduced proliferation were causative of NTDs, then a small reduction in proliferation may be sufficient to induce development of the defects in $Sp^{2H}/+$ embryos. If anti-mitotic agents are capable of inducing NTDs in $Sp^{2H}/+$ embryos, it could be an indication that the reduction in proliferation is causative of NTDs.

The *Pax3* gene encodes a transcription factor. Research has identified a number of *Pax3* target genes involved in proliferation, differentiation and apoptosis which could provide information on how it is able to regulate these processes (Wang et al., 2007). This could also indicate which pathways are being affected by *Pax3* mutation, and why proliferation is downregulated in the NTs of Sp^{2H}/Sp^{2H} embryos.

The expressions of several Cyclin proteins are upregulated by *Pax3* (Wang et al., 2007). These include Cyclin A and Cyclin E, which promote transition into S phase and DNA replication (Ohtsubo et al., 1995; Zindy et al., 1992), and Cyclin I, which is required for progression through S and G₂/M phases (Nagano et al., 2013). *Pax3* may increase cell proliferation through activation of genes such as the Cyclins, and promotion of progress through the cell cycle. Additionally, *Pax3* increases expression of other genes which promote proliferation, such as protein kinase C- γ , and Ybx1, thus acting in a less direct manner (Feng et al., 2009; Wouters et

al., 2009). This suggests that Pax3 acts through multiple pathways in order to robustly promote proliferation.

3.2.2 Consequences of the reduction in proliferation in the neural tube

The finding that proliferation is reduced in the neural folds of Sp^{2H}/Sp^{2H} embryos is supported by previously published research. For example, lower numbers of cells in sections of neural tube from Sp^{2H}/Sp^{2H} embryos compared to $+/+$ embryos has been reported (Kapron-Bras and Trasler, 1988). In addition, lower proliferation rates have been described in NTs from Sp^{2H}/Sp^{2H} embryos compared to $+/+$ embryos at certain stages of development (Keller-Peck and Mullen, 1997). Research appears to show that this defect in *Splotch* embryos is due to lengthening of the cell cycle comparative to wild type; previous work shows that neurepithelial cells from Sp^{2H}/Sp^{2H} embryos have extended cell cycles in comparison to wild type embryos (Wilson, 1974). Additionally, Pax3 protein has been found to upregulate expression of a number of Cyclin genes, which are known to aid progression through the cell cycle (Wang et al., 2007). Therefore, it seems likely that Pax3 increases proliferation through cell cycle regulation.

The reduction of proliferation in the neural folds of Sp^{2H}/Sp^{2H} embryos would be predicted to cause a reduction in cell number in the NT. This was found to be true; data showed a significant reduction in cell number in the NT as a whole in 14-15 somite stage Sp^{2H}/Sp^{2H} embryos, but also interestingly in both the dorsal and ventral regions separately. This shows that although the proliferation defect is only present in the dorsal region of the NT the effects are present throughout. This could suggest that either cells are translocating dorsally in the neural folds, or the dorsal region comprises a smaller proportion of the NT. This could be analysed using a dorsal NT marker, such as Wnt1 or Wnt3a, to observe the relative size of the dorsal region. Additionally, the reduction in cell number is still present in 19-20 somite stage embryos, when the proliferation is comparable in $+/+$ and Sp^{2H}/Sp^{2H} embryos. This suggests that at this stage, the embryos have been unable to compensate for the reduced proliferation through alternative mechanisms, such as reduced apoptosis. The reduction in cell number could result in morphological changes in the NT. For example, it could reduce the size of the NT, or it could alter the cell density of the tissue.

Measurements showed that the height and width of the NT are significantly reduced in the 14-15 somite stage Sp^{2H}/Sp^{2H} embryos. At the 19-20 somite stage the differences in height and width are less pronounced when comparing between the genotypes, and only the height is significantly reduced in Sp^{2H}/Sp^{2H} embryos. This suggests that the NT may be able to compensate to a small degree to recover size once the proliferation defect is no longer

present. The height/width ratio is comparable between the genotypes, which suggests that the size proportions of the NT are unchanged in Sp^{2H}/Sp^{2H} embryos.

The overall cross sectional area of the NT is reduced in Sp^{2H}/Sp^{2H} embryos at both the 14-15 and 19-20 somite stages. This is consistent with a smaller size. Likewise, the dorsal and ventral areas of the NT are smaller at the 14-15 somite stage, although this was expected since the height and width are reduced. Again, the difference in size is less pronounced at the 19-20 somite stage, as the dorsal and ventral surface areas demonstrate no significant differences between $+/+$ and Sp^{2H}/Sp^{2H} embryos, although Sp^{2H}/Sp^{2H} embryos show a trend towards a smaller NT size when compared to $+/+$ embryos.

A small increase in cell density in the NT is seen at the 14-15 somite stage. However, this difference only reaches significance in the dorsal region, where the reduction in proliferation is located. At the 19-20 somite stage no difference in cell density is seen either in the whole NT cross section, or in the dorsal and ventral regions considered separately. These results suggest that the reduction in cell number is likely to contribute to the reduction in NT size in Sp^{2H}/Sp^{2H} embryos, but a defect may also be present in the mechanisms controlling the dorso-ventral and lateral size of the NT. At the 14-15 somite stage, the cells are more densely packed into the smaller NT, but by the 19-20 somite stage the issue has been partially rectified, and both the size and cell density appear closer to wild type levels.

Another potential explanation for the size and cell density defects seen in Sp^{2H}/Sp^{2H} NTs involves cell-cell adhesion in the neurepithelium, which is known to require Pax3 signalling (Wiggan et al., 2002; Wiggan and Hamel, 2002). If the cells are somehow more tightly adhered in Sp^{2H}/Sp^{2H} NT then there would be less interstitial space, and the cells would be more densely packed. Additionally, the size of the NT would be reduced. If this were partially rectified before the 19-20 somite stage then the tissue would become less dense, and the size of the NT may more closely resemble that of $+/+$ embryos. This theory is supported by the fact that the defect is more pronounced in the dorsal *Pax3*-expression region, and also becomes less pronounced at the 19-20 somite stage in comparison to the 14-15 somite stage. However, Pax3 is associated with maintenance and formation of epithelia, and ectopic *Pax3* expression *in vitro* is associated with formation of epithelial structure and increased cell-cell adhesion (Wiggan et al., 2002). Additionally, Pax3 mutation *in vivo* causes loss of epithelial structure in the dermomyotome (Mansouri et al., 2001). Also, expression of the gene Cyclin A2 is upregulated by Pax3, and the Cyclin A2 protein promotes epithelial formation and cell-cell adhesion (Bendris et al., 2014; Wang et al., 2007). Therefore, increased cell density in the NT of Sp^{2H}/Sp^{2H} embryos was unexpected. Nonetheless, the NT itself retains epithelial integrity in

Sp^{2H}/Sp^{2H} embryos, and previous research does not exclude the possibility that Pax3 protein could function to decrease cell-cell adhesion in the NT.

The thickness of the NT was compared between $+/+$ and Sp^{2H}/Sp^{2H} embryos. A trend towards a thinner NT was apparent in 14-15 somite stage Sp^{2H}/Sp^{2H} embryos, although this data does not reach significance. As the NT is only a single cell in thickness this would suggest a potential defect in the mechanisms controlling the apico-basal length of the cells. Larger sample sizes could clarify if this is the case. Again, this defect appears to resolve by the 19-20 somite stage.

Sp^{2H}/Sp^{2H} embryos show a significant reduction in NT size, but no significant reduction in the thickness of the NT when compared to $+/+$ embryos. Therefore the ratio between dorsal thickness and NT area was compared between genotypes to observe any changes in proportions of the NT. This ratio was significantly increased in Sp^{2H}/Sp^{2H} embryos at both the 14-15 and 19-20 somite stages. This shows that the thickness of the NT is increased relative to NT size in Sp^{2H}/Sp^{2H} embryos compared to $+/+$ embryos, and that this defect is present during both early and late PNP closure. An increase in NT thickness may affect the mechanical properties of the NT during neurulation, potentially making it more resistant to bending and closure, and may contribute to the development of spina bifida in Sp^{2H}/Sp^{2H} embryos.

This theory was examined further through examination of the hinge points in $+/+$ and Sp^{2H}/Sp^{2H} embryos. No differences were observed in the angle of the MHP between $+/+$ and Sp^{2H}/Sp^{2H} embryos, but some differences were identified between the genotypes in the DLHPs. Greater bending is seen in the DLHPs of Sp^{2H}/Sp^{2H} embryos, and they are also positioned more dorsally in these embryos. These two observations could be linked, as the greater bending in the DLHPs could reduce the distance between these hinge points and the dorsal-most point of the NT, thus affecting their proportional position along the dorso-ventral axis.

This was an unexpected result. I hypothesised that the increase in the thickness of the neural folds in Sp^{2H}/Sp^{2H} embryos could reduce hinge point bending, and thus prevent NT closure. However, this is not what was observed. It is possible that the increased bending could prevent NT closure in Sp^{2H}/Sp^{2H} embryos, possibly by preventing the neural folds from making contact, and thus fusing correctly. This may or may not be linked to the relative thickening of the neural folds. Alternatively, it could be linked to the fact that the neural folds are actually slightly thinner in mutant neural folds compared to those of the wild type embryos, even though they are proportionally thicker. For example, the shorter cells could be more greatly affected by the basal positioning of the nucleus, making apical constriction more extreme. This could increase the bending of the hinge points. However, as this data did not reach significance more studies would need to be carried out to prove or disprove this theory. On the other hand, the

increased bending of the neural folds could be an artefact of the fixing and sectioning process, or alternatively the morphology of the neural tube could be unrelated to the failure of NT closure in Sp^{2H}/Sp^{2H} embryos.

Sections were compared proximal and more distal to the closure point of the PNP, but no differences were observed in the hinge points between these positions. However, the most distal sections studied were a maximum of 42 μm caudal of the closure point. It is possible that sections a greater distance caudally from the closure point could identify differences between the genotypes which could suggest a morphological mechanism for the development of spina bifida in Sp^{2H}/Sp^{2H} embryos.

3.2.3 The effects of folate deficiency on neural tube closure in *Spotch* mutant embryos

Sp^{2H}/Sp^{2H} embryos are responsive to folate deficiency in the frequency of NTD development; frequency of exencephaly is increased and the size of the PNP is reduced. The rescue of PNP closure was an unexpected result, and has not previously been reported. However, it is likely that the rescue was temporary, as previous research has reported no difference in the frequency of spina bifida in Sp^{2H}/Sp^{2H} or $Sp^{2H}/+$ embryos fed either ND or FD (Burren et al., 2008).

The folate deficiency could be acting on the embryo through either of two mechanisms; disruption in the donation of methyl groups to macromolecules, or the synthesis of pyrimidines and purines. It has previously been reported that folate supplementation rescued defective epigenetic marking in the Sp^{2H}/Sp^{2H} genome (Ichi et al., 2010). Therefore it is possible that folate deficiency worsens the epigenetic defects seen in these embryos. However, it is more likely that folate affects NTD development in Sp^{2H}/Sp^{2H} embryos through defective pyrimidine and purine synthesis.

It has been shown in this project that Sp^{2H}/Sp^{2H} embryos have reduced proliferation in the dorsal region of the spinal NT. If folate deficiency is reducing pyrimidine and purine synthesis, then this could further reduce the rate of proliferation, and potentially prolong the time the embryo has reduced proliferation. Assuming that the reduction in proliferation is causative of NTDs, this could worsen the NTDs, and induce NTDs in embryos which may not otherwise have developed them, including $Sp^{2H}/+$ embryos. This would explain the increase in exencephaly observed in the FD embryos. Furthermore, it could also explain research which has shown rescue of NTDs by folic acid in Sp^{2H}/Sp^{2H} embryos, as folate supplementation could increase purine and pyrimidine synthesis, and potentially increase proliferation in the *Pax3*-deficient regions of the NT.

The effects of folate deficiency on the rate of proliferation in the NT could be studied as described previously, using sections and an antibody against the proliferation marker phospho-histone H3. It would be informative to observe the effects of folate deficiency – and also potentially folate supplementation – on the rates of proliferation in the dorsal *Pax3*-expressing regions of the NT of Sp^{2H}/Sp^{2H} embryos. If folic acid does indeed rescue NTDs through rescue of the proliferation defect it would be expected that folate supplementation would increase proliferation in the NTs of Sp^{2H}/Sp^{2H} embryos to levels resembling those of wild type embryos. On the other hand, it would be expected that folate deficiency would further reduce proliferation in the NTs of Sp^{2H}/Sp^{2H} embryos, and would also reduce proliferation in the NTs of $Sp^{2H}/+$ embryos to levels resembling those of Sp^{2H}/Sp^{2H} embryos. It could also be interesting to repeat the apoptosis and neuronal differentiation experiments carried out in this chapter using folate deficient or folate supplemented embryos. This could be informative if folate is involved in either of these processes during embryonic development, possibly through epigenetic mechanisms.

On the other hand, folate deficiency may have effects on the mother which could affect embryonic development independently of effects on proliferation and epigenetics. For example, FD mothers tend to eat less and be more slender than their ND counterparts. This does not cause serious malnutrition or starvation as they are able to be on the diet for long periods of time without serious effects. However, it is possible that the small reduction in calorific or nutritional intake could affect embryonic development during gestation.

This folate deficient mouse model is not directly comparable to a human model. Minor reductions in folate intake, such as those seen in humans, have no effect on the folate levels in the mouse embryo (Burren et al., 2008). Additionally, in humans, although maternal folate deficiency is a risk factor in the development of NTDs, most mothers experiencing NTD pregnancies have folate levels within a healthy range (Kirke et al., 1993). It is highly unlikely that any human would be folate deficient to the degree induced in the mouse model described here. However, this model could be useful in deducing the mode of action of NTD rescue through folic acid supplementation, and thus could be useful in understanding why some NTDs are unaffected by folic acid.

3.2.4 The *Spotch* mutation and canonical Wnt signalling

Both *Pax3* signalling and canonical Wnt signalling are known to be important in the balance of proliferation and differentiation in the NT (Keller-Peck and Mullen, 1997; Megason and McMahon, 2002). Therefore it is likely that the two pathways are interlinked. Previous research appears to support this theory; it has been shown that canonical Wnt signalling acts

upstream of Pax3, and also that Pax3 induces expression of *Wnt1* (Fenby et al., 2008; Zhao et al., 2014). Therefore, *Spotch* mice were studied to determine if Pax3 acts upstream of canonical Wnt signalling.

Comparisons in Wnt gene expression were made between *+/+* and *Sp^{2H}/Sp^{2H}* samples using the SABiosciences RT² Profiler™ PCR Array Plate for the mouse Wnt signalling pathway. A number of genes demonstrated small differences in expression between the genotypes, and several of these were tested individually using RT-qPCR. However, none of the differences could be verified. Expression levels of the canonical Wnt signalling-related genes Axin1, Axin2, Cdx2, Fzd6, and Sfrp4 were compared between *+/+* and *Sp^{2H}/Sp^{2H}* whole embryos, but no significant differences were identified. Likewise, LacZ RT-qPCR of *+/+* and *Sp^{2H}/Sp^{2H}* embryos carrying the BatGal allele identified no significant difference in canonical Wnt signalling between the genotypes.

Taken together, these results suggest that canonical Wnt signalling does not act downstream of Pax3 signalling in the NT. This hypothesis could be verified using *Sp^{2H}/Sp^{2H}* embryos through study of more of the genes involved in canonical Wnt signalling, as only a small selection were studied. However, none of the data shown here suggests otherwise.

Additionally, it would be interesting to study the expression of these genes at an earlier stage in development, for example the 8-9 somite stage, prior to the onset of the morphological defect. It is possible that changes in gene expression which are causative for NTDs in *Spotch* mice are no longer detectable in the 23-24 somite stage embryos which were tested. Alternatively, different Wnt-related genes in addition to *Axin2* and *Cdx2* could be used to quantify the levels of canonical Wnt signalling in the embryos. For example, *Cyclin-D1* or *c-Myc* could also be used in this way, as they are targets of β -catenin transcription (He et al., 1998; Tetsu and McCormick, 1999). The combination of several genes could give a more accurate reading of canonical Wnt signalling levels in the different genotypes.

It is also possible that although whole embryos of different genotypes had similar expression of the genes tested, certain regions of the embryos may express them differently. A good way to examine this would be to carry out whole mount *in situ* hybridisation of the embryos using probes to detect the genes tested. This could show differences in the patterns of gene expression between genotypes. Additionally, RT-qPCR of select regions of the embryos – for example the NT – could identify differences in the levels of gene expression.

3.2.5 Conclusions

Splotch embryos have been found to have a significant reduction in proliferation in the *Pax3*-expressing dorsal region of the spinal NT. This appears to cause a number of morphological defects in the NT itself, although it is currently uncertain whether or not this is causative of the spinal NTDs seen in these embryos. In addition folate deficiency has been shown to worsen cranial NTDs in the *Splotch* mutants. This is likely to be through further reduction in proliferation in the T, but more studies are needed to confirm this.

Although a cellular defect has been identified in the *Splotch* mouse, it is also important to identify the molecular defects responsible for the development of NTDs. Evidence in the literature suggests that there could be interaction between the *Pax3* and canonical Wnt signalling pathways. Given the involvement of canonical Wnt signalling in the regulation of proliferation and differentiation, this could suggest a mechanism by which *Pax3* mutation causes reduced proliferation in the NT.

Initial studies described in this chapter suggest that *Pax3* mutation does not cause changes in the expression levels of the canonical Wnt-related genes tested. However, other Wnt genes may be affected, or alternatively protein levels or expression patterns of the Wnt components could be altered. It is also possible that canonical Wnt signalling acts upstream of *Pax3*. Therefore, in **Chapters 4** and **5** of this thesis I will be investigating the potential interaction between *Pax3* and canonical Wnt signalling, and observing the effects this interaction has on NT and NC development.

4 Pax3 and β -Catenin Gain-of-Function

4.1 Results

The experiments described in this chapter aim to use the β -catenin gain-of-function (β -catenin^{GOF}) allele to determine if an interaction exists between Pax3 and the canonical Wnt signalling pathway, and which cellular mechanisms may be involved in this interaction. They also attempt to elucidate the developmental processes which are affected by the interaction, and to describe the defects present in double mutant embryos. The research is based on the hypothesis: interaction between Pax3 and the canonical Wnt signalling pathway reduces proliferation and induces premature neuronal differentiation in the NT and NC, resulting in NTDs and NC defects.

Although data from the previous chapter suggests that canonical Wnt signalling is not disrupted in *Spotch* mutant embryos, this will be examined in more detail, looking at the mutant phenotype as well as gene expression, and using a β -catenin mutant allele to examine the effects of compound mutation. Evidence from the literature strongly suggests that there is an interaction between Pax3 and the canonical Wnt signalling pathway, and so this will be examined further. The link with NTDs will be studied through compound mutant embryos, and through cellular processes which are affected by the interaction between Pax3 and the canonical Wnt signalling pathway.

Previous publications indicate an interaction between canonical Wnt signalling and Pax3. The two pathways show overlapping function; Pax3 is important in the regulation of proliferation and differentiation, and canonical Wnt signalling is also known to play a role in the regulation of these processes (Keller-Peck and Mullen, 1997; Megason and McMahon, 2002). This interaction could either be direct communication between Pax3 and the canonical Wnt signalling pathway, or convergence of the processes on the same developmental pathway. For example, both Pax3 and canonical Wnt signalling act through the Notch pathway to regulate development of the NC and the nervous system (De Bellard et al., 2002; Ma et al., 1996; Nakazaki et al., 2008; Shimizu et al., 2008; Yun et al., 2002). Therefore, observed effects of interaction could be a summation of the effects of both Pax3 and canonical Wnt signalling on the Notch pathway.

Both canonical Wnt signalling and Pax3 are important for the development of the NC cells. Wnt1 and Wnt3a play a role in the induction and proliferation of the NC (Dickinson et al., 1994; Ikeya et al., 1997; Saint-Jeannet et al., 1997). In addition, Pax3 is necessary for NC

		Mouse 2: Pax3 ^{Cre/+} β-catenin ^{+/+}	
		Pax3 ^{Cre} β-catenin ⁺	Pax3 ⁺ β-catenin ⁺
Mouse 1: Pax3 ^{Sp2H/+} β-catenin	Pax3 ^{Sp2H} β-catenin ^{GOF}	Pax3 ^{Sp2H/Cre} β-catenin ^{GOF/+}	Pax3 ^{Sp2H/+} β-catenin ^{GOF/+}
	Pax3 ^{Sp2H} β-catenin ⁺	Pax3 ^{Sp2H/Cre} β-catenin ^{+/+}	Pax3 ^{Sp2H/+} β-catenin ^{+/+}
	Pax3 ⁺ β-catenin ^{GOF}	Pax3 ^{Cre/+} β-catenin ^{GOF/+}	Pax3 ^{+/+} β-catenin ^{GOF/+}
	Pax3 ⁺ β-catenin ⁺	Pax3 ^{Cre/+} β-catenin ^{+/+}	Pax3 ^{+/+} β-catenin ^{+/+}

Pax3 ^{+/+} β-catenin ^{+/+}
Pax3 ^{+/-} β-catenin ^{+/+}
Pax3 ^{Cre/+} β-catenin ^{GOF/+}
Pax3 ^{Sp2H/Cre} β-catenin ^{+/+}
Pax3 ^{Sp2H/Cre} β-catenin ^{GOF/+}

Figure 4.1: A punnet square demonstrating the progeny from the cross *Pax3*^{Sp2H/+} *β-catenin*^{GOF/+} x *Pax3*^{Cre/+} *β-catenin*^{+/+}. The key represents the five genotype groups used in the experiments described in this chapter. Colour coding demonstrates how the genotypes are distributed among the groups, as several genotypes have been pooled into the same genotype group (see also **Figure 4.2**).

specification, migration and differentiation; *Pax3* mutant mice have a reduced NC population and reduced NC-derivative tissues (Auerbach, 1954; Conway et al., 1997a; Lang et al., 2000; Moase and Trasler, 1989). Interestingly, *Pax3*-induced NC development appears to be Wnt-dependent (Monsoro-Burq et al., 2005; Sato et al., 2005).

Several publications also indicate interaction between the canonical Wnt signalling pathway and *Pax3* through the influence of one on the other. Evidence has been published which suggests that canonical Wnt signalling may act both upstream and downstream of *Pax3* (Fenby et al., 2008; Zhao et al., 2014). Additionally, *Pax3* may directly regulate expression of several components of the canonical Wnt signalling pathway (Wang et al., 2007).

Most of the experimental litters used in this chapter are generated using the cross *Pax3*^{Sp2H/+} *β-catenin*^{GOF/+} x *Pax3*^{Cre/+} *β-catenin*^{+/+} (**Figure 4.1**). Comparisons are drawn between different

genotypes, including *Pax3* heterozygous embryos, with or without β -catenin gain-of-function (GOF). As the β -catenin^{GOF} allele is conditional, and the ‘floxed’ region must be excised by Cre recombinase to become active, *Pax3* heterozygotes with β -catenin GOF are always of the genotype *Pax3*^{Cre/+} β -catenin^{GOF/+}. However, *Pax3* heterozygote embryos without β -catenin GOF may be of the genotypes *Pax3*^{Cre/+} β -catenin^{+/+}, *Pax3*^{Sp2H/+} β -catenin^{+/+} or *Pax3*^{Sp2H/+} β -catenin^{GOF/+}, as none of these genotypes have a floxed β -catenin^{GOF} allele. These three genotypes show no significant differences in rates of exencephaly or spina bifida (**Figure 4.2B and D**), therefore they will be pooled throughout the results, and referred to as *Pax3*^{+/-} β -catenin^{+/+}.

Likewise, neither *Pax3*^{+/+} β -catenin^{+/+} nor *Pax3*^{+/+} β -catenin^{GOF/+} embryos have a floxed β -catenin^{GOF} allele. They show no significant differences in rates of exencephaly or spina bifida, and so have been pooled as ‘wild type’ embryos (**Figure 4.2A and C**). They will be referred to as *Pax3*^{+/+} β -catenin^{+/+} embryos in these results.

4.1.1 Verification of the increase in canonical Wnt signalling in embryos carrying the β -catenin gain-of-function allele

The β -catenin^{GOF} allele has previously been generated and tested for effectiveness (Harada et al., 1999). However, it was important to check that the allele effectively increases canonical Wnt signalling in the mice being used for this research. Therefore, the levels of canonical Wnt signalling were evaluated in embryos carrying the β -catenin^{GOF} allele by analysing expression of downstream target genes, *Axin2* and *Cdx2*.

A probe which identifies the mRNA for *Axin2* was used in whole mount *in situ* hybridisations to compare levels of canonical Wnt signalling between embryos carrying the *Pax3* mutations, and embryos of the equivalent *Pax3* genotype also exhibiting β -catenin GOF (**Figure 4.3**). *Axin2* is a component of the destruction complex (Hart et al., 1998).

The *in situ* hybridisation was carried out on all embryos at the same time, and the colour development reaction had equal timings for all embryos. However, a darker staining is visible in embryos with β -catenin GOF. This is true when comparing the *Pax3*^{+/-} embryos with and without β -catenin GOF, and also when comparing the *Pax3*^{Sp2H/Cre} mutant embryos with and without β -catenin GOF (**Figure 4.3**). These results are relatively consistent. Therefore, *in situ* hybridisation suggests higher levels of *Axin2* expression, and thus higher levels of canonical Wnt signalling in embryos with β -catenin GOF. Sections of these embryos could have indicated the structures which show differences in *Axin2* expression, and negative controls could have demonstrated background staining.

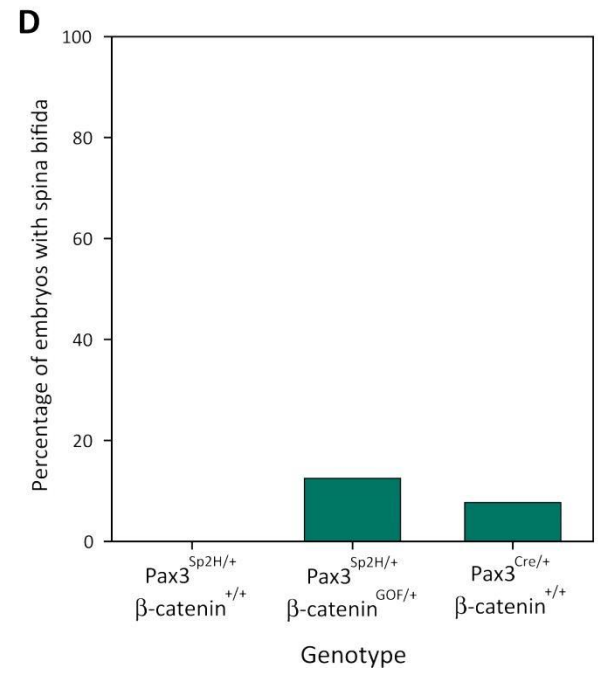
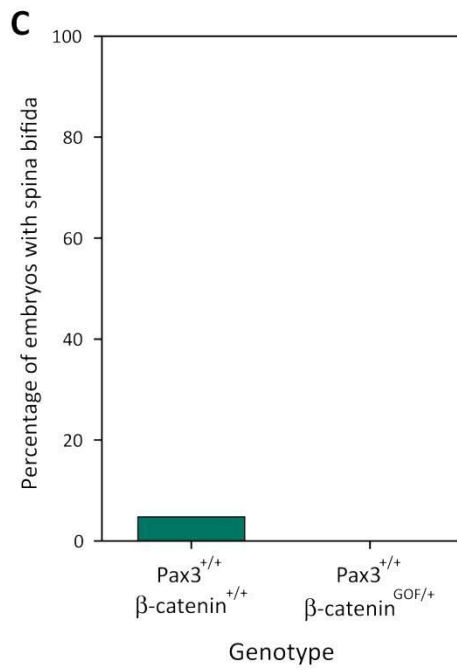
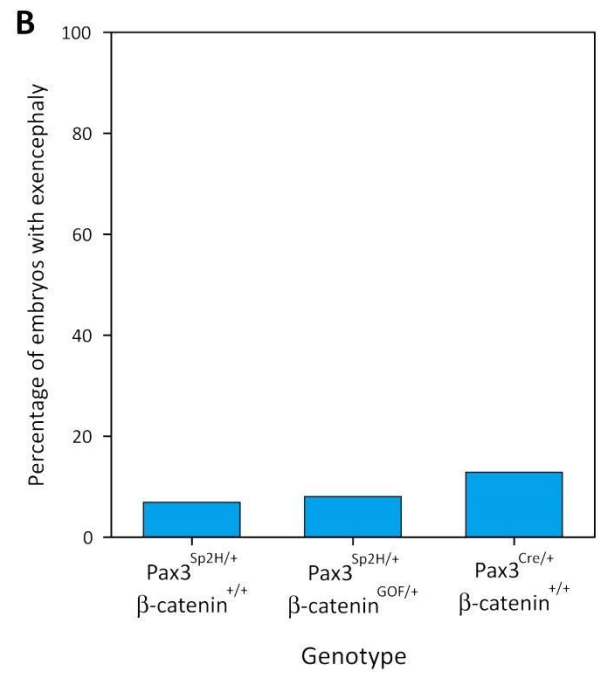
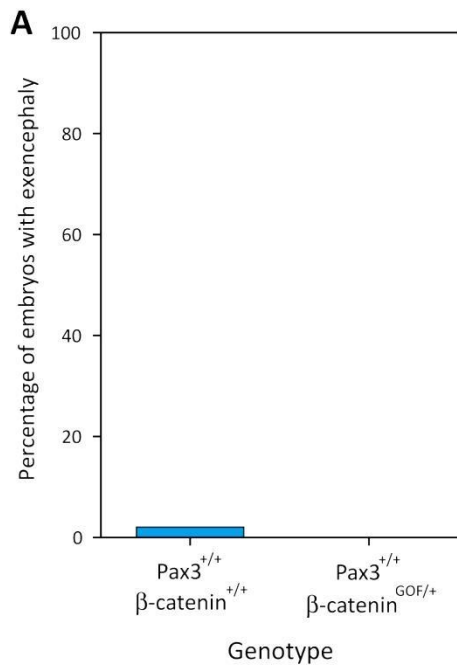
Figure 4.2: Pooling of embryo genotypes from the cross $Pax3^{Sp2H/+}$ β -catenin^{GOF/+} x $Pax3^{Cre/+}$ β -catenin^{+/+}. Several genotypes were pooled in experiments due to similar expression levels of wild type Pax3 and β -catenin, and to similar frequencies of exencephaly and spina bifida. Experimental litters were generated containing a mixture of genotypes through the cross $Pax3^{Sp2H/+}$ β -catenin^{GOF/+} x $Pax3^{Cre/+}$ β -catenin^{+/+}. Exencephaly was defined as an open cranial NT at the 18 somite stage or later. Spina bifida was defined as an open spinal NT at the 30 somite stage or later.

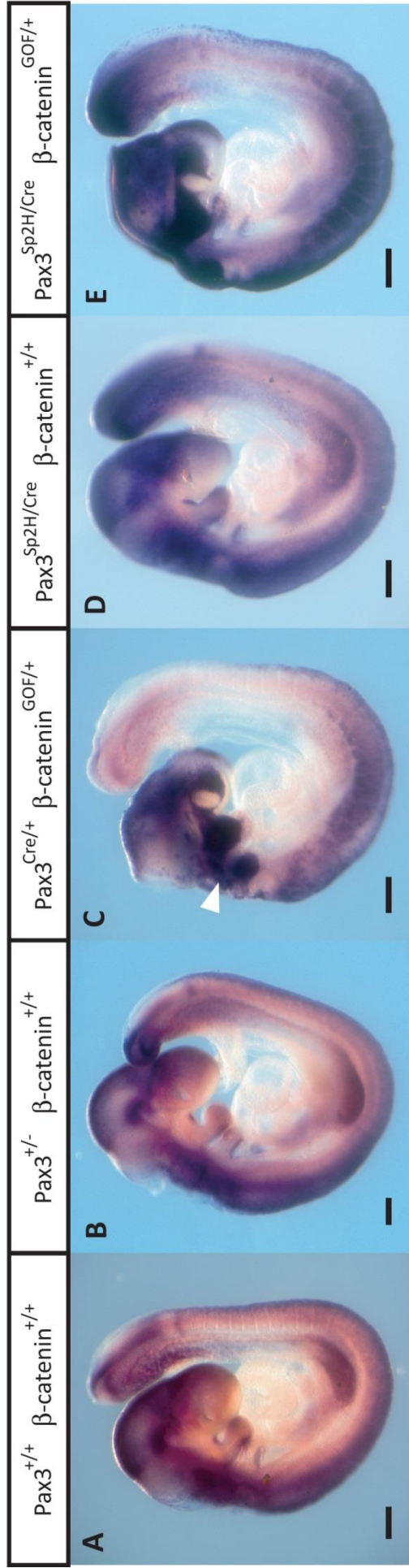
The frequencies of exencephaly and spina bifida were compared between $Pax3^{+/+}$ β -catenin^{+/+} and $Pax3^{+/+}$ β -catenin^{GOF/+} embryos (**A** and **C**), as these embryos have wild type Pax3 and wild type or unfloxed β -catenin. No significant differences were found in the frequencies of the NTDs, so these embryos are pooled in experiments as $Pax3^{+/+}$ β -catenin^{+/+} embryos.

The frequencies of exencephaly and spina bifida were compared between $Pax3^{Sp2H/+}$ β -catenin^{+/+}, $Pax3^{Sp2H/+}$ β -catenin^{GOF/+}, and $Pax3^{Cre/+}$ β -catenin^{+/+} embryos (**B** and **D**), as these embryos have heterozygous expression of Pax3, and wild type or unfloxed β -catenin. No significant differences were found in the frequencies of the NTDs, so these embryos are pooled in experiments as $Pax3^{+/-}$ β -catenin^{+/+} embryos.

Significance was assessed using the Chi-Square Test (**A**) or the Fisher Exact Test (**B**).

A - $Pax3^{+/+}$ β -catenin^{+/+}: n = 98. $Pax3^{+/+}$ β -catenin^{GOF/+}: n = 72. **B** - $Pax3^{Sp2H/+}$ β -catenin^{+/+}: n = 130. $Pax3^{Sp2H/+}$ β -catenin^{GOF/+}: n = 87. $Pax3^{Cre/+}$ β -catenin^{+/+}: n = 101. **C** - $Pax3^{+/+}$ β -catenin^{+/+}: n = 21. $Pax3^{+/+}$ β -catenin^{GOF/+}: n = 9. **D** - $Pax3^{Sp2H/+}$ β -catenin^{+/+}: n = 34. $Pax3^{Sp2H/+}$ β -catenin^{GOF/+}: n = 16. $Pax3^{Cre/+}$ β -catenin^{+/+}: n = 26.





174

Figure 4.3: β-catenin gain-of-function increases expression of Axin2. Experimental litters were generated containing a mixture of genotypes through the cross Pax3^{Sp2H/+} β-catenin^{GOF/+} x Pax3^{Cre/+} β-catenin^{+/+}. *in situ* hybridisation for Axin2 was carried out on embryos of multiple genotypes. Scale bars represent 250 μm. n = 2 for each genotype.

Pax3^{+/+} β-catenin^{+/+} embryos show Axin2 expression in a wide range of tissues, but it is most noticeable in the spinal and cranial regions (**A**). Pax3^{+/-} β-catenin^{+/+} (**B**) and Pax3^{Sp2H/Cre} β-catenin^{+/+} (**D**) embryos show the same expression pattern as Pax3^{+/+} β-catenin^{+/+} embryos.

Pax3^{Cre/+} β-catenin^{GOF/+} and Pax3^{Sp2H/Cre} β-catenin^{GOF/+} embryos show a similar pattern of Axin2 expression, but the staining present is slightly darker. This is particularly noticeable in the cranial region (White arrowhead, **C**).

However, whole mount *in situ* hybridisation is not a quantitative method of gene expression analysis. Therefore, RT-qPCR was used to quantify levels of canonical Wnt signalling in the embryos used for this research (**Figure 4.4**).

The genes *Axin2* and *Cdx2* were used as an indirect read-out of canonical Wnt signalling in the embryos of different genotypes. *Cdx2* is downstream of canonical Wnt signalling, and the gene may be a direct target of the β -catenin transcription complex (Benahmed et al., 2008; Wang and Shashikant, 2007). Embryos at the 22-24 somite stage were used for analysis; *Pax3* is still expressed at this stage, and so the canonical Wnt signalling GOF should still be in effect, and sufficient embryos were available at this stage to allow for replicates.

No significant differences were seen in the relative levels of *Cdx2* expression between embryos of differing genotypes (**Figure 4.4A**). However, a significant increase in relative *Axin2* expression was seen when comparing *Pax3*^{+/-} embryos with and without β -catenin GOF, and when comparing *Pax3*^{Sp2H/Cre} mutant embryos with and without β -catenin GOF. This was seen when using both *GAPDH* and *β -actin* as housekeeping genes for normalisation of expression (**Figure 4.4B** and **C**). These results suggest that β -catenin GOF does indeed increase levels of canonical Wnt signalling.

4.1.2 β -catenin gain-of-function alone is not able to induce neural tube defects

The β -catenin^{GOF} allele is conditional, and therefore requires a Cre recombinase enzyme to become 'floxed' and demonstrate β -catenin GOF. In the absence of Cre recombinase, the GOF protein functions as wild type β -catenin. The *Pax3*^{Cre} allele used in this study is a null *Pax3* allele. It is possible that the phenotypes observed represent a summation or interaction of the effects of *Pax3* mutation and β -catenin GOF. Alternatively, phenotypes may simply reflect an effect of β -catenin GOF. In order to distinguish these possibilities the effect of β -catenin GOF with wild type levels of *Pax3* was examined using a different Cre allele.

The allele used as a replacement was a *Sox-1*^{Cre} allele (Takashima et al., 2007). *Sox-1* is expressed throughout the neurepithelium from the specification of the neural plate (Pevny et al., 1998; Takashima et al., 2007). NTDs have not been reported in mice which are heterozygous or homozygous for *Sox-1* mutation (Nishiguchi et al., 1998).

Experimental litters were generated through the cross *Pax3*^{Sp2H/+} *β -catenin*^{GOF/+} x *Sox-1*^{Cre/+}, and the rates of spina bifida and exencephaly were analysed (**Figure 4.5**). Comparisons were drawn between embryos with and without β -catenin GOF in the NT, and with or without *Pax3* heterozygosity.

Figure 4.4: β -catenin gain-of-function increases the expression of Wnt markers. Experimental litters were generated containing a mixture of genotypes through the cross $Pax3^{Sp2H/+} \beta$ -catenin^{GOF/+} x $Pax3^{Cre/+} \beta$ -catenin^{+/+}. RT-qPCR was carried out using RNA prepared from whole embryos at the 22-24 somite stage.

Expression levels of two different genes were used to assess the level of canonical Wnt signalling – *Cdx2* (A) and *Axin2* (B and C). *Cdx2* was assessed using *GAPDH* as a housekeeping gene for normalisation (A). *Axin2* was assessed using *GAPDH* (B) and *β -actin* (C) for normalisation. *β -actin* was used for normalisation in addition to *GAPDH* to ensure that differences in expression levels of *Axin2* expression were not due to differences in expression levels of *GAPDH* between genotypes.

Graph A shows no significant differences in *Cdx2* expression between the genotypes. Graphs B and C show very similar results. $Pax3^{Cre/+} \beta$ -catenin^{GOF/+} embryos show a significant increase in *Axin2* expression compared to $Pax3^{+/-} \beta$ -catenin^{+/+} embryos, and $Pax3^{Sp2H/Cre} \beta$ -catenin^{GOF/+} embryos show a significant increase compared to $Pax3^{Sp2H/Cre} \beta$ -catenin^{+/+} embryos.

* $p < 0.05$. Significance was assessed using one way ANOVA. Only relevant differences have been labelled on the graphs. Error bars indicate standard error.

$Pax3^{+/+} \beta$ -catenin^{+/+}: n = 4. $Pax3^{+/-} \beta$ -catenin^{+/+}: n = 4 (n = 3 in C). $Pax3^{Cre/+} \beta$ -catenin^{GOF/+}: n = 3. $Pax3^{Sp2H/Cre} \beta$ -catenin^{+/+}: n = 4. $Pax3^{Sp2H/Cre} \beta$ -catenin^{GOF/+}: n = 3.

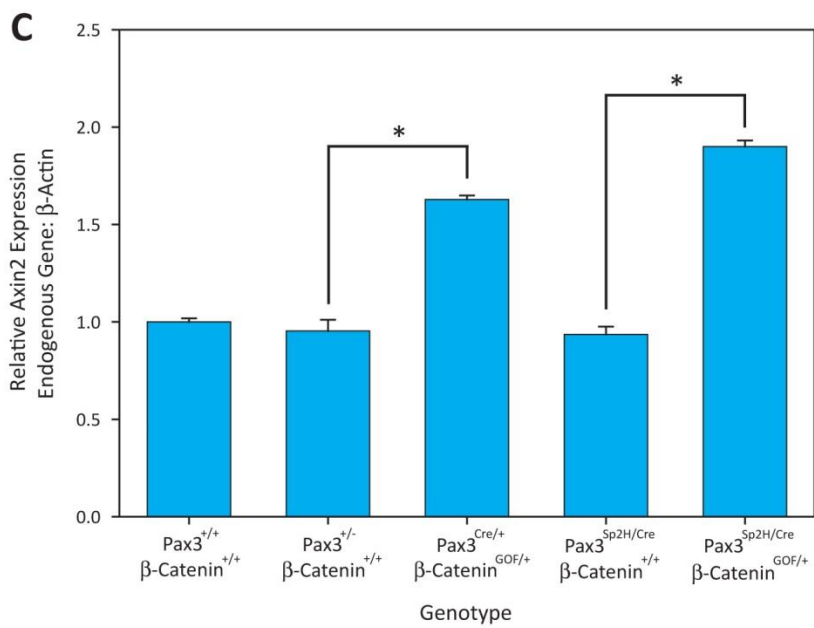
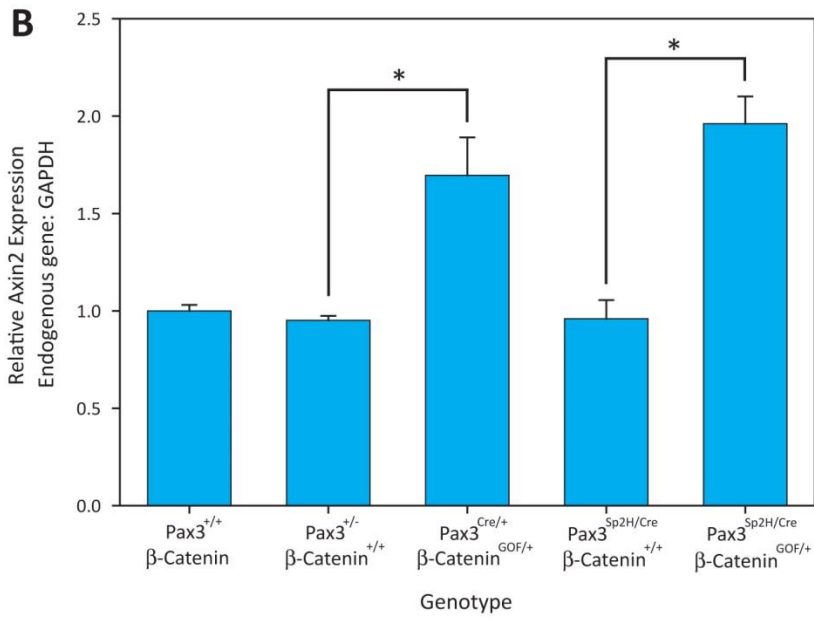
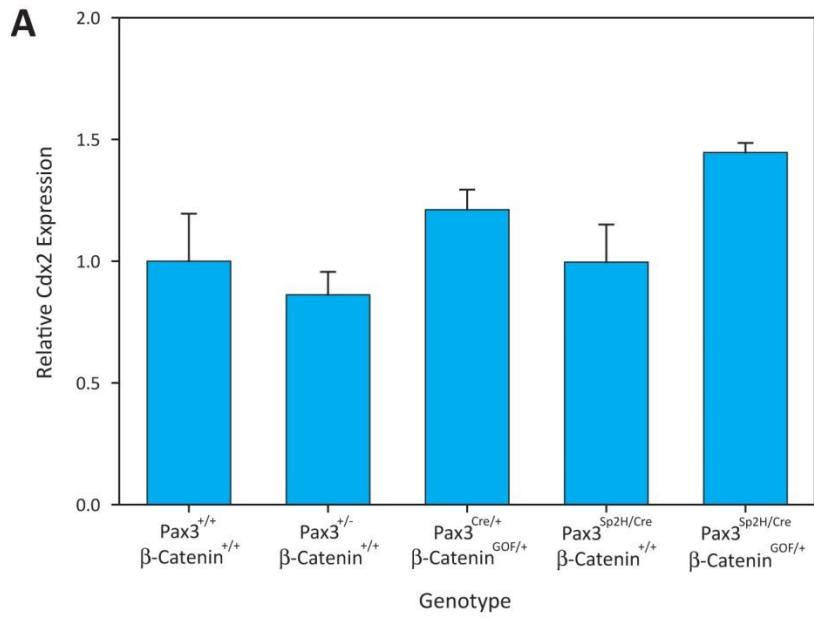


Figure 4.5: The effect of β -catenin gain-of-function on the development of neural tube defects in the absence of *Pax3* mutation. Experimental litters were generated through the cross *Pax3*^{Sp2H/+} β -catenin^{GOF/+} *Sox-1*^{+/+} x *Pax3*^{+/+} β -catenin^{+/+} *Sox-1*^{Cre/+}, and were collected at E10.5. Rates of spina bifida (**A**) and exencephaly (**B**) were analysed in each genotype in the offspring. Exencephaly has been defined as an open cranial region at the 18 somite stage or later. Spina bifida has been defined as an open spinal region at the 30 somite stage or later. Significance was assessed between genotypes with equivalent *Pax3* and *Sox1* status, but with different β -catenin genotypes.

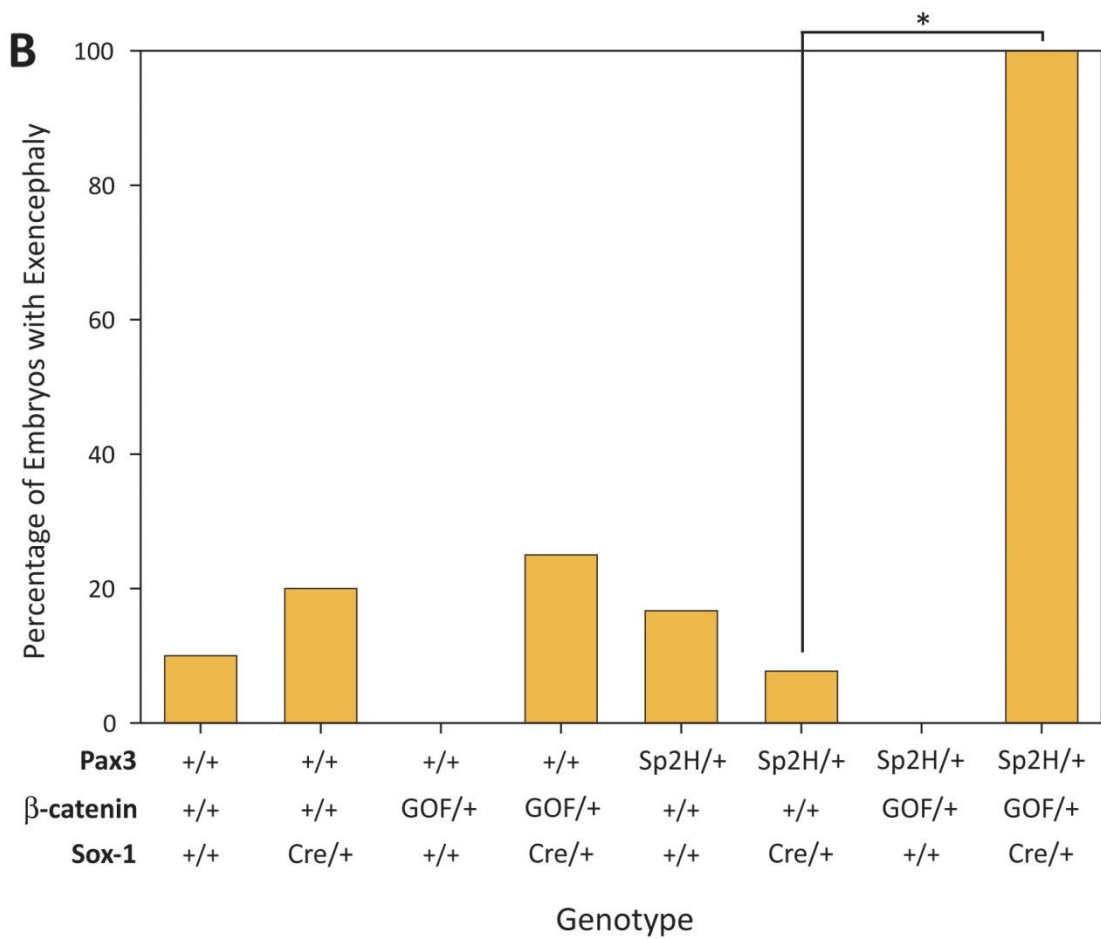
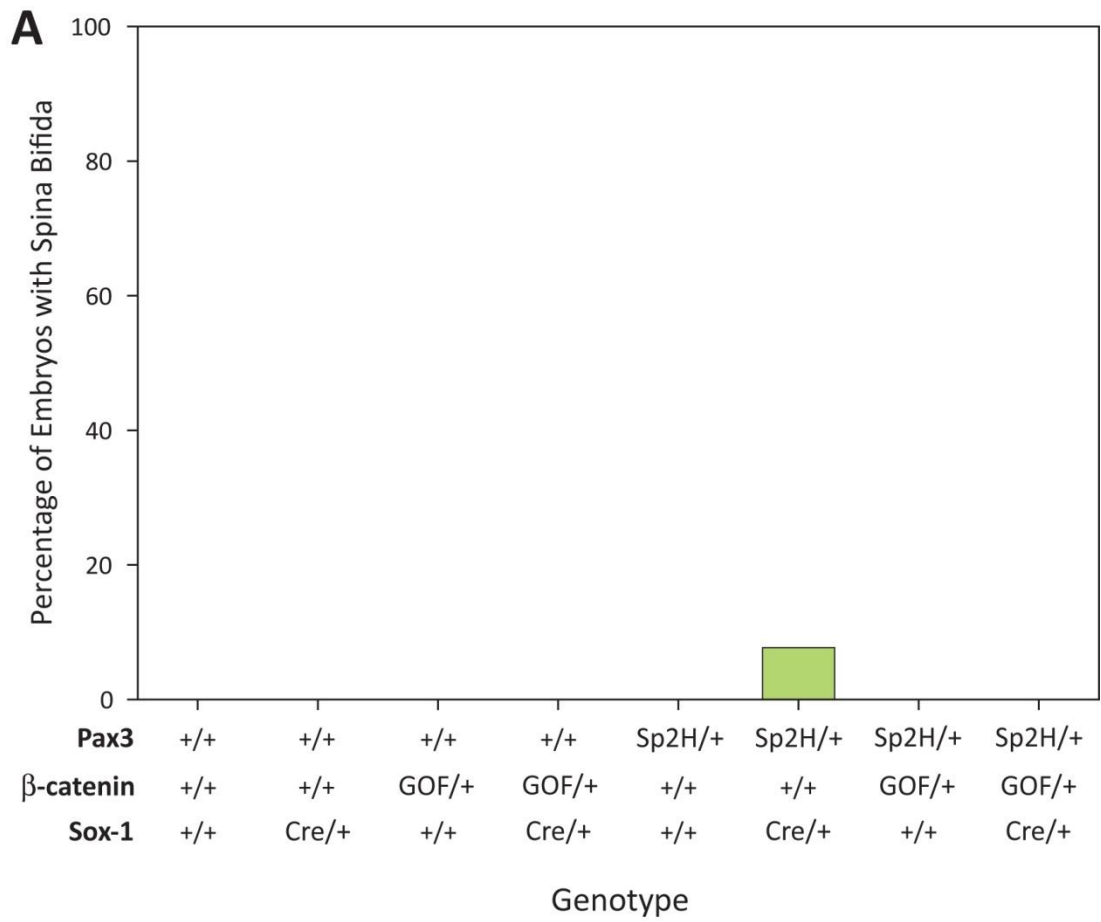
No significant differences were seen between genotypes in the frequency of spina bifida. This suggests that β -catenin GOF – with or without *Pax3* heterozygosity – does not induce spinal NTDs.

There are no significant differences observed in the frequency of exencephaly in the genotypes which do not include the *Pax3*^{Sp2H} allele (**B**). However, an increased frequency is seen between *Pax3*^{+/+} β -catenin^{GOF/+} *Sox-1*^{+/+} (0%) and *Pax3*^{+/+} β -catenin^{GOF/+} *Sox-1*^{Cre/+} (25%) embryos. This could suggest a slightly increased risk of exencephaly caused by β -catenin GOF independent of *Pax3* mutation.

When the embryos are heterozygous for *Pax3*^{Sp2H} the β -catenin GOF induces exencephaly. A significant increase in the rate of exencephaly is seen in *Pax3*^{Sp2H/+} β -catenin^{GOF/+} *Sox-1*^{Cre/+} embryos compared to *Pax3*^{Sp2H/+} β -catenin^{+/+} *Sox-1*^{Cre/+} embryos. These genotypes differ only in the presence or absence of β -catenin GOF.

* $p < 0.01$. Significance was assessed using the Fisher Exact Test.

Pax3^{+/+} β -catenin^{+/+} *Sox-1*^{+/+}: n = 10. *Pax3*^{+/+} β -catenin^{+/+} *Sox-1*^{Cre/+}: n = 15. *Pax3*^{+/+} β -catenin^{GOF/+} *Sox-1*^{+/+}: n = 3. *Pax3*^{+/+} β -catenin^{GOF/+} *Sox-1*^{Cre/+}: n = 4. *Pax3*^{Sp2H/+} β -catenin^{+/+} *Sox-1*^{+/+}: n = 6. *Pax3*^{Sp2H/+} β -catenin^{+/+} *Sox-1*^{Cre/+}: n = 13. *Pax3*^{Sp2H/+} β -catenin^{GOF/+} *Sox-1*^{+/+}: n = 1. *Pax3*^{Sp2H/+} β -catenin^{GOF/+} *Sox-1*^{Cre/+}: n = 2.



Rates of spina bifida were very low in all the genotypes studied, suggesting that defective Wnt signalling alone, or with *Pax3* heterozygosity, is not able to affect spinal NT closure. Additionally, the rates of exencephaly development were low in embryos with no *Pax3* mutation, but with β -catenin GOF in the NT. However, a small increase was observed in the frequency of exencephaly between *Pax3*^{+/+} *β -catenin*^{GOF/+} *Sox1*^{+/+} and *Pax3*^{+/+} *β -catenin*^{GOF/+} *Sox1*^{Cre/+} embryos. This difference did not reach significance, and more samples would be needed to confirm, but this could suggest that β -catenin GOF may slightly increase the risk of developing exencephaly independent of *Pax3* mutation. On the other hand, in combination with *Pax3* heterozygosity β -catenin GOF significantly increased the rate of exencephaly development in the embryos.

4.1.3 The effect of β -catenin gain-of-function on the development of neural tube defects in *Pax3*^{Sp2H/Cre} embryos

The effect of the *Pax3*^{Sp2H} allele on NT closure was studied in the previous chapter. Here the effect of the *β -catenin*^{GOF} allele on NT closure is studied, and in particular how it interacts with the mutant *Pax3* alleles *Pax3*^{Sp2H} and *Pax3*^{Cre} to influence the closure of the PNP and the cranial NT. Data regarding spina bifida and exencephaly in embryos of different genotypes are summarised in **Table 4.1**.

4.1.3.1 β -catenin gain-of-function affects spinal neurulation in *Pax3*^{Sp2H/Cre} and *Pax3*^{+/-} embryos, but does not cause spina bifida

Spinal neurulation was studied in the early stages of NT closure by measuring the size of the PNP. Additionally, the outcome of spinal neurulation is studied through analysis of the frequency of spina bifida in the embryos.

In order to assess the effects of β -catenin GOF on the caudal closure of the NT the closure rate of the PNP was studied in the same way as previously described for *Sp*^{2H}/*Sp*^{2H} embryos (see section 3.1.1.1). The size of the PNP was measured and plotted against the somite stage of the embryo (**Figure 4.6**).

In order to study the effects of β -catenin GOF on PNP closure *Pax3*^{+/-} *β -catenin*^{+/+} embryos were compared to *Pax3*^{Cre/+} *β -catenin*^{GOF/+} embryos, and also *Pax3*^{Sp2H/Cre} *β -catenin*^{+/+} embryos were compared to *Pax3*^{Sp2H/Cre} *β -catenin*^{GOF/+} embryos.

A significant increase in PNP size was seen in *Pax3*^{Cre/+} *β -catenin*^{GOF/+} embryos when compared to *Pax3*^{+/-} *β -catenin*^{+/+} embryos at the 12-13 somite stage, but the difference was then insignificant until the 20-21 somite stage. A significant increase in PNP size was seen in

Genotype	Number of embryos for exencephaly analysis	% embryos with exencephaly	Number of embryos for spina bifida analysis	% embryos with spina bifida
Pax3 ^{+/+} β-catenin ^{+/+}	178	1.7	34	0.0
Pax3 ^{+/-} β-catenin ^{+/+}	322	9.6	77	5.2
Pax3 ^{Cre/+} β-catenin ^{GOF/+}	82	80.5	9	11.1
Pax3 ^{Sp2H/Cre} β-catenin ^{+/+}	112	58.9	31	83.9
Pax3 ^{Sp2H/Cre} β-catenin ^{GOF/+}	82	98.8	17	88.2

Table 4.1: The frequency of neural tube defects in embryos of different genotypes.

Exencephaly is defined as an open cranial NT at the 18 somite stage or later. Spina bifida is defined as an open spinal NT at the 30 somite stage or later.

The genotypes are seen in the expected ratios (see **Figure 4.1** for information) except for embryos of the genotype Pax3^{Cre/+} β-catenin^{GOF/+} at the 30+ somite stage (the spina bifida column), which are present at a lower frequency than would be expected. This could be due to partial embryonic lethality between the 18 and 30 somite stages. However, as this reduction in frequency is not seen in the more severely affected Pax3^{Sp2H/Cre} β-catenin^{GOF/+} embryos, this result could be spurious.

Pax3^{Sp2H/Cre} β-catenin^{GOF/+} compared to Pax3^{Sp2H/Cre} β-catenin^{+/+} embryos at the 18-19 somite stage.

Spina bifida was significantly increased in frequency in Pax3^{Sp2H/Cre} β-catenin^{+/+} embryos compared to Pax3^{+/+} β-catenin^{+/+} embryos (**Figure 4.7B**). However, there appears to be no significant difference in spina bifida frequency when comparing Pax3^{+/-} β-catenin^{+/+} and Pax3^{Cre/+} β-catenin^{GOF/+} embryos, and also when comparing Pax3^{Sp2H/Cre} β-catenin^{+/+} and Pax3^{Sp2H/Cre} β-catenin^{GOF/+} embryos.

Figure 4.6A: β -catenin gain-of-function does not affect the size of the posterior neuropore. Experimental litters were generated containing a mixture of genotypes through the cross $Pax3^{Sp2H/+} \beta$ -catenin^{GOF/+} x $Pax3^{Cre/+} \beta$ -catenin^{+/+}. This graph begins in **Figure 4.6A** and continues in **Figure 4.6B**.

$Pax3^{+/-} \beta$ -catenin^{+/+} embryos were compared to $Pax3^{Cre/+} \beta$ -catenin^{GOF/+} embryos, and $Pax3^{Sp2H/Cre} \beta$ -catenin^{+/+} embryos were compared to $Pax3^{Sp2H/Cre} \beta$ -catenin^{GOF/+} embryos. A significant difference is first seen between $Pax3^{+/-} \beta$ -catenin^{+/+} and $Pax3^{Cre/+} \beta$ -catenin^{GOF/+} embryos at the 12-13 somite stage. However, significance is not seen again between these genotypes until the 20-21 somite stage. A significant difference between $Pax3^{Sp2H/Cre} \beta$ -catenin^{+/+} and $Pax3^{Sp2H/Cre} \beta$ -catenin^{GOF/+} embryos is first seen at the 18-19 somite stage.

* p < 0.05. Significance was assessed using one-way ANOVA, followed by a t-test if necessary. Only relevant significance is indicated on the graph.

- 8-9 somites – $Pax3^{+/+} \beta$ -catenin^{+/+}; n = 15. $Pax3^{+/-} \beta$ -catenin^{+/+}; n = 28. $Pax3^{Cre/+} \beta$ -catenin^{GOF/+}; n = 12. $Pax3^{Sp2H/Cre} \beta$ -catenin^{+/+}; n = 9. $Pax3^{Sp2H/Cre} \beta$ -catenin^{GOF/+}; n = 12.
- 10-11 somites – $Pax3^{+/+} \beta$ -catenin^{+/+}; n = 16. $Pax3^{+/-} \beta$ -catenin^{+/+}; n = 12. $Pax3^{Cre/+} \beta$ -catenin^{GOF/+}; n = 6. $Pax3^{Sp2H/Cre} \beta$ -catenin^{+/+}; n = 11. $Pax3^{Sp2H/Cre} \beta$ -catenin^{GOF/+}; n = 6.
- 12-13 somites – $Pax3^{+/+} \beta$ -catenin^{+/+}; n = 10. $Pax3^{+/-} \beta$ -catenin^{+/+}; n = 17. $Pax3^{Cre/+} \beta$ -catenin^{GOF/+}; n = 3. $Pax3^{Sp2H/Cre} \beta$ -catenin^{+/+}; n = 5. $Pax3^{Sp2H/Cre} \beta$ -catenin^{GOF/+}; n = 3.
- 14-15 somites – $Pax3^{+/+} \beta$ -catenin^{+/+}; n = 11. $Pax3^{+/-} \beta$ -catenin^{+/+}; n = 18. $Pax3^{Cre/+} \beta$ -catenin^{GOF/+}; n = 4. $Pax3^{Sp2H/Cre} \beta$ -catenin^{+/+}; n = 4. $Pax3^{Sp2H/Cre} \beta$ -catenin^{GOF/+}; n = 7.
- 16-17 somites – $Pax3^{+/+} \beta$ -catenin^{+/+}; n = 13. $Pax3^{+/-} \beta$ -catenin^{+/+}; n = 20. $Pax3^{Cre/+} \beta$ -catenin^{GOF/+}; n = 9. $Pax3^{Sp2H/Cre} \beta$ -catenin^{+/+}; n = 12. $Pax3^{Sp2H/Cre} \beta$ -catenin^{GOF/+}; n = 8.
- 18-19 somites – $Pax3^{+/+} \beta$ -catenin^{+/+}; n = 16. $Pax3^{+/-} \beta$ -catenin^{+/+}; n = 42. $Pax3^{Cre/+} \beta$ -catenin^{GOF/+}; n = 9. $Pax3^{Sp2H/Cre} \beta$ -catenin^{+/+}; n = 10. $Pax3^{Sp2H/Cre} \beta$ -catenin^{GOF/+}; n = 12.
- 20-21 somites – $Pax3^{+/+} \beta$ -catenin^{+/+}; n = 29. $Pax3^{+/-} \beta$ -catenin^{+/+}; n = 49. $Pax3^{Cre/+} \beta$ -catenin^{GOF/+}; n = 11. $Pax3^{Sp2H/Cre} \beta$ -catenin^{+/+}; n = 16. $Pax3^{Sp2H/Cre} \beta$ -catenin^{GOF/+}; n = 20.
- 22-23 somites – $Pax3^{+/+} \beta$ -catenin^{+/+}; n = 33. $Pax3^{+/-} \beta$ -catenin^{+/+}; n = 60. $Pax3^{Cre/+} \beta$ -catenin^{GOF/+}; n = 25. $Pax3^{Sp2H/Cre} \beta$ -catenin^{+/+}; n = 25. $Pax3^{Sp2H/Cre} \beta$ -catenin^{GOF/+}; n = 13.
- 24-25 somites – $Pax3^{+/+} \beta$ -catenin^{+/+}; n = 19. $Pax3^{+/-} \beta$ -catenin^{+/+}; n = 41. $Pax3^{Cre/+} \beta$ -catenin^{GOF/+}; n = 10. $Pax3^{Sp2H/Cre} \beta$ -catenin^{+/+}; n = 12. $Pax3^{Sp2H/Cre} \beta$ -catenin^{GOF/+}; n = 9.
- 26-27 somites – $Pax3^{+/+} \beta$ -catenin^{+/+}; n = 9. $Pax3^{+/-} \beta$ -catenin^{+/+}; n = 14. $Pax3^{Cre/+} \beta$ -catenin^{GOF/+}; n = 9. $Pax3^{Sp2H/Cre} \beta$ -catenin^{+/+}; n = 1. $Pax3^{Sp2H/Cre} \beta$ -catenin^{GOF/+}; n = 1.
- 28-29 somites – $Pax3^{+/+} \beta$ -catenin^{+/+}; n = 3. $Pax3^{+/-} \beta$ -catenin^{+/+}; n = 4. $Pax3^{Cre/+} \beta$ -catenin^{GOF/+}; n = 0. $Pax3^{Sp2H/Cre} \beta$ -catenin^{+/+}; n = 5. $Pax3^{Sp2H/Cre} \beta$ -catenin^{GOF/+}; n = 1.

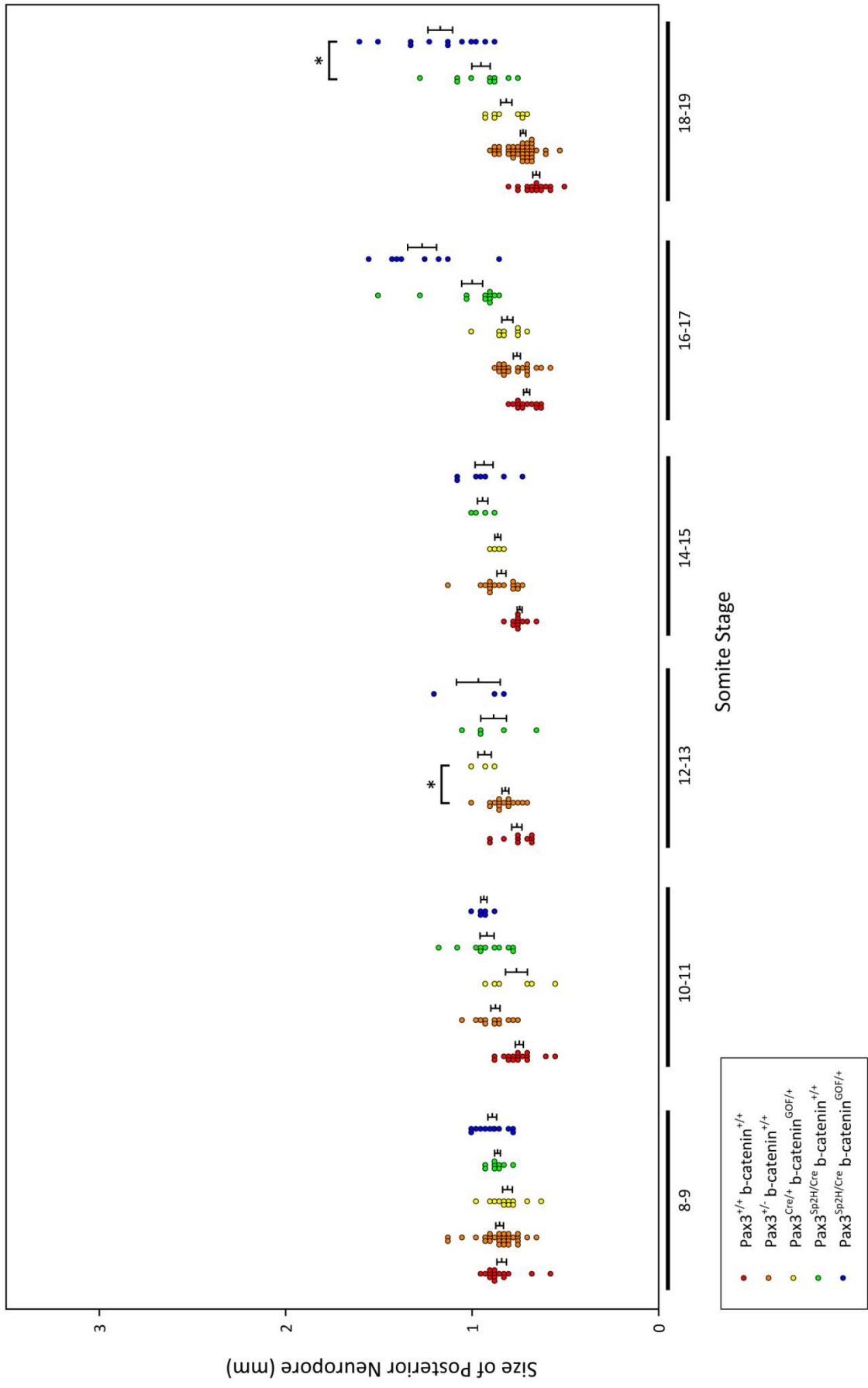


Figure 4.6B: β -catenin gain-of-function does not affect the size of the posterior neuropore, continued.

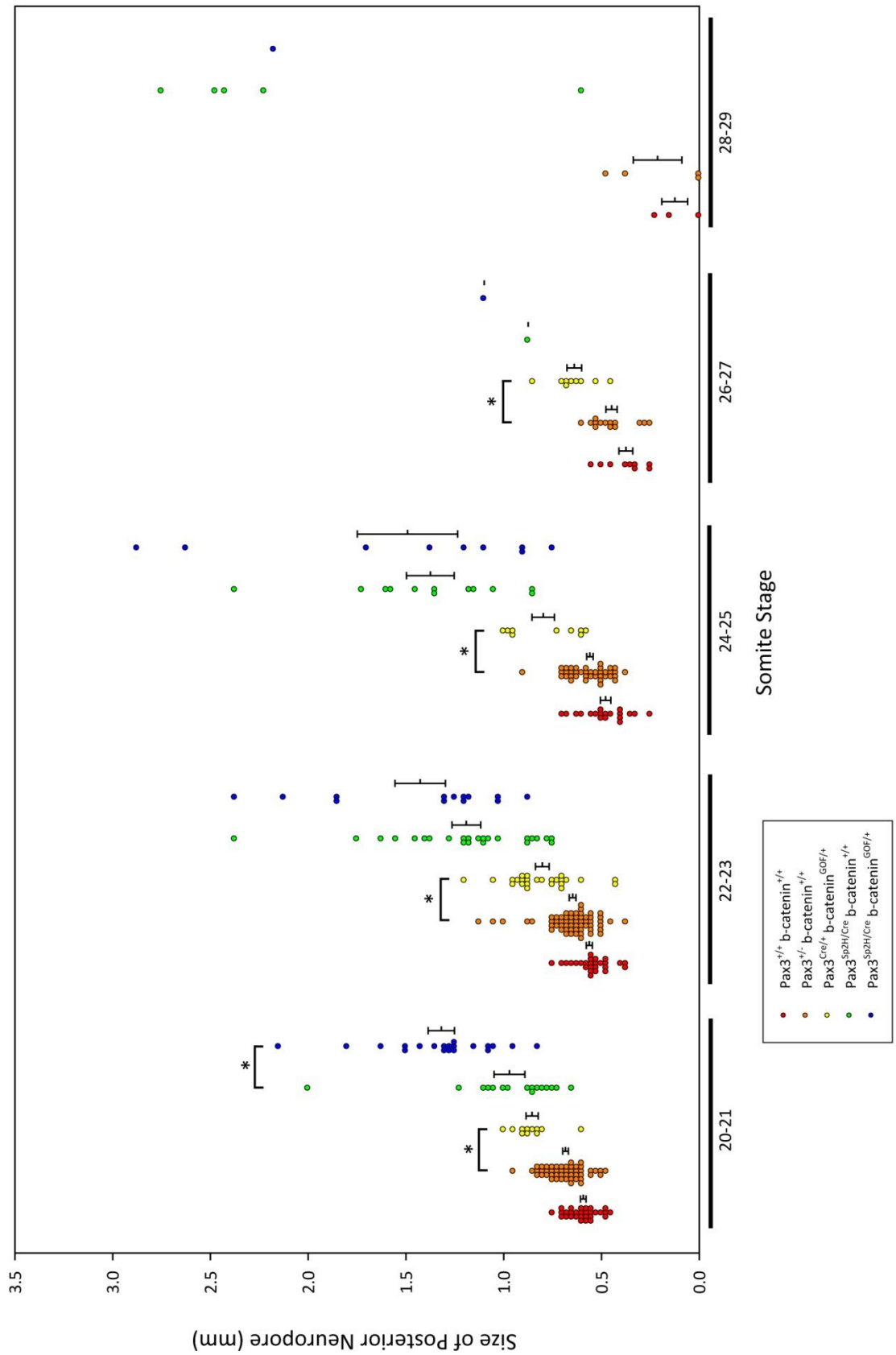


Figure 4.7: β -catenin gain-of-function increases the frequency of exencephaly but not spina bifida in *Pax3* mutant and heterozygous embryos. Experimental litters were generated containing a mixture of genotypes through the cross *Pax3*^{Sp2H/+} β -catenin^{GOF/+} x *Pax3*^{Cre/+} β -catenin^{+/+}. Exencephaly is defined as an open cranial NT at the 18 somite stage or later. Spina bifida is defined as an open spinal NT at the 30 somite stage or later.

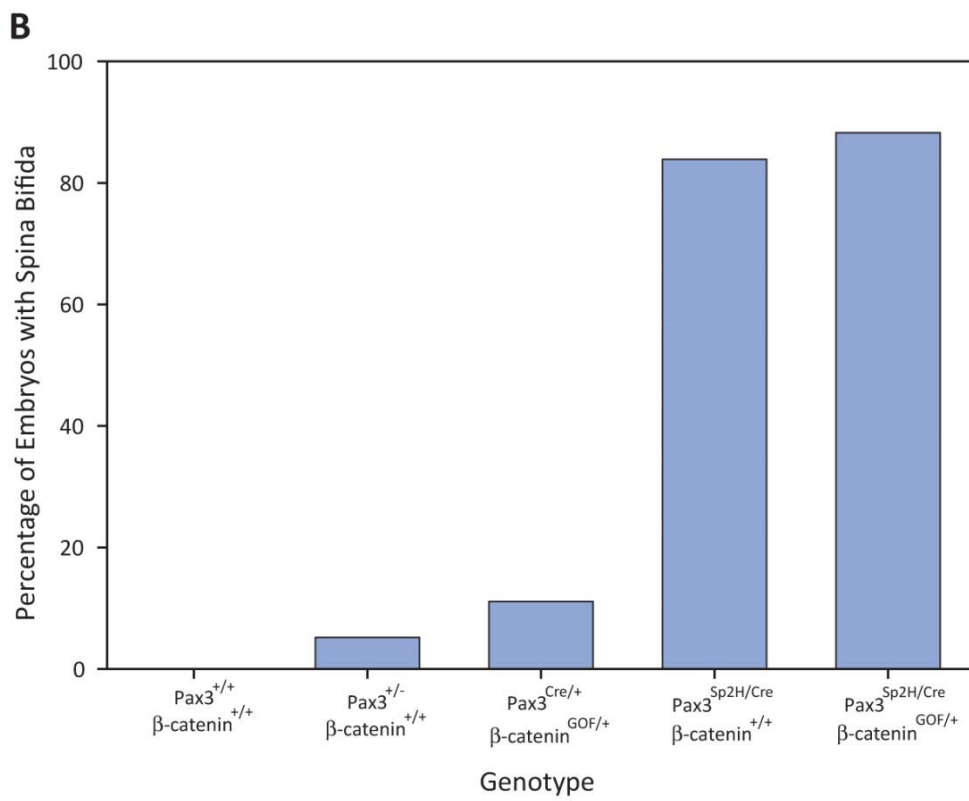
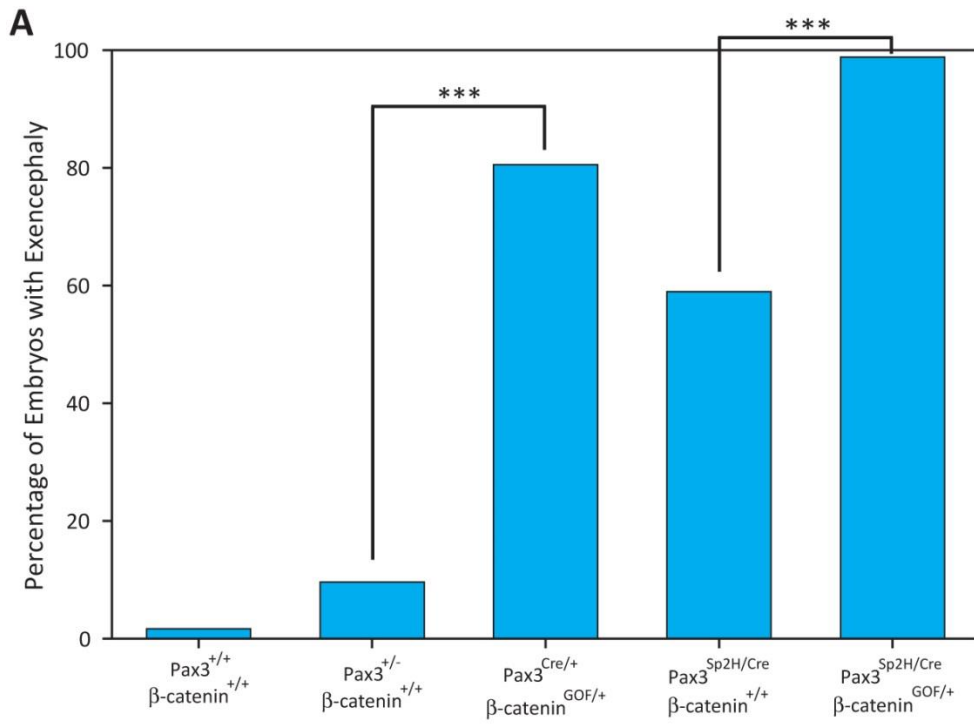
β -catenin GOF dramatically increases the frequency of exencephaly (**A**); *Pax3*^{Cre/+} β -catenin^{GOF/+} embryos have a significantly higher frequency of exencephaly than *Pax3*^{+/-} β -catenin^{+/+} embryos, and *Pax3*^{Sp2H/Cre} β -catenin^{GOF/+} have a significantly higher frequency than *Pax3*^{Sp2H/Cre} β -catenin^{+/+} embryos.

B compares the frequency of spina bifida in embryos of different genotypes from the same cross, as described for **A**. No significant difference in the frequencies of spina bifida are seen between *Pax3*^{+/-} β -catenin^{+/+} and *Pax3*^{Cre/+} β -catenin^{GOF/+} embryos, or between *Pax3*^{Sp2H/Cre} β -catenin^{+/+} and *Pax3*^{Sp2H/Cre} β -catenin^{GOF/+} embryos.

*** p < 0.001. Significance was assessed using the Chi-Square Test (**A**) or the Fisher Exact Test (**B**). Only relevant significant differences are shown.

A – *Pax3*^{+/+} β -catenin^{+/+}: n = 178. *Pax3*^{+/-} β -catenin^{+/+}: n = 322. *Pax3*^{Cre/+} β -catenin^{GOF/+}: n = 82. *Pax3*^{Sp2H/Cre} β -catenin^{+/+}: n = 112. *Pax3*^{Sp2H/Cre} β -catenin^{GOF/+}: n = 82.

B – *Pax3*^{+/+} β -catenin^{+/+}: n = 34. *Pax3*^{+/-} β -catenin^{+/+}: n = 77. *Pax3*^{Cre/+} β -catenin^{GOF/+}: n = 9. *Pax3*^{Sp2H/Cre} β -catenin^{+/+}: n = 31. *Pax3*^{Sp2H/Cre} β -catenin^{GOF/+}: n = 17.



4.1.3.2 β -catenin gain-of-function increases the rate of exencephaly in both $Pax3^{Sp2H/Cre}$ and $Pax3^{+/-}$ mutant embryos

In order to analyse the effect of β -catenin GOF on NTD development the frequency of exencephaly was compared between $Pax3^{+/-} \beta$ -catenin^{+/+} and $Pax3^{Cre/+} \beta$ -catenin^{GOF/+} embryos, and also between $Pax3^{Sp2H/Cre} \beta$ -catenin^{+/+} and $Pax3^{Sp2H/Cre} \beta$ -catenin^{GOF/+} embryos (**Figure 4.7A**).

$Pax3^{Cre/+} \beta$ -catenin^{GOF/+} embryos demonstrated a highly significant increase in the rate of exencephaly compared to $Pax3^{+/-} \beta$ -catenin^{+/+} embryos. Likewise, $Pax3^{Sp2H/Cre} \beta$ -catenin^{GOF/+} embryos showed a highly significant increase in the rate of exencephaly compared to $Pax3^{Sp2H/Cre} \beta$ -catenin^{+/+} embryos.

As an aside, the results of this analysis support the findings previously described in section 3.1.1.2; there is a highly significant increase in the rate of exencephaly in $Pax3^{Sp2H/Cre}$ mutant embryos when compared to the $Pax3^{+/-}$ embryos. Interestingly, there is a significant increase in the rate of exencephaly in $Pax3^{+/-}$ embryos compared to $Pax3^{+/+}$. This is in contrast to the results from section 3.1.1.2. This difference could be due to higher numbers of embryos, or to the involvement of the $Pax3^{Cre}$ allele in addition to the $Pax3^{Sp2H}$ allele.

4.1.4 Phenotypes resulting from β -catenin gain-of-function

β -catenin GOF alters the phenotype of the embryo; $Pax3^{Sp2H/Cre} \beta$ -catenin^{+/+} embryos have a frequency of 84% spina bifida and 59% exencephaly (**Figure 4.7** and **Table 4.1**). However, at E9.5 the exencephaly affects the midbrain and hindbrain, and the neural folds are usually fairly closely apposed. However, $Pax3^{Sp2H/Cre} \beta$ -catenin^{GOF/+} embryos have a different appearance (**Figure 4.8**). They too demonstrate high frequencies of spina bifida (88%), which is very similar in appearance to that seen in $Pax3^{Sp2H/Cre} \beta$ -catenin^{+/+} embryos, but also have exencephaly at a frequency of 99% (**Figure 4.7** and **Table 4.1**). At E9.5 the exencephaly almost always appears very different; the open region of the neural folds is more extensive, and often affects the forebrain in addition to the midbrain and hindbrain. The neural folds are widely splayed open, and the edges of the open region are more rippled in appearance compared to open neural folds in $Pax3^{Sp2H/Cre} \beta$ -catenin^{+/+} embryos. Haemorrhage is frequently seen in the region of the developing CNS, often in the cranial region, but also sometimes in the spinal region. This can affect both open and closed regions of the NT, and is seen in approximately 23% of $Pax3^{Sp2H/Cre} \beta$ -catenin^{GOF/+} embryos (**Figure 4.8E**). This represents a significant increase in frequency when compared to $Pax3^{Sp2H/Cre} \beta$ -catenin^{+/+} embryos, which develop CNS haemorrhage at a frequency of around 7% ($p < 0.001$, assessed using the Chi Square Test).

At E10.5 the difference is still apparent between $Pax3^{Sp2H/Cre}$ genotypes. The neural folds of $Pax3^{Sp2H/Cre} \beta$ -catenin^{+/+} embryos have usually taken on a more rippled appearance (**Figure**

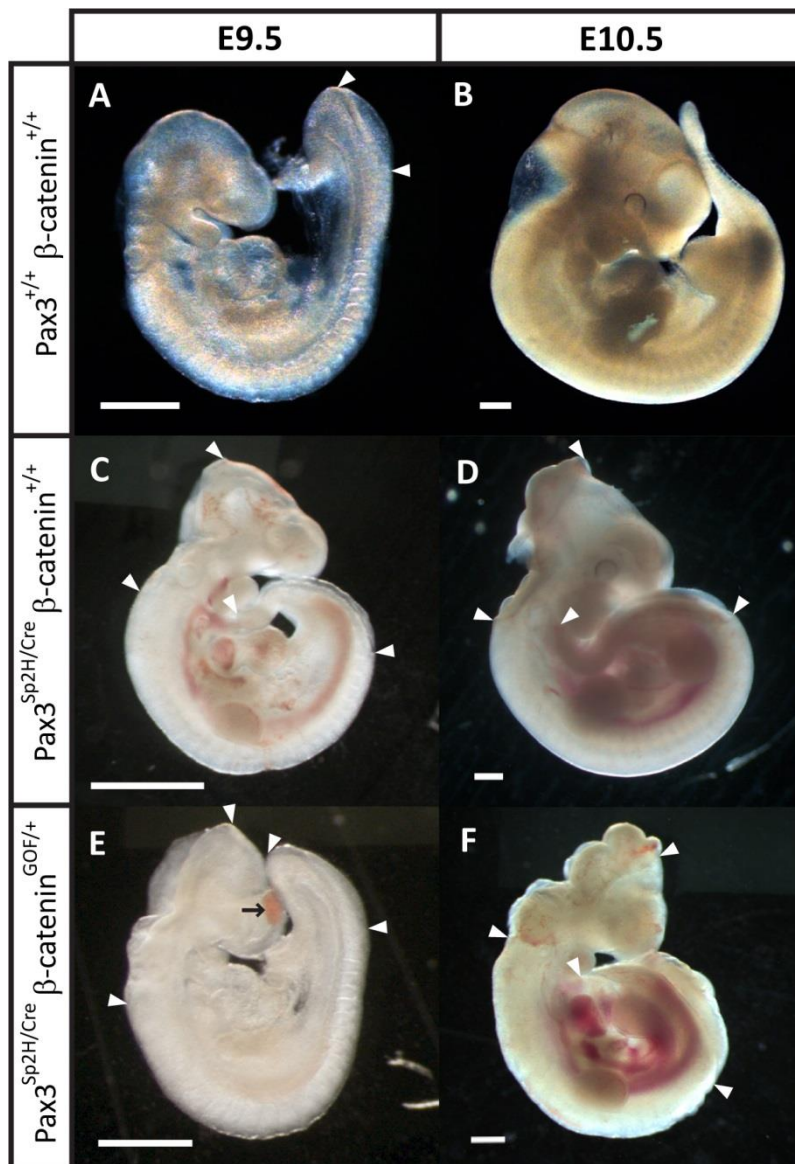


Figure 4.8: Phenotype of $Pax3^{Sp2H/Cre} \beta\text{-catenin}^{GOF/+}$ embryos. Experimental litters were generated through the cross $Pax3^{Sp2H/+} \beta\text{-catenin}^{GOF/+}$ x $Pax3^{Cre/+} \beta\text{-catenin}^{+/+}$. The scale bars represent 500 μm . White arrowheads indicate the open regions of the cranial NT, and the white arrows indicate the open region of the spinal NT.

A and **B** show embryos at E9.5 and E10.5 respectively with the genotype $Pax3^{+/+} \beta\text{-catenin}^{+/+}$ for comparison. Embryos at both of these stages have a closed cranial region, although at E9.5 (**A**) wild type embryos still have an open PNP. **C** and **D** show embryos with the genotype $Pax3^{Sp2H/Cre} \beta\text{-catenin}^{+/+}$ at E9.5 and E10.5 respectively. These embryos demonstrate open PNPs at both stages, and often have open cranial regions. **E** and **F** show embryos with the genotype $Pax3^{Sp2H/Cre} \beta\text{-catenin}^{GOF/+}$ at E9.5 and E10.5 respectively. These embryos have open cranial NTs and open spinal NTs at both stages. The black arrow in **E** indicates cranial haemorrhage. Note the flattened shape of the forebrain in **F**, and the more abnormal appearance of the open cranial region in **F** compared to **D**.

4.8D), much like those in $Pax3^{Sp2H/Cre} \beta\text{-catenin}^{GOF/+}$ embryos. $Pax3^{Sp2H/Cre} \beta\text{-catenin}^{+/+}$ embryos also occasionally develop haemorrhage in the NT, with a frequency of around 13%. However exencephaly seen in $Pax3^{Sp2H/Cre} \beta\text{-catenin}^{GOF/+}$ embryos is usually much larger and causes the cranial region to be very misshapen. Haemorrhage is also usually more extensive (**Figure 4.8F**).

A difference in phenotype is also often seen when comparing $Pax3^{+/-}$ embryos with and without β -catenin GOF. $Pax3^{+/-} \beta\text{-catenin}^{+/+}$ embryos have a wild type phenotype in respect to NT closure, rarely developing either spina bifida or exencephaly. However, $Pax3^{+/-} \beta\text{-catenin}^{GOF/+}$ embryos have a high frequency of exencephaly (80%, see **Figure 4.7** and **Table 4.1**), although they too rarely develop spina bifida. The exencephaly seen in $Pax3^{+/-} \beta\text{-catenin}^{GOF/+}$ embryos resembles that seen in $Pax3^{Sp2H/Cre} \beta\text{-catenin}^{GOF/+}$ embryos; the opening is large, often affecting the forebrain and midbrain as well as the hindbrain, and the neural fold edges in the open region are rippled in appearance. Haemorrhage in the region of the NT is also seen in 13% of $Pax3^{Cre/+} \beta\text{-catenin}^{GOF/+}$ embryos (compared to 5% of $Pax3^{Cre/+} \beta\text{-catenin}^{+/+}$ embryos), although this is usually less severe than in $Pax3^{Sp2H/Cre} \beta\text{-catenin}^{GOF/+}$ embryos.

There are multiple possible causes for these differences in phenotype. It is possible that the phenotypes are simply a summation of the individual phenotypes caused by β -catenin and Pax3 mutations. The mutations may affect different cellular or morphological mechanisms, which affect NT closure in different ways, and produce a compound phenotype.

Alternatively, the differences between phenotypes in $Pax3^{Sp2H/Cre} \beta\text{-catenin}^{+/+}$ and $Pax3^{Sp2H/Cre} \beta\text{-catenin}^{GOF/+}$ embryos could be caused by an interaction between Pax3 and canonical Wnt signalling. This is discussed in more detail in section **1.4.7**. The pathways could interact directly, or they could both act on a single cellular mechanism which affects NT closure, such as proliferation or neuronal differentiation.

Reduced canonical Wnt signalling in the CNS has been reported to cause abnormalities in angiogenesis and haemorrhage (Daneman et al., 2009). Although the embryos described here have an increase in canonical Wnt signalling, it is possible that the haemorrhage seen in $Pax3^{Cre/+} \beta\text{-catenin}^{GOF/+}$ and $Pax3^{Sp2H/Cre} \beta\text{-catenin}^{GOF/+}$ embryos could be due to disruption of the canonical Wnt signalling pathway, rather than an interaction between Pax3 and the canonical Wnt signalling pathway.

4.1.5 β -catenin gain-of-function does not affect proliferation during cranial neurulation

As shown previously (section **3.1.2.4**) a decrease in proliferation may be a causative element of spina bifida development in the Sp^{2H}/Sp^{2H} mouse. If canonical Wnt signalling acted directly on

Pax3 signalling it may also have an effect on proliferation of cells in the NT. Alternatively, canonical Wnt signalling may worsen NTDs in *Pax3* mutant embryos by acting further on an already defective cellular mechanism. The main effect of canonical Wnt signalling on NT closure appears to be in the cranial region. Therefore, proliferation in the cranial NT was analysed.

Embryos of multiple genotypes for study were generated from the cross *Pax3*^{Sp2H/+} β -catenin^{GOF/+} x *Pax3*^{Cre/+} β -catenin^{+/+}. They were collected at the 13-15 somite stage, as at this stage the cranial NT would be in the process of closing in *Pax3*^{+/+} β -catenin^{+/+} embryos. Therefore, the cranial tissue in mutant embryos which would go on to develop exencephaly will not yet show secondary effects resulting from exposure to the intra-uterine environment.

The anti-phospho histone H3 antibody stains cells in G2/M phase, and so was used as a marker for proliferating cells, as described in section 3.1.2.4. Coronal sections were taken of the cranial NT, and the dorsal 25% of the cranial NT was studied as the *Pax3*-positive region (see section 3.1.2.1 for cranial *Pax3* expression).

The mitotic index was calculated for *Pax3*-positive region of the cranial NT for the embryos of each genotype (Table 4.2 and Figure 4.9). Data shows that there are no significant differences in the rate of proliferation between the genotypes.

4.1.6 β -catenin gain-of-function does not affect neuronal differentiation during neurulation

It has been suggested previously that premature neuronal differentiation may contribute to the development of NTDs in *Pax3* mutant embryos (section 3.1.2.2). Although this was found not to be the case in *Sp*^{2H}/*Sp*^{2H} spinal neurulation, it is potentially true for the cranial region. Canonical Wnt signalling is known to be important in the initiation and timing of differentiation of many cell types during development. Therefore β -catenin GOF may worsen cranial NTDs in the *Pax3*^{Sp2H/Cre} embryos by acting through this mechanism.

Spinal neuronal differentiation is normal in *Sp*^{2H}/*Sp*^{2H} embryos. However, β -catenin GOF appears to slow closure of the PNP, although it doesn't increase the frequency of spina bifida. Therefore, β -catenin GOF may have this effect in the *Pax3* mutant homozygous and heterozygous embryos through causing premature neuronal differentiation in the spinal region.

4.1.6.1 Spinal neuronal differentiation in embryos with β -catenin gain-of-function

Whole mount antibody staining using the neuronal marker Tuj1 was used to detect neuronal differentiation in the spinal region as previously described in section 3.1.2.2; spinal neuronal

Genotype	Average number of cells per section	Average number of proliferating cells per section	% cells which are proliferating (mitotic index)
Pax3 ^{+/+} β-catenin ^{+/+}	65.0	3.35	5.13
Pax3 ^{+/-} β-catenin ^{+/+}	99.8	4.77	4.85
Pax3 ^{Cre/+} β-catenin ^{GOF/+}	87.8	5.52	6.04
Pax3 ^{Sp2H/Cre} β-catenin ^{+/+}	107.9	5.13	4.86
Pax3 ^{Sp2H/Cre} β-catenin ^{GOF/+}	143.7	7.44	5.19

Table 4.2: The number of proliferating cells in the dorsal region of the neural tube. The number of cells was calculated for the dorsal region of the NT by counting DAPI-stained nuclei in this region. The number of neurons was calculated by counting phospho-histone H3-positive cells in the same region. The antibody against phospho-histone H3 stains cells in G2 and M phase, and thus is used as a marker for proliferating cells. An average was calculated by totalling the number of cells and the number of proliferating cells per embryo, calculating the percentage of proliferating cells for each embryo, and then averaging this percentage between embryos of each genotype.

differentiation extends in a rostral-to-caudal manner. Therefore the caudal-most somite level which has robust Tuj1 staining was analysed for the embryos of each genotype (**Figure 4.10**).

No significant differences were found in the extent of spinal neuronal differentiation between the genotypes studied.

4.1.6.2 Cranial neuronal differentiation in embryos with β-catenin gain-of-function

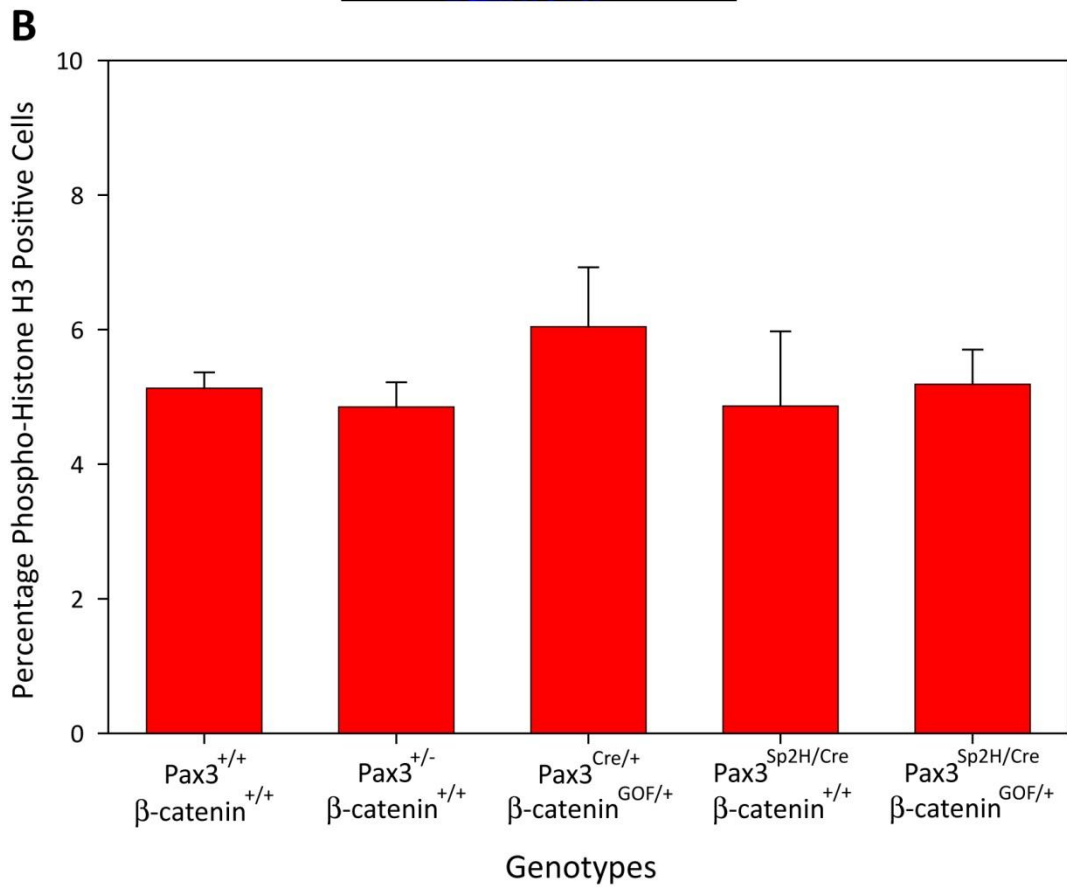
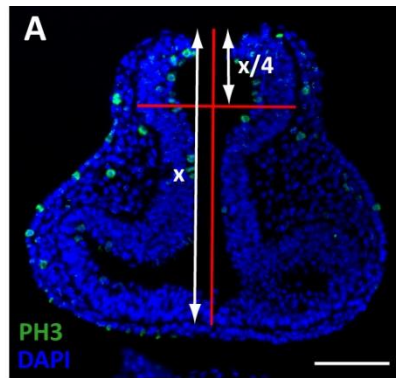
Neuronal differentiation was studied in embryos at the 13-15 somite stage, when the cranial NT is closing, and the tissue will not yet show secondary damage due to exposure to the intra-uterine environment. Coronal sections were taken of the cranial NT, and the antibody Tuj1, which binds βIII-tubulin, was used to mark differentiating neurons. The dorsal half of the NT was defined as the experimental region, and counts were taken of the number of Tuj1-positive cells in this region (**Table 4.3** and **Figure 4.11**). No significant differences were found in the number of Tuj1-positive cells in the dorsal half of the cranial NT.

Figure 4.9: β -catenin gain-of-function does not affect proliferation in the cranial neural tube. Experimental litters were generated containing a mixture of genotypes through the cross $Pax3^{Sp2H/+} \beta\text{-catenin}^{GOF/+}$ x $Pax3^{Cre/+} \beta\text{-catenin}^{+/+}$. Immunohistochemistry of sections using an antibody against phospho histone H3 was carried out on embryos of multiple genotypes. This antibody identifies cells in G2 and M phase, and therefore is used as a marker for proliferating cells. The scale bar represents 100 μm .

A demonstrates how the NT section was divided for proliferation cell counts. The height of the NT was measured (x), and then the dorsal-most quarter was demarcated (x/4). Phospho histone H3-positive cells were counted within this dorsal region. DAPI was used to mark all cells in the NT section. No significant differences were found between genotypes for the number of PH3-positive cells (**B**).

One way ANOVA was used to assess significance. Error bars indicate standard error.

4-6 sections per embryo. Number of embryos – $Pax3^{+/+} \beta\text{-catenin}^{+/+}$: n = 6. $Pax3^{+/-} \beta\text{-catenin}^{+/+}$: n = 6. $Pax3^{Cre/+} \beta\text{-catenin}^{GOF/+}$: n = 3. $Pax3^{Sp2H/Cre} \beta\text{-catenin}^{+/+}$: n = 4. $Pax3^{Sp2H/Cre} \beta\text{-catenin}^{GOF/+}$: n = 7.



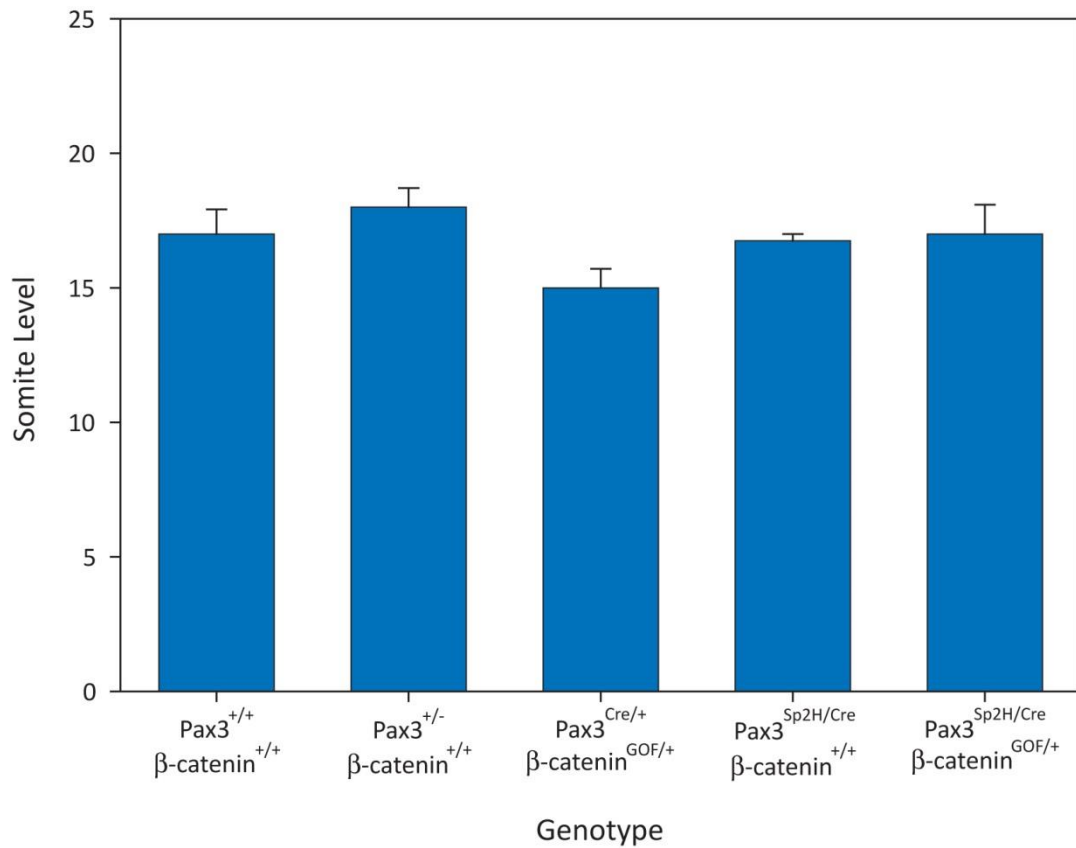


Figure 4.10: β -catenin gain-of-function does not affect the rostro-causal progression of spinal neuronal differentiation in $Pax3^{Cre/+}$ or $Pax3^{Sp2H/Cre}$ embryos. Experimental litters containing a mixture of the genotypes for study were generated using the cross $Pax3^{Sp2H/+} \beta\text{-catenin}^{GOF/+} \times Pax3^{Cre/+} \beta\text{-catenin}^{+/+}$. Embryos were studied at the 23 somite stage. $n = 4$ for each genotype. The antibody Tuj1 was used to mark neurons, as it binds β III-tubulin.

Neuronal differentiation in the spinal region develops in a rostro-caudal direction. Therefore, the extent to which neuronal differentiation had progressed was examined. The most caudal somite level which displayed robust Tuj1 staining was compared between the genotypes. No significant difference was seen between the genotypes in the extent of the neuronal differentiation.

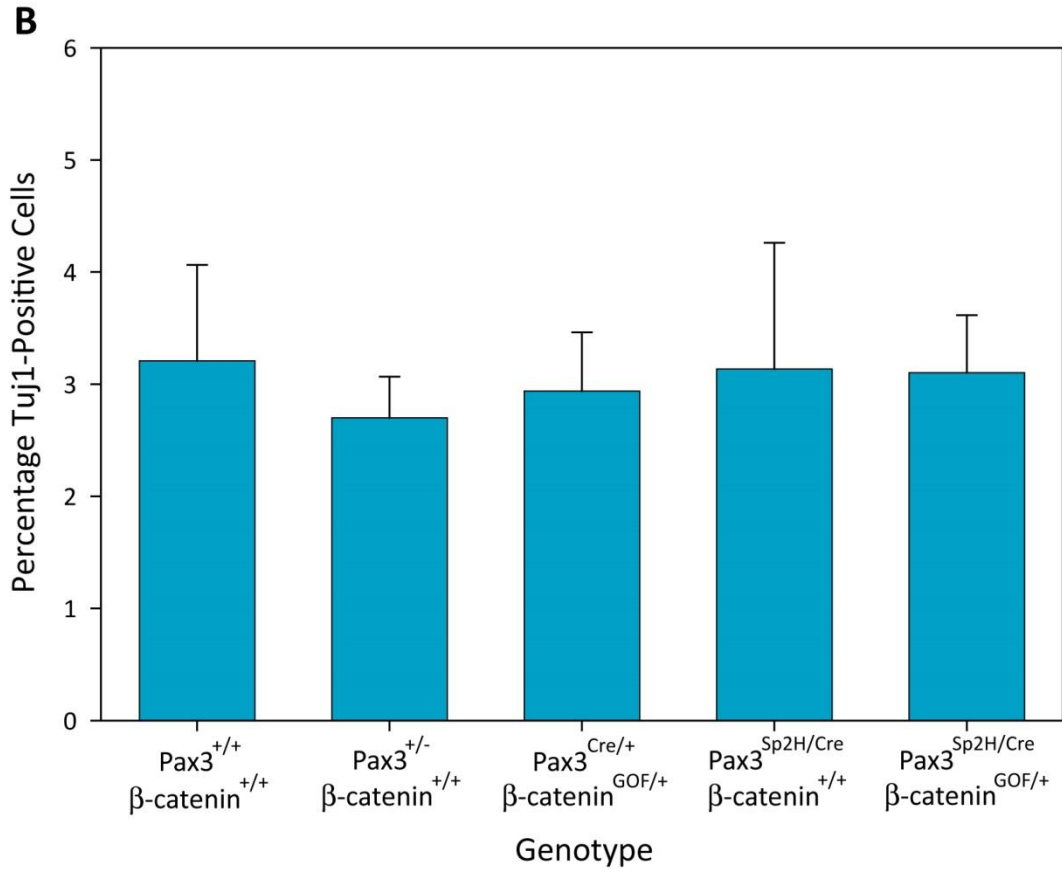
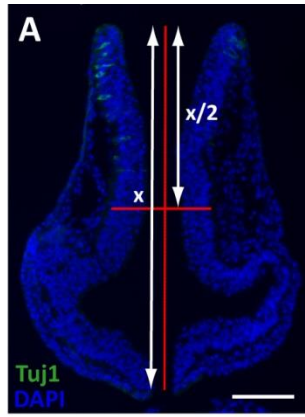
Significance was calculated using one-way ANOVA. Error bars indicate standard error.

Figure 4.11: β -catenin gain-of-function does not affect neuronal differentiation in the cranial neural tube. Experimental litters were generated containing a mixture of genotypes through the cross $Pax3^{Sp2H/+} \beta\text{-catenin}^{GOF/+}$ x $Pax3^{Cre/+} \beta\text{-catenin}^{+/+}$. Immunohistochemistry of sections using the Tuj1 antibody was carried out on progeny of multiple genotypes at the 13-15 somite stage. This antibody binds β III-tubulin, and marks differentiated neurons. The scale bar represents 100 μ m.

A demonstrates how the NT section was divided for differentiation cell counts. The height of the NT was measured (x), and then the dorsal-most half was demarcated (x/2). Tuj1-positive cells were counted within this dorsal region. DAPI was used to mark all cells in the NT section. No significant differences were found between genotypes for the number of PH3-positive cells (**B**).

One way ANOVA was used to assess significance. Error bars indicate standard error.

4-6 sections per embryo. Number of embryos – $Pax3^{+/+} \beta\text{-catenin}^{+/+}$: n = 4. $Pax3^{+/-} \beta\text{-catenin}^{+/+}$: n = 6. $Pax3^{Cre/+} \beta\text{-catenin}^{GOF/+}$: n = 2. $Pax3^{Sp2H/Cre} \beta\text{-catenin}^{+/+}$: n = 3. $Pax3^{Sp2H/Cre} \beta\text{-catenin}^{GOF/+}$: n = 5.



Genotype	Average number of cells per section	Average number of neurons per section	% cells which are neurons
Pax3 ^{+/+} β-catenin ^{+/+}	173.2	6.10	3.21
Pax3 ^{+/-} β-catenin ^{+/+}	185.3	4.77	2.70
Pax3 ^{Cre/+} β-catenin ^{GOF/+}	174.8	5.22	2.94
Pax3 ^{Sp2H/Cre} β-catenin ^{+/+}	204.2	7.72	3.13
Pax3 ^{Sp2H/Cre} β-catenin ^{GOF/+}	272.4	8.55	3.10

Table 4.3: The number of neurons in the dorsal region of the neural tube. The number of cells was calculated for the dorsal region of the NT by counting DAPI-stained nuclei in this region. The number of neurons was calculated by counting Tuj1-positive cells in the same region. Tuj1 stains βIII-tubulin and is used as a marker for neurons. An average was calculated by totalling the number of cells and the number of neurons per embryo, calculating the percentage of neurons for each embryo, and then averaging this percentage between embryos of each genotype.

4-6 sections per embryo. Number of embryos – Pax3^{+/+} β-catenin^{+/+}: n = 4. Pax3^{+/-} β-catenin^{+/+}: n = 6. Pax3^{Cre/+} β-catenin^{GOF/+}: n = 2. Pax3^{Sp2H/Cre} β-catenin^{+/+}: n = 3. Pax3^{Sp2H/Cre} β-catenin^{GOF/+}: n = 5.

4.1.7 The effects of β-catenin gain-of-function on the development of the neural crest

The data presented above analyse the effects of β-catenin GOF on the closure of the NT. However, *Sp^{2H}/Sp^{2H}* embryos have several additional abnormalities involving the limb musculature and the NC (Auerbach, 1954; Bober et al., 1994; Goulding et al., 1994).

The specification and migration of the NC, and the development of the subsequent NC-derived tissues were studied in mouse embryos carrying various combinations of *Pax3* and *β-catenin* mutations. The aim of this study was to determine if canonical Wnt signalling interacts with *Pax3* in the development and differentiation of the NC.

4.1.7.1 β-catenin gain-of-function causes abnormalities in the neural crest

Whole mount *in situ* hybridisation for the gene *ErbB3*, a marker for NC, was used to study NC in multiple genotypes, and from the 18 to 30+ somite stages (**Figure 4.12**). Embryos within a

Figure 4.12: β -catenin gain-of-function disrupts expression of *ErbB3*. Experimental litters were generated containing a mixture of genotypes through the cross *Pax3^{Sp2H/+} β -catenin^{GOF/+} x Pax3^{Cre/+} β -catenin^{+/+}*. Whole mount *in situ* hybridisation for *ErbB3* was carried out on embryos of multiple genotypes to mark the NC. The expression was studied at the 18-20 (**A-E**), 24-26 (**F-J**), and 30+ (**K-O**) somite stages. Scale bars represent 500 μ m.

Pax3^{+/+} β -catenin^{+/+} embryos (**A, F, and K**) show *ErbB3* expression in the DRG (black arrowhead), vagus nerve (red arrowhead), trigeminal ganglia (black arrow), and otic vesicle (red arrow). *Pax3^{+/-} β -catenin^{+/+}* embryos (**B, G, and L**) show the same expression pattern.

Pax3^{Sp2H/Cre} β -catenin^{+/+} embryos (**D, I, and N**) show weaker staining, which suggests lower *ErbB3* expression. The staining in the DRG is much weaker compared to *Pax3^{+/+} β -catenin^{+/+}* embryos. This is particularly noticeable in the older embryos, at the 24-26 (**I**) and 30+ (**N**) somite stages. However, segmentation in the DRG is still apparent, and expression in the vagus nerve, trigeminal ganglia and otic vesicle is present.

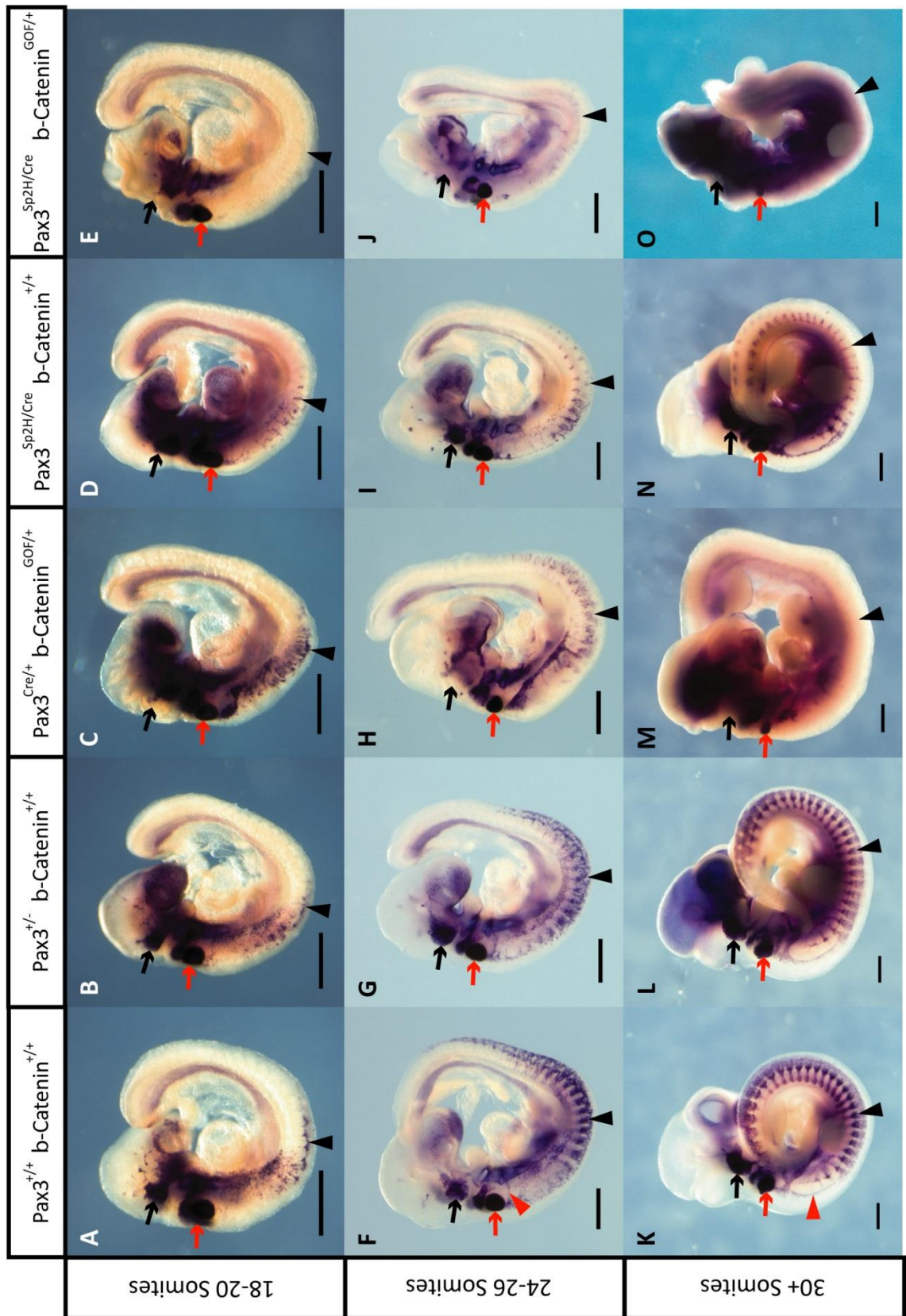
Pax3^{Cre/+} β -catenin^{GOF/+} embryos (**C, H, and M**) appear to show normal *ErbB3* expression in the DRG at the 18-20 somite stage (**C**). However, by the 24-26 somite stage (**H**) the DRG staining is fainter than in *Pax3^{+/+} β -catenin^{+/+}* embryos, and segmentation is much less obvious. By the 30+ somite stage (**M**) staining of the DRG has disappeared completely. *ErbB3* expression in the developing vagus nerve appears to be much stronger and more defined in *Pax3^{Cre/+} β -catenin^{GOF/+}* embryos compared to *Pax3^{+/+} β -catenin^{+/+}* embryos at the 18-20 and 24-26 somite stages (**C and H**). However, by the 30+ somite stage, only rudimentary nerve staining remains, and it appears that the vagus nerve fails to form properly. *ErbB3* expression in the trigeminal ganglia is absent in every stage studied.

Pax3^{Sp2H/Cre} β -catenin^{GOF/+} embryos (**E, J, and O**) also show absent *ErbB3* expression in the trigeminal ganglia throughout the stages studied. Staining in the developing vagus nerve is also completely absent. Some very sparse staining of the DRG is visible at the 18-20 and 24-26 somite stages, but this has disappeared by the 30+ somite stage.

18-20 somite stage – *Pax3^{+/+} β -catenin^{+/+}*; n = 1. *Pax3^{+/-} β -catenin^{+/+}*; n = 2. *Pax3^{Cre/+} β -catenin^{GOF/+}*; n = 2. *Pax3^{Sp2H/Cre} β -catenin^{+/+}*; n = 2. *Pax3^{Sp2H/Cre} β -catenin^{GOF/+}*; n = 2.

24-26 somite stage – *Pax3^{+/+} β -catenin^{+/+}*; n = 2. *Pax3^{+/-} β -catenin^{+/+}*; n = 2. *Pax3^{Cre/+} β -catenin^{GOF/+}*; n = 2. *Pax3^{Sp2H/Cre} β -catenin^{+/+}*; n = 2. *Pax3^{Sp2H/Cre} β -catenin^{GOF/+}*; n = 2.

30+ somite stage – *Pax3^{+/+} β -catenin^{+/+}*; n = 2. *Pax3^{+/-} β -catenin^{+/+}*; n = 2. *Pax3^{Cre/+} β -catenin^{GOF/+}*; n = 2. *Pax3^{Sp2H/Cre} β -catenin^{+/+}*; n = 2. *Pax3^{Sp2H/Cre} β -catenin^{GOF/+}*; n = 2.



genotype and somite stage show a high degree of consistency in the pattern of *ErbB3* expression.

Little difference is apparent in *ErbB3* expression between *Pax3*^{+/-} *β-catenin*^{+/-} and *Pax3*^{+/-} *β-catenin*^{+/-} embryos at any of the stages studied. Loss of *Pax3* expression results in reduced *ErbB3* expression in the DRG of *Pax3*^{Sp2H/Cre} *β-catenin*^{+/-} embryos. However, rudimentary DRG still form, and segmentation is clearly visible.

The addition of β -catenin GOF either to the *Pax3* heterozygous or homozygous mutant embryos has a profound effect on the expression of *ErbB3*. Both *Pax3*^{Cre/+} *β-catenin*^{GOF/+} and *Pax3*^{Sp2H/Cre} *β-catenin*^{GOF/+} embryos completely lack expression in the trigeminal ganglia, and both lack staining in the DRG by 30+ somite stage, although *Pax3*^{Cre/+} *β-catenin*^{GOF/+} embryos form rudimentary, badly segmented DRG at earlier stages. Additionally, *ErbB3* expression in the vagus nerve is affected; both genotypes lack staining in the vagus nerve at the 30+ somite stage. However, *Pax3*^{Sp2H/Cre} *β-catenin*^{GOF/+} embryos fail to express *ErbB3* in the vagus nerve throughout development, whereas *Pax3*^{Cre/+} *β-catenin*^{GOF/+} embryos first overexpress *ErbB3* in the developing vagus nerve, and then lose expression by 30+ somite stage. Both *Pax3*^{Cre/+} *β-catenin*^{GOF/+} and *Pax3*^{Sp2H/Cre} *β-catenin*^{GOF/+} embryos quickly developed dark, but seemingly non-specific staining in the cranial regions and the trunk. This makes it difficult to observe the expression pattern of *ErbB3*. Alternatively, the consistency of this staining across samples may suggest a defect in *ErbB3* expression. Sectioning through this region could help to identify stained tissues and clarify why this staining occurs.

In addition to studying the NC population, the antibody Tuj1 – a neuronal marker – was used to study the development of the PNS, which is largely NC-derived. *Pax3*^{+/-} *β-catenin*^{+/-} and *Pax3*^{+/-} *β-catenin*^{+/-} embryos show similar patterns of Tuj1 staining (**Figure 4.13**). *Pax3*^{Sp2H/Cre} *β-catenin*^{+/-} embryos also show similar patterning, but the DRG are not quite so clearly defined.

Comparable to the *ErbB3* expression patterns, the presence of β -catenin GOF severely disrupts the patterning of nerve differentiation in *Pax3* homozygous and heterozygous embryos. In both *Pax3*^{Cre/+} *β-catenin*^{GOF/+} and *Pax3*^{Sp2H/Cre} *β-catenin*^{GOF/+} embryos, the nerves in the cranial meshwork appear to clump into foci, and the vagus nerve shows disrupted patterning. The spinal DRG show very disrupted patterning, and segmentation is poorly defined.

These abnormalities in the spinal NC could be caused by failure of NC specification, differentiation, apoptosis of specified NC, or failure of NC migration. Presence of *ErbB3* expression in the spinal region of each of the genotypes at the 24-26 somite stage suggests

Figure 4.13: Neuronal differentiation is disrupted by β -catenin gain-of-function. Experimental litters were generated containing a mixture of genotypes through the cross $Pax3^{Sp2H/+} \beta$ -catenin^{GOF/+} x $Pax3^{Cre/+} \beta$ -catenin^{+/+}. Embryos of multiple genotypes have undergone whole mount antibody staining using the Tuj1 antibody, which binds β -tubulin and identifies differentiating neurons. Scale bars represent 500 μ m. n = 1-2 for each genotype.

In 23-24 somite stage $Pax3^{+/+} \beta$ -catenin^{+/+} embryos (**A**) neuronal differentiation has begun in the cranial region, and is spreading in a rostral-to-caudal direction down the spinal region. This appears to be fairly uniform throughout the genotypes of the same stage (**B-D**).

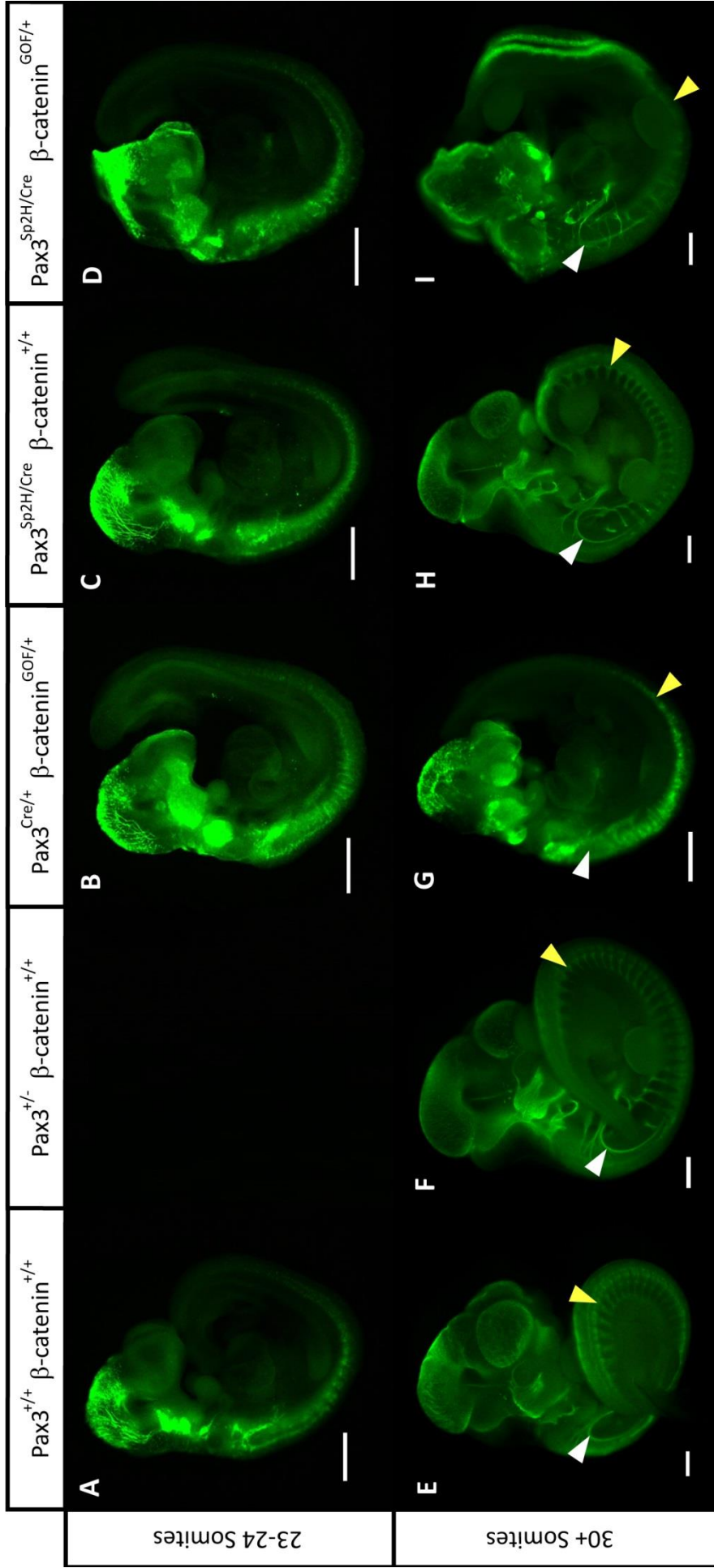
$Pax3^{+/+} \beta$ -catenin^{+/+} embryos at the 30+ somite stage (**E**) appear to have a fine meshwork of differentiated neurons in the cranial region, well defined vagus nerve formation (indicated by the white arrowheads), and well patterned DRG forming in the spinal region (indicated by the yellow arrowhead). This is also true for the $Pax3^{+/-} \beta$ -catenin^{+/+} embryo shown in **F**.

$Pax3^{Sp2H/Cre} \beta$ -catenin^{+/+} embryos (**H**) also appears to demonstrate similar definition and differentiation patterns. The cranial neurons are forming, and the vagus nerve is well defined. The DRG begin to lose definition in the caudal-most region, likely where neural tube closure has failed, but are otherwise well patterned.

On the other hand, β -catenin GOF appears to have a strong effect on neuronal differentiation in both the $Pax3$ heterozygous (**G**) and homozygous mutant (**I**) embryos. The developing neurons in the cranial region fail to form a fine meshwork, and instead appear clumped into foci. The vagus nerve shows less definition and patterning. The spinal neurons have failed to pattern into ganglia, instead forming a streak of Tuj1 staining resembling the spinal staining of 23-24 somite stage embryos.

23-24 somite stage – $Pax3^{+/+} \beta$ -catenin^{+/+}; n = 2. $Pax3^{Cre/+} \beta$ -catenin^{GOF/+}; n = 2. $Pax3^{Sp2H/Cre} \beta$ -catenin^{+/+}; n = 2. $Pax3^{Sp2H/Cre} \beta$ -catenin^{GOF/+}; n = 1.

30+ somite stage – $Pax3^{+/+} \beta$ -catenin^{+/+}; n = 1. $Pax3^{+/-} \beta$ -catenin^{+/+}; n = 2. $Pax3^{Cre/+} \beta$ -catenin^{+/+}; n = 2. $Pax3^{Sp2H/Cre} \beta$ -catenin^{+/+}; n = 2. $Pax3^{Sp2H/Cre} \beta$ -catenin^{GOF/+}; n = 2.



that migration still occurs. Therefore, studies were carried out to observe apoptosis, and NC specification and differentiation in the embryos of different genotypes.

4.1.7.2 β -catenin gain-of-function causes an increase in apoptosis in the neural crest

Whole mount TUNEL stains were carried out to compare the pattern and frequency of apoptotic cells in embryos of different genotypes. The purpose of this is to ascertain if β -catenin has any effect on apoptosis, in particular focussing on the NC. *in situ* hybridisation against the *ErbB3* gene has shown that NC cells are present at the 24-26 somite stage, but not at 30+ somites in *Pax3^{Cre/+} β -catenin^{GOF/+}* and *Pax3^{Sp2H/Cre} β -catenin^{GOF/+}* embryos. In order to determine if the NC are undergoing apoptosis between the 26 and 30 somite stage, TUNEL stains were carried out shortly prior to and during these stages, from 22 to 30+ somites. The results of these TUNEL stainings gave variable results, even within somite stages and genotypes. No common patterns have been discussed unless they are present on all embryos of a particular somite stage and genotype which have been tested. However, larger sample sizes and quantification through sectioning could further clarify the results. It is also assumed that TUNEL staining in regions known to contain NC cells mark apoptosing NC cells. However, the TUNEL staining also marks apoptotic cells of other tissues. TUNEL staining in combination with NC markers could further clarify the cell types undergoing apoptosis. In addition, negative controls could show background staining which occurs during TUNEL staining.

Apoptosis shows a similar pattern in *Pax3^{+/-} β -catenin^{+/-}* and *Pax3^{+/-} β -catenin^{+/-}* embryos; at the 22-24 somite stage (**Figure 4.14**) apoptosis is most obvious in a stream of migrating NC. At the 27-29 somite stage (**Figure 4.15**) this stream of apoptotic NC is still visible, and apoptosing NC-derived cells are visible in the DRG in a segmented pattern. Additionally, a clearly-defined line of apoptotic cells is visible in the midline of the forebrain NT. At the 30+ somite stage (**Figure 4.16**), the migrating stream of NC is less visible, but apoptotic cells in the DRG form the same segmented patterning seen at the 27-29 somite stage. However, even between embryos of the same genotype there is variation.

The pattern of apoptosis in *Pax3^{Sp2H/Cre} β -catenin^{+/-}* embryos does not appear to differ greatly from that of *Pax3^{+/-} β -catenin^{+/-}* embryos; at the 22-24 and 27-29 somite stages (**Figures 4.14** and **4.15**). Apoptosis in *Pax3^{Sp2H/Cre} β -catenin^{+/-}* embryos is indistinguishable from *Pax3^{+/-} β -catenin^{+/-}* embryos, apart from possibly a small increase in apoptosis at the cervical-hindbrain boundary (**Figure 4.14**), and a reduction in apoptotic cells at the midline of the forebrain NT (**Figure 4.15**). However, by the 30+ somite stage (**Figure 4.16**) apoptosis appears to be reduced. This is particularly obvious in the DRG.

Figure 4.14: TUNEL assay of 22-24 somite stage embryos. Experimental litters were generated containing a mixture of genotypes through the cross $Pax3^{Sp2H/+} \beta\text{-catenin}^{GOF/+} \times Pax3^{Cre/+} \beta\text{-catenin}^{+/+}$. TUNEL staining was carried out on embryos of multiple genotypes. Scale bars represent 250 μm . $n = 2$ for each genotype. **A'-E'** show zoomed in images of the spinal regions of **A-E** respectively.

$Pax3^{+/+} \beta\text{-catenin}^{+/+}$ (**A** and **A'**) embryos appear to show a small patch of apoptotic cells near the hindbrain-cervical boundary (arrowhead), and a stream of apoptotic cells in the migrating NC (arrows). There do not appear to be any differences in TUNEL staining in the migrating NC between the genotypes. However, there is potentially a higher level of apoptosis in the hindbrain-cervical boundary region in $Pax3^{Cre/+} \beta\text{-catenin}^{GOF/+}$ (**C**), $Pax3^{Sp2H/Cre} \beta\text{-catenin}^{+/+}$ (**D**) and $Pax3^{Sp2H/Cre} \beta\text{-catenin}^{GOF/+}$ (**E**) compared to $Pax3^{+/+} \beta\text{-catenin}^{+/+}$ (**A**) and $Pax3^{+/+} \beta\text{-catenin}^{+/+}$ (**B**) embryos. Additionally, $Pax3^{+/+} \beta\text{-catenin}^{+/+}$ embryos may have a slightly higher overall level of apoptosis.

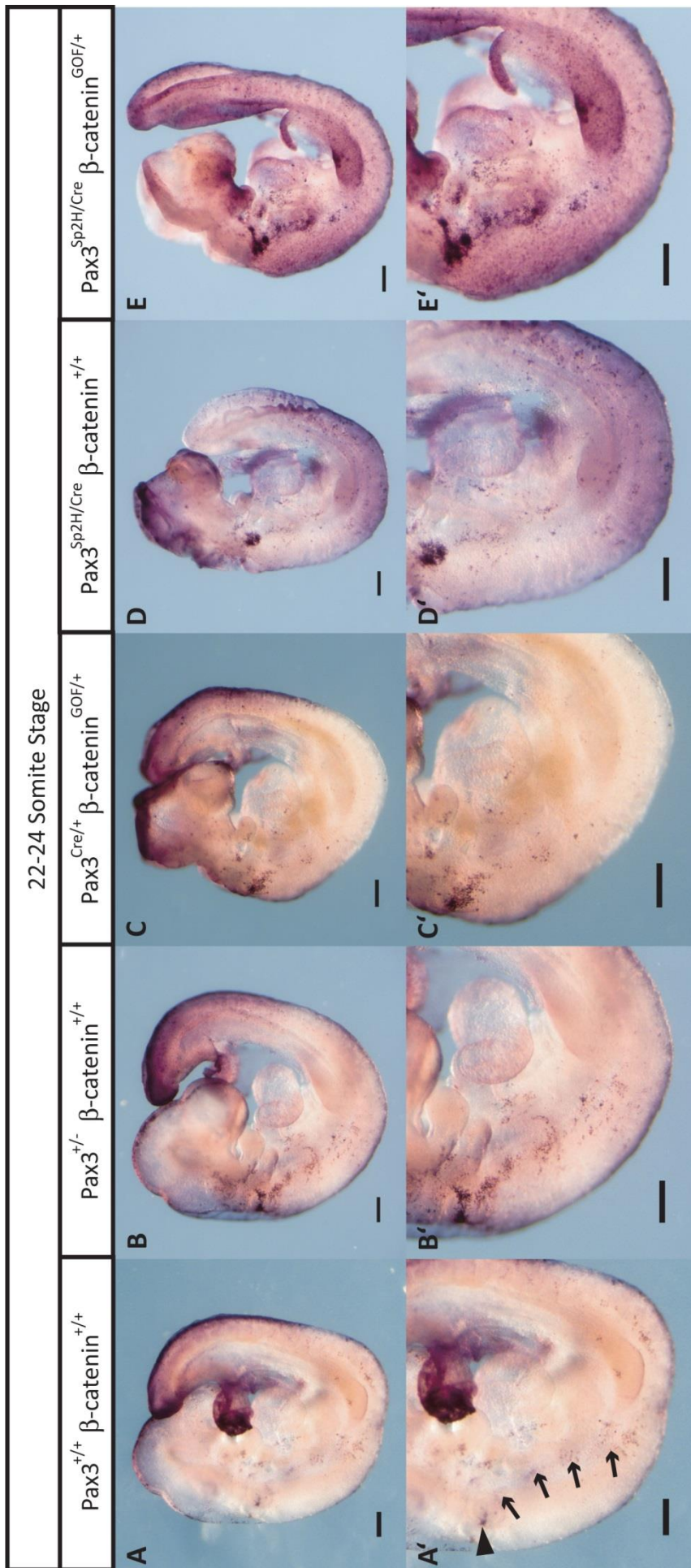


Figure 4.15: TUNEL assay of 27-29 somite stage embryos. Experimental litters were generated containing a mixture of genotypes through the cross $Pax3^{Sp2H/+} \beta\text{-catenin}^{GOF/+} \times Pax3^{Cre/+} \beta\text{-catenin}^{+/+}$. TUNEL staining was carried out on embryos of multiple genotypes. Scale bars represent 250 μm . **A'-E'** show zoomed in images of the spinal regions of **A-E** respectively. **F-J** show the rostral region of the forebrain.

$Pax3^{+/+} \beta\text{-catenin}^{+/+}$ (wild type; **A, A'** and **F**) and $Pax3^{+/-} \beta\text{-catenin}^{+/+}$ (**B, B'** and **G**) embryos show similar TUNEL staining patterns; well segmented apoptosis in the DRG (black arrowhead, **A'**), a stream of apoptotic cells in the migrating NC (arrows, **B'**), and a well-defined line of apoptotic cells in the midline of the forebrain NT (white arrowhead, **F**). The pattern of staining has common features between all stained embryos. However, the degree of staining was variable even between embryos of the same genotype.

$Pax3^{Cre/+} \beta\text{-catenin}^{GOF/+}$ (**C** and **C'**), $Pax3^{Sp2H/Cre} \beta\text{-catenin}^{+/+}$ (**D** and **D'**), and $Pax3^{Sp2H/Cre} \beta\text{-catenin}^{GOF/+}$ (**E** and **E'**) embryos all show wild type patterning of apoptosis in the migrating NC. $Pax3^{Cre/+} \beta\text{-catenin}^{GOF/+}$ and $Pax3^{Sp2H/Cre} \beta\text{-catenin}^{+/+}$ embryos also show wild type patterning of apoptosis in the DRG (although segmentation is less defined in the $Pax3^{Cre/+} \beta\text{-catenin}^{GOF/+}$ embryos), but $Pax3^{Sp2H/Cre} \beta\text{-catenin}^{GOF/+}$ embryos show a reduction in this region.

$Pax3^{Sp2H/Cre} \beta\text{-catenin}^{+/+}$ (**I**) embryos show a reduction in apoptosis in the midline of the forebrain NT, but it is still present. However $Pax3^{Cre/+} \beta\text{-catenin}^{GOF/+}$ (**H**) and $Pax3^{Sp2H/Cre} \beta\text{-catenin}^{GOF/+}$ (**J**) embryos lack apoptosis in the midline of the forebrain NT.

$Pax3^{+/+} \beta\text{-catenin}^{+/+}$; n = 2. $Pax3^{+/-} \beta\text{-catenin}^{+/+}$; n = 3. $Pax3^{Cre/+} \beta\text{-catenin}^{GOF/+}$; n = 2. $Pax3^{Sp2H/Cre} \beta\text{-catenin}^{+/+}$; n = 3. $Pax3^{Sp2H/Cre} \beta\text{-catenin}^{GOF/+}$; n = 2.

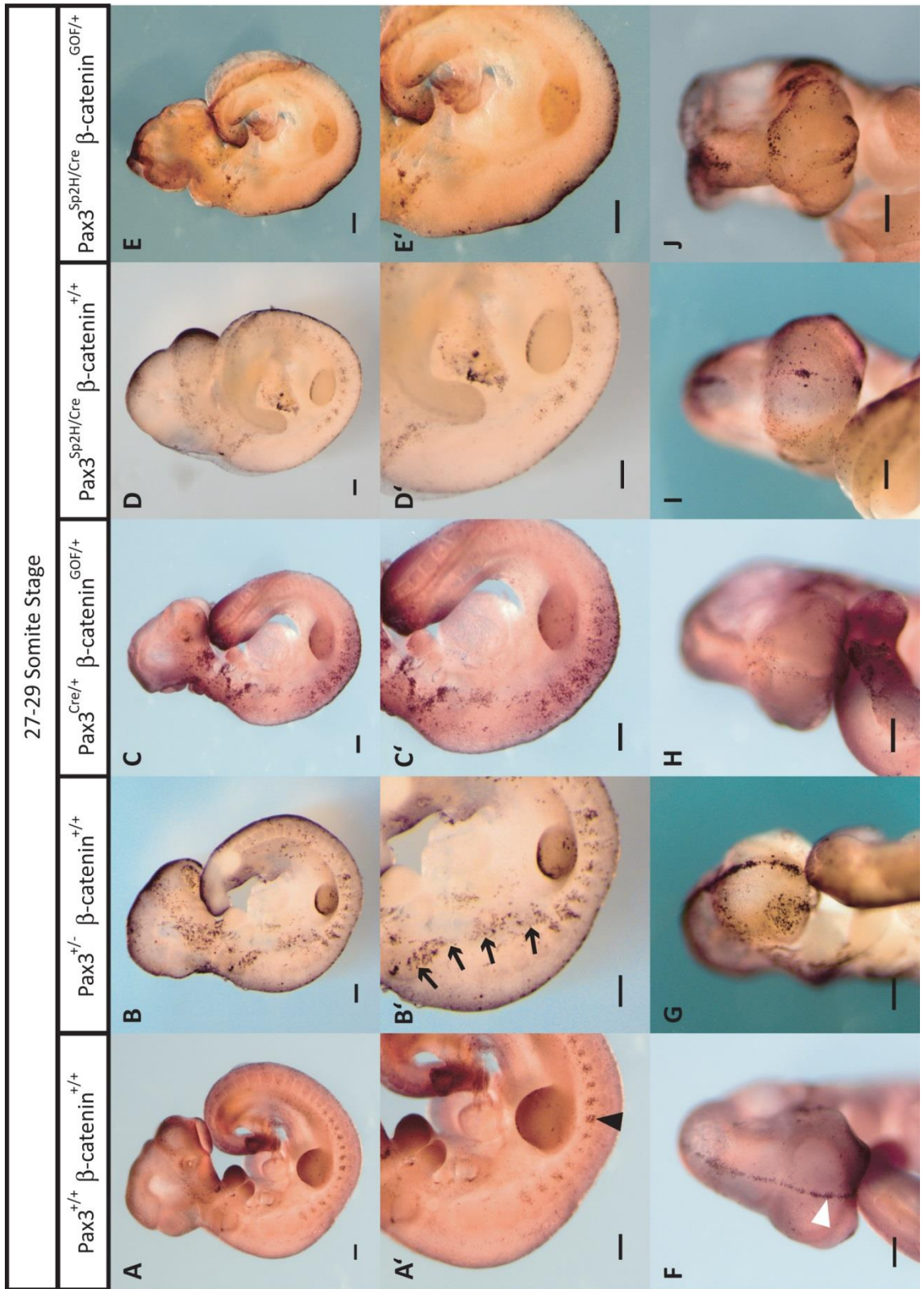
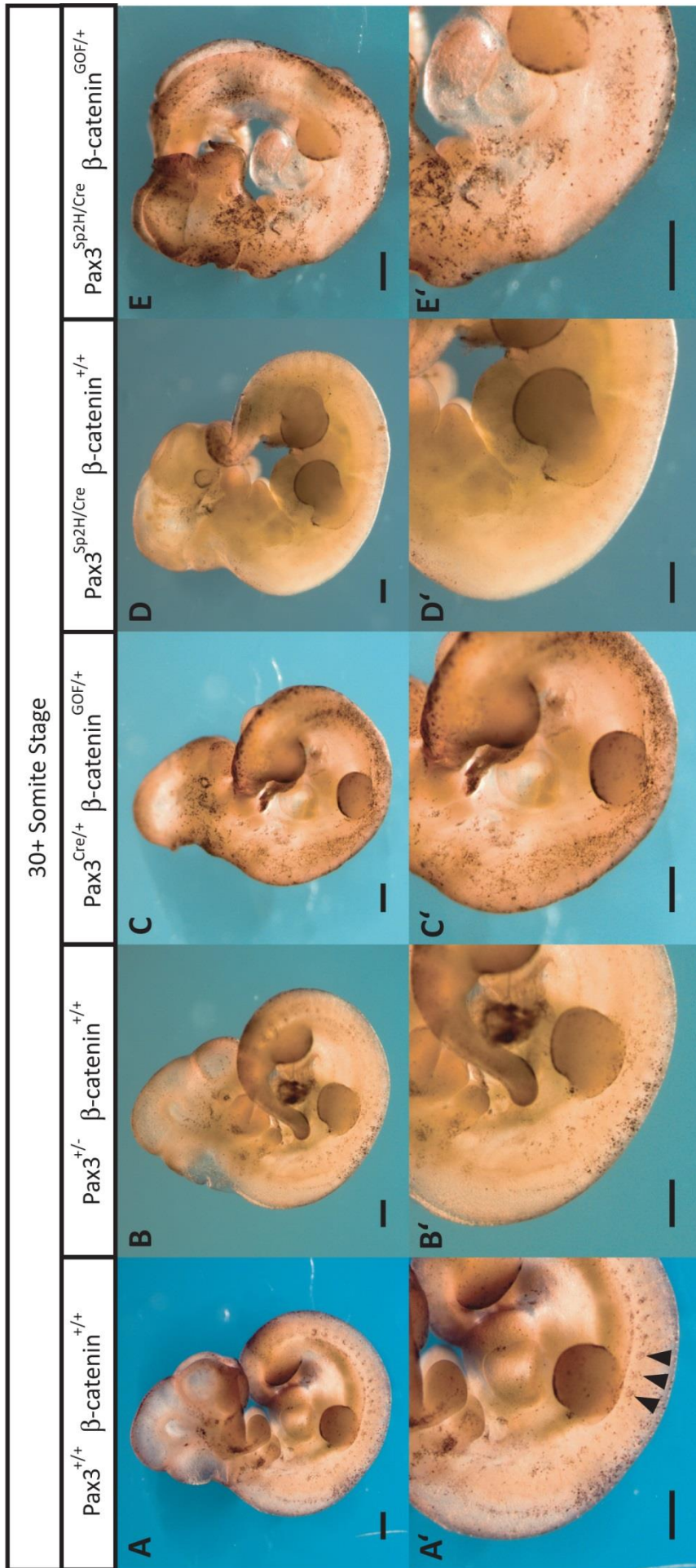


Figure 4.16: TUNEL assay of 30+ somite stage embryos. Experimental litters were generated containing a mixture of genotypes through the cross $Pax3^{Sp2H/+} \beta\text{-catenin}^{GOF/+}$ x $Pax3^{Cre/+} \beta\text{-catenin}^{+/+}$, which were collected at E10.5. TUNEL staining was carried out on embryos of multiple genotypes. Scale bars represent 500 μm . **A'-E'** show zoomed in images of the spinal regions of **A-E** respectively.

$Pax3^{+/+} \beta\text{-catenin}^{+/+}$ (**A** and **A'**) and $Pax3^{+/-} \beta\text{-catenin}^{+/+}$ (**B** and **B'**) embryos have a similar pattern of apoptosis, notably a segmented spinal pattern of apoptosis in the DRG (arrowheads, **A'**). $Pax3^{Sp2H/Cre} \beta\text{-catenin}^{+/+}$ embryos (**D** and **D'**) have a much reduced level of spinal apoptosis, although it is still visible in the caudal-most region. However, $Pax3^{Cre/+} \beta\text{-catenin}^{GOF/+}$ (**C** and **C'**) and $Pax3^{Sp2H/Cre} \beta\text{-catenin}^{GOF/+}$ (**E** and **E'**) embryos have normal-to-high levels of spinal apoptosis, which occurs with minimal or no segmentation.

$Pax3^{+/+} \beta\text{-catenin}^{+/+}$; n = 2. $Pax3^{+/-} \beta\text{-catenin}^{+/+}$; n = 2. $Pax3^{Cre/+} \beta\text{-catenin}^{GOF/+}$; n = 1. $Pax3^{Sp2H/Cre} \beta\text{-catenin}^{+/+}$; n = 2. $Pax3^{Sp2H/Cre} \beta\text{-catenin}^{GOF/+}$; n = 2.



Pax3^{Cre/+} *β-catenin*^{GOF/+} embryos show a largely wild type pattern of apoptosis at the 22-24 somite stage, but with possibly a small increase in apoptosis at the cervical-hindbrain boundary (**Figure 4.14**). However, at the 27-29 somite stage (**Figure 4.15**) the segmentation of apoptotic cells in the DRG begins to appear less defined. Furthermore, no apoptosis is seen in the midline of the forebrain NT. Apoptosis in the migrating NC appears to be normal. At the 30+ somite stage (**Figure 4.16**) the segmentation of the apoptotic DRG cells has reduced further, and overall apoptosis appears to be slightly increased when compared to both *Pax3*^{+/+} *β-catenin*^{+/+} and *Pax3*^{+/-} *β-catenin*^{+/+} embryos.

Apoptosis in *Pax3*^{Sp2H/Cre} *β-catenin*^{GOF/+} embryos is increased at the cervical-hindbrain boundary, and may be slightly increased overall at the 22-24 somite stage (**Figure 4.14**). At the 27-29 somite stage (**Figure 4.15**) apoptosis at the midline of the forebrain NT is absent. In addition, apoptosis in the DRG appears to be reduced compared to both *Pax3*^{+/+} *β-catenin*^{+/+} and *Pax3*^{Sp2H/Cre} *β-catenin*^{+/+} embryos. However, at the 30+ somite stage (**Figure 4.16**) apoptosis is increased in the DRG compared to *Pax3*^{+/+} *β-catenin*^{+/+} embryos, and very much compared to *Pax3*^{Sp2H/Cre} *β-catenin*^{+/+} embryos. Furthermore, the segmental pattern of apoptosis in the spinal region is lost.

A summary of the apoptosis data is given in **Table 4.4**.

4.1.7.3 β-catenin gain-of-function causes a slight decrease in neural crest specification

The gene *FoxD3* is an early marker for NC specification (Dottori et al., 2001). The expression pattern of *FoxD3* was studied through whole mount *in situ* hybridisation in embryos with and without β-catenin GOF at early stages of NC specification (**Figure 4.17**). The purpose of this is to determine whether β-catenin GOF affects the specification of the NC.

Embryos were analysed at the 7-9 and 10-12 somite stages, early in the specification of the NC, in order to observe the initial development of these cells. *Pax3*^{+/+} *β-catenin*^{+/+} and *Pax3*^{+/-} *β-catenin*^{+/+} embryos show similar *FoxD3* expression patterns. *Pax3*^{Cre/+} *β-catenin*^{GOF/+} embryos have a more broken pattern of *FoxD3* expression in the spinal region of the NT, suggesting that NC specification may not be continuous along the length of the NT. This is more apparent at the 7-9 somite stage than the 10-12 somite stage.

Pax3^{Sp2H/Cre} *β-catenin*^{+/+} and *Pax3*^{Sp2H/Cre} *β-catenin*^{GOF/+} embryos show similar patterns of *FoxD3* expression; expression in the cranial region and rhombomere 4 is unchanged from the wild type, but expression in the spinal NT is absent at both the 7-9 and 10-12 somite stages.

Genotype	Somite Stage	Change from <i>Pax3</i> ^{+/+} <i>β-catenin</i> ^{+/+} TUNEL Staining
<i>Pax3</i> ^{+/-} <i>β-catenin</i> ^{+/+}	22-24	None.
	27-29	None.
	30+	None.
<i>Pax3</i> ^{Cre/+} <i>β-catenin</i> ^{GOF/+}	22-24	Small increase at the cervical-hindbrain boundary.
	27-29	Reduced DRG segmentation. No apoptosis in the midline of the forebrain.
	30+	Reduced DRG segmentation. Slightly increased overall apoptosis.
<i>Pax3</i> ^{Sp2H/Cre} <i>β-catenin</i> ^{+/+}	22-24	None.
	27-29	Reduction at the midline of the forebrain.
	30+	Reduced.
<i>Pax3</i> ^{Sp2H/Cre} <i>β-catenin</i> ^{GOF/+}	22-24	Increased at the cervical-hindbrain boundary. Possibly slight overall increase.
	27-29	No apoptosis in the midline of the forebrain. Reduced apoptosis in the DRG.
	30+	Increased in the DRG. No segmentation in DRG.

Table 4.4: Summary of apoptosis data between the 22 and 30+ somite stages. The data given is a comparison to the pattern of TUNEL staining seen in *Pax3*^{+/+} *β-catenin*^{+/+} embryos at each given somite stage.

22-24 somite stage – n = 2 for each genotype.

27-29 somite stage – *β-catenin*^{+/+}: n = 2. *Pax3*^{+/-} *β-catenin*^{+/+}: n = 3. *Pax3*^{Cre/+} *β-catenin*^{GOF/+}: n = 2. *Pax3*^{Sp2H/Cre} *β-catenin*^{+/+}: n = 3. *Pax3*^{Sp2H/Cre} *β-catenin*^{GOF/+}: n = 2.

30+ somite stage – *Pax3*^{+/+} *β-catenin*^{+/+}: n = 2. *Pax3*^{+/-} *β-catenin*^{+/+}: n = 2. *Pax3*^{Cre/+} *β-catenin*^{GOF/+}: n = 1. *Pax3*^{Sp2H/Cre} *β-catenin*^{+/+}: n = 2. *Pax3*^{Sp2H/Cre} *β-catenin*^{GOF/+}: n = 2.

Figure 4.17: β -catenin gain-of-function slightly decreases spinal *FoxD3* expression in *Pax3* heterozygous embryos. Experimental litters were generated containing a mixture of genotypes through the cross *Pax3^{Sp2H/+} β -catenin^{GOF/+}* x *Pax3^{Cre/+} β -catenin^{+/+}*. Whole mount *in situ* hybridisation for *FoxD3* was carried out on embryos of multiple genotypes. The expression was studied at the 7-9 (A-E), and 10-12 (F-J) somite stages. Scale bars represent 250 μ m.

Pax3^{+/+} β -catenin^{+/+} embryos (A and F) show *FoxD3* expression in the midbrain (white arrowhead), rhombomere 4 (black arrowhead), and the spinal NT (black arrows). *Pax3^{+/-} β -catenin^{+/+}* embryos (B and G) show the same expression pattern.

Pax3^{Cre/+} β -catenin^{GOF/+} embryos (C and H) show a similar expression pattern, but the spinal NT expression appears to be a slightly broken line, in contrast to the strong, unbroken line seen in the wild type embryos (A and F). This difference is particularly noticeable in 7-9 somite stage embryos (C).

Both *Pax3^{Sp2H/Cre} β -catenin^{+/+}* and *Pax3^{Sp2H/Cre} β -catenin^{GOF/+}* embryos appear to have normal *FoxD3* expression in the cranial region and rhombomere 4. However, these embryos have no expression in the spinal NT at the 7-9 or 10-12 somite stages.

7-9 somite stage – *Pax3^{+/+} β -catenin^{+/+}*; n = 4. *Pax3^{+/-} β -catenin^{+/+}*; n = 2. *Pax3^{Cre/+} β -catenin^{+/+}*; n = 2. *Pax3^{Sp2H/Cre} β -catenin^{+/+}*; n = 2. *Pax3^{Sp2H/Cre} β -catenin^{GOF/+}*; n = 3.

10-12 somite stage – *Pax3^{+/+} β -catenin^{+/+}*; n = 4. *Pax3^{+/-} β -catenin^{+/+}*; n = 3. *Pax3^{Cre/+} β -catenin^{+/+}*; n = 3. *Pax3^{Sp2H/Cre} β -catenin^{+/+}*; n = 2. *Pax3^{Sp2H/Cre} β -catenin^{GOF/+}*; n = 2.

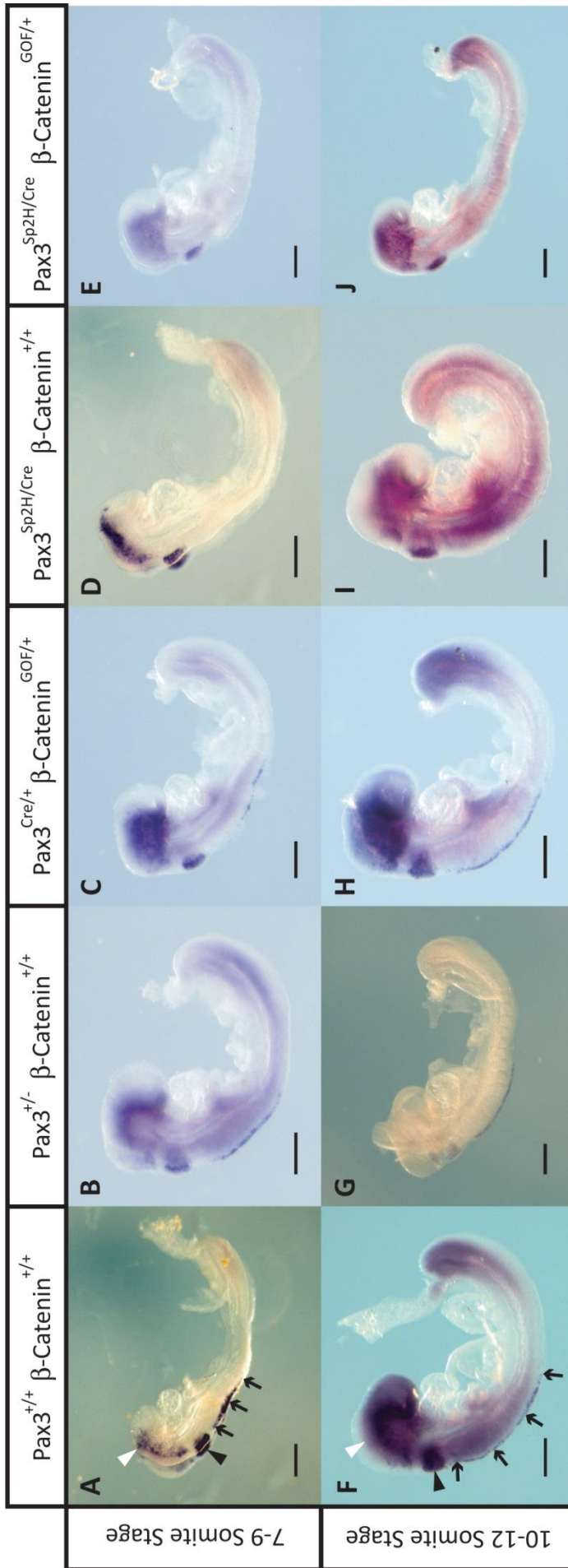


Figure 4.18: β -catenin gain-of-function does not affect expression of *Ngn2*. Experimental litters were generated containing a mixture of genotypes through the cross $Pax3^{Sp2H/+} \beta\text{-catenin}^{GOF/+} \times Pax3^{Cre/+} \beta\text{-catenin}^{+/+}$. Whole mount *in situ* hybridisation for *Ngn2* was carried out on 16-18 somite stage embryos of various genotypes. Sections were then taken of the caudal (A'-E') and cranial regions (A''-E'') of the NT. The dashed lines show the position of the NT in the sections. Scale bars represent 250 μ m.

$Pax3^{+/+} \beta\text{-catenin}^{+/+}$ embryos (A, A', and A'') shows expression of *Ngn2* in the mid region of the NT on the dorso-ventral axis. There is a small ventral region of no expression, and a larger dorsal region of low expression. Some expression is also seen in the lateral mesoderm directly adjacent to the dorsal region of the NT.

There appear to be no major differences in *Ngn2* expression between the genotypes at the 16-18 somite stage. The *Pax3* heterozygous and homozygous mutant embryos, with and without β -catenin GOF, appear to show very similar expression patterns of *Ngn2*.

$Pax3^{+/+} \beta\text{-catenin}^{+/+}$; n = 3. $Pax3^{Cre/+} \beta\text{-catenin}^{GOF/+}$; n = 2. $Pax3^{Sp2H/Cre} \beta\text{-catenin}^{GOF/+}$; n = 3. $Pax3^{Sp2H/Cre} \beta\text{-catenin}^{GOF/+}$; n = 3.

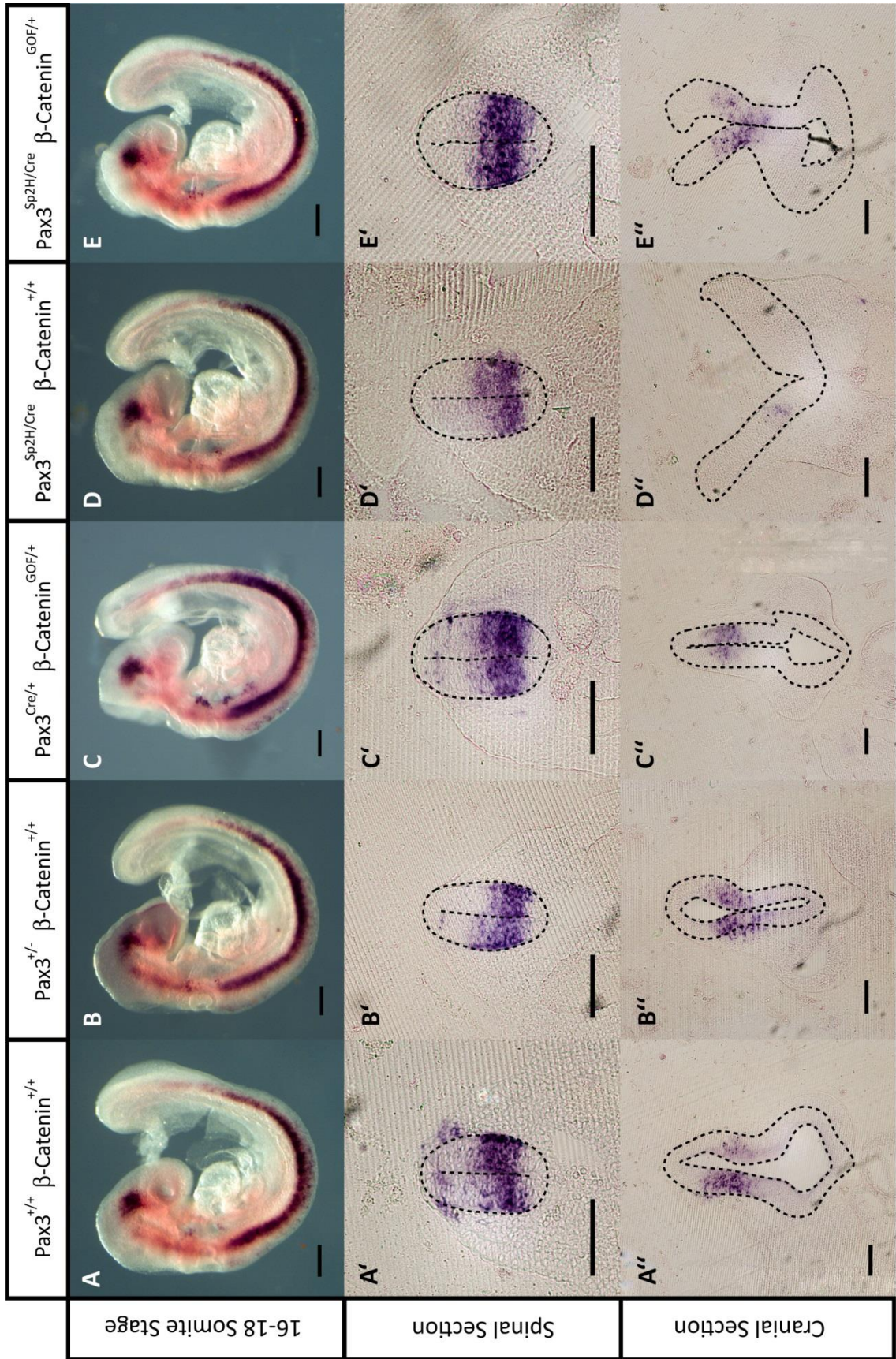


Figure 4.19: β -catenin gain-of-function reduces expression of *Brn3a* in the spinal region. Experimental litters were generated containing a mixture of genotypes through the cross *Pax3*^{Sp2H/+} β -catenin^{GOF/+} x *Pax3*^{Cre/+} β -catenin^{+/+}. *in situ* hybridisation for *Brn3a* was carried out on embryos of multiple genotypes. White scale bars represent 500 μ m, and black scale bars represent 100 μ m. **F'-J'** and **F''-J''** show transverse sections through 30+ somite stage embryos. **F'-J'** and **F''-J''** show cranial sections, and **F''-J''** show spinal sections. Dotted lines delineate the NT within sections.

Pax3^{+/+} β -catenin^{+/+} embryos at the 23-24 and 30+ somite stages (**A** and **F** respectively) show strong *Brn3a* expression in the NT (black arrowheads) and in the somites (white arrowheads), showing clearly defined segmentation. *Brn3a* expression appears to be expressed in the somites along the full length of the body in 23-24 somite stage embryos (**A**), but in 30+ somite stage embryos is reduced in the rostral-most somites and more strongly expressed in the caudal somites (**F**). *Brn3a* is expressed in approximately the dorsal half of the cranial NT (**F'**) and the dorsal third in the spinal NT (**F''**). Somitic *Brn3a* is clearly visible in the spinal region, and is expressed in a defined stripe in the dermomyotome (**F''**, arrows). *Brn3a* expression is *Pax3*^{+/-} β -catenin^{+/+} embryos (**B**, **G**, **G'** and **G''**) is identical to *Pax3*^{+/+} β -catenin^{+/+}.

Brn3a expression in 23-24 somite stage *Pax3*^{Sp2H/Cre} β -catenin^{+/+} embryos (**D**) appears to be reduced compared to *Pax3*^{+/+} β -catenin^{+/+} embryos. The staining is barely visible in the somites or the NT. Expression is slightly more visible in 30+ somite stage *Pax3*^{Sp2H/Cre} β -catenin^{+/+} embryos (**I**), but still appears to be reduced, particularly in the caudal NT and the somites, where staining is only faintly visible. Expression in the sections (**I'** and **I''**) corroborates these observations; the staining is present in the same regions as in *Pax3*^{+/+} β -catenin^{+/+} embryos, but appears much fainter.

Spinal NT expression of *Brn3a* appears to be reduced in *Pax3*^{Cre/+} β -catenin^{GOF/+} embryos at both the 23-24 somite stage (**C**) and the 30+ somite stage (**H**). The cranial region, however, appears to be less strongly affected. These results are verified by the sections; the cranial region (**H'**) shows *Brn3a* NT expression similar to *Pax3*^{+/+} β -catenin^{+/+} embryos, but the spinal section shows reduced NT expression (**H''**). *Brn3a* expression in the somites of *Pax3*^{Cre/+} β -catenin^{GOF/+} embryos appears similar to that in *Pax3*^{+/+} β -catenin^{+/+} embryos, or possibly slightly reduced (**C** and **H**). However, the sections (**H'** and **H''**) show that the somitic region of *Brn3a* expression is expanded ventrally compared to *Pax3*^{+/+} β -catenin^{+/+} embryos. There is an additional region of *Brn3a* expression in the cranial region of 23-24 somite stage *Pax3*^{Cre/+} β -catenin^{GOF/+} embryos, above the pharyngeal arches and into the forebrain (**C**, white asterisk). This aberrant expression appears to continue into 30+ somite stage (**H**).

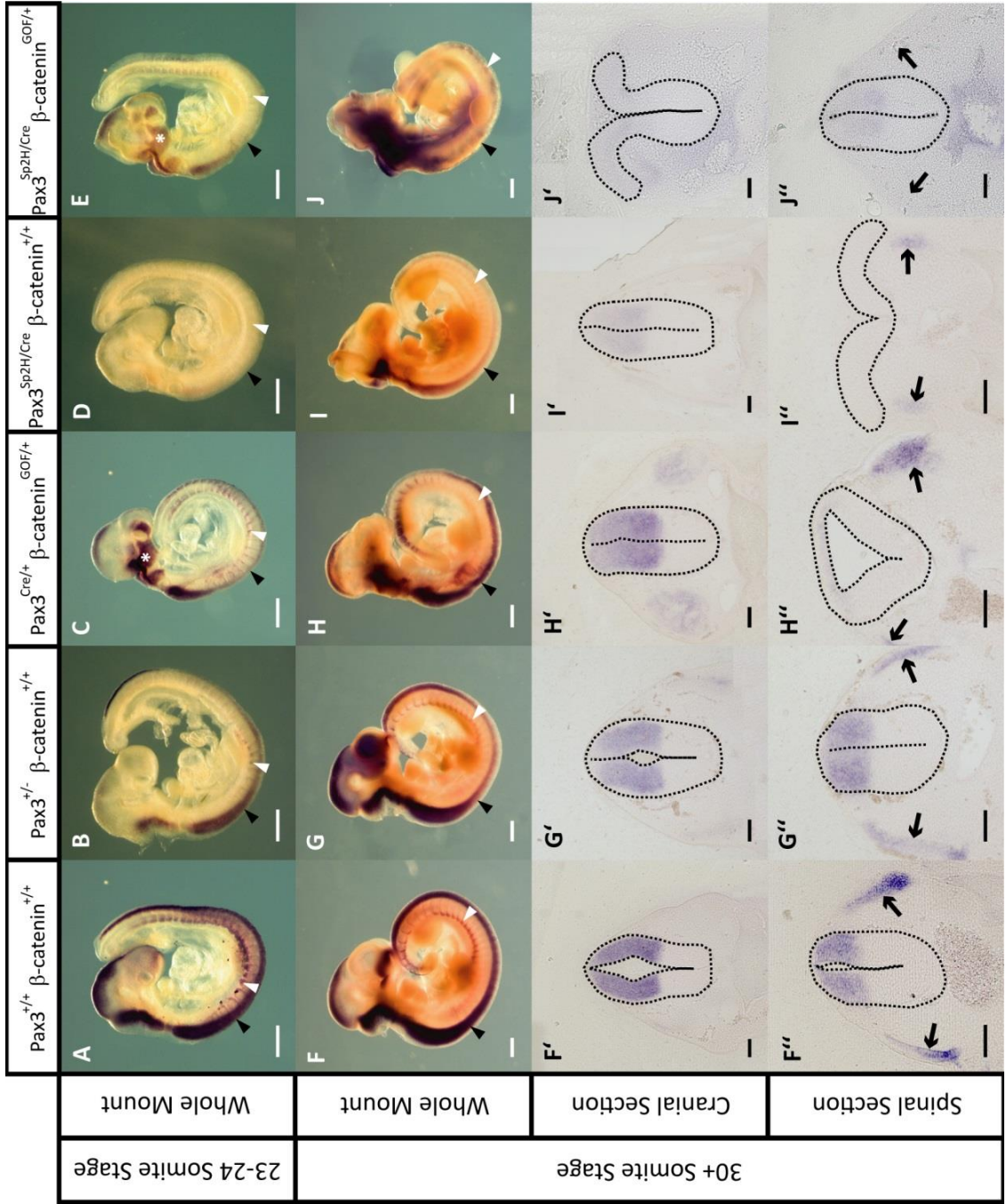


Figure 4.19: β-catenin gain-of-function reduces expression of *Brn3a* in the spinal region, continued.

Brn3a expression is greatly reduced in the spinal NT and somites of *Pax3^{Sp2H/Cre} β-catenin^{GOF/+}* embryos at 23-24 (E) and 30+ (J) somite stages. Spinal sections also show this (J''). The aberrant cranial expression seen in *Pax3^{Cre/+} β-catenin^{GOF/+}* embryos (C and H) is also present in *Pax3^{Sp2H/Cre} β-catenin^{GOF/+}* embryos (E and J). However, cranial sections (J') show that *Brn3a* expression is not present in the NT.

23-24 somite stage: *Pax3^{+/+} β-catenin^{+/+}*; n = 3.
Pax3^{+/-} β-catenin^{+/+}; n = 2. *Pax3^{Cre/+} β-catenin^{GOF/+}*; n = 2. *Pax3^{Sp2H/Cre} β-catenin^{+/+}*; n = 1.
Pax3^{Sp2H/Cre} β-catenin^{GOF/+}; n = 1.

30+ somite stage: *Pax3^{+/+} β-catenin^{+/+}*; n = 4.
Pax3^{+/-} β-catenin^{+/+}; n = 2. *Pax3^{Cre/+} β-catenin^{GOF/+}*; n = 2. *Pax3^{Sp2H/Cre} β-catenin^{+/+}*; n = 2.
Pax3^{Sp2H/Cre} β-catenin^{GOF/+}; n = 3.

4.1.7.4 Development of the peripheral nervous system

Expression of the genes *Ngn2* and *Brn3a* were used to study the development of the PNS. *Ngn2* is a proneural gene, and *Brn3a* is expressed in sensory neurons (Ninkina et al., 1993; Sommer et al., 1996). *Ngn2* expression was studied early in the development of the PNS, at the 16-18 somite stage (**Figure 4.18**). β -catenin GOF appears to have no effect on *Ngn2* expression at this stage.

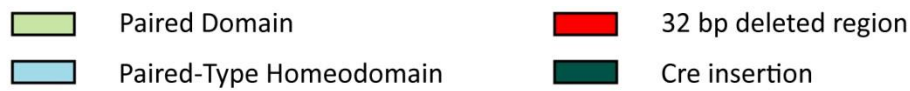
Brn3a expression was studied at a slightly later stage of PNS development, at the 23-24 and 30+ somite stages (**Figure 4.19**). *Pax3* mutation appears to cause a general reduction in *Brn3a* expression. However, β -catenin GOF appears to slightly reduce spinal NT *Brn3a* expression, but expand the region of cranial expression beyond the NT, such that staining was evident above the pharyngeal arches and in the forebrain. Additionally, β -catenin GOF expands the region of *Brn3a* expression in the somites ventrally, below the dermomyotome and into the sclerotome.

4.1.8 β -catenin gain-of-function does not affect *Pax3* expression

Evidence has suggested that canonical Wnt signalling may act upstream of *Pax3* signalling (Zhao et al., 2014). Therefore, the expression level of *Pax3* was studied to test whether it is influenced by β -catenin GOF. RT-qPCR was carried out using two different *Pax3* primers. Only *Pax3*^{Cre/+} β -catenin^{+/+} embryos were used as *Pax3* heterozygotes to eliminate the chance of error caused by possible differences in expression between the *Pax3*^{Cre} and *Pax3*^{Sp2H} alleles, and because the primer pairs used are only able to detect one of the two alleles.

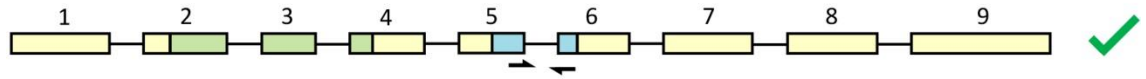
Pax3 primer pair 1 is positioned to overlap the 32bp region which is deleted in exon 5 of the *Pax3*^{Sp2H} allele (**Figure 4.20A-C**), so it detects *Pax3*⁺ and *Pax3*^{Cre}, but not *Pax3*^{Sp2H}. This primer pair detected no significant difference in *Pax3* expression between *Pax3*^{Cre/+} β -catenin^{+/+} and *Pax3*^{Cre/+} β -catenin^{GOF/+} embryos, or between *Pax3*^{Sp2H/Cre} β -catenin^{+/+} and *Pax3*^{Sp2H/Cre} β -catenin^{GOF/+} embryos (**Figure 4.21A**).

Pax3 primer 2 is positioned to amplify the region from exon 1 to exon 2 of *Pax3*, with the forward primer binding in exon 1, and the reverse primer in exon 2 (**Figure 4.20D-F**). Therefore it detects *Pax3*⁺ and *Pax3*^{Sp2H}, but not *Pax3*^{Cre}. This primer pair detected no significant difference in *Pax3* expression between *Pax3*^{Cre/+} β -catenin^{+/+} and *Pax3*^{Cre/+} β -catenin^{GOF/+} embryos, or between *Pax3*^{Sp2H/Cre} β -catenin^{+/+} and *Pax3*^{Sp2H/Cre} β -catenin^{GOF/+} embryos (**Figure 4.21B**).

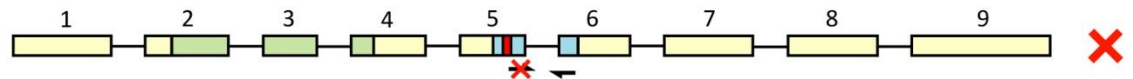


Primer Pair 1

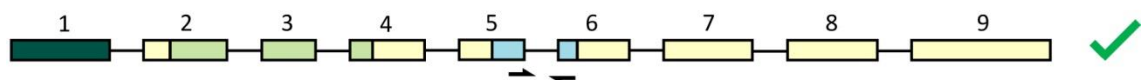
A *Pax3* Gene



B *Sp2H* Allele

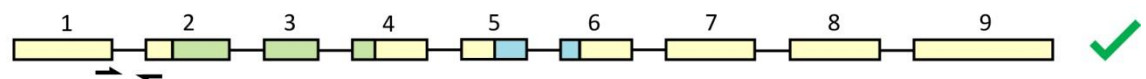


C *Pax3-Cre* Allele

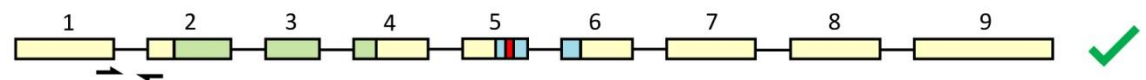


Primer Pair 2

D *Pax3* Gene



E *Sp2H* Allele



F *Pax3-Cre* Allele

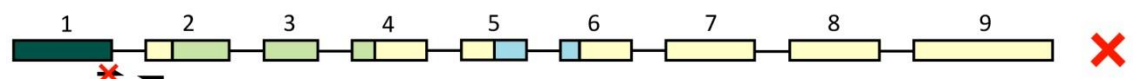


Figure 4.20: Positions of primer pairs 1 and 2 within the *Pax3* gene. The positions of the primer pairs are demonstrated by half arrows in the *Pax3*⁺ (A and D), *Pax3*^{Sp2H} (B and E) and *Pax3*^{Cre} (C and F) alleles.

Amplification by primer pair 1 occurs in the *Pax3*⁺ (A) and *Pax3*^{Cre} (C) alleles, but not the *Pax3*^{Sp2H} allele (B) as the forward primer binding site is positioned in the deleted region. Amplification by primer pair 2 occurs in the *Pax3*⁺ (D) and *Pax3*^{Sp2H} (E) alleles, but not the *Pax3*^{Cre} allele (F) as the forward primer binding site is positioned in exon 1, which is replaced by a Cre recombinase gene in this allele.

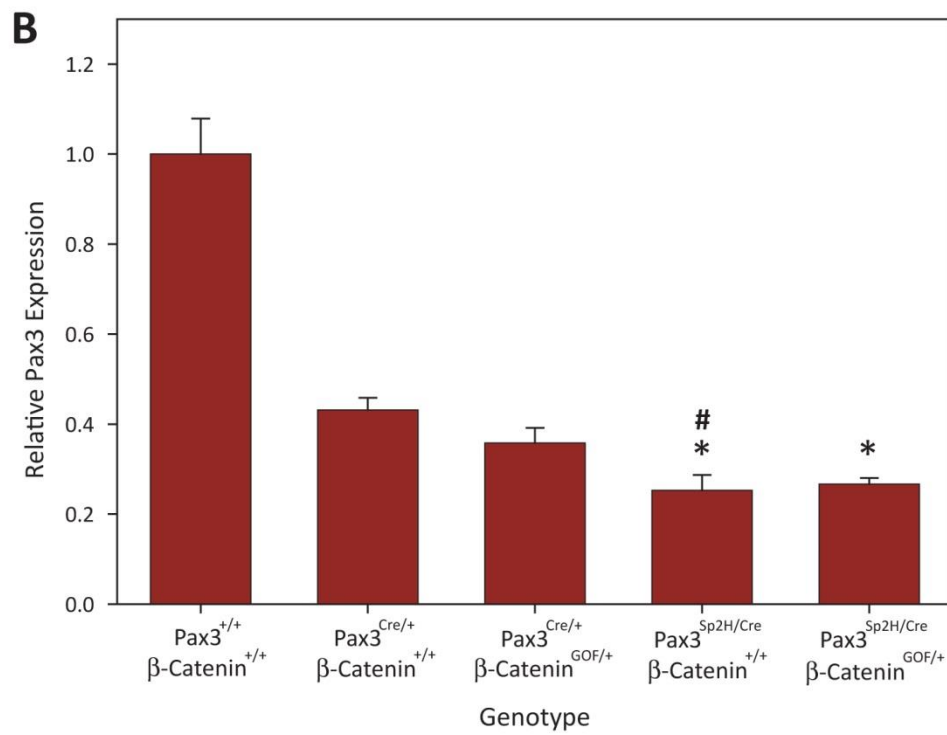
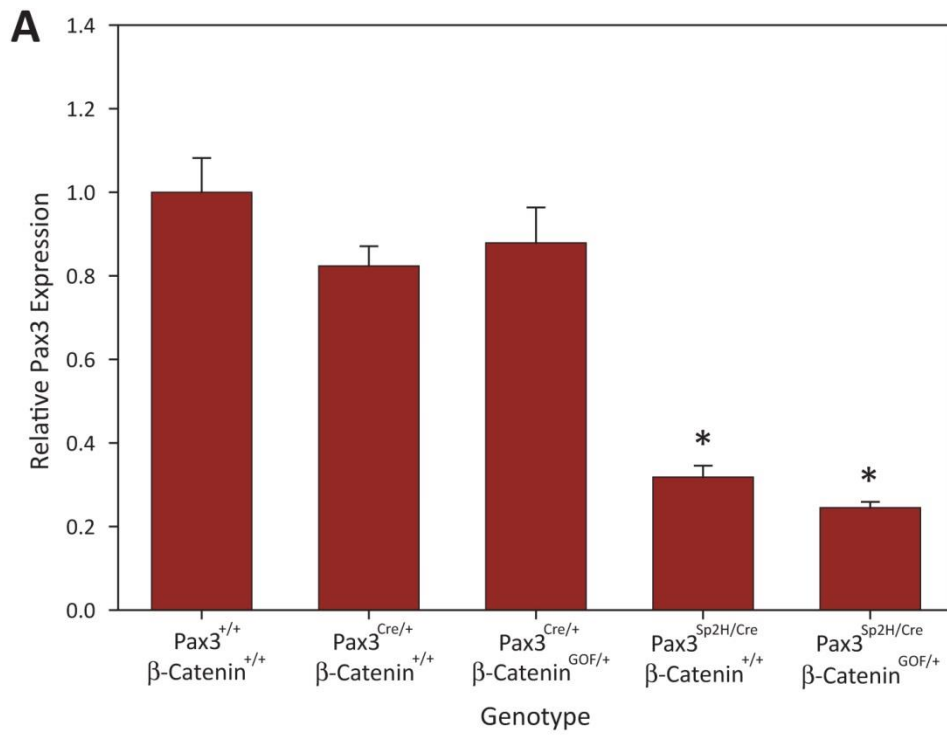
Figure 4.21: β -catenin gain-of-function does not affect Pax3 expression levels. Experimental litters were generated containing a mixture of genotypes through the cross $Pax3^{Sp2H/+} \beta\text{-catenin}^{GOF/+}$ x $Pax3^{Cre/+} \beta\text{-catenin}^{+/+}$. RT-qPCR was carried out on embryos of multiple genotypes at the 23-24 somite stage. * indicates significant difference from $Pax3^{+/+} \beta\text{-catenin}^{+/+}$. # indicates significant difference from $Pax3^{Cre/+} \beta\text{-catenin}^{+/+}$.

Graph **A** shows RT-qPCR results using Pax3 primer pair 1. This primer pair detects Pax3⁺ and Pax3^{Cre}, but not Pax3^{Sp2H}. A significant reduction in Pax3 expression is seen between $Pax3^{+/+} \beta\text{-catenin}^{+/+}$ and $Pax3^{Sp2H/Cre} \beta\text{-catenin}^{+/+}$ embryos, and between $Pax3^{+/+} \beta\text{-catenin}^{+/+}$ and $Pax3^{Sp2H/Cre} \beta\text{-catenin}^{GOF/+}$ embryos. However, no significant differences are seen between $Pax3^{+/-} \beta\text{-catenin}^{+/+}$ and $Pax3^{Cre/+} \beta\text{-catenin}^{GOF/+}$ embryos, or between $Pax3^{Sp2H/Cre} \beta\text{-catenin}^{+/+}$ and $Pax3^{Sp2H/Cre} \beta\text{-catenin}^{GOF/+}$ embryos.

Graph **B** shows RT-qPCR results using Pax3 primer pair 2. This primer pair detects Pax3⁺ and Pax3^{Sp2H}, but not Pax3^{Cre}. A significant reduction in Pax3 expression is seen between $Pax3^{+/+} \beta\text{-catenin}^{+/+}$ and both $Pax3^{Cre/+} \beta\text{-catenin}^{+/+}$ and $Pax3^{Sp2H/Cre} \beta\text{-catenin}^{+/+}$ embryos. However, no significant differences are seen between $Pax3^{+/-} \beta\text{-catenin}^{+/+}$ and $Pax3^{Cre/+} \beta\text{-catenin}^{GOF/+}$ embryos, or between $Pax3^{Sp2H/Cre} \beta\text{-catenin}^{+/+}$ and $Pax3^{Sp2H/Cre} \beta\text{-catenin}^{GOF/+}$ embryos. Additionally, Pax3 expression is significantly reduced in $Pax3^{Sp2H/Cre} \beta\text{-catenin}^{+/+}$ embryos compared to $Pax3^{Cre/+} \beta\text{-catenin}^{+/+}$ embryos.

*/# p < 0.05. Significance compared to $Pax3^{+/+} \beta\text{-catenin}^{+/+}$ was determined using one way ANOVA followed by the Holm Sidak test (**A**), or by one way ANOVA on ranks followed by Dunn's test (**B**). Pairwise significance was determined using the t-test. Only significance between relevant data is shown. Error bars show standard error.

For both **A** and **B** – $Pax3^{+/+} \beta\text{-catenin}^{+/+}$: n = 4. $Pax3^{Cre/+} \beta\text{-catenin}^{+/+}$: n = 3. $Pax3^{Cre/+} \beta\text{-catenin}^{GOF/+}$: n = 3. $Pax3^{Sp2H/Cre} \beta\text{-catenin}^{+/+}$: n = 4. $Pax3^{Sp2H/Cre} \beta\text{-catenin}^{GOF/+}$: n = 3.



4.2 Discussion

4.2.1 The β -catenin gain-of-function allele

The β -catenin GOF allele used in this research was first developed and described by the Taketo lab (Harada et al., 1999).

β -catenin is known to play a role in adherens junctions in addition to canonical Wnt signalling. Therefore it is possible that the mutation affects both functions, and not just the canonical Wnt signalling pathway. In the original paper describing this mutation (Harada et al., 1999) this is mentioned as a possibility, although it is also stated that the mutation does not appear to affect the interaction with adherens junctions. However, there remains a possibility that some of the effects of the mutation described in this thesis could be due to alterations in the adherens junctions. This could be further examined through study of the adherens junctions themselves in tissues affected by the mutation (i.e. *Pax3*-expressing tissues) in the different genotypes. For example, use of antibodies against components of the adherens junction, such as α -catenin, γ -catenin or E-cadherin could provide some insight into the integrity and density of adherens junctions within mutant tissue, including the neural tube.

For the purpose of this thesis several genotypes were pooled during analysis (see introduction to **Chapter 4 Results**, section 4.1). These pooled genotypes contained functionally equivalent combinations of alleles, and provided higher numbers of embryos for experiments and analysis. However, genotypes would have ideally been kept separate, as there is a chance that differences in the mutations could cause differences in the results. Analysis of the pooled genotypes showed no significant differences in the frequencies of spina bifida and exencephaly, but this does not completely rule out the possibility of differences between the genotypes, especially as sample numbers were often low.

As an example of potential differences, previous publications report different frequencies of exencephaly in *Pax3*^{Cre/Cre} and *Pax3*^{Sp2H/Sp2H} embryos, despite both mutations resulting in functionally null Pax3 protein; *Pax3*^{Cre/Cre} embryos have a frequency of 20-30% exencephaly, (Nick Greene, unpublished observations) compared to around 80% in *Pax3*^{Sp2H/Sp2H} embryos (Fleming and Copp, 2000). However, it has also been found that the frequency of exencephaly within *Pax3*^{Sp2H/Sp2H} embryos may vary considerably with time, despite all other factors being equal (Greene et al., 2009). Therefore, a certain amount of variability, even within a strain, is to be expected.

An additional issue is that the *Pax3*^{Cre} allele and the *Pax3*^{Sp2H} allele are carried on different genetic backgrounds. The effect of this during development is discussed in more detail in

section **1.2.2.1**. The combination of genetic backgrounds in the cross could create variations in modifier genes in the offspring, and it is possible that this could affect the results of the study. Ideally, the $Pax3^{Sp2H}$ allele would have been backcrossed onto the C57BL/6 background, which is the background of the $Pax3^{Cre}$ allele. Analysis of the embryos throughout the experiments described in this chapter showed fairly consistent results, which suggests that the difference in genetic background is not affecting the results to a large degree. However, this caveat should be taken into consideration for the results. Both alleles were used in the cross because, although the frequency of spina bifida was close to 100% in both genotypes, $Pax3^{Sp2H/Sp2H}$ embryos have a higher frequency of exencephaly than $Pax3^{Cre/Cre}$ embryos. At least one copy of the $Pax3^{Cre}$ allele was necessary to flox conditional alleles in the experiments, but combining this allele with the $Pax3^{Sp2H}$ allele increased the rate of exencephaly; $Pax3^{Sp2H/Cre}$ embryos have a higher frequency of exencephaly than $Pax3^{Cre/Cre}$ embryos. This made it easier and more efficient to study the development of exencephaly in the experiments.

4.2.2 β -catenin gain-of-function and neural tube defects

It was discussed in **Chapter 3** that Sp^{2H}/Sp^{2H} embryos exhibit a reduction in proliferation in the neural tube, and that this may be the cause of NTDs in these embryos. Evidence suggests a potential link between Pax3 and canonical Wnt signalling (see section **1.4.7**). Canonical Wnt signalling is associated with the maintenance of a proliferative, multipotent state (Megason and McMahon, 2002), and so it was hypothesised that an increase in canonical Wnt signalling levels may rescue NTDs in Sp^{2H}/Sp^{2H} embryos. However, this was not found to be the case.

β -catenin GOF appears to greatly affect the closure of the cranial NT. The resulting increase in canonical Wnt signalling causes a visible difference in the cranial neural folds of $Pax3^{Sp2H/Cre}$ β -catenin^{GOF/+} embryos compared to $Pax3^{Sp2H/Cre}$ β -catenin^{+/+} embryos (**Figure 4.8**). β -catenin GOF induced by Sox-1^{Cre} does not appear to increase NTDs to the same degree as when induced by Pax3^{Cre} (Sox1 is reported to be expressed in the NT, although this could be confirmed in the experimental mice through *in situ* hybridisation). The $Pax3^{+/+}$ β -catenin^{GOF/+} Sox-1^{Cre/+} genotype causes exencephaly in 25% of embryos (**Figure 4.5**), $Pax3^{Sp2H/Cre}$ β -catenin^{+/+} in 59% of embryos, and $Pax3^{Sp2H/Cre}$ β -catenin^{GOF/+} in 99% of embryos (**Figure 4.7**). In addition, β -catenin GOF induces exencephaly in Pax3 heterozygous embryos, as $Pax3^{+/-}$ β -catenin^{+/+} embryos have exencephaly at a rate of 10%, whereas $Pax3^{Cre/+}$ β -catenin^{GOF/+} embryos have exencephaly at a rate of 80% (**Figure 4.7**). Therefore, it is likely that the increase in the frequency of exencephaly is due to genetic interaction between the Pax3 and canonical Wnt signalling pathways, rather than an additive effect of the phenotypes.

Previously, neuronal differentiation and proliferation in the NT were studied in *Spotch* mice, as *Pax3* mutation was reported to affect the proliferation-differentiation balance (Keller-Peck and Mullen, 1997). Canonical Wnt signalling is reported as having a similar role (Miyake et al., 2012; Xie et al., 2011), so it is possible that the effects of β -catenin GOF are mediated through these same processes. It would be expected that β -catenin GOF-mediated upregulation of canonical Wnt signalling could therefore increase proliferation and decrease differentiation, as this effect has been reported previously (Miyake et al., 2012; Xie et al., 2011). However, spina bifida, and potentially exencephaly in Sp^{2H}/Sp^{2H} embryos is likely to be caused by a reduction in proliferation in the NT (**Chapter 3**), and β -catenin GOF worsens NTDs in *Pax3* mutant embryos (**Figures 4.7** and **4.8**). Therefore, it appears likely that β -catenin GOF is not rescuing the proliferation defect in the NTs of *Pax3* mutant embryos, but may still affect it.

Proliferation was studied in the *Pax3*-expressing dorsal regions of the cranial NT. Results were compared between $Pax3^{+/-} \beta\text{-catenin}^{+/+}$ and $Pax3^{Cre/+} \beta\text{-catenin}^{GOF/+}$ embryos, and between $Pax3^{Sp2H/Cre} \beta\text{-catenin}^{+/+}$ and $Pax3^{Sp2H/Cre} \beta\text{-catenin}^{GOF/+}$ embryos in order to determine how β -catenin GOF affects NT proliferation (**Figure 4.9**). However, no significant differences in the rates of proliferation were seen between any of the genotypes, including $Pax3^{+/-} \beta\text{-catenin}^{+/+}$ and $Pax3^{Sp2H/Cre} \beta\text{-catenin}^{+/+}$ embryos.

A significant difference in proliferation in the dorsal spinal NT was observed when comparing $+/+$ and Sp^{2H}/Sp^{2H} embryos, as the dorso-ventral gradient of proliferation is lost in Sp^{2H}/Sp^{2H} embryos at the 14-15 somite stage (see section **3.1.2.4**, **Figure 3.11**). Therefore, it is possible that a similar difference exists between genotypes in the cranial region, but that higher numbers of samples would be needed to detect differences in the rate of proliferation between genotypes. Alternatively, the differences between the results could be due to differences in the genetic background of the mice used in the study – embryos used in the study described in section **3.1.2.4** were generated through a $Sp^{2H}/+ \times Sp^{2H}/+$ cross, and were on a CBA genetic background. On the other hand, embryos used in the cranial proliferation study described in this chapter were generating using the cross $Pax3^{Sp2H/+} \beta\text{-catenin}^{GOF/+} \times Pax3^{Cre/+} \beta\text{-catenin}^{+/+}$, and were on a C57 genetic background. The different genetic backgrounds may affect the rate of proliferation observed in mutant embryos. It is also possible that the lack of difference between proliferation in $Pax3^{+/-} \beta\text{-catenin}^{+/+}$ and $Pax3^{Sp2H/Cre} \beta\text{-catenin}^{+/+}$ embryos suggests that although proliferation is abnormal and may underlie NTDs in the spinal NT, it might not be a factor in the cranial region.

On the other hand, β -catenin GOF has only a minor exacerbating effect on the closure of the PNP in $Pax3^{+/-}$ or $Pax3^{Sp2H/Cre}$ embryos. β -catenin GOF causes a significant increase in the size of

the PNP when compared to embryos of equivalent *Pax3* genotype but without β -catenin GOF (**Figure 4.6**). However, this difference does not occur until a slightly later stage of NT closure – the 18-19 or 20-21 somite stages for *Pax3*^{Sp2H/Cre} and *Pax3*^{+/-} respectively – when PNP closure is already delayed in embryos carrying the *Pax3* mutation compared with wild type embryos. Additionally, there are no significant differences in the frequency of spina bifida when comparing *Pax3*^{+/-} *β -catenin*^{+/+} to *Pax3*^{Cre/+} *β -catenin*^{GOF/+} embryos, and *Pax3*^{Sp2H/Cre} *β -catenin*^{+/+} to *Pax3*^{Sp2H/Cre} *β -catenin*^{GOF/+} embryos (**Figure 4.7**). This suggests that β -catenin GOF may delay closure, but does not prevent it from occurring.

Premature neuronal differentiation is not present in the spinal NT of *Sp*^{2H}/*Sp*^{2H} embryos. However, this does not preclude the phenotype being present in embryos with β -catenin GOF, and potentially contributing to NTD development. Nonetheless, no significant differences were seen in the level of neuronal differentiation between genotypes (**Figure 4.10 and 4.11**). Therefore it appears unlikely that β -catenin GOF induces neuronal differentiation, and such a mechanism is unlikely to cause spinal NTDs.

The data in **Tables 4.2 and 4.3** suggest that *Pax3*^{Sp2H/Cre} *β -catenin*^{GOF/+} embryos have higher numbers of cells in cross-sections of the NT compared to *Pax3*^{+/+} *β -catenin*^{+/+} embryos. However, since this is also apparent in *Pax3*^{Sp2H/Cre} *β -catenin*^{+/+} embryos, which do not carry the β -catenin^{GOF} allele, this is unlikely to be due to abnormalities in canonical Wnt signalling. It is possible that this is an artefact of sectioning, and differences in the angle of sectioning affect the size of the NT and number of cells observed in each section. No differences were observed in mitotic index in the cranial region between genotypes. Nonetheless, the antibody used to calculate mitotic index – against phospho histone h3 – labels cells in G2/M phase. This indicates that the proportion of cells in G2/M phase is unchanged in mutant embryos. However, it is possible that proliferation could be increased by a reduction in the length of S or G2 phase during the cell cycle. This could be studied using immunohistochemistry with both anti-phospho histone H3 and the antibody Ki-67, which labels cells in all active phases of the cell cycle. Therefore, cells in S or G2 phase would be Ki-67 positive, but phospho histone H3 negative. It is also possible that proliferation was increased in the mutant embryos prior to the stage of study, but had reduced to normal levels by the 13-15 somite stage. Proliferation studies using embryos from earlier stages of development, such as the 9-11 somite stage, could provide more information about this.

4.2.3 β -catenin gain-of-function and neural crest defects

Although this research initially focussed on the development of NTDs, a secondary aim was to determine whether there may be an interaction between Pax3 and canonical Wnt signalling.

Given the observed effects of β -catenin GOF on NTDs, there are two possible explanations; firstly, β -catenin GOF in the NT may exacerbate the deleterious effect of *Pax3* mutation. This could be due to interaction in a downstream mechanism, or possibly more than one, which summate to give the observed phenotype. Secondly, there may be a more direct interaction in which of the pathways is able to influence the activity of the other. To aid in determining the nature of the interaction, the effect of β -catenin GOF was studied in another *Pax3*-positive tissue in addition to the NT – the NC.

A more severe phenotype was observed in the NTs of *Pax3*^{Sp2H/Cre} *β -catenin*^{GOF/+} embryos when compared to *Pax3*^{Sp2H/Cre} *β -catenin*^{+/+} embryos, and in *Pax3*^{Cre/+} *β -catenin*^{GOF/+} embryos when compared to *Pax3*^{+/-} *β -catenin*^{+/+} embryos (**Figures 4.7** and **4.8**). Therefore, the NC were studied to determine what effect *Pax3* and β -catenin mutations have on the developing NC and the NC derivatives in compound mutant embryos.

ErbB3 was used as a marker for NC, and its expression was studied in embryos of different genotypes between 18 and 30+ somites (**Figure 4.12**). The Tuj1 antibody was also used as a neuronal marker in embryos of a similar somite stage to study the effect of β -catenin GOF on the development of the NC-derived PNS (**Figure 4.13**). In combination these assays provide information about the neuronal specification of the NC.

Pax3^{Sp2H/Cre} *β -catenin*^{+/+} embryos show weaker *ErbB3* expression. However, expression is present in all the appropriate tissues, and rudimentary DRG are present. This result is corroborated by Tuj1 immunohistochemistry. However, when comparing *Pax3*^{+/-} *β -catenin*^{+/+} to *Pax3*^{Cre/+} *β -catenin*^{GOF/+} embryos, and *Pax3*^{Sp2H/Cre} *β -catenin*^{+/+} to *Pax3*^{Sp2H/Cre} *β -catenin*^{GOF/+} embryos, differences are apparent, which are due to β -catenin GOF.

Both *Pax3*^{Cre/+} *β -catenin*^{GOF/+} and *Pax3*^{Sp2H/Cre} *β -catenin*^{GOF/+} embryos show some *ErbB3* expression in developing DRG until the 24-26 somite stage. However, in *Pax3*^{Sp2H/Cre} *β -catenin*^{GOF/+} embryos the segmental pattern of expression is less well defined, and expression is much fainter than in wild type embryos. Tuj1 immunohistochemistry suggests that neuronal differentiation in the spinal region at this stage resembles wild type, although the vagus nerve is less developed in both genotypes. Unlike the other genotypes, at the 30+ somite stage *ErbB3* expression is no longer visible in the spinal region of *Pax3*^{Cre/+} *β -catenin*^{GOF/+} and *Pax3*^{Sp2H/Cre} *β -catenin*^{GOF/+} embryos. Tuj1 immunohistochemistry shows that some neurons differentiate in this region, but are less numerous than in wild types, and segmentation of the DRG is less clear. Additionally, these genotypes continue to show abnormalities in the developing vagus nerve, and absent expression of *ErbB3* in the trigeminal ganglia. Evidence suggests that these abnormalities are due to β -catenin GOF, rather than the *Pax3* mutation alone. However, the

phenotype of $Pax3^{Sp2H/Cre} \beta\text{-catenin}^{GOF/+}$ embryos is consistently more abnormal than $Pax3^{Cre/+} \beta\text{-catenin}^{GOF/+}$ embryos, suggesting that $Pax3$ mutation still affects the phenotype in embryos with β -catenin GOF.

The mutant phenotypes seen in $Pax3^{Cre/+} \beta\text{-catenin}^{GOF/+}$ and $Pax3^{Sp2H/Cre} \beta\text{-catenin}^{GOF/+}$ embryos could potentially be caused by a number of abnormal mechanisms. The NC appear to migrate normally, as *ErbB3* expression is present in the appropriate regions in embryos with β -catenin GOF at the 18-20 somite stage (**Figure 4.12**). However, compared to wild type, expression in $Pax3^{Sp2H/Cre} \beta\text{-catenin}^{GOF/+}$ embryos appears to be weaker and both $Pax3^{Cre/+} \beta\text{-catenin}^{GOF/+}$ and $Pax3^{Sp2H/Cre} \beta\text{-catenin}^{GOF/+}$ embryos appear to form fewer neurons in the DRG, which could suggest that fewer NC cells have been specified. This theory is supported by the abnormal development of the vagus nerve, and the failure of *ErbB3* expression in the trigeminal ganglia, as it is possible that both of these abnormalities could be caused by insufficient population of the appropriate regions by NC.

Alternatively, the mutant phenotypes seen in embryos with β -catenin GOF could be caused by excess apoptosis of the NC following migration. This could explain the progressive loss of *ErbB3* expression, and also the reduction in neuronal differentiation observed in $Pax3^{Cre/+} \beta\text{-catenin}^{GOF/+}$ and $Pax3^{Sp2H/Cre} \beta\text{-catenin}^{GOF/+}$ embryos.

Another possible explanation could be premature differentiation of the spinal NC in embryos with β -catenin GOF. This would cause the cells to stop expressing *ErbB3*, and could also explain the lower numbers of differentiating neurons in $Pax3^{Cre/+} \beta\text{-catenin}^{GOF/+}$ and $Pax3^{Sp2H/Cre} \beta\text{-catenin}^{GOF/+}$ embryos, as early differentiation would prematurely halt proliferation.

$Pax3^{+/+} \beta\text{-catenin}^{+/+}$ and $Pax3^{+/-} \beta\text{-catenin}^{+/+}$ embryos show an unbroken line of spinal NC specification delineated by *FoxD3* expression at the 7-9 and 10-11 somite stages (**Figure 4.17**). In contrast, *FoxD3* expression was not detectable in the spinal region of $Pax3^{Sp2H/Cre} \beta\text{-catenin}^{+/+}$ embryos at these stages. As *ErbB3* expression is seen at later stages of development, this would suggest that NC specification is delayed in these mutant embryos, which may result in fewer NC cells being specified. $Pax3^{Cre/+} \beta\text{-catenin}^{GOF/+}$ embryos show a broken line of *FoxD3* expression. This suggests that although the initial specification does not appear to be delayed, the process may occur at a slower rate in these embryos. Therefore, fewer NC cells may be specified, as the environment may not be as conducive to specification at the later stage. For example, the morphogen gradients may change, resulting in altered environmental cues, or expression of ECM proteins may be less favourable to NC specification at the slightly later stages. $Pax3^{Sp2H/Cre} \beta\text{-catenin}^{GOF/+}$ embryos also show reduced *FoxD3* expression in the spine between the 7 and 11 somite stages, which again suggests a delay and/or failure of

specification. On the other hand, fewer cells may be competent to respond to specification signals, and thus fewer NC cells are specified. It would be interesting to observe NC specification through *FoxD3 in situ* hybridisation in embryos of a lower somite stage, for example the 5-6 somite stage. This would enable observation of the initial specification of the NC in *Pax3^{+/+} β-catenin^{+/+}* embryos, and would allow comparison of this point between the genotypes.

It is well documented that *Spotch* mice have a reduced population of NC, and it has often been attributed to a failure of NC migration, either through intrinsic or environmental mechanisms (Auerbach, 1954; Chan et al., 2004; Conway et al., 1997b; Henderson et al., 1997; Serbedzija and McMahon, 1997). It is likely that a NC migration defect is present in the *Spotch* mouse. Research has indicated that Pax3 may influence expression of both ECM proteins, such as Matrix metalloproteinase 14, Fibronectin, and Laminin A, and also intracellular proteins, such as Doublecortin and Claudin13, which act on cell migration and adhesion (Wang et al., 2007). Therefore, Pax3 is likely to play a role in both intracellular and environmental control of NC migration. However, research has shown that migration defects are unlikely to be the sole cause of NC defects seen in *Sp^{2H}/Sp^{2H}* mice. For example, other studies have suggested that reduced expansion of the NC population prior to migration is the cause of the defects (Conway et al., 2000). This data fits the findings of this study, but could potentially also be interpreted as a reduction in NC specification. Therefore it seems likely that NC cells in *Sp^{2H}/Sp^{2H}* mice either fail to proliferate pre-migration, or that fewer are initially specified. This may be due to a delay in the initiation of NC specification.

On the other hand, NC in *Pax3^{Cre/+} β-catenin^{GOF/+}* embryos appear to be specified at the appropriate time, but in fewer numbers, or the expansion of the NC population is reduced (**Figure 4.17**). The lack of NC specification in *Pax3^{Sp2H/Cre} β-catenin^{GOF/+}* embryos is likely to be caused by a combination of β-catenin GOF and Pax3 mutant NC defects; delayed specification, reduced specification, or a reduction in pre-migratory NC proliferation, or some combination of these. Study of NC specification at slightly older somite stages could indicate when it begins in *Pax3^{Sp2H/Cre} β-catenin^{+/+}* and *Pax3^{Sp2H/Cre} β-catenin^{GOF/+}* embryos; for example by *in situ* hybridisation for *FoxD3* at the 13-15 and 16-18 somite stages. This could provide more information about the timing of specification and numbers of specified cells.

Apoptosis was studied through TUNEL staining in embryos of various genotypes between 22 and 30+ somites (**Figures 4.14, 4.15 and 4.16**). In *Pax3^{Sp2H/Cre} β-catenin^{+/+}* at the 30+ somite stage, there is an apparent reduction in the characteristic pattern of apoptosis in regions containing high numbers of NC. This is interesting given the smaller population of NC in these

embryos. The reduction in apoptosis at the 30+ somite stage could be a reflection of the reduced abundance of NC. Alternatively, the TUNEL-positive cells may not be NC, and may be cells from other tissues. This could be assessed by using TUNEL staining in combination with an antibody to mark NC, such as anti-FoxD3 or anti-ErbB3. Sections of the NT following TUNEL staining could also be useful in quantifying the apoptosis present. It would also be interesting to study NC from *Spotch* embryos *in vitro* to observe rates and proportions of apoptosis.

Pax3^{Cre/+} *β-catenin*^{GOF/+} embryos show similar patterns of apoptosis to wild type embryos at the 22-24 and 27-29 somite stages, but by the 30+ somite stage they exhibit a generalised increase in apoptosis, in particular in a pattern corresponding to the DRGs. At the 27-29 somite stage, *Pax3*^{Sp2H/Cre} *β-catenin*^{GOF/+} embryos show a slight reduction in apoptosis, but by the 30+ somite stage, apoptosis is similar or slightly elevated compared with wild type levels. These results could provide an explanation for the lack of *ErbB3* expression in the spinal region at the 30+ somite stage: higher rates of apoptosis in this region could further reduce the size of the NC population, which is already diminished prior to migration. However, Tuj1 immunohistochemistry shows that some of the NC survive to form neurons in this region. Therefore, the lack of *ErbB3* expression cannot be completely explained by excess apoptosis of the NC.

Markers of PNS differentiation were analysed to indicate whether subsequent PNS differentiation is likely to be affected. *Ngn2* expression was used to study general neuronal differentiation (Sommer et al., 1996), and *Brn3a* was used as marker for sensory neurons specifically (Ninkina et al., 1993). Research suggests that *Pax3* mutation causes premature neuronal differentiation, but prevents the differentiation of sensory neurons (Dude et al., 2009). Therefore, it was of interest to determine the effect of *Pax3* mutation in combination with *β-catenin* GOF.

Ngn2 expression was studied fairly early during NT closure, at the 16-18 somite stage (**Figure 4.18**). There did not appear to be any difference in expression pattern between genotypes. This was surprising, as *Ngn2* is known to act downstream of *Pax3* (Nakazaki et al., 2008). However, research has shown that *Pax3* mutation affects *Ngn2* expression at later stages of development (Nakazaki et al., 2008). Therefore it is possible that both *Pax3* and canonical Wnt signalling may affect neurogenesis and *Ngn2* expression at a later stage, but that the 16-18 somite stage is too early to detect a difference.

Brn3a expression was studied at a slightly later stage in development, at the 23-24 and 30+ somite stages (**Figure 4.19**). *Pax3*^{Sp2H/Cre} *β-catenin*^{+/+} embryos appear to show reduced *Brn3a* expression compared with wild type, particularly in the spinal region. This may indicate a

reduced potential for differentiation, but most likely reflects reduction in the NC cell number. *Pax3^{Sp2H/Cre} β-catenin^{GOF/+}* and *Pax3^{Cre/+} β-catenin^{GOF/+}* embryos also show this reduction in *Brn3a* expression.

An interesting *Brn3a* expression pattern was observed in the cranial region of *Pax3^{Cre/+} β-catenin^{GOF/+}* and *Pax3^{Sp2H/Cre} β-catenin^{GOF/+}* embryos. Expression is not reduced in the cranial region, and an additional region of expression was observed above the pharyngeal arches and in the forebrain (**Figure 4.19**). These results suggest that β-catenin GOF causes an expansion of *Brn3a* expression in the cranial region. It appears likely that canonical Wnt signalling induces *Brn3a* expression in this region, and that overexpression of β-catenin results in an expansion of the *Brn3a* expression domain. It is interesting that *Brn3a* expression in *Pax3^{Cre/+} β-catenin^{GOF/+}* embryos is downregulated in the spinal region, but not the cranial region. This suggests that the canonical Wnt signalling pathway influences the differentiation of the NC differently in the cranial and spinal regions.

Additionally, the region of *Brn3a* expression in the somites is expanded ventrally in *Pax3^{Cre/+} β-catenin^{GOF/+}* and *Pax3^{Sp2H/Cre} β-catenin^{GOF/+}* embryos compared to wild type (**Figure 4.19**). This suggests that β-catenin GOF either causes an expansion of the expression domain of *Brn3a*, or interferes with the formation of the dermomyotome, thus causing a generalised expansion of dermomyotome markers, including *Brn3a*. Research suggests that Wnt1 and Wnt3a expression in the NT may affect dermomyotome formation (Fan et al., 1997), so the overexpression of β-catenin may interfere with this process. On the other hand, Pax3 has also been implicated in development of the dermomyotome (Goulding et al., 1994), and yet the faint *Brn3a* expression seen in the somites of *Pax3^{Sp2H/Cre} β-catenin^{+/+}* embryos suggests that it is localised to the dorsal region. Analysis with other markers of the dermomyotome, such as *Sim1*, could provide more information (Fan et al., 1997).

It is difficult to conclude whether β-catenin GOF has any effect on the differentiation of the NC population, either in timing or cell type generated. Both *β-catenin^{GOF}* and *Pax3* mutant alleles reduced the expression of *Brn3a* in differentiating NC. However, as it is also likely that they both decrease the size of the NC population, it is difficult to determine what causes the defects seen in these mice. *Ngn2* expression studies of embryos at similar somite stages could allow a comparison between the number of differentiating neurons and the number of differentiating sensory neurons, which would allow the sensory neuronal differentiation to be observed as a proportion of overall neuronal differentiation.

The most prominent NC defect seen in the embryos with β-catenin GOF is the premature disappearance of *ErbB3* expression at 30+ somite stage (**Figure 4.12**). There is evidence that

this defect could be caused by reduced specification of NC cells, increased apoptosis, or premature differentiation, or some combination of these. The *in vivo* experiments described here are important, as they allow the study of each of these processes in the presence of surrounding tissues and signals which are likely to influence them. However, the reduced populations of NC make analysis difficult, as the relative amounts of each of these processes are awkward to study *in vivo*. Therefore *in vitro* studies of NC could prove very useful, as it would be possible to quantify the processes as a function of the size of the NC population. These experiments would allow the study of the rates of apoptosis in the NC of the different genotypes, as well as research into the timing and cell types of neuronal differentiation in these embryos.

4.2.4 The effect of β -catenin gain-of-function on *Pax3* expression

Recent research suggests that canonical Wnt signalling may act upstream of *Pax3* signalling during NT closure (Zhao et al., 2014). Therefore, RT-qPCR was used to quantify *Pax3* expression in embryos of different genotypes to determine whether it was affected by β -catenin GOF.

Primers which detect expression from the *Pax3*⁺ (wild type) and *Pax3*^{Cre} alleles but not the *Pax3*^{Sp2H} allele showed a significant reduction of *Pax3* expression in embryos carrying the *Pax3*^{Sp2H} allele (**Figure 4.21A**). Thus, expression was lower in *Pax3*^{Sp2H/Cre} β -catenin^{+/+} and *Pax3*^{Sp2H/Cre} β -catenin^{GOF/+} embryos compared with *Pax3*^{+/+} β -catenin^{+/+}, *Pax3*^{Cre/+} β -catenin^{+/+} and *Pax3*^{Cre/+} β -catenin^{GOF/+} embryos. This difference was predicted although the magnitude of the loss of expression was greater than expected; the *Pax3* expression of *Pax3*^{Sp2H/Cre} β -catenin^{+/+} embryos would be expected to be around 0.5 of wild type, when it is actually 0.32. This could suggest that the *Pax3*^{Cre} mRNA is expressed at a lower level than wild type. This idea is supported by the fact that, while not statistically significant, there appeared to be lower *Pax3* expression in *Pax3*^{Cre/+} β -catenin^{+/+} than *Pax3*^{+/+} β -catenin^{+/+} embryos.

A second set of primers which amplify DNA from wild type and *Pax3*^{Sp2H} alleles, but not the *Pax3*^{Cre} allele showed an expected significant reduction in *Pax3* expression in *Pax3*^{Cre/+} β -catenin^{+/+} embryos when compared to *Pax3*^{+/+} β -catenin^{+/+} embryos (**Figure 4.21B**). In addition, *Pax3*^{Sp2H/Cre} β -catenin^{+/+} embryos exhibited significantly lower *Pax3* expression than *Pax3*^{Cre/+} β -catenin^{+/+}. These data suggests that *Pax3*^{Sp2H} mRNA is expressed at a lower level than wild type *Pax3* mRNA.

Neither set of primers detected any significant differences in *Pax3* expression between *Pax3*^{Cre/+} β -catenin^{+/+} and *Pax3*^{Cre/+} β -catenin^{GOF/+} embryos, or between *Pax3*^{Sp2H/Cre} β -catenin^{+/+} and *Pax3*^{Sp2H/Cre} β -catenin^{GOF/+} embryos. Therefore, β -catenin GOF does not appear to affect expression of *Pax3*.

It has been previously reported that β -catenin loss-of-function is able to downregulate the expression of *Pax3* (Zhao et al., 2014). Therefore, it might have been expected that β -catenin GOF could upregulate *Pax3* expression. However, this does not appear to be the case. This may be because β -catenin is not the limiting factor in the level of *Pax3* expression. If this was the case, then upregulating β -catenin would not increase the expression of *Pax3*. Alternatively, it could be because the β -catenin GOF is only present in certain tissues of the embryo. Therefore, any effect this mutation would have on *Pax3* expression will also only occur in these certain tissues, and may be undetectable using qPCR of the whole embryo.

4.2.5 Conclusions

Evidence in this chapter suggests that an interaction occurs between the *Pax3* and canonical Wnt signalling pathways which causes compound mutations to affect the embryos differently compared to *Pax3* or canonical Wnt mutations alone. For example, the compound mutant embryos have much higher frequencies of NTDs in comparison to the separate mutations.

However, the nature of this interaction remains uncertain. Proliferation and neuronal differentiation in the cranial NT appear unchanged by both the *Pax3* and β -catenin^{GOF} mutations. The development of the NC is severely affected by the combination of the mutations, but the processes behind the defects are currently unclear. However, evidence suggests that the interaction between the pathways may affect multiple cellular mechanisms in the NC, including specification, proliferation, apoptosis and migration. Further studies, should clarify which defects are present, and their relative contributions to the development of the NT and NC defects.

It is also unclear how β -catenin GOF affects the expression of *Pax3*. Previously described literature suggests that β -catenin GOF might upregulate *Pax3* expression, but this was not detected. However, this does not necessarily mean that a change in expression does not occur.

In order to provide balance to these studies, and to further examine the interaction between the *Pax3* and canonical Wnt signalling pathways, it is also important to observe the effects of β -catenin loss-of-function. Abnormally low levels of canonical Wnt signalling is likely to affect the embryo differently to abnormally high levels, and may interact with *Pax3* differently. Therefore, complementary experiments using embryos with β -catenin loss-of-function are described in **Chapter 5** of this thesis.

5 Pax3 and β -Catenin Loss-of-Function

5.1 Results

Previous research has indicated the possibility of an interaction between Pax3 and the canonical Wnt signalling pathway. The two pathways play overlapping roles during development, as both are important in maintaining cells in an undifferentiated, proliferative state (Keller-Peck and Mullen, 1997; Megason and McMahon, 2002). In addition, both pathways are involved in the specification and development of the NC and NC-derived tissues (Bondurand et al., 2000; Conway et al., 1997b; Nakazaki et al., 2008; Saint-Jeannet et al., 1997; Shimizu et al., 2008).

The interaction between Pax3 and the canonical Wnt signalling pathway could be direct, with one pathway affecting the expression of components of the other pathway. Published research suggests that this is possible, as β -catenin LOF has been shown to reduce the expression of *Pax3* in the NT (Zhao et al., 2014). Additionally, studies have shown several genes encoding components of the canonical Wnt signalling pathway to be direct targets of Pax3 (Fenby et al., 2008; Wang et al., 2007).

Alternatively, the interaction between Pax3 and the canonical Wnt signalling pathway could be indirect, with the processes converging on a common mechanism or pathway. For example, both Pax3 and the canonical Wnt signalling pathway are known to act on Notch signalling to regulate the development of the NC and nervous system (De Bellard et al., 2002; Ma et al., 1996; Nakazaki et al., 2008; Shimizu et al., 2008; Yun et al., 2002). In this case, the interaction would reflect a summation of the effects of Pax3 and the canonical Wnt signalling pathway.

Both Pax3 and canonical Wnt signalling have important roles in the specification and development of the NC. Wnt1 and Wnt3a are involved in specification and proliferation (Dickinson et al., 1994; Ikeya et al., 1997; Saint-Jeannet et al., 1997), and Pax3 is important for specification, migration and differentiation of the NC (Auerbach, 1954; Conway et al., 1997a; Lang et al., 2000; Moase and Trasler, 1989). Pax3-induced NC development appears to be Wnt-dependent, which may suggest interaction between the pathways during NC development (Monsoro-Burq et al., 2005; Sato et al., 2005).

The aim of this study is to determine whether an interaction exists between Pax3 and the canonical Wnt signalling pathway, and if so, to determine the nature of the interaction. The hypothesis being tested is the same as that described in **Chapter 4**: interaction between Pax3

		Mouse 2: Pax3 ^{Cre/+} β-catenin ^{+/-}			
		Pax3 ^{Cre} β-catenin ⁻	Pax3 ^{Cre} β-catenin ⁺	Pax3 ⁺ β-catenin ⁻	Pax3 ⁺ β-catenin ⁺
Mouse 1: Pax3 ^{Sp2H/+} β-catenin ^{LOF/+}	Pax3 ^{Sp2H} β-catenin ^{LOF}	Pax3 ^{Sp2H/Cre} β-catenin ^{LOF/-}	Pax3 ^{Sp2H/Cre} β-catenin ^{LOF/+}	Pax3 ^{Sp2H/+} β-catenin ^{LOF/-}	Pax3 ^{Sp2H/+} β-catenin ^{LOF/+}
	Pax3 ^{Sp2H} β-catenin ⁺	Pax3 ^{Sp2H/Cre} β-catenin ^{+/-}	Pax3 ^{Sp2H/Cre} β-catenin ^{+/+}	Pax3 ^{Sp2H/+} β-catenin ^{+/-}	Pax3 ^{Sp2H/+} β-catenin ^{+/+}
	Pax3 ⁺ β-catenin ^{LOF}	Pax3 ^{Cre/+} β-catenin ^{LOF/-}	Pax3 ^{Cre/+} β-catenin ^{LOF/+}	Pax3 ^{+/+} β-catenin ^{LOF/-}	Pax3 ^{+/+} β-catenin ^{LOF/+}
	Pax3 ⁺ β-catenin ⁺	Pax3 ^{Cre/+} β-catenin ^{+/-}	Pax3 ^{Cre/+} β-catenin ^{+/+}	Pax3 ^{+/+} β-catenin ^{+/-}	Pax3 ^{+/+} β-catenin ^{+/+}

Pax3 ^{+/+} β-catenin ^{+/+}	Pax3 ^{+/-} β-catenin ^{-/-}
Pax3 ^{+/+} β-catenin ^{+/-}	Pax3 ^{-/-} β-catenin ^{+/+}
Pax3 ^{+/-} β-catenin ^{+/+}	Pax3 ^{-/-} β-catenin ^{+/-}
Pax3 ^{+/-} β-catenin ^{+/-}	Pax3 ^{-/-} β-catenin ^{-/-}

Figure 5.1: Punnett square demonstrating genotypes and ratios of offspring from the cross $Pax3^{Sp2H/+} \beta\text{-catenin}^{LOF/+} \times Pax3^{Cre/+} \beta\text{-catenin}^{+/-}$. The key represents the genotype groups used in the experiments described in this chapter. Colour coding demonstrates how the genotypes are distributed among the groups, as several genotypes have been pooled into the same genotype group (see **Figures 5.4** and **5.5**).

		Mouse 2: Pax3 ^{Cre/+} β-catenin ^{LOF/+}			
		Pax3 ^{Cre} β-catenin ^{LOF}	Pax3 ^{Cre} β-catenin ⁺	Pax3 ⁺ β-catenin ^{LOF}	Pax3 ⁺ β-catenin ⁺
Mouse 1: Pax3 ^{Sp2H/+} β-catenin ^{LOF/+}	Pax3 ^{Sp2H} β-catenin ^{LOF}	Pax3 ^{Sp2H/Cre} β-catenin ^{LOF/LOF}	Pax3 ^{Sp2H/Cre} β-catenin ^{LOF/+}	Pax3 ^{Sp2H/+} β-catenin ^{LOF/LOF}	Pax3 ^{Sp2H/+} β-catenin ^{LOF/+}
	Pax3 ^{Sp2H} β-catenin ⁺	Pax3 ^{Sp2H/Cre} β-catenin ^{LOF/+}	Pax3 ^{Sp2H/Cre} β-catenin ^{+/+}	Pax3 ^{Sp2H/+} β-catenin ^{LOF/+}	Pax3 ^{Sp2H/+} β-catenin ^{+/+}
	Pax3 ⁺ β-catenin ^{LOF}	Pax3 ^{Cre/+} β-catenin ^{LOF/LOF}	Pax3 ^{Cre/+} β-catenin ^{LOF/+}	Pax3 ^{+/+} β-catenin ^{LOF/LOF}	Pax3 ^{+/+} β-catenin ^{LOF/+}
	Pax3 ⁺ β-catenin ⁺	Pax3 ^{Cre/+} β-catenin ^{LOF/+}	Pax3 ^{Cre/+} β-catenin ^{+/+}	Pax3 ^{+/+} β-catenin ^{LOF/+}	Pax3 ^{+/+} β-catenin ^{+/+}

Pax3 ^{+/+} β-catenin ^{+/+}	Pax3 ^{Sp2H/Cre} β-catenin ^{+/+}
Pax3 ^{+/-} β-catenin ^{+/+}	Pax3 ^{Sp2H/Cre} β-catenin ^{LOF/+}
Pax3 ^{Cre/+} β-catenin ^{LOF/+}	Pax3 ^{Sp2H/Cre} β-catenin ^{LOF/LOF}
Pax3 ^{Cre/+} β-catenin ^{LOF/LOF}	

Figure 5.2: Punnet square demonstrating genotypes and ratios of offspring from the cross Pax3^{Sp2H/+} β-catenin^{LOF/+} x Pax3^{Cre/+} β-catenin^{LOF/+}. The key represents the genotype groups used in the experiments described in this chapter. Colour coding demonstrates how the genotypes are distributed among the groups, as several genotypes have been pooled into the same genotype group (see **Figure 5.3**).

the canonical Wnt signalling pathway reduces proliferation and induces premature neuronal differentiation in the NT and NC, resulting in NTDs and NC defects. Two different genetic crosses were carried out to generate the embryos used for these results. The initial cross was Pax3^{Sp2H/+} β-catenin^{LOF/+} x Pax3^{Cre/+} β-catenin^{+/-} (**Figure 5.1**), but due to and breeding problems the experiments were continued using embryos from the cross Pax3^{Sp2H/+} β-catenin^{LOF/+} x Pax3^{Cre/+} β-catenin^{LOF/+} (**Figure 5.2**). **Figures 5.1 and 5.2** also provide information on genotype

pooling (described below). Information in figure legends states which cross was used for the experiment described.

$Pax3^{+/-} \beta\text{-catenin}^{+/+}$ has been used to denote either $Pax3^{Cre/+} \beta\text{-catenin}^{+/+}$, $Pax3^{Sp2H/+} \beta\text{-catenin}^{+/+}$, $Pax3^{Sp2H/+} \beta\text{-catenin}^{LOF/+}$, or $Pax3^{Sp2H/+} \beta\text{-catenin}^{LOF/LOF}$. In the absence of Cre recombinase the $\beta\text{-catenin}^{LOF}$ allele is not recombined, and acts as a wild type $\beta\text{-catenin}$ allele. Thus the genotypes listed above are functionally equivalent, and there are no significant differences in the rates of spina bifida or exencephaly between these genotypes (**Figures 5.3, 5.4 and 5.5, and Table 5.1**).

In addition, $\beta\text{-catenin}^{+/-}$ may refer to a single copy of the $\beta\text{-catenin}$ -null allele, or it may refer to $\beta\text{-catenin}^{LOF/+}$ if Cre recombinase is expressed (the $\beta\text{-catenin}^{LOF}$ allele has been recombined) or to $\beta\text{-catenin}^{LOF/-}$ if Cre is not present (one copy of $\beta\text{-catenin}^{-/-}$, one un-recombined $\beta\text{-catenin}^{LOF}$ allele). These alleles are functionally equivalent in the Cre-expressing regions, and there are no significant differences in the rates of spina bifida or exencephaly between the genotypes (**Figures 5.3, 5.4 and 5.5, and Table 5.1**).

Likewise, neither $Pax3^{+/+} \beta\text{-catenin}^{+/+}$, $Pax3^{+/+} \beta\text{-catenin}^{LOF/+}$, nor $Pax3^{+/+} \beta\text{-catenin}^{LOF/LOF}$ embryos have recombined $\beta\text{-catenin}^{LOF}$ alleles. They show no significant differences in rates of exencephaly or spina bifida (**Figures 5.3, 5.4 and 5.5, and Table 5.1**), and so have been pooled as 'wild type' embryos. They will be referred to as $Pax3^{+/+} \beta\text{-catenin}^{+/+}$ embryos in these results.

5.1.1 Verification of the decrease in canonical Wnt signalling caused by the $\beta\text{-catenin}$ loss-of-function allele

As with the $\beta\text{-catenin}^{GOF}$ allele, the $\beta\text{-catenin}^{LOF}$ allele has previously been generated and examined (Brault et al., 2001). However, the effects of this allele were further verified in the embryos used for this research.

A probe which identified *Axin2* mRNA was used in whole mount *in situ* hybridisation as a marker to indicate levels of canonical Wnt signalling. Embryos were compared with different *Pax3* genotypes, and carrying two, one or no mutant copies of the $\beta\text{-catenin}$ allele.

Embryos which carried one or no $\beta\text{-catenin}$ mutant alleles showed the same expression patterns of *Axin2*, suggesting a wild type level of canonical Wnt signalling. However, embryos with two mutant $\beta\text{-catenin}$ alleles – $Pax3^{Cre/+} \beta\text{-catenin}^{LOF/-}$ and $Pax3^{Sp2H/Cre} \beta\text{-catenin}^{LOF/-}$ embryos – show reduced expression of *Axin2*. This suggests reduced canonical Wnt signalling (**Figure 5.6**).

Genotype group	Cross	Genotype	Number of embryos for exencephaly study	% embryos with exencephaly	Number of embryos for spina bifida study	% embryos with spina bifida
Pax3 ^{+/+} β-catenin ^{+/+}	LOF	Pax3 ^{+/+} β-catenin ^{+/+}	16	0.00	9	0.00
		Pax3 ^{+/+} β-catenin ^{LOF/+}	38	2.63	19	5.26
		Pax3 ^{+/+} β-catenin ^{LOF/LOF}	13	7.69	7	0.00
Null	Null	Pax3 ^{+/+} β-catenin ^{+/+}	19	0.00	2	0.00
		Pax3 ^{+/+} β-catenin ^{LOF/+}	15	0.00	5	0.00
		Pax3 ^{Cre/+} β-catenin ^{+/+}	9	11.1	4	0.00
Pax3 ^{+/-} β-catenin ^{+/+}	LOF	Pax3 ^{Sp2H/+} β-catenin ^{+/+}	25	8.00	12	25
		Pax3 ^{Sp2H/+} β-catenin ^{LOF/+}	34	5.88	22	9.09
		Pax3 ^{Sp2H/+} β-catenin ^{LOF/LOF}	14	7.14	4	25
Null	Null	Pax3 ^{Cre/+} β-catenin ^{+/+}	14	7.14	4	0.00
		Pax3 ^{Sp2H/+} β-catenin ^{+/+}	11	0.00	6	0.00
		Pax3 ^{Sp2H/+} β-catenin ^{LOF/+}	17	0.00	7	0.00

Table 5.1: Pooling genotypes from the crosses Pax3^{Sp2H/+} β-catenin^{LOF/+} x Pax3^{Cre/+} β-catenin^{LOF/+} and Pax3^{Sp2H/+} β-catenin^{LOF/+} x Pax3^{Cre/+} β-catenin^{+/-}.

Data is shown from each resulting genotype to demonstrate lack of significant difference between pooled genotypes (assessed by the Chi-Square Test). In the

'Cross' column, LOF refers to the cross Pax3^{Sp2H/+} β-catenin^{LOF/+} x Pax3^{Cre/+} β-catenin^{LOF/+}, and Null refers to the cross Pax3^{Sp2H/+} β-catenin^{LOF/+} x Pax3^{Cre/+} β-catenin^{+/-}.

The table is continued on the following page.

Genotype group	Cross	Genotype	Number of embryos for exencephaly study	% embryos with exencephaly	Number of embryos for spina bifida study	% embryos with spina bifida
Pax3 ^{+/-} β-catenin ^{+/-}	LOF	Pax3 ^{Cre/+} β-catenin ^{LOF/+}	31	0.00	18	5.56
	Null	Pax3 ^{Cre/+} β-catenin ^{LOF/+}	10	0.00	3	0.00
		Pax3 ^{Cre/+} β-catenin ^{+/-}	15	6.67	5	0.00
		Pax3 ^{Sp2H/+} β-catenin ^{+/-}	17	5.88	4	50.0
		Pax3 ^{Sp2H/+} β-catenin ^{LOF/-}	19	15.8	4	25
Pax3 ^{+/-} β-catenin ^{-/-}	LOF	Pax3 ^{Cre/+} β-catenin ^{LOF/LOF}	18	16.7	10	80.0
	Null	Pax3 ^{Cre/+} β-catenin ^{LOF/-}	10	10.0	6	100
		Pax3 ^{Sp2H/Cre} β-catenin ^{+/+}	20	45.0	9	100
Pax3 ^{-/-} β-catenin ^{+/-}	Null	Pax3 ^{Sp2H/Cre} β-catenin ^{+/+}	13	69.2	5	100
	LOF	Pax3 ^{Sp2H/Cre} β-catenin ^{LOF/+}	32	43.8	14	92.9
	Null	Pax3 ^{Sp2H/Cre} β-catenin ^{LOF/+}	17	41.2	9	100
		Pax3 ^{Sp2H/Cre} β-catenin ^{+/-}	5	60.0	3	100
		Pax3 ^{Sp2H/Cre} β-catenin ^{LOF/LOF}	16	12.5	11	100
Pax3 ^{-/-} β-catenin ^{-/-}	LOF	Pax3 ^{Sp2H/Cre} β-catenin ^{LOF/-}	14	50.0	5	100

Table 5.1: Pooling genotypes from the crosses Pax3^{Sp2H/+} β-catenin^{LOF/+} x Pax3^{Cre/+} β-catenin^{LOF/+} and Pax3^{Sp2H/+} β-catenin^{LOF/+} x Pax3^{Cre/+} β-catenin^{+/-}, continued from previous page. Data is shown from each resulting genotype to demonstrate lack of significant difference between pooled genotypes (assessed by the Chi-Square Test). In the 'Cross' column, LOF refers to the cross Pax3^{Sp2H/+} β-catenin^{LOF/+} x Pax3^{Cre/+} β-catenin^{LOF/+}, and Null refers to the cross Pax3^{Sp2H/+} β-catenin^{LOF/+} x Pax3^{Cre/+} β-catenin^{+/-}.

Figure 5.3: Pooling of embryo genotypes from the cross $Pax3^{Sp2H/+}$ β -catenin^{LOF/+} x $Pax3^{Cre/+}$ β -catenin^{LOF/+}. Several genotypes were pooled in experiments due to similar expression levels of wild type Pax3 and β -catenin, and to similar frequencies of exencephaly and spina bifida. Experimental litters were generated containing a mixture of genotypes through the cross $Pax3^{Sp2H/+}$ β -catenin^{LOF/+} x $Pax3^{Cre/+}$ β -catenin^{LOF/+}. Exencephaly was defined as an open cranial NT at the 18 somite stage or later. Spina bifida was defined as an open spinal NT at the 30 somite stage or later.

The frequencies of exencephaly and spina bifida were compared between $Pax3^{+/+}$ β -catenin^{+/+}, $Pax3^{+/+}$ β -catenin^{LOF/+} and $Pax3^{+/+}$ β -catenin^{LOF/LOF} embryos (**A** and **C**), as these embryos have wild type Pax3 and wild type or unfloxed β -catenin. No significant differences were found in the frequencies of the NTDs, so these embryos are pooled in experiments as $Pax3^{+/+}$ β -catenin^{+/+} embryos.

The frequencies of exencephaly and spina bifida were compared between $Pax3^{Sp2H/+}$ β -catenin^{+/+}, $Pax3^{Sp2H/+}$ β -catenin^{LOF/+}, $Pax3^{Sp2H/+}$ β -catenin^{LOF/LOF}, and $Pax3^{Cre/+}$ β -catenin^{+/+} embryos (**B** and **D**), as these embryos have heterozygous expression of Pax3, and wild type or unfloxed β -catenin. No significant differences were found in the frequencies of the NTDs, so these embryos are pooled in experiments as $Pax3^{+/-}$ β -catenin^{+/+} embryos.

Significance was assessed using the Fisher Exact Test.

A – $Pax3^{+/+}$ β -catenin^{+/+} : n = 16. $Pax3^{+/+}$ β -catenin^{LOF/+} : n = 38. $Pax3^{+/+}$ β -catenin^{LOF/LOF} : n = 13. **B** – $Pax3^{Sp2H/+}$ β -catenin^{+/+} : n = 25. $Pax3^{Sp2H/+}$ β -catenin^{LOF/+} : n = 34. $Pax3^{Sp2H/+}$ β -catenin^{LOF/LOF} : n = 14. $Pax3^{Cre/+}$ β -catenin^{+/+} : n = 9. **C** – $Pax3^{+/+}$ β -catenin^{+/+} : n = 9. $Pax3^{+/+}$ β -catenin^{LOF/+} : n = 19. $Pax3^{+/+}$ β -catenin^{LOF/LOF} : n = 7. **D** – $Pax3^{Sp2H/+}$ β -catenin^{+/+} : n = 12. $Pax3^{Sp2H/+}$ β -catenin^{LOF/+} : n = 22. $Pax3^{Sp2H/+}$ β -catenin^{LOF/LOF} : n = 4. $Pax3^{Cre/+}$ β -catenin^{+/+} : n = 4.

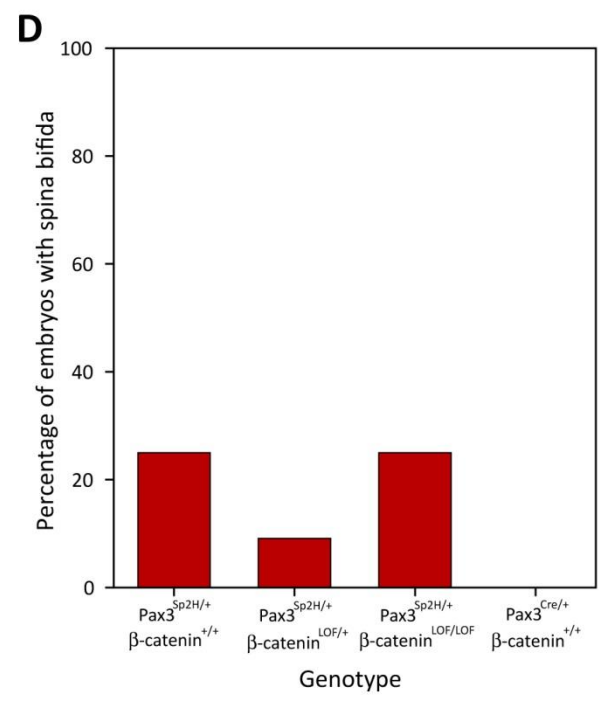
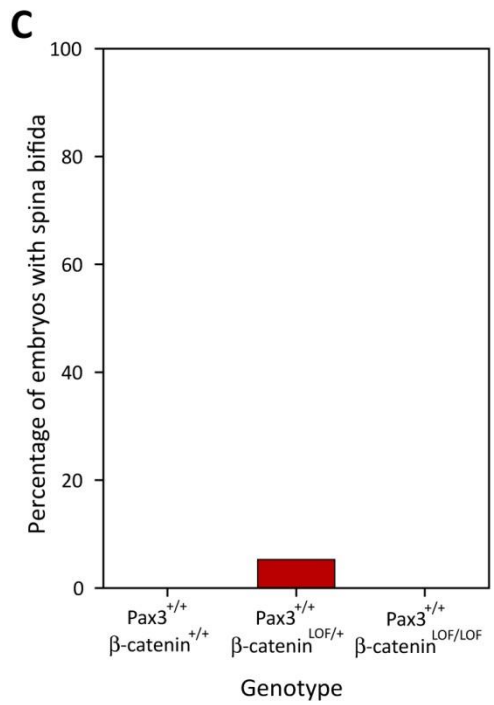
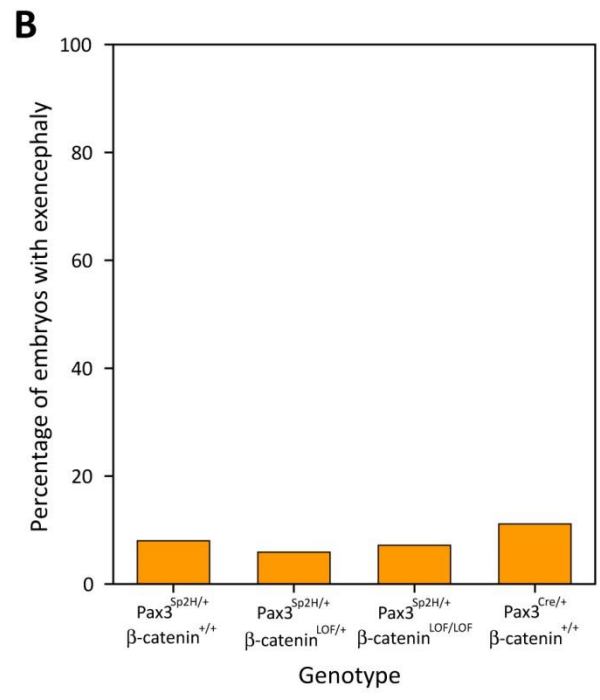
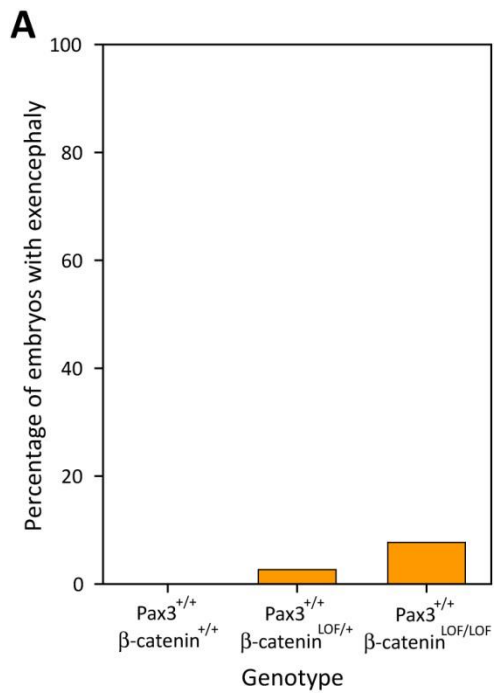


Figure 5.4: Pooling of embryo genotypes from the cross $Pax3^{Sp2H/+}$ β -catenin^{LOF/+} x $Pax3^{Cre/+}$ β -catenin^{+/-} - exencephaly. Several genotypes were pooled in experiments due to similar expression levels of wild type Pax3 and β -catenin, and to similar frequencies of exencephaly and spina bifida. Experimental litters were generated containing a mixture of genotypes through the cross $Pax3^{Sp2H/+}$ β -catenin^{LOF/+} x $Pax3^{Cre/+}$ β -catenin^{+/-}. Exencephaly was defined as an open cranial NT at the 18 somite stage or later.

The frequency of exencephaly was compared between $Pax3^{+/+}$ β -catenin^{+/+} and $Pax3^{+/+}$ β -catenin^{LOF/+} embryos (**A**), as these embryos have wild type Pax3 and wild type or unfloxed β -catenin. No significant differences were found in the frequencies of the NTD, so these embryos are pooled in experiments as $Pax3^{+/+}$ β -catenin^{+/+} embryos. The frequency of exencephaly was also compared between $Pax3^{+/+}$ β -catenin^{+/-} and $Pax3^{+/+}$ β -catenin^{LOF/-} embryos (**B**), as these genotypes have wild type expression of Pax3 and one null allele of β -catenin. No significant differences were found in the frequencies of the NTD, so these embryos are pooled in experiments as $Pax3^{+/+}$ β -catenin^{+/-} embryos.

The frequency of exencephaly was compared between $Pax3^{Sp2H/+}$ β -catenin^{+/+}, $Pax3^{Sp2H/+}$ β -catenin^{LOF/+}, and $Pax3^{Cre/+}$ β -catenin^{+/+} embryos (**C**), as these embryos have heterozygous expression of Pax3, and wild type or unfloxed β -catenin. No significant differences were found in the frequencies of the NTD, so these embryos are pooled in experiments as $Pax3^{+/-}$ β -catenin^{+/+} embryos. The frequency of exencephaly was also compared between $Pax3^{Cre/+}$ β -catenin^{LOF/+}, $Pax3^{Cre/+}$ β -catenin^{+/-}, $Pax3^{Sp2H/+}$ β -catenin^{+/-}, and $Pax3^{Sp2H/+}$ β -catenin^{LOF/-} embryos (**D**), as these genotypes have one mutant allele of Pax3 and one null allele of β -catenin. No significant differences were found in the frequencies of the NTD, so these embryos are pooled in experiments as $Pax3^{+/-}$ β -catenin^{+/-} embryos.

Significance was assessed using the Fisher Exact Test.

A - $Pax3^{+/+}$ β -catenin^{+/+}: n = 19. $Pax3^{+/+}$ β -catenin^{LOF/+}: n = 15. **B** - $Pax3^{+/+}$ β -catenin^{+/-}: n = 19. $Pax3^{+/+}$ β -catenin^{LOF/-}: n = 15. **C** - $Pax3^{Cre/+}$ β -catenin^{+/+}: n = 14. $Pax3^{Sp2H/+}$ β -catenin^{+/+}: n = 11. $Pax3^{Sp2H/+}$ β -catenin^{LOF/+}: n = 17. **D** - $Pax3^{Cre/+}$ β -catenin^{LOF/+}: n = 10. $Pax3^{Cre/+}$ β -catenin^{+/-}: n = 15. $Pax3^{Sp2H/+}$ β -catenin^{+/-}: n = 17. $Pax3^{Sp2H/+}$ β -catenin^{LOF/-}: n = 19.

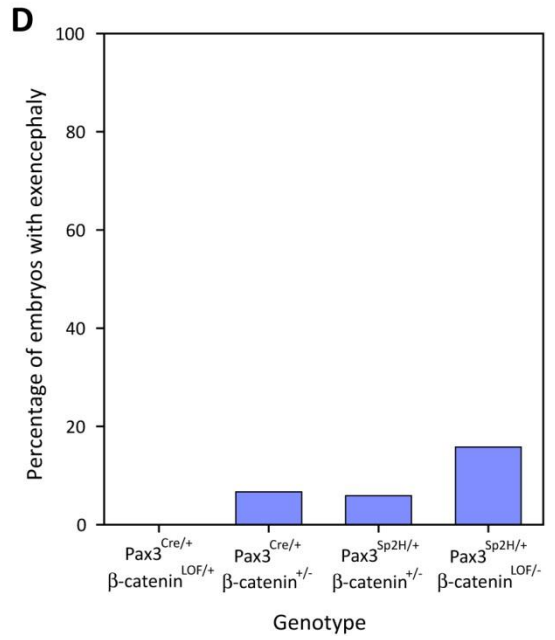
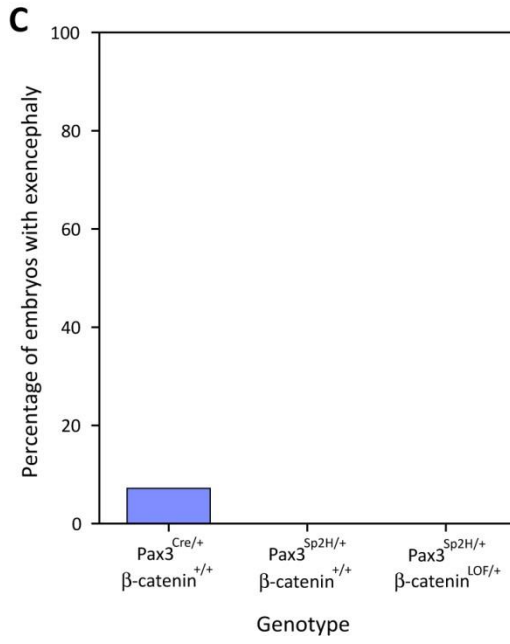
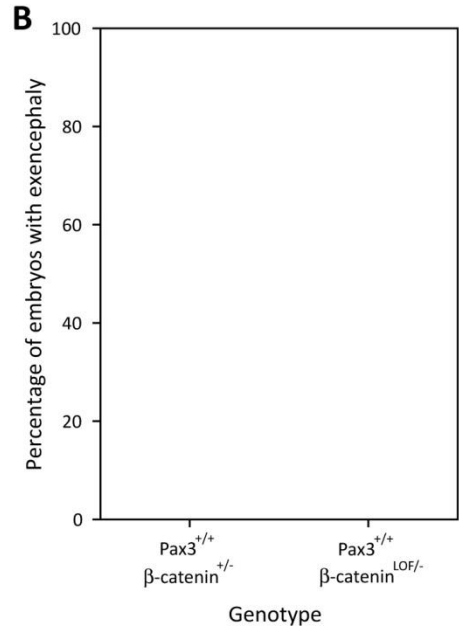
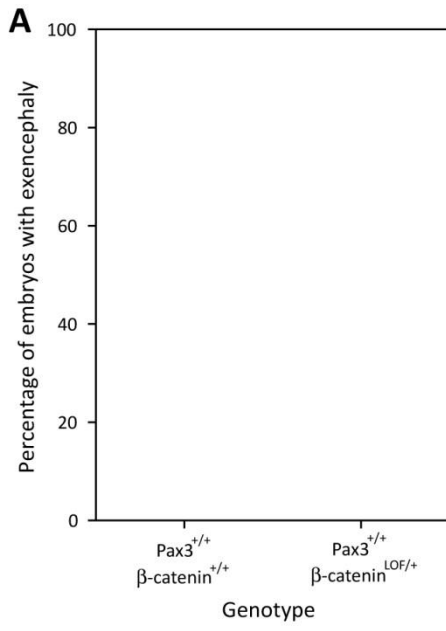


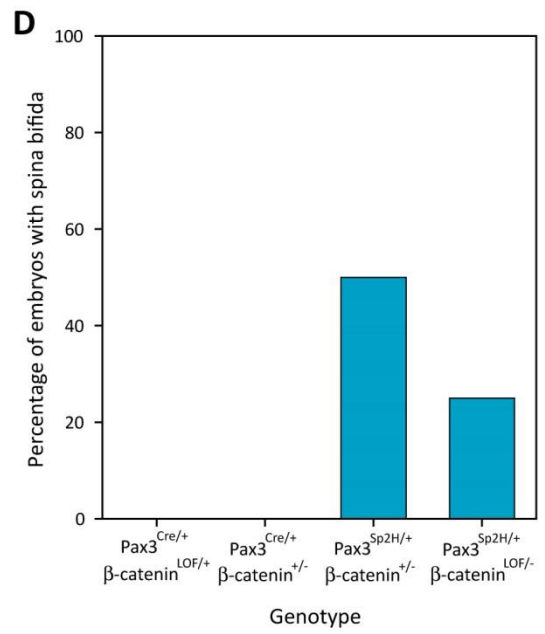
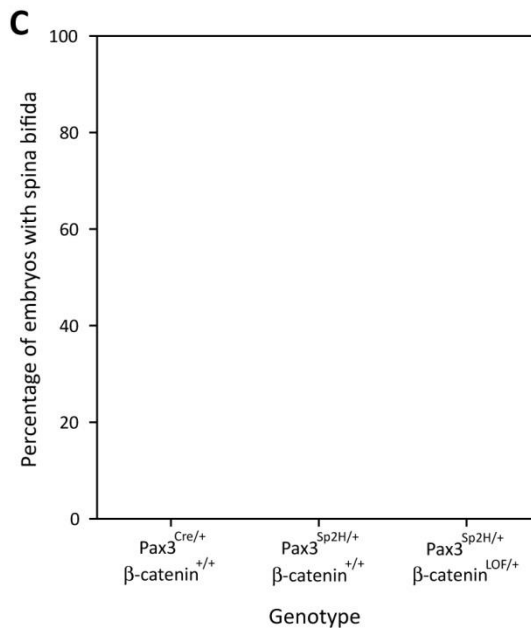
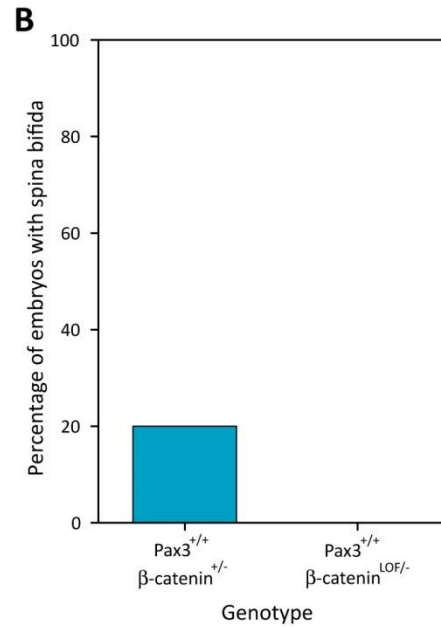
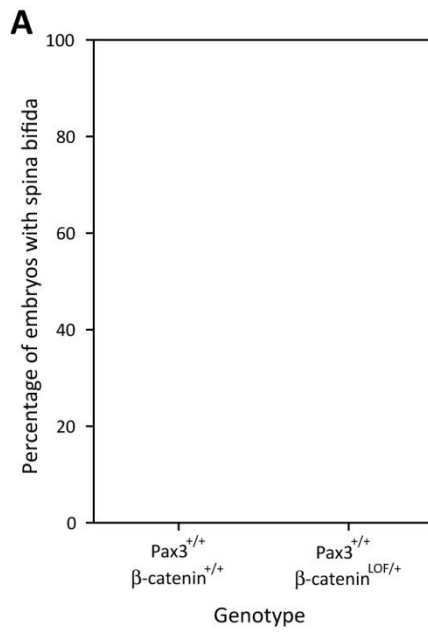
Figure 5.5: Pooling of embryo genotypes from the cross $Pax3^{Sp2H/+}$ β -catenin^{LOF/+} x $Pax3^{Cre/+}$ β -catenin^{+/-} - spina bifida. Several genotypes were pooled in experiments due to similar expression levels of wild type Pax3 and β -catenin, and to similar frequencies of exencephaly and spina bifida. Experimental litters were generated containing a mixture of genotypes through the cross $Pax3^{Sp2H/+}$ β -catenin^{LOF/+} x $Pax3^{Cre/+}$ β -catenin^{+/-}. Spina bifida was defined as an open spinal NT at the 30 somite stage or later.

The frequency of spina bifida was compared between $Pax3^{+/+}$ β -catenin^{+/+} and $Pax3^{+/+}$ β -catenin^{LOF/+} embryos (**A**), as these embryos have wild type Pax3 and wild type or unfloxed β -catenin. No significant differences were found in the frequencies of the NTD, so these embryos are pooled in experiments as $Pax3^{+/+}$ β -catenin^{+/+} embryos. The frequency of spina bifida was also compared between $Pax3^{+/+}$ β -catenin^{+/-} and $Pax3^{+/+}$ β -catenin^{LOF/-} embryos (**B**), as these genotypes have wild type expression of Pax3 and one null allele of β -catenin. No significant differences were found in the frequencies of the NTD, so these embryos are pooled in experiments as $Pax3^{+/+}$ β -catenin^{+/-} embryos.

The frequency of spina bifida was compared between $Pax3^{Sp2H/+}$ β -catenin^{+/+}, $Pax3^{Sp2H/+}$ β -catenin^{LOF/+}, and $Pax3^{Cre/+}$ β -catenin^{+/+} embryos (**C**), as these embryos have heterozygous expression of Pax3, and wild type or unfloxed β -catenin. No significant differences were found in the frequencies of the NTD, so these embryos are pooled in experiments as $Pax3^{+/-}$ β -catenin^{+/+} embryos. The frequency of spina bifida was also compared between $Pax3^{Cre/+}$ β -catenin^{LOF/+}, $Pax3^{Cre/+}$ β -catenin^{+/-}, $Pax3^{Sp2H/+}$ β -catenin^{+/-}, and $Pax3^{Sp2H/+}$ β -catenin^{LOF/-} embryos (**D**), as these genotypes have one mutant allele of Pax3 and one null allele of β -catenin. No significant differences were found in the frequencies of the NTD, so these embryos are pooled in experiments as $Pax3^{+/-}$ β -catenin^{+/-} embryos.

Significance was assessed using the Fisher Exact Test.

A - $Pax3^{+/+}$ β -catenin^{+/+}: n = 2. $Pax3^{+/+}$ β -catenin^{LOF/+}: n = 5. **B** - $Pax3^{+/+}$ β -catenin^{+/-}: n = 5. $Pax3^{+/+}$ β -catenin^{LOF/-}: n = 6. **C** - $Pax3^{Cre/+}$ β -catenin^{+/+}: n = 4. $Pax3^{Sp2H/+}$ β -catenin^{+/+}: n = 6. $Pax3^{Sp2H/+}$ β -catenin^{LOF/+}: n = 7. **D** - $Pax3^{Cre/+}$ β -catenin^{LOF/+}: n = 3. $Pax3^{Cre/+}$ β -catenin^{+/-}: n = 5. $Pax3^{Sp2H/+}$ β -catenin^{+/-}: n = 4. $Pax3^{Sp2H/+}$ β -catenin^{LOF/-}: n = 4.



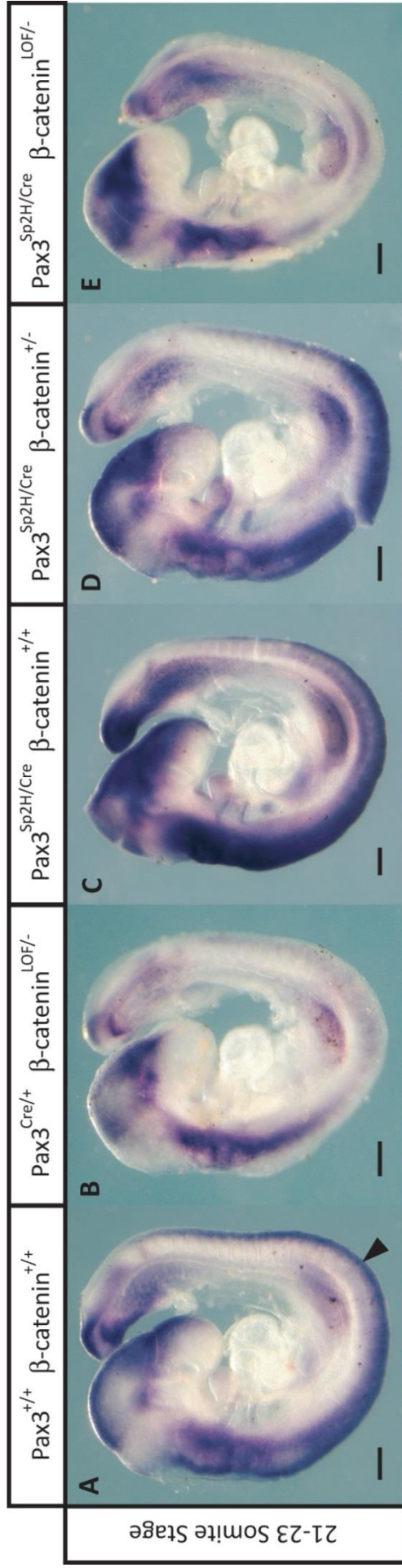


Figure 5.6: β-catenin loss-of-function results in reduced expression of Axin2. Experimental litters were generated containing a mixture of genotypes through the cross Pax3^{Sp2H/+} β-catenin^{LOF/+} x Pax3^{Cre/+} β-catenin^{+/-}. Whole mount *in situ* hybridisation for Axin2 was carried out on embryos of multiple genotypes. n = 2 for each genotype. Scale bars represent 250 μm.

Pax3^{+/+} β-catenin^{+/+} embryos (A) show Axin2 expression in a variety of tissues. However, it is most clearly expressed in the cranial region and the spinal region (arrowhead). Pax3^{Sp2H/Cre} β-catenin^{+/+} (C) and Pax3^{Sp2H/Cre} β-catenin^{+/-} (D) embryos show the same expression pattern. However Pax3^{Sp2H/Cre} β-catenin^{LOF/-} and Pax3^{Sp2H/Cre} β-catenin^{LOF/-} embryos both show reduced Axin2 expression. This is most obvious in the spinal region.

RT-qPCR was used as a quantitative measure of downstream targets of canonical Wnt signalling in the embryos used for this research. The genes *Cdx2* and *Axin2* were used to measure the levels of canonical Wnt signalling. The gene *GAPDH* was used as a housekeeping gene for normalisation for both *Cdx2* and *Axin2*. In addition, *Axin2* expression was measured using *β-actin* as a housekeeping gene for normalisation to ensure that results were not due to differences in *GAPDH* expression between genotypes.

No significant differences were seen in expression levels of *Cdx2* or *Axin2* between the genotypes (**Figure 5.7**). This does not necessarily show that β -catenin LOF does not cause reduced canonical Wnt signalling, as the β -catenin^{LOF} allele is only recombined in *Pax3*-expressing tissues. Therefore, the reduction in canonical Wnt signalling will only be present in certain tissues, including the NT and NC. RT-qPCR of whole embryos may not be sensitive enough to detect the reduction in expression of downstream targets.

5.1.2 The effect of β -catenin loss-of-function on the development of neural tube defects in the *Pax3* mutant embryo

β -catenin GOF appears to have a significant effect on the development of NTDs in *Pax3* heterozygous and mutant mice (**Chapter 4**). Therefore, the effects of β -catenin LOF in *Pax3* mutant mice were also examined.

5.1.2.1 β -catenin loss-of-function may delay spinal neurulation in *Pax3* heterozygous mutant embryos

The closure of the PNP was studied to observe whether β -catenin LOF has an effect on spinal neurulation. Data in this analysis has been pooled from two separate genetic crosses: *Pax3*^{Sp2H/+} β -catenin^{LOF/+} x *Pax3*^{Cre/+} β -catenin^{+/-} and *Pax3*^{Sp2H/+} β -catenin^{LOF/+} x *Pax3*^{Cre/+} β -catenin^{LOF/+} (**Figure 5.8**). In **Figure 5.9**, which displays this data, mutant *Pax3* alleles have all been designated *Pax3*⁻, and mutant β -catenin alleles have all been designated β -catenin⁻. This is to demonstrate, in a simplified manner, how the data has been pooled. No significant differences in NTD frequency which could affect the data when pooled were detected between embryos of equivalent *Pax3* and β -catenin genotype from different crosses (**Table 5.1**).

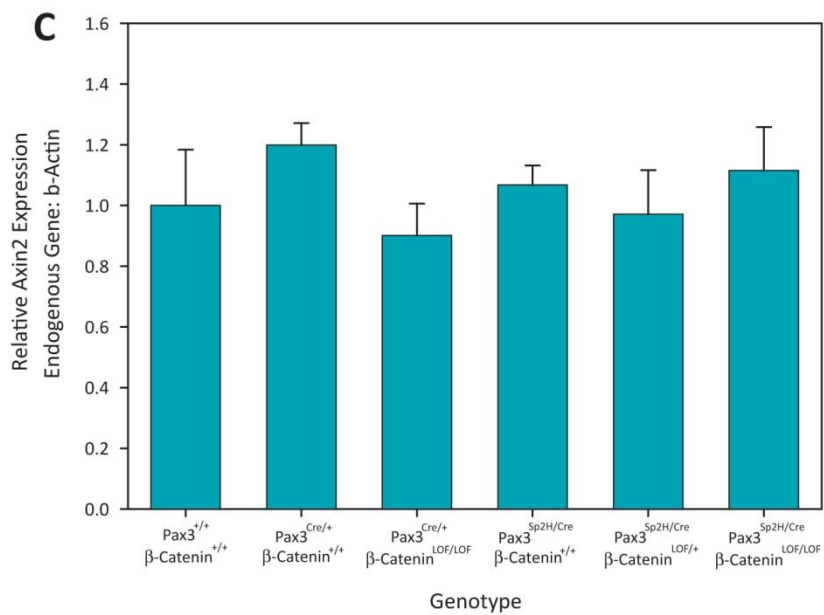
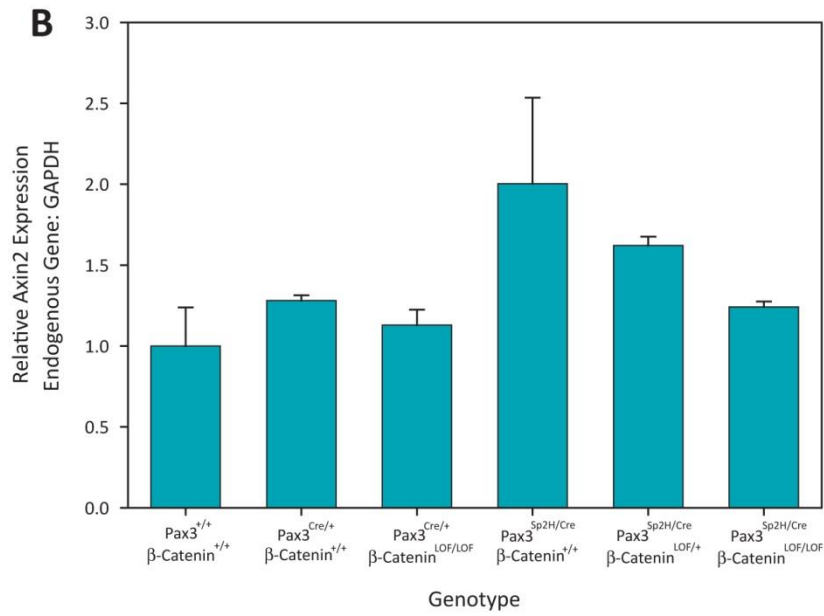
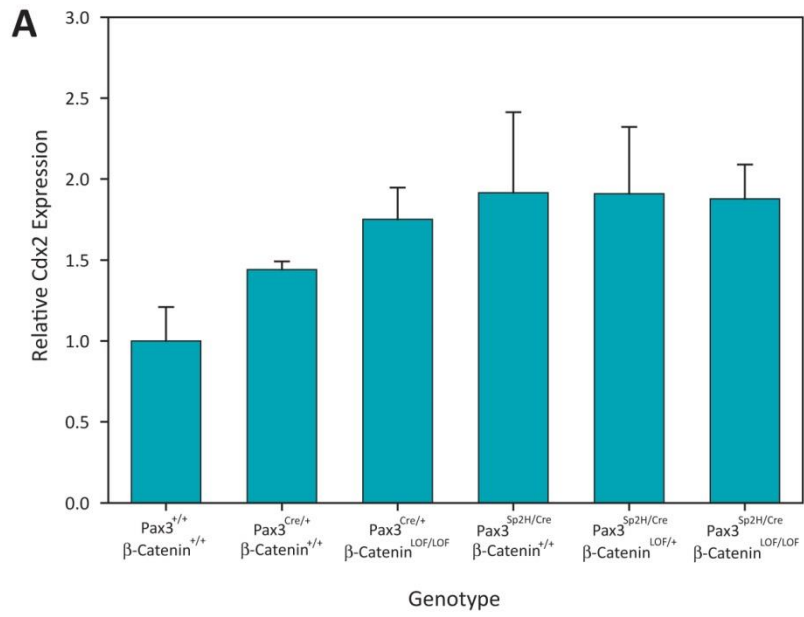
As expected, significant differences were seen between embryos with equivalent β -catenin genotypes but different *Pax3* genotypes; *Pax3* mutant embryos have larger PNPs from an early somite stage, consistent with previous data (section **3.1.1.1**). However, the β -catenin genotype appears to have little effect on PNP size in early somite stages; embryos with equivalent *Pax3* genotype but different β -catenin genotypes show similarly sized PNPs. However, a significant increase in PNP size is seen in *Pax3*^{+/-} β -catenin^{-/-} embryos in comparison to *Pax3*^{+/-} β -catenin^{+/-}

Figure 5.7: RT-qPCR was unable to determine if β -catenin loss-of-function reduces the level of canonical Wnt signalling. Experimental litters were generated containing a mixture of genotypes through the cross $Pax3^{Sp2H/+} \beta\text{-catenin}^{LOF/+}$ x $Pax3^{Cre/+} \beta\text{-catenin}^{LOF/+}$. RT-qPCR was carried out using RNA prepared from whole embryos at the 23-24 somite stage.

Graph **A** shows results for the gene *Cdx2* using *GAPDH* as an endogenous gene. No significant differences are seen between genotypes. Graphs **B** and **C** show data for *Axin2*; graph **B** shows data using *GAPDH* as the endogenous gene, and graph **C** shows data using β -actin as the endogenous gene. No significant differences in gene expression are seen between the genotypes in either of these graphs.

Significance was assessed using one-way ANOVA. Error bars indicate standard error.

$Pax3^{+/+} \beta\text{-catenin}^{+/+}$: n = 3. $Pax3^{Cre/+} \beta\text{-catenin}^{+/+}$: n = 3. $Pax3^{Cre/+} \beta\text{-catenin}^{LOF/LOF}$: n = 2. $Pax3^{Sp2H/Cre} \beta\text{-catenin}^{+/+}$: n = 3. $Pax3^{Sp2H/Cre} \beta\text{-catenin}^{LOF/+}$: n = 3. $Pax3^{Sp2H/Cre} \beta\text{-catenin}^{LOF/LOF}$: n = 3.



A

		Mouse 2: Pax3 ^{Cre/+} β-catenin ^{LOF/+}				
		Pax3 ^{Cre} β-catenin ^{LOF}	Pax3 ^{Cre} β-catenin ⁺	Pax3 ⁺ β-catenin ^{LOF}	Pax3 ⁺ β-catenin ⁺	
Mouse 1: Pax3	β-catenin ^{LOF/+}	Pax3 ^{Sp2H} β-catenin ^{LOF}	Pax3 ^{Sp2H/Cre} β-catenin ^{LOF/LOF}	Pax3 ^{Sp2H/Cre} β-catenin ^{LOF/+}	Pax3 ^{Sp2H/+} β-catenin ^{LOF/LOF}	Pax3 ^{Sp2H/+} β-catenin ^{LOF/+}
	β-catenin ^{Sp2H/+}	Pax3 ^{Sp2H} β-catenin ⁺	Pax3 ^{Sp2H/Cre} β-catenin ^{LOF/+}	Pax3 ^{Sp2H/Cre} β-catenin ^{+/+}	Pax3 ^{Sp2H/+} β-catenin ^{LOF/+}	Pax3 ^{Sp2H/+} β-catenin ^{+/+}
	β-catenin ⁺	Pax3 ⁺ β-catenin ^{LOF}	Pax3 ^{Cre/+} β-catenin ^{LOF/LOF}	Pax3 ^{Cre/+} β-catenin ^{LOF/+}	Pax3 ^{+/+} β-catenin ^{LOF/LOF}	Pax3 ^{+/+} β-catenin ^{LOF/+}
	β-catenin ⁺	Pax3 ⁺ β-catenin ⁺	Pax3 ^{Cre/+} β-catenin ^{LOF/+}	Pax3 ^{Cre/+} β-catenin ^{+/+}	Pax3 ^{+/+} β-catenin ^{LOF/+}	Pax3 ^{+/+} β-catenin ^{+/+}
	β-catenin ⁺	Pax3 ⁺ β-catenin ⁺	Pax3 ^{Cre/+} β-catenin ^{LOF/+}	Pax3 ^{Cre/+} β-catenin ^{+/+}	Pax3 ^{+/+} β-catenin ^{LOF/+}	Pax3 ^{+/+} β-catenin ^{+/+}

B

		Mouse 2: Pax3 ^{Cre/+} β-catenin ^{+/-}				
		Pax3 ^{Cre} β-catenin ⁻	Pax3 ^{Cre} β-catenin ⁺	Pax3 ⁺ β-catenin ⁻	Pax3 ⁺ β-catenin ⁺	
Mouse 1: Pax3	β-catenin ^{LOF/+}	Pax3 ^{Sp2H} β-catenin ^{LOF}	Pax3 ^{Sp2H/Cre} β-catenin ^{LOF/-}	Pax3 ^{Sp2H/Cre} β-catenin ^{LOF/+}	Pax3 ^{Sp2H/+} β-catenin ^{LOF/-}	Pax3 ^{Sp2H/+} β-catenin ^{LOF/+}
	β-catenin ^{Sp2H/+}	Pax3 ^{Sp2H} β-catenin ⁺	Pax3 ^{Sp2H/Cre} β-catenin ^{+/-}	Pax3 ^{Sp2H/Cre} β-catenin ^{+/+}	Pax3 ^{Sp2H/+} β-catenin ^{+/-}	Pax3 ^{Sp2H/+} β-catenin ^{+/+}
	β-catenin ⁺	Pax3 ⁺ β-catenin ^{LOF}	Pax3 ^{Cre/+} β-catenin ^{LOF/-}	Pax3 ^{Cre/+} β-catenin ^{LOF/+}	Pax3 ^{+/+} β-catenin ^{LOF/-}	Pax3 ^{+/+} β-catenin ^{LOF/+}
	β-catenin ⁺	Pax3 ⁺ β-catenin ⁺	Pax3 ^{Cre/+} β-catenin ^{+/-}	Pax3 ^{Cre/+} β-catenin ^{+/+}	Pax3 ^{+/+} β-catenin ^{+/-}	Pax3 ^{+/+} β-catenin ^{+/+}
	β-catenin ⁺	Pax3 ⁺ β-catenin ⁺	Pax3 ^{Cre/+} β-catenin ^{+/-}	Pax3 ^{Cre/+} β-catenin ^{+/+}	Pax3 ^{+/+} β-catenin ^{+/-}	Pax3 ^{+/+} β-catenin ^{+/+}

Pax3 ^{+/+} β-catenin ^{+/+}	Pax3 ^{+/-} β-catenin ^{-/-}
Pax3 ^{+/+} β-catenin ^{+/-}	Pax3 ^{-/-} β-catenin ^{+/+}
Pax3 ^{+/-} β-catenin ^{+/+}	Pax3 ^{-/-} β-catenin ^{+/-}
Pax3 ^{+/-} β-catenin ^{+/-}	Pax3 ^{-/-} β-catenin ^{-/-}

Figure 5.8: Punnett squares demonstrating the pooling of genotypes of offspring from the crosses Pax3^{Sp2H/+} β-catenin^{LOF/+} x Pax3^{Cre/+} β-catenin^{LOF/+} (A) and Pax3^{Sp2H/+} β-catenin^{LOF/+} x Pax3^{Cre/+} β-catenin^{+/-} (B). The key represents the genotype groups used in Figure 5.11. Colour coding demonstrates how the genotypes are distributed among the groups, as several genotypes have been pooled into the same genotype group (see Table 5.1).

Figure 5.9A: β -catenin loss-of-function causes minor delays in the closure of the posterior neuropore. Experimental litters were generated containing a mixture of genotypes through the crosses $Pax3^{Sp2H/+} \beta\text{-catenin}^{LOF/+}$ x $Pax3^{Cre/+} \beta\text{-catenin}^{LOF/+}$ and $Pax3^{Sp2H/+} \beta\text{-catenin}^{LOF/+}$ x $Pax3^{Cre/+} \beta\text{-catenin}^{LOF/+}$. The genotypes from both crosses have been pooled, and the data pooled accordingly (see **Figure 5.8** and **Table 5.1**). The graph begins in **Figure 5.9A** and continues in **Figure 5.9B**.

Data indicates that the only significant differences between embryos of different $\beta\text{-catenin}$ genotypes are seen between $Pax3^{+/-} \beta\text{-catenin}^{+/+}$ and $Pax3^{+/-} \beta\text{-catenin}^{-/-}$ embryos at 24-26 somite stage. Otherwise, embryos with the same $Pax3$ genotype but different $\beta\text{-catenin}$ genotypes show no significant differences in PNP size. However, significant differences are seen between embryos with the same $\beta\text{-catenin}$ genotype but different $Pax3$ genotypes (significant differences not shown on graph).

* $p < 0.05$. Significance was assessed using one-way ANOVA. Significant differences are only shown between genotypes with equivalent $Pax3$ genotype, but different $\beta\text{-catenin}$ genotype. Error bars show standard error.

9-11 somites stage – $Pax3^{+/+} \beta\text{-catenin}^{+/+}$; n = 3. $Pax3^{+/+} \beta\text{-catenin}^{+/-}$; n = 1. $Pax3^{+/-} \beta\text{-catenin}^{+/+}$; n = 2. $Pax3^{+/-} \beta\text{-catenin}^{+/-}$; n = 4. $Pax3^{+/-} \beta\text{-catenin}^{-/-}$; n = 1. $Pax3^{-/-} \beta\text{-catenin}^{+/+}$; n = 2. $Pax3^{-/-} \beta\text{-catenin}^{+/-}$; n = 12.

12-14 somite stage – $Pax3^{+/+} \beta\text{-catenin}^{+/+}$; n = 2. $Pax3^{+/+} \beta\text{-catenin}^{+/-}$; n = 1. $Pax3^{+/-} \beta\text{-catenin}^{+/+}$; n = 5. $Pax3^{+/-} \beta\text{-catenin}^{+/-}$; n = 2. $Pax3^{+/-} \beta\text{-catenin}^{-/-}$; n = 1. $Pax3^{-/-} \beta\text{-catenin}^{+/+}$; n = 2. $Pax3^{-/-} \beta\text{-catenin}^{+/-}$; n = 1.

15-17 somite stage – $Pax3^{+/+} \beta\text{-catenin}^{+/+}$; n = 5. $Pax3^{+/+} \beta\text{-catenin}^{+/-}$; n = 1. $Pax3^{+/-} \beta\text{-catenin}^{+/+}$; n = 7. $Pax3^{+/-} \beta\text{-catenin}^{+/-}$; n = 5. $Pax3^{+/-} \beta\text{-catenin}^{-/-}$; n = 1. $Pax3^{-/-} \beta\text{-catenin}^{+/+}$; n = 4. $Pax3^{-/-} \beta\text{-catenin}^{+/-}$; n = 3. $Pax3^{-/-} \beta\text{-catenin}^{-/-}$; n = 4.

18-20 somite stage – $Pax3^{+/+} \beta\text{-catenin}^{+/+}$; n = 7. $Pax3^{+/+} \beta\text{-catenin}^{+/-}$; n = 5. $Pax3^{+/-} \beta\text{-catenin}^{+/+}$; n = 12. $Pax3^{+/-} \beta\text{-catenin}^{+/-}$; n = 11. $Pax3^{+/-} \beta\text{-catenin}^{-/-}$; n = 4. $Pax3^{-/-} \beta\text{-catenin}^{+/+}$; n = 1. $Pax3^{-/-} \beta\text{-catenin}^{+/-}$; n = 4. $Pax3^{-/-} \beta\text{-catenin}^{-/-}$; n = 3.

Continued in the legend of **Figure 5.9B**.

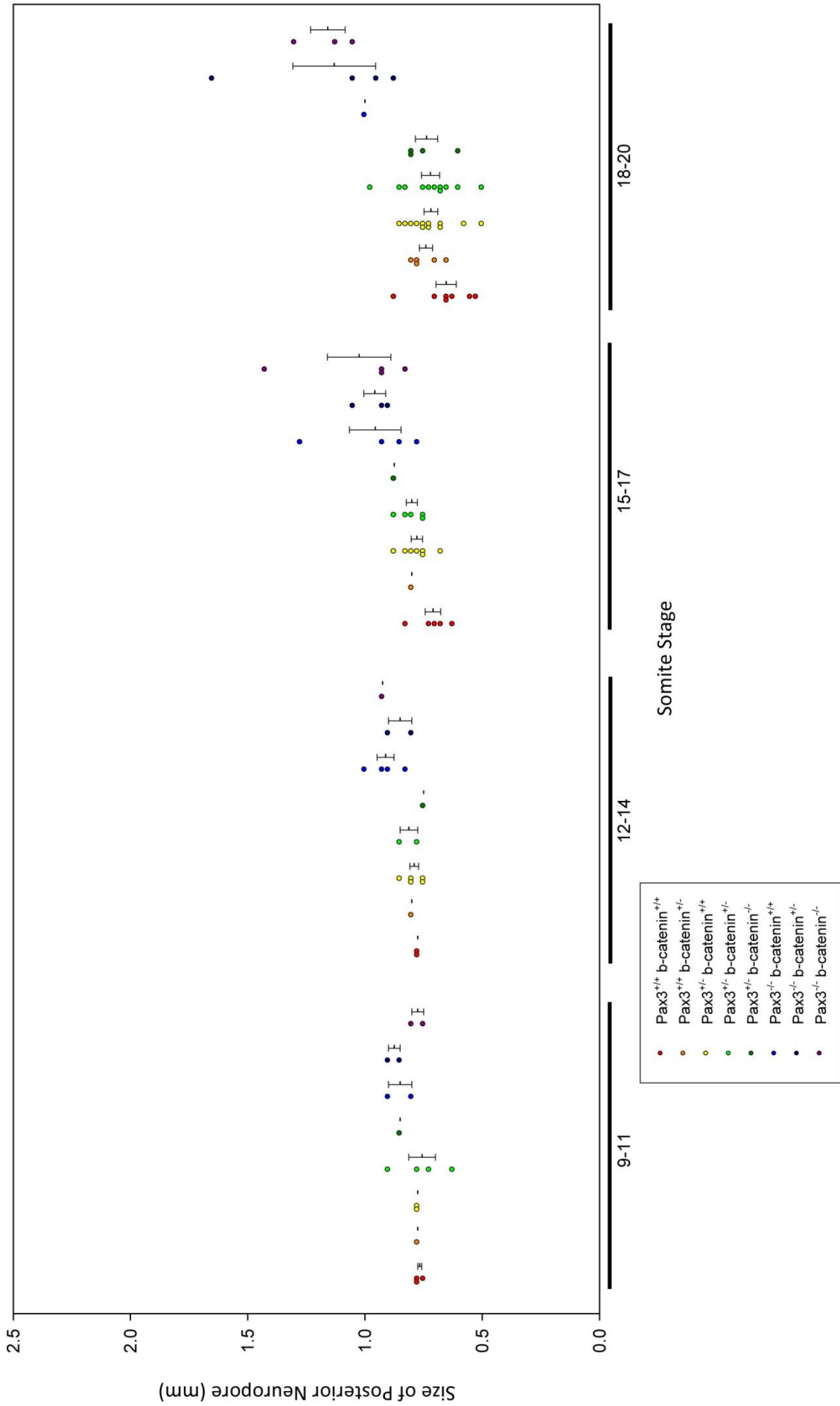
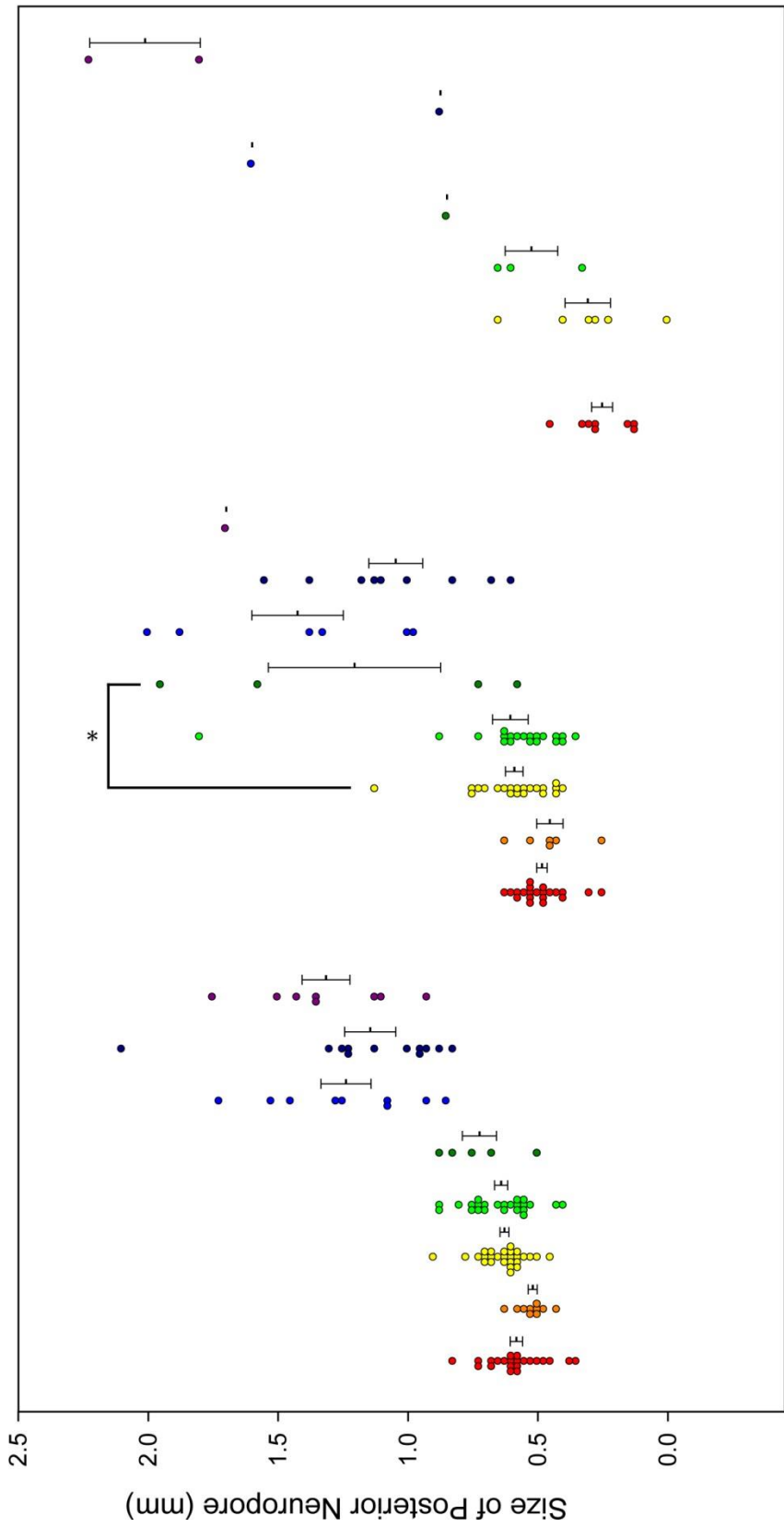


Figure 5.9B: β -catenin loss-of-function causes minor delays in the closure of the posterior neuropore, continued.

21-23 somites stage – Pax3^{+/+} β -catenin^{+/+}; n = 22. Pax3^{+/+} β -catenin^{+/-}; n = 10. Pax3^{+/-} β -catenin^{+/+}; n = 27. Pax3^{+/-} β -catenin^{+/-}; n = 24. Pax3^{+/-} β -catenin^{-/-}; n = 5. Pax3^{-/-} β -catenin^{+/+}; n = 9. Pax3^{-/-} β -catenin^{+/-}; n = 12. Pax3^{-/-} β -catenin^{-/-}; n = 8.

24-26 somite stage – Pax3^{+/+} β -catenin^{+/+}; n = 21. Pax3^{+/+} β -catenin^{+/-}; n = 6. Pax3^{+/-} β -catenin^{+/+}; n = 22. Pax3^{+/-} β -catenin^{+/-}; n = 20. Pax3^{+/-} β -catenin^{-/-}; n = 4. Pax3^{-/-} β -catenin^{+/+}; n = 6. Pax3^{-/-} β -catenin^{+/-}; n = 9. Pax3^{-/-} β -catenin^{-/-}; n = 1.

27-29 somite stage – Pax3^{+/+} β -catenin^{+/+}; n = 8. Pax3^{+/+} β -catenin^{+/-}; n = 0. Pax3^{+/-} β -catenin^{+/+}; n = 6. Pax3^{+/-} β -catenin^{+/-}; n = 3. Pax3^{+/-} β -catenin^{-/-}; n = 1. Pax3^{-/-} β -catenin^{+/+}; n = 1. Pax3^{-/-} β -catenin^{+/-}; n = 2.



21-23

24-26

27-29

Somite Stage

- Pax3^{+/+} b-catenin^{+/+}
- Pax3^{+/+} b-catenin^{-/-}
- Pax3^{-/-} b-catenin^{+/+}
- Pax3^{-/-} b-catenin^{-/-}
- Pax3^{-/-} b-catenin^{+/+}
- Pax3^{-/-} b-catenin^{-/-}
- Pax3^{-/-} b-catenin^{-/-}
- Pax3^{-/-} b-catenin^{-/-}

embryos at 24-26 somite stage (**Figure 5.9**). This could indicate that β -catenin LOF delays PNP closure in *Pax3* heterozygous mutant embryos.

The frequency of spina bifida has also been studied in embryos generated by the cross *Pax3*^{Sp2H/+} *β -catenin*^{LOF/+} x *Pax3*^{Cre/+} *β -catenin*^{LOF/+} (**Figure 5.10**). This allows observation of the long-term effects of β -catenin LOF on spinal neurulation. β -catenin LOF did not affect the frequency of spina bifida in *Pax3* mutant embryos. However, a significant increase in the frequency of spina bifida is seen in *Pax3*^{Cre/+} *β -catenin*^{LOF/LOF} embryos compared to *Pax3*^{+/-} *β -catenin*^{+/+} embryos, suggesting that β -catenin LOF affects spinal neurulation in *Pax3* heterozygous embryos.

5.1.2.2 β -catenin loss-of-function may decrease the frequency of exencephaly in *Pax3* mutant embryos

Cranial NT closure was studied to observe whether β -catenin LOF affects cranial neurulation (**Figure 5.11**). No significant differences in the frequency of exencephaly were observed between genotypes. However, the frequency in *Pax3*^{Sp2H/Cre} *β -catenin*^{LOF/LOF} embryos is 13%, compared to 45% in *Pax3*^{Sp2H/Cre} *β -catenin*^{+/+} embryos. This reduction suggests that β -catenin LOF may rescue the exencephaly seen in *Pax3* mutant mice. Proportion sample size calculation suggests that a sample size of 36 per genotype would be required to produce a significant difference.

5.1.2.3 The β -catenin loss-of-function phenotype

β -catenin LOF alters the phenotype of *Pax3* mutant embryos (**Figure 5.12**). *Pax3*^{Sp2H/Cre} *β -catenin*^{LOF/LOF} embryos frequently have spina bifida, but exencephaly appears to be less common in *Pax3*^{Sp2H/Cre} *β -catenin*^{LOF/LOF} embryos than in *Pax3*^{Sp2H/Cre} *β -catenin*^{+/+} embryos. In *Pax3*^{Sp2H/Cre} *β -catenin*^{LOF/LOF} embryos which have a closed cranial NT, the cranial region may appear slightly misshapen, and haemorrhage is common in both the cranial NT and the spinal NT (**Figure 5.12C**). Reduced canonical Wnt signalling in the CNS has been previously shown to cause haemorrhage and abnormalities in angiogenesis (Daneman et al., 2009). Therefore, the haemorrhage seen in *Pax3*^{Sp2H/Cre} *β -catenin*^{LOF/LOF} may be due to the reduction in canonical Wnt signalling affecting angiogenesis, rather than an interaction between *Pax3* and the canonical Wnt signalling pathway.

The phenotype of *Pax3*^{Sp2H/Cre} *β -catenin*^{LOF/+} embryos resembles that of *Pax3*^{Sp2H/Cre} *β -catenin*^{+/+} embryos. This suggests that one copy of wild type β -catenin is able to compensate for β -catenin LOF in the NT.

Figure 5.10: β -catenin loss-of-function increases the frequency of spina bifida in Pax3 heterozygotes. Experimental litters were generated containing a mixture of genotypes through the cross $Pax3^{Sp2H/+} \beta\text{-catenin}^{LOF/+} \times Pax3^{Cre/+} \beta\text{-catenin}^{LOF/+}$. Spina bifida was defined as an open spinal NT at 30+ somite stage.

A significant increase in the frequency of spina bifida is seen in $Pax3^{Cre/+} \beta\text{-catenin}^{LOF/LOF}$ embryos compared to $Pax3^{+/-} \beta\text{-catenin}^{+/+}$ embryos. However, β -catenin genotype has no effect on the frequency of spina bifida in $Pax3^{Sp2H/Cre}$ embryos; there are no significant differences in spina bifida frequency between $Pax3^{Sp2H/Cre} \beta\text{-catenin}^{+/+}$, $Pax3^{Sp2H/Cre} \beta\text{-catenin}^{LOF/+}$ and $Pax3^{Sp2H/Cre} \beta\text{-catenin}^{LOF/LOF}$ embryos. However, since the frequency of spina bifida is 100% in $Pax3^{Sp2H/Cre} \beta\text{-catenin}^{+/+}$ embryos β -catenin LOF cannot not increase the frequency of the defect.

*** $p < 0.001$. Significance was assessed using the Fisher Exact Test. Significant differences are only shown between genotypes with equivalent Pax3 genotype, but different β -catenin genotypes.

$Pax3^{+/+} \beta\text{-catenin}^{+/+}$; n = 35. $Pax3^{+/-} \beta\text{-catenin}^{+/+}$; n = 42. $Pax3^{Cre/+} \beta\text{-catenin}^{LOF/+}$; n = 18. $Pax3^{Sp2H/Cre} \beta\text{-catenin}^{LOF/LOF}$; n = 10. $Pax3^{Sp2H/Cre} \beta\text{-catenin}^{LOF/+}$; n = 14. $Pax3^{Sp2H/Cre} \beta\text{-catenin}^{LOF/LOF}$; n = 11.

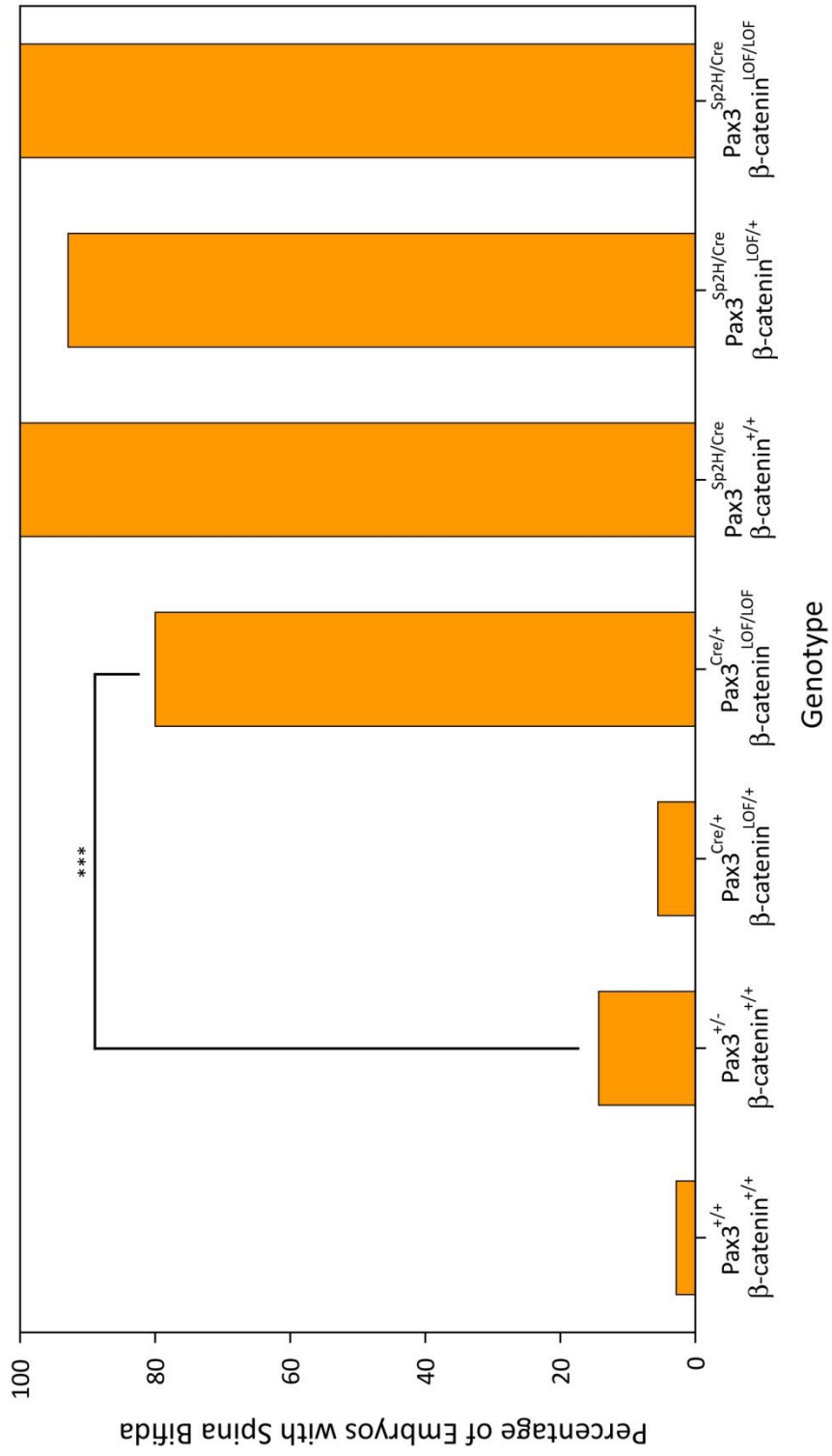
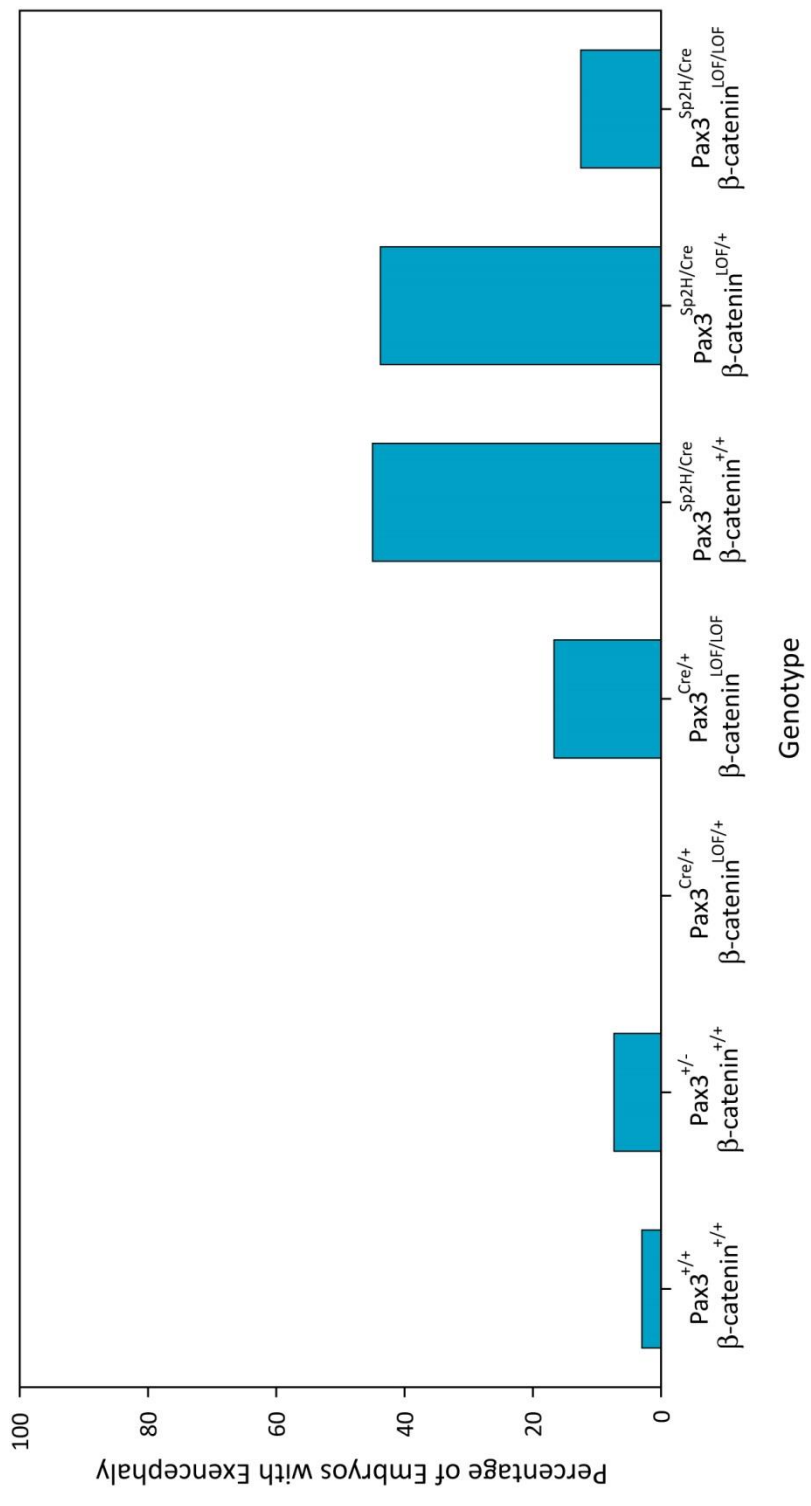


Figure 5.11: β -catenin loss-of-function decreases the frequency of exencephaly in Pax3 mutant embryos. Experimental litters were generated containing a mixture of genotypes through the cross $Pax3^{Sp2H/+} \beta\text{-catenin}^{LOF/+}$ x $Pax3^{Cre/+} \beta\text{-catenin}^{LOF/+}$. Exencephaly was defined as an open cranial NT at the 18 somite stage or later.

Significance is assessed between embryos of a particular genotype and embryos of equivalent Pax3 genotype, but wild type β -catenin. No significant differences are seen in the frequency of exencephaly between genotypes. However, there is a decrease in the frequency of exencephaly in $Pax3^{Sp2H/Cre} \beta\text{-catenin}^{LOF/LOF}$ embryos when compared to $Pax3^{Sp2H/Cre} \beta\text{-catenin}^{+/+}$ embryos.

Significance was assessed using either the Fisher Exact Test or the Chi Square test, depending on the number of samples being analysed.

$Pax3^{+/+} \beta\text{-catenin}^{+/+}$; n = 67. $Pax3^{+/-} \beta\text{-catenin}^{+/+}$; n = 88. $Pax3^{Cre/+} \beta\text{-catenin}^{LOF/+}$; n = 31. $Pax3^{Cre/+} \beta\text{-catenin}^{LOF/LOF}$; n = 18. $Pax3^{Sp2H/Cre} \beta\text{-catenin}^{+/+}$; n = 20. $Pax3^{Sp2H/Cre} \beta\text{-catenin}^{LOF/+}$; n = 32. $Pax3^{Sp2H/Cre} \beta\text{-catenin}^{LOF/LOF}$; n = 16.



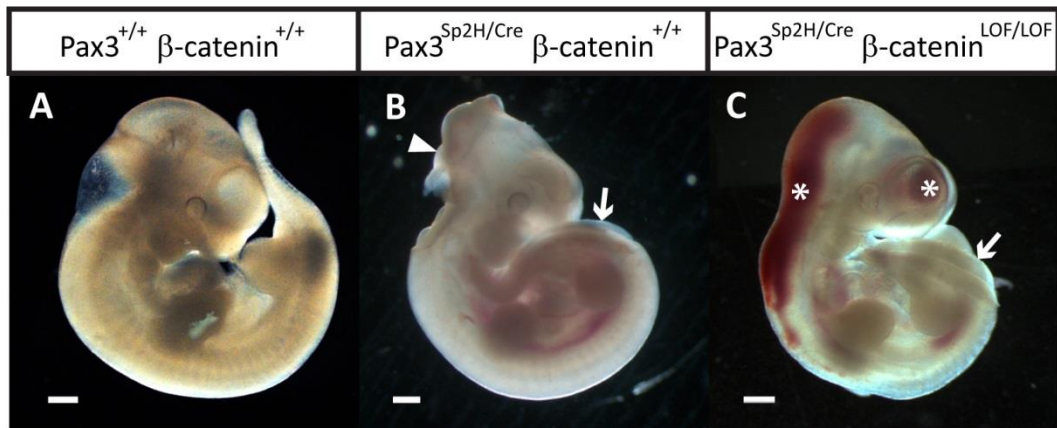


Figure 5.12: Phenotype of a $Pax3^{Sp2H/Cre} \beta\text{-catenin}^{LOF/LOF}$ embryo. This image shows a $Pax3^{+/+} \beta\text{-catenin}^{+/+}$ embryo for reference (A), a typical $Pax3^{Sp2H/Cre} \beta\text{-catenin}^{+/+}$ embryo (B), and a typical $Pax3^{Sp2H/Cre} \beta\text{-catenin}^{LOF/LOF}$ embryo (C). All embryos are at E10.5. All genotypes were generated through the cross $Pax3^{Sp2H/+} \beta\text{-catenin}^{LOF/+} \times Pax3^{Cre/+} \beta\text{-catenin}^{LOF/+}$. Scale bars indicate 500 μm .

The arrowhead indicates the cranial NT, which is open in the $Pax3^{Sp2H/Cre} \beta\text{-catenin}^{+/+}$ embryo (B) and closed in the $Pax3^{+/+} \beta\text{-catenin}^{+/+}$ (A) and $Pax3^{Sp2H/Cre} \beta\text{-catenin}^{LOF/LOF}$ embryos (C). The arrow indicates the spinal NT, which is closed in the $Pax3^{+/+} \beta\text{-catenin}^{+/+}$ embryo (A), but open in both the $Pax3^{Sp2H/Cre} \beta\text{-catenin}^{+/+}$ (B) and $Pax3^{Sp2H/Cre} \beta\text{-catenin}^{LOF/LOF}$ (C) embryos. The asterisk indicates haemorrhage in the hindbrain, forebrain and spinal NT of the $Pax3^{Sp2H/Cre} \beta\text{-catenin}^{LOF/LOF}$ embryo (B).

5.1.2.4 An inhibitor of Wnt signalling has no effect on the frequency of exencephaly in cultured $Pax3$ mutant embryos

The aim of this experiment was to chemically inhibit canonical Wnt signalling to investigate whether reduced Wnt signalling has an effect on the development of exencephaly in *Spotch* embryos. The inhibitor XAV939 was used in embryo culture to achieve the knock-down of canonical Wnt signalling during NT closure.

Xav939 inhibits canonical Wnt signalling through the stabilisation of Axin, which promotes β -catenin degradation (see section 1.6.2). The enzymes tankyrase 1 and tankyrase 2 bind and promote the degradation of Axin. XAV939 stabilises Axin by inhibiting the activity of the tankyrase enzymes (Huang et al., 2009).

Embryos were cultured in concentrations of 25 μM and 100 μM XAV939, to estimate a threshold concentration above which the inhibitor causes generalised toxic effects. These toxic effects included stunted growth of the tail bud, exencephaly, tailbud externalised from the yolk sac, reduced yolk sac circulation, small somites, and failure of the embryos to turn during development. Control embryos were cultured in an equivalent concentration of vehicle (DMSO). At 100 μM XAV939 all the embryos (9/9) showed severe abnormalities caused by generalised toxicity. At 25 μM XAV939 17/30 embryos still showed abnormalities due to generalised toxicity. Therefore, further tests were carried out to further refine the dose required. Cultures were carried out using doses of 5 μM , 10 μM , 15 μM and 20 μM XAV939. Abnormalities were seen in 2/3 embryos at 20 μM , 1/3 embryos at 15 μM , 0/4 at 10 μM , and 2/4 embryos at 5 μM . Although abnormalities were seen at 5 μM Xav939, it is possible that these were due to suboptimal culture conditions, rather than toxic effects from the inhibitor. A concentration of 10 μM XAV939 was chosen for use in embryo culture, as this was the highest concentration tested which produced no generalised toxic effects.

XAV939 had no effect on the development of exencephaly in *Spotch* embryos. A very similar proportion of Sp^{2H}/Sp^{2H} embryos developed exencephaly in inhibitor culture as in the control culture (**Figure 5.13**).

In order to determine if the lack of phenotypic difference was a genuine effect or could be due to lack of Wnt inhibition, $Sp^{2H}/+$ embryos were assessed for inhibition of canonical Wnt signalling as a result of culture in XAV939, compared to culture in vehicle. *In situ* hybridisation was used to detect *Axin2* expression, but no differences were identified between culture conditions (**Figure 5.14A and B**). Relative expressions of the genes *Axin2* and *Cdx2* were also analysed by RT-qPCR, but there were no significant differences in the expression level of either gene when comparing culture conditions (**Figure 5.14C and D**).

5.1.3 The effect of β -catenin loss-of-function on the development of the neural crest in *Pax3* mutant embryos

The effect of β -catenin GOF on NC development and differentiation was studied in detail in the previous chapter (see section 4.1.7). Therefore, study of β -catenin LOF was performed on the NC for comparison. The effects of β -catenin LOF have been reported previously in the NC using *Wnt1-Cre* (Brault et al., 2001). A study using *Pax3-Cre* could provide information about the effect of suppressing β -catenin function in the *Pax3* expression domain in comparison to the *Wnt1* expression domain, enabling comparison of the roles of β -catenin at different developmental times and in slightly different regions. It also enables study of potential interactions of β -catenin LOF with *Pax3* heterozygosity.

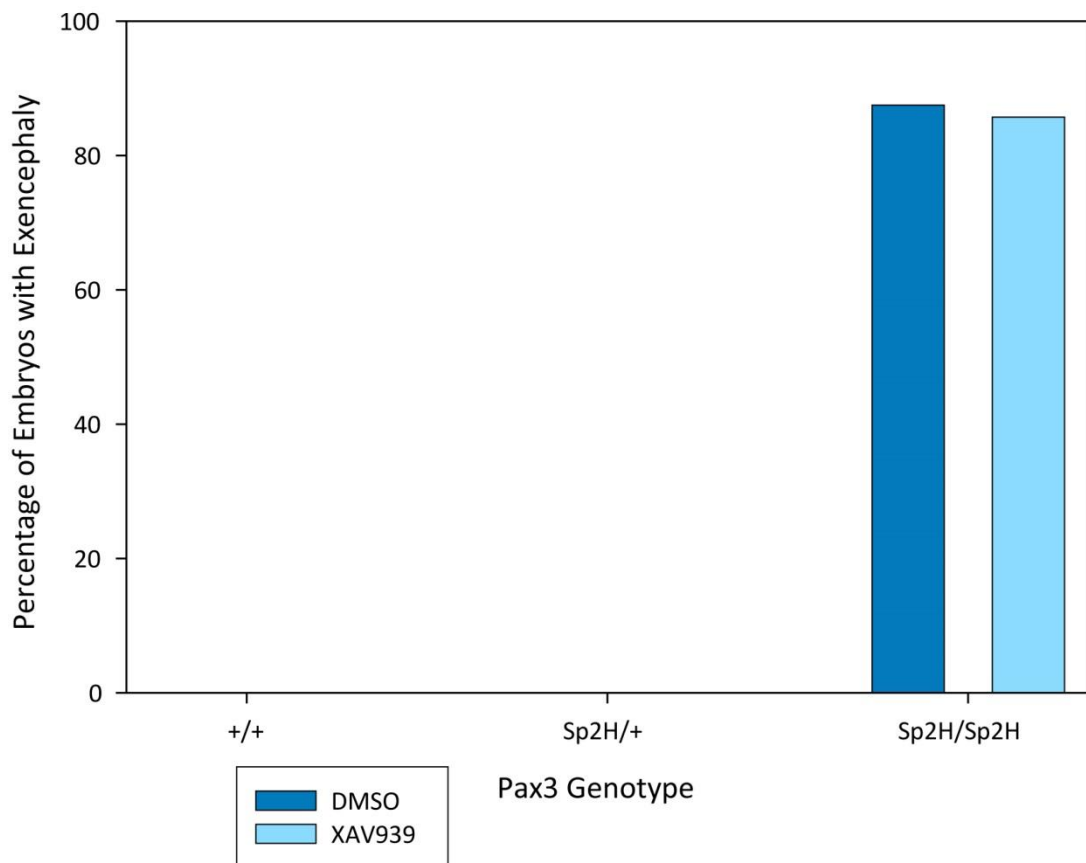


Figure 5.13: Culture of *Spitch* embryos with XAV939 does not affect the frequency of exencephaly. Experimental litters were generated containing a mixture of genotypes through intercross of $Sp^{2H}/+$ embryos. Embryos were cultured through the period of NT closure in the presence of either canonical Wnt inhibitor (XAV939) at $10\mu\text{M}$ concentration, or vehicle (DMSO) at an equivalent concentration. Exencephaly was defined as an open cranial NT at the 18 somite stage or later.

No significant differences were observed in the frequency of exencephaly when comparing culture conditions within a genotype. None of the $+/+$ or $Sp^{2H}/+$ embryos developed exencephaly in either culture condition, and very similar proportions of Sp^{2H}/Sp^{2H} embryos developed exencephaly in vehicle and inhibitor culture conditions.

Significance was assessed using the Fisher Exact Test.

DMSO – $+/+$: $n = 4$. $Sp^{2H}/+$: $n = 11$. Sp^{2H}/Sp^{2H} : $n = 8$. XAV939 – $+/+$: $n = 3$. $Sp^{2H}/+$: $n = 16$. Sp^{2H}/Sp^{2H} : $n = 7$.

Figure 5.14: Culture in 10 μ M XAV939 has no detectable effect on canonical Wnt signalling. Experimental litters were generated containing a mixture of genotypes through the cross $Sp^{2H}/Sp^{2H} \times Sp^{2H}/Sp^{2H}$. Whole mount *in situ* hybridisation for *Axin2* was carried out on $Sp^{2H}/+$ embryos at the 21-26 somite stage (**A** and **B**). RT-qPCR was carried out on $Sp^{2H}/+$ embryos at the 24-28 somite stage (**C** and **D**). Scale bars represent 500 μ m.

No differences in the expression of *Axin2* were detected using *in situ* hybridisation (**A** and **B**) when comparing embryos which have undergone treatment with vehicle (DMSO, **A**) or inhibitor (10 μ M XAV939, **B**). DMSO: n = 3. XAV939: n = 4.

RT-qPCR was carried out on whole embryo RNA preparations using the genes *Axin2* and *Cdx2* as indicators of canonical Wnt signalling levels (**C** and **D**) (n = 4). *GAPDH* was used as the housekeeping gene for normalisation. No significant differences were detected in relative expression levels of either *Axin2* (**C**) or *Cdx2* (**D**) between embryos which have undergone treatment with vehicle or inhibitor. n = 4 per condition.

Significance was assessed using the t-test. Error bars indicate standard error.

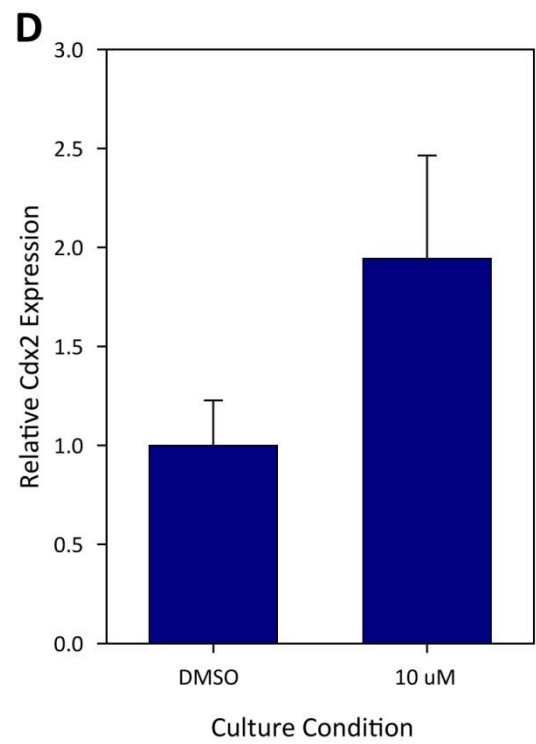
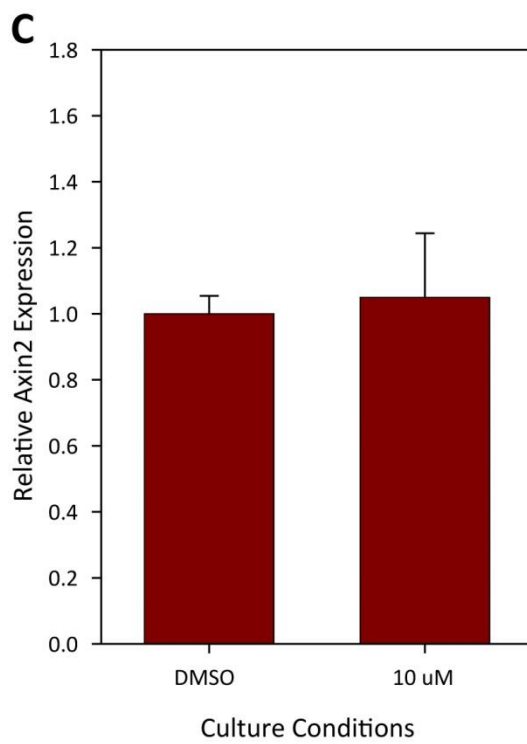
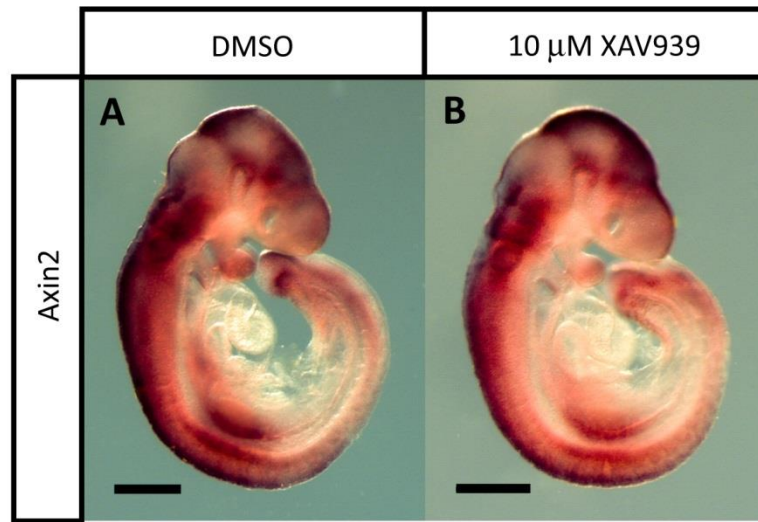


Figure 5.15: β -catenin loss-of-function disrupts expression of *ErbB3*. Experimental litters were generated containing a mixture of genotypes through the cross *Pax3^{Sp2H/+} β -catenin^{GOF/+}* x *Pax3^{Cre/+} β -catenin^{LOF/+}*. Whole mount *in situ* hybridisation for *ErbB3* was carried out on embryos of multiple genotypes to mark the NC. The expression was studied at the 30+ somite stage (E10.5). Scale bars represent 500 μ m. **A-E** show whole embryo views, and **A'-E'** show zoomed in images of the spinal regions.

Wild type (*Pax3^{+/+} β -catenin^{+/+}*) embryos (**A** and **A'**) show *ErbB3* expression in the DRG (black arrowhead), vagus nerve (blue arrowhead), trigeminal ganglia (black arrow), and otic vesicle (blue arrow).

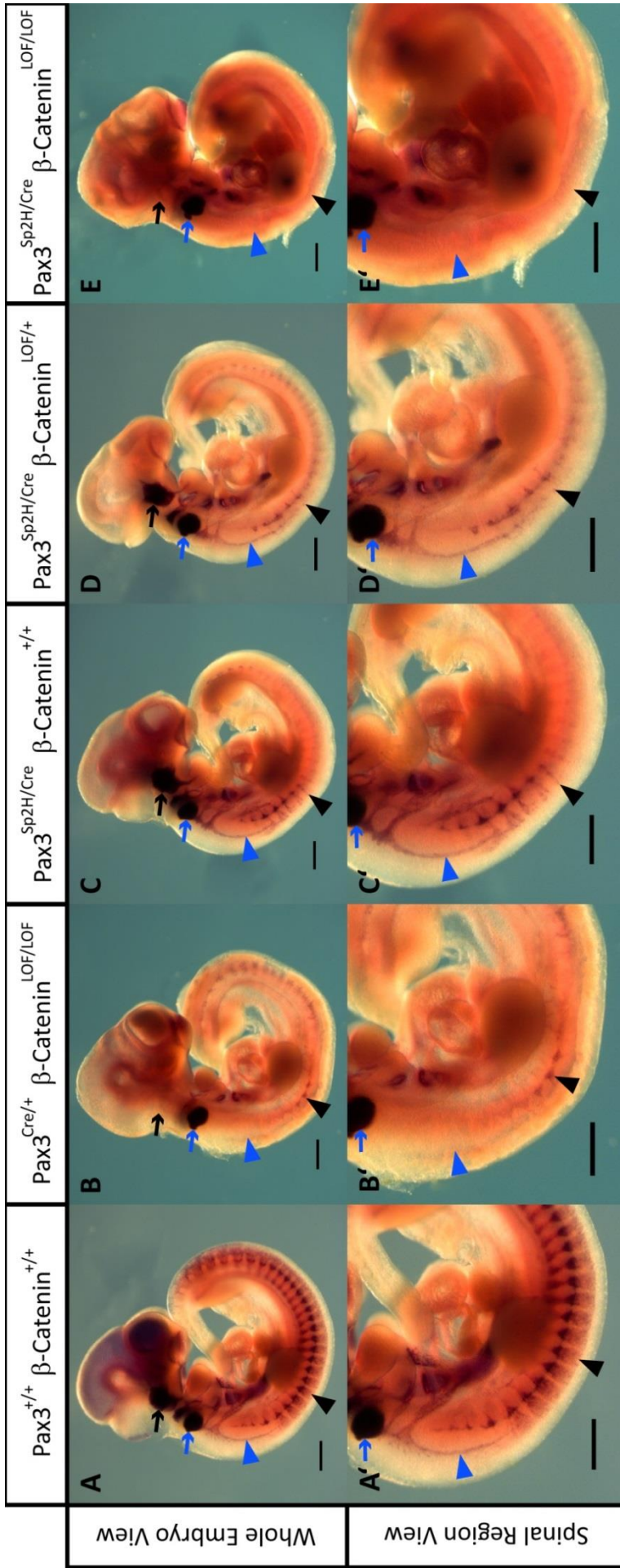
Pax3^{Sp2H/Cre} β -catenin^{+/+} embryos (**C** and **C'**) show weaker staining, which suggests lower *ErbB3* expression. The staining in the DRG is much weaker compared to wild type, but is still present, particularly more rostrally. Segmentation in the DRG is still apparent, and expression in the vagus nerve, trigeminal ganglia and otic vesicle is present.

Pax3^{Sp2H/Cre} β -catenin^{LOF/+} embryos (**D** and **D'**) show very similar *ErbB3* expression to *Pax3^{Sp2H/Cre} β -catenin^{+/+}* embryos.

Pax3^{Cre/+} β -catenin^{LOF/LOF} embryos (**B** and **B'**) show *ErbB3* expression in the otic vesicle faint, and also faint, but still segmented expression in the DRG. However, *ErbB3* expression in the vagus nerve and trigeminal ganglia is completely absent.

Pax3^{Sp2H/Cre} β -catenin^{LOF/LOF} embryos (**E** and **E'**) show similar *ErbB3* expression to *Pax3^{Cre/+} β -catenin^{LOF/LOF}* embryos; expression is present in the otic vesicle, but absent from the trigeminal ganglia and the vagus nerve. However, additionally expression is absent from the DRG.

Pax3^{+/+} β -catenin^{LOF/LOF}; n = 3. *Pax3^{Cre/+} β -catenin^{LOF/LOF}*; n = 2. *Pax3^{Sp2H/Cre} β -catenin^{+/+}*; n = 3. *Pax3^{Sp2H/Cre} β -catenin^{LOF/+}*; n = 3. *Pax3^{Sp2H/Cre} β -catenin^{LOF/LOF}*; n = 3.



ErbB3 expression was used as a marker for the NC (**Figure 5.15**). Study of embryos at the 30+ somite stage showed that *Pax3*^{Sp2H/Cre} *β-catenin*^{+/+} embryos had weaker expression throughout the embryo compared to *Pax3*^{+/+} *β-catenin*^{+/+} embryos. However, *β-catenin* LOF resulted in the absence of *ErbB3* expression in the trigeminal ganglia and the vagus nerve. Additionally, expression in the DRG was much reduced in *Pax3*^{Cre/+} *β-catenin*^{LOF/LOF} embryos compared with *Pax3*^{+/+} *β-catenin*^{+/+} and *Pax3*^{Cre/+} *β-catenin*^{+/+} embryos, and was absent in *Pax3*^{Sp2H/Cre} *β-catenin*^{LOF/LOF} embryos.

5.1.4 Pax3 signalling is reduced by *β-catenin* loss-of-function

As discussed in the previous chapter, evidence has suggested that canonical Wnt signalling may act upstream of *Pax3* signalling (Zhao et al., 2014). Therefore, expression levels of *Pax3* were studied to determine whether they were influenced by *β-catenin* LOF (**Figure 5.16**). RT-qPCR was carried out using two different sets of primers to amplify the *Pax3* gene. Only *Pax3*^{Cre/+} *β-catenin*^{+/+} embryos were used as *Pax3* heterozygotes to eliminate the chance of error caused by possible differences in expression between the *Pax3*^{Cre} and *Pax3*^{Sp2H} alleles, and because the primer pairs used are only able to detect one of the two alleles.

Pax3 primer pair 1 detects *Pax3*⁺ and *Pax3*^{Cre}, but not *Pax3*^{Sp2H} (as previously described in section 4.1.8). As would be expected, there is no difference in *Pax3* expression between *Pax3*^{+/+} *β-catenin*^{+/+} and *Pax3*^{Cre/+} *β-catenin*^{+/+} embryos, and *Pax3*^{Sp2H/Cre} *β-catenin*^{+/+} embryos show a significant reduction in *Pax3* expression when compared to *Pax3*^{+/+} *β-catenin*^{+/+} embryos (**Figure 5.16A**). However, there is also a significant reduction in *Pax3* expression of *Pax3*^{Cre/+} *β-catenin*^{LOF/LOF} embryos compared to *Pax3*^{Cre/+} *β-catenin*^{+/+} embryos, which is attributable to the presence of the *β-catenin*^{LOF} allele. There is also a reduction in *Pax3*^{Sp2H/Cre} *β-catenin*^{LOF/LOF} embryos compared to *Pax3*^{Sp2H/Cre} *β-catenin*^{+/+} embryos, although this difference does not reach significance. Together these data suggest that *β-catenin* LOF causes downregulation of *Pax3* expression.

Pax3 primer pair 2 detects *Pax3*⁺ and *Pax3*^{Sp2H}, but not *Pax3*^{Cre} (as previously described in section 4.1.8). As would be expected, there is a significant reduction in *Pax3* expression in *Pax3*^{Sp2H/Cre} *β-catenin*^{+/+} embryos when compared to *Pax3*^{+/+} *β-catenin*^{+/+} embryos (**Figure 5.16B**). However, a significant reduction in *Pax3* expression would be expected in *Pax3*^{Cre/+} *β-catenin*^{+/+} embryos compared to *Pax3*^{+/+} *β-catenin*^{+/+} embryos, but this was not observed, although a small reduction in expression is apparent. There is significantly decreased *Pax3* expression in *Pax3*^{Cre/+} *β-catenin*^{LOF/LOF} embryos compared to *Pax3*^{Cre/+} *β-catenin*^{+/+} embryos.

Interestingly, the data from the *β-catenin* GOF cross shows that *Pax3*^{Cre/+} *β-catenin*^{+/+} embryos have around half the *Pax3* expression of *Pax3*^{+/+} *β-catenin*^{+/+} embryos shown by RT-qPCR with

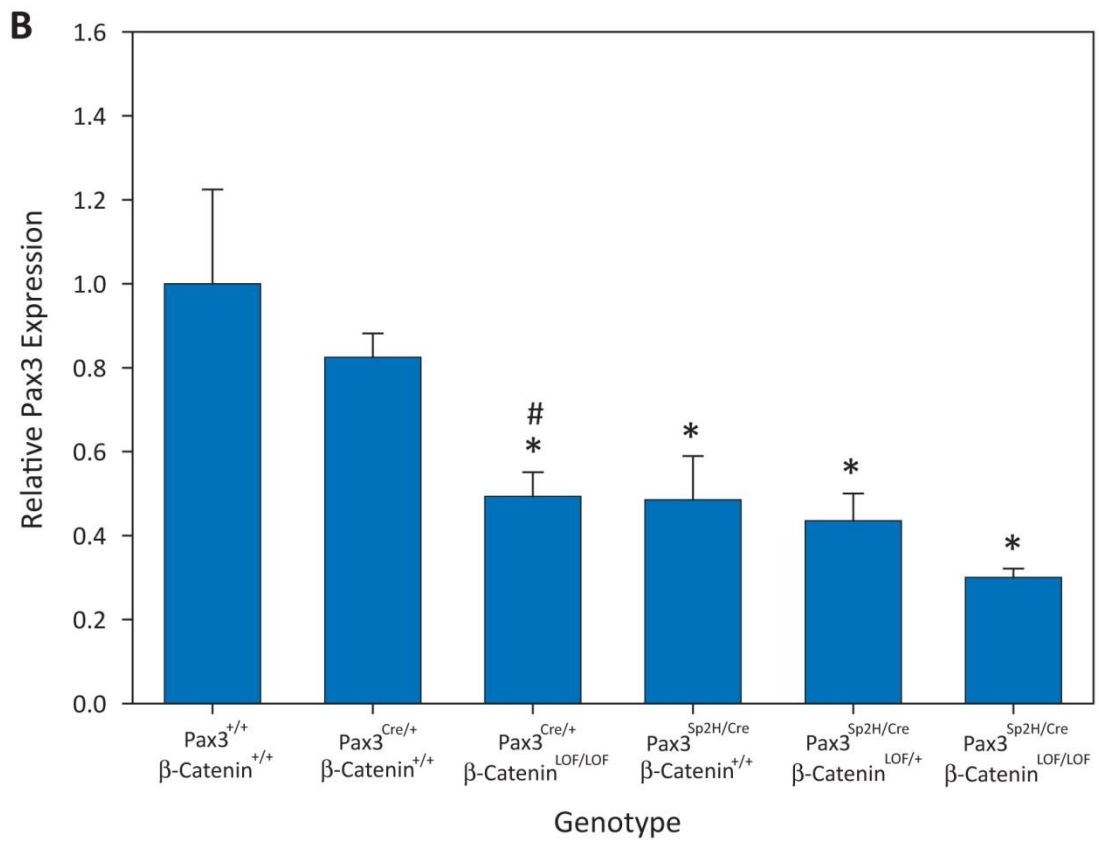
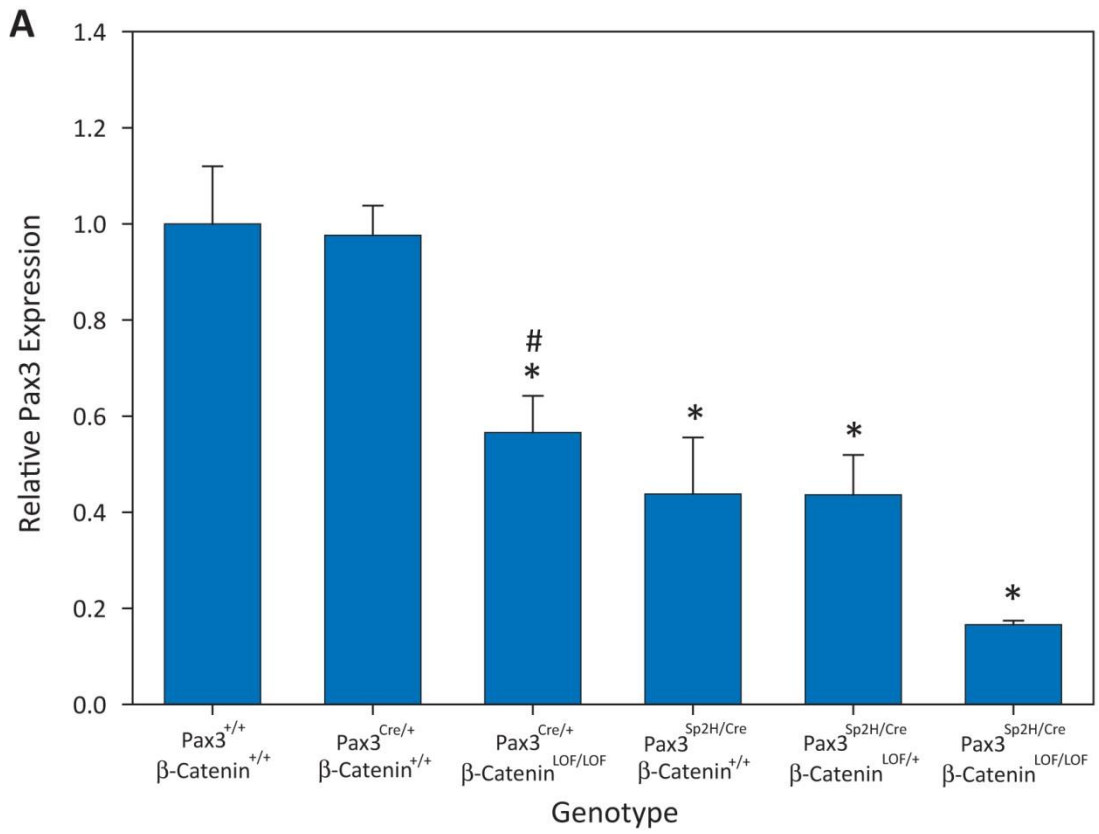
Figure 5.16: β -catenin loss-of-function reduces Pax3 expression levels. Experimental litters were generated containing a mixture of genotypes through the cross $Pax3^{Sp2H/+} \beta\text{-catenin}^{LOF/+}$ x $Pax3^{Cre/+} \beta\text{-catenin}^{LOF/+}$. RT-qPCR was carried out on embryos of multiple genotypes at the 23-24 somite stage. * indicates significant difference from $Pax3^{+/+} \beta\text{-catenin}^{+/+}$, and # indicates statistical significance from $Pax3^{Cre/+} \beta\text{-catenin}^{+/+}$.

Graph **A** shows RT-qPCR results using Pax3 primer pair 1 which detects Pax3⁺ and Pax3^{Cre}, but not Pax3^{Sp2H}. A significant reduction in Pax3 expression is seen in $Pax3^{Cre/+} \beta\text{-catenin}^{LOF/LOF}$, $Pax3^{Sp2H/Cre} \beta\text{-catenin}^{+/+}$, $Pax3^{Sp2H/Cre} \beta\text{-catenin}^{LOF/+}$, and $Pax3^{Sp2H/Cre} \beta\text{-catenin}^{LOF/LOF}$ embryos when compared to $Pax3^{+/+} \beta\text{-catenin}^{+/+}$ embryos. A significant reduction is also seen in $Pax3^{Cre/+} \beta\text{-catenin}^{LOF/LOF}$ embryos when compared to $Pax3^{Cre/+} \beta\text{-catenin}^{+/+}$ embryos. There is also a reduction in Pax3 expression in $Pax3^{Sp2H/Cre} \beta\text{-catenin}^{LOF/LOF}$ embryos when compared to $Pax3^{Sp2H/Cre} \beta\text{-catenin}^{+/+}$ embryos, but this difference does not reach statistical significance.

Graph **B** shows RT-qPCR results using Pax3 primer pair 2 which detects Pax3⁺ and Pax3^{Sp2H}, but not Pax3^{Cre}. A significant reduction in Pax3 expression is seen in $Pax3^{Cre/+} \beta\text{-catenin}^{LOF/LOF}$, $Pax3^{Sp2H/Cre} \beta\text{-catenin}^{+/+}$, $Pax3^{Sp2H/Cre} \beta\text{-catenin}^{LOF/+}$, and $Pax3^{Sp2H/Cre} \beta\text{-catenin}^{LOF/LOF}$ embryos when compared to $Pax3^{+/+} \beta\text{-catenin}^{+/+}$ embryos. A significant reduction is also seen in $Pax3^{Cre/+} \beta\text{-catenin}^{LOF/LOF}$ embryos when compared to $Pax3^{Cre/+} \beta\text{-catenin}^{+/+}$ embryos. There is a reduction in Pax3 expression in $Pax3^{Sp2H/Cre} \beta\text{-catenin}^{LOF/LOF}$ embryos when compared to $Pax3^{Sp2H/Cre} \beta\text{-catenin}^{+/+}$ embryos, but this difference does not reach statistical significance.

*/# $p < 0.05$. Significance compared to $Pax3^{+/+} \beta\text{-catenin}^{+/+}$ was determined using one way ANOVA followed by the Holm Sidak test. Pairwise significance was determined using the t-test. Only significance between relevant data is shown. Error bars show standard error.

$Pax3^{+/+} \beta\text{-catenin}^{+/+}$: n = 3. $Pax3^{Cre/+} \beta\text{-catenin}^{+/+}$: n = 3. $Pax3^{Cre/+} \beta\text{-catenin}^{LOF/LOF}$: n = 2. $Pax3^{Sp2H/Cre} \beta\text{-catenin}^{+/+}$: n = 3. $Pax3^{Sp2H/Cre} \beta\text{-catenin}^{LOF/+}$: n = 3. $Pax3^{Sp2H/Cre} \beta\text{-catenin}^{LOF/LOF}$: n = 3.



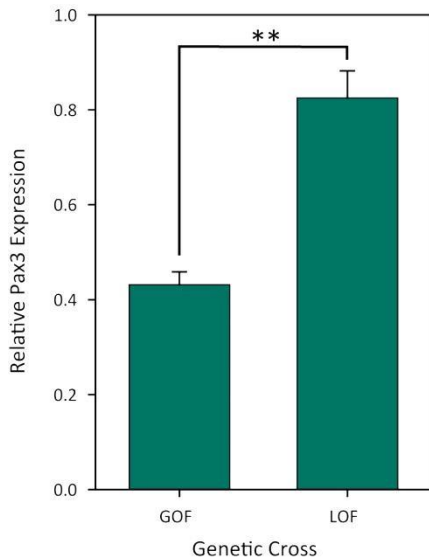


Figure 5.17: $Pax3^{Cre/+}$ β -catenin^{+/+} embryos from two different genetic crosses have significantly different expression levels of $Pax3$. GOF refers to embryos from the cross $Pax3^{Sp2H/+}$ β -catenin^{GOF/+} x $Pax3^{Cre/+}$ β -catenin^{+/+}, and LOF refers to embryos from the cross $Pax3^{Sp2H/+}$ β -catenin^{LOF/+} x $Pax3^{Cre/+}$ β -catenin^{LOF/+}. RT-qPCR was carried out on 23-24 somite stage $Pax3^{Cre/+}$ β -catenin^{+/+} embryos using RNA prepared from whole embryos. *GAPDH* was used as a housekeeping gene for normalisation, and *Pax3* primer pair 2 was used to determine relative *Pax3* expression. *Pax3* expression for embryos within each cross was normalised using *Pax3* expression of wild type embryos from the same cross. n = 3 for each group.

A significant decrease in *Pax3* expression is seen when comparing $Pax3^{Cre/+}$ β -catenin^{+/+} embryos from the cross $Pax3^{Sp2H/+}$ β -catenin^{GOF/+} x $Pax3^{Cre/+}$ β -catenin^{+/+} to embryos of the same genotype from the cross $Pax3^{Sp2H/+}$ β -catenin^{LOF/+} x $Pax3^{Cre/+}$ β -catenin^{LOF/+}.

** p < 0.01. Significance was calculated using the t-test. Error bars show standard error.

Pax3 primer pair 2. When the data is normalised to $Pax3^{+/+}$ β -catenin^{+/+} embryos from the relevant genetic cross, comparing $Pax3^{Cre/+}$ β -catenin^{+/+} embryos from the β -catenin GOF and LOF crosses shows a significant difference in *Pax3* expression (**Figure 5.17**). This could be due to slight differences in genetic background, or could be due to random variation.

5.2 Discussion

5.2.1 The β -catenin Loss-of-Function allele

The β -catenin LOF allele used in this research was first developed and described by the Kemler lab (Brault et al., 2001).

As discussed previously (see section 1.6.3.2) β -catenin is known to play a role in adherens junctions in addition to canonical Wnt signalling. Therefore it is possible that β -catenin LOF affects both functions, and not just the canonical Wnt signalling pathway. Again, study of the adherens junctions themselves could provide information about the integrity and density of the junctions in tissues with β -catenin LOF.

Two different genetic crosses were used for study of embryos with β -catenin LOF. The initial cross carried out was $Pax3^{Sp2H/+} \beta\text{-catenin}^{LOF/+} \times Pax3^{Cre/+} \beta\text{-catenin}^{+/-}$. However, the mice used for this cross did not breed well, and had small litters. Therefore, the cross was changed to $Pax3^{Sp2H/+} \beta\text{-catenin}^{LOF/+} \times Pax3^{Cre/+} \beta\text{-catenin}^{LOF/+}$. The mice used for this cross bred better and had larger litters. Mice carrying the $\beta\text{-catenin}^{LOF/+}$ allele had the same genetic background as mice carrying the $\beta\text{-catenin}^{+/-}$ allele (see section 2.4.2), so there was no change in genetic background in the new cross. However, it is possible that the difference in allele use could give slightly different results. Figure legends give information about which genetic cross was used for the experiments. The majority of the experiments use the second genetic cross described here. The embryos of both crosses were pooled for **Figure 5.9**, as analysis showed no significant differences in the rates of NTDs between embryos from the different crosses (see **Table 5.1**). However, sample numbers are relatively low, so it is possible that differences in the rates of NTDs would be evident with larger samples. This pooling was not ideal, but it allowed for more thorough analysis of the existing data.

In addition, genotypes were pooled within the crosses for experiments (see introduction to **Chapter 5 Results**, section 5.1). Again, the data showed no significant differences between genotypes within the pooled groups, although again it is possible that differences would have been found with larger sample sizes. Ideally, pooling would not have been necessary. However, this pooling allowed for better analysis of existing data. On the other hand, it should be considered that the pooling could possibly affect the results seen in this thesis.

As previously discussed in section 4.2.1, the $Pax3^{Cre}$ allele and the $Pax3^{Sp2H}$ allele are carried on different genetic backgrounds, which could create variations in modifier genes in the offspring. As mentioned, the consistency of the described results suggests that this isn't having a significant effect, but it should be considered when interpreting the data.

5.2.2 β -catenin loss-of-function and neural tube defects

The effect of β -catenin LOF has been previously studied in the neural tube using a *Wnt1*-Cre line (Brault et al., 2001). *Wnt1* is expressed in a similar domain of the NT to *Pax3*; both are expressed in the dorsal region, although *Pax3* expression may extend slightly more ventrally in the NT (Megason and McMahon, 2002). However, *Wnt1*^{Cre/+} *β -catenin*^{LOF/LOF} embryos did not develop NTDs. This suggests that β -catenin LOF alone does not cause NTDs. Conversely, β -catenin LOF appears to have an effect on NTD development when in combination with *Pax3* mutation.

β -catenin LOF does not appear to affect the frequency of spinal NTDs in wild type or *Pax3* mutant embryos, but greatly increases the frequency of spina bifida in *Pax3* heterozygous mutant embryos (**Figure 5.10**). *Pax3* heterozygotes do not usually develop spina bifida, but have demonstrated vulnerability to cranial NTD development in comparison to wild type embryos. For example, folate deficiency increases the frequency of exencephaly in *Pax3* heterozygous embryos (see section 3.1.3.1) (Burren et al., 2008). Additionally, *Pax3* heterozygous embryos are highly susceptible to β -catenin GOF-induced exencephaly (see section 4.1.3.2). It appears that *Pax3* heterozygous embryos are also vulnerable to spinal NTDs under specific conditions, such as β -catenin LOF. *Pax3*^{+/-} *β -catenin*^{-/-} embryos have significantly increased PNP size in comparison to *Pax3*^{+/-} *β -catenin*^{+/+} embryos at the 24-26 somite stage, and a significantly higher proportion of these embryos develop spina bifida at later stages of development (**Figures 5.9 and 5.10**). *Pax3*^{+/+} and *Pax3*^{Sp2H/Cre} embryos show no such increase in spinal NTD development in response to β -catenin LOF. However, *Pax3*^{Sp2H/Cre} embryos have 100% frequency of spina bifida without β -catenin LOF, so no further increase is possible. This data suggests that although β -catenin LOF in the NT does not in itself cause spina bifida, as demonstrated in *Wnt1*^{Cre/+} *β -catenin*^{LOF/LOF} embryos (Megason and McMahon, 2002), it is able to induce spinal NTD development in embryos which are vulnerable due to *Pax3* heterozygosity.

β -catenin LOF has a very different effect on closure of the cranial NT. Although the differences did not reach significance, a clear trend was visible which suggests that β -catenin LOF decreases the frequency of exencephaly in *Pax3*^{Sp2H/Cre} embryos; *Pax3*^{Sp2H/Cre} *β -catenin*^{+/+} embryos showed a frequency of 45%, whereas *Pax3*^{Sp2H/Cre} *β -catenin*^{LOF/LOF} embryos had a frequency of 13% (**Figure 5.11**). This is strong evidence for an interaction between *Pax3* and canonical Wnt signalling; generalised developmental abnormalities may worsen an existing defect, but a rescue effect suggests a more specific interaction.

Evidence suggests that canonical Wnt signalling induces *Pax3* expression (Zhao et al., 2014). Therefore, it would be logical to assume that β -catenin LOF would compromise expression of *Pax3*. However, *Pax3*^{Sp^{2H}/Cre} embryos are already Pax3-null. Therefore, it appears that β -catenin LOF is able to compensate for the loss of Pax3 in the cranial region. This could be through a mechanism such as increased proliferation, or delayed neuronal differentiation, which could offset defects previously observed in the cranial regions of Sp^{2H}/Sp^{2H} embryos (Greene et al., unpublished data). It is also possible that the deleterious effects of *Pax3* mutation are dependent on an intact canonical Wnt signalling pathway. This would place Pax3 both up- and down-stream of the canonical Wnt signalling pathway.

The aim of *Spotch* embryo culture with the canonical Wnt inhibitor XAV939 was to determine if chemically reducing canonical Wnt signalling could rescue exencephaly in the mutant embryos. The inhibitor was found to have no effect on the development of exencephaly in any of the genotypes studied (**Figure 5.13**).

This lack of effect could be because the inhibitor did not affect NT closure, or it could be because the inhibitor failed to downregulate canonical Wnt signalling. Therefore, Sp^{2H}/+ embryos were assessed for *Axin2* expression using *in situ* hybridisation and RT-qPCR, and *Cdx2* expression was assessed using RT-qPCR (**Figure 5.14**). No differences were observed in the expression of either of these genes using any method. In the original paper it was reported that XAV939 increased the protein levels but not mRNA levels of Axin (Huang et al., 2009). This could explain why no difference was seen in *Axin2* expression. However, if Axin2 protein was upregulated, a downregulation of *Cdx2* would be expected. *Cdx2* has not proven to be an especially good marker for canonical Wnt activity, but the embryo-wide downregulation should result in reduced *Cdx2* expression.

These results suggest that XAV939 did not successfully downregulate canonical Wnt signalling in *Spotch* embryos. This could be for a number of reasons. For example, the concentration used may have been too low. The 10 μ M concentration was chosen for its lack of a generalised toxic effect, but this may have meant that the concentration was too low to sufficiently inhibit canonical Wnt signalling. Alternatively, the inhibitor may have degraded prior to use, or may degrade quickly in embryo culture. Therefore, XAV939 may not be the best choice of canonical Wnt signalling inhibitor for use in embryo culture. Better results may be gained by using an alternative inhibitor. For example PMED-1 inhibits canonical Wnt signalling by reducing β -catenin binding to CREB (cAMP response element-binding protein), which is a component of the core transcriptional machinery of the cell. This has been used to inhibit signalling in

zebrafish embryos (Delgado et al., 2014). Alternatively, BAS1 alters the transcription of several microRNA molecules which mediate posttranscriptional β -catenin silencing (Shi et al., 2014).

5.2.3 β -catenin loss-of-function and neural crest defects

Given the rescue effect of β -catenin LOF on cranial NT closure in *Spotch* embryos, NC development was studied to observe if defects were also rescued in this system. However, β -catenin LOF appeared to worsen the NC defects observed in *Pax3*^{Sp2H/Cre} embryos.

Pax3^{Sp2H/Cre} *β -catenin*^{+/+} embryos show reduced *ErbB3* expression throughout the embryos, but the vagus nerve, trigeminal ganglia and DRG all show expression, and appear to be developing to some degree (**Figure 5.15**). *Pax3*^{Sp2H/Cre} *β -catenin*^{LOF/+} embryos show similar *ErbB3* expression to *Pax3*^{Sp2H/Cre} *β -catenin*^{+/+} embryos, which suggests that a single copy of wild type β -catenin is able to compensate for β -catenin LOF. However, both *Pax3*^{Cre/+} *β -catenin*^{LOF/LOF} and *Pax3*^{Sp2H/Cre} *β -catenin*^{LOF/LOF} embryos appear to show severe NC defects; both genotypes lack *ErbB3* expression in the vagus nerve and the trigeminal ganglia, which could indicate that these structures are not developing. Additionally, *Pax3*^{Cre/+} *β -catenin*^{LOF/LOF} embryos show weak spinal *ErbB3* expression in the DRG (although segmentation is clearly evident), and *Pax3*^{Sp2H/Cre} *β -catenin*^{LOF/LOF} embryos show no expression in the DRG. Again, this suggests that these structures may have formed improperly, or not at all. These data suggest that canonical Wnt signalling is necessary for correct development of several NC-derived tissues, including the DRG, trigeminal ganglia and the vagus nerve.

Further research into the specification, migration and differentiation of the NC could provide a more complete picture of the role of β -catenin in the NC. *FoxD3 in situ* hybridisation early in NC specification could provide insight into its role in early NC development, and Tuj1 antibody staining alongside *Brn3a* and *Ngn2 in situ* hybridisation could give more information about the fate of these cells. Additionally, TUNEL staining would provide data on survival of the NC cells.

Evidence so far suggests that deletion of genes involved in canonical Wnt signalling results in the specification of fewer NC cells, and thus abnormal development of NC derivatives (Ikeya et al., 1997). It would be interesting to observe the more localised effects of β -catenin downregulation in the NT and NC enabled by conditional LOF and *Pax3*^{Cre}.

As mentioned previously, research has previously been carried out in which the conditional β -catenin^{LOF} allele was combined with *Wnt1*^{Cre} (Brault et al., 2001). *Wnt1* has a similar expression pattern to *Pax3* in the NT and NC (Brault et al., 2001; Megason and McMahon, 2002). Therefore, *Wnt1*^{Cre/+} *β -catenin*^{LOF/LOF} embryos will have reduced β -catenin expression in a similar region to *Pax3*^{Cre/+} *β -catenin*^{LOF/LOF} embryos. However, *Wnt1*^{Cre/+} *β -catenin*^{LOF/LOF} embryos

have more severe CNS and NC defects in comparison to *Pax3*^{Cre/+} *β-catenin*^{LOF/LOF} embryos described in this thesis. *Wnt1*^{Cre/+} *β-catenin*^{LOF/LOF} embryos failed to develop craniofacial structures and the forebrain, midbrain and hindbrain were all grossly abnormal. Greatly increased apoptosis was also visible in the cranial region (Brault et al., 2001). On the other hand, *Pax3*^{Cre/+} *β-catenin*^{LOF/LOF} embryos show far fewer cranial defects.

These differences could be caused by a number of factors. For example, *Wnt1* may be expressed slightly earlier in NC and NT development than *Pax3*, as canonical Wnt signalling is involved in the specification of these cells, whilst *Pax3* is expressed in the specified cells (Monsoro-Burq et al., 2005; Saint-Jeannet et al., 1997; Wilson et al., 2001). A small change in the timing of expression could be crucial during NC specification. Additionally, small changes in the region or level of expression could also be crucial. Therefore, the differences in phenotype between *Wnt1*^{Cre/+} *β-catenin*^{LOF/LOF} and *Pax3*^{Cre/+} *β-catenin*^{LOF/LOF} embryos indicate a greater influence of Wnt1 than Pax3 in the development of the cranial NC, or it could indicate that slightly earlier canonical Wnt signalling has a greater effect on craniofacial development.

5.2.4 The effects of β-catenin loss-of-function on Pax3 expression

Recent research suggests that canonical Wnt signalling may act upstream of *Pax3* signalling during NT closure (Zhao et al., 2014). RT-qPCR was used to quantify *Pax3* expression in embryos of different genotypes to determine whether it was affected by β-catenin LOF (**Figure 5.16**).

Two different primer pairs were used which distinguished between the *Pax3*^{Cre} and *Pax3*^{Sp2H} alleles (see section 4.1.8). RT-qPCR using these primer pairs largely gave the expected results when comparing between embryos with wild type β-catenin. However, the data agrees with the findings from the β-catenin^{GOF} allele (section 4.1.8) that the *Pax3*^{Cre} allele appears to have slightly lower expression levels than *Pax3*⁺.

Pax3 primer pair 1, which detects *Pax3*⁺ and *Pax3*^{Cre}, but not *Pax3*^{Sp2H}, detects some very interesting results when comparing *Pax3* genotypes with or without β-catenin LOF. *Pax3*^{Cre/+} *β-catenin*^{LOF/LOF} embryos have significantly reduced *Pax3* expression in comparison to *Pax3*^{Cre/+} *β-catenin*^{+/+} embryos. Additionally, *Pax3*^{Sp2H/Cre} *β-catenin*^{LOF/LOF} embryos have reduced expression of *Pax3* in comparison to *Pax3*^{Sp2H/Cre} *β-catenin*^{+/+} embryos, although this difference does not reach significance. These data suggest that β-catenin signalling increases expression of *Pax3*. Interestingly, *Pax3*^{Sp2H/Cre} *β-catenin*^{LOF/+} embryos have very similar levels of *Pax3* expression to *Pax3*^{Sp2H/Cre} *β-catenin*^{+/+} embryos, which suggests that one copy of wild type β-catenin is able to compensate for the β-catenin LOF caused by a single copy of the recombined β-catenin^{LOF} allele.

Pax3 primer pair 2 detects Pax3⁺ and Pax3^{Sp2H}, but not Pax3^{Cre}. As expected using this primer pair Pax3^{Sp2H/Cre} β-catenin^{+/+} embryos have a significantly reduced Pax3 expression of around half that of Pax3^{+/+} β-catenin^{+/+} embryos. However, it would be expected for Pax3^{Cre/+} β-catenin^{+/+} embryos to have a similar reduction, but the relative expression level of these embryos is 0.82. This could be an indication of Pax3 compensation through autoregulation, if the Pax3⁺ allele were upregulated to compensate for loss of Pax3 expression due to the Pax3^{Cre} allele. On the other hand, the data from the β-catenin GOF cross shows that Pax3^{Cre/+} β-catenin^{+/+} embryos have around half the Pax3 expression of Pax3^{+/+} β-catenin^{+/+} embryos shown by RT-qPCR with Pax3 primer pair 2 (see section 4.1.8). Indeed, when normalised to Pax3^{+/+} β-catenin^{+/+} embryos from the relevant genetic cross, comparing Pax3^{Cre/+} β-catenin^{+/+} embryos from the β-catenin GOF and LOF crosses shows a significant difference in Pax3 expression (Figure 5.17). This suggests that the higher-than-expected expression shown by Pax3^{Cre/+} β-catenin^{+/+} embryos in the β-catenin LOF cross could be due to slight differences in genetic background, or could be due to random variation. However, it is unlikely to be due to autoregulation.

RT-qPCR data from Pax3 primer pair 2 shows similar results to Pax3 primer pair 1 regarding the effects of β-catenin LOF; Pax3^{Cre/+} β-catenin^{LOF/LOF} embryos have significantly reduced Pax3 expression compared to Pax3^{Cre/+} β-catenin^{+/+} embryos, and Pax3^{Sp2H/Cre} β-catenin^{LOF/LOF} embryos have lower expression than Pax3^{Sp2H/Cre} β-catenin^{+/+} embryos, although this difference doesn't reach significance. Again, these data suggest that β-catenin increases Pax3 expression. Additionally, Pax3 primer pair 2 shows that Pax3^{Sp2H/Cre} β-catenin^{LOF/+} and Pax3^{Sp2H/Cre} β-catenin^{+/+} embryos have similar expression levels of Pax3, which suggests that one copy of β-catenin⁺ is able to compensate for β-catenin LOF caused by a single copy of the recombined β-catenin^{LOF} allele.

In summary, both previously published findings (Zhao et al., 2014) and the research described in this chapter suggest that β-catenin is necessary for upregulation of Pax3 expression. This could have implications for the findings described above, which suggest that β-catenin LOF both increases the frequency of spinal NTDs and worsens NC defects in Pax3 heterozygous embryos. It is possible that because β-catenin LOF results in downregulation of wild type Pax3 expression, Pax3 heterozygous embryos with β-catenin LOF more closely resemble Pax3 homozygous mutant embryos; the further reduction in Pax3 expression results in higher frequencies of defects associated with Pax3 mutation.

Conversely, β-catenin LOF appears to rescue cranial NTDs in Pax3 mutant embryos. In the absence of Pax3 function β-catenin LOF in the cranial region may be able to compensate. This

could be through direct means, if β -catenin LOF affected the same mechanism which causes cranial NTDs in *Pax3* mutant embryos. Alternatively, the rescue could occur through less direct means, such as a summation of the downstream effects of the *Pax3* and *β -catenin* mutations.

5.2.5 Conclusions

Evidence discussed in this chapter supports data from **Chapter 4** that an interaction occurs between *Pax3* and the canonical Wnt signalling pathway, as β -catenin LOF may rescue *Pax3*-induced cranial NTDs.

However, the nature of this interaction still remains uncertain, and will take further experiments to decipher. β -catenin LOF appears to affect similar cellular processes to β -catenin GOF in *Pax3* mutant embryos, including neuronal differentiation and the development of the NC. This suggests that β -catenin acts in a dose-dependent manner. However, as suggested before, *in vitro* analysis of the NC could clarify which processes are affected, and their relative contribution to NC defect development. Additionally, quantification of proliferation, apoptosis and neuronal differentiation in the NT could provide information on the processes involved in rescue of cranial NTDs.

β -catenin LOF has been found to decrease expression of *Pax3*. This supports recently published findings (Zhao et al., 2014), and could provide an explanation for the worsening on spinal NTDs in *Pax3* heterozygous embryos. However, the mechanism for the β -catenin LOF-induced rescue of cranial NTDs in *Pax3* mutant embryos is unclear. Further study into cellular processes in the NTs of these embryos could shed light on the matter.

6 General Discussion

The studies described in this thesis have investigated different aspects of the phenotype of *Spotch* (*Pax3* mutant) embryos, with particular focus on the development of NTDs. The research was divided into two main areas; mechanisms underlying spinal NTDs in *Spotch* embryos (**Chapter 3**), and interaction between *Pax3* and the canonical Wnt signalling pathway in NTDs (**Chapters 4 and 5**). An interaction was also observed between *Pax3* and the canonical Wnt signalling pathway in NC development, and so this was explored further.

Findings from the research on mechanisms of spina bifida development in *Spotch* embryos suggest that a reduction in proliferation in the NT may be causative. Morphological alterations were observed in the NT of *Sp^{2H}/Sp^{2H}* embryos, which could provide a connection between the reduction in proliferation and failure of NT closure.

The overall findings of the research on potential interactions between *Pax3* and canonical Wnt signalling does not support the hypothesis that a canonical Wnt signalling defect exists in *Spotch* embryos, as no differences were seen in the expression of downstream target genes of canonical Wnt signalling. However, β -catenin mutation did appear to alter the expression of *Pax3*. This suggests that canonical Wnt signalling acts upstream of *Pax3*, and recently published data supports this theory (Zhao et al., 2014).

6.1 Neural tube defects

NTDs are an extremely heterogeneous group of birth defects, which in humans are usually caused by a combination of environmental and genetic factors. This makes the prediction, prevention and study of NTDs very difficult, and few genes have been linked with human NTD development.

Many different mouse models are available for studying NTDs. They have a wide range of mutations, which result in many different phenotypes, different NTDs, and different penetrance. A huge variety of cellular and morphological alterations have been found in these mice, which result in the development of NTDs (see section 1.2 for more information). In a few cases the genes responsible for NTDs in these models – such as *AMT*, *SCRIB* and *CELSR1* – have been associated with development of NTDs in humans, suggesting that NTD-causing genes in mice may play a role in some human NTDs (Lei et al., 2013; Lei et al., 2014; Narisawa et al., 2012). Other genes, including *MTHFR*, have been linked to NTDs in humans, but mice carrying

mutations in these genes do not develop NTDs (van der Put et al., 1995). For still other genes – such as *Pax3* – the link with NTD development in humans is less clear (See section 1.5); evidence suggests that *Pax3* is not a major causative gene for NTDs in humans, but variations and polymorphisms in *Pax3* may contribute to human NTD development in some cases (Agopian et al., 2013; Chatkupt et al., 1995; Lu et al., 2007). These discrepancies may be due to differences between protein function in humans and mice, but also may be because NTD mouse models usually carry a single gene mutation, whereas human NTDs are generally thought to be multigenic. Human NTD patients may carry variations and mutations in multiple risk genes, which can make them difficult to identify. Additionally, many risk genes are not fully sequenced in human NTD cases, and the studies are often small scale. Therefore, it is not possible to draw firm conclusions about the genetics underlying human NTDs.

Due to these difficulties, mouse models of NTDs are usually used as examples of cellular and morphological defects which can occur in NTDs, rather than genetic models of mutations which can cause NTDs in humans. *Spotch* mice are an example of this – *Pax3* mutations, such as those found in *Spotch* mice, are not thought to be major risk factors of human NTDs (Chatkupt et al., 1995). However, it is studied as an NTD model given the high frequency of NTDs in mutant embryos. Any defective cellular or morphological mechanisms which occur in these mice may be applicable to understanding the mechanistic basis of human NTDs. In addition, *Spotch* NTDs are preventable by folic acid, providing a model to examine the mechanisms involved in folate-induced rescue of human NTDs.

The hypothesis used in this section of the research was: premature neuronal differentiation and reduced proliferation in the NT of the *Spotch* embryo cause spina bifida. The research described in this thesis suggests that *Spotch* mutant embryos have reduced proliferation in the dorsal region of the spinal NT, although they show no premature differentiation. I also found that *Spotch* embryos have altered morphology of the NT – the NT is smaller due to fewer cell numbers, but proportionally thicker than wild type embryos. It appears likely that the smaller size of the NT is caused by the reduced proliferation rate. It also seems plausible that these features have a causative role in the development of spina bifida in these mutant embryos. For example, it is likely that reduced proliferation in the neural folds of *Spotch* mutant embryos causes morphological differences, which in turn could cause spina bifida. Experiments which manipulate the rate of proliferation in the NT would allow for study of the NT morphology and NTD frequency in *Spotch* embryos, and may allow a causative relationship to be proved or disproved. For instance, given more time, I would like to culture *Spotch* embryos in anti-mitotic agents, such as Mitomycin. This would further reduce proliferation in the NT, and could provide information about the effect of the proliferation defect on the

morphology of the NT. It could also produce data on the effect of proliferation specifically on the development of NTDs. It would be especially interesting to observe if *Sp^{2H}/+* embryos develop NTDs after being treated with anti-mitotics. These embryos are more susceptible than *+/+* embryos to developing NTDs, and treatment with anti-mitotics could be very informative about the role of proliferation in NT development.

Both Pax3 and canonical Wnt signalling are associated with the maintenance of cells in a proliferative, multipotent state (Keller-Peck and Mullen, 1997; Megason and McMahon, 2002). Therefore, the loss of either of these pathways might be expected to have a similar effect on phenotype – loss of proliferation and potentially premature differentiation. Additionally, as discussed previously, spina bifida in *Spotch* embryos may be caused by reduced proliferation. The hypothesis for this research was: interaction between Pax3 and the canonical Wnt signalling pathway reduces proliferation and induces premature neuronal differentiation in the NT and NC, resulting in NTDs and NC defects.

Consequently, the observation that β -catenin LOF rescued certain NTDs whereas β -catenin GOF worsened NTDs in *Pax3* mutant embryos was the opposite of the expected results. The data described in this thesis has shown that mutations in canonical Wnt signalling alone cause NTDs only at a low frequency. Therefore the rescue effect suggests a more specific interaction between Pax3 and canonical Wnt signalling.

Research published in 2014 highlighted the potential link between Pax3 and canonical Wnt signalling (Zhao et al., 2014). In this paper, β -catenin LOF was used in combination with Pax3^{Cre}, as in the research described in **Chapter 5** of this thesis. The researchers found that β -catenin LOF reduced the expression of *Pax3* and *Cdx2* using *in situ* hybridisation, and that both of these genes contained upstream Tcf/Lef1 binding activation sites. This suggests that the expression of both *Pax3* and *Cdx2* is directly induced by canonical Wnt signalling. Furthermore, expression of a *Pax3* transgene was able to rescue spina bifida in embryos with β -catenin LOF, which suggests that NTDs in these embryos are mediated by an alteration in *Pax3* expression. This paper supports the data found in this thesis which suggests a link between Pax3 and the canonical Wnt signalling pathways. It also corroborates the finding in Chapter 5 that Pax3 expression is reduced in embryos with β -catenin LOF, although I was unable to replicate the effects of β -catenin LOF on *Cdx2* expression. Additionally, the discovery of Tcf/Lef1 binding sites upstream of the *Pax3* gene, and the effect of the Pax3 transgene are evidence of interaction between Pax3 and the canonical Wnt signalling pathway.

In **Chapter 5** of this thesis, β -catenin LOF was shown to reduce *Pax3* expression, and yet it rescues exencephaly in *Pax3* mutant embryos. In addition to a role upstream of Pax3, this data

suggests that canonical Wnt signalling may also act on a mechanism downstream of Pax3. Pax3 expression does not affect canonical Wnt signalling, so this is not a direct interaction. However, the pathways may converge and act antagonistically on a particular cellular mechanism.

My data suggests that β -catenin GOF does not affect proliferation or neuronal differentiation in the cranial NT. However, this does not preclude the possibility that β -catenin LOF may act on these pathways. For example, if canonical Wnt signalling were to inhibit proliferation, β -catenin GOF may have no effect, but β -catenin LOF might. It is less likely that canonical Wnt signalling would promote neuronal differentiation, as it would be expected that β -catenin GOF would cause an increase in neuronal cell numbers, which was not observed. Cell counts of proliferating and differentiating cells in the cranial NT of embryos with β -catenin LOF could provide more information about these theories.

However, it is unlikely that canonical Wnt signalling acts through inhibition of proliferation, as this is a mechanism which affects spinal NT closure, and β -catenin LOF has no rescue effect on spinal NT closure. Therefore, it is more likely that canonical Wnt signalling acts on a mechanism which is essential for cranial NT closure, but not spinal neurulation. Alternatively, there may be a difference in requirement for β -catenin in proliferation between the cranial and spinal regions of the NT. Furthermore, spina bifida occurs at a higher frequency than exencephaly in *Spotch* mutant embryos. Thus spina bifida could be more resistant to rescue than exencephaly.

Both β -catenin GOF and β -catenin LOF appear to affect the frequency of exencephaly more profoundly than the frequency of spina bifida in *Pax3* mutant and heterozygous embryos. This supports the evidence that canonical Wnt signalling affects different processes in the cranial and spinal NTs. Research has shown that different mechanisms are employed in the closure of these two distinct regions (Massa et al., 2009; Ybot-Gonzalez and Copp, 1999). Therefore, it is probable that canonical Wnt signalling interacts with one of these differential mechanisms, thus affecting the regions very differently.

It was shown that the actin cytoskeleton is essential for cranial, but not spinal, neurulation (Ybot-Gonzalez and Copp, 1999). Previous research has demonstrated interactions between canonical Wnt signalling and the actin cytoskeleton. For example, canonical Wnt signalling may have a role in wound healing by initiating an increase in α -actin-positive stress fibre formation (Carthy et al., 2011). Therefore it is possible that disrupted canonical Wnt signalling may affect the actin cytoskeleton formation enough to induce exencephaly in vulnerable embryos, such as *Pax3* mutant embryos. It would be interesting to study the *Pax3* and canonical Wnt mutant

embryos using markers for the actin cytoskeleton, to observe any changes which may occur. It would also potentially be informative to culture *Spotch* embryos in agents which affect the actin cytoskeleton, such as Cytochalasin or Latrunculin to prevent polymerisation of actin. This could produce information about the role of the actin cytoskeleton in *Pax3*-related NTDs.

It is likely there are a large number of differences in morphology and signalling between cranial and spinal NT closure which have not yet been described. Therefore the interaction between *Pax3* and canonical Wnt signalling may affect one of these processes. Further research into closure mechanisms which differ between regions of the NT may help to shed light on the process or processes which link the two pathways.

In addition to previously discussed mechanisms, it is possible that β -catenin LOF and GOF may affect adherens junctions in the mutant embryos, which could be responsible for some aspects of the phenotype observed. Further study of adherens junctions in these embryos, possibly through the use of adherens junction markers, or *in vitro* cell assays, could provide more information about the potential effects of this defect on the mutant embryos.

6.2 *Pax3*, Canonical Wnt signalling, and the neural crest

I found that loss of canonical Wnt signalling rescues cranial NTDs in *Pax3* mutant embryos. Therefore the NC were examined as another *Pax3*-expressing population of cells which may be affected by canonical Wnt signalling. This research has shown that in combination with *Pax3* mutation both β -catenin LOF and GOF appear to reduce the NC population and their derivative tissues.

Research on embryos with β -catenin GOF suggests that in combination with the *Pax3* mutation β -catenin GOF appears to limit specification and/or expansion of the premigratory population of NC, as shown by reduced expression of the NC marker *FoxD3* in the spinal region of *Pax3*^{Cre/+} β -catenin^{GOF/+} and *Pax3*^{Sp2H/Cre} β -catenin^{GOF/+} embryos compared to *Pax3*^{+/+} β -catenin^{+/+} embryos. These NC cells also appeared to have higher rates of apoptosis and premature NC differentiation. These defects results in massive reduction of NC derivatives, such as the DRG, trigeminal ganglia and vagus nerve.

Data from β -catenin LOF suggests that in combination with *Pax3* mutation, reduced canonical Wnt signalling also results in a reduction in size or in a failure of NC-derived tissues to develop, although the mechanisms behind this were not determined.

Together these data show that both LOF and GOF of canonical Wnt signalling cause reduced contribution of cells to NC derivative tissues. This suggests that normal development of the NC requires carefully balanced canonical Wnt signalling. It would be interesting to see if β -catenin LOF had similar effects on differentiation, apoptosis and differentiation in the NC population to β -catenin GOF, or if LOF causes reduced NC derivatives through alternative mechanisms.

Several aspects of the β -catenin LOF and GOF NC phenotypes were very similar. For example, both caused complete loss of vagal nerve and trigeminal ganglion development. This data suggests that these structures are particularly sensitive to the balance of canonical Wnt signalling.

On the other hand, some aspects of the β -catenin LOF and GOF NC phenotypes differ slightly. For instance, both β -catenin LOF and GOF appear to reduce DRG development. However, β -catenin LOF embryos retain segmentation of the DRG, whereas segmentation is largely lost in the DRG of β -catenin GOF embryos. This could suggest that lower levels of canonical Wnt signalling are necessary in some areas for the correct segmentation of the DRG, and that the higher levels caused by β -catenin GOF makes this impossible. Additionally, β -catenin LOF embryos retain a small amount of *ErbB3* expression in the DRG at 30+ somite stage, whereas β -catenin GOF embryos have lost all *ErbB3* expression in the DRG at this stage. Again this could suggest that slightly lower levels of canonical Wnt signalling are necessary for DRG development. This could be due to the effect of β -catenin GOF on levels of apoptosis or differentiation in the DRG, compared to the effect of β -catenin LOF. Alternatively, this could suggest that canonical Wnt signalling aids development of the DRG, but is not essential, whereas over-activation of signalling inhibits DRG development. This inhibition could be due to ectopic activation of downstream targets, or activation of an inhibitory pathway.

On the other hand, the differences seen in the degree of NC abnormality between β -catenin LOF and GOF embryos could be due to the degree of difference in canonical Wnt signalling caused by the recombined β -catenin^{LOF} and β -catenin^{GOF} alleles. Recombined β -catenin^{LOF} causes a reduction in the NC and the NT, but this was not detectable by RT-qPCR on whole embryos. On the other hand, the GOF in canonical Wnt signalling caused by the recombined β -catenin^{GOF} allele was detectable by RT-qPCR, although present in the same regions. This suggests that the recombined β -catenin^{GOF} allele causes a huge increase in canonical Wnt signalling of several fold difference. The more severe NC phenotype seen in β -catenin GOF embryos could be due to the greater difference in canonical Wnt signalling caused by the β -catenin^{GOF} allele in comparison to the β -catenin^{LOF} allele. Additionally, β -catenin LOF causes a

simple loss of signalling, whereas β -catenin GOF may cause ectopic activation or inhibition of downstream targets.

Determining the cellular causes of the NC defects in embryos with β -catenin LOF and GOF could offer more information about whether the defects are different due to the mechanisms involved, or whether they are different due to the degree of signalling abnormality. It could also provide information on the various cellular effects that can influence NT closure, some of which could be relevant to corresponding birth defects in humans. If I had more time, I would like to isolate and culture NC cells from the different genotypes, including embryos with β -catenin LOF and GOF. These cultures could be used to study a number of cellular processes, including proliferation, differentiation, apoptosis and migration. Comparison of these processes between the genotypes could indicate the cellular processes which are abnormal in *Pax3* mutant embryos, as well as those with β -catenin LOF and GOF. It could also indicate if there is an interaction between *Pax3* and the canonical Wnt signalling pathway in the development of the NC.

7 References

- Abdul-Aziz,N.M., Turmaine,M., Greene,N.D., and Copp,A.J.** (2009). EphrinA-EphA receptor interactions in mouse spinal neurulation: implications for neural fold fusion. *Int. J. Dev. Biol.* **53**, 559-568.
- Aberle,H., Bauer,A., Stappert,J., Kispert,A., and Kemler,R.** (1997). beta-catenin is a target for the ubiquitin-proteasome pathway. *EMBO J.* **16**, 3797-3804.
- Aberle,H., Schwartz,H., Hoschuetzky,H., and Kemler,R.** (1996). Single amino acid substitutions in proteins of the armadillo gene family abolish their binding to alpha-catenin. *J. Biol. Chem.* **271**, 1520-1526.
- Adams,B., Dorfler,P., Aguzzi,A., Kozmik,Z., Urbanek,P., Maurer-Fogy,I., and Busslinger,M.** (1992). Pax-5 encodes the transcription factor BSAP and is expressed in B lymphocytes, the developing CNS, and adult testis. *Genes Dev.* **6**, 1589-1607.
- Adzick,N.S., Thom,E.A., Spong,C.Y., Brock,J.W., III, Burrows,P.K., Johnson,M.P., Howell,L.J., Farrell,J.A., Dabrowiak,M.E., Sutton,L.N. et al.** (2011). A randomized trial of prenatal versus postnatal repair of myelomeningocele. *N. Engl. J. Med.* **364**, 993-1004.
- Afman,L.A., Blom,H.J., Driittij,M.J., Brouns,M.R., and van Straaten,H.W.** (2005). Inhibition of transmethylation disturbs neurulation in chick embryos. *Brain Res. Dev. Brain Res.* **158**, 59-65.
- Agathon,A., Thisse,C., and Thisse,B.** (2003). The molecular nature of the zebrafish tail organizer. *Nature.* **424**, 448-452.
- Agopian,A.J., Bhalla,A.D., Boerwinkle,E., Finnell,R.H., Grove,M.L., Hixson,J.E., Shimmin,L.C., Sewda,A., Stuart,C., Zhong,Y. et al.** (2013). Exon sequencing of PAX3 and T (brachyury) in cases with spina bifida. *Birth Defects Res. A Clin. Mol. Teratol.* **97**, 597-601.
- Ai,D., Fu,X., Wang,J., Lu,M.F., Chen,L., Baldini,A., Klein,W.H., and Martin,J.F.** (2007). Canonical Wnt signaling functions in second heart field to promote right ventricular growth. *Proc. Natl. Acad. Sci. U. S. A.* **104**, 9319-9324.
- Akiyama,H., Lyons,J.P., Mori-Akiyama,Y., Yang,X., Zhang,R., Zhang,Z., Deng,J.M., Taketo,M.M., Nakamura,T., Behringer,R.R. et al.** (2004). Interactions between Sox9 and beta-catenin control chondrocyte differentiation. *Genes Dev.* **18**, 1072-1087.
- Amit,S., Hatzubai,A., Birman,Y., Andersen,J.S., Ben-Shushan,E., Mann,M., Ben-Neriah,Y., and Alkalay,I.** (2002). Axin-mediated CKI phosphorylation of beta-catenin at Ser 45: a molecular switch for the Wnt pathway. *Genes Dev.* **16**, 1066-1076.
- Anderson,D.J.** (1994). Stem cells and transcription factors in the development of the mammalian neural crest. *FASEB J.* **8**, 707-713.
- Angers,S. and Moon,R.T.** (2009). Proximal events in Wnt signal transduction. *Nat. Rev. Mol. Cell Biol.* **10**, 468-477.
- Aoki,Y., Saint-Germain,N., Gyda,M., Magner-Fink,E., Lee,Y.H., Credidio,C., and Saint-Jeannet,J.P.** (2003). Sox10 regulates the development of neural crest-derived melanocytes in *Xenopus*. *Dev. Biol.* **259**, 19-33.

- Apuzzo,S. and Gros,P.** (2002). Site-specific modification of single cysteine Pax3 mutants reveals reciprocal regulation of DNA binding activity of the paired and homeo domain. *Biochemistry* **41**, 12076-12085.
- Apuzzo,S. and Gros,P.** (2007). Cooperative interactions between the two DNA binding domains of Pax3: helix 2 of the paired domain is in the proximity of the amino terminus of the homeodomain. *Biochemistry* **46**, 2984-2993.
- Arber,N., Doki,Y., Han,E.K., Sgambato,A., Zhou,P., Kim,N.H., Delohery,T., Klein,M.G., Holt,P.R., and Weinstein,I.B.** (1997). Antisense to cyclin D1 inhibits the growth and tumorigenicity of human colon cancer cells. *Cancer Res.* **57**, 1569-1574.
- Arias,S.** (1993). Mutations of PAX3 unlikely in Waardenburg syndrome type 2. *Nat. Genet.* **5**, 8.
- Aruga,J.** (2004). The role of Zic genes in neural development. *Mol. Cell Neurosci.* **26**, 205-221.
- Aruga,J., Inoue,T., Hoshino,J., and Mikoshiba,K.** (2002a). Zic2 controls cerebellar development in cooperation with Zic1. *J. Neurosci.* **22**, 218-225.
- Aruga,J., Tohmonda,T., Homma,S., and Mikoshiba,K.** (2002b). Zic1 promotes the expansion of dorsal neural progenitors in spinal cord by inhibiting neuronal differentiation. *Dev. Biol.* **244**, 329-341.
- Asher,J.H., Jr. and Friedman,T.B.** (1990). Mouse and hamster mutants as models for Waardenburg syndromes in humans. *J. Med. Genet.* **27**, 618-626.
- Auerbach,R.** (1954). Analysis of the developmental effects of a lethal mutation in the house mouse. *J. Exp. Zool.* **127**, 305-329.
- Aulehla,A., Wiegraebe,W., Baubet,V., Wahl,M.B., Deng,C., Taketo,M., Lewandoski,M., and Pourquie,O.** (2008). A beta-catenin gradient links the clock and wavefront systems in mouse embryo segmentation. *Nat. Cell Biol.* **10**, 186-193.
- Aybar,M.J., Nieto,M.A., and Mayor,R.** (2003). Snail precedes slug in the genetic cascade required for the specification and migration of the Xenopus neural crest. *Development* **130**, 483-494.
- Ayme,S. and Philip,N.** (1995). Possible homozygous Waardenburg syndrome in a fetus with exencephaly. *Am. J. Med. Genet.* **59**, 263-265.
- Baeg,G.H., Lin,X., Khare,N., Baumgartner,S., and Perrimon,N.** (2001). Heparan sulfate proteoglycans are critical for the organization of the extracellular distribution of Wingless. *Development.* **128**, 87-94.
- Baeg,G.H., Selva,E.M., Goodman,R.M., DasGupta,R., and Perrimon,N.** (2004). The Wingless morphogen gradient is established by the cooperative action of Frizzled and Heparan Sulfate Proteoglycan receptors. *Dev. Biol.* **276**, 89-100.
- Bajard,L., Relaix,F., Lagha,M., Rocancourt,D., Daubas,P., and Buckingham,M.E.** (2006). A novel genetic hierarchy functions during hypaxial myogenesis: Pax3 directly activates Myf5 in muscle progenitor cells in the limb. *Genes Dev.* **20**, 2450-2464.
- Baker,J.C., Beddington,R.S., and Harland,R.M.** (1999). Wnt signaling in Xenopus embryos inhibits bmp4 expression and activates neural development. *Genes Dev.* **13**, 3149-3159.

- Balczarek, K.A., Lai, Z.C., and Kumar, S.** (1997). Evolution of functional diversification of the paired box (Pax) DNA-binding domains. *Mol. Biol. Evol.* **14**, 829-842.
- Banerjee, A.K.** (1986). Waardenburg's syndrome associated with ostium secundum atrial septal defect. *J. R. Soc. Med.* **79**, 677-678.
- Bang, A.G., Papalopulu, N., Goulding, M.D., and Kintner, C.** (1999). Expression of Pax-3 in the lateral neural plate is dependent on a Wnt-mediated signal from posterior nonaxial mesoderm. *Dev. Biol.* **212**, 366-380.
- Banting, G.S., Barak, O., Ames, T.M., Burnham, A.C., Kardel, M.D., Cooch, N.S., Davidson, C.E., Godbout, R., McDermid, H.E., and Shiekhata, R.** (2005). CECR2, a protein involved in neurulation, forms a novel chromatin remodeling complex with SNF2L. *Hum. Mol. Genet.* **14**, 513-524.
- Banziger, C., Soldini, D., Schutt, C., Zipperlen, P., Hausmann, G., and Basler, K.** (2006). Wntless, a conserved membrane protein dedicated to the secretion of Wnt proteins from signaling cells. *Cell* **125**, 509-522.
- Bartscherer, K., Pelte, N., Ingelfinger, D., and Boutros, M.** (2006). Secretion of Wnt ligands requires Evi, a conserved transmembrane protein. *Cell* **125**, 523-533.
- Basch, M.L., Bronner-Fraser, M., and Garcia-Castro, M.I.** (2006). Specification of the neural crest occurs during gastrulation and requires Pax7. *Nature* **441**, 218-222.
- Basch, M.L., Garcia-Castro, M.I., and Bronner-Fraser, M.** (2004). Molecular mechanisms of neural crest induction. *Birth Defects Res. C. Embryo. Today* **72**, 109-123.
- Beaudin, A.E. and Stover, P.J.** (2007). Folate-mediated one-carbon metabolism and neural tube defects: balancing genome synthesis and gene expression. *Birth Defects Res. C. Embryo. Today* **81**, 183-203.
- Beechey, C.V. and Searle, A.G.** (1986). Mutations at the Sp locus. *Mouse News Letter* 7526.
- Begleiter, M.L. and Harris, D.J.** (1992). Waardenburg syndrome and meningocele. *Am. J. Med. Genet.* **44**, 541.
- Behrens, J., Jerchow, B.A., Wurtele, M., Grimm, J., Asbrand, C., Wirtz, R., Kuhl, M., Wedlich, D., and Birchmeier, W.** (1998). Functional interaction of an axin homolog, conductin, with beta-catenin, APC, and GSK3beta. *Science* **280**, 596-599.
- Behrens, J., von Kries, J.P., Kuhl, M., Bruhn, L., Wedlich, D., Grosschedl, R., and Birchmeier, W.** (1996). Functional interaction of beta-catenin with the transcription factor LEF-1. *Nature* **382**, 638-642.
- Bellmeyer, A., Kruse, J., Lindgren, J., and LaBonne, C.** (2003). The protooncogene c-myc is an essential regulator of neural crest formation in xenopus. *Dev. Cell* **4**, 827-839.
- Ben-Yair, R. and Kalcheim, C.** (2005). Lineage analysis of the avian dermomyotome sheet reveals the existence of single cells with both dermal and muscle progenitor fates. *Development* **132**, 689-701.
- Benahmed, F., Gross, I., Gaunt, S.J., Beck, F., Jehan, F., Domon-Dell, C., Martin, E., Keding, M., Freund, J.N., and Duluc, I.** (2008). Multiple regulatory regions control the complex expression pattern of the mouse Cdx2 homeobox gene. *Gastroenterology*. **135**, 1238-1247, 1247.

- Bendris,N., Cheung,C.T., Leong,H.S., Lewis,J.D., Chambers,A.F., Blanchard,J.M., and Lemmers,B.** (2014). Cyclin A2, a novel regulator of EMT. *Cell Mol. Life Sci.*
- Bennett,G.D., An,J., Craig,J.C., Gefrides,L.A., Calvin,J.A., and Finnell,R.H.** (1998). Neurulation abnormalities secondary to altered gene expression in neural tube defect susceptible Splotch embryos. *Teratology* **57**, 17-29.
- Bernasconi,M., Remppis,A., Fredericks,W.J., Rauscher,F.J., III, and Schafer,B.W.** (1996). Induction of apoptosis in rhabdomyosarcoma cells through down-regulation of PAX proteins. *Proc. Natl. Acad. Sci. U. S. A* **93**, 13164-13169.
- Bhanot,P., Brink,M., Samos,C.H., Hsieh,J.C., Wang,Y., Macke,J.P., Andrew,D., Nathans,J., and Nusse,R.** (1996). A new member of the frizzled family from Drosophila functions as a Wingless receptor. *Nature* **382**, 225-230.
- Bhatt,S., Diaz,R., and Trainor,P.A.** (2013). Signals and switches in Mammalian neural crest cell differentiation. *Cold Spring Harb. Perspect. Biol.* **5**.
- Bienz,M. and He,X.** (2012). Biochemistry. A lipid linchpin for Wnt-Fz docking. *Science* **337**, 44-45.
- Bierie,B., Nozawa,M., Renou,J.P., Shillingford,J.M., Morgan,F., Oka,T., Taketo,M.M., Cardiff,R.D., Miyoshi,K., Wagner,K.U. et al.** (2003). Activation of beta-catenin in prostate epithelium induces hyperplasias and squamous transdifferentiation. *Oncogene*. **19**;22, 3875-3887.
- Bierkamp,C., Schwarz,H., Huber,O., and Kemler,R.** (1999). Desmosomal localization of beta-catenin in the skin of plakoglobin null-mutant mice. *Development*. **126**, 371-381.
- Bilic,J., Huang,Y.L., Davidson,G., Zimmermann,T., Cruciat,C.M., Biern,M., and Niehrs,C.** (2007). Wnt induces LRP6 signalosomes and promotes dishevelled-dependent LRP6 phosphorylation. *Science* **316**, 1619-1622.
- Birrane,G., Soni,A., and Ladias,J.A.** (2009). Structural basis for DNA recognition by the human PAX3 homeodomain. *Biochemistry* **48**, 1148-1155.
- Bladt,F., Riethmacher,D., Isenmann,S., Aguzzi,A., and Birchmeier,C.** (1995). Essential role for the c-met receptor in the migration of myogenic precursor cells into the limb bud. *Nature* **376**, 768-771.
- Blake,J.A. and Ziman,M.R.** (2014). Pax genes: regulators of lineage specification and progenitor cell maintenance. *Development*. **141**, 737-751.
- Bober,E., Franz,T., Arnold,H.H., Gruss,P., and Tremblay,P.** (1994). Pax-3 is required for the development of limb muscles: a possible role for the migration of dermomyotomal muscle progenitor cells. *Development* **120**, 603-612.
- Bolos,V., Peinado,H., Perez-Moreno,M.A., Fraga,M.F., Esteller,M., and Cano,A.** (2003). The transcription factor Slug represses E-cadherin expression and induces epithelial to mesenchymal transitions: a comparison with Snail and E47 repressors. *J. Cell Sci.* **116**, 499-511.
- Bondurand,N., Pingault,V., Goerich,D.E., Lemort,N., Sock,E., Le,C.C., Wegner,M., and Goossens,M.** (2000). Interaction among SOX10, PAX3 and MITF, three genes altered in Waardenburg syndrome. *Hum. Mol. Genet.* **9**, 1907-1917.

- Bonstein,L., Elias,S., and Frank,D.** (1998). Paraxial-fated mesoderm is required for neural crest induction in *Xenopus* embryos. *Dev. Biol.* **193**, 156-168.
- Borycki,A.G., Li,J., Jin,F., Emerson,C.P., and Epstein,J.A.** (1999). Pax3 functions in cell survival and in pax7 regulation. *Development* **126**, 1665-1674.
- Boulet,S.L., Yang,Q., Mai,C., Kirby,R.S., Collins,J.S., Robbins,J.M., Meyer,R., Canfield,M.A., and Mulinare,J.** (2008). Trends in the postfortification prevalence of spina bifida and anencephaly in the United States. *Birth Defects Res. A Clin. Mol. Teratol.* **82**, 527-532.
- Bourhis,E., Tam,C., Franke,Y., Bazan,J.F., Ernst,J., Hwang,J., Costa,M., Cochran,A.G., and Hannoush,R.N.** (2010). Reconstitution of a frizzled8.Wnt3a.LRP6 signaling complex reveals multiple Wnt and Dkk1 binding sites on LRP6. *J. Biol. Chem.* **285**, 9172-9179.
- Boyles,A.L., Hammock,P., and Speer,M.C.** (2005). Candidate gene analysis in human neural tube defects. *Am. J. Med. Genet. C. Semin. Med. Genet.* **135C**, 9-23.
- Brade,T., Pane,L.S., Moretti,A., Chien,K.R., and Laugwitz,K.L.** (2013). Embryonic heart progenitors and cardiogenesis. *Cold Spring Harb. Perspect. Med.* **3**, a013847.
- Brannon,M., Gomperts,M., Sumoy,L., Moon,R.T., and Kimelman,D.** (1997). A beta-catenin/XTcf-3 complex binds to the siamois promoter to regulate dorsal axis specification in *Xenopus*. *Genes Dev.* **11**, 2359-2370.
- Brantjes,H., Roose,J., van De,W.M., and Clevers,H.** (2001). All Tcf HMG box transcription factors interact with Groucho-related co-repressors. *Nucleic Acids Res.* **29**, 1410-1419.
- Brault,V., Moore,R., Kutsch,S., Ishibashi,M., Rowitch,D.H., McMahon,A.P., Sommer,L., Boussadia,O., and Kemler,R.** (2001). Inactivation of the beta-catenin gene by Wnt1-Cre-mediated deletion results in dramatic brain malformation and failure of craniofacial development. *Development* **128**, 1253-1264.
- Braunstein,M., Rose,A.B., Holmes,S.G., Allis,C.D., and Broach,J.R.** (1993). Transcriptional silencing in yeast is associated with reduced nucleosome acetylation. *Genes Dev.* **7**, 592-604.
- Brembeck,F.H., Schwarz-Romond,T., Bakkers,J., Wilhelm,S., Hammerschmidt,M., and Birchmeier,W.** (2004). Essential role of BCL9-2 in the switch between beta-catenin's adhesive and transcriptional functions. *Genes Dev.* **18**, 2225-2230.
- Brieher,W.M. and Gumbiner,B.M.** (1994). Regulation of C-cadherin function during activin induced morphogenesis of *Xenopus* animal caps. *J. Cell Biol.* **126**, 519-527.
- Britsch,S., Goerich,D.E., Riethmacher,D., Peirano,R.I., Rossner,M., Nave,K.A., Birchmeier,C., and Wegner,M.** (2001). The transcription factor Sox10 is a key regulator of peripheral glial development. *Genes Dev.* **15**, 66-78.
- Britsch,S., Li,L., Kirchhoff,S., Theuring,F., Brinkmann,V., Birchmeier,C., and Riethmacher,D.** (1998). The ErbB2 and ErbB3 receptors and their ligand, neuregulin-1, are essential for development of the sympathetic nervous system. *Genes Dev.* **12**, 1825-1836.
- Bronner-Fraser,M.** (1985). Alterations in neural crest migration by a monoclonal antibody that affects cell adhesion. *J. Cell Biol.* **101**, 610-617.

- Brook,F.A., Estibeiro,J.P., and Copp,A.J.** (1994). Female predisposition to cranial neural tube defects is not because of a difference between the sexes in the rate of embryonic growth or development during neurulation. *J. Med. Genet.* **31**, 383-387.
- Brouns,M.R., De Castro,S.C., Terwindt-Rouwenhorst,E.A., Massa,V., Hekking,J.W., Hirst,C.S., Savery,D., Munts,C., Partridge,D., Lamers,W. et al.** (2011). Over-expression of Grhl2 causes spina bifida in the Axial defects mutant mouse. *Hum. Mol. Genet.* **20**, 1536-1546.
- Brouns,M.R., Matheson,S.F., Hu,K.Q., Delalle,I., Caviness,V.S., Silver,J., Bronson,R.T., and Settleman,J.** (2000). The adhesion signaling molecule p190 RhoGAP is required for morphogenetic processes in neural development. *Development* **127**, 4891-4903.
- Brown,S.D., Twells,R.C., Hey,P.J., Cox,R.D., Levy,E.R., Soderman,A.R., Metzker,M.L., Caskey,C.T., Todd,J.A., and Hess,J.F.** (1998). Isolation and characterization of LRP6, a novel member of the low density lipoprotein receptor gene family. *Biochem. Biophys. Res. Commun.* **248**, 879-888.
- Bruner,J.P., Tulipan,N., Paschall,R.L., Boehm,F.H., Walsh,W.F., Silva,S.R., Hernanz-Schulman,M., Lowe,L.H., and Reed,G.W.** (1999). Fetal surgery for myelomeningocele and the incidence of shunt-dependent hydrocephalus. *JAMA* **282**, 1819-1825.
- Bryja,V., Schulte,G., Rawal,N., Grahn,A., and Arenas,E.** (2007). Wnt-5a induces Dishevelled phosphorylation and dopaminergic differentiation via a CK1-dependent mechanism. *J. Cell Sci.* **120**, 586-595.
- Buckingham,M. and Relaix,F.** (2007). The role of Pax genes in the development of tissues and organs: Pax3 and Pax7 regulate muscle progenitor cell functions. *Annu. Rev. Cell Dev. Biol.* **23**, 645-673.
- Buckiova,D. and Syka,J.** (2004). Development of the inner ear in Splotch mutant mice. *Neuroreport* **15**, 2001-2005.
- Budi,E.H., Patterson,L.B., and Parichy,D.M.** (2008). Embryonic requirements for ErbB signaling in neural crest development and adult pigment pattern formation. *Development.* **135**, 2603-2614.
- Burren,K.A., Savery,D., Massa,V., Kok,R.M., Scott,J.M., Blom,H.J., Copp,A.J., and Greene,N.D.** (2008). Gene-environment interactions in the causation of neural tube defects: folate deficiency increases susceptibility conferred by loss of Pax3 function. *Hum. Mol. Genet.* **17**, 3675-3685.
- Cai,C. and Shi,O.** (2014). Genetic evidence in planar cell polarity signaling pathway in human neural tube defects. *Front Med.* **8**, 68-78.
- Cano,A., Perez-Moreno,M.A., Rodrigo,I., Locascio,A., Blanco,M.J., del Barrio,M.G., Portillo,F., and Nieto,M.A.** (2000). The transcription factor snail controls epithelial-mesenchymal transitions by repressing E-cadherin expression. *Nat. Cell Biol.* **2**, 76-83.
- Cao,Y., Liu,R., Jiang,X., Lu,J., Jiang,J., Zhang,C., Li,X., and Ning,G.** (2009). Nuclear-cytoplasmic shuttling of menin regulates nuclear translocation of {beta}-catenin. *Mol. Cell Biol.* **29**, 5477-5487.
- Capaldo,C.T., Farkas,A.E., and Nusrat,A.** (2014). Epithelial adhesive junctions. *F1000Prime. Rep.* **6:1**. doi: [10.12703/P6-1](https://doi.org/10.12703/P6-1). eCollection;2014., 1.

- Carezani-Gavin,M., Clarren,S.K., and Steege,T.** (1992). Waardenburg syndrome associated with meningomyelocele. *Am. J. Med. Genet.* **42**, 135-136.
- Carl,T.F., Dufton,C., Hanken,J., and Klymkowsky,M.W.** (1999). Inhibition of neural crest migration in *Xenopus* using antisense slug RNA. *Dev. Biol.* **213**, 101-115.
- Carmona-Fontaine,C., Matthews,H.K., Kuriyama,S., Moreno,M., Dunn,G.A., Parsons,M., Stern,C.D., and Mayor,R.** (2008). Contact inhibition of locomotion in vivo controls neural crest directional migration. *Nature.* **456**, 957-961.
- Carmona-Fontaine,C., Theveneau,E., Tzekou,A., Tada,M., Woods,M., Page,K.M., Parsons,M., Lambris,J.D., and Mayor,R.** (2011). Complement fragment C3a controls mutual cell attraction during collective cell migration. *Dev. Cell.* **21**, 1026-1037.
- Carraway,K.L., III and Cantley,L.C.** (1994). A new acquaintance for erbB3 and erbB4: a role for receptor heterodimerization in growth signaling. *Cell.* **78**, 5-8.
- Carter,C.O. and Evans,K.** (1973). Spina bifida and anencephalus in greater London. *J. Med. Genet.* **10**, 209-234.
- Carthy,J.M., Garmaroudi,F.S., Luo,Z., and McManus,B.M.** (2011). Wnt3a induces myofibroblast differentiation by upregulating TGF-beta signaling through SMAD2 in a beta-catenin-dependent manner. *PLoS. One.* **6**, e19809.
- Castano,J., Raurell,I., Piedra,J.A., Miravet,S., Dunach,M., and Garcia de,H.A.** (2002). Beta-catenin N- and C-terminal tails modulate the coordinated binding of adherens junction proteins to beta-catenin. *J. Biol. Chem.* **277**, 31541-31550.
- Cavallo,R.A., Cox,R.T., Moline,M.M., Roose,J., Polevoy,G.A., Clevers,H., Peifer,M., and Bejsovec,A.** (1998). Drosophila Tcf and Groucho interact to repress Wingless signalling activity. *Nature* **395**, 604-608.
- Chan,W.Y., Cheung,C.S., Yung,K.M., and Copp,A.J.** (2004). Cardiac neural crest of the mouse embryo: axial level of origin, migratory pathway and cell autonomy of the splotch (Sp2H) mutant effect. *Development.* **131**, 3367-3379.
- Chang,T.I., Horal,M., Jain,S.K., Wang,F., Patel,R., and Loeken,M.R.** (2003). Oxidant regulation of gene expression and neural tube development: Insights gained from diabetic pregnancy on molecular causes of neural tube defects. *Diabetologia.* **46**, 538-545.
- Chappell,J.H., Jr., Wang,X.D., and Loeken,M.R.** (2009). Diabetes and apoptosis: neural crest cells and neural tube. *Apoptosis.* **14**, 1472-1483.
- Chatkupt,S., Chatkupt,S., and Johnson,W.G.** (1993). Waardenburg syndrome and myelomeningocele in a family. *J. Med. Genet.* **30**, 83-84.
- Chatkupt,S., Hol,F.A., Shugart,Y.Y., Geurds,M.P., Stenroos,E.S., Koenigsberger,M.R., Hamel,B.C., Johnson,W.G., and Mariman,E.C.** (1995). Absence of linkage between familial neural tube defects and PAX3 gene. *J. Med. Genet.* **32**, 200-204.
- Chen,B., Mao,H.H., Chen,L., Zhang,F.L., Li,K., and Xue,Z.F.** (2013). Loop-tail phenotype in heterozygous mice and neural tube defects in homozygous mice result from a nonsense mutation in the *Vangl2* gene. *Genet. Mol. Res.* **12**, 3157-3165.

- Chen,G., Fernandez,J., Mische,S., and Courey,A.J.** (1999). A functional interaction between the histone deacetylase Rpd3 and the corepressor groucho in *Drosophila* development. *Genes Dev.* **13**, 2218-2230.
- Chen,W., ten,B.D., Brown,J., Ahn,S., Hu,L.A., Miller,W.E., Caron,M.G., Barak,L.S., Nusse,R., and Lefkowitz,R.J.** (2003). Dishevelled 2 recruits beta-arrestin 2 to mediate Wnt5A-stimulated endocytosis of Frizzled 4. *Science.* **301**, 1391-1394.
- Chen,Z., Trotman,L.C., Shaffer,D., Lin,H.K., Dotan,Z.A., Niki,M., Koutcher,J.A., Scher,H.I., Ludwig,T., Gerald,W. et al.** (2005). Crucial role of p53-dependent cellular senescence in suppression of Pten-deficient tumorigenesis. *Nature.* **436**, 725-730.
- Chen,Z.F. and Behringer,R.R.** (1995). twist is required in head mesenchyme for cranial neural tube morphogenesis. *Genes Dev.* **9**, 686-699.
- Cheng,Y., Cheung,M., Abu-Elmagd,M.M., Orme,A., and Scotting,P.J.** (2000). Chick sox10, a transcription factor expressed in both early neural crest cells and central nervous system. *Brain Res. Dev. Brain Res.* **121**, 233-241.
- Cheung,M. and Briscoe,J.** (2003). Neural crest development is regulated by the transcription factor Sox9. *Development.* **130**, 5681-5693.
- Cheung,M., Chaboissier,M.C., Mynett,A., Hirst,E., Schedl,A., and Briscoe,J.** (2005). The transcriptional control of trunk neural crest induction, survival, and delamination. *Dev. Cell.* **8**, 179-192.
- Choi,S.H., Choi,K.M., and Ahn,H.J.** (2010). Coexpression and protein-protein complexing of DIX domains of human Dvl1 and Axin1 protein. *BMB. Rep.* **43**, 609-613.
- Chong,J.A., Tapia-Ramirez,J., Kim,S., Toledo-Aral,J.J., Zheng,Y., Boutros,M.C., Altshuler,Y.M., Frohman,M.A., Kraner,S.D., and Mandel,G.** (1995). REST: a mammalian silencer protein that restricts sodium channel gene expression to neurons. *Cell* **80**, 949-957.
- Clevers,H. and Nusse,R.** (2012). Wnt/beta-Catenin Signaling and Disease. *Cell* **149**, 1192-1205.
- Cliffe,A., Hamada,F., and Bienz,M.** (2003). A role of Dishevelled in relocating Axin to the plasma membrane during wingless signaling. *Curr. Biol.* **13**, 960-966.
- Collins,C.A., Gnocchi,V.F., White,R.B., Boldrin,L., Perez-Ruiz,A., Relaix,F., Morgan,J.E., and Zammit,P.S.** (2009). Integrated functions of Pax3 and Pax7 in the regulation of proliferation, cell size and myogenic differentiation. *PLoS. One.* **4**, e4475.
- Colman,H., Giannini,C., Huang,L., Gonzalez,J., Hess,K., Bruner,J., Fuller,G., Langford,L., Pelloski,C., Aaron,J. et al.** (2006). Assessment and prognostic significance of mitotic index using the mitosis marker phospho-histone H3 in low and intermediate-grade infiltrating astrocytomas. *Am. J. Surg. Pathol.* **30**, 657-664.
- Cong,F. and Varmus,H.** (2004). Nuclear-cytoplasmic shuttling of Axin regulates subcellular localization of beta-catenin. *Proc. Natl. Acad. Sci. U. S. A* **101**, 2882-2887.
- Conway,S.J., Bundy,J., Chen,J., Dickman,E., Rogers,R., and Will,B.M.** (2000). Decreased neural crest stem cell expansion is responsible for the conotruncal heart defects within the splotch (Sp(2H))/Pax3 mouse mutant. *Cardiovasc. Res.* **47**, 314-328.

- Conway,S.J., Henderson,D.J., and Copp,A.J.** (1997a). Pax3 is required for cardiac neural crest migration in the mouse: evidence from the splotch (Sp2H) mutant. *Development* **124**, 505-514.
- Conway,S.J., Henderson,D.J., Kirby,M.L., Anderson,R.H., and Copp,A.J.** (1997b). Development of a lethal congenital heart defect in the splotch (Pax3) mutant mouse. *Cardiovasc. Res.* **36**, 163-173.
- Coombs,G.S., Yu,J., Canning,C.A., Veltri,C.A., Covey,T.M., Cheong,J.K., Utomo,V., Banerjee,N., Zhang,Z.H., Jadulco,R.C. et al.** (2010). WLS-dependent secretion of WNT3A requires Ser209 acylation and vacuolar acidification. *J. Cell Sci.* **123**, 3357-3367.
- Copp,A.J., Brook,F.A., Estibeiro,J.P., Shum,A.S., and Cockroft,D.L.** (1990). The embryonic development of mammalian neural tube defects. *Prog. Neurobiol.* **35**, 363-403.
- Copp,A.J., Brook,F.A., and Roberts,H.J.** (1988a). A cell-type-specific abnormality of cell proliferation in mutant (curly tail) mouse embryos developing spinal neural tube defects. *Development* **104**, 285-295.
- Copp,A.J., Crolla,J.A., and Brook,F.A.** (1988b). Prevention of spinal neural tube defects in the mouse embryo by growth retardation during neurulation. *Development.* **104**, 297-303.
- Copp,A.J., Greene,N.D., and Murdoch,J.N.** (2003). The genetic basis of mammalian neurulation. *Nat. Rev. Genet.* **4**, 784-793.
- Copp,A.J., Stanier,P., and Greene,N.D.** (2013). Neural tube defects: recent advances, unsolved questions, and controversies. *Lancet Neurol.* **12**, 799-810.
- Corada,M., Nyqvist,D., Orsenigo,F., Caprini,A., Giampietro,C., Taketo,M.M., Iruela-Arispe,M.L., Adams,R.H., and Dejana,E.** (2010). The Wnt/beta-catenin pathway modulates vascular remodeling and specification by upregulating Dll4/Notch signaling. *Dev. Cell* **18**, 938-949.
- Correa,A., Gilboa,S.M., Besser,L.M., Botto,L.D., Moore,C.A., Hobbs,C.A., Cleves,M.A., Riehle-Colarusso,T.J., Waller,D.K., and Reece,E.A.** (2008). Diabetes mellitus and birth defects. *Am. J. Obstet. Gynecol.* **199**, 237-239.
- Cox,R.T., Pai,L.M., Kirkpatrick,C., Stein,J., and Peifer,M.** (1999). Roles of the C terminus of Armadillo in Wingless signaling in *Drosophila*. *Genetics* **153**, 319-332.
- Crider,K.S., Bailey,L.B., and Berry,R.J.** (2011). Folic acid food fortification-its history, effect, concerns, and future directions. *Nutrients.* **3**, 370-384.
- Curtin,J.A., Quint,E., Tsiouri,V., Arkell,R.M., Cattnach,B., Copp,A.J., Henderson,D.J., Spurr,N., Stanier,P., Fisher,E.M. et al.** (2003). Mutation of *Celsr1* disrupts planar polarity of inner ear hair cells and causes severe neural tube defects in the mouse. *Curr. Biol.* **13**, 1129-1133.
- Dajani,R., Fraser,E., Roe,S.M., Yeo,M., Good,V.M., Thompson,V., Dale,T.C., and Pearl,L.H.** (2003). Structural basis for recruitment of glycogen synthase kinase 3beta to the axin-APC scaffold complex. *EMBO J.* **22**, 494-501.
- Dajani,R., Fraser,E., Roe,S.M., Young,N., Good,V., Dale,T.C., and Pearl,L.H.** (2001). Crystal structure of glycogen synthase kinase 3 beta: structural basis for phosphate-primed substrate specificity and autoinhibition. *Cell* **105**, 721-732.

- Dale,L., Howes,G., Price,B.M., and Smith,J.C.** (1992). Bone morphogenetic protein 4: a ventralizing factor in early *Xenopus* development. *Development* **115**, 573-585.
- Daneman,R., Agalliu,D., Zhou,L., Kuhnert,F., Kuo,C.J., and Barres,B.A.** (2009). Wnt/beta-catenin signaling is required for CNS, but not non-CNS, angiogenesis. *Proc. Natl. Acad. Sci. U. S. A* **106**, 641-646.
- Dann,C.E., Hsieh,J.C., Rattner,A., Sharma,D., Nathans,J., and Leahy,D.J.** (2001). Insights into Wnt binding and signalling from the structures of two Frizzled cysteine-rich domains. *Nature* **412**, 86-90.
- Das,S., Yu,S., Sakamori,R., Stypulkowski,E., and Gao,N.** (2012). Wntless in Wnt secretion: molecular, cellular and genetic aspects. *Front Biol. (Beijing)* **7**, 587-593.
- Daston,G., Lamar,E., Olivier,M., and Goulding,M.** (1996). Pax-3 is necessary for migration but not differentiation of limb muscle precursors in the mouse. *Development* **122**, 1017-1027.
- David,G.** (1993). Integral membrane heparan sulfate proteoglycans. *FASEB J.* **7**, 1023-1030.
- Davidson,C.E., Li,Q., Churchill,G.A., Osborne,L.R., and McDermid,H.E.** (2007). Modifier locus for exencephaly in *Cecr2* mutant mice is syntenic to the 10q25.3 region associated with neural tube defects in humans. *Physiol Genomics* **31**, 244-251.
- Davidson,G., Wu,W., Shen,J., Bilic,J., Fenger,U., Stanek,P., Glinka,A., and Niehrs,C.** (2005). Casein kinase 1 gamma couples Wnt receptor activation to cytoplasmic signal transduction. *Nature* **438**, 867-872.
- Davis,N., Yoffe,C., Raviv,S., Antes,R., Berger,J., Holzmann,S., Stoykova,A., Overbeek,P.A., Tamm,E.R., and Ashery-Padan,R.** (2009). Pax6 dosage requirements in iris and ciliary body differentiation. *Dev. Biol.* **333**, 132-142.
- De Bellard,M.E., Ching,W., Gossler,A., and Bronner-Fraser,M.** (2002). Disruption of segmental neural crest migration and ephrin expression in delta-1 null mice. *Dev. Biol.* **249**, 121-130.
- de la Pompa,J.L., Wakeham,A., Correia,K.M., Samper,E., Brown,S., Aguilera,R.J., Nakano,T., Honjo,T., Mak,T.W., Rossant,J. et al.** (1997). Conservation of the Notch signalling pathway in mammalian neurogenesis. *Development.* **124**, 1139-1148.
- De,C.J., Araya,C., Marchant,L., Riaz,C.F., and Mayor,R.** (2005). Essential role of non-canonical Wnt signalling in neural crest migration. *Development.* **132**, 2587-2597.
- de,C.N., Maczkowiak,F., and Monsoro-Burq,A.H.** (2011). Reiterative AP2a activity controls sequential steps in the neural crest gene regulatory network. *Proc. Natl. Acad. Sci. U. S. A.* **108**, 155-160.
- Deardorff,M.A., Tan,C., Saint-Jeannet,J.P., and Klein,P.S.** (2001). A role for frizzled 3 in neural crest development. *Development* **128**, 3655-3663.
- del Barrio,M.G. and Nieto,M.A.** (2002). Overexpression of Snail family members highlights their ability to promote chick neural crest formation. *Development.* **129**, 1583-1593.
- Delaune,E., Lemaire,P., and Kodjabachian,L.** (2005). Neural induction in *Xenopus* requires early FGF signalling in addition to BMP inhibition. *Development* **132**, 299-310.

- Delezoide,A.L. and Vekemans,M.** (1994). Waardenburg syndrome in man and splotch mutants in the mouse: a paradigm of the usefulness of linkage and syntenic homologies in mouse and man for the genetic analysis of human congenital malformations. *Biomed. Pharmacother.* **48**, 335-339.
- Delgado,E.R., Yang,J., So,J., Leimgruber,S., Kahn,M., Ishitani,T., Shin,D., Wilson,G.M., and Monga,S.P.** (2014). Identification and Characterization of a Novel Small-Molecule Inhibitor of beta-Catenin Signaling. *Am. J. Pathol.* **10**.
- Deol,M.S.** (1966). Influence of the neural tube on the differentiation of the inner ear in the mammalian embryo. *Nature* **209**, 219-220.
- Detrait,E.R., George,T.M., Etchevers,H.C., Gilbert,J.R., Vekemans,M., and Speer,M.C.** (2005). Human neural tube defects: developmental biology, epidemiology, and genetics. *Neurotoxicol. Teratol.* **27**, 515-524.
- Detrick,R.J., Dickey,D., and Kintner,C.R.** (1990). The effects of N-cadherin misexpression on morphogenesis in *Xenopus* embryos. *Neuron* **4**, 493-506.
- DICKIE,M.M.** (1964). NEW SPLOTCH ALLELES IN THE MOUSE. *J. Hered.* **55**, 97-101.
- Dickinson,M.E., Krumlauf,R., and McMahon,A.P.** (1994). Evidence for a mitogenic effect of Wnt-1 in the developing mammalian central nervous system. *Development* **120**, 1453-1471.
- Donehower,L.A., Harvey,M., Slagle,B.L., McArthur,M.J., Montgomery,C.A., Jr., Butel,J.S., and Bradley,A.** (1992). Mice deficient for p53 are developmentally normal but susceptible to spontaneous tumours. *Nature* **356**, 215-221.
- Dottori,M., Gross,M.K., Labosky,P., and Goulding,M.** (2001). The winged-helix transcription factor *Foxd3* suppresses interneuron differentiation and promotes neural crest cell fate. *Development.* **128**, 4127-4138.
- Dressler,G.R., Deutsch,U., Chowdhury,K., Nornes,H.O., and Gruss,P.** (1990). *Pax2*, a new murine paired-box-containing gene and its expression in the developing excretory system. *Development.* **109**, 787-795.
- Dude,C.M., Kuan,C.Y., Bradshaw,J.R., Greene,N.D., Relaix,F., Stark,M.R., and Baker,C.V.** (2009). Activation of *Pax3* target genes is necessary but not sufficient for neurogenesis in the ophthalmic trigeminal placode. *Dev. Biol.* **326**, 314-326.
- Dutton,K.A., Pauliny,A., Lopes,S.S., Elworthy,S., Carney,T.J., Rauch,J., Geisler,R., Haffter,P., and Kelsh,R.N.** (2001). Zebrafish *colourless* encodes *sox10* and specifies non-ectomesenchymal neural crest fates. *Development.* **128**, 4113-4125.
- Eblaghie,M.C., Lunn,J.S., Dickinson,R.J., Munsterberg,A.E., Sanz-Ezquerro,J.J., Farrell,E.R., Mathers,J., Keyse,S.M., Storey,K., and Tickle,C.** (2003). Negative feedback regulation of FGF signaling levels by *Pyst1/MKP3* in chick embryos. *Curr. Biol.* **13**, 1009-1018.
- Echelard,Y., Epstein,D.J., St-Jacques,B., Shen,L., Mohler,J., McMahon,J.A., and McMahon,A.P.** (1993). Sonic hedgehog, a member of a family of putative signaling molecules, is implicated in the regulation of CNS polarity. *Cell.* **75**, 1417-1430.
- Edelman,G.M.** (1986). Cell adhesion molecules in the regulation of animal form and tissue pattern. *Annu. Rev. Cell Biol.* **2:81-116.**, 81-116.

- Ederly,P., Attie,T., Amiel,J., Pelet,A., Eng,C., Hofstra,R.M., Martelli,H., Bidaud,C., Munnich,A., and Lyonnet,S.** (1996). Mutation of the endothelin-3 gene in the Waardenburg-Hirschsprung disease (Shah-Waardenburg syndrome). *Nat. Genet.* **12**, 442-444.
- Eickholt,B.J., Mackenzie,S.L., Graham,A., Walsh,F.S., and Doherty,P.** (1999). Evidence for collapsin-1 functioning in the control of neural crest migration in both trunk and hindbrain regions. *Development.* **126**, 2181-2189.
- el-Deiry,W.S.** (1998). Regulation of p53 downstream genes. *Semin. Cancer Biol.* **8**, 345-357.
- Ellies,D.L., Church,V., Francis-West,P., and Lumsden,A.** (2000). The WNT antagonist cSFRP2 modulates programmed cell death in the developing hindbrain. *Development.* **127**, 5285-5295.
- Elul,T., Koehl,M.A., and Keller,R.** (1997). Cellular mechanism underlying neural convergent extension in *Xenopus laevis* embryos. *Dev. Biol.* **191**, 243-258.
- Endo,Y., Osumi,N., and Wakamatsu,Y.** (2002). Bimodal functions of Notch-mediated signaling are involved in neural crest formation during avian ectoderm development. *Development.* **129**, 863-873.
- Engleka,K.A., Gitler,A.D., Zhang,M., Zhou,D.D., High,F.A., and Epstein,J.A.** (2005). Insertion of Cre into the Pax3 locus creates a new allele of Splotch and identifies unexpected Pax3 derivatives. *Dev. Biol.* **280**, 396-406.
- Eom,D.S., Amarnath,S., and Agarwala,S.** (2013). Apicobasal polarity and neural tube closure. *Dev. Growth Differ.* **55**, 164-172.
- Eom,D.S., Amarnath,S., Fogel,J.L., and Agarwala,S.** (2011). Bone morphogenetic proteins regulate neural tube closure by interacting with the apicobasal polarity pathway. *Development* **138**, 3179-3188.
- Eom,D.S., Amarnath,S., Fogel,J.L., and Agarwala,S.** (2012). Bone morphogenetic proteins regulate hinge point formation during neural tube closure by dynamic modulation of apicobasal polarity. *Birth Defects Res. A Clin. Mol. Teratol.* **94**, 804-816.
- Epstein,D.J., Vekemans,M., and Gros,P.** (1991). Splotch (Sp2H), a mutation affecting development of the mouse neural tube, shows a deletion within the paired homeodomain of Pax-3. *Cell* **67**, 767-774.
- Epstein,D.J., Vogan,K.J., Trasler,D.G., and Gros,P.** (1993). A mutation within intron 3 of the Pax-3 gene produces aberrantly spliced mRNA transcripts in the splotch (Sp) mouse mutant. *Proc. Natl. Acad. Sci. U. S. A* **90**, 532-536.
- Ericson,J., Morton,S., Kawakami,A., Roelink,H., and Jessell,T.M.** (1996). Two critical periods of Sonic Hedgehog signaling required for the specification of motor neuron identity. *Cell* **87**, 661-673.
- Estibeiro,J.P., Brook,F.A., and Copp,A.J.** (1993). Interaction between splotch (Sp) and curly tail (ct) mouse mutants in the embryonic development of neural tube defects. *Development* **119**, 113-121.
- Fagotto,F., Jho,E., Zeng,L., Kurth,T., Joos,T., Kaufmann,C., and Costantini,F.** (1999). Domains of axin involved in protein-protein interactions, Wnt pathway inhibition, and intracellular localization. *J. Cell Biol.* **145**, 741-756.

- Fairchild,C.L., Conway,J.P., Schiffmacher,A.T., Taneyhill,L.A., and Gammill,L.S.** (2014). FoxD3 regulates cranial neural crest EMT via downregulation of tetraspanin18 independent of its functions during neural crest formation. *Mech. Dev.* **132:1-12**. doi: **10.1016/j.mod.2014.02.004**. Epub;2014 Feb 28., 1-12.
- Fairchild,C.L. and Gammill,L.S.** (2013). Tetraspanin18 is a FoxD3-responsive antagonist of cranial neural crest epithelial-to-mesenchymal transition that maintains cadherin-6B protein. *J. Cell Sci.* **126**, 1464-1476.
- Fan,C.M., Lee,C.S., and Tessier-Lavigne,M.** (1997). A role for WNT proteins in induction of dermomyotome. *Dev. Biol.* **191**, 160-165.
- Farmer,D.L., von Koch,C.S., Peacock,W.J., Danielpour,M., Gupta,N., Lee,H., and Harrison,M.R.** (2003). In utero repair of myelomeningocele: experimental pathophysiology, initial clinical experience, and outcomes. *Arch. Surg.* **138**, 872-878.
- Farrer,L.A., Arnos,K.S., Asher,J.H., Jr., Baldwin,C.T., Diehl,S.R., Friedman,T.B., Greenberg,J., Grundfast,K.M., Hoth,C., Lalwani,A.K. et al.** (1994). Locus heterogeneity for Waardenburg syndrome is predictive of clinical subtypes. *Am. J. Hum. Genet.* **55**, 728-737.
- Fenby,B.T., Fotaki,V., and Mason,J.O.** (2008). Pax3 regulates Wnt1 expression via a conserved binding site in the 5' proximal promoter. *Biochim. Biophys. Acta.* **1779**, 115-121.
- Feng,Q., Huang,S., Zhang,A., Chen,Q., Guo,X., Chen,R., and Yang,T.** (2009). Y-box protein 1 stimulates mesangial cell proliferation via activation of ERK1/2. *Nephron Exp. Nephrol.* **113**, e16-e25.
- Fine,E.L., Horal,M., Chang,T.I., Fortin,G., and Loeken,M.R.** (1999). Evidence that elevated glucose causes altered gene expression, apoptosis, and neural tube defects in a mouse model of diabetic pregnancy. *Diabetes* **48**, 2454-2462.
- Finnell,R.H., Bennett,G.D., Karras,S.B., and Mohl,V.K.** (1988). Common hierarchies of susceptibility to the induction of neural tube defects in mouse embryos by valproic acid and its 4-propyl-4-pentenoic acid metabolite. *Teratology.* **38**, 313-320.
- Finnell,R.H., Moon,S.P., Abbott,L.C., Golden,J.A., and Chernoff,G.F.** (1986). Strain differences in heat-induced neural tube defects in mice. *Teratology.* **33**, 247-252.
- Fleming,A. and Copp,A.J.** (1998). Embryonic folate metabolism and mouse neural tube defects. *Science* **280**, 2107-2109.
- Fleming,A. and Copp,A.J.** (2000). A genetic risk factor for mouse neural tube defects: defining the embryonic basis. *Hum. Mol. Genet.* **9**, 575-581.
- Fode,C., Gradwohl,G., Morin,X., Dierich,A., LeMeur,M., Golidis,C., and Guillemot,F.** (1998). The bHLH protein NEUROGENIN 2 is a determination factor for epibranchial placode-derived sensory neurons. *Neuron.* **20**, 483-494.
- Food and Drug Administration** (1996). Food Standards: Amendment of Standards of Identity for Enriched Grain Products to Require Addition of Folic Acid. *Federal Register* **61**, 8781-8797.
- Franz,T.** (1989). Persistent truncus arteriosus in the Splotch mutant mouse. *Anat. Embryol. (Berl).* **180**, 457-464.

- Franz,T., Kothary,R., Surani,M.A., Halata,Z., and Grim,M.** (1993). The Splotch mutation interferes with muscle development in the limbs. *Anat. Embryol. (Berl)* **187**, 153-160.
- Freyer,L., Aggarwal,V., and Morrow,B.E.** (2011). Dual embryonic origin of the mammalian otic vesicle forming the inner ear. *Development*. **138**, 5403-5414.
- Fu,J., Tay,S.S., Ling,E.A., and Dheen,S.T.** (2006). High glucose alters the expression of genes involved in proliferation and cell-fate specification of embryonic neural stem cells. *Diabetologia*. **49**, 1027-1038.
- Galili,N., Davis,R.J., Fredericks,W.J., Mukhopadhyay,S., Rauscher,F.J., III, Emanuel,B.S., Rovera,G., and Barr,F.G.** (1993). Fusion of a fork head domain gene to PAX3 in the solid tumour alveolar rhabdomyosarcoma. *Nat. Genet.* **5**, 230-235.
- Gan,X.Q., Wang,J.Y., Xi,Y., Wu,Z.L., Li,Y.P., and Li,L.** (2008). Nuclear Dvl, c-Jun, beta-catenin, and TCF form a complex leading to stabilization of beta-catenin-TCF interaction. *J. Cell Biol.* **180**, 1087-1100.
- Garcia-Castro,M.I., Marcelle,C., and Bronner-Fraser,M.** (2002). Ectodermal Wnt function as a neural crest inducer. *Science* **297**, 848-851.
- Gat,U., DasGupta,R., Degenstein,L., and Fuchs,E.** (1998). De Novo hair follicle morphogenesis and hair tumors in mice expressing a truncated beta-catenin in skin. *Cell* **95**, 605-614.
- Giese,K., Cox,J., and Grosschedl,R.** (1992). The HMG domain of lymphoid enhancer factor 1 bends DNA and facilitates assembly of functional nucleoprotein structures. *Cell* **69**, 185-195.
- Giese,K., Kingsley,C., Kirshner,J.R., and Grosschedl,R.** (1995). Assembly and function of a TCR alpha enhancer complex is dependent on LEF-1-induced DNA bending and multiple protein-protein interactions. *Genes Dev.* **9**, 995-1008.
- Glogarova,K. and Buckiova,D.** (2004). Changes in sialylation in homozygous Sp2H mouse mutant embryos. *Birth Defects Res. A Clin. Mol. Teratol.* **70**, 142-152.
- Gonsalvez,D.G., Li-Yuen-Fong,M., Cane,K.N., Stamp,L.A., Young,H.M., and Anderson,C.R.** (2014). Different neural crest populations exhibit diverse proliferative behaviors. *Dev. Neurobiol.* **10**.
- Goulding,M.** (1992). Paired box genes in vertebrate neurogenesis. *Semin. Neurosci.* **4**, 327-335.
- Goulding,M., Lumsden,A., and Paquette,A.J.** (1994). Regulation of Pax-3 expression in the dermomyotome and its role in muscle development. *Development* **120**, 957-971.
- Goulding,M., Sterrer,S., Fleming,J., Balling,R., Nadeau,J., Moore,K.J., Brown,S.D., Steel,K.P., and Gruss,P.** (1993). Analysis of the Pax-3 gene in the mouse mutant splotch. *Genomics* **17**, 355-363.
- Goulding,M.D., Chalepakis,G., Deutsch,U., Erselius,J.R., and Gruss,P.** (1991). Pax-3, a novel murine DNA binding protein expressed during early neurogenesis. *EMBO J.* **10**, 1135-1147.
- Gouti,M., Briscoe,J., and Gavalas,A.** (2011). Anterior Hox genes interact with components of the neural crest specification network to induce neural crest fates. *Stem Cells.* **29**, 858-870.
- Graham,A., Francis-West,P., Brickell,P., and Lumsden,A.** (1994). The signalling molecule BMP4 mediates apoptosis in the rhombencephalic neural crest. *Nature.* **372**, 684-686.

- Graham,A., Heyman,I., and Lumsden,A.** (1993). Even-numbered rhombomeres control the apoptotic elimination of neural crest cells from odd-numbered rhombomeres in the chick hindbrain. *Development*. **119**, 233-245.
- Graham,T.A., Weaver,C., Mao,F., Kimelman,D., and Xu,W.** (2000). Crystal structure of a beta-catenin/Tcf complex. *Cell*. **103**, 885-896.
- Gravel,M., Iliescu,A., Horth,C., Apuzzo,S., and Gros,P.** (2010). Molecular and cellular mechanisms underlying neural tube defects in the loop-tail mutant mouse. *Biochemistry* **49**, 3445-3455.
- Gray,J.D., Kholmanskikh,S., Castaldo,B.S., Hansler,A., Chung,H., Klotz,B., Singh,S., Brown,A.M., and Ross,M.E.** (2013). LRP6 exerts non-canonical effects on Wnt signaling during neural tube closure. *Hum. Mol. Genet.* **22**, 4267-4281.
- Gray,S., Szymanski,P., and Levine,M.** (1994). Short-range repression permits multiple enhancers to function autonomously within a complex promoter. *Genes Dev.* **8**, 1829-1838.
- Greene,N.D. and Copp,A.J.** (2009). Development of the vertebrate central nervous system: formation of the neural tube. *Prenat. Diagn.* **29**, 303-311.
- Greene,N.D., Massa,V., and Copp,A.J.** (2009). Understanding the causes and prevention of neural tube defects: Insights from the splotch mouse model. *Birth Defects Res. A Clin. Mol. Teratol.* **85**, 322-330.
- Greene,N.D., Stanier,P., and Moore,G.E.** (2011). The emerging role of epigenetic mechanisms in the etiology of neural tube defects. *Epigenetics*. **6**, 875-883.
- Grigoryan,T., Wend,P., Klaus,A., and Birchmeier,W.** (2008). Deciphering the function of canonical Wnt signals in development and disease: conditional loss- and gain-of-function mutations of beta-catenin in mice. *Genes Dev.* **22**, 2308-2341.
- Groden,J., Thliveris,A., Samowitz,W., Carlson,M., Gelbert,L., Albertsen,H., Joslyn,G., Stevens,J., Spirio,L., Robertson,M. et al.** (1991). Identification and characterization of the familial adenomatous polyposis coli gene. *Cell* **66**, 589-600.
- Guger,K.A. and Gumbiner,B.M.** (1995). beta-Catenin has Wnt-like activity and mimics the Nieuwkoop signaling center in *Xenopus* dorsal-ventral patterning. *Dev. Biol.* **172**, 115-125.
- Guo,X., Day,T.F., Jiang,X., Garrett-Beal,L., Topol,L., and Yang,Y.** (2004). Wnt/beta-catenin signaling is sufficient and necessary for synovial joint formation. *Genes Dev.* **18**, 2404-2417.
- Gustavsson,P., Greene,N.D., Lad,D., Pauws,E., De Castro,S.C., Stanier,P., and Copp,A.J.** (2007). Increased expression of Grainyhead-like-3 rescues spina bifida in a folate-resistant mouse model. *Hum. Mol. Genet.* **16**, 2640-2646.
- Hadeball,B., Borchers,A., and Wedlich,D.** (1998). *Xenopus* cadherin-11 (Xcadherin-11) expression requires the Wg/Wnt signal. *Mech. Dev.* **72**, 101-113.
- Haegel,H., Larue,L., Ohsugi,M., Fedorov,L., Herrenknecht,K., and Kemler,R.** (1995). Lack of beta-catenin affects mouse development at gastrulation. *Development* **121**, 3529-3537.
- Han,Z.J., Song,G., Cui,Y., Xia,H.F., and Ma,X.** (2011). Oxidative stress is implicated in arsenic-induced neural tube defects in chick embryos. *Int. J. Dev. Neurosci.* **29**, 673-680.

- Harada,N., Tamai,Y., Ishikawa,T., Sauer,B., Takaku,K., Oshima,M., and Taketo,M.M.** (1999). Intestinal polyposis in mice with a dominant stable mutation of the beta-catenin gene. *EMBO J.* **18**, 5931-5942.
- Hari,L., Brault,V., Kleber,M., Lee,H.Y., Ille,F., Leimeroth,R., Paratore,C., Suter,U., Kemler,R., and Sommer,L.** (2002). Lineage-specific requirements of beta-catenin in neural crest development. *J. Cell Biol.* **159**, 867-880.
- Harris,M.J. and Juriloff,D.M.** (2010). An update to the list of mouse mutants with neural tube closure defects and advances toward a complete genetic perspective of neural tube closure. *Birth Defects Res. A Clin. Mol. Teratol.* **88**, 653-669.
- Hart,M., Concordet,J.P., Lassot,I., Albert,I., del los,S.R., Durand,H., Perret,C., Rubinfeld,B., Margottin,F., Benarous,R. et al.** (1999). The F-box protein beta-TrCP associates with phosphorylated beta-catenin and regulates its activity in the cell. *Curr. Biol.* **9**, 207-210.
- Hart,M.J., de los,S.R., Albert,I.N., Rubinfeld,B., and Polakis,P.** (1998). Downregulation of beta-catenin by human Axin and its association with the APC tumor suppressor, beta-catenin and GSK3 beta. *Curr. Biol.* **8**, 573-581.
- Hayashi,K., Erikson,D.W., Tilford,S.A., Bany,B.M., Maclean,J.A., Rucker,E.B., III, Johnson,G.A., and Spencer,T.E.** (2009). Wnt genes in the mouse uterus: potential regulation of implantation. *Biol. Reprod.* **80**, 989-1000.
- He,T.C., Sparks,A.B., Rago,C., Hermeking,H., Zawel,L., da Costa,L.T., Morin,P.J., Vogelstein,B., and Kinzler,K.W.** (1998). Identification of c-MYC as a target of the APC pathway. *Science* **281**, 1509-1512.
- He,X., Saint-Jeannet,J.P., Woodgett,J.R., Varmus,H.E., and Dawid,I.B.** (1995). Glycogen synthase kinase-3 and dorsoventral patterning in *Xenopus* embryos. *Nature*. **374**, 617-622.
- Heasman,J., Crawford,A., Goldstone,K., Garner-Hamrick,P., Gumbiner,B., McCrea,P., Kintner,C., Noro,C.Y., and Wylie,C.** (1994). Overexpression of cadherins and underexpression of beta-catenin inhibit dorsal mesoderm induction in early *Xenopus* embryos. *Cell*. **79**, 791-803.
- Hebbes,T.R., Thorne,A.W., and Crane-Robinson,C.** (1988). A direct link between core histone acetylation and transcriptionally active chromatin. *EMBO J.* **7**, 1395-1402.
- Hecht,A., Litterst,C.M., Huber,O., and Kemler,R.** (1999). Functional characterization of multiple transactivating elements in beta-catenin, some of which interact with the TATA-binding protein in vitro. *J. Biol. Chem.* **274**, 18017-18025.
- Hecht,A., Vleminckx,K., Stemmler,M.P., van,R.F., and Kemler,R.** (2000). The p300/CBP acetyltransferases function as transcriptional coactivators of beta-catenin in vertebrates. *EMBO J.* **19**, 1839-1850.
- Hegarty,S.V., O'Keeffe,G.W., and Sullivan,A.M.** (2013). BMP-Smad 1/5/8 signalling in the development of the nervous system. *Prog. Neurobiol.*
- Hemavathy,K., Ashraf,S.I., and Ip,Y.T.** (2000). Snail/slug family of repressors: slowly going into the fast lane of development and cancer. *Gene* **257**, 1-12.
- Henderson,B.R.** (2000). Nuclear-cytoplasmic shuttling of APC regulates beta-catenin subcellular localization and turnover. *Nat. Cell Biol.* **2**, 653-660.

- Henderson,D.J., Ybot-Gonzalez,P., and Copp,A.J.** (1997). Over-expression of the chondroitin sulphate proteoglycan versican is associated with defective neural crest migration in the Pax3 mutant mouse (splotch). *Mech. Dev.* **69**, 39-51.
- Hendriksen,J., Fagotto,F., van,d., V, van,S.M., Noordermeer,J., and Fornerod,M.** (2005). RanBP3 enhances nuclear export of active (beta)-catenin independently of CRM1. *J. Cell Biol.* **171**, 785-797.
- Herbarth,B., Pingault,V., Bondurand,N., Kuhlbrodt,K., Hermans-Borgmeyer,I., Puliti,A., Lemort,N., Goossens,M., and Wegner,M.** (1998). Mutation of the Sry-related Sox10 gene in Dominant megacolon, a mouse model for human Hirschsprung disease. *Proc. Natl. Acad. Sci. U. S. A.* **95**, 5161-5165.
- Hernandez-Diaz,S., Werler,M.M., Walker,A.M., and Mitchell,A.A.** (2001). Neural tube defects in relation to use of folic acid antagonists during pregnancy. *Am. J. Epidemiol.* **153**, 961-968.
- Heseker,H.B., Mason,J.B., Selhub,J., Rosenberg,I.H., and Jacques,P.F.** (2009). Not all cases of neural-tube defect can be prevented by increasing the intake of folic acid. *Br. J. Nutr.* **102**, 173-180.
- Hierholzer,A. and Kemler,R.** (2010). Beta-catenin-mediated signaling and cell adhesion in postgastrulation mouse embryos. *Dev. Dyn.* **239**, 191-199.
- Hildebrand,J.D. and Soriano,P.** (1999). Shroom, a PDZ domain-containing actin-binding protein, is required for neural tube morphogenesis in mice. *Cell* **99**, 485-497.
- Hill,T.P., Taketo,M.M., Birchmeier,W., and Hartmann,C.** (2006). Multiple roles of mesenchymal beta-catenin during murine limb patterning. *Development.* **133**, 1219-1229.
- Hinck,L., Nelson,W.J., and Papkoff,J.** (1994). Wnt-1 modulates cell-cell adhesion in mammalian cells by stabilizing beta-catenin binding to the cell adhesion protein cadherin. *J. Cell Biol.* **124**, 729-741.
- Hochgreb-Hagele,T. and Bronner,M.E.** (2013). A novel FoxD3 gene trap line reveals neural crest precursor movement and a role for FoxD3 in their specification. *Dev. Biol.* **374**, 1-11.
- Hofmann,K.** (2000). A superfamily of membrane-bound O-acyltransferases with implications for wnt signaling. *Trends Biochem. Sci.* **25**, 111-112.
- Hol,F.A., Hamel,B.C., Geurds,M.P., Mullaart,R.A., Barr,F.G., Macina,R.A., and Mariman,E.C.** (1995). A frameshift mutation in the gene for PAX3 in a girl with spina bifida and mild signs of Waardenburg syndrome. *J. Med. Genet.* **32**, 52-56.
- Hol,F.A., Schepens,M.T., van Beersum,S.E., Redolfi,E., Affer,M., Vezzoni,P., Hamel,B.C., Karnes,P.S., Mariman,E.C., and Zucchi,I.** (2000). Identification and characterization of an Xq26-q27 duplication in a family with spina bifida and panhypopituitarism suggests the involvement of two distinct genes. *Genomics* **69**, 174-181.
- Holmberg,J., Clarke,D.L., and Frisen,J.** (2000). Regulation of repulsion versus adhesion by different splice forms of an Eph receptor. *Nature* **408**, 203-206.
- Holmes,N.M., Nguyen,H.T., Harrison,M.R., Farmer,D.L., and Baskin,L.S.** (2001). Fetal intervention for myelomeningocele: effect on postnatal bladder function. *J. Urol.* **166**, 2383-2386.

- Hong,C.S. and Saint-Jeannet,J.P.** (2005). Sox proteins and neural crest development. *Semin. Cell Dev. Biol.* **16**, 694-703.
- Honjo,Y., Kniss,J., and Eisen,J.S.** (2008). Neuregulin-mediated ErbB3 signaling is required for formation of zebrafish dorsal root ganglion neurons. *Development.* **135**, 2615-2625.
- Hopwood,N.D., Pluck,A., and Gurdon,J.B.** (1989). A *Xenopus* mRNA related to *Drosophila* twist is expressed in response to induction in the mesoderm and the neural crest. *Cell.* **59**, 893-903.
- Hoth,C.F., Milunsky,A., Lipsky,N., Sheffer,R., Clarren,S.K., and Baldwin,C.T.** (1993). Mutations in the paired domain of the human PAX3 gene cause Klein-Waardenburg syndrome (WS-III) as well as Waardenburg syndrome type I (WS-I). *Am. J. Hum. Genet.* **52**, 455-462.
- Hsieh,J.C., Rattner,A., Smallwood,P.M., and Nathans,J.** (1999). Biochemical characterization of Wnt-frizzled interactions using a soluble, biologically active vertebrate Wnt protein. *Proc. Natl. Acad. Sci. U. S. A.* **96**, 3546-3551.
- Hu,Q., Ueno,N., and Behringer,R.R.** (2004). Restriction of BMP4 activity domains in the developing neural tube of the mouse embryo. *EMBO Rep.* **5**, 734-739.
- Hu,W., Zhang,C., Wu,R., Sun,Y., Levine,A., and Feng,Z.** (2010). Glutaminase 2, a novel p53 target gene regulating energy metabolism and antioxidant function. *Proc. Natl. Acad. Sci. U. S. A.* **107**, 7455-7460.
- Huang,S.M., Mishina,Y.M., Liu,S., Cheung,A., Stegmeier,F., Michaud,G.A., Charlat,O., Wiелlette,E., Zhang,Y., Wiessner,S. et al.** (2009). Tankyrase inhibition stabilizes axin and antagonizes Wnt signalling. *Nature* **461**, 614-620.
- Huber,A.H., Nelson,W.J., and Weis,W.I.** (1997). Three-dimensional structure of the armadillo repeat region of beta-catenin. *Cell* **90**, 871-882.
- Hume,R.F., Jr., Drugan,A., Reichler,A., Lampinen,J., Martin,L.S., Johnson,M.P., and Evans,M.I.** (1996). Aneuploidy among prenatally detected neural tube defects. *Am. J. Med. Genet.* **61**, 171-173.
- Hunt,P., Wilkinson,D., and Krumlauf,R.** (1991). Patterning the vertebrate head: murine Hox 2 genes mark distinct subpopulations of premigratory and migrating cranial neural crest. *Development.* **112**, 43-50.
- Ichi,S., Costa,F.F., Bischof,J.M., Nakazaki,H., Shen,Y.W., Boshnjaku,V., Sharma,S., Mania-Farnell,B., McLone,D.G., Tomita,T. et al.** (2010). Folic acid remodels chromatin on Hes1 and Neurog2 promoters during caudal neural tube development. *J. Biol. Chem.* **285**, 36922-36932.
- Ichi,S., Nakazaki,H., Boshnjaku,V., Singh,R.M., Mania-Farnell,B., Xi,G., McLone,D.G., Tomita,T., and Mayanil,C.S.** (2012). Fetal neural tube stem cells from Pax3 mutant mice proliferate, differentiate, and form synaptic connections when stimulated with folic acid. *Stem Cells Dev.* **21**, 321-330.
- Ikeda,S., Kishida,S., Yamamoto,H., Murai,H., Koyama,S., and Kikuchi,A.** (1998). Axin, a negative regulator of the Wnt signaling pathway, forms a complex with GSK-3beta and beta-catenin and promotes GSK-3beta-dependent phosphorylation of beta-catenin. *EMBO J.* **17**, 1371-1384.
- Ikeya,M., Lee,S.M., Johnson,J.E., McMahon,A.P., and Takada,S.** (1997). Wnt signalling required for expansion of neural crest and CNS progenitors. *Nature* **389**, 966-970.

- Inukai,T., Inoue,A., Kurosawa,H., Goi,K., Shinjyo,T., Ozawa,K., Mao,M., Inaba,T., and Look,A.T.** (1999). SLUG, a ces-1-related zinc finger transcription factor gene with antiapoptotic activity, is a downstream target of the E2A-HLF oncoprotein. *Mol. Cell* **4**, 343-352.
- Itoh,K., Brott,B.K., Bae,G.U., Ratcliffe,M.J., and Sokol,S.Y.** (2005). Nuclear localization is required for Dishevelled function in Wnt/beta-catenin signaling. *J. Biol.* **4**, 3.
- Jacobson,A.G. and Gordon,R.** (1976). Changes in the shape of the developing vertebrate nervous system analyzed experimentally, mathematically and by computer simulation. *J. Exp. Zool.* **197**, 191-246.
- Janda,C.Y., Waghray,D., Levin,A.M., Thomas,C., and Garcia,K.C.** (2012). Structural basis of Wnt recognition by Frizzled. *Science* **337**, 59-64.
- Janerich,D.T.** (1975). Female excess in anencephaly and spina bifida: possible gestational influences. *Am. J. Epidemiol.* **101**, 70-76.
- Jarvinen,E., Salazar-Ciudad,I., Birchmeier,W., Taketo,M.M., Jernvall,J., and Thesleff,I.** (2006). Continuous tooth generation in mouse is induced by activated epithelial Wnt/beta-catenin signaling. *Proc. Natl. Acad. Sci. U. S. A.* **103**, 18627-18632.
- Jessen,K.R. and Mirsky,R.** (1998). Origin and early development of Schwann cells. *Microsc. Res. Tech.* **41**, 393-402.
- Jho,E.H., Zhang,T., Domon,C., Joo,C.K., Freund,J.N., and Costantini,F.** (2002). Wnt/beta-catenin/Tcf signaling induces the transcription of Axin2, a negative regulator of the signaling pathway. *Mol. Cell Biol.* **22**, 1172-1183.
- Jia,L., Cheng,L., and Raper,J.** (2005). Slit/Robo signaling is necessary to confine early neural crest cells to the ventral migratory pathway in the trunk. *Dev. Biol.* **282**, 411-421.
- Jiang,Y., Liu,M.T., and Gershon,M.D.** (2003). Netrins and DCC in the guidance of migrating neural crest-derived cells in the developing bowel and pancreas. *Dev. Biol.* **258**, 364-384.
- Jin,J., Kittanakom,S., Wong,V., Reyes,B.A., Van Bockstaele,E.J., Stagljar,I., Berrettini,W., and Levenson,R.** (2010). Interaction of the mu-opioid receptor with GPR177 (Wntless) inhibits Wnt secretion: potential implications for opioid dependence. *BMC. Neurosci.* **11**, 33.
- Johnson,M.P., Sutton,L.N., Rintoul,N., Crombleholme,T.M., Flake,A.W., Howell,L.J., Hedrick,H.L., Wilson,R.D., and Adzick,N.S.** (2003). Fetal myelomeningocele repair: short-term clinical outcomes. *Am. J. Obstet. Gynecol.* **189**, 482-487.
- Johnston,J., Ramos-Valdes,Y., Stanton,L.A., Ladhani,S., Beier,F., and Dimattia,G.E.** (2010). Human stanniocalcin-1 or -2 expressed in mice reduces bone size and severely inhibits cranial intramembranous bone growth. *Transgenic Res.* **19**, 1017-1039.
- Johnstone,R.W.** (2002). Histone-deacetylase inhibitors: novel drugs for the treatment of cancer. *Nat. Rev. Drug Discov.* **1**, 287-299.
- Jonkers,J., Meuwissen,R., van der Gulden,H., Peterse,H., van,d, V, and Berns,A.** (2001). Synergistic tumor suppressor activity of BRCA2 and p53 in a conditional mouse model for breast cancer. *Nat. Genet.* **29**, 418-425.
- Joslyn,G., Richardson,D.S., White,R., and Alber,T.** (1993). Dimer formation by an N-terminal coiled coil in the APC protein. *Proc. Natl. Acad. Sci. U. S. A* **90**, 11109-11113.

- Jostes,B., Walther,C., and Gruss,P.** (1990). The murine paired box gene, Pax7, is expressed specifically during the development of the nervous and muscular system. *Mech. Dev.* **33**, 27-37.
- Julius,M.A., Schelbert,B., Hsu,W., Fitzpatrick,E., Jho,E., Fagotto,F., Costantini,F., and Kitajewski,J.** (2000). Domains of axin and disheveled required for interaction and function in wnt signaling. *Biochem. Biophys. Res. Commun.* **276**, 1162-1169.
- Juriloff,D.M. and Harris,M.J.** (2012). Hypothesis: the female excess in cranial neural tube defects reflects an epigenetic drag of the inactivating X chromosome on the molecular mechanisms of neural fold elevation. *Birth Defects Res. A Clin. Mol. Teratol.* **94**, 849-855.
- Kageyama,R., Ohtsuka,T., Shimojo,H., and Imayoshi,I.** (2008). Dynamic Notch signaling in neural progenitor cells and a revised view of lateral inhibition. *Nat. Neurosci.* **11**, 1247-1251.
- Kajita,M., McClinic,K.N., and Wade,P.A.** (2004). Aberrant expression of the transcription factors snail and slug alters the response to genotoxic stress. *Mol. Cell Biol.* **24**, 7559-7566.
- Kanzler,B., Foreman,R.K., Labosky,P.A., and Mallo,M.** (2000). BMP signaling is essential for development of skeletogenic and neurogenic cranial neural crest. *Development.* **127**, 1095-1104.
- Kapron-Bras,C.M. and Trasler,D.G.** (1988). Histological comparison of the effects of the splotch gene and retinoic acid on the closure of the mouse neural tube. *Teratology.* **37**, 389-399.
- Karfunkel,P.** (1971). The role of microtubules and microfilaments in neurulation in *Xenopus*. *Dev. Biol.* **25**, 30-56.
- Karfunkel,P.** (1972). The activity of microtubules and microfilaments in neurulation in the chick. *J. Exp. Zool.* **181**, 289-301.
- Karfunkel,P.** (1974). The mechanisms of neural tube formation. *Int. Rev. Cytol.* **38**, 245-271.
- Kashef,J., Kohler,A., Kuriyama,S., Alfandari,D., Mayor,R., and Wedlich,D.** (2009). Cadherin-11 regulates protrusive activity in *Xenopus* cranial neural crest cells upstream of Trio and the small GTPases. *Genes Dev.* **23**, 1393-1398.
- Kawakami,A., Kimura-Kawakami,M., Nomura,T., and Fujisawa,H.** (1997). Distributions of PAX6 and PAX7 proteins suggest their involvement in both early and late phases of chick brain development. *Mech. Dev.* **66**, 119-130.
- Kee,Y. and Bronner-Fraser,M.** (2005). To proliferate or to die: role of Id3 in cell cycle progression and survival of neural crest progenitors. *Genes Dev.* **19**, 744-755.
- Keller,R., Davidson,L., Edlund,A., Elul,T., Ezin,M., Shook,D., and Skoglund,P.** (2000). Mechanisms of convergence and extension by cell intercalation. *Philos. Trans. R. Soc. Lond B Biol. Sci.* **355**, 897-922.
- Keller,R.E., Danilchik,M., Gimlich,R., and Shih,J.** (1985). The function and mechanism of convergent extension during gastrulation of *Xenopus laevis*. *J. Embryol. Exp. Morphol.* **89 Suppl**, 185-209.
- Keller-Peck,C.R. and Mullen,R.J.** (1996). Patterns of neuronal differentiation in neural tube mutant mice: curly tail and Pax3 splotch-delayed. *J. Comp Neurol.* **368**, 516-526.

- Keller-Peck,C.R. and Mullen,R.J.** (1997). Altered cell proliferation in the spinal cord of mouse neural tube mutants curly tail and Pax3 splotch-delayed. *Brain Res. Dev. Brain Res.* **102**, 177-188.
- Kelsh,R.N. and Eisen,J.S.** (2000). The zebrafish colourless gene regulates development of non-ectomesenchymal neural crest derivatives. *Development.* **127**, 515-525.
- Kiecker,C. and Niehrs,C.** (2001). A morphogen gradient of Wnt/beta-catenin signalling regulates anteroposterior neural patterning in *Xenopus*. *Development* **128**, 4189-4201.
- Kil,S.H. and Bronner-Fraser,M.** (1996). Expression of the avian alpha 7-integrin in developing nervous system and myotome. *Int. J. Dev. Neurosci.* **14**, 181-190.
- Kim,D.H., Inagaki,Y., Suzuki,T., Ioka,R.X., Yoshioka,S.Z., Magoori,K., Kang,M.J., Cho,Y., Nakano,A.Z., Liu,Q. et al.** (1998). A new low density lipoprotein receptor related protein, LRP5, is expressed in hepatocytes and adrenal cortex, and recognizes apolipoprotein E. *J. Biochem.* **124**, 1072-1076.
- Kim,K.C., Friso,S., and Choi,S.W.** (2009). DNA methylation, an epigenetic mechanism connecting folate to healthy embryonic development and aging. *J. Nutr. Biochem.* **20**, 917-926.
- Kim,T.H., Goodman,J., Anderson,K.V., and Niswander,L.** (2007). Phactr4 regulates neural tube and optic fissure closure by controlling PP1-, Rb-, and E2F1-regulated cell-cycle progression. *Dev. Cell.* **13**, 87-102.
- Kinoshita,N., Sasai,N., Misaki,K., and Yonemura,S.** (2008). Apical accumulation of Rho in the neural plate is important for neural plate cell shape change and neural tube formation. *Mol. Biol. Cell* **19**, 2289-2299.
- Kioussi,C., Gross,M.K., and Gruss,P.** (1995). Pax3: a paired domain gene as a regulator in PNS myelination. *Neuron* **15**, 553-562.
- Kirke,P.N., Molloy,A.M., Daly,L.E., Burke,H., Weir,D.G., and Scott,J.M.** (1993). Maternal plasma folate and vitamin B12 are independent risk factors for neural tube defects. *Q. J. Med.* **86**, 703-708.
- Kishida,S., Yamamoto,H., Hino,S., Ikeda,S., Kishida,M., and Kikuchi,A.** (1999). DIX domains of Dvl and axin are necessary for protein interactions and their ability to regulate beta-catenin stability. *Mol. Cell Biol.* **19**, 4414-4422.
- Kissinger,C.R., Liu,B.S., Martin-Blanco,E., Kornberg,T.B., and Pabo,C.O.** (1990). Crystal structure of an engrailed homeodomain-DNA complex at 2.8 Å resolution: a framework for understanding homeodomain-DNA interactions. *Cell* **63**, 579-590.
- Knudsen,K.A. and Wheelock,M.J.** (1992). Plakoglobin, or an 83-kD homologue distinct from beta-catenin, interacts with E-cadherin and N-cadherin. *J. Cell Biol.* **118**, 671-679.
- Koblar,S.A., Murphy,M., Barrett,G.L., Underhill,A., Gros,P., and Bartlett,P.F.** (1999). Pax-3 regulates neurogenesis in neural crest-derived precursor cells. *J. Neurosci. Res.* **56**, 518-530.
- Koch,Y., van,F.B., Kaiser,S., Klein,D., Kibschull,M., Schorle,H., Carpinteiro,A., Gellhaus,A., and Winterhager,E.** (2012). Connexin 31 (GJB3) deficiency in mouse trophoblast stem cells alters giant cell differentiation and leads to loss of oxygen sensing. *Biol. Reprod.* **87**, 37.

- Komekado,H., Yamamoto,H., Chiba,T., and Kikuchi,A.** (2007). Glycosylation and palmitoylation of Wnt-3a are coupled to produce an active form of Wnt-3a. *Genes Cells*. **12**, 521-534.
- Kos,R., Reedy,M.V., Johnson,R.L., and Erickson,C.A.** (2001). The winged-helix transcription factor FoxD3 is important for establishing the neural crest lineage and repressing melanogenesis in avian embryos. *Development*. **128**, 1467-1479.
- Kuriyama,S. and Mayor,R.** (2008). Molecular analysis of neural crest migration. *Philos. Trans. R. Soc. Lond B Biol. Sci.* **363**, 1349-1362.
- Kwok,R.P., Lundblad,J.R., Chrvia,J.C., Richards,J.P., Bachinger,H.P., Brennan,R.G., Roberts,S.G., Green,M.R., and Goodman,R.H.** (1994). Nuclear protein CBP is a coactivator for the transcription factor CREB. *Nature* **370**, 223-226.
- LaBonne,C. and Bronner-Fraser,M.** (1998). Neural crest induction in *Xenopus*: evidence for a two-signal model. *Development* **125**, 2403-2414.
- LaBonne,C. and Bronner-Fraser,M.** (1999). Molecular mechanisms of neural crest formation. *Annu. Rev. Cell Dev. Biol.* **15**, 81-112.
- LaBonne,C. and Bronner-Fraser,M.** (2000). Snail-related transcriptional repressors are required in *Xenopus* for both the induction of the neural crest and its subsequent migration. *Dev. Biol.* **221**, 195-205.
- Lakkis,M.M., Golden,J.A., O'Shea,K.S., and Epstein,J.A.** (1999). Neurofibromin deficiency in mice causes exencephaly and is a modifier for *Splotch* neural tube defects. *Dev. Biol.* **212**, 80-92.
- Lammer,E.J., Sever,L.E., and Oakley,G.P., Jr.** (1987). Teratogen update: valproic acid. *Teratology* **35**, 465-473.
- Lammi,L., Arte,S., Somer,M., Jarvinen,H., Lahermo,P., Thesleff,I., Pirinen,S., and Nieminen,P.** (2004). Mutations in AXIN2 cause familial tooth agenesis and predispose to colorectal cancer. *Am. J. Hum. Genet.* **74**, 1043-1050.
- Landman,K.A., Fernando,A.E., Zhang,D., and Newgreen,D.F.** (2011). Building stable chains with motile agents: Insights into the morphology of enteric neural crest cell migration. *J. Theor. Biol.* **276**, 250-268.
- Lang,D., Chen,F., Milewski,R., Li,J., Lu,M.M., and Epstein,J.A.** (2000). Pax3 is required for enteric ganglia formation and functions with Sox10 to modulate expression of c-ret. *J. Clin. Invest* **106**, 963-971.
- Lang,D., Lu,M.M., Huang,L., Engleka,K.A., Zhang,M., Chu,E.Y., Lipner,S., Skoultchi,A., Millar,S.E., and Epstein,J.A.** (2005). Pax3 functions at a nodal point in melanocyte stem cell differentiation. *Nature*. **433**, 884-887.
- Launay,C., Fromentoux,V., Shi,D.L., and Boucaut,J.C.** (1996). A truncated FGF receptor blocks neural induction by endogenous *Xenopus* inducers. *Development* **122**, 869-880.
- Le Douarin,N.M. and Teillet,M.A.** (1974). Experimental analysis of the migration and differentiation of neuroblasts of the autonomic nervous system and of neurectodermal mesenchymal derivatives, using a biological cell marking technique. *Dev. Biol.* **41**, 162-184.

- Lee,C.H. and Gumbiner,B.M.** (1995). Disruption of gastrulation movements in *Xenopus* by a dominant-negative mutant for C-cadherin. *Dev. Biol.* **171**, 363-373.
- Lee,H.Y., Kleber,M., Hari,L., Brault,V., Suter,U., Taketo,M.M., Kemler,R., and Sommer,L.** (2004). Instructive role of Wnt/beta-catenin in sensory fate specification in neural crest stem cells. *Science* **303**, 1020-1023.
- Lei,Y., Zhu,H., Duhon,C., Yang,W., Ross,M.E., Shaw,G.M., and Finnell,R.H.** (2013). Mutations in planar cell polarity gene SCRIB are associated with spina bifida. *PLoS. One.* **8**, e69262.
- Lei,Y., Zhu,H., Yang,W., Ross,M.E., Shaw,G.M., and Finnell,R.H.** (2014). Identification of novel CELSR1 mutations in spina bifida. *PLoS. One.* **9**, e92207.
- Leptin,M.** (1991). twist and snail as positive and negative regulators during *Drosophila* mesoderm development. *Genes Dev.* **5**, 1568-1576.
- Li,L., Yuan,H., Xie,W., Mao,J., Caruso,A.M., McMahon,A., Sussman,D.J., and Wu,D.** (1999). Dishevelled proteins lead to two signaling pathways. Regulation of LEF-1 and c-Jun N-terminal kinase in mammalian cells. *J. Biol. Chem.* **274**, 129-134.
- Li,R., Chase,M., Jung,S.K., Smith,P.J., and Loeken,M.R.** (2005). Hypoxic stress in diabetic pregnancy contributes to impaired embryo gene expression and defective development by inducing oxidative stress. *Am. J. Physiol Endocrinol. Metab* **289**, E591-E599.
- Li,Z., Ren,A., Zhang,L., Ye,R., Li,S., Zheng,J., Hong,S., Wang,T., and Li,Z.** (2006). Extremely high prevalence of neural tube defects in a 4-county area in Shanxi Province, China. *Birth Defects Res. A Clin. Mol. Teratol.* **76**, 237-240.
- Light,W., Vernon,A.E., Lasorella,A., Iavarone,A., and LaBonne,C.** (2005). *Xenopus* Id3 is required downstream of Myc for the formation of multipotent neural crest progenitor cells. *Development* **132**, 1831-1841.
- Lin,X. and Perrimon,N.** (1999). Dally cooperates with *Drosophila* Frizzled 2 to transduce Wingless signalling. *Nature* **400**, 281-284.
- Lister,J.A., Cooper,C., Nguyen,K., Modrell,M., Grant,K., and Raible,D.W.** (2006). Zebrafish Foxd3 is required for development of a subset of neural crest derivatives. *Dev. Biol.* **290**, 92-104.
- Liu,C., Kato,Y., Zhang,Z., Do,V.M., Yankner,B.A., and He,X.** (1999). beta-Trcp couples beta-catenin phosphorylation-degradation and regulates *Xenopus* axis formation. *Proc. Natl. Acad. Sci. U. S. A* **96**, 6273-6278.
- Liu,C., Li,Y., Semenov,M., Han,C., Baeg,G.H., Tan,Y., Zhang,Z., Lin,X., and He,X.** (2002). Control of beta-catenin phosphorylation/degradation by a dual-kinase mechanism. *Cell* **108**, 837-847.
- Liu,F., Thirumangalathu,S., Gallant,N.M., Yang,S.H., Stoick-Cooper,C.L., Reddy,S.T., Andl,T., Taketo,M.M., Dlugosz,A.A., Moon,R.T. et al.** (2007). Wnt-beta-catenin signaling initiates taste papilla development. *Nat. Genet.* **39**, 106-112.
- Liu,J.P. and Jessell,T.M.** (1998). A role for rhoB in the delamination of neural crest cells from the dorsal neural tube. *Development.* **125**, 5055-5067.

- Lofberg,J., Nynas-McCoy,A., Olsson,C., Jonsson,L., and Perris,R.** (1985). Stimulation of initial neural crest cell migration in the axolotl embryo by tissue grafts and extracellular matrix transplanted on microcarriers. *Dev. Biol.* **107**, 442-459.
- Londin,E.R., Niemiec,J., and Sirotkin,H.I.** (2005). Chordin, FGF signaling, and mesodermal factors cooperate in zebrafish neural induction. *Dev. Biol.* **279**, 1-19.
- Lu,W., Zhu,H., Wen,S., Laurent,C., Shaw,G.M., Lammer,E.J., and Finnell,R.H.** (2007). Screening for novel PAX3 polymorphisms and risks of spina bifida. *Birth Defects Res. A Clin. Mol. Teratol.* **79**, 45-49.
- Luo,H., Liu,X., Wang,F., Huang,Q., Shen,S., Wang,L., Xu,G., Sun,X., Kong,H., Gu,M. et al.** (2005). Disruption of palladin results in neural tube closure defects in mice. *Mol. Cell Neurosci.* **29**, 507-515.
- Lynberg,M.C., Khoury,M.J., Lu,X., and Cocian,T.** (1994). Maternal flu, fever, and the risk of neural tube defects: a population-based case-control study. *Am. J. Epidemiol.* **140**, 244-255.
- Ma,Q., Kintner,C., and Anderson,D.J.** (1996). Identification of neurogenin, a vertebrate neuronal determination gene. *Cell.* **87**, 43-52.
- MacDonald,B.T., Tamai,K., and He,X.** (2009). Wnt/beta-catenin signaling: components, mechanisms, and diseases. *Dev. Cell* **17**, 9-26.
- Mansouri,A., Pla,P., Larue,L., and Gruss,P.** (2001). Pax3 acts cell autonomously in the neural tube and somites by controlling cell surface properties. *Development* **128**, 1995-2005.
- Mansouri,A., Stoykova,A., Torres,M., and Gruss,P.** (1996). Dysgenesis of cephalic neural crest derivatives in Pax7^{-/-} mutant mice. *Development* **122**, 831-838.
- Mao,J., Wang,J., Liu,B., Pan,W., Farr,G.H., III, Flynn,C., Yuan,H., Takada,S., Kimelman,D., Li,L. et al.** (2001). Low-density lipoprotein receptor-related protein-5 binds to Axin and regulates the canonical Wnt signaling pathway. *Mol. Cell* **7**, 801-809.
- Maretto,S., Cordenosi,M., Dupont,S., Braghetta,P., Broccoli,V., Hassan,A.B., Volpin,D., Bressan,G.M., and Piccolo,S.** (2003). Mapping Wnt/beta-catenin signaling during mouse development and in colorectal tumors. *Proc. Natl. Acad. Sci. U. S. A* **100**, 3299-3304.
- Margolis,B. and Borg,J.P.** (2005). Apicobasal polarity complexes. *J. Cell Sci.* **118**, 5157-5159.
- Marose,T.D., Merkel,C.E., McMahan,A.P., and Carroll,T.J.** (2008). Beta-catenin is necessary to keep cells of ureteric bud/Wolffian duct epithelium in a precursor state. *Dev. Biol.* **314**, 112-126.
- Maroto,M., Reshef,R., Munsterberg,A.E., Koester,S., Goulding,M., and Lassar,A.B.** (1997). Ectopic Pax-3 activates MyoD and Myf-5 expression in embryonic mesoderm and neural tissue. *Cell* **89**, 139-148.
- Martin,L.J., Machado,A.F., Loza,M.A., Mao,G.E., Lee,G.S., Hovland,D.N., Jr., Cantor,R.M., and Collins,M.D.** (2003). Effect of arsenite, maternal age, and embryonic sex on spina bifida, exencephaly, and resorption rates in the splotch mouse. *Birth Defects Res. A Clin. Mol. Teratol.* **67**, 231-239.
- Maschhoff,K.L. and Baldwin,H.S.** (2000). Molecular determinants of neural crest migration. *Am. J. Med. Genet.* **97**, 280-288.

- Mason,J.O., Kitajewski,J., and Varmus,H.E.** (1992). Mutational analysis of mouse Wnt-1 identifies two temperature-sensitive alleles and attributes of Wnt-1 protein essential for transformation of a mammary cell line. *Mol. Biol. Cell* **3**, 521-533.
- Massa,V., Savery,D., Ybot-Gonzalez,P., Ferraro,E., Rongvaux,A., Cecconi,F., Flavell,R., Greene,N.D., and Copp,A.J.** (2009). Apoptosis is not required for mammalian neural tube closure. *Proc. Natl. Acad. Sci. U. S. A* **106**, 8233-8238.
- Mastroiacovo,P. and Leoncini,E.** (2011). More folic acid, the five questions: why, who, when, how much, and how. *Biofactors* **37**, 272-279.
- Mathieu,M., Bourges,E., Caron,F., and Piussan,C.** (1990). [Waardenburg's syndrome and severe cyanotic cardiopathy]. *Arch. Fr. Pediatr.* **47**, 657-659.
- Matoba,S., Kang,J.G., Patino,W.D., Wragg,A., Boehm,M., Gavrilova,O., Hurley,P.J., Bunz,F., and Hwang,P.M.** (2006). p53 regulates mitochondrial respiration. *Science.* **312**, 1650-1653.
- Matteson,P.G., Desai,J., Korstanje,R., Lazar,G., Borsuk,T.E., Rollins,J., Kadambi,S., Joseph,J., Rahman,T., Wink,J. et al.** (2008). The orphan G protein-coupled receptor, Gpr161, encodes the vacuolated lens locus and controls neurulation and lens development. *Proc. Natl. Acad. Sci. U. S. A* **105**, 2088-2093.
- Matthews,H.K., Marchant,L., Carmona-Fontaine,C., Kuriyama,S., Larrain,J., Holt,M.R., Parsons,M., and Mayor,R.** (2008). Directional migration of neural crest cells in vivo is regulated by Syndecan-4/Rac1 and non-canonical Wnt signaling/RhoA. *Development.* **135**, 1771-1780.
- Mayor,R., Guerrero,N., and Martinez,C.** (1997). Role of FGF and noggin in neural crest induction. *Dev. Biol.* **189**, 1-12.
- Mayor,R., Morgan,R., and Sargent,M.G.** (1995). Induction of the prospective neural crest of *Xenopus*. *Development* **121**, 767-777.
- McKendry,R., Hsu,S.C., Harland,R.M., and Grosschedl,R.** (1997). LEF-1/TCF proteins mediate wnt-inducible transcription from the *Xenopus* nodal-related 3 promoter. *Dev. Biol.* **192**, 420-431.
- McKeown,S.J., Wallace,A.S., and Anderson,R.B.** (2013). Expression and function of cell adhesion molecules during neural crest migration. *Dev. Biol.* **373**, 244-257.
- McLaughlin,M.E., Kruger,G.M., Slocum,K.L., Crowley,D., Michaud,N.A., Huang,J., Magendantz,M., and Jacks,T.** (2007). The Nf2 tumor suppressor regulates cell-cell adhesion during tissue fusion. *Proc. Natl. Acad. Sci. U. S. A* **104**, 3261-3266.
- McLone,D.G., Dias,M.S., Goossens,W., and Knepper,P.A.** (1997). Pathological changes in exposed neural tissue of fetal delayed splotch (Spd) mice. *Childs Nerv. Syst.* **13**, 1-7.
- McMahon,A.P. and Moon,R.T.** (1989). Ectopic expression of the proto-oncogene int-1 in *Xenopus* embryos leads to duplication of the embryonic axis. *Cell.* **58**, 1075-1084.
- McMahon,J.A., Takada,S., Zimmerman,L.B., Fan,C.M., Harland,R.M., and McMahon,A.P.** (1998). Noggin-mediated antagonism of BMP signaling is required for growth and patterning of the neural tube and somite. *Genes Dev.* **12**, 1438-1452.

- Megason,S.G. and McMahon,A.P.** (2002). A mitogen gradient of dorsal midline Wnts organizes growth in the CNS. *Development* **129**, 2087-2098.
- Memberg,S.P. and Hall,A.K.** (1995). Dividing neuron precursors express neuron-specific tubulin. *J. Neurobiol.* **27**, 26-43.
- Menegola,E., Di,R.F., Broccia,M.L., Prudenziati,M., Minucci,S., Massa,V., and Giavini,E.** (2005). Inhibition of histone deacetylase activity on specific embryonic tissues as a new mechanism for teratogenicity. *Birth Defects Res. B Dev. Reprod. Toxicol.* **74**, 392-398.
- Messier,P.E.** (1969). Effects of beta-mercaptoethanol on the fine structure of the neural plate cells of the chick embryo. *J. Embryol. Exp. Morphol.* **21**, 309-329.
- Mikels,A.J. and Nusse,R.** (2006). Wnts as ligands: processing, secretion and reception. *Oncogene* **25**, 7461-7468.
- Miller,K.A., Barrow,J., Collinson,J.M., Davidson,S., Lear,M., Hill,R.E., and Mackenzie,A.** (2007). A highly conserved Wnt-dependent TCF4 binding site within the proximal enhancer of the anti-myogenic Msx1 gene supports expression within Pax3-expressing limb bud muscle precursor cells. *Dev. Biol.* **311**, 665-678.
- Mills,J.L., McPartlin,J.M., Kirke,P.N., Lee,Y.J., Conley,M.R., Weir,D.G., and Scott,J.M.** (1995). Homocysteine metabolism in pregnancies complicated by neural-tube defects. *Lancet* **345**, 149-151.
- Mitchell,L.E.** (2005). Epidemiology of neural tube defects. *Am. J. Med. Genet. C. Semin. Med. Genet.* **135C**, 88-94.
- Miyake,A., Nihno,S., Murakoshi,Y., Satsuka,A., Nakayama,Y., and Itoh,N.** (2012). Neucrin, a novel secreted antagonist of canonical Wnt signaling, plays roles in developing neural tissues in zebrafish. *Mech. Dev.* **128**, 577-590.
- Miyoshi,A., Kitajima,Y., Sumi,K., Sato,K., Hagiwara,A., Koga,Y., and Miyazaki,K.** (2004). Snail and SIP1 increase cancer invasion by upregulating MMP family in hepatocellular carcinoma cells. *Br. J. Cancer.* **90**, 1265-1273.
- Mo,R., Chew,T.L., Maher,M.T., Bellipanni,G., Weinberg,E.S., and Gottardi,C.J.** (2009). The terminal region of beta-catenin promotes stability by shielding the Armadillo repeats from the axin-scaffold destruction complex. *J. Biol. Chem.* **284**, 28222-28231.
- Moase,C.E. and Trasler,D.G.** (1989). Spinal ganglia reduction in the splotch-delayed mouse neural tube defect mutant. *Teratology* **40**, 67-75.
- Moase,C.E. and Trasler,D.G.** (1990). Delayed neural crest cell emigration from Sp and Spd mouse neural tube explants. *Teratology.* **42**, 171-182.
- Moase,C.E. and Trasler,D.G.** (1991). N-CAM alterations in splotch neural tube defect mouse embryos. *Development* **113**, 1049-1058.
- Molenaar,M., van de Wetering,M., Oosterwegel,M., Peterson-Maduro,J., Godsave,S., Korinek,V., Roose,J., Destree,O., and Clevers,H.** (1996). XTcf-3 transcription factor mediates beta-catenin-induced axis formation in *Xenopus* embryos. *Cell* **86**, 391-399.
- Moline,M.L. and Sandlin,C.** (1993). Waardenburg syndrome and meningomyelocele. *Am. J. Med. Genet.* **47**, 126.

- Monsoro-Burq,A.H., Wang,E., and Harland,R.** (2005). Msx1 and Pax3 cooperate to mediate FGF8 and WNT signals during *Xenopus* neural crest induction. *Dev. Cell* **8**, 167-178.
- Morales,A.V., Barbas,J.A., and Nieto,M.A.** (2005). How to become neural crest: from segregation to delamination. *Semin. Cell Dev. Biol.* **16**, 655-662.
- Morgan,S.C., Lee,H.Y., Relaix,F., Sandell,L.L., Levorse,J.M., and Loeken,M.R.** (2008). Cardiac outflow tract septation failure in Pax3-deficient embryos is due to p53-dependent regulation of migrating cardiac neural crest. *Mech. Dev.* **125**, 757-767.
- Mori-Akiyama,Y., Akiyama,H., Rowitch,D.H., and de,C.B.** (2003). Sox9 is required for determination of the chondrogenic cell lineage in the cranial neural crest. *Proc. Natl. Acad. Sci. U. S. A.* **100**, 9360-9365.
- Morriss,G.M. and Solorsh,M.** (1978). Regional differences in mesenchymal cell morphology and glycosaminoglycans in early neural-fold stage rat embryos. *J. Embryol. Exp. Morphol.* **46**, 37-52.
- Mosimann,C., Hausmann,G., and Basler,K.** (2009). Beta-catenin hits chromatin: regulation of Wnt target gene activation. *Nat. Rev. Mol. Cell Biol.* **10**, 276-286.
- Moury,J.D. and Jacobson,A.G.** (1990). The origins of neural crest cells in the axolotl. *Dev. Biol.* **141**, 243-253.
- MRC** (1991). Prevention of neural tube defects: results of the Medical Research Council Vitamin Study. MRC Vitamin Study Research Group. *Lancet* **338**, 131-137.
- Munsterberg,A.E., Kitajewski,J., Bumcrot,D.A., McMahon,A.P., and Lassar,A.B.** (1995). Combinatorial signaling by Sonic hedgehog and Wnt family members induces myogenic bHLH gene expression in the somite. *Genes Dev.* **9**, 2911-2922.
- Murko,C., Lagger,S., Steiner,M., Seiser,C., Schoefer,C., and Pusch,O.** (2013). Histone deacetylase inhibitor Trichostatin A induces neural tube defects and promotes neural crest specification in the chicken neural tube. *Differentiation* **85**, 55-66.
- Murray,S.A. and Gridley,T.** (2006). Snail family genes are required for left-right asymmetry determination, but not neural crest formation, in mice. *Proc. Natl. Acad. Sci. U. S. A* **103**, 10300-10304.
- Nagai,T., Aruga,J., Minowa,O., Sugimoto,T., Ohno,Y., Noda,T., and Mikoshiba,K.** (2000). Zic2 regulates the kinetics of neurulation. *Proc. Natl. Acad. Sci. U. S. A* **97**, 1618-1623.
- Nagano,T., Hashimoto,T., Nakashima,A., Hisanaga,S., Kikkawa,U., and Kamada,S.** (2013). Cyclin I is involved in the regulation of cell cycle progression. *Cell Cycle.* **12**, 2617-2624.
- Nakagawa,S. and Takeichi,M.** (1995). Neural crest cell-cell adhesion controlled by sequential and subpopulation-specific expression of novel cadherins. *Development.* **121**, 1321-1332.
- Nakamura,Y., Nishisho,I., Kinzler,K.W., Vogelstein,B., Miyoshi,Y., Miki,Y., Ando,H., and Horii,A.** (1992). Mutations of the APC (adenomatous polyposis coli) gene in FAP (familial polyposis coli) patients and in sporadic colorectal tumors. *Tohoku J. Exp. Med.* **168**, 141-147.
- Nakazaki,H., Reddy,A.C., Mania-Farnell,B.L., Shen,Y.W., Ichi,S., McCabe,C., George,D., McLone,D.G., Tomita,T., and Mayanil,C.S.** (2008). Key basic helix-loop-helix transcription

factor genes Hes1 and Ngn2 are regulated by Pax3 during mouse embryonic development. *Dev. Biol.* **316**, 510-523.

Narisawa,A., Komatsuzaki,S., Kikuchi,A., Niihori,T., Aoki,Y., Fujiwara,K., Tanemura,M., Hata,A., Suzuki,Y., Relton,C.L. et al. (2012). Mutations in genes encoding the glycine cleavage system predispose to neural tube defects in mice and humans. *Hum. Mol. Genet.* **21**, 1496-1503.

Neave,B., Holder,N., and Patient,R. (1997). A graded response to BMP-4 spatially coordinates patterning of the mesoderm and ectoderm in the zebrafish. *Mech. Dev.* **62**, 183-195.

Nevin,N.C. and Johnston,W.P. (1980). A family study of spina bifida and anencephalus in Belfast, Northern Ireland (1964 to 1968). *J. Med. Genet.* **17**, 203-211.

Nguyen,D.X., Chiang,A.C., Zhang,X.H., Kim,J.Y., Kris,M.G., Ladanyi,M., Gerald,W.L., and Massague,J. (2009). WNT/TCF signaling through LEF1 and HOXB9 mediates lung adenocarcinoma metastasis. *Cell.* **138**, 51-62.

Nichane,M., de,C.N., Ren,X., Souopgui,J., Monsoro-Burq,A.H., and Bellefroid,E.J. (2008a). Hairy2-Id3 interactions play an essential role in *Xenopus* neural crest progenitor specification. *Dev. Biol.* **322**, 355-367.

Nichane,M., Ren,X., Souopgui,J., and Bellefroid,E.J. (2008b). Hairy2 functions through both DNA-binding and non DNA-binding mechanisms at the neural plate border in *Xenopus*. *Dev. Biol.* **322**, 368-380.

Nieto,M.A., Sargent,M.G., Wilkinson,D.G., and Cooke,J. (1994). Control of cell behavior during vertebrate development by Slug, a zinc finger gene. *Science* **264**, 835-839.

Ninkina,N.N., Stevens,G.E., Wood,J.N., and Richardson,W.D. (1993). A novel Brn3-like POU transcription factor expressed in subsets of rat sensory and spinal cord neurons. *Nucleic Acids Res.* **21**, 3175-3182.

Nishiguchi,S., Wood,H., Kondoh,H., Lovell-Badge,R., and Episkopou,V. (1998). Sox1 directly regulates the gamma-crystallin genes and is essential for lens development in mice. *Genes Dev.* **12**, 776-781.

Nitzan,E., Krispin,S., Pfaltzgraff,E.R., Klar,A., Labosky,P.A., and Kalcheim,C. (2013). A dynamic code of dorsal neural tube genes regulates the segregation between neurogenic and melanogenic neural crest cells. *Development.* **140**, 2269-2279.

Nutt,S.L., Heavey,B., Rolink,A.G., and Busslinger,M. (1999). Commitment to the B-lymphoid lineage depends on the transcription factor Pax5. *Nature.* **401**, 556-562.

O'Rourke,M.P. and Tam,P.P. (2002). Twist functions in mouse development. *Int. J. Dev. Biol.* **46**, 401-413.

Odelberg,S.J., Kollhoff,A., and Keating,M.T. (2000). Dedifferentiation of mammalian myotubes induced by msx1. *Cell* **103**, 1099-1109.

Ohtsubo,M., Theodoras,A.M., Schumacher,J., Roberts,J.M., and Pagano,M. (1995). Human cyclin E, a nuclear protein essential for the G1-to-S phase transition. *Mol. Cell Biol.* **15**, 2612-2624.

- Okano,M., Bell,D.W., Haber,D.A., and Li,E.** (1999). DNA methyltransferases Dnmt3a and Dnmt3b are essential for de novo methylation and mammalian development. *Cell* **99**, 247-257.
- Ordahl,C.P. and Le Douarin,N.M.** (1992). Two myogenic lineages within the developing somite. *Development* **114**, 339-353.
- Orford,K., Crockett,C., Jensen,J.P., Weissman,A.M., and Byers,S.W.** (1997). Serine phosphorylation-regulated ubiquitination and degradation of beta-catenin. *J. Biol. Chem.* **272**, 24735-24738.
- Pai,Y.J., Abdullah,N.L., Mohd-Zin,S.W., Mohammed,R.S., Rolo,A., Greene,N.D., Abdul-Aziz,N.M., and Copp,A.J.** (2012). Epithelial fusion during neural tube morphogenesis. *Birth Defects Res. A Clin. Mol. Teratol.* **94**, 817-823.
- Panakova,D., Sprong,H., Marois,E., Thiele,C., and Eaton,S.** (2005). Lipoprotein particles are required for Hedgehog and Wingless signalling. *Nature* **435**, 58-65.
- Pani,L., Horal,M., and Loeken,M.R.** (2002). Rescue of neural tube defects in Pax-3-deficient embryos by p53 loss of function: implications for Pax-3- dependent development and tumorigenesis. *Genes Dev.* **16**, 676-680.
- Parle-McDermott,A., Pangilinan,F., O'Brien,K.K., Mills,J.L., Magee,A.M., Troendle,J., Sutton,M., Scott,J.M., Kirke,P.N., Molloy,A.M. et al.** (2009). A common variant in MTHFD1L is associated with neural tube defects and mRNA splicing efficiency. *Hum. Mutat.* **30**, 1650-1656.
- Parr,B.A., Shea,M.J., Vassileva,G., and McMahon,A.P.** (1993). Mouse Wnt genes exhibit discrete domains of expression in the early embryonic CNS and limb buds. *Development* **119**, 247-261.
- Partington,M.D. and McLone,D.G.** (1995). Hereditary factors in the etiology of neural tube defects. Results of a survey. *Pediatr. Neurosurg.* **23**, 311-316.
- Patel,S.R., Kim,D., Levitan,I., and Dressler,G.R.** (2007). The BRCT-domain containing protein PTIP links PAX2 to a histone H3, lysine 4 methyltransferase complex. *Dev. Cell.* **13**, 580-592.
- Patterson,E.S., Waller,L.E., and Kroll,K.L.** (2014). Geminin loss causes neural tube defects through disrupted progenitor specification and neuronal differentiation. *Dev. Biol.* **393**, 44-56.
- Peifer,M. and Polakis,P.** (2000). Wnt signaling in oncogenesis and embryogenesis--a look outside the nucleus. *Science* **287**, 1606-1609.
- Pevny,L.H., Sockanathan,S., Placzek,M., and Lovell-Badge,R.** (1998). A role for SOX1 in neural determination. *Development.* **125**, 1967-1978.
- Phelan,S.A., Ito,M., and Loeken,M.R.** (1997). Neural tube defects in embryos of diabetic mice: role of the Pax-3 gene and apoptosis. *Diabetes* **46**, 1189-1197.
- Piedra,J., Martinez,D., Castano,J., Miravet,S., Dunach,M., and de Herreros,A.G.** (2001). Regulation of beta-catenin structure and activity by tyrosine phosphorylation. *J. Biol. Chem.* **276**, 20436-20443.
- Piedrahita,J.A., Oetama,B., Bennett,G.D., van,W.J., Kamen,B.A., Richardson,J., Lacey,S.W., Anderson,R.G., and Finnell,R.H.** (1999). Mice lacking the folic acid-binding protein Folbp1 are defective in early embryonic development. *Nat. Genet.* **23**, 228-232.

- Pingault,V., Bondurand,N., Kuhlbrodt,K., Goerich,D.E., Prehu,M.O., Puliti,A., Herbarth,B., Hermans-Borgmeyer,I., Legius,E., Matthijs,G. et al.** (1998). SOX10 mutations in patients with Waardenburg-Hirschsprung disease. *Nat. Genet.* **18**, 171-173.
- Pinson,K.I., Brennan,J., Monkley,S., Avery,B.J., and Skarnes,W.C.** (2000). An LDL-receptor-related protein mediates Wnt signalling in mice. *Nature* **407**, 535-538.
- Polakis,P.** (1997). The adenomatous polyposis coli (APC) tumor suppressor. *Biochim. Biophys. Acta* **1332**, F127-F147.
- Puffenberger,E.G., Hosoda,K., Washington,S.S., Nakao,K., deWit,D., Yanagisawa,M., and Chakravart,A.** (1994). A missense mutation of the endothelin-B receptor gene in multigenic Hirschsprung's disease. *Cell* **79**, 1257-1266.
- Pyrgaki,C., Liu,A., and Niswander,L.** (2011). Grainyhead-like 2 regulates neural tube closure and adhesion molecule expression during neural fold fusion. *Dev. Biol.* **353**, 38-49.
- Quintin,S., Gally,C., and Labouesse,M.** (2008). Epithelial morphogenesis in embryos: asymmetries, motors and brakes. *Trends Genet.* **24**, 221-230.
- Ray,H.J. and Niswander,L.** (2012). Mechanisms of tissue fusion during development. *Development* **139**, 1701-1711.
- Ray,J.G. and Blom,H.J.** (2003). Vitamin B12 insufficiency and the risk of fetal neural tube defects. *QJM.* **96**, 289-295.
- Read,A.P. and Newton,V.E.** (1997). Waardenburg syndrome. *J. Med. Genet.* **34**, 656-665.
- Reeves,F.C., Burdge,G.C., Fredericks,W.J., Rauscher,F.J., and Lillycrop,K.A.** (1999). Induction of antisense Pax-3 expression leads to the rapid morphological differentiation of neuronal cells and an altered response to the mitogenic growth factor bFGF. *J. Cell Sci.* **112 (Pt 2)**, 253-261.
- Reichsman,F., Smith,L., and Cumberledge,S.** (1996). Glycosaminoglycans can modulate extracellular localization of the wingless protein and promote signal transduction. *J. Cell Biol.* **135**, 819-827.
- Relaix,F., Montarras,D., Zaffran,S., Gayraud-Morel,B., Rocancourt,D., Tajbakhsh,S., Mansouri,A., Cumano,A., and Buckingham,M.** (2006). Pax3 and Pax7 have distinct and overlapping functions in adult muscle progenitor cells. *J. Cell Biol.* **172**, 91-102.
- Relaix,F., Rocancourt,D., Mansouri,A., and Buckingham,M.** (2005). A Pax3/Pax7-dependent population of skeletal muscle progenitor cells. *Nature* **435**, 948-953.
- Ridenour,D.A., McLennan,R., Teddy,J.M., Semerad,C.L., Haug,J.S., and Kulesa,P.M.** (2014). The neural crest cell cycle is related to phases of migration in the head. *Development.* **141**, 1095-1103.
- Rios-Esteves,J. and Resh,M.D.** (2013). Stearoyl CoA Desaturase Is Required to Produce Active, Lipid-Modified Wnt Proteins. *Cell Rep.*
- Rockman,S.P., Currie,S.A., Ciavarella,M., Vincan,E., Dow,C., Thomas,R.J., and Phillips,W.A.** (2001). Id2 is a target of the beta-catenin/T cell factor pathway in colon carcinoma. *J. Biol. Chem.* **276**, 45113-45119.

- Roelink,H. and Nusse,R.** (1991). Expression of two members of the Wnt family during mouse development--restricted temporal and spatial patterns in the developing neural tube. *Genes Dev.* **5**, 381-388.
- Roszko,I., Sawada,A., and Solnica-Krezel,L.** (2009). Regulation of convergence and extension movements during vertebrate gastrulation by the Wnt/PCP pathway. *Semin. Cell Dev. Biol.* **20**, 986-997.
- Roura,S., Miravet,S., Piedra,J., Garcia de,H.A., and Dunach,M.** (1999). Regulation of E-cadherin/Catenin association by tyrosine phosphorylation. *J. Biol. Chem.* **274**, 36734-36740.
- Rubinfeld,B., Albert,I., Porfiri,E., Fiol,C., Munemitsu,S., and Polakis,P.** (1996). Binding of GSK3beta to the APC-beta-catenin complex and regulation of complex assembly. *Science* **272**, 1023-1026.
- Rubinfeld,B., Albert,I., Porfiri,E., Munemitsu,S., and Polakis,P.** (1997). Loss of beta-catenin regulation by the APC tumor suppressor protein correlates with loss of structure due to common somatic mutations of the gene. *Cancer Res.* **57**, 4624-4630.
- Rubinfeld,B., Souza,B., Albert,I., Muller,O., Chamberlain,S.H., Masiarz,F.R., Munemitsu,S., and Polakis,P.** (1993). Association of the APC gene product with beta-catenin. *Science* **262**, 1731-1734.
- Rubinfeld,B., Souza,B., Albert,I., Munemitsu,S., and Polakis,P.** (1995). The APC protein and E-cadherin form similar but independent complexes with alpha-catenin, beta-catenin, and plakoglobin. *J. Biol. Chem.* **270**, 5549-5555.
- Rudloff,S. and Kemler,R.** (2012). Differential requirements for beta-catenin during mouse development. *Development.* **139**, 3711-3721.
- Russell,W.L.** (1947). Splotch, a new mutation in the house mouse, *Mus musculus*. *Genetics* **32**, 107.
- Sah,V.P., Attardi,L.D., Mulligan,G.J., Williams,B.O., Bronson,R.T., and Jacks,T.** (1995). A subset of p53-deficient embryos exhibit exencephaly. *Nat. Genet.* **10**, 175-180.
- Saint-Jeannet,J.P., He,X., Varmus,H.E., and Dawid,I.B.** (1997). Regulation of dorsal fate in the neuraxis by Wnt-1 and Wnt-3a. *Proc. Natl. Acad. Sci. U. S. A* **94**, 13713-13718.
- Santiago,A. and Erickson,C.A.** (2002). Ephrin-B ligands play a dual role in the control of neural crest cell migration. *Development.* **129**, 3621-3632.
- Sasai,N., Mizuseki,K., and Sasai,Y.** (2001). Requirement of FoxD3-class signaling for neural crest determination in *Xenopus*. *Development.* **128**, 2525-2536.
- Sato,A., Scholl,A.M., Kuhn,E.N., Stadt,H.A., Decker,J.R., Pegram,K., Hutson,M.R., and Kirby,M.L.** (2011). FGF8 signaling is chemotactic for cardiac neural crest cells. *Dev. Biol.* **354**, 18-30.
- Sato,T., Sasai,N., and Sasai,Y.** (2005). Neural crest determination by co-activation of Pax3 and Zic1 genes in *Xenopus* ectoderm. *Development.* **132**, 2355-2363.
- Schilling,T.F. and Kimmel,C.B.** (1994). Segment and cell type lineage restrictions during pharyngeal arch development in the zebrafish embryo. *Development.* **120**, 483-494.

- Schoenherr,C.J. and Anderson,D.J.** (1995). The neuron-restrictive silencer factor (NRSF): a coordinate repressor of multiple neuron-specific genes. *Science* **267**, 1360-1363.
- Schoenwolf,G.C.** (1985). Shaping and bending of the avian neuroepithelium: morphometric analyses. *Dev. Biol.* **109**, 127-139.
- Schoenwolf,G.C. and Alvarez,I.S.** (1989). Roles of neuroepithelial cell rearrangement and division in shaping of the avian neural plate. *Development* **106**, 427-439.
- Schoenwolf,G.C. and Powers,M.L.** (1987). Shaping of the chick neuroepithelium during primary and secondary neurulation: role of cell elongation. *Anat. Rec.* **218**, 182-195.
- Scholl,F.A., Kamarashev,J., Murmann,O.V., Geertsen,R., Dummer,R., and Schafer,B.W.** (2001). PAX3 is expressed in human melanomas and contributes to tumor cell survival. *Cancer Res.* **61**, 823-826.
- Schroeder,T.E.** (1970). Neurulation in *Xenopus laevis*. An analysis and model based upon light and electron microscopy. *J. Embryol. Exp. Morphol.* **23**, 427-462.
- Sefton,M., Sanchez,S., and Nieto,M.A.** (1998). Conserved and divergent roles for members of the Snail family of transcription factors in the chick and mouse embryo. *Development* **125**, 3111-3121.
- Sela-Donenfeld,D. and Kalcheim,C.** (1999). Regulation of the onset of neural crest migration by coordinated activity of BMP4 and Noggin in the dorsal neural tube. *Development.* **126**, 4749-4762.
- Selleck,M.A. and Bronner-Fraser,M.** (1995). Origins of the avian neural crest: the role of neural plate-epidermal interactions. *Development* **121**, 525-538.
- Seller,M.J.** (1975). Prenatal diagnosis of a neural tube defect: Meckel syndrome. *J. Med. Genet.* **12**, 109-110.
- Seller,M.J. and Perkins,K.J.** (1986). Effect of mitomycin C on the neural tube defects of the curly-tail mouse. *Teratology* **33**, 305-309.
- Serbedzija,G.N. and McMahon,A.P.** (1997). Analysis of neural crest cell migration in Splotch mice using a neural crest-specific LacZ reporter. *Dev. Biol.* **185**, 139-147.
- Sergi,C., Gekas,J., and Kamnasaran,D.** (2013). Recurrent anencephaly: a case report and examination of the VANGL1 and FOXN1 genes. *Fetal Pediatr. Pathol.* **32**, 293-297.
- Shaham,O., Menuchin,Y., Farhy,C., and Ashery-Padan,R.** (2012). Pax6: a multi-level regulator of ocular development. *Prog. Retin. Eye Res.* **31**, 351-376.
- Shapiro,D.N., Sublett,J.E., Li,B., Downing,J.R., and Naeve,C.W.** (1993). Fusion of PAX3 to a member of the forkhead family of transcription factors in human alveolar rhabdomyosarcoma. *Cancer Res.* **53**, 5108-5112.
- Shariatmadari,M., Peyronnet,J., Papachristou,P., Horn,Z., Sousa,K.M., Arenas,E., and Ringstedt,T.** (2005). Increased Wnt levels in the neural tube impair the function of adherens junctions during neurulation. *Mol. Cell Neurosci.* **30**, 437-451.
- Shi,J., Severson,C., Yang,J., Wedlich,D., and Klymkowsky,M.W.** (2011). Snail2 controls mesodermal BMP/Wnt induction of neural crest. *Development* **138**, 3135-3145.

- Shi,Z.D., Qian,X.M., Zhang,J.X., Han,L., Zhang,K.L., Chen,L.Y., Zhou,X., Zhang,J.N., and Kang,C.S.** (2014). BASI, A Potent Small Molecular Inhibitor, Inhibits Glioblastoma Progression by Targeting microRNA-mediated beta-Catenin Signaling. *CNS. Neurosci. Ther.* **10**.
- Shimizu,H., Julius,M.A., Giarre,M., Zheng,Z., Brown,A.M., and Kitajewski,J.** (1997). Transformation by Wnt family proteins correlates with regulation of beta-catenin. *Cell Growth Differ.* **8**, 1349-1358.
- Shimizu,T., Kagawa,T., Inoue,T., Nonaka,A., Takada,S., Aburatani,H., and Taga,T.** (2008). Stabilized beta-catenin functions through TCF/LEF proteins and the Notch/RBP-Jkappa complex to promote proliferation and suppress differentiation of neural precursor cells. *Mol. Cell Biol.* **28**, 7427-7441.
- Shimojo,H., Ohtsuka,T., and Kageyama,R.** (2008). Oscillations in notch signaling regulate maintenance of neural progenitors. *Neuron.* **58**, 52-64.
- Shum,A.S. and Copp,A.J.** (1996). Regional differences in morphogenesis of the neuroepithelium suggest multiple mechanisms of spinal neurulation in the mouse. *Anat. Embryol. (Berl).* **194**, 65-73.
- Sierra,J., Yoshida,T., Joazeiro,C.A., and Jones,K.A.** (2006). The APC tumor suppressor counteracts beta-catenin activation and H3K4 methylation at Wnt target genes. *Genes Dev.* **20**, 586-600.
- Simons,M., Gault,W.J., Gotthardt,D., Rohatgi,R., Klein,T.J., Shao,Y., Lee,H.J., Wu,A.L., Fang,Y., Satlin,L.M. et al.** (2009). Electrochemical cues regulate assembly of the Frizzled/Dishevelled complex at the plasma membrane during planar epithelial polarization. *Nat. Cell Biol.* **11**, 286-294.
- Smith,A., Robinson,V., Patel,K., and Wilkinson,D.G.** (1997). The EphA4 and EphB1 receptor tyrosine kinases and ephrin-B2 ligand regulate targeted migration of branchial neural crest cells. *Curr. Biol.* **7**, 561-570.
- Smith,A.N., Miller,L.A., Song,N., Taketo,M.M., and Lang,R.A.** (2005). The duality of beta-catenin function: a requirement in lens morphogenesis and signaling suppression of lens fate in periocular ectoderm. *Dev. Biol.* **285**, 477-489.
- Smith,J.L. and Schoenwolf,G.C.** (1987). Cell cycle and neuroepithelial cell shape during bending of the chick neural plate. *Anat. Rec.* **218**, 196-206.
- Smith,J.L. and Schoenwolf,G.C.** (1988). Role of cell-cycle in regulating neuroepithelial cell shape during bending of the chick neural plate. *Cell Tissue Res.* **252**, 491-500.
- Smith,K.J., Levy,D.B., Maupin,P., Pollard,T.D., Vogelstein,B., and Kinzler,K.W.** (1994). Wild-type but not mutant APC associates with the microtubule cytoskeleton. *Cancer Res.* **54**, 3672-3675.
- Sokol,S.Y., Klingensmith,J., Perrimon,N., and Itoh,K.** (1995). Dorsalizing and neuralizing properties of Xdsh, a maternally expressed Xenopus homolog of dishevelled. *Development.* **121**, 1637-1647.
- Solanas,G., Miravet,S., Casagolda,D., Castano,J., Raurell,I., Corrienero,A., de Herreros,A.G., and Dunach,M.** (2004). beta-Catenin and plakoglobin N- and C-tails determine ligand specificity. *J. Biol. Chem.* **279**, 49849-49856.

- Sommer,L., Ma,Q., and Anderson,D.J.** (1996). neurogenins, a novel family of atonal-related bHLH transcription factors, are putative mammalian neuronal determination genes that reveal progenitor cell heterogeneity in the developing CNS and PNS. *Mol. Cell Neurosci.* **8**, 221-241.
- Soo,K., O'Rourke,M.P., Khoo,P.L., Steiner,K.A., Wong,N., Behringer,R.R., and Tam,P.P.** (2002). Twist function is required for the morphogenesis of the cephalic neural tube and the differentiation of the cranial neural crest cells in the mouse embryo. *Dev. Biol.* **247**, 251-270.
- Soshnikova,N., Zechner,D., Huelsken,J., Mishina,Y., Behringer,R.R., Taketo,M.M., Crenshaw,E.B., III, and Birchmeier,W.** (2003). Genetic interaction between Wnt/beta-catenin and BMP receptor signaling during formation of the AER and the dorsal-ventral axis in the limb. *Genes Dev.* **17**, 1963-1968.
- Southard-Smith,E.M., Kos,L., and Pavan,W.J.** (1998). Sox10 mutation disrupts neural crest development in Dom Hirschsprung mouse model. *Nat. Genet.* **18**, 60-64.
- Spokony,R.F., Aoki,Y., Saint-Germain,N., Magner-Fink,E., and Saint-Jeannet,J.P.** (2002). The transcription factor Sox9 is required for cranial neural crest development in Xenopus. *Development.* **129**, 421-432.
- Steel,K.P. and Smith,R.J.** (1992). Normal hearing in Splotch (Sp/+), the mouse homologue of Waardenburg syndrome type 1. *Nat. Genet.* **2**, 75-79.
- Steventon,B., Carmona-Fontaine,C., and Mayor,R.** (2005). Genetic network during neural crest induction: from cell specification to cell survival. *Semin. Cell Dev. Biol.* **16**, 647-654.
- Stewart,R.A., Arduini,B.L., Berghmans,S., George,R.E., Kanki,J.P., Henion,P.D., and Look,A.T.** (2006). Zebrafish foxd3 is selectively required for neural crest specification, migration and survival. *Dev. Biol.* **292**, 174-188.
- Stiefel,D., Copp,A.J., and Meuli,M.** (2007). Fetal spina bifida in a mouse model: loss of neural function in utero. *J. Neurosurg.* **106**, 213-221.
- Stiefel,D. and Meuli,M.** (2007). Scanning electron microscopy of fetal murine myelomeningocele reveals growth and development of the spinal cord in early gestation and neural tissue destruction around birth. *J. Pediatr. Surg.* **42**, 1561-1565.
- Stottmann,R.W., Berrong,M., Matta,K., Choi,M., and Klingensmith,J.** (2006). The BMP antagonist Noggin promotes cranial and spinal neurulation by distinct mechanisms. *Dev. Biol.* **295**, 647-663.
- Streit,A., Lee,K.J., Woo,I., Roberts,C., Jessell,T.M., and Stern,C.D.** (1998). Chordin regulates primitive streak development and the stability of induced neural cells, but is not sufficient for neural induction in the chick embryo. *Development* **125**, 507-519.
- Streit,A. and Stern,C.D.** (1999). Establishment and maintenance of the border of the neural plate in the chick: involvement of FGF and BMP activity. *Mech. Dev.* **82**, 51-66.
- Stumpo,D.J., Bock,C.B., Tuttle,J.S., and Blackshear,P.J.** (1995). MARCKS deficiency in mice leads to abnormal brain development and perinatal death. *Proc. Natl. Acad. Sci. U. S. A* **92**, 944-948.
- Su,L.K., Vogelstein,B., and Kinzler,K.W.** (1993). Association of the APC tumor suppressor protein with catenins. *Science* **262**, 1734-1737.

- Suarez,L., Felkner,M., and Hendricks,K.** (2004). The effect of fever, febrile illnesses, and heat exposures on the risk of neural tube defects in a Texas-Mexico border population. *Birth Defects Res. A Clin. Mol. Teratol.* **70**, 815-819.
- Sun,J.H., Zhang,Y., Yin,B.Y., Li,J.X., Liu,G.S., Xu,W., and Tang,S.** (2012). Differential expression of Axin1, Cdc25c and Cdkn2d mRNA in 2-cell stage mouse blastomeres. *Zygote.* **20**, 305-310.
- Sutherland,C., Leighton,I.A., and Cohen,P.** (1993). Inactivation of glycogen synthase kinase-3 beta by phosphorylation: new kinase connections in insulin and growth-factor signalling. *Biochem. J.* **296 (Pt 1)**, 15-19.
- Sutton,L.N., Adzick,N.S., Bilaniuk,L.T., Johnson,M.P., Crombleholme,T.M., and Flake,A.W.** (1999). Improvement in hindbrain herniation demonstrated by serial fetal magnetic resonance imaging following fetal surgery for myelomeningocele. *JAMA* **282**, 1826-1831.
- Suzuki,A., Ueno,N., and Hemmati-Brivanlou,A.** (1997). Xenopus msx1 mediates epidermal induction and neural inhibition by BMP4. *Development* **124**, 3037-3044.
- Tabata,T. and Takei,Y.** (2004). Morphogens, their identification and regulation. *Development* **131**, 703-712.
- Tada,M. and Heisenberg,C.P.** (2012). Convergent extension: using collective cell migration and cell intercalation to shape embryos. *Development.* **139**, 3897-3904.
- Taelman,V.F., Dobrowolski,R., Plouhinec,J.L., Fuentealba,L.C., Vorwald,P.P., Gumper,I., Sabatini,D.D., and De Robertis,E.M.** (2010). Wnt signaling requires sequestration of glycogen synthase kinase 3 inside multivesicular endosomes. *Cell* **143**, 1136-1148.
- Tajbakhsh,S., Rocancourt,D., Cossu,G., and Buckingham,M.** (1997). Redefining the genetic hierarchies controlling skeletal myogenesis: Pax-3 and Myf-5 act upstream of MyoD. *Cell* **89**, 127-138.
- Takada,R., Satomi,Y., Kurata,T., Ueno,N., Norioka,S., Kondoh,H., Takao,T., and Takada,S.** (2006). Monounsaturated fatty acid modification of Wnt protein: its role in Wnt secretion. *Dev. Cell* **11**, 791-801.
- Takada,S., Stark,K.L., Shea,M.J., Vassileva,G., McMahon,J.A., and McMahon,A.P.** (1994). Wnt-3a regulates somite and tailbud formation in the mouse embryo. *Genes Dev.* **8**, 174-189.
- Takashima,Y., Era,T., Nakao,K., Kondo,S., Kasuga,M., Smith,A.G., and Nishikawa,S.** (2007). Neuroepithelial cells supply an initial transient wave of MSC differentiation. *Cell.* **129**, 1377-1388.
- Tamai,K., Semenov,M., Kato,Y., Spokony,R., Liu,C., Katsuyama,Y., Hess,F., Saint-Jeannet,J.P., and He,X.** (2000). LDL-receptor-related proteins in Wnt signal transduction. *Nature* **407**, 530-535.
- Tamai,K., Zeng,X., Liu,C., Zhang,X., Harada,Y., Chang,Z., and He,X.** (2004). A mechanism for Wnt coreceptor activation. *Mol. Cell* **13**, 149-156.
- Tanaka,K., Kitagawa,Y., and Kadowaki,T.** (2002). Drosophila segment polarity gene product porcupine stimulates the posttranslational N-glycosylation of wingless in the endoplasmic reticulum. *J. Biol. Chem.* **277**, 12816-12823.

- Taneyhill, L.A. and Bronner-Fraser, M.** (2005). Dynamic alterations in gene expression after Wnt-mediated induction of avian neural crest. *Mol. Biol. Cell.* **16**, 5283-5293.
- Taneyhill, L.A., Coles, E.G., and Bronner-Fraser, M.** (2007). Snail2 directly represses cadherin6B during epithelial-to-mesenchymal transitions of the neural crest. *Development.* **134**, 1481-1490.
- Tang, X., Wu, Y., Belenkaya, T.Y., Huang, Q., Ray, L., Qu, J., and Lin, X.** (2012). Roles of N-glycosylation and lipidation in Wg secretion and signaling. *Dev. Biol.* **364**, 32-41.
- Tassabehji, M., Newton, V.E., and Read, A.P.** (1994). Waardenburg syndrome type 2 caused by mutations in the human microphthalmia (MITF) gene. *Nat. Genet.* **8**, 251-255.
- Tassabehji, M., Read, A.P., Newton, V.E., Harris, R., Balling, R., Gruss, P., and Strachan, T.** (1992). Waardenburg's syndrome patients have mutations in the human homologue of the Pax-3 paired box gene. *Nature* **355**, 635-636.
- Tassabehji, M., Read, A.P., Newton, V.E., Patton, M., Gruss, P., Harris, R., and Strachan, T.** (1993). Mutations in the PAX3 gene causing Waardenburg syndrome type 1 and type 2. *Nat. Genet.* **3**, 26-30.
- Teng, L., Mundell, N.A., Frist, A.Y., Wang, Q., and Labosky, P.A.** (2008). Requirement for Foxd3 in the maintenance of neural crest progenitors. *Development.* **135**, 1615-1624.
- Tennant, P.W., Samarasekera, S.D., Pless-Mulloli, T., and Rankin, J.** (2011). Sex differences in the prevalence of congenital anomalies: a population-based study. *Birth Defects Res. A Clin. Mol. Teratol.* **91**, 894-901.
- Tetsu, O. and McCormick, F.** (1999). Beta-catenin regulates expression of cyclin D1 in colon carcinoma cells. *Nature* **398**, 422-426.
- Theocharis, A.D., Skandalis, S.S., Tzanakakis, G.N., and Karamanos, N.K.** (2010). Proteoglycans in health and disease: novel roles for proteoglycans in malignancy and their pharmacological targeting. *FEBS J.* **277**, 3904-3923.
- Theveneau, E. and Mayor, R.** (2012). Neural crest delamination and migration: From epithelium-to-mesenchyme transition to collective cell migration. *Dev. Biol.*
- Thierry, J.P., Duband, J.L., and Delouee, A.** (1982). Pathways and mechanisms of avian trunk neural crest cell migration and localization. *Dev. Biol.* **93**, 324-343.
- Thompson, J.A. and Ziman, M.** (2011). Pax genes during neural development and their potential role in neuroregeneration. *Prog. Neurobiol.* **95**, 334-351.
- Toriello, H.V. and Higgins, J.V.** (1985). Possible causal heterogeneity in spina bifida cystica. *Am. J. Med. Genet.* **21**, 13-20.
- Torres, M., Gomez-Pardo, E., Dressler, G.R., and Gruss, P.** (1995). Pax-2 controls multiple steps of urogenital development. *Development.* **121**, 4057-4065.
- Tsukamoto, K., Nakamura, Y., and Niikawa, N.** (1994). Isolation of two isoforms of the PAX3 gene transcripts and their tissue-specific alternative expression in human adult tissues. *Hum. Genet.* **93**, 270-274.

- Tubbs,R.S., Chambers,M.R., Smyth,M.D., Bartolucci,A.A., Bruner,J.P., Tulipan,N., and Oakes,W.J.** (2003). Late gestational intrauterine myelomeningocele repair does not improve lower extremity function. *Pediatr. Neurosurg.* **38**, 128-132.
- Tung,E.W. and Winn,L.M.** (2011). Valproic acid increases formation of reactive oxygen species and induces apoptosis in postimplantation embryos: a role for oxidative stress in valproic acid-induced neural tube defects. *Mol. Pharmacol.* **80**, 979-987.
- Underhill,D.A. and Gros,P.** (1997). The paired-domain regulates DNA binding by the homeodomain within the intact Pax-3 protein. *J. Biol. Chem.* **272**, 14175-14182.
- Underhill,D.A., Vogan,K.J., and Gros,P.** (1995). Analysis of the mouse Splotch-delayed mutation indicates that the Pax-3 paired domain can influence homeodomain DNA-binding activity. *Proc. Natl. Acad. Sci. U. S. A* **92**, 3692-3696.
- Underwood,T.J., Amin,J., Lillycrop,K.A., and Blaydes,J.P.** (2007). Dissection of the functional interaction between p53 and the embryonic proto-oncoprotein PAX3. *FEBS Lett.* **581**, 5831-5835.
- Urbanek,P., Wang,Z.Q., Fetka,I., Wagner,E.F., and Busslinger,M.** (1994). Complete block of early B cell differentiation and altered patterning of the posterior midbrain in mice lacking Pax5/BSAP. *Cell.* **79**, 901-912.
- Valenta,T., Gay,M., Steiner,S., Draganova,K., Zemke,M., Hoffmans,R., Cinelli,P., Aguet,M., Sommer,L., and Basler,K.** (2011). Probing transcription-specific outputs of beta-catenin in vivo. *Genes Dev.* **25**, 2631-2643.
- Vallin,J., Girault,J.M., Thiery,J.P., and Broders,F.** (1998). Xenopus cadherin-11 is expressed in different populations of migrating neural crest cells. *Mech. Dev.* **75**, 171-174.
- Vallin,J., Thuret,R., Giacomello,E., Faraldo,M.M., Thiery,J.P., and Broders,F.** (2001). Cloning and characterization of three Xenopus slug promoters reveal direct regulation by Lef/beta-catenin signaling. *J. Biol. Chem.* **276**, 30350-30358.
- van de Wetering,M., Cavallo,R., Dooijes,D., van,B.M., van,E.J., Loureiro,J., Ypma,A., Hursh,D., Jones,T., Bejsovec,A. et al.** (1997). Armadillo coactivates transcription driven by the product of the Drosophila segment polarity gene dTCF. *Cell* **88**, 789-799.
- van der Put,N.M., Steegers-Theunissen,R.P., Frosst,P., Trijbels,F.J., Eskes,T.K., van den Heuvel,L.P., Mariman,E.C., den,H.M., Rozen,R., and Blom,H.J.** (1995). Mutated methylenetetrahydrofolate reductase as a risk factor for spina bifida. *Lancet* **346**, 1070-1071.
- van Straaten,H.W., Hekking,J.W., Consten,C., and Copp,A.J.** (1993). Intrinsic and extrinsic factors in the mechanism of neurulation: effect of curvature of the body axis on closure of the posterior neuropore. *Development* **117**, 1163-1172.
- van Straaten,H.W., Hekking,J.W., Thors,F., Wiertz-Hoessels,E.L., and Drukker,J.** (1985). Induction of an additional floor plate in the neural tube. *Acta Morphol. Neerl. Scand.* **23**, 91-97.
- Van,C.G., Van Thienen,M.N., Handig,I., Van,R.B., Rao,V.S., Milunsky,A., Read,A.P., Baldwin,C.T., Farrer,L.A., Bonduelle,M. et al.** (1995). Chromosome 13q deletion with Waardenburg syndrome: further evidence for a gene involved in neural crest function on 13q. *J. Med. Genet.* **32**, 531-536.

- Vega,S., Morales,A.V., Ocana,O.H., Valdes,F., Fabregat,I., and Nieto,M.A.** (2004a). Snail blocks the cell cycle and confers resistance to cell death. *Genes Dev.* **18**, 1131-1143.
- Vega,S., Morales,A.V., Ocana,O.H., Valdes,F., Fabregat,I., and Nieto,M.A.** (2004b). Snail blocks the cell cycle and confers resistance to cell death. *Genes Dev.* **18**, 1131-1143.
- Verbeek,R.J., Heep,A., Maurits,N.M., Cremer,R., Hoving,E.W., Brouwer,O.F., van der Hoeven,J.H., and Sival,D.A.** (2012). Fetal endoscopic myelomeningocele closure preserves segmental neurological function. *Dev. Med. Child Neurol.* **54**, 15-22.
- Verras,M., Papandreou,I., Lim,A.L., and Denko,N.C.** (2008). Tumor hypoxia blocks Wnt processing and secretion through the induction of endoplasmic reticulum stress. *Mol. Cell Biol.* **28**, 7212-7224.
- Vincentz,J.W., Firulli,B.A., Lin,A., Spicer,D.B., Howard,M.J., and Firulli,A.B.** (2013). Twist1 controls a cell-specification switch governing cell fate decisions within the cardiac neural crest. *PLoS. Genet.* **9**, e1003405.
- Vogan,K.J., Epstein,D.J., Trasler,D.G., and Gros,P.** (1993). The splotch-delayed (Spd) mouse mutant carries a point mutation within the paired box of the Pax-3 gene. *Genomics.* **17**, 364-369.
- WAARDENBURG,P.J.** (1951). A new syndrome combining developmental anomalies of the eyelids, eyebrows and nose root with pigmentary defects of the iris and head hair and with congenital deafness. *Am. J. Hum. Genet.* **3**, 195-253.
- Wallingford,J.B., Niswander,L.A., Shaw,G.M., and Finnell,R.H.** (2013). The continuing challenge of understanding, preventing, and treating neural tube defects. *Science* **339**, 1222002.
- Walther,C. and Gruss,P.** (1991). Pax-6, a murine paired box gene, is expressed in the developing CNS. *Development* **113**, 1435-1449.
- Walther,C., Guenet,J.L., Simon,D., Deutsch,U., Jostes,B., Goulding,M.D., Plachov,D., Balling,R., and Gruss,P.** (1991). Pax: a murine multigene family of paired box-containing genes. *Genomics.* **11**, 424-434.
- Wang,J., Hamblet,N.S., Mark,S., Dickinson,M.E., Brinkman,B.C., Segil,N., Fraser,S.E., Chen,P., Wallingford,J.B., and Wynshaw-Boris,A.** (2006). Dishevelled genes mediate a conserved mammalian PCP pathway to regulate convergent extension during neurulation. *Development.* **133**, 1767-1778.
- Wang,Q., Kumar,S., Mitsios,N., Slevin,M., and Kumar,P.** (2007). Investigation of downstream target genes of PAX3c, PAX3e and PAX3g isoforms in melanocytes by microarray analysis. *Int. J. Cancer.* **120**, 1223-1231.
- Wang,W.C. and Shashikant,C.S.** (2007). Evidence for positive and negative regulation of the mouse Cdx2 gene. *J. Exp. Zool. B Mol. Dev. Evol.* **308**, 308-321.
- Wang,X., Wang,J., Guan,T., Xiang,Q., Wang,M., Guan,Z., Li,G., Zhu,Z., Xie,Q., Zhang,T. et al.** (2013). Role of methotrexate exposure in apoptosis and proliferation during early neurulation. *J. Appl. Toxicol.*
- Wang,X.D., Morgan,S.C., and Loeken,M.R.** (2011). Pax3 stimulates p53 ubiquitination and degradation independent of transcription. *PLoS. One.* **6**, e29379.

- Watanabe,T., Tanaka,G., Hamada,S., Namiki,C., Suzuki,T., Nakajima,M., and Furihata,C.** (2009). Dose-dependent alterations in gene expression in mouse liver induced by diethylnitrosamine and ethylnitrosourea and determined by quantitative real-time PCR. *Mutat. Res.* **673**, 9-20.
- Waterland,R.A. and Jirtle,R.L.** (2003). Transposable elements: targets for early nutritional effects on epigenetic gene regulation. *Mol. Cell Biol.* **23**, 5293-5300.
- Watkins,M.L., Rasmussen,S.A., Honein,M.A., Botto,L.D., and Moore,C.A.** (2003). Maternal obesity and risk for birth defects. *Pediatrics* **111**, 1152-1158.
- Watkins,M.L., Scanlon,K.S., Mulinare,J., and Khoury,M.J.** (1996). Is maternal obesity a risk factor for anencephaly and spina bifida? *Epidemiology* **7**, 507-512.
- Wehrli,M., Dougan,S.T., Caldwell,K., O'Keefe,L., Schwartz,S., Vaizel-Ohayon,D., Schejter,E., Tomlinson,A., and DiNardo,S.** (2000). *arrow* encodes an LDL-receptor-related protein essential for Wingless signalling. *Nature* **407**, 527-530.
- Wei,D. and Loeken,M.R.** (2014). Increased DNA methyltransferase 3b (Dnmt3b)-mediated CpG island methylation stimulated by oxidative stress inhibits expression of a gene required for neural tube and neural crest development in diabetic pregnancy. *Diabetes.* **63**, 3512-3522.
- Wei,X., Li,H., Miao,J., Zhou,F., Liu,B., Wu,D., Li,S., Wang,L., Fan,Y., Wang,W. et al.** (2012). Disturbed apoptosis and cell proliferation in developing neuroepithelium of lumbo-sacral neural tubes in retinoic acid-induced spina bifida aperta in rat. *Int. J. Dev. Neurosci.* **30**, 375-381.
- Werth,M., Walentin,K., Aue,A., Schonheit,J., Wuebken,A., Pode-Shakked,N., Vilianovitch,L., Erdmann,B., Dekel,B., Bader,M. et al.** (2010). The transcription factor grainyhead-like 2 regulates the molecular composition of the epithelial apical junctional complex. *Development* **137**, 3835-3845.
- Wickline,E.D., Awuah,P.K., Behari,J., Ross,M., Stolz,D.B., and Monga,S.P.** (2011). Hepatocyte gamma-catenin compensates for conditionally deleted beta-catenin at adherens junctions. *J. Hepatol.* **55**, 1256-1262.
- Wickline,E.D., Du,Y., Stolz,D.B., Kahn,M., and Monga,S.P.** (2013). gamma-Catenin at adherens junctions: mechanism and biologic implications in hepatocellular cancer after beta-catenin knockdown. *Neoplasia.* **15**, 421-434.
- Wiechens,N., Heinle,K., Englmeier,L., Schohl,A., and Fagotto,F.** (2004). Nucleo-cytoplasmic shuttling of Axin, a negative regulator of the Wnt-beta-catenin Pathway. *J. Biol. Chem.* **279**, 5263-5267.
- Wiggan,O., Fadel,M.P., and Hamel,P.A.** (2002). Pax3 induces cell aggregation and regulates phenotypic mesenchymal-epithelial interconversion. *J. Cell Sci.* **115**, 517-529.
- Wiggan,O. and Hamel,P.A.** (2002). Pax3 regulates morphogenetic cell behavior in vitro coincident with activation of a PCP/non-canonical Wnt-signaling cascade. *J. Cell Sci.* **115**, 531-541.
- Wilcox,E.R., Rivolta,M.N., Ploplis,B., Potterf,S.B., and Fex,J.** (1992). The PAX3 gene is mapped to human chromosome 2 together with a highly informative CA dinucleotide repeat. *Hum. Mol. Genet.* **1**, 215.

- Willert,J., Epping,M., Pollack,J.R., Brown,P.O., and Nusse,R.** (2002). A transcriptional response to Wnt protein in human embryonic carcinoma cells. *BMC. Dev. Biol.* **2**, 8.
- Willert,K., Brink,M., Wodarz,A., Varmus,H., and Nusse,R.** (1997). Casein kinase 2 associates with and phosphorylates Dishevelled. *EMBO J.* **16**, 3089-3096.
- Willert,K., Brown,J.D., Danenberg,E., Duncan,A.W., Weissman,I.L., Reya,T., Yates,J.R., III, and Nusse,R.** (2003). Wnt proteins are lipid-modified and can act as stem cell growth factors. *Nature* **423**, 448-452.
- Willert,K. and Nusse,R.** (1998). Beta-catenin: a key mediator of Wnt signaling. *Curr. Opin. Genet. Dev.* **8**, 95-102.
- Willert,K., Shibamoto,S., and Nusse,R.** (1999). Wnt-induced dephosphorylation of axin releases beta-catenin from the axin complex. *Genes Dev.* **13**, 1768-1773.
- Williams,L.J., Mai,C.T., Edmonds,L.D., Shaw,G.M., Kirby,R.S., Hobbs,C.A., Sever,L.E., Miller,L.A., Meaney,F.J., and Levitt,M.** (2002). Prevalence of spina bifida and anencephaly during the transition to mandatory folic acid fortification in the United States. *Teratology* **66**, 33-39.
- Wilson,D.B.** (1974). Proliferation in the neural tube of the splotch (Sp) mutant mouse. *J. Comp Neurol.* **154**, 249-255.
- Wilson,L. and Maden,M.** (2005). The mechanisms of dorsoventral patterning in the vertebrate neural tube. *Dev. Biol.* **282**, 1-13.
- Wilson,P.A. and Hemmati-Brivanlou,A.** (1995). Induction of epidermis and inhibition of neural fate by Bmp-4. *Nature* **376**, 331-333.
- Wilson,S.I. and Edlund,T.** (2001). Neural induction: toward a unifying mechanism. *Nat. Neurosci.* **4 Suppl:1161-8.**, 1161-1168.
- Wilson,S.I., Graziano,E., Harland,R., Jessell,T.M., and Edlund,T.** (2000). An early requirement for FGF signalling in the acquisition of neural cell fate in the chick embryo. *Curr. Biol.* **10**, 421-429.
- Wilson,S.I., Rydstrom,A., Trimborn,T., Willert,K., Nusse,R., Jessell,T.M., and Edlund,T.** (2001). The status of Wnt signalling regulates neural and epidermal fates in the chick embryo. *Nature* **411**, 325-330.
- Winyard,P.J., Risdon,R.A., Sams,V.R., Dressler,G.R., and Woolf,A.S.** (1996). The PAX2 transcription factor is expressed in cystic and hyperproliferative dysplastic epithelia in human kidney malformations. *J. Clin. Invest* **98**, 451-459.
- Wlodarczyk,B.C., Craig,J.C., Bennett,G.D., Calvin,J.A., and Finnell,R.H.** (1996). Valproic acid-induced changes in gene expression during neurulation in a mouse model. *Teratology.* **54**, 284-297.
- Wolda,S.L., Moody,C.J., and Moon,R.T.** (1993). Overlapping expression of Xwnt-3A and Xwnt-1 in neural tissue of *Xenopus laevis* embryos. *Dev. Biol.* **155**, 46-57.
- Wong,H.C., Bourdelas,A., Krauss,A., Lee,H.J., Shao,Y., Wu,D., Mlodzik,M., Shi,D.L., and Zheng,J.** (2003). Direct binding of the PDZ domain of Dishevelled to a conserved internal sequence in the C-terminal region of Frizzled. *Mol. Cell* **12**, 1251-1260.

- Wouters,M.M., Roeder,J.L., Tharayil,V.S., Stanich,J.E., Strege,P.R., Lei,S., Bardsley,M.R., Ordog,T., Gibbons,S.J., and Farrugia,G.** (2009). Protein kinase C $\{\gamma\}$ mediates regulation of proliferation by the serotonin 5-hydroxytryptamine receptor 2B. *J. Biol. Chem.* **284**, 21177-21184.
- Wu,X., Tu,X., Joeng,K.S., Hilton,M.J., Williams,D.A., and Long,F.** (2008). Rac1 activation controls nuclear localization of beta-catenin during canonical Wnt signaling. *Cell* **133**, 340-353.
- Xie,Z., Chen,Y., Li,Z., Bai,G., Zhu,Y., Yan,R., Tan,F., Chen,Y.G., Guillemot,F., Li,L. et al.** (2011). Smad6 promotes neuronal differentiation in the intermediate zone of the dorsal neural tube by inhibition of the Wnt/beta-catenin pathway. *Proc. Natl. Acad. Sci. U. S. A.* **108**, 12119-12124.
- Xing,Y., Takemaru,K., Liu,J., Berndt,J.D., Zheng,J.J., Moon,R.T., and Xu,W.** (2008). Crystal structure of a full-length beta-catenin. *Structure.* **16**, 478-487.
- Xu,W., Baribault,H., and Adamson,E.D.** (1998). Vinculin knockout results in heart and brain defects during embryonic development. *Development* **125**, 327-337.
- Xu,W., Rould,M.A., Jun,S., Desplan,C., and Pabo,C.O.** (1995). Crystal structure of a paired domain-DNA complex at 2.5 Å resolution reveals structural basis for Pax developmental mutations. *Cell* **80**, 639-650.
- Yamamoto,H., Kishida,S., Kishida,M., Ikeda,S., Takada,S., and Kikuchi,A.** (1999). Phosphorylation of axin, a Wnt signal negative regulator, by glycogen synthase kinase-3 β regulates its stability. *J. Biol. Chem.* **274**, 10681-10684.
- Yamashita,M.** (2013). From neuroepithelial cells to neurons: changes in the physiological properties of neuroepithelial stem cells. *Arch. Biochem. Biophys.* **534**, 64-70.
- Yanagawa,S., van,L.F., Wodarz,A., Klingensmith,J., and Nusse,R.** (1995). The dishevelled protein is modified by wingless signaling in Drosophila. *Genes Dev.* **9**, 1087-1097.
- Yang,J., Mani,S.A., Donaher,J.L., Ramaswamy,S., Itzykson,R.A., Come,C., Savagner,P., Gitelman,I., Richardson,A., and Weinberg,R.A.** (2004). Twist, a master regulator of morphogenesis, plays an essential role in tumor metastasis. *Cell.* **117**, 927-939.
- Ybot-Gonzalez,P. and Copp,A.J.** (1999). Bending of the neural plate during mouse spinal neurulation is independent of actin microfilaments. *Dev. Dyn.* **215**, 273-283.
- Ybot-Gonzalez,P., Gaston-Massuet,C., Girdler,G., Klingensmith,J., Arkell,R., Greene,N.D., and Copp,A.J.** (2007). Neural plate morphogenesis during mouse neurulation is regulated by antagonism of Bmp signalling. *Development* **134**, 3203-3211.
- Yin,Y., White,A.C., Huh,S.H., Hilton,M.J., Kanazawa,H., Long,F., and Ornitz,D.M.** (2008). An FGF-WNT gene regulatory network controls lung mesenchyme development. *Dev. Biol.* **319**, 426-436.
- Yokoyama,S. and Asahara,H.** (2011). The myogenic transcriptional network. *Cell Mol. Life Sci.* **68**, 1843-1849.
- Yoshida,H., Kong,Y.Y., Yoshida,R., Elia,A.J., Hakem,A., Hakem,R., Penninger,J.M., and Mak,T.W.** (1998). Apaf1 is required for mitochondrial pathways of apoptosis and brain development. *Cell* **94**, 739-750.

- Yost,C., Torres,M., Miller,J.R., Huang,E., Kimelman,D., and Moon,R.T.** (1996). The axis-inducing activity, stability, and subcellular distribution of beta-catenin is regulated in *Xenopus* embryos by glycogen synthase kinase 3. *Genes Dev.* **10**, 1443-1454.
- Young,H.M., Hearn,C.J., Farlie,P.G., Canty,A.J., Thomas,P.Q., and Newgreen,D.F.** (2001). GDNF is a chemoattractant for enteric neural cells. *Dev. Biol.* **229**, 503-516.
- Yuan,W., Condorelli,G., Caruso,M., Felsani,A., and Giordano,A.** (1996). Human p300 protein is a coactivator for the transcription factor MyoD. *J. Biol. Chem.* **271**, 9009-9013.
- Yun,K., Fischman,S., Johnson,J., Hrabe de,A.M., Weinmaster,G., and Rubenstein,J.L.** (2002). Modulation of the notch signaling by Mash1 and Dlx1/2 regulates sequential specification and differentiation of progenitor cell types in the subcortical telencephalon. *Development.* **129**, 5029-5040.
- Zechner,D., Fujita,Y., Hulsken,J., Muller,T., Walther,I., Taketo,M.M., Crenshaw,E.B., III, Birchmeier,W., and Birchmeier,C.** (2003). beta-Catenin signals regulate cell growth and the balance between progenitor cell expansion and differentiation in the nervous system. *Dev. Biol.* **258**, 406-418.
- Zeng,L., Fagotto,F., Zhang,T., Hsu,W., Vasicek,T.J., Perry,W.L., III, Lee,J.J., Tilghman,S.M., Gumbiner,B.M., and Costantini,F.** (1997). The mouse Fused locus encodes Axin, an inhibitor of the Wnt signaling pathway that regulates embryonic axis formation. *Cell* **90**, 181-192.
- Zeng,X., Huang,H., Tamai,K., Zhang,X., Harada,Y., Yokota,C., Almeida,K., Wang,J., Doble,B., Woodgett,J. et al.** (2008). Initiation of Wnt signaling: control of Wnt coreceptor Lrp6 phosphorylation/activation via frizzled, dishevelled and axin functions. *Development* **135**, 367-375.
- Zeng,X., Tamai,K., Doble,B., Li,S., Huang,H., Habas,R., Okamura,H., Woodgett,J., and He,X.** (2005). A dual-kinase mechanism for Wnt co-receptor phosphorylation and activation. *Nature* **438**, 873-877.
- Zhai,L., Chaturvedi,D., and Cumberledge,S.** (2004). *Drosophila* wnt-1 undergoes a hydrophobic modification and is targeted to lipid rafts, a process that requires porcupine. *J. Biol. Chem.* **279**, 33220-33227.
- Zhang,N., Wei,P., Gong,A., Chiu,W.T., Lee,H.T., Colman,H., Huang,H., Xue,J., Liu,M., Wang,Y. et al.** (2011). FoxM1 promotes beta-catenin nuclear localization and controls Wnt target-gene expression and glioma tumorigenesis. *Cancer Cell* **20**, 427-442.
- Zhao,T., Gan,Q., Stokes,A., Lassiter,R.N., Wang,Y., Chan,J., Han,J.X., Pleasure,D.E., Epstein,J.A., and Zhou,C.J.** (2014). beta-catenin regulates Pax3 and Cdx2 for caudal neural tube closure and elongation. *Development.* **141**, 148-157.
- Zhao,W., Mosley,B.S., Cleves,M.A., Melnyk,S., James,S.J., and Hobbs,C.A.** (2006). Neural tube defects and maternal biomarkers of folate, homocysteine, and glutathione metabolism. *Birth Defects Res. A Clin. Mol. Teratol.* **76**, 230-236.
- Zhong,Y., Brieher,W.M., and Gumbiner,B.M.** (1999). Analysis of C-cadherin regulation during tissue morphogenesis with an activating antibody. *J. Cell Biol.* **144**, 351-359.
- Zhou,H.M., Wang,J., Rogers,R., and Conway,S.J.** (2008). Lineage-specific responses to reduced embryonic Pax3 expression levels. *Dev. Biol.* **315**, 369-382.

- Zhou,J., Qu,J., Yi,X.P., Graber,K., Huber,L., Wang,X., Gerdes,A.M., and Li,F.** (2007). Upregulation of gamma-catenin compensates for the loss of beta-catenin in adult cardiomyocytes. *Am. J. Physiol Heart Circ. Physiol.* **292**, H270-H276.
- Zhu,H., Fearnhead,H.O., and Cohen,G.M.** (1995). An ICE-like protease is a common mediator of apoptosis induced by diverse stimuli in human monocytic THP.1 cells. *FEBS Lett.* **374**, 303-308.
- Zimmermann,D.R. and Ruoslahti,E.** (1989). Multiple domains of the large fibroblast proteoglycan, versican. *EMBO J.* **8**, 2975-2981.
- Zindy,F., Lamas,E., Chenivesse,X., Sobczak,J., Wang,J., Fesquet,D., Henglein,B., and Brechot,C.** (1992). Cyclin A is required in S phase in normal epithelial cells. *Biochem. Biophys. Res. Commun.* **182**, 1144-1154.
- Zlotogora,J., Lerer,I., Bar-David,S., Ergaz,Z., and Abeliovich,D.** (1995). Homozygosity for Waardenburg syndrome. *Am. J. Hum. Genet.* **56**, 1173-1178.
- Zoltewicz,J.S., Ashique,A.M., Choe,Y., Lee,G., Taylor,S., Phamluong,K., Solloway,M., and Peterson,A.S.** (2009). Wnt signaling is regulated by endoplasmic reticulum retention. *PLoS. One.* **4**, e6191.